

World Journal of *Gastrointestinal Oncology*

World J Gastrointest Oncol 2023 December 15; 15(12): 2049-2241



EDITORIAL

- 2049 Dual primary gastric and colorectal cancer: A complex challenge in surgical oncology
Marano L

MINIREVIEWS

- 2053 Identification of genes associated with gall bladder cell carcinogenesis: Implications in targeted therapy of gall bladder cancer
Ghosh I, Dey Ghosh R, Mukhopadhyay S

ORIGINAL ARTICLE**Clinical and Translational Research**

- 2064 Transient receptor potential-related risk model predicts prognosis of hepatocellular carcinoma patients
Mei XC, Chen Q, Zuo S

Retrospective Cohort Study

- 2077 Cohort study to assess geographical variation in cholangiocarcinoma treatment in England
Jose S, Zalin-Miller A, Knott C, Paley L, Tataru D, Morement H, Toledano MB, Khan SA

Retrospective Study

- 2093 Effect of ultrasound-guided lumbar square muscle block on stress response in patients undergoing radical gastric cancer surgery
Wang XR, Xu DD, Guo MJ, Wang YX, Zhang M, Zhu DX

- 2101 Application of remimazolam transversus abdominis plane block in gastrointestinal tumor surgery
Liu J, Tian JM, Liu GZ, Sun JN, Gao PF, Zhang YQ, Yue XQ

- 2111 The efficacy of full-thickness endoscopic resection of subepithelial tumors in the gastric cardia
Xu EP, Qi ZP, Li B, Ren Z, Cai MY, Cai SL, Lyv ZT, Chen ZH, Liu JY, Shi Q, Zhong YS

Basic Study

- 2120 Hsa_circ_0136666 mediates the antitumor effect of curcumin in colorectal carcinoma by regulating CXCL1 via miR-1301-3p

Chen S, Li W, Ning CG, Wang F, Wang LX, Liao C, Sun F

- 2138 Combined TIM-3 and PD-1 blockade restrains hepatocellular carcinoma development by facilitating CD4+ and CD8+ T cell-mediated antitumor immune responses

Zhang XS, Zhou HC, Wei P, Chen L, Ma WH, Ding L, Liang SC, Chen BD

- 2150** Association between heat shock factor protein 4 methylation and colorectal cancer risk and potential molecular mechanisms: A bioinformatics study
Zhang WJ, Yue KL, Wang JZ, Zhang Y
- 2169** Evaluating the causal relationship between human blood metabolites and gastroesophageal reflux disease
Hu JY, Lv M, Zhang KL, Qiao XY, Wang YX, Wang FY
- 2185** Paired-related homeobox 1 induces epithelial-mesenchymal transition in oesophageal squamous cancer
Guo JB, Du M, Wang B, Zhong L, Fu ZX, Wei JL

META-ANALYSIS

- 2197** Intensive follow-up *vs* conventional follow-up for patients with non-metastatic colorectal cancer treated with curative intent: A meta-analysis
Cui LL, Cui SQ, Qu Z, Ren ZQ
- 2212** Prognostic value of T cell immunoglobulin and mucin-domain containing-3 expression in upper gastrointestinal tract tumors: A meta-analysis
Yan JJ, Liu BB, Yang Y, Liu MR, Wang H, Deng ZQ, Zhang ZW
- 2225** Association of MBOAT7 rs641738 polymorphism with hepatocellular carcinoma susceptibility: A systematic review and meta-analysis
Lai M, Qin YL, Jin QY, Chen WJ, Hu J

CASE REPORT

- 2237** Conversion immunotherapy for deficient mismatch repair locally unresectable colon cancer: A case report
Sun Z, Liu H, Zhang GN, Xiao Y

ABOUT COVER

Editorial Board Member of *World Journal of Gastrointestinal Oncology*, Luigi Marano, MD, PhD, Professor, Department of Medicine, Academy of Medical and Social Applied Sciences-AMiSNS: Akademia Medycznych i Społecznych Nauk Stosowanych-2 Lotnicza Street, Elbląg 82-300, Poland. l.marano@amisns.edu.pl

AIMS AND SCOPE

The primary aim of *World Journal of Gastrointestinal Oncology* (*WJGO*, *World J Gastrointest Oncol*) is to provide scholars and readers from various fields of gastrointestinal oncology with a platform to publish high-quality basic and clinical research articles and communicate their research findings online.

WJGO mainly publishes articles reporting research results and findings obtained in the field of gastrointestinal oncology and covering a wide range of topics including liver cell adenoma, gastric neoplasms, appendiceal neoplasms, biliary tract neoplasms, hepatocellular carcinoma, pancreatic carcinoma, cecal neoplasms, colonic neoplasms, colorectal neoplasms, duodenal neoplasms, esophageal neoplasms, gallbladder neoplasms, *etc.*

INDEXING/ABSTRACTING

The *WJGO* is now abstracted and indexed in PubMed, PubMed Central, Science Citation Index Expanded (SCIE, also known as SciSearch®), Journal Citation Reports/Science Edition, Scopus, Reference Citation Analysis, China Science and Technology Journal Database, and Superstar Journals Database. The 2023 edition of Journal Citation Reports® cites the 2022 impact factor (IF) for *WJGO* as 3.0; IF without journal self cites: 2.9; 5-year IF: 3.0; Journal Citation Indicator: 0.49; Ranking: 157 among 241 journals in oncology; Quartile category: Q3; Ranking: 58 among 93 journals in gastroenterology and hepatology; and Quartile category: Q3. The *WJGO*'s CiteScore for 2022 is 4.1 and Scopus CiteScore rank 2022: Gastroenterology is 71/149; Oncology is 197/366.

RESPONSIBLE EDITORS FOR THIS ISSUE

Production Editor: *Xiang-Di Zhang*; Production Department Director: *Xu Guo*; Editorial Office Director: *Jia-Ru Fan*.

NAME OF JOURNAL

World Journal of Gastrointestinal Oncology

ISSN

ISSN 1948-5204 (online)

LAUNCH DATE

February 15, 2009

FREQUENCY

Monthly

EDITORS-IN-CHIEF

Monjur Ahmed, Florin Burada

POLICY OF CO-AUTHORS**EDITORIAL BOARD MEMBERS**

<https://www.wjgnet.com/1948-5204/editorialboard.htm>

PUBLICATION DATE

December 15, 2023

COPYRIGHT

© 2024 Baishideng Publishing Group Inc

INSTRUCTIONS TO AUTHORS

<https://www.wjgnet.com/bpg/gerinfo/204>

GUIDELINES FOR ETHICS DOCUMENTS

<https://www.wjgnet.com/bpg/GerInfo/287>

GUIDELINES FOR NON-NATIVE SPEAKERS OF ENGLISH

<https://www.wjgnet.com/bpg/gerinfo/240>

PUBLICATION ETHICS

<https://www.wjgnet.com/bpg/GerInfo/288>

PUBLICATION MISCONDUCT

<https://www.wjgnet.com/bpg/gerinfo/208>

<https://www.wjgnet.com/bpg/GerInfo/310>

ARTICLE PROCESSING CHARGE

<https://www.wjgnet.com/bpg/gerinfo/242>

STEPS FOR SUBMITTING MANUSCRIPTS

<https://www.wjgnet.com/bpg/GerInfo/239>

ONLINE SUBMISSION

<https://www.f6publishing.com>



Dual primary gastric and colorectal cancer: A complex challenge in surgical oncology

Luigi Marano

Specialty type: Oncology

Provenance and peer review:

Invited article; Externally peer reviewed.

Peer-review model: Single blind

Peer-review report's scientific quality classification

Grade A (Excellent): A

Grade B (Very good): 0

Grade C (Good): C

Grade D (Fair): 0

Grade E (Poor): 0

P-Reviewer: Liu Z, China; Wan XH, China

Received: October 17, 2023

Peer-review started: October 17, 2023

First decision: November 1, 2023

Revised: November 1, 2023

Accepted: November 17, 2023

Article in press: November 17, 2023

Published online: December 15, 2023



Luigi Marano, Medical Department, Academy of Applied Medical and Social Sciences - Akademia Medycznych i Społecznych Nauk Stosowanych, Elbląg 82-300, Poland

Corresponding author: Luigi Marano, MD, PhD, Professor, Medical Department, Academy of Applied Medical and Social Sciences - Akademia Medycznych i Społecznych Nauk Stosowanych, Lotnicza 2, Elbląg 82-300, Poland. l.marano@amisns.edu.pl

Abstract

The intricate interplay of colorectal cancer (CRC) and gastric cancer (GC) as dual primary malignancies presents a significant challenge in surgical oncology. CRC is the most common secondary malignancy in GC patients, and vice versa, evidence highlighted by advances in diagnostic procedures and therapy modalities that impact patient survival. A recent study titled "Features of synchronous and metachronous dual primary gastric and colorectal cancer" explores this enigmatic dual malignancy, uncovering crucial insights into the clinical characteristics and prognostic distinctions between synchronous and metachronous presentations. Notably, metachronous cases with a second primary cancer discovered more than six months after the first diagnosis have a better outcome, emphasizing the importance of early detection and treatment. This study underscores the prognostic role of GC stage in patient outcomes. It also sheds light on the complexities faced by synchronous cases, often presenting with unresectable CRC. Surgery-related procedures, like gastrectomy and colon resection, stand out as important predictors of increased survival, necessitating a reevaluation of current therapeutic approaches. A tailored and patient-centered strategy, considering the health of each patient individually and the feasibility of radical treatments, is essential. Continuous follow-up and monitoring are crucial as most second primary cancers arise within five years. In conclusion, early diagnosis, surgical intervention, and watchful surveillance are pivotal in managing dual primary gastric and colorectal cancer patients. Since the incidence of gastric and colorectal cancers continues to rise, the imperative need for further research, ideally with larger sample sizes, becomes evident in our pursuit of comprehensive insights that will refine clinical approaches for this intricate dual malignancy.

Key Words: Multiple primary cancers; Colorectal cancer; Gastric cancer; Dual primary cancers; Synchronous cancers; Metachronous cancers

Core Tip: This editorial explores the complex landscape of dual primary gastric and colorectal cancer (DPGCC), investigating synchronous and metachronous cases. It uncovers a clear prognostic gap, emphasizing the need of early detection. The research underlines the pivotal role of surgical interventions, with gastric cancer stage significantly impacting patient outcomes. It also highlights the need for regular follow-up due to the majority of second primary cancers occurring within five years. The current literature provides guidance for individualized therapeutic approaches, enhancing patient prognoses, and underscores the intricate and multifaceted character of managing DPGCC.

Citation: Marano L. Dual primary gastric and colorectal cancer: A complex challenge in surgical oncology. *World J Gastrointest Oncol* 2023; 15(12): 2049-2052

URL: <https://www.wjgnet.com/1948-5204/full/v15/i12/2049.htm>

DOI: <https://dx.doi.org/10.4251/wjgo.v15.i12.2049>

INTRODUCTION

The intersection of colorectal cancer (CRC) and gastric cancer (GC) as dual primary cancers presents a significant challenge in surgical oncology[1]. CRC, with an incidence of 11.4%, ranks among the most frequent tumors associated with multiple primary cancers[2], while GC can evolve into a second primary cancer, with an incidence ranging from 1% to 4.2% in GC patients[3-5]. The intricate relationship between these malignancies is bidirectional, with CRC being the most common second primary cancer in GC patients, and GC the most common second primary cancer in CRC patients [6-8]. Advances in diagnostic techniques and treatment modalities leading to extended patient survival will likely increase the detection and incidence of multiple primary cancers. This necessitates a comprehensive approach to the evaluation and management of dual primary gastric and CC (DPGCC). A recent study by Lin *et al*[9], titled "Features of synchronous and metachronous dual primary gastric and colorectal cancer", addresses this complex aspect of surgical oncology, providing valuable insights into the clinical characteristics and prognosis of DPGCC patients. Notably, the study reveals a distinct difference in prognosis between synchronous and metachronous DPGCCs. Patients with metachronous DPGCC exhibited a more favorable prognosis, underlining the significance of early diagnosis and intervention. The study also highlights the high rate of unresectable CC in synchronous DPGCC patients, emphasizing the complexity of managing this dual malignancy. Additionally, it underscores the critical influence of GC stage on patient outcomes, with stage III-IV patients experiencing a considerably worse prognosis. Surgical interventions, such as gastrectomy and colorectal resection, significantly improved survival rates. Regular follow-up and surveillance emerged as crucial components, with the majority of second primary cancers in DPGCC cases occurring within five years. The study's findings have important implications for tailoring treatment strategies and improving patient outcomes in DPGCC.

SYNCHRONOUS VS METACHRONOUS DPGCC: A PROGNOSTIC GAP

The theory of the etiologic field effect, frequently invoked in the field of multiple primary cancers, offers valuable insights into the pathogenesis and evolution of DPGCC[10]. This theoretical framework postulates that the epithelium of the gastrointestinal tract is subjected to a dynamic interplay of genetic and environmental variables, which increases the tendency for carcinogenesis. Both the stomach and the colorectum are equally sensitive to these factors' effect because they are both essential parts of the continuous mucosal epithelium lining the digestive tract, exposing patients to synchronous or metachronous carcinogenesis. Empirical research confirms a detectable relationship between the initial primary cancer and the second primary cancer in patients with multiple primary neoplasms, highlighting the intricate multifactorial etiology of DPGCC[11-13]. This enriches our understanding of the intricate dynamics at play in the DPGCC landscape, shedding light on the relationships governing its occurrence. Importantly, the study's primary finding, that patients with metachronous DPGCC exhibit a more favorable prognosis compared to synchronous cases, is consistent with previous studies on multiple primary cancers' prognosis[14-16]. This observation underscores the need for tailored treatment strategies and watchful surveillance for patients with synchronous DPGCC, further illuminating the factors influencing this gap in prognosis and refining our approach to managing these challenging cases.

RESECTION AS A PROGNOSTIC KEY FACTOR

The study emphasizes the central role of clinicopathologic characteristics of DPGCC and the inclusion of therapeutic factors in the prognostic analysis[16]. Gastrectomy and colorectal resection were associated with better prognosis, highlighting the importance of early diagnosis and surgical intervention. The identification of GC resection as an

independent predictor of overall survival aligns with the benefits of surgical intervention in GC[17]. This underscores the value of radical surgery in synchronous DPGCC cases, encouraging a reconsideration of treatment strategies and the need for improved diagnostic and therapeutic approaches for this specific dual malignancy.

On the other hand, the research also highlights the high rate of unresectable CC in synchronous DPGCC patients as well as the significant impact of GC stage on patient prognosis, underscoring the importance of early detection and further investigation to identify contributing factors. It is essential to emphasize that the treatment approach for DPGCC remains challenging and multifaceted, requiring individualized evaluation and consideration of patient health and the feasibility of perioperative multidisciplinary treatments associated with radical surgeries.

INTENSIVE FOLLOW-UP: A KEY ISSUE

Early diagnosis and timely intervention are essential in the clinical management of DPGCC[14]. The research demonstrates that most second primary cancers in DPGCC cases occur within five years, highlighting the importance of intensive surveillance and follow-up for patients with gastric or CC. Postoperative monitoring of the entire digestive tract is essential, and patients who have extensive resections might need protracted monitoring, underlining the importance of thorough, long-term follow-up to achieve the best outcomes.

CONCLUSION

In conclusion, early diagnosis, surgical resection, and watchful follow-up are essential for managing DPGCC patients. The current literature conclusions call for a reevaluation of therapeutic approaches, particularly in synchronous cases when radical surgery may hold the key to improved outcomes. Furthermore, economic considerations should also be explored to determine the cost-benefit ratio of surveillance strategies. As the incidence of gastric and colorectal cancers continues to rise, the insights derived from this research, as well as the current body of literature, will steer us toward more effective treatment and follow-up strategies for DPGCC. Further research, ideally with larger sample sizes, is imperative to corroborate and expand upon these findings, thereby offering a more comprehensive understanding of DPGCC and guiding more effective clinical approaches in the future.

FOOTNOTES

Author contributions: Marano L designed the overall concept and outline of the manuscript, wrote and edited the manuscript and review of literature.

Conflict-of-interest statement: The author reports no relevant conflicts of interest for this article.

Open-Access: This article is an open-access article that was selected by an in-house editor and fully peer-reviewed by external reviewers. It is distributed in accordance with the Creative Commons Attribution NonCommercial (CC BY-NC 4.0) license, which permits others to distribute, remix, adapt, build upon this work non-commercially, and license their derivative works on different terms, provided the original work is properly cited and the use is non-commercial. See: <https://creativecommons.org/licenses/by-nc/4.0/>

Country/Territory of origin: Poland

ORCID number: Luigi Marano [0000-0002-9777-9588](https://orcid.org/0000-0002-9777-9588).

S-Editor: Wang JJ

L-Editor: A

P-Editor: Zhang XD

REFERENCES

- Vogt A, Schmid S, Heinimann K, Frick H, Herrmann C, Cerny T, Omlin A. Multiple primary tumours: challenges and approaches, a review. *ESMO Open* 2017; **2**: e000172 [PMID: 28761745 DOI: 10.1136/esmoopen-2017-000172]
- Tanjak P, Suktitipat B, Vorasan N, Juengwiwattanakit P, Thientrong B, Songjang C, Therasakvichya S, Laiteerapong S, Chinswangwatanakul V. Risks and cancer associations of metachronous and synchronous multiple primary cancers: a 25-year retrospective study. *BMC Cancer* 2021; **21**: 1045 [PMID: 34556087 DOI: 10.1186/s12885-021-08766-9]
- Ikeda Y, Saku M, Kawanaka H, Nonaka M, Yoshida K. Features of second primary cancer in patients with gastric cancer. *Oncology* 2003; **65**: 113-117 [PMID: 12931016 DOI: 10.1159/000072335]
- Eom BW, Lee HJ, Yoo MW, Cho JJ, Kim WH, Yang HK, Lee KU. Synchronous and metachronous cancers in patients with gastric cancer. *J Surg Oncol* 2008; **98**: 106-110 [PMID: 18452218 DOI: 10.1002/jso.21027]
- Ha TK, An JY, Youn HG, Noh JH, Sohn TS, Kim S. Surgical outcome of synchronous second primary cancer in patients with gastric cancer.

- Yonsei Med J* 2007; **48**: 981-987 [PMID: 18159590 DOI: 10.3349/ymj.2007.48.6.981]
- 6 **Lee JH**, Bae JS, Ryu KW, Lee JS, Park SR, Kim CG, Kook MC, Choi IJ, Kim YW, Park JG, Bae JM. Gastric cancer patients at high-risk of having synchronous cancer. *World J Gastroenterol* 2006; **12**: 2588-2592 [PMID: 16688807 DOI: 10.3748/wjg.v12.i16.2588]
 - 7 **Lim SB**, Jeong SY, Choi HS, Sohn DK, Hong CW, Jung KH, Chang HJ, Park JG, Choi IJ, Kim CG. Synchronous gastric cancer in primary sporadic colorectal cancer patients in Korea. *Int J Colorectal Dis* 2008; **23**: 61-65 [PMID: 17724601 DOI: 10.1007/s00384-007-0366-z]
 - 8 **Yoon SN**, Oh ST, Lim SB, Kim TW, Kim JH, Yu CS, Kim JC. Clinicopathologic characteristics of colorectal cancer patients with synchronous and metachronous gastric cancer. *World J Surg* 2010; **34**: 2168-2176 [PMID: 20532772 DOI: 10.1007/s00268-010-0623-0]
 - 9 **Lin YJ**, Chen HX, Zhang FX, Hu XS, Cheng YZ, Peng JS, Lian L. Features of synchronous and metachronous dual primary gastric and colorectal cancer. *World J Gastrointest Oncol* 2023; **15**: 1864-1873 [DOI: 10.4251/wjgo.v15.i11.1864]
 - 10 **Lochhead P**, Chan AT, Nishihara R, Fuchs CS, Beck AH, Giovannucci E, Ogino S. Etiologic field effect: reappraisal of the field effect concept in cancer predisposition and progression. *Mod Pathol* 2015; **28**: 14-29 [PMID: 24925058 DOI: 10.1038/modpathol.2014.81]
 - 11 **Samowitz WS**, Albertsen H, Sweeney C, Herrick J, Caan BJ, Anderson KE, Wolff RK, Slattery ML. Association of smoking, CpG island methylator phenotype, and V600E BRAF mutations in colon cancer. *J Natl Cancer Inst* 2006; **98**: 1731-1738 [PMID: 17148775 DOI: 10.1093/jnci/djj468]
 - 12 **Toyomura K**, Yamaguchi K, Kawamoto H, Tabata S, Shimizu E, Mineshita M, Ogawa S, Lee KY, Kono S. Relation of cigarette smoking and alcohol use to colorectal adenomas by subsite: the self-defense forces health study. *Cancer Sci* 2004; **95**: 72-76 [PMID: 14720330 DOI: 10.1111/j.1349-7006.2004.tb03173.x]
 - 13 **Leggett BA**, Worthley DL. Synchronous colorectal cancer: not just bad luck? *Gastroenterology* 2009; **137**: 1559-1562 [PMID: 19789087 DOI: 10.1053/j.gastro.2009.09.025]
 - 14 **Park JH**, Baek JH, Yang JY, Lee WS, Lee WK. Clinicopathologic characteristics and survival rate in patients with synchronous or metachronous double primary colorectal and gastric cancer. *Korean J Clin Oncol* 2018; **14**: 83-88 [DOI: 10.14216/kjco.18015]
 - 15 **Ueno M**, Muto T, Oya M, Ota H, Azekura K, Yamaguchi T. Multiple primary cancer: an experience at the Cancer Institute Hospital with special reference to colorectal cancer. *Int J Clin Oncol* 2003; **8**: 162-167 [PMID: 12851840 DOI: 10.1007/s10147-003-0322-z]
 - 16 **Watanabe M**, Kochi M, Fujii M, Kaiga T, Mihara Y, Funada T, Tamegai H, Shimizu H, Takayama T. Dual primary gastric and colorectal cancer: is the prognosis better for synchronous or metachronous? *Am J Clin Oncol* 2012; **35**: 407-410 [PMID: 21659834 DOI: 10.1097/COC.0b013e318218585a]
 - 17 **Wu J**, Yu J, Chen Z, Zhu H, Zhong C, Liang Y, Mai Z, Lin Z, Wan Y, Li G. Survival benefit of primary tumor resection for gastric cancer with liver metastasis: A propensity score-matched, population-based study. *Front Oncol* 2022; **12**: 1039086 [PMID: 36465378 DOI: 10.3389/fonc.2022.1039086]



Identification of genes associated with gall bladder cell carcinogenesis: Implications in targeted therapy of gall bladder cancer

Ishita Ghosh, Ruma Dey Ghosh, Soma Mukhopadhyay

Specialty type: Oncology

Provenance and peer review:

Unsolicited article; Externally peer reviewed.

Peer-review model: Single blind

Peer-review report's scientific quality classification

Grade A (Excellent): 0
Grade B (Very good): 0
Grade C (Good): 0
Grade D (Fair): D, D
Grade E (Poor): 0

P-Reviewer: Dumitrașcu T, Romania; Yu PF, China

Received: July 27, 2023

Peer-review started: July 27, 2023

First decision: September 26, 2023

Revised: October 11, 2023

Accepted: November 10, 2023

Article in press: November 10, 2023

Published online: December 15, 2023



Ishita Ghosh, Ruma Dey Ghosh, Soma Mukhopadhyay, Department of Molecular Biology, Netaji Subhas Chandra Bose Cancer Research Institute, Kolkata 700094, India

Corresponding author: Soma Mukhopadhyay, BSc, MSc, PhD, Director, Senior Scientist, Department of Molecular Biology, Netaji Subhas Chandra Bose Cancer Research Institute, 3081 Nayabad, Kolkata 700094, India. soma.nscri@gmail.com

Abstract

Gall bladder cancer (GBC) is becoming a very devastating form of hepatobiliary cancer in India. Every year new cases of GBC are quite high in India. Despite recent advanced multimodality treatment options, the survival of GBC patients is very low. If the disease is diagnosed at the advanced stage (with local nodal metastasis or distant metastasis) or surgical resection is inoperable, the prognosis of those patients is very poor. So, perspectives of targeted therapy are being taken. Targeted therapy includes hormone therapy, proteasome inhibitors, signal transduction and apoptosis inhibitors, angiogenesis inhibitors, and immunotherapeutic agents. One such signal transduction inhibitor is the specific short interfering RNA (siRNA) or short hairpin RNA (shRNA). For developing siRNA-mediated therapy shRNA, although several preclinical studies to evaluate the efficacy of these key molecules have been performed using gall bladder cells, many more clinical trials are required. To date, many such genes have been identified. This review will discuss the recently identified genes associated with GBC and those that have implications in its treatment by siRNA or shRNA.

Key Words: Gall bladder cancer; Gene biomarker; Targeted therapy; siRNA mediated therapy; Prognosis; Advanced therapy of gall bladder cancer

©The Author(s) 2023. Published by Baishideng Publishing Group Inc. All rights reserved.

Core Tip: The frequency of gall bladder cancer (GBC) in India has increased. The survival of GBC patients is also poor. In this context, some genes have been recognized which are involved in the carcinogenesis of GBCs. In this review, we have discussed such genes which could be aimed for the development of targeted therapy for GBC.

Citation: Ghosh I, Dey Ghosh R, Mukhopadhyay S. Identification of genes associated with gall bladder cell carcinogenesis: Implications in targeted therapy of gall bladder cancer. *World J Gastrointest Oncol* 2023; 15(12): 2053-2063

URL: <https://www.wjgnet.com/1948-5204/full/v15/i12/2053.htm>

DOI: <https://dx.doi.org/10.4251/wjgo.v15.i12.2053>

INTRODUCTION

Gall bladder cancer (GBC) is the most common among hepatobiliary cancers. In India every year approximately 19570 new cases are detected and approximately 14736 death occurs due to GBC. According to the Cancer Registry, the rate of GBC is highest in Bolivia (14/100000) and Chile (9.3/100000)[1]. Recently, the occurrence of GBC in India is comparable and close to these countries. In 2001-2004, 6-7 individuals suffered from GBC among 100000 individuals, but in 2012-2014, 10-11 individuals suffered from GBC among 100000 individuals[2]. The total number of GBC cases in India is about 10% of the total GBC cases in the world. The rate of GBC is increasing in India in both males and females. If only the north and northeast are considered, the rates are even higher, which are 11.8/100000 and 17.1/10000 respectively (National Cancer Registry Program, 2012-2014). GBC is found to have a poor prognosis. Among the patients diagnosed with GBC, the average 5-year survival rate is as low as 19%. Unfortunately, most of the GBCs are detected after malignant cells have spread to other organs. In that case, chemotherapy and palliative treatment are the only options (Figure 1). Other approaches of tailored treatment are necessary for the treatment of this disease (Figure 1). Next-generation sequencing, whole exome sequencing, RNA sequencing, single cell isolation, and proteomics are some of the approaches to tailored treatment. This has been applied to specific target treatment, immunotherapy, vaccine therapy, and treatment with nanoparticles, which are already in clinical trials[3]. Therefore, a detailed study of the key molecules involved in the process of carcinogenesis of GBC is necessary for the tailored treatment of this disease.

Short interfering RNA (siRNA) is a small double-stranded RNA interfering molecule whereas, short hairpin RNA (shRNA) is a single-stranded RNA molecule folded into a hairpin or stem-loop-like structure. siRNA can be endogenous, exogenous, or artificial in origin for transient expression. Primarily, siRNA is to provide viral/bacterial defense and genomic stability. It is very similar to microRNA (miRNA), which mainly functions as an endogenous regulator of gene expression through gene silencing. ShRNA is an artificial molecule integrated into genomic DNA for long-term gene silencing of a specific gene expression. The shRNA is processed by DICER to generate siRNA. These siRNAs are then untwisted by helicases into two single strands, one is called the passenger strand and the other is called the guide strand. The guide strand combines with other components to form the RNA-induced silencing complex (RISC). The other main components of RISC are transactivation response RNA binding protein, protein activator of protein kinase R, and Argonaute2 (Ago2). The guide strand binds to its complementary mRNA strand. Ago2 cuts and removes the targeted mRNA. This mRNA becomes inactive and then cannot be translated and expressed. So, when a specific siRNA is introduced into the cell, it stops the translation of the corresponding mRNA.

In this review, we will describe some siRNA-based gene therapeutic techniques that have yielded positive results for the implication of treatment of GBC. In the present review, we have identified some genes that are responsible for the spread of GBC cells. Approaches for silencing these genes could have the potential for the treatment of this disease. One approach to silencing these genes is by constructing and delivering specific short-interfering RNAs or siRNAs. Technology for the construction of specific siRNA has already been developed and is in practice.

TARGET GENES FOR siRNA-MEDIATED GBC THERAPY

Genes related to the development of gall bladder tumor

KRAS (Kirsten sarcoma viral oncogene homolog): The gene *KRAS* encodes a protein which is 21 kDa and occurs in the inner side of the plasma membrane of those cells which could bind GTP and have the ability to convert GTP into GDP. However, when *KRAS* is attached to GTP, it remains active and plays an important role in the cell signaling pathways[4]. When GTP is converted to GDP, *KRAS* becomes inactive. Mutations in the *KRAS* gene result in the loss of the ability of the *KRAS* protein to return to its inactive form. This affects cell signaling pathways[5]. It was evident from a set of experiments that mutation of *KRAS* causes the development of gall bladder adenoma[6]. The possible mechanism is that *KRAS* activates the NOTCH signaling pathway and leads to tumor development.

PIK3CA (Phosphatidylinositol-4,5-bisphosphate 3-kinase catalytic subunit alpha): The gene *PIK3CA* encodes a protein (p110), which is the stimulating subunit of the enzyme PI3K. It is well known now that PI3K participates in many events of cell signaling and is well-linked to cell growth and proliferation[7]. In a set of experiments examining the role of PI3K-AKT in gall bladder tumorigenesis, it was observed that the PI3K-AKT pathway is disturbed when *PIK3CA* is mutated. The gall bladder epithelial cells are directed towards mesenchymal transition and lead to tumor formation[8].

Genes related to invasive metastasis

CD44 (Cluster of differentiation 44): CD44 is a glycoprotein which is found in the lipid bilayer. It is encoded by the gene *CD44* present on chromosome 11[9]. This glycoprotein is required in the interplay between the cells, mainly in cell attachment and migration. It is found to have a function in the activation of lymphocytes, formation of blood cell

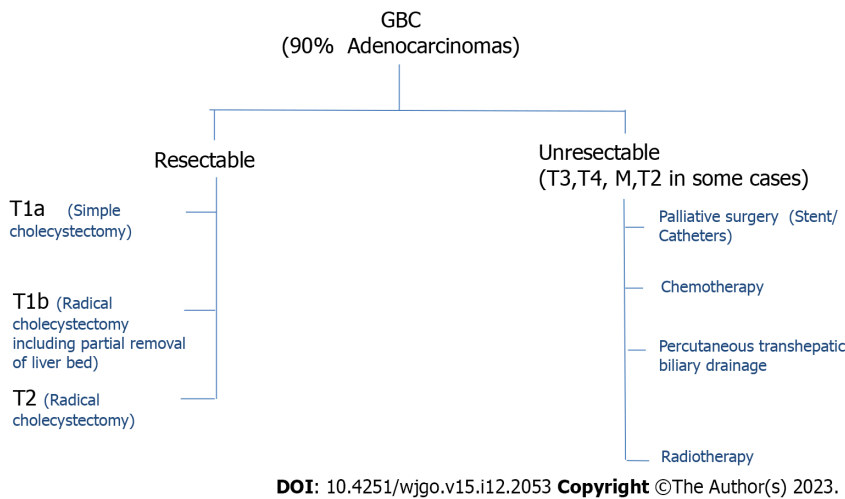


Figure 1 Current scenario of gall bladder cancer treatment strategies. T1a, T1b, T2, T3, and T4 stand for the different T stages of gall bladder cancer. Usually, the T1a, T1b, and T2 tumors could be removed by surgery but this should be confirmed only after a CT scan. T3 and T4 tumors usually cannot be removed by surgery and other approaches are taken to treat them. GBC: Gall bladder cancer.

components, cell proliferation, cell differentiation, and angiogenesis. Though, CD44 has a few other ligands, mainly hyaluronan binds to CD44 and activates it for the regulation of many pathways like the RAS, MAPK, and PI3K pathways which are associated with cell proliferation, cell differentiation, and angiogenesis[10,11]. **Figure 2** shows how CD44 is linked to the MAPK pathway.

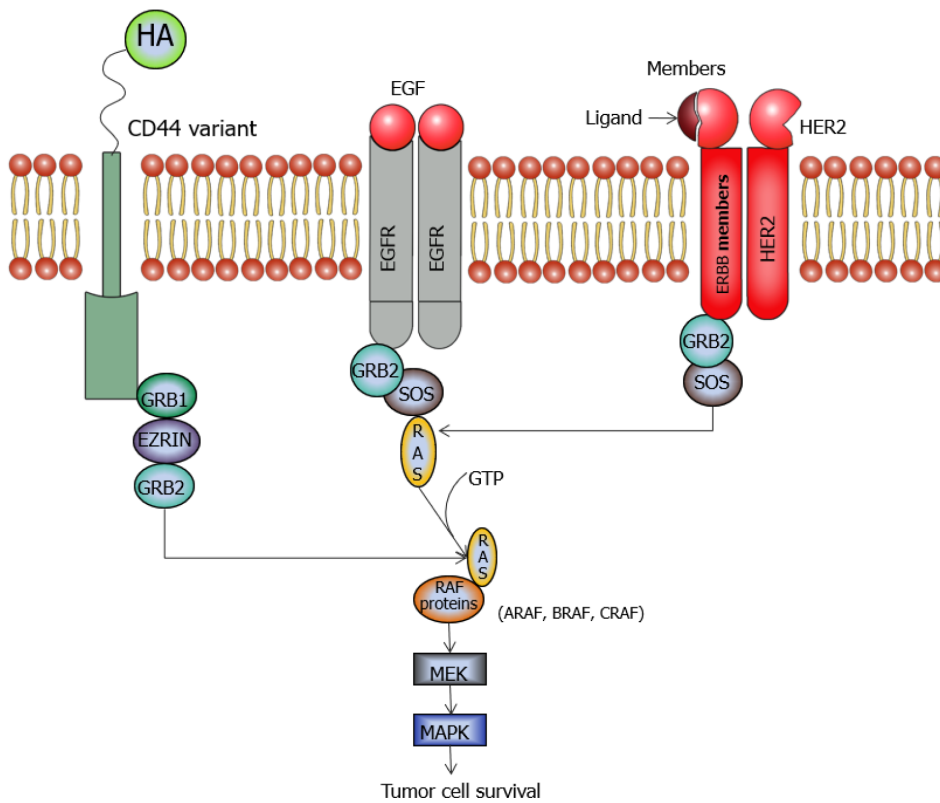
It is overexpressed in many cancers including those of the liver and gall bladder. The movement and occupation of the stroma by the GBC cells are also decreased on CD44 inactivation. CD44/CD133 positive cells also behave as cancer stem cells. CD44, in union with NANOG (another cancer stem cell marker), is found to have stimulated some multidrug-resistant genes and thus tumor development[12]. When tested for cancer stem cells, they were found to be reduced in activation of CD44 by CD44-siRNA. The total life span of patients in whom CD44 was overexpressed was much less than those who did not express CD44[13].

In a set of experiments by He *et al*[13], CD44-siRNA constructs were prepared by Sangon Biotech. A GBC cell line (GBC-SD) was transfected with CD44-siRNA. The expression of CD44 decreased significantly in the CD44-siRNA transfected cells as revealed by immunohistochemical staining, Western blot, and real-time PCR. The apoptosis of these cells increased considerably, which was detected by flow cytometry, while the proliferation capacity of these cells was considerably decreased as observed by cell counting kit-8 (CCK-8) assay. In this study involving CD44-mRNA it was found that CD44 is unhindered in hepatobiliary tumors and CD44 protein is expressed much more in gall bladder carcinoma tissues than non-malignant tissues. The overall survival of these patients is also poor. Silencing of the CD44 gene by delivering the corresponding siRNA in the cells has led to decreased expression of CD44.

EGFR (Epidermal growth factor receptor): EGFR/ErBB1 is a member of the receptor tyrosine kinase family. It is a transmembrane protein that is turned by the binding of its ligand (epidermal growth factor or transforming growth factor). When EGFR is turned on, it forms a dimer with itself or with another member of the receptor tyrosine kinase family, leading to its phosphorylation. This phosphorylation, in turn, leads to the activation of its target proteins which are the components of either the MAPK or AKT, or JNK pathways, and ultimately cell proliferation occurs[14,15]. **Figure 2** shows how EGFR could activate the MAPK pathway.

In a set of experiments by Iyer *et al*[16], exome analysis and sequencing were performed to detect tumor-specific mutations in GBC tissues. EGFR and ERBB2 were turned off using EGFR-specific shRNA and ERBB2-specific shRNA. Cell proliferation of the transfected cells was assessed by MTT colorimetric assay. Expression of various tumor markers in the transfected cells including EGFR was estimated by Western blot assay and Immunohistochemistry. Migration assays of the transfected cells revealed that there was a considerable decrease in migration and invasive abilities of the transfected cells.

ERBB2 (erythroblastic oncogene B 2): It is a tyrosine kinase, also known as HER2/neu or receptor tyrosine-protein kinase ERBB-2 or CD340, belonging to the Erb family of receptor tyrosine kinases. In humans this Erb family consists of Her1 (EGFR/Erbb1), Her2 (Neu/Erbb2), Her3 (Erbb3) and Her4 (Erbb4)[17,18]. HER2/neu is a protein encoded by the gene ERBB2, present in the long arm of chromosome 17. When a ligand binds to this receptor, it undergoes dimerization activates many signaling pathways, and finally leads to cell proliferation and growth[19]. It has been found that HER2/neu could initiate the PI3K/Akt[20,21] and also the MAP kinase pathway[22]. **Figure 2** shows how HER2/neu could activate the MAP kinase pathway. In an experimental setup by Kiguchi *et al*[23], HER2 was overexpressed in Gall bladder adenocarcinoma of mice. Silencing of ERBB2 was found to curb the penetrating, relocating, and docking free growth properties of human GBC-SDs, provided that KRAS (G12V) is not mutated in these GBC-SDs[16], as visualized by proliferation and migration assays. It was also visualized that due to the silencing of ERBB2, it was unable to signal target proteins of the MAPK pathway.



DOI: 10.4251/wjgo.v15.i12.2053 Copyright ©The Author(s) 2023.

Figure 2 Mechanism of MAP kinase activation by some of the target genes. ERBB members: EGFR/ Her2/ErbB3/ErbB4; GRB: A serine protease and shortened form of Granzyme B; EZRIN: A protein needed for activation of RAS; SOS: Guanine nucleotide exchange factor helps in the activation of RAS, the name derived from Son of Sevenless gene; RAS: A G protein, the name is derived from rat sarcoma virus; RAF: Serine threonine protein kinases and shortened form of rapidly accelerated fibrosarcoma; MAP kinase: Protein kinases and shortened form of mitogen-activated protein kinase; EGFR, HER2/neu, and CD44 are receptors embedded in the phospholipid bilayer and A-RAF protein is present in the cytoplasm; EGFR, HER2/neu, CD44, and ARAF activate the protein kinase, MAPK which ultimately results in the survival of tumor cells; HA: Hyaluronic acid; EGF: Epidermal growth factor; EGFR: Epidermal growth factor receptors.

ARAF: It is a serine-threonine kinase of the Raf-kinase family. There are three members of the Raf (rapidly accelerated fibrosarcoma) kinase family - ARAF, BRAF, and CRAF. These three enzymes have roles in the MAP kinase pathway (Figure 2). In humans, ARAF is encoded by the *ARAF* gene, located on the X chromosome (xp11.3)[24]. ARAF activates MEK proteins, which in turn activates extracellular regulated kinase (ERK) which is known to activate many transcription factors and drive the MAPK pathway toward cell proliferation[25,26]. In a set of experiments by Lin *et al*[27], the *ARAF* gene was found to be elevated in GBC cells. Silencing of ARAF by *ARAF*-siRNA hinders the proliferation of GBC cells in a GBC-SD, as studied by the CCK-8 assay. The drifting and intruding nature of GBC cells declined, as estimated from transwell and wound healing assays. When the GBC-SD was used for tumor formation in athymic nude mice, *ARAF*-siRNA was injected. On regular monitoring of tumor size and volume, it was found that *ARAF*-siRNA was able to reduce the tumor volume remarkably.

Genes related to apoptosis

BMI1 (B-cell specific Moloney murine leukemia virus integration site 1): BMI1 is a member of the polycomb group family proteins which suppresses transcription. To date, many such polycomb proteins are known[28,29]. Some of the common ones are PRC1, PRC2, PHC1, PHC2, HP1, BMI1, PCGF1, PCGF2, RYBP, RING1, SUV39H1, L3MBT12, EZH2, EE2, SUZ12, JARID2, REST, RNF2, CBF-β and YY1. Basically, they organize the chromatin of the specific gene in such a way that they are suppressed for a long period of time and during cell division. The human *BMI1* gene is placed at the short arm of chromosome 10[30].

BMI1 gene has been found to interact with p16 and p19[31], which are inhibitors of cyclin-dependent kinases (CDK4 and CDK6). P16 is a protein that disallows the cell from the G1 phase to the S-phase. P19 is a protein that has been found to direct p53 to stop the cell cycle at G1 and apoptosis in fibroblast cells[32]. BMI1 has been found to downregulate these inhibitors[33] and thus plays an important role in the progression of the cell cycle and sustaining cell division[34]. In a set of experiments by Jiao *et al*[35], *BMI1*-siRNA constructs were prepared by Shanghai Biotech. A GBC-SD was transfected with *BMI1*-siRNA. Initially, BMI1 was found to be expressed in a majority (84%) of the GBC patients as compared to 40% of normal patients who were taken up for the study. The expression of BMI1 decreased significantly in the *BMI1*-siRNA transfected cells as revealed by immunohistochemical staining, Western blot, and real-time PCR. The apoptosis of these cells increased considerably, which was detected by flow cytometry, while the proliferation capacity of these cells was considerably decreased as observed by the CCK-8 assay. Silencing of *BMI1* by specific siRNA could induce apoptosis of

the GBC cells and decrease the proliferation of GBC cells, which could hinder the growth of GBC cells.

BCL2 (B-cell lymphoma 2): BCL2 belongs to the Bcl-2 family of proteins. It is present in the outer mitochondrial membrane, embedded in it, and plays an important role in the suppression of the pro-apoptotic proteins BAX and BAK [36,37]. Thus, it plays a role in cell growth and proliferation. Overexpression of this gene with the upregulation of the proto-oncogene MYC has been found to be associated with some cancers[38]. In a set of experiments, GBC-SD were transfected with BCL2-siRNA according to the standard procedure by Lipofectamine[39]. The cells were cultured in media. The growth and the morphology of the resultant cells were observed. After a certain period of culture, expression of BCL2 was measured in the resulting cells by quantitative real time PCR (qRT-PCR) and Western blot. Expression of the BCL2 gene was found to be significantly lower in the BCL2-siRNA transfected group. On silencing of this gene, the GBC cells were found to be more responsive to chemotherapy drugs. In the nude mouse model experiments, the tumor volume also significantly decreased in the experimental group where this gene was silenced.

JAB1 (c-JUN activation domain binding protein 1): The gene JAB1 is positioned on chromosome 8. JAB1 is a co-activator of c-JUN, which is a well-known oncogene[40,41]. JAB1 is a member of a complex called constitutive photomorphogenic-9 signalosome (CSN) complex, which positively controls cell proliferation and transcription of various genes[42]. It is essential in the advancement of the cell cycle from the G1 phase to the S-phase, as c-JUN controls the level of Cyclin D1. If c-JUN is not activated, the expression of p53 and p21 could be upregulated to prevent the cell cycle from advancing farther[43,44]. Activating factor AP1 binds to the promoter region of JUN and transcription of JUN begins[45]. AP1 is a transcription factor consisting of mainly four groups of proteins *i.e.* Jun (C-Jun, Jun-B, and Jun-D), Fos (FosC, FosB, Fra1, and Fra2), ATF/cyclic AMP responsive element, and Maf family proteins. Thus, c-JUN transcription is also controlled by c-JUN itself. JUN transcription could also be started with active ERK[46]. In a set of experiments by Pandey *et al*[47], increased levels of JAB1 were found in GBC tissues. JAB1-siRNA constructs were prepared and used to transfect GBC cells. JAB1 expression, cell growth, and apoptosis of these GBC cells were studied by qRT-PCR, Western blot, MTT, reactive oxygen species, Hoechst, and FITC/Annexin-V staining. In the cells in which JAB1 is expressed highly, proliferation is turned on in these cells. GBC cells when transfected with JAB1-SiRNA decreased this proliferation considerably and programmed cell death was initiated. The cell cycle was found to halt at the G1 phase. Expression of the apoptotic gene CASP 3 and apoptotic regulatory genes p27, P53, and BAX were evident.

Genes related to the immune system

MIF (Macrophage migration inhibitory factor): MIF is a protein that plays a role in inflammatory responses. It has been found that though inflammation is a mechanism of the body's defense if it occurs for a prolonged period, which occurs in the case of chronic inflammation could lead to cancer in some cases. One way, that chronic inflammation could be linked to cancer is thought to be through MIF[48,49]. MIF binds to its receptor CD74 and activates it and it then activates PI3K-AKT, ERK, and NF-kappa B pathways[50,51]. It has been found to subdue the anti-inflammatory cytokines and enhance the other inflammatory cytokines[52]. MIF has been found to be upregulated in many cancers including GBC[53,54]. Inactivation of the MIF gene using MIF-siRNA reduces the proliferation and intruding properties of cancer cells as observed in the colony formation assays.

CD73: CD73 resists the proper functioning of the T-cells by interfering with their clonal expansion, their activation, and their cytolytic activities. It plays an important role in the process due to which tumors can escape the immune system. CD73 is a cell surface enzyme that induces the dephosphorylation of AMP into adenosine[55]. Adenosine activates the G-protein coupled receptors (A2AR and A2BR) and plays a role in the escape of tumor cells by the immune system[56,57]. NOZ cells, a human GBC-SD were transfected with specific CD73-siRNA by Cao *et al*[58], and the expression of CD73 was found to be reduced in transfected cells as observed by quantitative reverse transcription PCR and Western blot. Adherent cells and spherical aggregates of cancer cells were found to decrease when CD73 was silenced. When CD73 was silenced by CD73-siRNA, epithelial to mesenchymal transition was found to reduce in GBC cells. It could be one of the important reasons for the opposition to drugs by cancer stem cells. The growth of GBC cells in single layers and attached to the surface and also those which can grow without embankment were retarded. The migrating nature of the GBC-NOZ cells was found to be reduced as detected by trans well assays.

PDL1 (Programmed cell death protein 1 ligand): PDL1 binds to its receptor programmed cell death protein 1 (PD1) which is found on activated T-cells' and B-cells' surfaces[59]. The interplay between PD1 and PDL1 hinders the proper functioning of the T-cells[60]. PDL1 is expressed on the surface of many cancer cells[61]. The interaction of PD1 with PDL1 interrupts major histocompatibility complex and thus obstructs the interaction of PDL1 with its receptor PD1, as a result, antigen presentation to cytotoxic T-lymphocytes[3]. PDL1 is overexpressed in the GBC-NOZ cells. When PDL1 was silenced with PDL1-siRNA cell growth and transportability of GBC-NOZ cells were diminished. This was revealed by proliferation as well as wound healing assays[58].

Other genes: miRNA is short (about 20 nucleotides), single-stranded, intrinsic, and non-coding sequences of RNA found in all tissues or blood. They could silence a gene by binding it to the specific RNA, complementary to it. Their mechanism of action is similar to that of siRNA. However, miRNAs are procured from different regions of DNA than siRNA. About more than 2500 miRNAs have been found in humans. In GBC several miRNAs have been found to be uncontrolled.

In a microarray analysis of GBC tissues from patients who survived for a long period after diagnosis and those who survived for a short time[62], changes in the expression of miRNA were identified. It was found that only two miRNAs (hsa-miR-30a-3p and hsa-miR-660-5p) were suppressed in patients who survived long. However, 11 miRNAs were suppressed and 11 were stimulated in patients who did not survive long. This recommended the possible roles of these

miRNAs in GBC. In some other microarray analyses, changes in the expression of many other miRNAs have been detected in GBC. The table below (Table 1) lists the important ones and the genes associated with these miRNAs.

Some of the miRNAs including the miR-55 and miR-20a have been considered as oncogenic miRNA or onco-miR as when they were expression levels were increased, the cell proliferation and intruding capabilities of the Gall bladder cells also increased[63]. The status of the important miRNAs in the GBC tissue of a particular patient could determine his response to a particular kind of therapy and prognosis.

TRANSLATIONAL RESEARCH AND CLINICAL TRIALS RELATED TO GBC

Mutations of *KRAS*, *INK4A* (p16), *TP53*, and *HER 2/neu* have been commonly noticed in GBC[5,64-66]. Mutations of *PIK3CA* in GBC are also not rare[65]. *BRAF* and *PI3K* mutations also have been detected in GBC but they are not as common as *KRAS*[8,67,68]. There have been attempts to develop drugs against *KRAS* but the chemical nature of these drugs was such that they could not be controlled, so they were not approved. Some therapeutic drugs, targeting some genes are under development for the treatment of GBC. They are in different phases of clinical trials (Table 2). Many immune checkpoint inhibitors against *PDL1* and *CTLA4* for the treatment of GBC are also under various stages of clinical trial[69,70].

CONCLUSION

The combined chemotherapy regimens have been found to increase the overall survival of patients in clinical trials, but still, they have been found to have toxic effects, and resistance is developed later[3,71,72]. Whenever clinical trials were performed some unforeseen hurdles were found, including the side effects and development of resistance to a particular drug. The cause of this resistance to a particular drug could be diversity within the same tumor and genetic differences among the patients[73].

The siRNAs have been found to be capable of silencing a specific gene in experimental models. However, there are certain constraints for the siRNA-mediated therapy. These are mainly the firmness and delivery of siRNA. Choosing the gene to be silenced is another issue with siRNA-mediated therapy. All these issues have to be answered before starting clinical trials in patients. As the siRNA molecules are negatively charged and have an inflexible structure, their diffusion across the membrane becomes difficult. So, they are taken up by the cell through endocytosis. In this case, there is a huge chance of the collection of many molecules in the endosomal compartments rather than reaching the cytosol where it can form the RISC. In the past few years, scientists have attempted to prepare strategies for the endosomal escape of these molecules, and a few have been reported[74]. Few endosomolytic media have been obtained from natural substances or manufactured and many other agents like polymers, liposomes, nano-particles, and other coupling agents have also been developed for the successful carriage of siRNA. Some recent clinical trials have disclosed the safety of nano-particle-based delivery of siRNA in some other cancers[62]. Still, there have been issues regarding the delivery of shRNA[75,76]. However, various attempts have been made to optimize the delivery of shRNA by viral vectors. Many vectors have been studied for their efficiency in the delivery of shRNAs within the target cell[77,78]. These viral vectors have improved the delivery of shRNAs but the safety of these vectors is in question as they are based on viruses. Consequently, these approaches are not applicable to clinical trials. Selection of the gene to be silenced is another important aspect of these siRNA-based technologies. It is suggested by experts to select such a combination therapy for patients which targets the important molecular pathways governing cancer metastasis and also would have less toxicity. To date, many genes have been identified which are responsible for the cells being able to avoid senescence and those which are responsible for metastasis. Genes that are linked to multiple pathways and have been expressed in many cancers are perhaps suitable for targeting. In the case of GBC, a recent study suggests that there are predominantly mutations of the genes *ARID1A*, *ARID2*, *ATM*, *CTNNB1*, *ERBB2*, *ERBB3*, *KMT2C*, *KMT2D*, *KRAS*, *PIK3CA*, *SMAD4*, *TERT*, *TP53*, and *ZNF521*[65]. High expression of the gene *GLI2* has also been found to increase the number of GBC cells and their aggressive property[79].

All the genes mentioned in this review are linked to important cell signaling pathways. Among them, *CD44*, *EGFR*, and *MIF* have been found to be linked to multiple pathways. *CD44* has been found to activate the *MAPK*, *PI3K-AKT* pathways, *MIF* has been linked with the *MAPK*, *PI3K-AKT*, and the *NF-κB* pathways and *EGFR* has been found to stimulate the *MAPK*, *PI3K-AKT*, and *JNK* pathways. The genes *ERBB2*, *ERBB3*, *KRAS*, and *PIK3CA* were already known to have been linked with multiple pathways. So, these genes which could activate multiple pathways could be potential targets for si-RNA/shRNA mediated knockdown. siRNA and shRNA-mediated knockdown of the genes mentioned above has shown to have decreased the invasiveness of the GBC considerably. The question of delivery of specific siRNA/shRNA in patients is expected to be answered. If the question is answered, they seem to have the potential for the tailored treatment of GBC. In that case, the toxicity resulting from the knockdown of the selected gene has also to be tested in preclinical models. Another aspect is the high cost of this siRNA/shRNA-mediated therapy. Therefore, before it comes to regular clinical practice all these issues need to be resolved. All these challenges have made it quite far from commercialization.

Table 1 MicroRNAs identified to have changed expression in gall bladder cancer

miRNA	Status in gall bladder cancer	Target genes
miR-146b-5p	Suppressed	EGFR[80]
miR-124	Suppressed	CDK6, ROCK1[81]
miR20a	Stimulated	SMAD7[82]
miR155	Stimulated	[82]
miR182	Stimulated	CADM1[82]
miR122	Stimulated	BMI1[82]
miR34a	Suppressed	PNUTS[82]
miR335	Suppressed	[82]
miR130a	Suppressed	HOTAIR[82]
miR135a5p	Suppressed	VLDLR[82]
miR-145-5p	Suppressed	STAT1[83]
miR26a	Suppressed	HMGGA2[82]
miR145	Suppressed	AXL[82]
miR143	Suppressed	[82]
miR2185p	Suppressed	BMI1[84]

miRNA: MicroRNA.

Table 2 Target genes for treating gall bladder cancer (under investigation and those under clinical trial)

Target genes silenced by siRNA (under investigation)	Target genes for GBC treatment (under clinical trial)
BMI1, CD44, CLIC1, JAB1, EGFR	EGFR and Her/2 together (Afatnib-NCT04183712, Apatinib-NCT03702491)
HER 2/neu, ARAF	HER/2 (Trastuzumab-NCT00478140)
MIF	MEK (Trametinib-NCT02042443)
CD73, PDL1	DNMT (Guadecitabine-NCT03257761)

GBC: Gall bladder cancer.

FOOTNOTES

Co-corresponding authors: Ruma Dey Ghosh and Soma Mukhopadhyay.

Author contributions: Ghosh I, Dey Ghosh R, Mukhopadhyay S conceived the idea and designed the manuscript; Ghosh I and Dey Ghosh R, collected information, analyzed the data, constructed figures and tables, and wrote the manuscript; Ghosh I drafted the manuscript; Dey Ghosh R critically reviewed, edited and corrected the manuscript; All authors were involved in the critical review of the results and have contributed to, read, and approved the final manuscript. Dey Ghosh R, and Mukhopadhyay S contributed equally to this work as co-corresponding authors. The reasons for designating Dey Ghosh R, and Mukhopadhyay S as co-corresponding authors are threefold. First, the research was performed as a collaborative effort, and the designation of co-corresponding authorship accurately reflects the distribution of responsibilities and burdens associated with the time and effort required to complete the study and the resultant paper. This also ensures effective communication and management of post-submission matters, ultimately enhancing the paper's quality and reliability. Second, the overall research team encompassed authors with a variety of expertise and skills from different fields, and the designation of co-corresponding authors best reflects this diversity. This also promotes the most comprehensive and in-depth examination of the research topic, ultimately enriching readers' understanding by offering various expert perspectives. Third, Dey Ghosh R, and Mukhopadhyay S contributed efforts of equal substance throughout the research process. The choice of these researchers as co-corresponding authors acknowledges and respects this equal contribution, while recognizing the spirit of teamwork and collaboration of this study. In summary, we believe that designating Dey Ghosh R, and Mukhopadhyay S as co-corresponding authors of is fitting for our manuscript as it accurately reflects our team's collaborative spirit, equal contributions, and diversity.

Conflict-of-interest statement: The authors declare no conflict-of interest.

Open-Access: This article is an open-access article that was selected by an in-house editor and fully peer-reviewed by external reviewers. It is distributed in accordance with the Creative Commons Attribution NonCommercial (CC BY-NC 4.0) license, which permits others to

distribute, remix, adapt, build upon this work non-commercially, and license their derivative works on different terms, provided the original work is properly cited and the use is non-commercial. See: <https://creativecommons.org/licenses/by-nc/4.0/>

Country/Territory of origin: India

ORCID number: Ruma Dey Ghosh 0000-0002-9775-8170; Soma Mukhopadhyay 0000-0002-8945-891X.

S-Editor: Lin C

L-Editor: A

P-Editor: Zhao S

REFERENCES

- 1 **Bray F**, Ferlay J, Soerjomataram I, Siegel RL, Torre LA, Jemal A. Global cancer statistics 2018: GLOBOCAN estimates of incidence and mortality worldwide for 36 cancers in 185 countries. *CA Cancer J Clin* 2018; **68**: 394-424 [PMID: 30207593 DOI: 10.3322/caac.21492]
- 2 **Phadke PR**, Mhatre SS, Budukh AM, Dikshit RP. Trends in gallbladder cancer incidence in the high-and low-risk regions of India. *Indian J Med Paediatr Oncol* 2019; **40**: 90-93 [DOI: 10.4103/ijmpo.ijmpo_164_18]
- 3 **Song X**, Hu Y, Li Y, Shao R, Liu F, Liu Y. Overview of current targeted therapy in gallbladder cancer. *Signal Transduct Target Ther* 2020; **5**: 230 [PMID: 33028805 DOI: 10.1038/s41392-020-00324-2]
- 4 **Verma K**, Dixit R, Singh J, Tiwary SK, Khanna AK, Narayan G, Kumar P. Molecular genetic changes in gall bladder carcinoma. *Int J Mol Immuno Oncol* 2020; **5**: 49-61 [DOI: 10.25259/IJMIO_19_2019]
- 5 **Rashid A**, Ueki T, Gao YT, Houlihan PS, Wallace C, Wang BS, Shen MC, Deng J, Hsing AW. K-ras mutation, p53 overexpression, and microsatellite instability in biliary tract cancers: a population-based study in China. *Clin Cancer Res* 2002; **8**: 3156-3163 [PMID: 12374683]
- 6 **Chung WC**, Wang J, Zhou Y, Xu K. Kras(G12D) upregulates Notch signaling to induce gallbladder tumorigenesis in mice. *Oncoscience* 2017; **4**: 131-138 [PMID: 29142904 DOI: 10.18632/oncoscience.368]
- 7 **Kuipers H**, de Bitter TJJ, de Boer MT, van der Post RS, Nijkamp MW, de Reuver PR, Fehrmann RSN, Hoogwater FJH. Gallbladder Cancer: Current Insights in Genetic Alterations and Their Possible Therapeutic Implications. *Cancers (Basel)* 2021; **13** [PMID: 34771420 DOI: 10.3390/cancers13215257]
- 8 **Lunardi A**, Webster KA, Papa A, Padmani B, Clohessy JG, Bronson RT, Pandolfi PP. Role of aberrant PI3K pathway activation in gallbladder tumorigenesis. *Oncotarget* 2014; **5**: 894-900 [PMID: 24658595 DOI: 10.18632/oncotarget.1808]
- 9 **Spring FA**, Dalchau R, Daniels GL, Mallinson G, Judson PA, Parsons SF, Fabre JW, Anstee DJ. The Ina and Inb blood group antigens are located on a glycoprotein of 80,000 MW (the CDw44 glycoprotein) whose expression is influenced by the In(Lu) gene. *Immunology* 1988; **64**: 37-43 [PMID: 2454887]
- 10 **Herishanu Y**, Gibellini F, Njuguna N, Hazan-Halevy I, Farooqui M, Bern S, Keyvanfar K, Lee E, Wilson W, Wiestner A. Activation of CD44, a receptor for extracellular matrix components, protects chronic lymphocytic leukemia cells from spontaneous and drug induced apoptosis through MCL-1. *Leuk Lymphoma* 2011; **52**: 1758-1769 [PMID: 21649540 DOI: 10.3109/10428194.2011.569962]
- 11 **Cheng C**, Yaffe MB, Sharp PA. A positive feedback loop couples Ras activation and CD44 alternative splicing. *Genes Dev* 2006; **20**: 1715-1720 [PMID: 16818603 DOI: 10.1101/gad.1430906]
- 12 **Bourguignon LY**, Singleton PA, Zhu H, Zhou B. Hyaluronan promotes signaling interaction between CD44 and the transforming growth factor beta receptor I in metastatic breast tumor cells. *J Biol Chem* 2002; **277**: 39703-39712 [PMID: 12145287 DOI: 10.1074/jbc.M204320200]
- 13 **He Y**, Xue C, Yu Y, Chen J, Chen X, Ren F, Ren Z, Cui G, Sun R. CD44 is overexpressed and correlated with tumor progression in gallbladder cancer. *Cancer Manag Res* 2018; **10**: 3857-3865 [PMID: 30288117 DOI: 10.2147/CMAR.S175681]
- 14 **Wee P**, Wang Z. Epidermal Growth Factor Receptor Cell Proliferation Signaling Pathways. *Cancers (Basel)* 2017; **9** [PMID: 28513565 DOI: 10.3390/cancers9050052]
- 15 **Terakado M**, Gon Y, Sekiyama A, Takeshita I, Kozu Y, Matsumoto K, Takahashi N, Hashimoto S. The Rac1/JNK pathway is critical for EGFR-dependent barrier formation in human airway epithelial cells. *Am J Physiol Lung Cell Mol Physiol* 2011; **300**: L56-L63 [PMID: 21036915 DOI: 10.1152/ajplung.00159.2010]
- 16 **Iyer P**, Shrikhande SV, Ranjan M, Joshi A, Gardi N, Prasad R, Dharavath B, Thorat R, Salunkhe S, Sahoo B, Chandrani P, Kore H, Mohanty B, Chaudhari V, Choughule A, Kawle D, Chaudhari P, Ingle A, Banavali S, Gera P, Ramadwar MR, Prabhaskar K, Barreto SG, Dutt S, Dutt A. ERBB2 and KRAS alterations mediate response to EGFR inhibitors in early stage gallbladder cancer. *Int J Cancer* 2019; **144**: 2008-2019 [PMID: 30304546 DOI: 10.1002/ijc.31916]
- 17 **Vermeulen Z**, Segers VF, De Keulenaer GW. ErbB2 signaling at the crossing between heart failure and cancer. *Basic Res Cardiol* 2016; **111**: 60 [PMID: 27596216 DOI: 10.1007/s00395-016-0576-z]
- 18 **Riese DJ 2nd**, Stern DF. Specificity within the EGF family/ErbB receptor family signaling network. *Bioessays* 1998; **20**: 41-48 [PMID: 9504046 DOI: 10.1002/(SICI)1521-1878(199801)20:1<41::AID-BIES7>3.0.CO;2-V]
- 19 **Iqbal N**, Iqbal N. Human Epidermal Growth Factor Receptor 2 (HER2) in Cancers: Overexpression and Therapeutic Implications. *Mol Biol Int* 2014; **2014**: 852748 [PMID: 25276427 DOI: 10.1155/2014/852748]
- 20 **Mishra R**, Patel H, Alanazi S, Yuan L, Garrett JT. HER3 signaling and targeted therapy in cancer. *Oncol Rev* 2018; **12**: 355 [PMID: 30057690 DOI: 10.4081/oncol.2018.355]
- 21 **Ortega-Cava CF**, Raja SM, Laiq Z, Bailey TA, Luan H, Mohapatra B, Williams SH, Ericsson AC, Goswami R, Dimri M, Duan L, Band V, Naramura M, Band H. Continuous requirement of ErbB2 kinase activity for loss of cell polarity and lumen formation in a novel ErbB2/Neu-driven murine cell line model of metastatic breast cancer. *J Carcinog* 2011; **10**: 29 [PMID: 22190871 DOI: 10.4103/1477-3163.90443]
- 22 **Lenferink AE**, Busse D, Flanagan WM, Yakes FM, Arteaga CL. ErbB2/neu kinase modulates cellular p27(Kip1) and cyclin D1 through multiple signaling pathways. *Cancer Res* 2001; **61**: 6583-6591 [PMID: 11522658]
- 23 **Kiguchi K**, Carbajal S, Chan K, Beltrán L, Ruffino L, Shen J, Matsumoto T, Yoshimi N, DiGiovanni J. Constitutive expression of ErbB-2 in

- gallbladder epithelium results in development of adenocarcinoma. *Cancer Res* 2001; **61**: 6971-6976 [PMID: 11585718]
- 24 **Robinson MJ**, Cobb MH. Mitogen-activated protein kinase pathways. *Curr Opin Cell Biol* 1997; **9**: 180-186 [PMID: 9069255 DOI: 10.1016/s0955-0674(97)80061-0]
- 25 **Garnett MJ**, Marais R. Guilty as charged: B-RAF is a human oncogene. *Cancer Cell* 2004; **6**: 313-319 [PMID: 15488754 DOI: 10.1016/j.ccr.2004.09.022]
- 26 **Rebocho AP**, Marais R. ARAF acts as a scaffold to stabilize BRAF:CRAF heterodimers. *Oncogene* 2013; **32**: 3207-3212 [PMID: 22926515 DOI: 10.1038/onc.2012.330]
- 27 **Lin W**, Tong C, Zhang W, Cen W, Wang Y, Li J, Zhu Z, Yu J, Lu B. Silencing ARAF Suppresses the Malignant Phenotypes of Gallbladder Cancer Cells. *Biomed Res Int* 2020; **2020**: 3235786 [PMID: 32923479 DOI: 10.1155/2020/3235786]
- 28 **Di Croce L**, Helin K. Transcriptional regulation by Polycomb group proteins. *Nat Struct Mol Biol* 2013; **20**: 1147-1155 [PMID: 24096405 DOI: 10.1038/nsmb.2669]
- 29 **Chan HL**, Morey L. Emerging Roles for Polycomb-Group Proteins in Stem Cells and Cancer. *Trends Biochem Sci* 2019; **44**: 688-700 [PMID: 31085088 DOI: 10.1016/j.tibs.2019.04.005]
- 30 **Beà S**, Tort F, Pinyol M, Puig X, Hernández L, Hernández S, Fernandez PL, van Lohuizen M, Colomer D, Campo E. BMI-1 gene amplification and overexpression in hematological malignancies occur mainly in mantle cell lymphomas. *Cancer Res* 2001; **61**: 2409-2412 [PMID: 11289106]
- 31 **Meng S**, Luo M, Sun H, Yu X, Shen M, Zhang Q, Zhou R, Ju X, Tao W, Liu D, Deng H, Lu Z. Identification and characterization of Bmi-1-responder element within the human p16 promoter. *J Biol Chem* 2010; **285**: 33219-33229 [PMID: 20551323 DOI: 10.1074/jbc.M110.133686]
- 32 **Radfar A**, Unnikrishnan I, Lee HW, DePinho RA, Rosenberg N. p19(Arf) induces p53-dependent apoptosis during abelson virus-mediated pre-B cell transformation. *Proc Natl Acad Sci U S A* 1998; **95**: 13194-13199 [PMID: 9789064 DOI: 10.1073/pnas.95.22.13194]
- 33 **Abdous H**, Facchino S, Chatoov W, Balasingam V, Ferreira J, Bernier G. BMI1 sustains human glioblastoma multiforme stem cell renewal. *J Neurosci* 2009; **29**: 8884-8896 [PMID: 19605626 DOI: 10.1523/JNEUROSCI.0968-09.2009]
- 34 **Fatma H**, Akhtar MS, Ali S, Ahmad M, Siddique HR. BMI-1 expression as a marker for gallbladder cancer progression. *Journal of Medicine Surgery and Public Health* 2023; **1**: 100002-100009 [DOI: 10.1016/j.gjmedi.2023.100002]
- 35 **Jiao K**, Jiang W, Zhao C, Su D, Zhang H. Bmi-1 in gallbladder carcinoma: Clinicopathology and mechanism of regulation of human gallbladder carcinoma proliferation. *Oncol Lett* 2019; **18**: 1365-1371 [PMID: 31423199 DOI: 10.3892/ol.2019.10408]
- 36 **Hardwick JM**, Soane L. Multiple functions of BCL-2 family proteins. *Cold Spring Harb Perspect Biol* 2013; **5** [PMID: 23378584 DOI: 10.1101/cshperspect.a008722]
- 37 **Kale J**, Osterlund EJ, Andrews DW. BCL-2 family proteins: changing partners in the dance towards death. *Cell Death Differ* 2018; **25**: 65-80 [PMID: 29149100 DOI: 10.1038/cdd.2017.186]
- 38 **Otake Y**, Soundararajan S, Sengupta TK, Kio EA, Smith JC, Pineda-Roman M, Stuart RK, Spicer EK, Fernandes DJ. Overexpression of nucleolin in chronic lymphocytic leukemia cells induces stabilization of bcl2 mRNA. *Blood* 2007; **109**: 3069-3075 [PMID: 17179226 DOI: 10.1182/blood-2006-08-043257]
- 39 **Geng ZM**, Zhang M, Pan XT, Wang L. Bcl-2 gene silencing by RNA interference inhibits the growth of the human gallbladder carcinoma cell line GBC-SD *in vitro* and *in vivo*. *Oncol Rep* 2013; **30**: 793-800 [PMID: 23784204 DOI: 10.3892/or.2013.2539]
- 40 **Chopra S**, Fernandez De Mattos S, Lam EW, Mann DJ. Jab1 co-activation of c-Jun is abrogated by the serine 10-phosphorylated form of p27Kip1. *J Biol Chem* 2002; **277**: 32413-32416 [PMID: 12119282 DOI: 10.1074/jbc.C200311200]
- 41 **Pandey P**, Khan F, Mishra R, Singh R, Upadhyay TK, Singh SK. Jab1 (COPSS) as an Emerging Prognostic, Diagnostic and Therapeutic Biomarker for Human Cancer. *Biointerface Research in Applied Chemistry* 2022; **12**: 7001-7011 [DOI: 10.33263/BRIAC125.70017011]
- 42 **Shackleford TJ**, Claret FX. JAB1/CSN5: a new player in cell cycle control and cancer. *Cell Div* 2010; **5**: 26 [PMID: 20955608 DOI: 10.1186/1747-1028-5-26]
- 43 **Oh W**, Lee EW, Sung YH, Yang MR, Ghim J, Lee HW, Song J. Jab1 induces the cytoplasmic localization and degradation of p53 in coordination with Hdm2. *J Biol Chem* 2006; **281**: 17457-17465 [PMID: 16624822 DOI: 10.1074/jbc.M601857200]
- 44 **Berg JP**, Zhou Q, Breuhahn K, Schirmacher P, Patil MA, Chen X, Schäfer N, Höller TT, Fischer HP, Büttner R, Gütgemann I. Inverse expression of Jun activation domain binding protein 1 and cell cycle inhibitor p27Kip1: influence on proliferation in hepatocellular carcinoma. *Hum Pathol* 2007; **38**: 1621-1627 [PMID: 17651785 DOI: 10.1016/j.humpath.2007.03.007]
- 45 **Claret FX**, Hibi M, Dhut S, Toda T, Karin M. A new group of conserved coactivators that increase the specificity of AP-1 transcription factors. *Nature* 1996; **383**: 453-457 [PMID: 8837781 DOI: 10.1038/383453a0]
- 46 **Gazon H**, Barbeau B, Mesnard JM, Peloponese JM Jr. Hijacking of the AP-1 Signaling Pathway during Development of ATL. *Front Microbiol* 2017; **8**: 2686 [PMID: 29379481 DOI: 10.3389/fmicb.2017.02686]
- 47 **Pandey P**, Siddiqui MH, Behari A, Kapoor VK, Mishra K, Sayeed U, Tiwari RK, Shekh R, Bajpai P. Jab1-siRNA Induces Cell Growth Inhibition and Cell Cycle Arrest in Gall Bladder Cancer Cells via Targeting Jab1 Signalosome. *Anticancer Agents Med Chem* 2019; **19**: 2019-2033 [PMID: 31345154 DOI: 10.2174/1871520619666190725122400]
- 48 **Hudson JD**, Shoabi MA, Maestro R, Carnero A, Hannon GJ, Beach DH. A proinflammatory cytokine inhibits p53 tumor suppressor activity. *J Exp Med* 1999; **190**: 1375-1382 [PMID: 10562313 DOI: 10.1084/jem.190.10.1375]
- 49 **Calandra T**, Roger T. Macrophage migration inhibitory factor: a regulator of innate immunity. *Nat Rev Immunol* 2003; **3**: 791-800 [PMID: 14502271 DOI: 10.1038/nri1200]
- 50 **Farr L**, Ghosh S, Moonah S. Role of MIF Cytokine/CD74 Receptor Pathway in Protecting Against Injury and Promoting Repair. *Front Immunol* 2020; **11**: 1273 [PMID: 32655566 DOI: 10.3389/fimmu.2020.01273]
- 51 **Wen Y**, Cai W, Yang J, Fu X, Putha L, Xia Q, Windsor JA, Phillips AR, Tyndall JDA, Du D, Liu T, Huang W. Targeting Macrophage Migration Inhibitory Factor in Acute Pancreatitis and Pancreatic Cancer. *Front Pharmacol* 2021; **12**: 638950 [PMID: 33776775 DOI: 10.3389/fphar.2021.638950]
- 52 **Harris J**, VanPatten S, Deen NS, Al-Abed Y, Morand EF. Rediscovering MIF: New Tricks for an Old Cytokine. *Trends Immunol* 2019; **40**: 447-462 [PMID: 30962001 DOI: 10.1016/j.it.2019.03.002]
- 53 **Kindt N**, Laurent G, Nonclercq D, Journé F, Ghanem G, Duvillier H, Gabius HJ, Lechien J, Saussez S. Pharmacological inhibition of macrophage migration inhibitory factor interferes with the proliferation and invasiveness of squamous carcinoma cells. *Int J Oncol* 2013; **43**: 185-193 [PMID: 23677331 DOI: 10.3892/ijo.2013.1944]
- 54 **Subbannayya T**, Leal-Rojas P, Barbhuiya MA, Raja R, Renuse S, Sathe G, Pinto SM, Syed N, Nanjappa V, Patil AH, Garcia P,

- Sahasrabudhe NA, Nair B, Guerrero-Preston R, Navani S, Tiwari PK, Santosh V, Sidransky D, Prasad TS, Gowda H, Roa JC, Pandey A, Chatterjee A. Macrophage migration inhibitory factor - a therapeutic target in gallbladder cancer. *BMC Cancer* 2015; **15**: 843 [PMID: 26530123 DOI: 10.1186/s12885-015-1855-z]
- 55 **Regateiro FS**, Cobbold SP, Waldmann H. CD73 and adenosine generation in the creation of regulatory microenvironments. *Clin Exp Immunol* 2013; **171**: 1-7 [PMID: 23199317 DOI: 10.1111/j.1365-2249.2012.04623.x]
- 56 **Sun C**, Wang B, Hao S. Adenosine-A2A Receptor Pathway in Cancer Immunotherapy. *Front Immunol* 2022; **13**: 837230 [PMID: 35386701 DOI: 10.3389/fimmu.2022.837230]
- 57 **Zhang B**. CD73: a novel target for cancer immunotherapy. *Cancer Res* 2010; **70**: 6407-6411 [PMID: 20682793 DOI: 10.1158/0008-5472.CAN-10-1544]
- 58 **Cao L**, Bridle KR, Shrestha R, Prithviraj P, Crawford DHG, Jayachandran A. CD73 and PD-L1 as Potential Therapeutic Targets in Gallbladder Cancer. *Int J Mol Sci* 2022; **23** [PMID: 35163489 DOI: 10.3390/ijms23031565]
- 59 **Ahmadzadeh M**, Johnson LA, Heemskerck B, Wunderlich JR, Dudley ME, White DE, Rosenberg SA. Tumor antigen-specific CD8 T cells infiltrating the tumor express high levels of PD-1 and are functionally impaired. *Blood* 2009; **114**: 1537-1544 [PMID: 19423728 DOI: 10.1182/blood-2008-12-195792]
- 60 **Han Y**, Liu D, Li L. PD-1/PD-L1 pathway: current researches in cancer. *Am J Cancer Res* 2020; **10**: 727-742 [PMID: 32266087]
- 61 **Ohaegbulam KC**, Assal A, Lazar-Molnar E, Yao Y, Zang X. Human cancer immunotherapy with antibodies to the PD-1 and PD-L1 pathway. *Trends Mol Med* 2015; **21**: 24-33 [PMID: 25440090 DOI: 10.1016/j.molmed.2014.10.009]
- 62 **Wang Y**, Xie Y, Kilchrist KV, Li J, Duvall CL, Oupický D. Endosomolytic and Tumor-Penetrating Mesoporous Silica Nanoparticles for siRNA/miRNA Combination Cancer Therapy. *ACS Appl Mater Interfaces* 2020; **12**: 4308-4322 [PMID: 31939276 DOI: 10.1021/acsami.9b21214]
- 63 **Li Z**, Yu X, Shen J, Law PT, Chan MT, Wu WK. MicroRNA expression and its implications for diagnosis and therapy of gallbladder cancer. *Oncotarget* 2015; **6**: 13914-13921 [PMID: 26040010 DOI: 10.18632/oncotarget.4227]
- 64 **Ueki T**, Hsing AW, Gao YT, Wang BS, Shen MC, Cheng J, Deng J, Fraumeni JF Jr, Rashid A. Alterations of p16 and prognosis in biliary tract cancers from a population-based study in China. *Clin Cancer Res* 2004; **10**: 1717-1725 [PMID: 15014024 DOI: 10.1158/1078-0432.ccr-1137-3]
- 65 **D'Afonseca V**, Arencebia AD, Echeverría-Vega A, Cerpa L, Cayún JP, Varela NM, Salazar M, Quiñones LA. Identification of Altered Genes in Gallbladder Cancer as Potential Driver Mutations for Diagnostic and Prognostic Purposes: A Computational Approach. *Cancer Inform* 2020; **19**: 1176935120922154 [PMID: 32546937 DOI: 10.1177/1176935120922154]
- 66 **Kawamoto T**, Krishnamurthy S, Tarco E, Trivedi S, Wistuba II, Li D, Roa I, Roa JC, Thomas MB. HER Receptor Family: Novel Candidate for Targeted Therapy for Gallbladder and Extrahepatic Bile Duct Cancer. *Gastrointestinal Cancer Res* 2007; **1**: 221-227 [PMID: 19262900]
- 67 **Rizzo A**, Federico AD, Ricci AD, Frega G, Palloni A, Pagani R, Tavolari S, Marco MD, Brandi G. Targeting BRAF-Mutant Biliary Tract Cancer: Recent Advances and Future Challenges. *Cancer Control* 2020; **27**: 1073274820983013 [PMID: 33356500 DOI: 10.1177/1073274820983013]
- 68 **Saetta AA**, Papanastasiou P, Michalopoulos NV, Gigelou F, Korkolopoulou P, Bei T, Patsouris E. Mutational analysis of BRAF in gallbladder carcinomas in association with K-ras and p53 mutations and microsatellite instability. *Virchows Arch* 2004; **445**: 179-182 [PMID: 15221372 DOI: 10.1007/s00428-004-1046-9]
- 69 **Kim JH**, Kim K, Kim M, Kim YM, Suh JH, Cha HJ, Choi HJ. Programmed death-ligand 1 expression and its correlation with clinicopathological parameters in gallbladder cancer. *J Pathol Transl Med* 2020; **54**: 154-164 [PMID: 32028754 DOI: 10.4132/jptm.2019.11.13]
- 70 **Xie C**, Duffy AG, Mabry-Hrones D, Wood B, Levy E, Krishnasamy V, Khan J, Wei JS, Agdashian D, Tyagi M, Gangalapudi V, Fioravanti S, Walker M, Anderson V, Venzon D, Figg WD, Sandhu M, Kleiner DE, Morelli MP, Floudas CS, Brar G, Steinberg SM, Korangy F, Greten TF. Tremelimumab in Combination With Microwave Ablation in Patients With Refractory Biliary Tract Cancer. *Hepatology* 2019; **69**: 2048-2060 [PMID: 30578687 DOI: 10.1002/hep.30482]
- 71 **Azizi AA**, Lamarca A, McNamara MG, Valle JW. Chemotherapy for advanced gallbladder cancer (GBC): A systematic review and meta-analysis. *Crit Rev Oncol Hematol* 2021; **163**: 103328 [PMID: 33862244 DOI: 10.1016/j.critrevonc.2021.103328]
- 72 **Zaidi A**, Chandna N, Narasimhan G, Moser M, Haider K, Chalchal H, Shaw J, Ahmed S. Second-line Chemotherapy Prolongs Survival in Real World Patients With Advanced Biliary Tract and Gallbladder Cancers: A Multicenter Retrospective Population-based Cohort Study. *Am J Clin Oncol* 2021; **44**: 93-98 [PMID: 33350678 DOI: 10.1097/COC.0000000000000789]
- 73 **Zhou Y**, Yuan K, Yang Y, Ji Z, Zhou D, Ouyang J, Wang Z, Wang F, Liu C, Li Q, Zhang Q, Shan X, Zhou J. Gallbladder cancer: current and future treatment options. *Front Pharmacol* 2023; **14**: 1183619 [PMID: 37251319 DOI: 10.3389/fphar.2023.1183619]
- 74 **Du Rietz H**, Hedlund H, Wilhelmson S, Nordenfelt P, Wittrup A. Imaging small molecule-induced endosomal escape of siRNA. *Nat Commun* 2020; **11**: 1809 [PMID: 32286269 DOI: 10.1038/s41467-020-15300-1]
- 75 **Silva JM**, Li MZ, Chang K, Ge W, Golding MC, Rickles RJ, Siolas D, Hu G, Paddison PJ, Schlabach MR, Sheth N, Bradshaw J, Burchard J, Kulkarni A, Cavet G, Sachidanandam R, McCombie WR, Cleary MA, Elledge SJ, Hannon GJ. Second-generation shRNA libraries covering the mouse and human genomes. *Nat Genet* 2005; **37**: 1281-1288 [PMID: 16200065 DOI: 10.1038/ng1650]
- 76 **Li L**, Lin X, Khvorova A, Fesik SW, Shen Y. Defining the optimal parameters for hairpin-based knockdown constructs. *RNA* 2007; **13**: 1765-1774 [PMID: 17698642 DOI: 10.1261/ma.599107]
- 77 **Sliva K**, Schnierle BS. Selective gene silencing by viral delivery of short hairpin RNA. *Virol J* 2010; **7**: 248 [PMID: 20858246 DOI: 10.1186/1743-422X-7-248]
- 78 **Varas-Godoy M**, Lladser A, Farfan N, Villota C, Villegas J, Tapia JC, Burzio LO, Burzio VA, Valenzuela PDT. In vivo knockdown of antisense non-coding mitochondrial RNAs by a lentiviral-encoded shRNA inhibits melanoma tumor growth and lung colonization. *Pigment Cell Melanoma Res* 2018; **31**: 64-72 [PMID: 28707763 DOI: 10.1111/pcmr.12615]
- 79 **Ichimiya S**, Onishi H, Nagao S, Koga S, Sakihama K, Nakayama K, Fujimura A, Oyama Y, Imaizumi A, Oda Y, Nakamura M. GLI2 but not GLI1/GLI3 plays a central role in the induction of malignant phenotype of gallbladder cancer. *Oncol Rep* 2021; **45**: 997-1010 [PMID: 33650666 DOI: 10.3892/or.2021.7947]
- 80 **Cai J**, Xu L, Cai Z, Wang J, Zhou B, Hu H. MicroRNA-146b-5p inhibits the growth of gallbladder carcinoma by targeting epidermal growth factor receptor. *Mol Med Rep* 2015; **12**: 1549-1555 [PMID: 25760482 DOI: 10.3892/mmr.2015.3461]
- 81 **Kai D**, Yannian L, Yitian C, Dinghao G, Xin Z, Wu J. Circular RNA HIPK3 promotes gallbladder cancer cell growth by sponging microRNA-124. *Biochem Biophys Res Commun* 2018; **503**: 863-869 [PMID: 29928876 DOI: 10.1016/j.bbrc.2018.06.088]

- 82 **Yang G**, Zhang L, Li R, Wang L. The role of microRNAs in gallbladder cancer. *Mol Clin Oncol* 2016; **5**: 7-13 [PMID: [27330755](#) DOI: [10.3892/mco.2016.905](#)]
- 83 **Goepfert B**, Truckenmueller F, Ori A, Fritz V, Albrecht T, Fraas A, Scherer D, Silos RG, Sticht C, Gretz N, Mehrabi A, Bewerunge-Hudler M, Pusch S, Bermejo JL, Dietrich P, Schirmacher P, Renner M, Roessler S. Profiling of gallbladder carcinoma reveals distinct miRNA profiles and activation of STAT1 by the tumor suppressive miRNA-145-5p. *Sci Rep* 2019; **9**: 4796 [PMID: [30886199](#) DOI: [10.1038/s41598-019-40857-3](#)]
- 84 **Chandra V**, Kim JJ, Mittal B, Rai R. MicroRNA aberrations: An emerging field for gallbladder cancer management. *World J Gastroenterol* 2016; **22**: 1787-1799 [PMID: [26855538](#) DOI: [10.3748/wjg.v22.i5.1787](#)]

Clinical and Translational Research

Transient receptor potential-related risk model predicts prognosis of hepatocellular carcinoma patients

Xiao-Cai Mei, Qian Chen, Shi Zuo

Specialty type: Oncology**Provenance and peer review:**

Unsolicited article; Externally peer reviewed.

Peer-review model: Single blind**Peer-review report's scientific quality classification**

Grade A (Excellent): 0

Grade B (Very good): B

Grade C (Good): C, C

Grade D (Fair): 0

Grade E (Poor): 0

P-Reviewer: Elshimi E, Egypt; Hori T, Japan; Moldogazieva NT, Russia**Received:** July 6, 2023**Peer-review started:** July 6, 2023**First decision:** October 9, 2023**Revised:** October 17, 2023**Accepted:** November 10, 2023**Article in press:** November 10, 2023**Published online:** December 15, 2023**Xiao-Cai Mei, Shi Zuo**, Department of Hepatobiliary Surgery, Affiliated Hospital of Guizhou Medical University, Guiyang 550000, Guizhou Province, China**Qian Chen**, Department of Organ Transplantation, Affiliated Hospital of Guizhou Medical University, Guiyang 550000, Guizhou Province, China**Corresponding author:** Shi Zuo, PhD, Chief Physician, Department of Hepatobiliary Surgery, Affiliated Hospital of Guizhou Medical University, No. 28 Gui Medical Street, Yunyan District, Guiyang 550000, Guizhou Province, China. 1056659393@qq.com**Abstract****BACKGROUND**

Members of the transient receptor potential (TRP) protein family shape oncogenic development, but the specific relevance of TRP-related genes in hepatocellular carcinoma (HCC) has yet to be defined.

AIM

To investigate the role of TRP genes in HCC, their association with HCC development and treatment was examined.

METHODS

HCC patient gene expression and clinical data were downloaded from The Cancer Genome Atlas database, and univariate and least absolute shrinkage and selection operator Cox regression models were employed to explore the TRP-related risk spectrum. Based on these analyses, clinically relevant TRP family genes were selected, and the association between the key TRP canonical type 1 (TRPC1) gene and HCC patient prognosis was evaluated.

RESULTS

In total, 28 TRP family genes were screened for clinical relevance, with multivariate analyses ultimately revealing three of these genes (TRPC1, TRP cation channel subfamily M member 2, and TRP cation channel subfamily M member 6) to be significantly associated with HCC patient prognosis ($P < 0.05$). These genes were utilized to establish a TRP-related risk model. Patients were separated into low- and high-risk groups based on the expression of these genes, and high-risk patients exhibited a significantly poorer prognosis ($P = 0.001$). Functional analyses highlighted pronounced differences in the immune status of patients in these two groups and associated enriched immune pathways. TRPC1 was identified as a

candidate gene in this family worthy of further study, with HCC patients expressing higher TRPC1 levels exhibiting poorer survival outcomes. Consistently, quantitative, immunohistochemistry, and western blot analyses revealed increased TRPC1 expression in HCC.

CONCLUSION

These three TRP genes help determine HCC patient prognosis, providing insight into tumor immune status and immunological composition. These findings will help design combination therapies including immunotherapeutic and anti-TRP agents.

Key Words: Transient receptor potential family genes; Hepatocellular carcinoma; Transient receptor potential canonical type 1; Novel oncogene

©The Author(s) 2023. Published by Baishideng Publishing Group Inc. All rights reserved.

Core Tip: The most common form of primary liver cancer is hepatocellular carcinoma (HCC). People with chronic liver conditions, such as cirrhosis caused by hepatitis B or hepatitis C infection, are most likely to develop HCC. Although the predictive value of transient receptor potential (TRP)-related genes in HCC is unknown, TRP family gene proteins influence tumor progression. Our current study assessed the family-related TRP factors to establish the prognosis and treatment plan for HCC.

Citation: Mei XC, Chen Q, Zuo S. Transient receptor potential-related risk model predicts prognosis of hepatocellular carcinoma patients. *World J Gastrointest Oncol* 2023; 15(12): 2064-2076

URL: <https://www.wjgnet.com/1948-5204/full/v15/i12/2064.htm>

DOI: <https://dx.doi.org/10.4251/wjgo.v15.i12.2064>

INTRODUCTION

Liver cancer is the sixth most prevalent cancer globally, with 840000 diagnoses and 780000 deaths annually[1-3]. Rising incidence rates and poor survival rates for hepatocellular carcinoma (HCC) patients in China[4,5] have made it a leading type of primary liver malignancy[6,7]. As HCC tumors exhibit a prolonged latency period and are generally not symptomatic during the early stages of disease, many patients already present with advanced or metastatic disease upon initial diagnosis[8-10]. Thus, the identification of new biomarkers capable of guiding the prognostic evaluation of HCC patients is critical to improve clinical outcomes for this deadly disease.

Ion channels play essential roles in the maintenance of cellular physiology and responsiveness, and their dysregulation is common in cancers and other diseases. Proteins in the transient receptor potential (TRP) channel family function as non-selective cationic channels on the cell surface involved in regulating calcium homeostasis and signaling[11-13]. The regulation of calcium stores is directly associated with how tumor cells, including HCC cells, proliferate[14], migrate, invade[15], and tolerate drug treatment[16]. TRP family genes have previously been implicated in the pathogenesis of diseases and cancers, including breast[17], pancreatic[18], ovarian[19], and prostate malignancies[20].

HCC has a high infiltration of immune cells, and immune responses and immune checkpoints are co-stimulators or co-suppressors required for an immune response to take place in HCC tumor cells. HCC is comprised of multiple cells, including tumor cells and non-tumor cells, with non-tumor cells containing regulatory factors, such as cytokines, growth factors, and certain hormones, which make up the tumor microenvironment (TME). Most immune cells, including macrophages, are critical for initiating tumor immune responses, such as immune surveillance, immune self-stabilization, and immune regulation. Wu *et al*[21] demonstrated important roles for TRP family gene members in pan-cancer analyses, indicating an intricate association between these genes and the TME. Takahashi *et al*[16] additionally demonstrated the ability of nuclear factor erythroid 2-related factor 2 to promote the upregulation of TRP cation channel, subfamily A, member 1 (TRPA1), thus promoting oxidative stress within tumor cells, and such efforts to target TRPA1 may represent a viable means of treating certain cancers.

At present, systematic bioinformatics-based studies of TRP family genes are lacking in the HCC research field. Accordingly, the present study was designed to comprehensively explore the prognostic relevance of TRP family genes in HCC by utilizing data from public databases, with further analyses aimed at the exploration of biological processes through which these genes may impact HCC patient prognosis to provide an effective foundation for the individualized treatment of HCC patients.

MATERIALS AND METHODS

The Cancer Genome Atlas database analyses

The Cancer Genome Atlas (TCGA), <https://portal.gdc.cancer.gov/>, a project developed by the National Cancer Institute and the National Human Genome Research Institute, provides transcriptomic and clinical data on patients with many different cancer types. In the present study, we queried TCGA-HCC patient data and used TCGAbiolinks to download the quantitative gene expression data and clinical information of HCC patients in TCGA database. From these data, the expression data of the 28 TRP family genes were extracted for subsequent analyses.

Survival analysis

Gene expression data of HCC patients (370 cases) and related clinical information were downloaded from TCGA website for further analyses. All statistical analyses were performed using R. Logistic regression and receiver operating characteristic (ROC) methods were used to analyze the relationship between clinicopathological features and TRP family genes. The Kaplan-Meier method and Cox regression analysis were used to determine the clinicopathologic characteristics associated with overall survival (OS) of patients in TCGA database. Critical values for TRP family gene expression were based on median expression values. Kaplan-Meier curves were used to estimate the effect of 28 TRP family genes on OS in HCC patients. Based on the optimal segregation results, patients were categorized into TRP family gene low expression and TRP family gene high expression groups. $P < 0.05$ were considered statistically significant.

Protein-protein interaction network construction and hub gene identification

The STRING database (<https://string-db.org/>) enables the analysis of complex interactions among proteins, and Cytoscape is an open-source bioinformatics tool for creating and visualizing molecular interaction networks. A confidence level of 0.4 was used to construct protein-protein interaction (PPI) network maps for the identified differential genes of the TRP family. Cytoscape software was then used to visualize and construct the interaction network map, and the key gene modules in the network map were screened using the Molecular Complex Detection (MCODE) plug-in, which identifies the key gene modules in the network. The following settings were used in MCODE: Degree cutoff of 2, node score cutoff of 0.2, K-core of 2, and maximum depth of 10024.

Construction of a TRP family gene-based risk score prognostic model

To examine the prognosis of patients with HCC in TCGA dataset, a Cox proportional hazards regression model was constructed. Initially, HCC patient prognosis-related TRP family genes were screened through one-way Cox regression analyses with a significance threshold of $P < 0.05$ using the survival package in R. A least absolute shrinkage and selection operator (LASSO) regression analysis was then implemented using the glmnet package in R to eliminate any overfitted genes included within this model. A prognostic nomogram was further generated based on a multifactorial Cox proportional risk regression analysis.

Patients with HCC were separated into two groups according to whether they were above or below the median risk score value (high risk and low risk) in an effort to clarify the prognostic relevance of this risk score. Patients' OS was then analyzed with Kaplan-Meier curves. Moreover, the sensitivity and specificity of column plots were estimated based on the area under the ROC curve (AUC), with an AUC > 0.06 considered indicative of good predictive validity.

TRP family gene-based nomogram construction

The rms package in R was utilized to generate a nomogram incorporating clinical characteristics and risk score values related to patient outcomes in an effort to establish a tool capable of predicting HCC patient prognosis. The accuracy and predictive performance of this model were assessed using calibration curves.

Immune cell type score analyses

The cell-type identification by estimating relative subsets of RNA transcripts (CIBERSORT) anti-convolution algorithm is a machine learning method based on linear support vector regression to assess the percentage of 22 immune cells in a tissue or cell. We used the CIBERSORT deconvolution method to simulate the transcriptionally characterized substrates of 22 immune cells including B cells, plasma cells, T cells, natural killer (NK) cells, monocytes, macrophages, dendritic cells (DC), mast cells, eosinophils, and neutrophils. The immune cell infiltration of the TRP family gene-expressing HCC patient samples was compared to normal samples to investigate the relationship between TRP family genes and the infiltration of 22 immune cell types in HCC patients in the high- and low-risk groups.

Cell lines and cell culture

The Huh7, HepG2, MHCC-97H, and LM3 HCC cell lines, as well as the control immortalized LO2 hepatic epithelial cell line, were cultured in Dulbecco's Modified Eagle Medium (Hyclone, Logan, UT, United States) containing 10 g/L fetal bovine serum (Gibco, Waltham, MA, United States) and 1 g/L penicillin/streptomycin in a 37 °C 5% CO₂ incubator. A Mycoprobe Mycoplasma Detection Kit (R&D Systems, Minneapolis, MN, United States) was used to confirm that cells were mycoplasma-free.

Western blot

HCC cells with good cell growth were collected and lysed using radioimmunoprecipitation assay buffer, and protein concentration was determined using a bicinchoninic acid protein assay kit. Proteins were separated using sodium

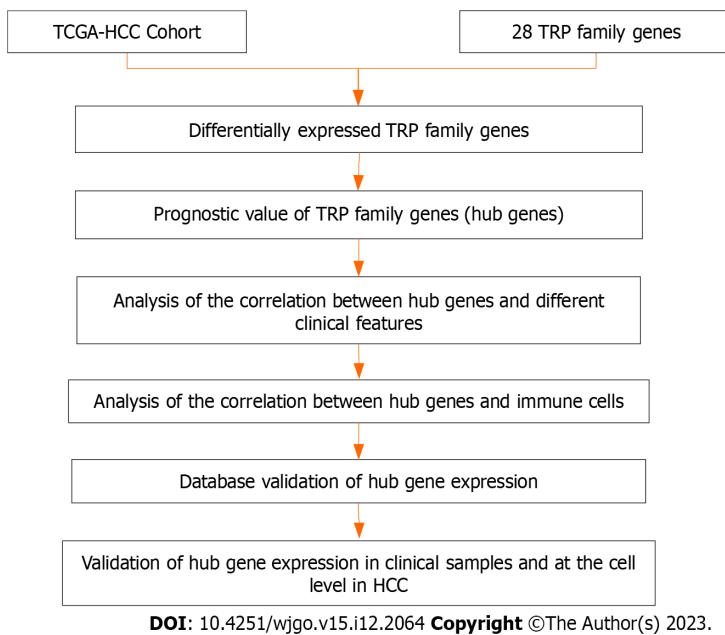


Figure 1 Study flow chart. HCC: Hepatocellular carcinoma; TCGA-HCC: The Cancer Genome Atlas-hepatocellular carcinoma; TRP: Transient receptor potential.

dodecyl sulfate polyacrylamide gel electrophoresis and then transferred to polyvinylidene difluoride membranes. The membranes were blocked in blocking buffer for 1 h and then incubated overnight with the following primary antibodies: Anti-TRP canonical type 1 (TRPC1) (ab192091; Abcam, Cambridge, MA, United States) and anti-GAPDH (10494-1-AP; Proteintech, Rosemont, IL, United States). Then the membranes were incubated with secondary antibodies. The protein bands were visualized using enhanced chemical reagents and analyzed with ImageJ software (V1.8.0.0).

Quantitative polymerase chain reaction

Following treatment with actinomycin D (1 g/mL) for the appropriate intervals, the RNAiso Plus Kit (Cat# 108-95-2; Takara Bio, Beijing, China) was used to extract total cellular RNA. The RT Reagent Kit (Cat# RR047A, Takara Bio; Cat# KR211-02, TIANGEN Biotech, Beijing, China) was used to prepare the cDNA, and quantitative PCR (qPCR) reactions were performed with the FastStart Universal SYBR Green Master Mix (Cat# 04194194001, Roche, Basel, Switzerland; Cat# FP411-02, TIANGEN Biotech) and the Applied Biosystems 7500 Real-Time PCR System (Applied Biosystems, Foster City, CA, United States). The following primers were used: TRPC1 forward, 5'-AAACGGGGATTATTAGTAG-3'; TRPC1 reverse, 5'-TATCTTCTACAGGTGCT-3'; GAPDH forward, 5'-GGAGCGAGATCCCTCCAAAAT-3'; and GAPDH reverse, 5'-GGCTGTTGTCACTTCTCATGG-3'.

Immunohistochemical staining

Tissue sections were deparaffinized using xylene, rehydrated using an ethanol gradient, and incubated for 20 min in sodium citrate buffer (pH 6.0) at 95 °C, followed by treatment for 20 min each with 3% hydrogen peroxide and 10% goat serum in phosphate-buffered saline (PBS) + 0.2% Tween. Sections were probed overnight at 4 °C with an appropriate primary antibody (ab110837; Abcam) in 5 g/L goat serum, washed with PBS, incubated for 40 min at room temperature with secondary antibodies, and developed using 3,3-diaminobenzidine tetrahydrochloride. All tissue samples were obtained from patients under the approval of the Ethical Review Committee of the Affiliated Hospital of Guizhou Medical University (Research Ethics Committee, 2021039; Guizhou, China), with patients providing written informed consent (Supplementary Table 1). Two pathologists independently scored all tissue and immunohistochemistry (IHC) sections based on the staining intensity (0, negative; 1, weak; 2, moderate; and 3, strong) and positive staining area (0, 10%; 1, 10%-25%; 2, 26%-50%; 3, 50%-75%; and 4, 75%-100%). These scores were multiplied to yield a final score, with high expression indicated by a score ≥ 6 .

Statistical analyses

R 3.6.2 was used for the statistical analyses, with differences in prognosis between low- and high-risk groups being assessed *via* the Kaplan-Meier method. $P < 0.05$ was the significance threshold.

RESULTS

Analyses of TRP family gene expression in HCC patients included within TCGA database

A flow chart outlining the present study process is provided in Figure 1. In total, 28 TRP family genes were retrieved from the literature and TCGA database (Supplementary Table 1). The limma package in R was used to analyze TCGA-

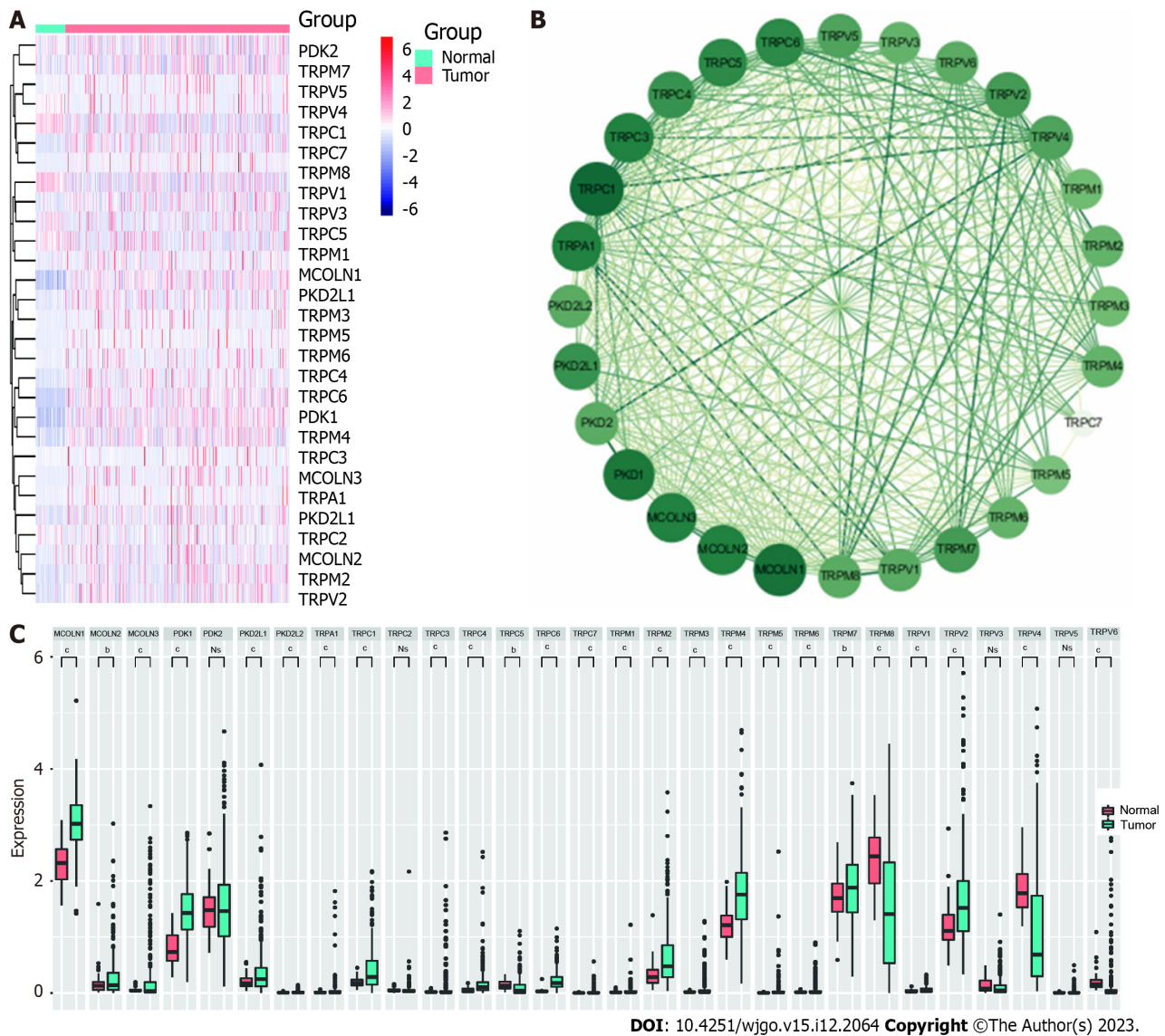
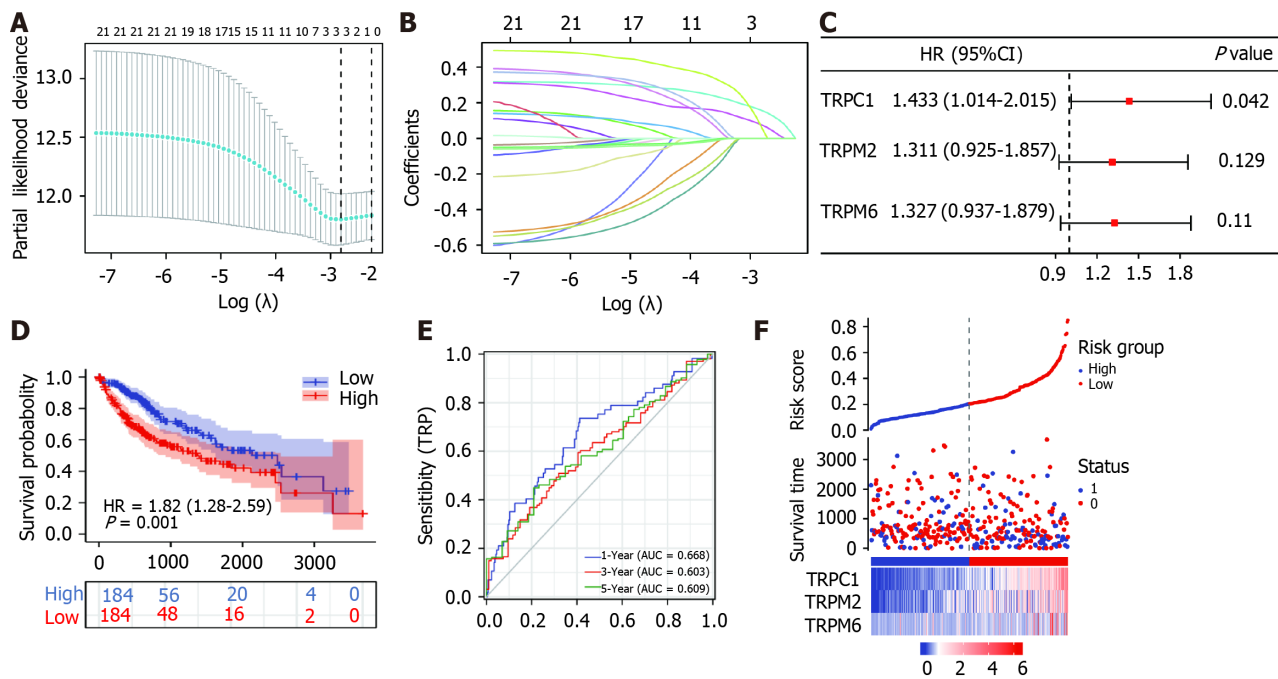


Figure 2 Analyses of differential transient receptor potential family gene expression in hepatocellular carcinoma. A: Heatmap representing the relative expression levels of 28 transient receptor potential (TRP) family genes in hepatocellular carcinoma (HCC) patients and control individuals in The Cancer Genome Atlas-HCC (TCGA-HCC) cohort; B: Violin plots representing the expression of 28 TRP family genes in HCC patients and control individuals from TCGA-HCC cohort; C: Protein-protein interaction network highlighting interactions among differentially expressed TRP family genes. ^b*P* < 0.01; ^c*P* < 0.001; NS: Not significant.

HCC patient RNA sequencing data with the goal of assessing the expression of these TRP genes in 374 HCC samples and 50 normal control tissue samples (Figure 2A). Among the 28 TRP family genes, only polycystin-2, TRP cation channel subfamily C member 2, TRP vanilloid-3, and TRP vanilloid-6 were not differentially expressed in HCC tumor tissues and adjacent tissues, but 24 TRP family genes were differentially expressed in cancer tissues and adjacent paracancerous tissues of HCC patients (Figure 2B). A PPI network was then constructed to assess interactions among these genes (Figure 2C), and additional details regarding the roles and scores of these genes are provided in Supplementary Table 2. These results highlighted the important roles that TRP family genes may play as regulators of key processes in HCC patients.

To identify prognosis-related TRP family-related genes, we performed Cox regression modeling using the LASSO algorithm on the 24 differentially expressed genes between HCC patients and normal healthy controls. Using the best λ parameter in the 10-fold validation, three TRP family-related genes, namely, TRPC1, TRP cation channel subfamily M member 2 (TRPM2), and TRP cation channel subfamily M member 2 (TRPM6), were selected (Figure 3A and B). As expected, univariate Cox analysis showed that some of the 24 genes were associated with OS in HCC patients, and multifactorial regression analysis indicated that TRPC1 was one of the independent prognostic factors in HCC patients (Figure 3C). A risk score was computed using the following model: Risk score = (TRPC1 × 0.156495) + (TRPM2 × 0.075215) + (TRPM6 × 0.058265). Median risk score values were then used to stratify patients into low and high-risk groups, with Kaplan-Meier curves revealing a shorter OS among high-risk patients compared to low-risk individuals (*P* = 0.001; Figure 3D). ROC curve analyses demonstrated the accuracy of this risk scoring model (Figure 3E), and risk score distributions for these HCC patients together with their survival status are presented in Figure 3F. These results suggested that TRPC1 may serve as a valuable prognostic marker in individuals diagnosed with HCC either alone or in a



DOI: 10.4251/wjgo.v15.i12.2064 Copyright ©The Author(s) 2023.

Figure 3 Prognostic analyses of hepatocellular carcinoma patients based on transient receptor potential family gene expression. A: Cross-validation of tuning parameter selection in the least absolute shrinkage and selection operator model by a factor of 10 using The Cancer Genome Atlas-hepatocellular carcinoma (HCC) data; B: Least absolute shrinkage and selection operator coefficients for selected transient receptor potential (TRP) family-related genes; C: Forest plots representing risk associated with prognostic TRP family genes in HCC; D: Kaplan-Meier curves comparing outcomes for low- and high-risk HCC patients classified according to risk scores; E: Receiver operating characteristic curves corresponding to HCC patient 1-, 3-, and 5-year survival rates based on TRP family gene expression; F: Relationship between TRP family gene expression and survival status. HR: Hazard ratio; TRPC1: Transient receptor potential canonical type 1; TRPM: Transient receptor potential cation channel subfamily M.

3-TRP gene signature.

Analysis of the prognostic relevance of the 3-TRP gene signature in HCC

The ability of the developed 3-TRP gene signature to serve as a predictor of HCC patient OS independent of other clinical characteristics (T stage, M stage, pathological grade, residual tumor, and risk score) was examined through univariate and multivariate Cox regression approaches. Factors significantly associated with patient OS in the univariate analyses included T stage, M stage, pathological grade, and risk score values ($P < 0.05$) (Figure 4A), while only risk score values remained independently associated with OS in multivariate analyses of TCGA patient cohort (Figure 4B). These results suggested that the developed risk scoring model can be utilized as a tool to independently predict HCC patient disease outcomes. A nomogram was additionally constructed with the rms package in R, which incorporated this 3-TRP gene signature-based risk score and other clinical characteristics to gauge survival odds (Figure 4C). In this model, higher scores were indicative of a poorer prognosis. Calibration curves revealed good consistency of actual patient 1-, 3-, and 5-year OS with that predicted by this nomogram (Figure 4D-F). Therefore, this predictive model is a valuable tool for the evaluation of HCC patient long-term prognosis.

Association between TRP family genes and the tumor immune microenvironment

To fully explore immune cell distributions and their relationships with established risk groups in individuals with HCC, the CIBERSORT algorithm was employed to approximate tumor infiltration of 22 different immune cell types and the relationship between such infiltration and TRP family genes in TCGA HCC patient cohort and corresponding control samples. The degree of immune cell infiltration was higher in the high-risk group than in the low-risk group, especially in γ - δ T cells and M0 macrophages (Figure 5A and B). We further analyzed the correlation of risk scores with the degree of immune cell infiltration. Core TRP family genes were closely correlated with the infiltration of important immune cell types including T cells, NK cells, DCs, and memory T cells ($|\text{cor}| > 0.3$) (Figure 5C and D). γ - δ T cells ($P = 0.02$, $r = 0.34$) and activated CD4 memory T cells ($P = 0.05$, $r = 0.29$) were positively correlated with the risk scores, whereas activated NK cells ($P = 0.01$, $r = 0.36$) and activated DCs ($P = 0.02$, $r = 0.33$) were negatively correlated with the risk scores (Figure 5C and D). Of these cell types, only T cells exhibited both a significant correlation with TRP family genes and differential infiltration levels between sample types (Figure 5E). Thus, these data indicated that core TRP family genes are closely related to immune cell infiltration, with individuals in the TRP-based high-risk group exhibiting upregulation of most immune-related cell activities (Figure 5F).

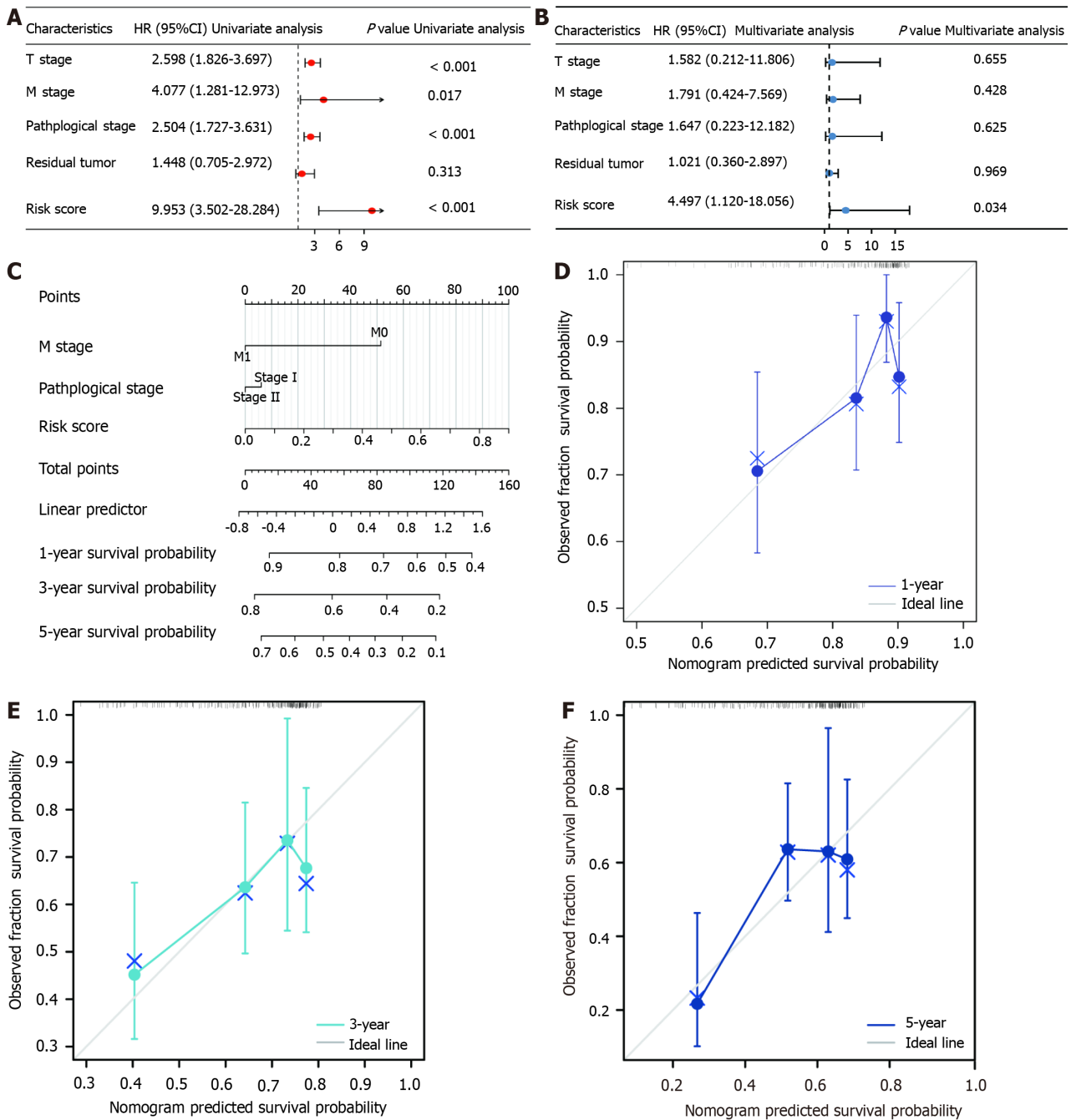
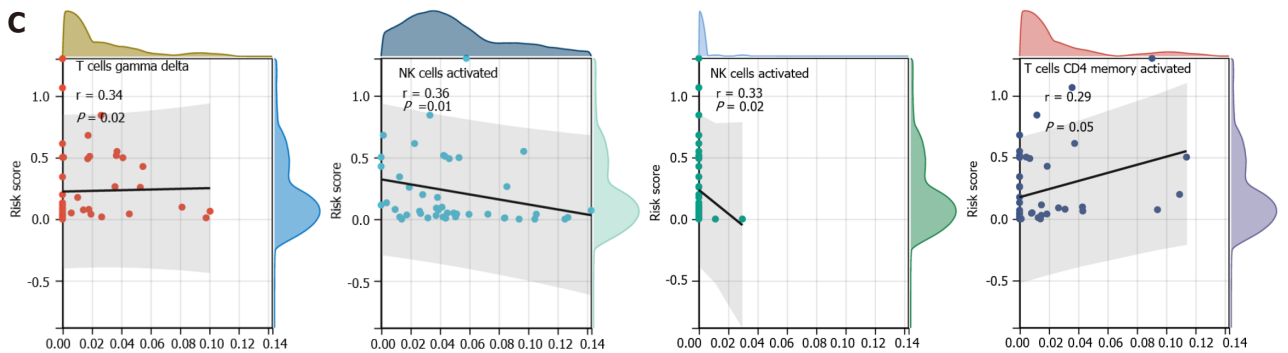
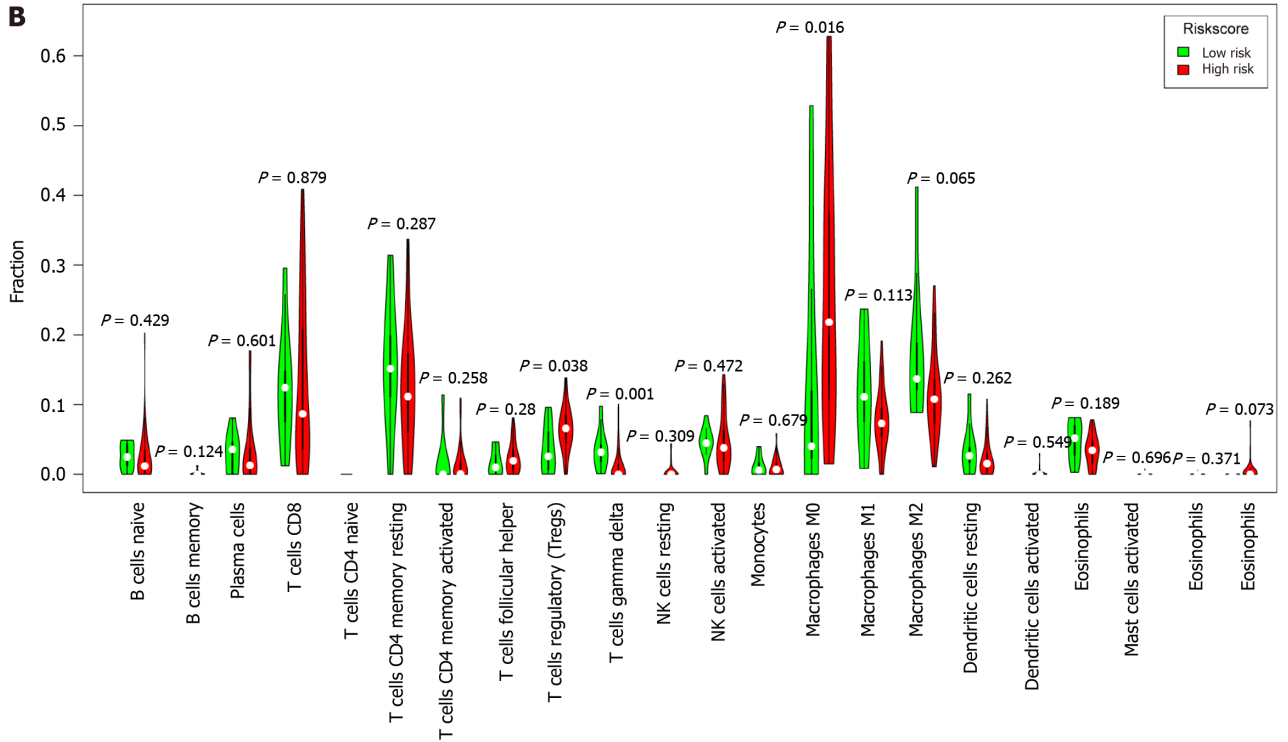
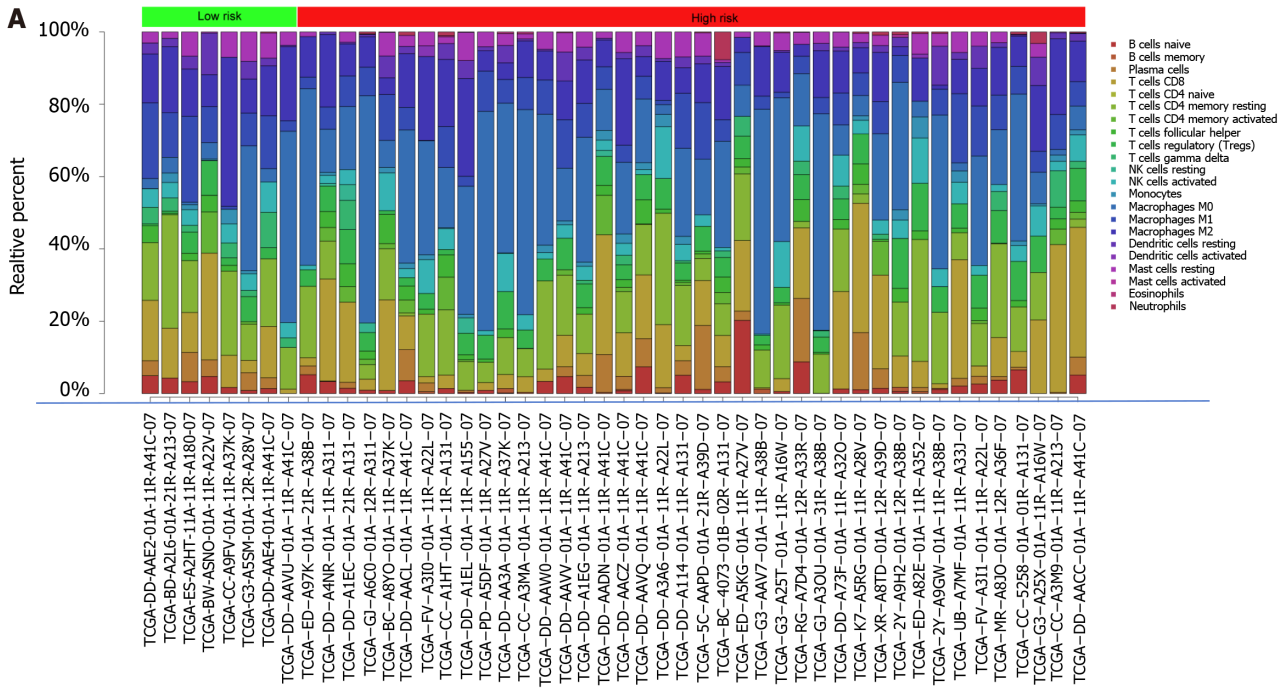


Figure 4 Analyses of the independent prognostic significance of transient receptor potential family gene expression. A and B: Univariate and multivariate Cox regression analyses of hepatocellular carcinoma (HCC) patients included within The Cancer Genome Atlas database; C: Model developed based on a combination of HCC patient clinical characteristics and risk signatures; D-F: Calibration curve plots demonstrating model predictive performance for 1-, 3-, and 5-year overall survival. HR: Hazard ratio.

Analysis of TRPC1 expression in HCC

While TRPC1, TRPM2, and TRPM6 were identified as core TRP family genes potentially associated with HCC pathogenesis, no significant differences in HCC patient prognosis were observed as a function of TRPM2 or TRPM6 expression. As such, TRPC1 expression and prognostic significance were further explored in greater detail. Initial pan-cancer analyses highlighted high levels of TRPC1 expression in most tumor types relative to corresponding normal tissue controls, including HCC (Figure 6A). Consistently, significantly higher levels of TRPC1 expression were detected in liver cancer samples relative to paired paracancerous tissues (Figure 6B), and the HCC patients exhibiting higher TRPC1 expression levels also had a poorer prognosis (Figure 6C). To independently confirm these results, qPCR and western blot analyses were conducted using the LM3, Huh7, MHCC-97H, and HepG2 HCC cell lines, as well as immortalized liver epithelial cells. In line with patient data, TRPC1 expression at the mRNA and protein levels was increased in HCC cells compared to epithelial controls (Figure 6D and E). Additional tissue samples were also collected from liver cancer patients at the Guizhou Medical University Affiliated Hospital and used for IHC staining, confirming that TRPC1



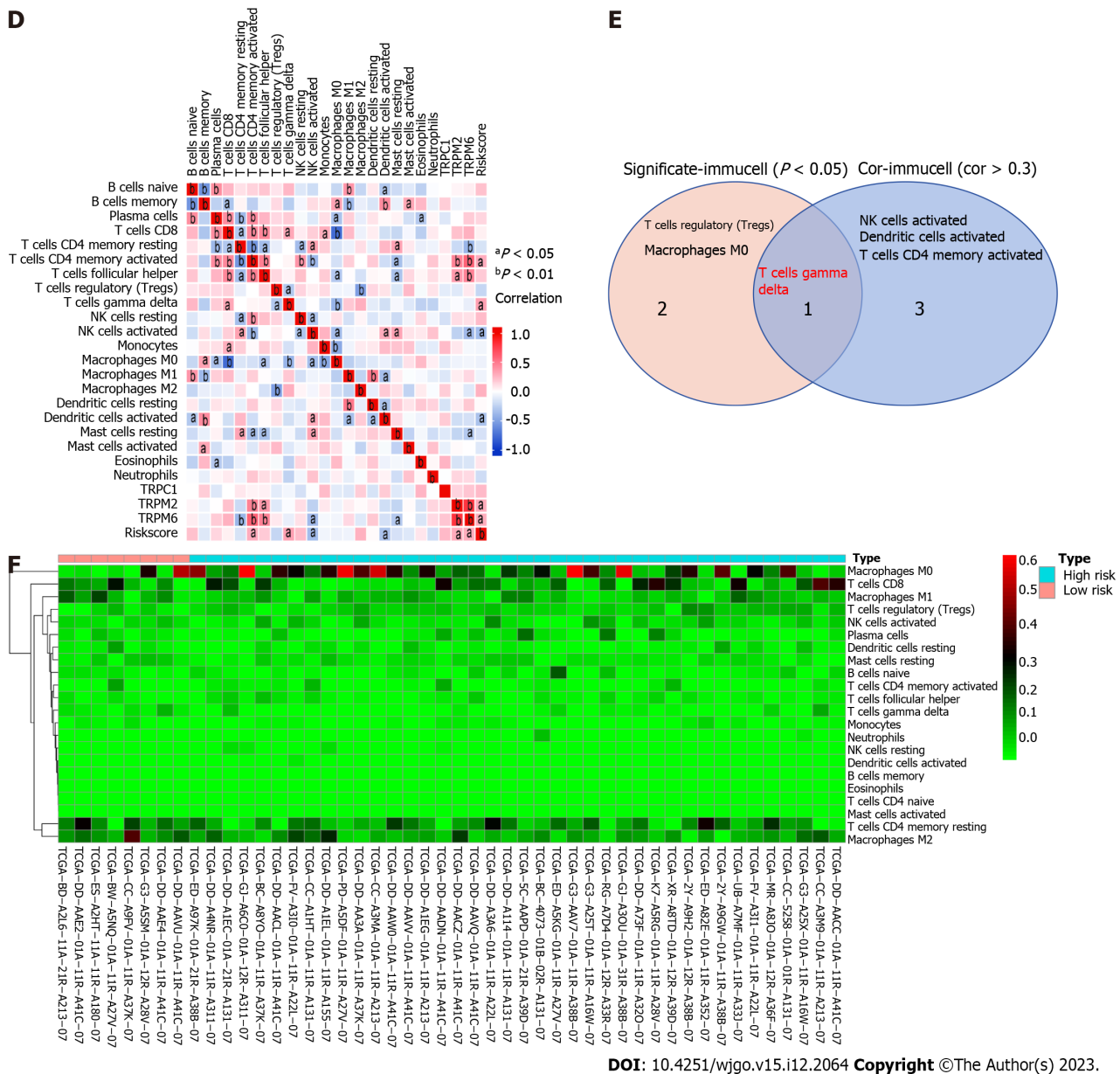


Figure 5 Analyses of the association between transient receptor potential family genes and the tumor immune microenvironment. A: Immune cell infiltration analysis for 22 types of immune cells in hepatocellular carcinoma (HCC) and control patient samples from The Cancer Genome Atlas-HCC cohort; B: Violin plot revealing differences in the relative infiltration of 22 immune cell types in HCC and control patient samples; C: Scatter plot exhibiting correlations between hub transient receptor potential family genes and 22 different immune cell types; D: Heatmap revealing correlations between hub gene expression and 22 different immune cell types; E: Venn diagram revealing overlapping immune cell types exhibiting differential expression and relevance; F: Heatmap corresponding to the association of high- and low-risk groups with immune cell infiltration. NK: Natural killer.

expression was upregulated in HCC patient tumors relative to adjacent healthy tissue (Figure 6F). In summary, HCC patients who have elevated TRPC1 expression have poorer prognostic outcomes.

DISCUSSION

Unlike many other gene families, TRP family members have been largely overlooked in oncological studies despite their strong associations with the onset and progression of other disease types[22-24]. Here, TRP family gene expression profiles were analyzed for the first time in HCC, underscoring potentially important roles for these genes as mediators of oncogenesis. Moreover, TRPC1 expression was experimentally confirmed to be dysregulated in HCC, suggesting that this protein may be a viable target for pharmaceutical intervention.

TCGA database is widely utilized throughout the world to study patterns of gene expression across many tumor types [25,26]. In the present study, 28 TRP family genes were selected, and their expression levels were analyzed in TCGA-HCC cohort. The majority of these genes were upregulated in HCC, and multivariate Cox regression analysis demonstrated that three of these genes (TRPC1, TRPM2, and TRPM6) were related to patient OS. These genes were then incorporated

While these results offer a valuable new foundation for studies focused on the association between TRPC1 and HCC, these findings are subject to certain limitations. First, only TCGA database was analyzed in the present study, potentially introducing some degree of sample bias into the results. Additional studies that include more HCC patient samples and additional clinical parameters will be conducted in the future to enhance the accuracy of these findings. Second, experimental evidence explaining the mechanistic role of TRPC1 as a regulator of HCC progression is currently lacking and warrants further study. Although these results offered new perspectives regarding the role of TRP family genes in HCC, more work is necessary to clarify the underlying mechanisms and the potential value of TRPC1 as a target for pharmacological intervention.

CONCLUSION

In summary, the present comprehensive study of the part of TRP-related genes led to the successful establishment of a TRP-related gene signature associated with HCC patient outcomes. Moreover, TRPC1 was identified as a potential oncogenic driver and candidate target for therapeutic intervention in this cancer type.

ARTICLE HIGHLIGHTS

Research background

The most typical form of primary liver cancer is hepatocellular carcinoma (HCC). People with chronic liver conditions, such as cirrhosis caused by hepatitis B or hepatitis C infection, are most likely to develop HCC. Although the predictive value of TRP-related genes in HCC is unknown, transient receptor potential (TRP) family gene proteins influence tumor progression. Our current study aimed to assess the family-related TRP factors to establish the prognosis and treatment plan for HCC. We downloaded the mRNA expression profiles and corresponding clinical information for the HCC patients from the cancer genome atlas (TCGA) database. Univariate and least absolute contraction and selection operator (LASSO) Cox regression models were used to construct the TRP risk spectrum, infer the clinically significant TRP family core genes, and examine the correlation between the core gene TRP canonical type 1 (TRPC1) and the expression and prognosis of HCC. Our findings propose that the predictive characteristics of the 3-TRP gene discussed in this study are not only effective for prognosis prediction but also related to the tumor's immune status and the infiltration of various immune cells in the tumor microenvironment. These results may provide significant clinical indications for HCC patients to propose a new combination therapy consisting of targeted anti-TRP treatment and immunotherapy.

Research motivation

To investigate the role of TRP genes in HCC, their association with HCC development and treatment was examined.

Research objectives

To investigate the role of TRP genes in HCC, their association with HCC development and treatment was examined.

Research methods

HCC patient gene expression and clinical data were downloaded from The Cancer Genome Atlas database, and univariate and LASSO Cox regression models were employed to explore the TRP-related risk spectrum. Based on these analyses, clinically relevant TRP family genes were selected, and the association between the key TRPC1 gene and HCC patient prognosis was evaluated.

Research results

In total, 28 TRP family genes were screened for clinical relevance, with multivariate analyses ultimately revealing three of these genes (TRPC1, TRP cation channel subfamily M member 2, and TRP cation channel subfamily M member 6) to be significantly associated with HCC patient prognosis ($P < 0.05$). These genes were utilized to establish a TRP-related risk model. Patients were separated into low and high-risk groups based on the expression of these genes, and high-risk patients exhibited a significantly poorer prognosis ($P = 0.001$). Functional analyses highlighted pronounced differences in the immune status of patients in these two groups and associated enriched immune pathways. TRPC1 was identified as a candidate gene in this family worthy of further study, with HCC patients expressing higher TRPC1 levels exhibiting poorer survival outcomes. Consistently, quantitative, immunohistochemistry, and western blot analyses revealed increased TRPC1 expression in HCC.

Research conclusions

These three TRP genes help determine HCC patient prognosis, providing insight into tumor immune status and immunological composition. These findings will help design combination therapies including immunotherapeutic and anti-TRP agents.

Research perspectives

In the future, we will focus on in-depth studies on the mechanism of how TRPC1 regulates the development of HCC.

ACKNOWLEDGEMENTS

We would like to thank all our colleagues in the Department of Hepatobiliary Surgery and Organ Transplantation of the Affiliated Hospital of Guizhou Medical University for their help.

FOOTNOTES

Co-first authors: Xiao-Cai Mei, and Qian Chen.

Author contributions: Zuo S designed the experiments and revised the manuscript, Mei XC, and Chen Q performed the data analysis and wrote the manuscript; Mei XC and Chen Q contributed to the conception of the study; Mei XC and Chen Q worked together on the data analysis of this article, including the analysis of the database and subsequent collaboration together on PCR and western blotting; Mei XC and Chen Q worked together to conceptualize the framework of the article, and in the revision process, the two authors also worked together to complete the reviewer's response; all authors read and agreed on the final manuscript.

Supported by National Natural Science Foundation of China, No. 82260535; and National Natural Science Foundation of Guizhou Medical University Hospital Incubation Program, No. gyfynsc-2022-07.

Institutional review board statement: This study was reviewed and approved by the Institutional Review Board of Guizhou Medical University Hospital.

Informed consent statement: All study participants, or their legal guardian, provided informed written consent prior to study enrollment.

Conflict-of-interest statement: The authors have no conflicts of interest to declare.

Data sharing statement: No additional data are available.

Open-Access: This article is an open-access article that was selected by an in-house editor and fully peer-reviewed by external reviewers. It is distributed in accordance with the Creative Commons Attribution NonCommercial (CC BY-NC 4.0) license, which permits others to distribute, remix, adapt, build upon this work non-commercially, and license their derivative works on different terms, provided the original work is properly cited and the use is non-commercial. See: <https://creativecommons.org/licenses/by-nc/4.0/>

Country/Territory of origin: China

ORCID number: Shi Zuo [0000-0002-8595-5062](https://orcid.org/0000-0002-8595-5062).

S-Editor: Qu XL

L-Editor: Filipodia

P-Editor: Zhao S

REFERENCES

- 1 Siegel RL, Miller KD, Fuchs HE, Jemal A. Cancer Statistics, 2021. *CA Cancer J Clin* 2021; **71**: 7-33 [PMID: [33433946](https://pubmed.ncbi.nlm.nih.gov/33433946/) DOI: [10.3322/caac.21654](https://doi.org/10.3322/caac.21654)]
- 2 Ferlay J, Colombet M, Soerjomataram I, Parkin DM, Piñeros M, Znaor A, Bray F. Cancer statistics for the year 2020: An overview. *Int J Cancer* 2021 [PMID: [33818764](https://pubmed.ncbi.nlm.nih.gov/33818764/) DOI: [10.1002/ijc.33588](https://doi.org/10.1002/ijc.33588)]
- 3 Lee S, Kang TW, Song KD, Lee MW, Rhim H, Lim HK, Kim SY, Sinn DH, Kim JM, Kim K, Ha SY. Effect of Microvascular Invasion Risk on Early Recurrence of Hepatocellular Carcinoma After Surgery and Radiofrequency Ablation. *Ann Surg* 2021; **273**: 564-571 [PMID: [31058694](https://pubmed.ncbi.nlm.nih.gov/31058694/) DOI: [10.1097/SLA.0000000000003268](https://doi.org/10.1097/SLA.0000000000003268)]
- 4 Chidambaranathan-Reghupaty S, Fisher PB, Sarkar D. Hepatocellular carcinoma (HCC): Epidemiology, etiology and molecular classification. *Adv Cancer Res* 2021; **149**: 1-61 [PMID: [33579421](https://pubmed.ncbi.nlm.nih.gov/33579421/) DOI: [10.1016/bs.acr.2020.10.001](https://doi.org/10.1016/bs.acr.2020.10.001)]
- 5 Kim E, Viatour P. Hepatocellular carcinoma: old friends and new tricks. *Exp Mol Med* 2020; **52**: 1898-1907 [PMID: [33268834](https://pubmed.ncbi.nlm.nih.gov/33268834/) DOI: [10.1038/s12276-020-00527-1](https://doi.org/10.1038/s12276-020-00527-1)]
- 6 Lin YL, Li Y. Study on the hepatocellular carcinoma model with metastasis. *Genes Dis* 2020; **7**: 336-350 [PMID: [32884988](https://pubmed.ncbi.nlm.nih.gov/32884988/) DOI: [10.1016/j.gendis.2019.12.008](https://doi.org/10.1016/j.gendis.2019.12.008)]
- 7 Liu J, Geng W, Sun H, Liu C, Huang F, Cao J, Xia L, Zhao H, Zhai J, Li Q, Zhang X, Kuang M, Shen S, Xia Q, Wong VW, Yu J. Integrative metabolomic characterisation identifies altered portal vein serum metabolome contributing to human hepatocellular carcinoma. *Gut* 2022; **71**: 1203-1213 [PMID: [34344785](https://pubmed.ncbi.nlm.nih.gov/34344785/) DOI: [10.1136/gutjnl-2021-325189](https://doi.org/10.1136/gutjnl-2021-325189)]
- 8 Wang J, Li CD, Sun L. Recent Advances in Molecular Mechanisms of the NKG2D Pathway in Hepatocellular Carcinoma. *Biomolecules* 2020; **10** [PMID: [32075046](https://pubmed.ncbi.nlm.nih.gov/32075046/) DOI: [10.3390/biom10020301](https://doi.org/10.3390/biom10020301)]
- 9 Gentile D, Donadon M, Lleo A, Aghemo A, Roncalli M, di Tommaso L, Torzilli G. Surgical Treatment of Hepatocholeangiocarcinoma: A Systematic Review. *Liver Cancer* 2020; **9**: 15-27 [PMID: [32071906](https://pubmed.ncbi.nlm.nih.gov/32071906/) DOI: [10.1159/000503719](https://doi.org/10.1159/000503719)]
- 10 Hashimoto A, Sarker D, Reebye V, Jarvis S, Sodergren MH, Kossenkov A, Sanseviero E, Raulf N, Vasara J, Andrikakou P, Meyer T, Huang KW, Plummer R, Chee CE, Spalding D, Pai M, Khan S, Pinato DJ, Sharma R, Basu B, Palmer D, Ma YT, Evans J, Habib R, Martirosyan A,

- Elasri N, Reynaud A, Rossi JJ, Cobbold M, Habib NA, Gabrilovich DI. Upregulation of C/EBP α Inhibits Suppressive Activity of Myeloid Cells and Potentiates Antitumor Response in Mice and Patients with Cancer. *Clin Cancer Res* 2021; **27**: 5961-5978 [PMID: 34407972 DOI: 10.1158/1078-0432.CCR-21-0986]
- 11 **Zhao Y**, McVeigh BM, Moiseenkova-Bell VY. Structural Pharmacology of TRP Channels. *J Mol Biol* 2021; **433**: 166914 [PMID: 33676926 DOI: 10.1016/j.jmb.2021.166914]
- 12 **Zhong T**, Zhang W, Guo H, Pan X, Chen X, He Q, Yang B, Ding L. The regulatory and modulatory roles of TRP family channels in malignant tumors and relevant therapeutic strategies. *Acta Pharm Sin B* 2022; **12**: 1761-1780 [PMID: 35847486 DOI: 10.1016/j.apsb.2021.11.001]
- 13 **Diver MM**, Lin King JV, Julius D, Cheng Y. Sensory TRP Channels in Three Dimensions. *Annu Rev Biochem* 2022; **91**: 629-649 [PMID: 35287474 DOI: 10.1146/annurev-biochem-032620-105738]
- 14 **Farfariello V**, Gordienko DV, Mesilmany L, Touil Y, Germain E, Fliniaux I, Desruelles E, Gkika D, Roudbaraki M, Shapovalov G, Noyer L, Lebas M, Allart L, Zienthal-Gelus N, Iamshanova O, Bonardi F, Figeac M, Laine W, Kluza J, Marchetti P, Quesnel B, Metzger D, Bernard D, Parys JB, Lemonnier L, Prevarskaya N. TRPC3 shapes the ER-mitochondria Ca(2+) transfer characterizing tumour-promoting senescence. *Nat Commun* 2022; **13**: 956 [PMID: 35177596 DOI: 10.1038/s41467-022-28597-x]
- 15 **Xing Y**, Wei X, Liu Y, Wang MM, Sui Z, Wang X, Zhu W, Wu M, Lu C, Fei YH, Jiang Y, Zhang Y, Wang Y, Guo F, Cao JL, Qi J, Wang W. Autophagy inhibition mediated by MCOLN1/TRPML1 suppresses cancer metastasis *via* regulating a ROS-driven TP53/p53 pathway. *Autophagy* 2022; **18**: 1932-1954 [PMID: 34878954 DOI: 10.1080/15548627.2021.2008752]
- 16 **Takahashi N**, Chen HY, Harris IS, Stover DG, Selfors LM, Bronson RT, Deraedt T, Cichowski K, Welm AL, Mori Y, Mills GB, Brugge JS. Cancer Cells Co-opt the Neuronal Redox-Sensing Channel TRPA1 to Promote Oxidative-Stress Tolerance. *Cancer Cell* 2018; **33**: 985-1003.e7 [PMID: 29805077 DOI: 10.1016/j.ccell.2018.05.001]
- 17 **Saldías MP**, Maureira D, Orellana-Serradell O, Silva I, Lavanderos B, Cruz P, Torres C, Cáceres M, Cerda O. TRP Channels Interactome as a Novel Therapeutic Target in Breast Cancer. *Front Oncol* 2021; **11**: 621614 [PMID: 34178620 DOI: 10.3389/fonc.2021.621614]
- 18 **Mesquita G**, Prevarskaya N, Schwab A, Lehen'kyi V. Role of the TRP Channels in Pancreatic Ductal Adenocarcinoma Development and Progression. *Cells* 2021; **10** [PMID: 33925979 DOI: 10.3390/cells10051021]
- 19 **Wang X**, Li G, Zhang Y, Li L, Qiu L, Qian Z, Zhou S, Wang X, Li Q, Zhang H. Pan-Cancer Analysis Reveals Genomic and Clinical Characteristics of TRPV Channel-Related Genes. *Front Oncol* 2022; **12**: 813100 [PMID: 35174089 DOI: 10.3389/fonc.2022.813100]
- 20 **Günther T**, Konrad M, Stopper L, Kunert JP, Fischer S, Beck R, Casini A, Wester HJ. Optimization of the Pharmacokinetic Profile of [(99m)Tc]Tc-N(4)-Bombesin Derivatives by Modification of the Pharmacophoric Gln-Trp Sequence. *Pharmaceuticals (Basel)* 2022; **15** [PMID: 36145354 DOI: 10.3390/ph15091133]
- 21 **Wu G**, He M, Yin X, Wang W, Zhou J, Ren K, Chen X, Xue Q. The Pan-Cancer Landscape of Crosstalk Between TRP Family and Tumour Microenvironment Relevant to Prognosis and Immunotherapy Response. *Front Immunol* 2022; **13**: 837665 [PMID: 35493463 DOI: 10.3389/fimmu.2022.837665]
- 22 **Fang C**, Xu H, Liu Y, Huang C, Wang X, Zhang Z, Xu Y, Yuan L, Zhang A, Shao A, Lou M. TRP Family Genes Are Differently Expressed and Correlated with Immune Response in Glioma. *Brain Sci* 2022; **12** [PMID: 35625048 DOI: 10.3390/brainsci12050662]
- 23 **Jimenez I**, Prado Y, Marchant F, Otero C, Eltit F, Cabello-Verrugio C, Cerda O, Simon F. TRPM Channels in Human Diseases. *Cells* 2020; **9** [PMID: 33291725 DOI: 10.3390/cells9122604]
- 24 **Pan F**, Wang K, Zheng M, Ren Y, Hao W, Yan J. A TRP Family Based Signature for Prognosis Prediction in Head and Neck Squamous Cell Carcinoma. *J Oncol* 2022; **2022**: 8757656 [PMID: 35140788 DOI: 10.1155/2022/8757656]
- 25 **Poore GD**, Kopylova E, Zhu Q, Carpenter C, Fraraccio S, Wandro S, Kosciolk T, Janssen S, Metcalf J, Song SJ, Kanbar J, Miller-Montgomery S, Heaton R, McKay R, Patel SP, Swafford AD, Knight R. Microbiome analyses of blood and tissues suggest cancer diagnostic approach. *Nature* 2020; **579**: 567-574 [PMID: 32214244 DOI: 10.1038/s41586-020-2095-1]
- 26 **Kuzu OF**, Noory MA, Robertson GP. The Role of Cholesterol in Cancer. *Cancer Res* 2016; **76**: 2063-2070 [PMID: 27197250 DOI: 10.1158/0008-5472.CAN-15-2613]
- 27 **Hanahan D**. Hallmarks of Cancer: New Dimensions. *Cancer Discov* 2022; **12**: 31-46 [PMID: 35022204 DOI: 10.1158/2159-8290.CD-21-1059]
- 28 **Peng S**, Xiao F, Chen M, Gao H. Tumor-Microenvironment-Responsive Nanomedicine for Enhanced Cancer Immunotherapy. *Adv Sci (Weinh)* 2022; **9**: e2103836 [PMID: 34796689 DOI: 10.1002/advs.202103836]
- 29 **Downs-Canner SM**, Meier J, Vincent BG, Serody JS. B Cell Function in the Tumor Microenvironment. *Annu Rev Immunol* 2022; **40**: 169-193 [PMID: 35044794 DOI: 10.1146/annurev-immunol-101220-015603]
- 30 **Kwiatkowska I**, Hermanowicz JM, Przybyszewska-Podstawka A, Pawlak D. Not Only Immune Escape-The Confusing Role of the TRP Metabolic Pathway in Carcinogenesis. *Cancers (Basel)* 2021; **13** [PMID: 34071442 DOI: 10.3390/cancers13112667]
- 31 **Parenti A**, De Logu F, Geppetti P, Benemei S. What is the evidence for the role of TRP channels in inflammatory and immune cells? *Br J Pharmacol* 2016; **173**: 953-969 [PMID: 26603538 DOI: 10.1111/bph.13392]
- 32 **Partida-Sanchez S**, Desai BN, Schwab A, Zierler S. Editorial: TRP Channels in Inflammation and Immunity. *Front Immunol* 2021; **12**: 684172 [PMID: 33936122 DOI: 10.3389/fimmu.2021.684172]
- 33 **Bertin S**, Raz E. Transient Receptor Potential (TRP) channels in T cells. *Semin Immunopathol* 2016; **38**: 309-319 [PMID: 26468011 DOI: 10.1007/s00281-015-0535-z]
- 34 **Huang T**, Xu T, Wang Y, Zhou Y, Yu D, Wang Z, He L, Chen Z, Zhang Y, Davidson D, Dai Y, Hang C, Liu X, Yan C. Cannabidiol inhibits human glioma by induction of lethal mitophagy through activating TRPV4. *Autophagy* 2021; **17**: 3592-3606 [PMID: 33629929 DOI: 10.1080/15548627.2021.1885203]
- 35 **Sun Y**, Ye C, Tian W, Ye W, Gao YY, Feng YD, Zhang HN, Ma GY, Wang SJ, Cao W, Li XQ. TRPC1 promotes the genesis and progression of colorectal cancer *via* activating CaM-mediated PI3K/AKT signaling axis. *Oncogenesis* 2021; **10**: 67 [PMID: 34642309 DOI: 10.1038/s41389-021-00356-5]

Retrospective Cohort Study

Cohort study to assess geographical variation in
cholangiocarcinoma treatment in England

Sophie Jose, Amy Zalin-Miller, Craig Knott, Lizz Paley, Daniela Tataru, Helen Morement, Mireille B Toledano, Shahid A Khan

Specialty type: Oncology

Provenance and peer review:

Unsolicited article; Externally peer reviewed.

Peer-review model: Single blind

Peer-review report's scientific quality classification

Grade A (Excellent): 0

Grade B (Very good): B

Grade C (Good): C

Grade D (Fair): 0

Grade E (Poor): 0

P-Reviewer: Lim YC, Brunei Darussalam; Wang L, China

Received: August 7, 2023

Peer-review started: August 7, 2023

First decision: September 1, 2023

Revised: September 22, 2023

Accepted: October 30, 2023

Article in press: October 30, 2023

Published online: December 15, 2023



Sophie Jose, Amy Zalin-Miller, Craig Knott, Health Data Analysis, Health Data Insight CIC, Cambridge CB21 5XE, United Kingdom

Sophie Jose, Amy Zalin-Miller, Craig Knott, Lizz Paley, Daniela Tataru, National Disease Registration Service, National Health Service England, London SE1 8UG, United Kingdom

Helen Morement, Department of Executive, AMMF-The Cholangiocarcinoma Charity, Essex CM24 1QW, United Kingdom

Mireille B Toledano, MRC Centre for Environment and Health, Imperial College London, London SW7 2BX, United Kingdom

Mireille B Toledano, Mohn Centre for Children's Health and Wellbeing, Imperial College London, London SW7 2BX, United Kingdom

Shahid A Khan, Liver Unit, Division of Digestive Diseases, Imperial College London, London SW7 2BX, United Kingdom

Corresponding author: Sophie Jose, PhD, Senior Statistician, Health Data Analysis, Health Data Insight CIC, CPC4 Capital Park, Cambridge CB21 5XE, United Kingdom. sophie.jose@nhs.net

Abstract**BACKGROUND**

Outcomes for cholangiocarcinoma (CCA) are extremely poor owing to the complexities in diagnosing and managing a rare disease with heterogenous sub-types. Beyond curative surgery, which is only an option for a minority of patients diagnosed at an early stage, few systemic therapy options are currently recommended to relieve symptoms and prolong life. Stent insertion to manage disease complications requires highly specialised expertise. Evidence is lacking as to how CCA patients are managed in a real-world setting and whether there is any variation in treatments received by CCA patients.

AIM

To assess geographic variation in treatments received amongst CCA patients in England.

METHODS

Data used in this cohort study were drawn from the National Cancer Registration Dataset (NCRD), Hospital Episode Statistics and the Systemic Anti-Cancer Therapy Dataset. A cohort of 8853 CCA patients diagnosed between 2014–2017 in the National Health Service in England was identified from the NCRD. Potentially curative surgery for all patients and systemic therapy and stent insertion for 7751 individuals who did not receive surgery were identified as three end-points of interest. Linear probability models assessed variation in each of the three treatment modalities according to Cancer Alliance of residence at diagnosis, and for socio-demographic and clinical characteristics at diagnosis.

RESULTS

Of 8853 CCA patients, 1102 (12.4%) received potentially curative surgery. The mean [95% confidence interval (CI)] percentage-point difference from the population average ranged from -3.96 (-6.34 to -1.59)% to 3.77 (0.54 to 6.99)% across Cancer Alliances in England after adjustment for patient sociodemographic and clinical characteristics, showing statistically significant variation. Amongst 7751 who did not receive surgery, 1542 (19.9%) received systemic therapy, with mean [95%CI] percentage-point difference from the population average between -3.84 (-8.04 to 0.35)% to 9.28 (1.76 to 16.80)% across Cancer Alliances after adjustment, again showing the presence of statistically significant variation for some regions. Stent insertion was received by 2156 (27.8%), with mean [95%CI] percentage-point difference from the population average between -10.54 (-12.88 to -8.20)% to 13.64 (9.22 to 18.06)% across Cancer Alliances after adjustment, showing wide and statistically significant variation from the population average. Half of 8853 patients ($n = 4468$) received no treatment with either surgery, systemic therapy or stent insertion.

CONCLUSION

Substantial regional variation in treatments received by CCA patients was observed in England. Such variation could be due to differences in case-mix, clinical practice or access to specialist expertise.

Key Words: Cholangiocarcinoma; Biliary tract cancer; Liver cancer; Treatment; Surgery; Systemic therapy; Chemotherapy; Stent; England

©The Author(s) 2023. Published by Baishideng Publishing Group Inc. All rights reserved.

Core Tip: Outcomes for cholangiocarcinoma (CCA) are extremely poor, with late presentation meaning curative surgery is not an option for many. Systemic therapies to prolong life are limited and stent insertion for disease management is complex. In a national cohort, treatments received (surgery, systemic therapy, stent insertion) by CCA patients across geographic areas were investigated. Half of patients did not receive any of the treatments considered. The proportion that received treatments significantly varied across England. These data provide novel evidence of low and varied treatment rates for CCA patients, warranting further investigation by healthcare providers to try to improve outcomes and reduce inequality.

Citation: Jose S, Zalin-Miller A, Knott C, Paley L, Tataru D, Morement H, Toledano MB, Khan SA. Cohort study to assess geographical variation in cholangiocarcinoma treatment in England. *World J Gastrointest Oncol* 2023; 15(12): 2077-2092

URL: <https://www.wjgnet.com/1948-5204/full/v15/i12/2077.htm>

DOI: <https://dx.doi.org/10.4251/wjgo.v15.i12.2077>

INTRODUCTION

Cholangiocarcinoma (CCA) is a malignancy arising from epithelial cells along the biliary tree within or external to the liver[1,2]. CCA are sub-classified into three main sub-types according to their anatomical site of origin: Intrahepatic CCA (iCCA), within the liver parenchyma, proximal to the second order bile ducts, perihilar, and distal CCA, often collectively referred to as extrahepatic CCA (eCCA)[3-5]. iCCA comprise the second most common form of primary liver cancer worldwide, after hepatocellular carcinoma[6]. The CCA sub-types exhibit some differences in their respective clinical presentations, risk factors, routes to diagnosis and clinical management, as well as exhibiting distinct epidemiological, clinical, molecular and genetic characteristics[3,7]. Of note, multiple epidemiological studies have reported rising incidence and mortality rates for CCA over the past few decades[8-10].

All CCA carries a high mortality as it typically presents at an advanced stage, usually too late for surgical resection or transplantation, the only potentially curative treatment options. Most cases are sporadic *i.e.*, they do not occur on the background of known risk factors and no screening strategy has been proven effective at reducing mortality[3]. Most CCA patients require systemic chemotherapy, with the current standard of care first line treatment being combination gemcitabine and cisplatin, or capecitabine in an adjuvant setting[3,4]. The other main treatment required by most patients is stenting to relieve biliary obstruction. In patients with high levels of jaundice, endoscopic or percutaneous stent placement is commonly used to reduce hyperbilirubinaemia prior to surgery in patients with resectable disease, or before

systemic therapy, or for palliation[3,4]. Although the overall prognosis of CCA is poor, with only a minority of patients surviving more than 3 years after diagnosis, these treatments have been shown to improve overall survival[3,6].

The management of CCA is complex, requiring a highly specialised multi-disciplinary approach and should be carried out at centres of expertise to achieve the best clinical outcomes[3]. Data on CCA patients' access to cancer-specific treatment is lacking. One recent United Kingdom study assessed variation in the surgical management of iCCA patients only, in selected hepatobiliary centres, finding variation in surgery volumes and in the proportions of patients treated with adjuvant chemotherapy[11]. A recent observational study from the European Reference Network for the Study of CCA investigated the clinical course of 2234 CCA patients from 26 referral Healthcare Centres from 11 European countries over a 10-year period (from 2010)[12]. The study found that CCA was frequently diagnosed at an advanced stage with almost 60% of patients presenting with locally advanced or metastatic disease. Furthermore, around 20% did not receive any specific cancer therapy, but best supportive care only. Although this was an important and large multi-centre study, data was collected from self-selected expert centres and the findings may not be representative of the whole population of individual participating countries.

Variation in access to cancer-specific treatment for CCA across England has not previously been reported. The aim of this study was to investigate if there is geographical variation across England of access to surgery, systemic therapy and stenting. Results are reported at the Cancer Alliance level, representing distinct geographic areas within which key health and social care stakeholders collaborate to plan and coordinate local cancer pathways.

MATERIALS AND METHODS

CCA patients were selected from the National Cancer Registration Dataset[13]. The following ICD-10 diagnosis codes were used to define CCA: C221, C240, C248, C249 of any morphology or C220, C222, C223, C224, C227, C229 with ICD-O2 histology code 8160. Patients were considered if resident in England at the time of diagnosis and were diagnosed between 2014 and 2017. This was the most recent diagnostic period at the time of the analysis with sufficient follow-up available to assess treatment initiation. Patients were followed to the earliest of death or 15 mo following recorded date of diagnosis. The first registered tumour per individual in this time period was used for the analysis and patient and tumour characteristics associated with this diagnosis are reported. Further inclusion criteria were recorded male or female gender, and age at diagnosis between 0 and 200 years. Individuals diagnosed with cancer on their death certificate only were excluded as such patients would not have been offered treatment.

Linked patient records from the Hospital Episode Statistics (HES) Admitted Patient Care (APC) dataset, Systemic Anti-Cancer Therapy dataset and National Radiotherapy Dataset[14-16] were used to determine the treatment received by each patient. Potentially curative surgery was defined based on a list of OPCS-4 procedure codes (Supplementary Table 1) dated between one month prior and 12 mo following the date of CCA diagnosis, irrespective of any other treatments received, as per the National Disease Registration Services' standard operating procedure[17]. Amongst individuals with no evidence of surgery as defined above, the presence of systemic therapy and/or stent insertion was assessed. Systemic therapy was defined as the delivery of any systemic anti-cancer therapy regimen initiated between the one month prior and 15 mo following diagnosis. A second list of OPCS-4 codes was used to define stent insertion (Supplementary Table 1), and these were similarly searched for in the interval two months prior to and up to 15 mo following diagnosis.

Geographic variation in treatment was analysed at the Cancer Alliance level according to boundaries defined in 2020. The Cancer Alliance for each tumour was assigned according to the main residence of the patient on the date of diagnosis. Other patient characteristics of interest, identified a priori as possible confounding variables of the relationship between geography and receipt of treatment were: Person-stated gender (male/female); age at diagnosis (0-44/45-54/55-64/65-74/75-84/85+ years); area income deprivation component of the index of multiple deprivation, 2019 (quintiles); year of diagnosis; tumour sub-type (iCCA/eCCA/other); tumour morphology (adenocarcinoma/other); Charlson comorbidity index (score 0/1/2/3+)[18]; underlying liver disease (yes/no) and route to diagnosis (urgent two-week wait general practitioner referral (TWW)/emergency presentation/other/unknown)[19]. To identify underlying liver disease, HES APC episodes from 5 years prior to 1 year after diagnosis were searched for diagnostic codes indicative of chronic hepatitis C or B, primary biliary cholangitis, autoimmune hepatitis, haemochromatosis, alcoholic liver disease, or non-alcoholic liver disease (NAFLD). NAFLD was defined as fatty (change of) liver, not elsewhere classified, or by the presence of cirrhosis combined with obesity or diabetes without the presence of any other underlying liver disease[20].

Linear probability models were performed for each of the following three binary outcomes: Potentially curative surgery regardless of other treatments received (yes/no); systemic therapy where no surgery was received (yes/no); stent insertion where no surgery was received (yes/no). For each outcome, bivariate models were conducted to assess the association with each covariate of interest without adjustment for other patient and tumour factors (referred to as 'unadjusted'). An adjusted model was then fit for each outcome that included all covariates, defined a priori as being of interest, concurrently. No interactions between covariates were assessed. Covariates were Cancer Alliance, age at diagnosis, gender, area income deprivation quintile, Charlson comorbidity score, prior liver disease, tumour sub-type, tumour morphology, route to diagnosis.

Weighted effect coding was applied such that estimates generated by each linear probability model are interpretable as percentage-point deviations from the sample mean[21]. Results from the linear probability models are presented as funnel plots with significance thresholds denoting two and three SD from the sample mean, being approximately equivalent to 95.0% and 99.7% confidence intervals, respectively. A statistical significance threshold of 5% was used.

A sensitivity analysis was undertaken that additionally adjusted for stage at diagnosis in a subgroup of the cohort who had a known stage at diagnosis. This was due to the high level of missing data for this variable (45.5%). The adjusted

models for each outcome were repeated in this subgroup to determine how reducing the cohort to patients with known stage impacted model estimates, before stage was additionally adjusted for in this group.

RESULTS

There were 8872 people diagnosed with CCA between 2014 and 2017. No exclusions were made due to age or gender data quality checks. After excluding 19 (0.2%) individuals diagnosed on death certificate only, a final cohort of 8853 individuals was available for analysis. Of these, 20.9% were under 65 years old and 50.9% were women (Table 1). The majority were diagnosed with an iCCA (77.6%). Comorbidities as measured by the Charlson comorbidity index were present in 29.7% of individuals and 9.1% were classified as having underlying liver disease. The largest proportion of diagnoses were situated in the West Midlands Cancer Alliance (11.4%), with the smallest in North Central London Cancer Alliance (1.6%).

Of the 8853 patients, 12.4% ($n = 1102$) received potentially curative surgery. In the 7751 patients with no evidence of surgery, 19.9% ($n = 1542$) received systemic therapy, 27.8% ($n = 2156$) received a stent insertion, and 42.4% ($n = 3283$) received either modality alone or in combination. Of note, half (50.5%) of the initial cohort received none of the three treatments considered (Table 1).

Geographic variation in potentially curative surgery

Variation in the unadjusted percentage of patients who received potentially curative surgery was observed across the Cancer Alliances, ranging from 8.8% to 16.2% ($P < 0.001$). In a linear probability model that included only Cancer Alliance, the percentage treated with surgery was more than two SD higher than the sample mean in one Cancer Alliance ($P < 0.05$), but more than two SD lower than average for two Cancer Alliances [Table 2A (unadjusted) and Figure 1A]. This finding remained present after adjustment for all patient and tumour characteristics being considered [Table 2A (adjusted) and Figure 1B].

Geographic variation in systemic therapy

Amongst those not treated with surgery, variation in the crude percentage of patients treated with systemic therapy was observed. Across Cancer Alliances the percentage in receipt of systemic therapy ranged from 12.4% to 29.4%. In a linear probability model that included Cancer Alliance as the only independent variable, the percentage treated with systemic therapy was more than two SD above the sample mean for two Cancer Alliances, and below the mean for two Cancer Alliances [Table 2B (unadjusted) and Figure 2A, $P < 0.001$]. Adjustment for patient and tumour characteristics attenuated this difference for two Cancer Alliances such that only one was observed to have a significantly lower percentage of patients receiving systemic therapy than the sample mean [Table 2B (adjusted) and Figure 2B].

Geographic variation in stent insertion

There was wide variation in the percentage of individuals who received a stent insertion amongst those not treated with potentially curative surgery. The unadjusted percentage across all Cancer Alliances ranged from 29.7% to 55.0% and was significantly higher than the sample mean for six Cancer Alliances, and significantly lower than the sample mean for five Cancer Alliances [Table 2C (unadjusted) and Figure 3A]. Adjustment for patient demographics, comorbidities and tumour characteristics did not alter this finding [Table 2C (adjusted) and Figure 3B].

Treatment associations with patient and tumour characteristics

The lowest percentage treated with potentially curative surgery was observed in the 85+ age group (Table 2A unadjusted). Age remained associated with the likelihood of surgery in a model that included all other cofactors of interest, with the highest proportion amongst those aged 0-44 [adjusted percentage point difference (pp): 20.69, 95% confidence interval (CI): 13.91 to 27.47]. Likewise, in those who did not receive surgery, older age at diagnosis was associated with a lower likelihood of systemic therapy in both unadjusted and adjusted analyses (adjusted pp: -17.16, 95%CI: -18.08 to -16.23 for age 85+ years). However, the relationship between age and likelihood of stent insertion was not similarly linear (Table 2C adjusted).

Although there was a difference between male and female gender in the crude percentage that received surgery (Table 2A unadjusted), this was attenuated after adjustment (adjusted pp: -0.49, 95%CI: -1.13 to 0.16 for women). Amongst those who did not receive surgery, women were less likely than men to receive a stent insertion (adjusted pp: -1.18, 95%CI: -2.13 to -0.24), but more likely to receive systemic therapy (adjusted pp: 1.21, 95%CI: 0.43 to 2.00).

High area income deprivation was associated with a lower probability of both surgery (adjusted pp: -2.77, 95%CI: -4.10 to -1.43 for most deprived areas) and systemic therapy in the absence of surgery (adjusted pp: -2.91, 95%CI: -4.59 to -1.22) but was not strongly associated with the probability of stent insertion in those who did not receive surgery (adjusted pp: -0.34, 95%CI: -2.33 to 1.65).

Compared to the population average, iCCA patients had a lower probability of treatment with surgery (adjusted pp: -2.65, 95%CI: -3.09 to -2.22), systemic therapy amongst those without surgery (adjusted pp: -0.47, 95%CI: -0.92 to -0.02) and stent insertion amongst those without surgery (adjusted pp: -3.89, 95%CI: -4.47 to -3.31) in adjusted models.

Those diagnosed *via* an emergency route had a lower-than-average probability of surgery (adjusted pp: -3.75, 95%CI: -4.42 to -3.08) and systemic therapy in those without surgery (adjusted pp: -5.31, 95%CI: -6.11 to -4.51), but a higher probability of stent insertion without surgery (adjusted pp: =2.10, 95%CI: 1.14 to 3.07) than the population average. Whilst a TWW referral route was not strongly associated with the probability of surgery (adjusted pp: -0.58, 95%CI: -2.08

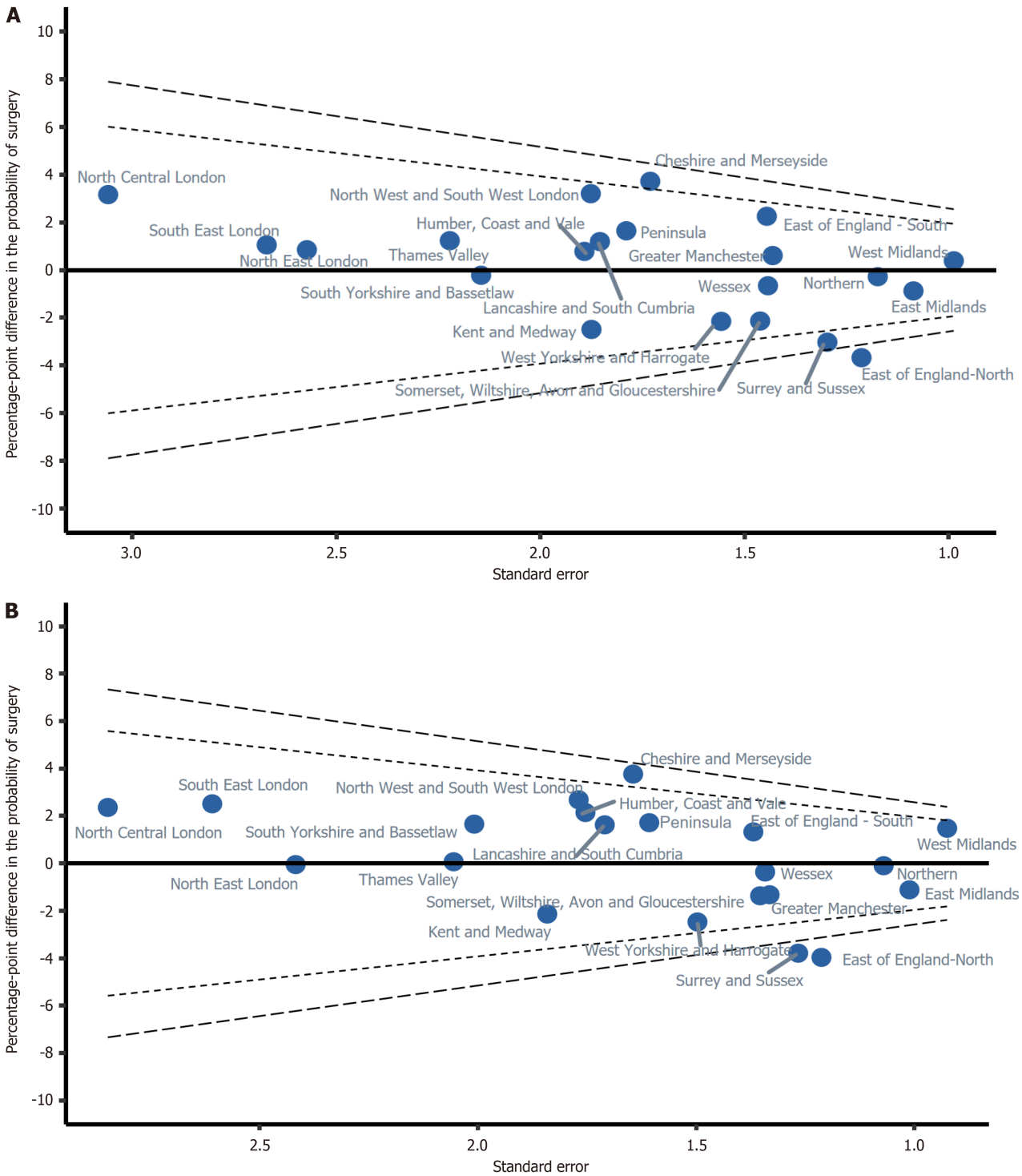


Figure 1 Percentage of cholangiocarcinoma patients treated with potentially curative surgery in each Cancer Alliance in England, 2014-2017. A: Unadjusted; B: Adjusted. Adjustment for: age, gender, income deprivation quintile, Charlson comorbidity index, underlying liver disease at diagnosis, diagnosis year, tumour morphology, tumour sub-type, and routes to diagnosis. Inner dashed line = two standard deviations difference from average. Outer dashed line = three standard deviations difference from average.

to 0.91), a TWW referral route was associated with a higher probability of systemic therapy (adjusted pp: 8.57, 95%CI: 6.55 to 10.59) and stent insertion (adjusted pp: 2.29, 95%CI: 0.06 to 4.51) among patients that did not receive surgery.

Patients with the highest categorised burden of comorbidities (3+) had a lower-than-average probability of surgery (adjusted pp: -3.19, 95%CI: -4.79 to -1.60), systemic therapy (adjusted pp: -7.06, 95%CI: -8.93 to -5.20) and stent insertion (adjusted pp: -5.53, 95%CI: -8.33 to -2.74). Conversely, of patients with evidence of liver disease specifically, there was no association with systemic therapy (adjusted pp: -0.43, 95%CI: -3.55 to 2.69), a higher-than-average probability of treatment with surgery (adjusted pp: 3.47, 95%CI: 0.96 to 5.97) and lower than average probability of stent insertion without surgery (adjusted pp: -4.19, 95%CI: -7.29 to -1.08).

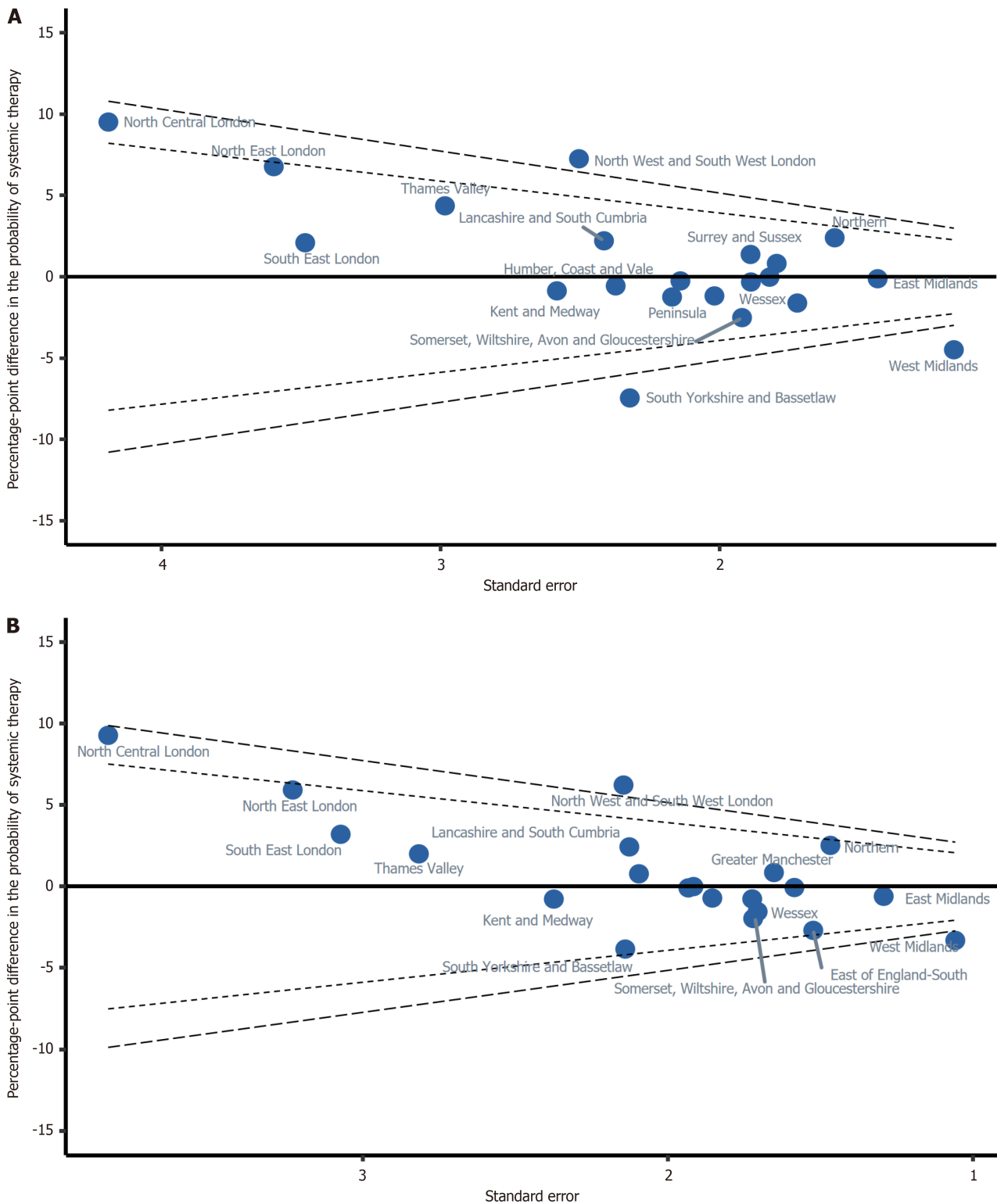


Figure 2 Percentage of cholangiocarcinoma patients treated with systemic therapy amongst those who did not receive surgery in each Cancer Alliance in England, 2014-2017. A: Unadjusted; B: Adjusted. Adjustment for: age, gender, income deprivation quintile, Charlson comorbidity index, underlying liver disease at diagnosis, diagnosis year, tumour morphology, tumour sub-type, and routes to diagnosis. Inner dashed line = two standard deviations difference from average. Outer dashed line = three standard deviations difference from average.

Sensitivity analysis

Of the 8853 CCA patients in the study cohort, 4832 (54.5%) had a known stage at diagnosis and were included in the sensitivity analysis for potentially curative surgery. Of these, 3925 (81.2%) did not receive curative surgery and were analysed for the probability of treatment with systemic therapy or stent insertion.

Table 1 Description of cholangiocarcinoma patients diagnosed between 2014 and 2017 in England, and subgroup who did not receive surgery up to 12 mo after diagnosis

Characteristics	Total	Did not receive surgery
Total patients (n, %)	8853 (100.0)	7751 (100.0)
Age at diagnosis (yr)		
0-44	180 (2.0)	117 (1.5)
45-54	442 (5.0)	320 (4.1)
55-64	1231 (13.9)	962 (12.4)
65-74	2407 (27.2)	1963 (25.3)
75-84	2814 (31.8)	2615 (33.7)
> 84	1779 (20.1)	1774 (22.9)
Gender		
Male	4343 (49.1)	3721 (48.0)
Female	4510 (50.9)	4030 (52.0)
Year of diagnosis		
2014	2055 (23.2)	1802 (23.2)
2015	2213 (25.0)	1951 (25.2)
2016	2259 (25.5)	1983 (25.6)
2017	2326 (26.3)	2015 (26.0)
Route to diagnosis		
Emergency presentation	4276 (48.3)	3975 (51.3)
TWW referral	1490 (16.8)	1306 (16.8)
Other GP referral	1844 (20.8)	1500 (19.4)
Other	979 (11.1)	729 (9.4)
Unknown	264 (3.0)	241 (3.1)
Stage at diagnosis		
1	310 (3.5)	203 (2.6)
2	686 (7.7)	283 (3.7)
3	330 (3.7)	26 (2.9)
4	3506 (39.6)	3213 (41.5)
Missing	4021 (45.4)	3826 (49.4)
Tumour sub-type		
CCA Other	391 (4.4)	378 (4.9)
eCCA	1595 (18.0)	1200 (15.5)
iCCA	6867 (77.6)	6173 (79.6)
Tumour morphology		
Adenomas and adenocarcinomas	8570 (96.8)	7484 (96.6)
Other	283 (3.2)	267 (3.4)
English Index of Multiple Deprivation, income component		
Quintile 1 (least deprived)	1715 (19.4)	1466 (18.9)
Quintile 2	1863 (21.0)	1609 (20.8)
Quintile 3	1797 (20.3)	1589 (20.5)
Quintile 4	1806 (20.4)	1590 (20.5)

Quintile 5 (most deprived)	1672 (18.9)	1497 (19.3)
Charlson comorbidity index		
0	6220 (70.3)	5340 (68.9)
1	1140 (12.9)	1025 (13.2)
2	678 (7.7)	623 (8.0)
3+	815 (9.2)	763 (9.8)
Underlying liver disease		
No	8044 (90.9)	7101 (91.6)
Yes	809 (9.1)	650 (8.4)
Cancer Alliance at diagnosis		
Cheshire and Merseyside	427 (4.8)	358 (4.6)
East Midlands	795 (9.0)	703 (9.1)
East of England-North	524 (5.9)	478 (6.2)
East of England-South	558 (6.3)	476 (6.1)
Greater Manchester	521 (5.9)	453 (5.8)
Humber, Coast and Vale	310 (3.5)	269 (3.5)
Kent and Medway	251 (2.8)	226 (2.9)
Lancashire and South Cumbria	330 (3.7)	285 (3.7)
North Central London	141 (1.6)	119 (1.5)
North East London	173 (2.0)	150 (1.9)
North West and South West London	358 (4.0)	302 (3.9)
Northern	715 (8.1)	628 (8.1)
Peninsula	362 (4.1)	311 (4.0)
Somerset, Wiltshire, Avon and Gloucestershire	417 (4.7)	374 (4.8)
South East London	163 (1.8)	141 (1.8)
South Yorkshire and Bassetlaw	229 (2.6)	201 (2.6)
Surrey and Sussex	488 (5.5)	442 (5.7)
Thames Valley	234 (2.6)	202 (2.6)
Wessex	475 (5.4)	419 (5.4)
West Midlands	1013 (11.4)	883 (11.4)
West Yorkshire and Harrogate	369 (4.2)	331 (4.3)
Treatment received		
Surgery only	507 (5.7)	0 (0.0)
Surgery + systemic therapy	367 (4.1)	0 (0.0)
Surgery + stent insertion	118 (1.3)	0 (0.0)
Surgery + systemic therapy + stent insertion	110 (1.2)	0 (0.0)
Systemic therapy only	1127 (12.7)	1127 (14.5)
Stent insertion only	1741 (19.7)	1741 (22.5)
Systemic therapy + stent insertion	415 (4.7)	415 (5.4)
None of surgery, systemic therapy or stent insertion	4468 (50.5)	4468 (57.6)

iCCA: Intrahepatic cholangiocarcinoma; eCCA: Extrahepatic cholangiocarcinoma; GP: General practitioner; TWW: Two week wait.

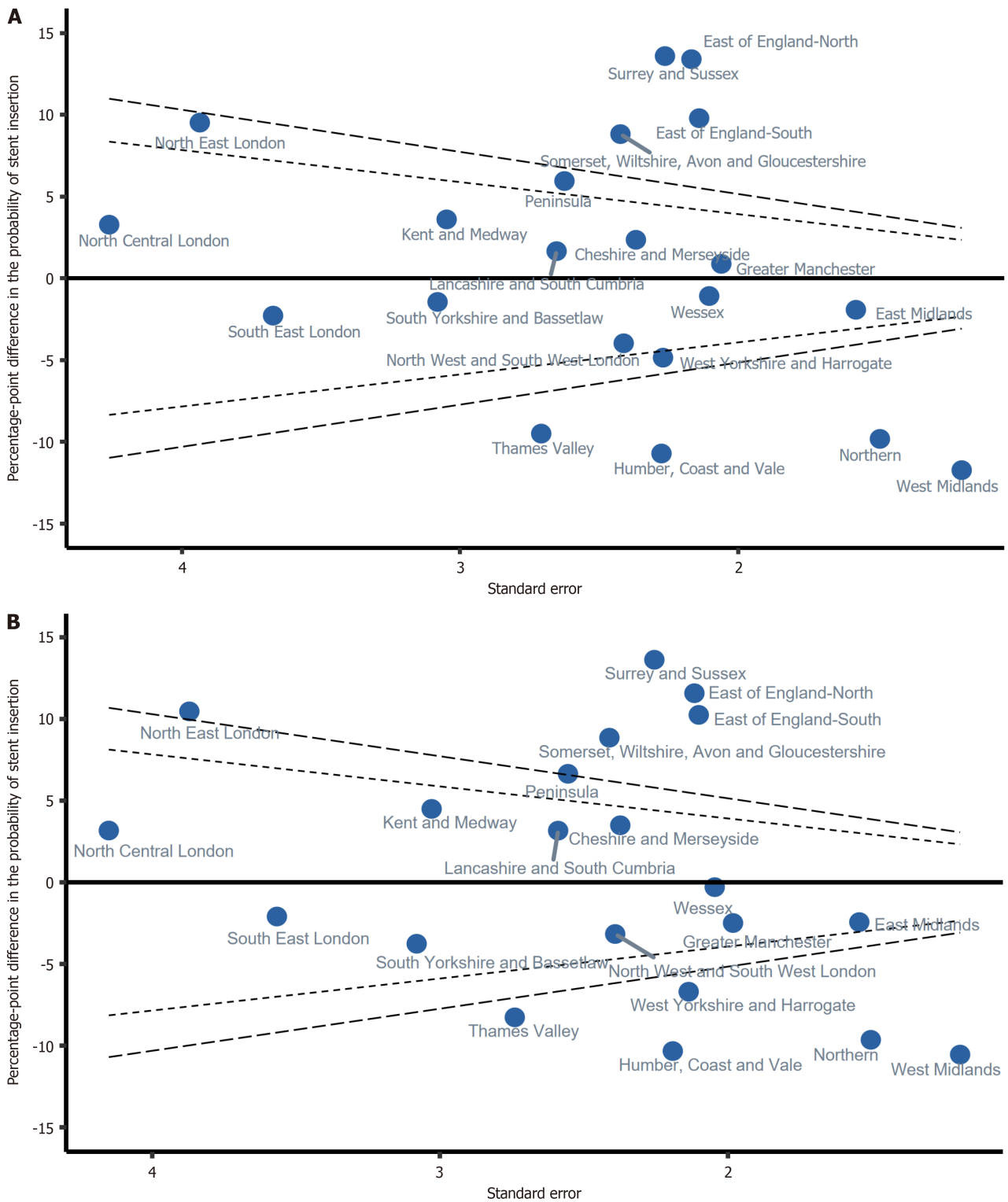


Figure 3 Percentage of cholangiocarcinoma patients treated with stent insertion amongst those who did not receive surgery in each Cancer Alliance in England, 2014-2017. A: Unadjusted; B: Adjusted. Adjustment for: age, gender, income deprivation quintile, Charlson comorbidity index, underlying liver disease at diagnosis, diagnosis year, tumour morphology, tumour sub-type, and routes to diagnosis. Inner dashed line = two standard deviations difference from average. Outer dashed line = three standard deviations difference from average.

The proportion of people staged varied by Cancer Alliance, from 36.7% to 74.7% ($P < 0.001$). Those with unknown stage at diagnosis were more likely to be older, diagnosed in an earlier year, have a high comorbidity score and an ‘other’ tumour sub-type or morphology (all $P < 0.001$, results not shown). Repeating the adjusted model of the main analysis in these subgroups identified different Cancer Alliances as having treatment probabilities that varied significantly (>2 SD) from the population average (Supplementary Table 2). This suggests that the subgroup of individuals with known stage at diagnosis was not generalisable to the whole cohort of individuals with CCA.

Table 2 Estimated percentage of cholangiocarcinoma patients in England 2014-2017 that received

	A: Potentially curative surgery				B: Systemic therapy in those who did not receive surgery				C: Stent insertion in those who did not receive surgery			
	Unadjusted		Adjusted		Unadjusted		Adjusted		Unadjusted		Adjusted	
	Estimate (95%CI)	Estimate (95%CI)	Estimate (95%CI)	Estimate (95%CI)	Estimate (95%CI)	Estimate (95%CI)	Estimate (95%CI)	Estimate (95%CI)	Estimate (95%CI)	Estimate (95%CI)	Estimate (95%CI)	Estimate (95%CI)
Population average (intercept)	12.45	(11.76, 13.14)	12.45	(11.81, 13.09)	19.89	(19.01, 20.78)	19.89	(19.1, 20.69)	27.82	(26.85, 28.78)	27.82	(26.85, 28.78)
Cheshire and Merseyside	3.71	(0.32, 7.10)	3.77	(0.54, 6.99)	-1.18	(-5.13, 2.78)	-0.09	(-3.88, 3.70)	2.35	(-2.29, 6.99)	3.50	(-1.15, 8.16)
East Midlands	-0.88	(-3.00, 1.25)	-1.11	(-3.10, 0.87)	-0.12	(-2.93, 2.69)	-0.60	(-3.14, 1.93)	-1.93	(-5.02, 1.16)	-2.43	(-5.45, 0.60)
East of England - North	-3.67	(-6.05, -1.29)	-3.96	(-6.34, -1.59)	0.82	(-2.70, 4.34)	-0.06	(-3.17, 3.04)	13.40	(9.15, 17.65)	11.59	(7.44, 15.74)
East of England - South	2.25	(-0.59, 5.08)	1.33	(-1.36, 4.01)	-1.62	(-4.99, 1.76)	-2.70	(-5.68, 0.29)	9.79	(5.59, 13.98)	10.26	(6.14, 14.38)
Greater Manchester	0.60	(-2.20, 3.41)	-1.32	(-3.93, 1.29)	-0.03	(-3.59, 3.54)	0.86	(-2.38, 4.09)	0.88	(-3.16, 4.92)	-2.48	(-6.37, 1.40)
Humber, Coast and Vale	0.78	(-2.93, 4.49)	2.14	(-1.29, 5.58)	-0.56	(-5.21, 4.09)	0.78	(-3.33, 4.88)	-10.72	(-15.18, -6.25)	-10.32	(-14.62, -6.03)
Kent and Medway	-2.49	(-6.16, 1.19)	-2.14	(-5.75, 1.47)	-0.87	(-5.93, 4.19)	-0.77	(-5.43, 3.88)	3.60	(-2.38, 9.58)	4.51	(-1.43, 10.44)
Lancashire and South Cumbria	1.19	(-2.45, 4.82)	1.63	(-1.72, 4.98)	2.21	(-2.52, 6.94)	2.43	(-1.74, 6.60)	1.66	(-3.54, 6.86)	3.18	(-1.90, 8.25)
North Central London	3.16	(-2.84, 9.15)	2.36	(-3.22, 7.94)	9.52	(1.30, 17.73)	9.28	(1.76, 16.80)	3.28	(-5.08, 11.63)	3.18	(-4.95, 11.32)
North East London	0.85	(-4.19, 5.89)	-0.05	(-4.79, 4.69)	6.77	(-0.28, 13.82)	5.93	(-0.41, 12.26)	9.52	(1.80, 17.23)	10.48	(2.89, 18.06)
North West and South West London	3.19	(-0.48, 6.87)	2.68	(-0.79, 6.15)	7.26	(2.35, 12.17)	6.23	(2.02, 10.43)	-3.97	(-8.70, 0.75)	-3.16	(-7.84, 1.53)
Northern	-0.28	(-2.58, 2.02)	-0.10	(-2.20, 2.00)	2.40	(-0.71, 5.51)	2.52	(-0.35, 5.40)	-9.82	(-12.74, -6.90)	-9.63	(-12.58, -6.69)
Peninsula	1.64	(-1.87, 5.15)	1.72	(-1.43, 4.87)	-1.24	(-5.50, 3.01)	-0.01	(-3.76, 3.75)	5.95	(0.80, 11.09)	6.65	(1.64, 11.66)
Somerset, Wiltshire, Avon and Gloucestershire	-2.14	(-5.00, 0.73)	-1.37	(-4.02, 1.29)	-2.51	(-6.28, 1.25)	-1.97	(-5.34, 1.41)	8.82	(4.07, 13.57)	8.87	(4.14, 13.59)
South East London	1.05	(-4.19, 6.28)	2.51	(-2.6, 7.62)	2.09	(-4.74, 8.92)	3.20	(-2.82, 9.23)	-2.28	(-9.48, 4.91)	-2.08	(-9.08, 4.91)
South Yorkshire and Bassetlaw	-0.22	(-4.43, 3.98)	1.66	(-2.28, 5.59)	-7.46	(-12.01, -2.91)	-3.84	(-8.04, 0.35)	-1.45	(-7.49, 4.59)	-3.75	(-9.79, 2.29)
Surrey and Sussex	-3.02	(-5.56, -0.48)	-3.79	(-6.27, -1.30)	1.37	(-2.33, 5.07)	-0.76	(-4.14, 2.61)	13.59	(9.15, 18.02)	13.64	(9.22, 18.06)
Thames Valley	11.23	(-3.13, 5.58)	0.07	(-3.96, 4.10)	4.36	(-1.49, 10.21)	2.00	(-3.52, 7.52)	-9.50	(-14.81, -4.19)	-8.26	(-13.63, -2.89)
Wessex	-0.66	(-3.49, 2.17)	-0.36	(-2.99, 2.27)	-0.32	(-4.02, 3.38)	-1.55	(-4.89, 1.80)	-1.09	(-5.21, 3.04)	-0.29	(-4.30, 3.72)
West Midlands	0.39	(-1.55, 2.32)	1.48	(-0.33, 3.29)	-4.49	(-6.77, -2.22)	-3.31	(-5.39, -1.24)	-11.73	(-14.08, -9.39)	-10.54	(-12.88, -8.20)
West Yorkshire and Harrogate	-2.15	(-5.20, 0.90)	-2.47	(-5.40, 0.46)	-0.26	(-4.45, 3.94)	-0.71	(-4.35, 2.92)	-4.86	(-9.31, -0.40)	-6.69	(-10.88, -2.50)
Age 0-44	22.14	(15.21, 29.08)	20.69	(13.91, 27.47)	37.29	(28.28, 46.31)	36.41	(27.47, 45.35)	-1.37	(-9.44, 6.70)	-1.59	(-9.41, 6.24)

Age 45-54	15.07	(11.03, 19.11)	13.24	(9.38, 17.11)	30.34	(24.98, 35.70)	28.96	(23.77, 34.15)	-4.91	(-9.47, -0.34)	-5.80	(-10.26, -1.34)
Age 55-64	9.38	(7.31, 11.46)	7.59	(5.58, 9.61)	23.18	(20.34, 26.03)	21.61	(18.82, 24.40)	-0.07	(-2.73, 2.59)	-0.39	(-3.00, 2.21)
Age 65-74	6.11	(4.86, 7.36)	4.84	(3.64, 6.04)	10.60	(8.94, 12.26)	9.59	(7.97, 11.21)	1.47	(-0.27, 3.21)	1.75	(0.06, 3.44)
Age 75-84	-5.41	(-6.29, -4.53)	-4.83	(-5.69, -3.96)	-8.88	(-9.95, -7.81)	-8.68	(-9.73, -7.63)	1.49	(0.07, 2.90)	1.53	(0.16, 2.90)
Age 85+	-12.21	(-12.9, -11.52)	-9.55	(-10.28, -8.83)	-19.18	(-20.05, -18.30)	-17.16	(-18.08, -16.23)	-2.81	(-4.6, -1.01)	-2.83	(-4.64, -1.02)
Female	-1.81	(-2.49, -1.13)	-0.49	(-1.13, 0.16)	-0.30	(-1.16, 0.56)	1.21	(0.43, 2.00)	-1.09	(-2.05, -0.12)	-1.18	(-2.13, -0.24)
Male	1.88	(1.17, 2.58)	0.51	(-0.16, 1.18)	0.33	(-0.60, 1.26)	-1.32	(-2.16, -0.47)	1.18	(0.13, 2.22)	1.28	(0.25, 2.31)
Income deprivation quintile 1 (least deprived)	2.12	(0.63, 3.61)	2.04	(0.64, 3.43)	3.15	(1.22, 5.08)	3.17	(1.41, 4.92)	0.98	(-1.11, 3.08)	0.47	(-1.59, 2.52)
Income deprivation quintile 2	1.23	(-0.15, 2.61)	1.17	(-0.11, 2.45)	1.44	(-0.34, 3.22)	1.88	(0.29, 3.47)	1.07	(-0.91, 3.04)	0.30	(-1.60, 2.20)
Income deprivation quintile 3	-0.90	(-2.24, 0.43)	-0.21	(-1.47, 1.05)	-0.21	(-1.96, 1.54)	0.24	(-1.32, 1.79)	1.14	(-0.85, 3.13)	0.66	(-1.26, 2.59)
Income deprivation quintile 4	-0.50	(-1.84, 0.85)	-0.38	(-1.63, 0.88)	-2.53	(-4.23, -0.84)	-2.32	(-3.85, -0.79)	-0.98	(-2.93, 0.98)	-1.08	(-2.98, 0.82)
Income deprivation quintile 5 (most deprived)	-2.03	(-3.38, -0.68)	-2.77	(-4.10, -1.43)	-1.70	(-3.48, 0.07)	-2.91	(-4.59, -1.22)	-2.28	(-4.28, -0.27)	-0.34	(-2.33, 1.65)
Diagnosis year 2014	-0.16	(-1.41, 1.08)	0.49	(-0.67, 1.65)	-1.46	(-3.05, 0.12)	0.08	(-1.35, 1.50)	-1.85	(-3.64, -0.06)	-1.81	(-3.53, -0.09)
Diagnosis year 2015	-0.64	(-1.81, 0.54)	-0.48	(-1.57, 0.61)	-0.77	(-2.29, 0.75)	-0.56	(-1.93, 0.81)	-0.55	(-2.27, 1.16)	-0.29	(-1.95, 1.36)
Diagnosis year 2016	-0.24	(-1.42, 0.93)	-0.30	(-1.41, 0.80)	0.69	(-0.85, 2.22)	0.08	(-1.29, 1.46)	0.82	(-0.90, 2.53)	1.04	(-0.62, 2.69)
Diagnosis year 2017	1.00	(-0.19, 2.20)	0.32	(-0.79, 1.43)	1.41	(-0.14, 2.95)	0.39	(-0.99, 1.77)	1.42	(-0.31, 3.14)	0.88	(-0.77, 2.53)
Adenomas and adenocarcinomas	0.23	(0.14, 0.32)	0.24	(0.14, 0.35)	0.49	(0.38, 0.59)	0.23	(0.10, 0.36)	-0.04	(-0.23, 0.15)	0.40	(0.18, 0.61)
Other morphology	-6.82	(-9.54, -4.10)	-7.35	(-10.55, -4.16)	-13.58	(-16.57, -10.59)	-6.38	(-10.05, -2.72)	1.08	(-4.31, 6.48)	-11.15	(-17.12, -5.18)
eCCA sub-type	12.40	(10.56, 14.23)	12.34	(10.58, 14.10)	1.64	(-0.50, 3.78)	2.89	(0.92, 4.87)	19.07	(16.51, 21.62)	19.28	(16.7, 21.86)
iCCA sub-type	-2.35	(-2.78, -1.93)	-2.65	(-3.09, -2.22)	0.10	(-0.35, 0.55)	-0.47	(-0.92, -0.02)	-3.66	(-4.20, -3.13)	-3.89	(-4.47, -3.31)
Other sub-type	-9.17	(-11.00, -7.33)	-3.70	(-6.01, -1.38)	-6.74	(-10.12, -3.36)	-1.52	(-4.98, 1.94)	-0.62	(-5.01, 3.78)	2.37	(-2.50, 7.24)
Emergency presentation diagnosis route	-5.45	(-6.14, -4.76)	-3.75	(-4.42, -3.08)	-7.95	(-8.80, -7.09)	-5.31	(-6.11, -4.51)	1.52	(0.55, 2.49)	2.10	(1.14, 3.07)
GP referral diagnosis route	6.16	(4.65, 7.68)	4.61	(3.17, 6.05)	6.10	(4.15, 8.04)	4.18	(2.39, 5.97)	-4.60	(-6.54, -2.65)	-5.28	(-7.16, -3.40)
IP and OP diagnosis route	13.04	(10.54, 15.55)	9.44	(7.09, 11.79)	12.54	(9.35, 15.73)	7.65	(4.69, 10.61)	-2.76	(-5.77, 0.25)	-2.75	(-5.69, 0.18)
TWW referral diagnosis route	-0.14	(-1.66, 1.37)	-0.58	(-2.08, 0.91)	10.96	(8.75, 13.18)	8.57	(6.55, 10.59)	2.92	(0.65, 5.19)	2.29	(0.06, 4.51)
Unknown diagnosis route	-2.99	(-7.06, 1.07)	-3.21	(-6.51, 0.08)	-5.61	(-10.73, -0.49)	-8.05	(-11.96, -4.15)	-5.21	(-11.31, 0.89)	-5.94	(-11.07, -0.81)

Charlson score - 0	1.69	(1.28, 2.10)	0.69	(0.30, 1.09)	3.19	(2.65, 3.73)	1.02	(0.51, 1.53)	1.52	(0.86, 2.18)	1.38	(0.73, 2.04)
Charlson score - 1	-2.31	(-3.98, -0.64)	-0.28	(-1.85, 1.29)	-3.40	(-5.56, -1.25)	0.42	(-1.52, 2.37)	-1.73	(-4.26, 0.80)	-2.00	(-4.45, 0.45)
Charlson score - 2	-4.32	(-6.35, -2.29)	-2.06	(-3.96, -0.17)	-6.06	(-8.71, -3.40)	-0.81	(-3.25, 1.63)	-1.97	(-5.30, 1.35)	-1.77	(-4.94, 1.40)
Charlson score - 3+	-6.07	(-7.74, -4.39)	-3.19	(-4.79, -1.60)	-12.84	(-14.71, -10.97)	-7.06	(-8.93, -5.20)	-6.73	(-9.52, -3.93)	-5.53	(-8.33, -2.74)
Liver disease-no	-0.73	(-0.99, -0.47)	-0.35	(-0.60, -0.10)	-0.51	(-0.80, -0.21)	0.04	(-0.25, 0.32)	0.46	(0.17, 0.75)	0.38	(0.10, 0.67)
Liver disease-yes	7.23	(4.65, 9.82)	3.47	(0.96, 5.97)	5.53	(2.33, 8.73)	-0.43	(-3.55, 2.69)	-4.99	(-8.11, -1.86)	-4.19	(-7.29, -1.08)

Apart from the intercept, estimates represent the percentage-point difference from the weighted cohort average probability of each route. CI: Confidence interval; iCCA: Intrahepatic cholangiocarcinoma; eCCA: Extrahepatic cholangiocarcinoma; GP: General Practitioner; IP: Inpatient; OP: Outpatient; TWW: Two week wait.

Adding adjustment for stage at diagnosis did not appear to explain much of the variation in the probability of surgery observed between Cancer Alliances. (Supplementary Table 2, model A). One Cancer Alliance no longer had a probability of potentially curative surgery that was >2 SD higher than average, but two additional Cancer Alliances were identified as having higher probabilities of surgery. Amongst patients who were not treated with surgery but had a known stage at diagnosis, adjustment for stage identified one additional Cancer Alliance that had a lower-than-average probability of systemic therapy, again indicating that adjustment for stage did not explain variation observed in the main analysis (Supplementary Table 2, model B). One less Cancer Alliance was observed to have a lower-than-average probability of stent insertion after adjusting for stage at diagnosis, leaving three Cancer Alliances with a significantly lower probability of stent insertion than average (Supplementary Table 2, model C).

DISCUSSION

After adjustment for patient and tumour factors, there was significant variation amongst English Cancer Alliances in CCA patients receiving cancer-specific treatments, including potentially curative surgery, systemic therapy without curative surgery or stent insertion without curative surgery. To our knowledge, this is the first study to look at potential variation in CCA treatment at a national level. There was evidence of significant variation amongst Cancer Alliances in the percentage receiving surgery, or systemic therapy in the absence of surgery. Most variation however was observed in the percentage receiving stent insertion in the absence of surgery, suggesting there may be gaps in expertise, access and/or clinical expertise for this treatment modality. In so far as we were able to adjust for differences in patient populations between Cancer Alliances, this adjustment did not reduce the level of variation observed. However, not every CCA patient will be clinically eligible or in need of stent insertion and our inability to account for clinical status with the available data means the observed variation might still be explainable by differences in clinical case-mix and not necessarily evidence of varied or poor practice.

Whilst we have analysed treatment modalities separately, there is a possibility that the propensity toward each treatment within an area is linked, due to local expertise, protocols or capacity. An area with lower rates of surgery may have correspondingly higher rates of systemic therapy, for example. This did not often appear to be borne out in the data, with no such correspondence between Cancer Alliances that significantly varied from average in the proportion who received systemic therapy compared to either stent insertion or surgery. Two Cancer Alliances that showed lower than

average proportions receiving surgery showed higher than average proportions receiving stent insertion in the absence of surgery.

In terms of patient factors that we were able to adjust for, higher income deprivation was associated with a lower likelihood of receiving surgery or systemic therapy, independently of geography. There is already evidence that socioeconomic factors play a powerful role in determining the health of individuals[22,23]. As regards cancer, the importance of socioeconomic factors has been demonstrated in association with screening, incidence, stage at diagnosis, and survival, especially in private health care settings[24,25]. However, relatively little has been reported on how socioeconomic factors affect access to cancer system therapies, especially in publicly funded health systems such as the United Kingdom National Health Service (NHS), where cancer care at the point of service is free of charge[26,27]. A study conducted in Canada's Public payer Universal healthcare system examined the association between material deprivation and receipt of cancer care among patients with advanced gastrointestinal cancer. It found that patients from the most deprived communities were significantly less likely to see an oncology specialist after a diagnosis and significantly less likely to receive radiation and/or chemotherapy compared to those living in the least materially deprived communities [28]. To our knowledge, this is the first study to report a similar theme in patients with CCA.

Increasing co-morbidities and emergency presentation were both associated with a lower probability of surgery, in keeping with the fact that higher surgical risk may preclude treatment for the former group and likely advanced CCA stage at presentation may preclude treatment for the latter.

That half of CCA patients in England received none of the main treatments for CCA is of interest. To our knowledge, regarding CCA, no previous study of national data has studied or reported this before. The Surveillance, Epidemiology and End Results (SEER) cancer registry, representing around 28% of the population of the United States, recently showed that approximately 50% of eCCA patients and 40% of iCCA patients did not receive surgery or adjuvant therapy over a comparable calendar period[29]. This indicates a higher proportion of CCA patients receive surgical treatment in the United States than our data showed for England. However, differences in the treatment end-points defined, differences between the healthcare systems and CCA populations of the United States and England, and the select coverage of the SEER study make these findings difficult to directly compare and interpret. In the European Reference Network for the Study of CCA study, 20% of patients did not receive any specific cancer therapy, but best supportive care only[12]. Data for their study was collected from self-selected expert centres in those hospitals who chose to send in their data. These centres are large expert referral centres and the study data is not therefore reflective of "real world" overall public healthcare. Our study involved the entire NHS (all public, government-funded hospitals), so all patients from all NHS hospitals were included. The high rates of short-term mortality observed in this group may well explain the observed lack of treatment, as their case may have been too advanced for any active treatment to be considered beneficial. Further studies are warranted to explore if this high proportion of patients had adequate clinical reasons to not receive any of the main treatments for CCA. Nonetheless, this highlights the importance of increasing the therapeutic options available to those diagnosed with CCA to prolong survival, either through earlier diagnosis to preserve current treatment options or through increased research into more effective systemic therapy options.

With the available data we were unable to account for certain relevant features of clinical status, such as degree of liver disease and performance status at the time of diagnosis, which could be key prognostic factors for treatment options. Performance status data were missing for 75.1% of the cohort at diagnosis, whereas degree of liver disease is not possible to abstract from the data sources available. Our intention to account for differences in the stage at diagnosis was hindered due to missing data for 45.5% of the cohort. Although a sensitivity analysis in those with reported stage was performed, the subgroup of individuals with known stage could have been highly selected and therefore their findings may not be generalisable to the entire CCA population. This highlights the importance of documenting and collecting information on stage of CCA at diagnosis in the future. It is unclear why completeness is relatively poor for this tumour site compared to other cancers. That said, in the group where CCA stage was known, the stage at diagnosis did not appear to explain much, if any, of the variation observed.

Based on a national cohort of CCA patients, these data are highly representative of CCA patients and treatment in England, where treatment is free at point of access *via* the NHS. However, these findings will be less generalisable to other countries that have different healthcare systems and guidelines as to the management of CCA.

CONCLUSION

Certainly, some Cancer Alliances appear to have lower than average rates of treatment for CCA patients. The reasons for this require further investigation that would be aided by more detail on patient clinical status and clinical case-mix than was available *via* this national registration database. It is important to understand whether observed differences are due to differences in clinical practice, case mix or geographical differences in access to expert facilities, in order to successfully implement evidence-based solutions to reduce variation and inequality in treatments received.

ARTICLE HIGHLIGHTS

Research background

Cholangiocarcinoma (CCA) is a cancer with poor survival outcomes that is increasing in incidence worldwide. In clinical practice there can be barriers to providing treatments that can improve outcomes for those with CCA. Potentially curative

surgery is not an option for those diagnosed with advanced disease, which represents the majority of patients. Stent insertion to manage disease complications is a complex procedure requiring access to specialist expertise that is not routinely available in all areas. There are currently relatively few recommended systemic treatment options available that can prolong survival.

Research motivation

Due to the complexity of treating CCA, we hypothesise that there could be variation in the treatments received by CCA patients. Such variation could contribute to the poor outcomes experienced by CCA patients. There is very little data to evidence variation in the care and management of CCA in England, so research into this area is needed. Identifying variation that could point to inequality is the first step toward improving patient outcomes, leading to further research into understanding why this variation exists and ultimately improvement strategies to reduce these variations in care.

Research objectives

We aimed to investigate whether there was evidence of geographic variation in the proportion of CCA patients that received each of three main cancer-specific treatments: potentially curative surgery; systemic therapy amongst those that did not receive surgery; stent insertion amongst those that did not receive surgery.

Research methods

We conducted a retrospective cohort study including patients diagnosed with CCA from 2014-2017 in England. We used linear probability models to investigate geographic variation in the proportions of that received either potentially curative surgery, systemic therapy (in the absence of surgery) or stent insertion (in the absence of surgery) across Cancer Alliance areas in England, adjusting for potential confounders.

Research results

Half of CCA patients in England received none of the cancer treatments we investigated in this study. Only 12.4% received potentially curative surgery. Across all Cancer Alliance areas, the mean percentage-point difference from the population average [95% confidence interval (CI)] ranged from -3.96 (-6.34 to -1.59)% to 3.77 (0.54 to 6.99)% after adjustment for patient sociodemographic and clinical characteristics, showing statistically significant variation.

Amongst those who did not receive surgery, 19.9% received systemic therapy, with mean percentage-point difference from the population average [95%CI] ranging from -3.84 (-8.04 to 0.35)% to 9.28 (1.76 to 16.80)% across Cancer Alliances after adjustment. Stent insertion was received by 27.8%. Across Cancer Alliances, after adjustment for confounders, the mean percentage-point difference from population average [95%CI] ranged between -10.54 (-12.88 to -8.20)% and 13.64 (9.22 to 18.06)%, showing wide and statistically significant variation from the population average.

It is unknown whether the observed variation is evidence of inequality in access to treatment and differing clinical practice or can be explained by factors we were unable to account for in our analysis, such as patient choice and differences in the clinical case-mix of patients in these areas.

Research conclusions

We found statistically significant geographic variation in the proportions of CCA patients receiving surgery, systemic therapy and stent insertion across Cancer Alliance areas in England.

Research perspectives

Local detailed review of treatment pathways should be undertaken to understand in more detail why rates of treatment were low and whether the observed variation indicates disparities in access to care or differences in clinical practice. Greater understanding of why variation in care is present can support the development of future strategies to reduce unwarranted variation and improve outcomes.

ACKNOWLEDGEMENTS

This work uses data that has been provided by patients and collected by the NHS as part of their care and support. The data are collated, maintained and quality assured by the National Disease Registration Service, which is part of NHS England.

FOOTNOTES

Author contributions: Jose S, Knott C, Khan SA, Morement H and Zalin-Miller A designed the study; Paley L and Toledano MB advised on the study design; Jose S, Zalin-Miller A and Knott C had full access to the underlying data in the study; all authors contributed to the interpretation of results; Jose S and Khan SA drafted the manuscript; Knott C, Morement H, Paley L, Tataru D, Toledano MB and Zalin-Miller A reviewed and revised the manuscript; all authors approved the final version of the manuscript had access to the study data and accept responsibility to submit for publication.

Supported by AMMF; National Disease Registration Service, National Health Service England.

Institutional review board statement: The study was reviewed and approved for publication by our Institutional Reviewer.

Informed consent statement: NHS England and has a special legal instruction to collect patient data without needing informed consent. This instruction is granted under section 254 of the Health and Social Care Act 2012.

Conflict-of-interest statement: Dr Jose reports grants from AMMF-The Cholangiocarcinoma Charity, during the conduct of the study.

Data sharing statement: The data that support the findings of this study are available from NHS England. Restrictions apply to the access and use of the data used to undertake this study. A data dictionary is available at <https://digital.nhs.uk/ndrs/data/access-to-data>.

STROBE statement: The authors have read the STROBE Statement-checklist of items, and the manuscript was prepared and revised according to the STROBE Statement-checklist of items.

Open-Access: This article is an open-access article that was selected by an in-house editor and fully peer-reviewed by external reviewers. It is distributed in accordance with the Creative Commons Attribution NonCommercial (CC BY-NC 4.0) license, which permits others to distribute, remix, adapt, build upon this work non-commercially, and license their derivative works on different terms, provided the original work is properly cited and the use is non-commercial. See: <https://creativecommons.org/licenses/by-nc/4.0/>

Country/Territory of origin: United Kingdom

ORCID number: Sophie Jose 0000-0002-3536-4344; Amy Zalin-Miller 0000-0002-3123-3566; Craig Knott 0000-0002-8593-6216; Lizz Paley 0000-0002-3879-5377; Daniela Tataru 0009-0002-2655-4717; Helen Morement 0000-0001-6141-2816; Mireille B Toledano 0000-0001-5695-6210; Shahid A Khan 0000-0003-2538-0911.

S-Editor: Qu XL

L-Editor: A

P-Editor: Xu ZH

REFERENCES

- 1 **Khan SA**, Thomas HC, Davidson BR, Taylor-Robinson SD. Cholangiocarcinoma. *Lancet* 2005; **366**: 1303-1314 [PMID: 16214602 DOI: 10.1016/S0140-6736(05)67530-7]
- 2 **Brindley PJ**, Bachini M, Ilyas SI, Khan SA, Loukas A, Sirica AE, Teh BT, Wongkham S, Gores GJ. Cholangiocarcinoma. *Nat Rev Dis Primers* 2021; **7**: 65 [PMID: 34504109 DOI: 10.1038/s41572-021-00300-2]
- 3 **Rushbrook S**. BSG Guidelines for the diagnosis and treatment of cholangiocarcinoma. *Gut* 2023; In press
- 4 **Khan SA**, Davidson BR, Goldin RD, Heaton N, Karani J, Pereira SP, Rosenberg WM, Tait P, Taylor-Robinson SD, Thillainayagam AV, Thomas HC, Wasan H; British Society of Gastroenterology. Guidelines for the diagnosis and treatment of cholangiocarcinoma: an update. *Gut* 2012; **61**: 1657-1669 [PMID: 22895392 DOI: 10.1136/gutjnl-2011-301748]
- 5 **Nakeeb A**, Pitt HA, Sohn TA, Coleman J, Abrams RA, Piantadosi S, Hruban RH, Lillemoe KD, Yeo CJ, Cameron JL. Cholangiocarcinoma. A spectrum of intrahepatic, perihilar, and distal tumors. *Ann Surg* 1996; **224**: 463-73; discussion 473 [PMID: 8857851 DOI: 10.1097/0000658-199610000-00005]
- 6 **Banales JM**, Marin JGG, Lamarca A, Rodrigues PM, Khan SA, Roberts LR, Cardinale V, Carpino G, Andersen JB, Braconi C, Calvisi DF, Perugorria MJ, Fabris L, Boulter L, Macias RIR, Gaudio E, Alvaro D, Gradilone SA, Strazzabosco M, Marzioni M, Couloouam C, Fouassier L, Raggi C, Invernizzi P, Mertens JC, Moncek A, Rizvi S, Heimbach J, Koerkamp BG, Bruix J, Forner A, Bridgewater J, Valle JW, Gores GJ. Cholangiocarcinoma 2020: the next horizon in mechanisms and management. *Nat Rev Gastroenterol Hepatol* 2020; **17**: 557-588 [PMID: 32606456 DOI: 10.1038/s41575-020-0310-z]
- 7 **Khan SA**, Tavolari S, Brandi G. Cholangiocarcinoma: Epidemiology and risk factors. *Liver Int* 2019; **39** Suppl 1: 19-31 [PMID: 30851228 DOI: 10.1111/liv.14095]
- 8 **Taylor-Robinson SD**, Toledano MB, Arora S, Keegan TJ, Hargreaves S, Beck A, Khan SA, Elliott P, Thomas HC. Increase in mortality rates from intrahepatic cholangiocarcinoma in England and Wales 1968-1998. *Gut* 2001; **48**: 816-820 [PMID: 11358902 DOI: 10.1136/gut.48.6.816]
- 9 **Khan SA**, Taylor-Robinson SD, Toledano MB, Beck A, Elliott P, Thomas HC. Changing international trends in mortality rates for liver, biliary and pancreatic tumours. *J Hepatol* 2002; **37**: 806-813 [PMID: 12445422 DOI: 10.1016/S0168-8278(02)00297-0]
- 10 **Vithayathil M**, Khan SA. Current epidemiology of cholangiocarcinoma in Western countries. *J Hepatol* 2022; **77**: 1690-1698 [PMID: 35977611 DOI: 10.1016/j.jhep.2022.07.022]
- 11 **McClements J**, Valle JW, Blackburn L, Brooks A, Prachalias A, Dasari BVM, Jones C, Harrison E, Malik H, Prasad KR, Sodergren M, Silva M, Kumar N, Shah N, Bhardwaj N, Nunes Q, Bhogal RH, Pandanaboyana S, Aroori S, Hamady Z, Gomez D; UK HPB Research Collaborative Group. Variation in treatment of intrahepatic cholangiocarcinoma: a nationwide multicentre study. *Br J Surg* 2023 [PMID: 37611144 DOI: 10.1093/bjs/znad259]
- 12 **Izquierdo-Sanchez L**, Lamarca A, La Casta A, Buettner S, Utpatel K, Klumpen HJ, Adeva J, Vogel A, Lleo A, Fabris L, Ponz-Sarvisse M, Brustia R, Cardinale V, Braconi C, Vidili G, Jamieson NB, Macias RI, Jonas JP, Marzioni M, Hołowko W, Folseraas T, Kupčinskas J, Sparchez Z, Krawczyk M, Krupa Ł, Scripcariu V, Grazi GL, Landa-Magdalena A, Ijzermans JN, Evert K, Erdmann JI, López-López F, Saborowski A, Scheiter A, Santos-Laso A, Carpino G, Andersen JB, Marin JJ, Alvaro D, Bujanda L, Forner A, Valle JW, Koerkamp BG, Banales JM. Cholangiocarcinoma landscape in Europe: Diagnostic, prognostic and therapeutic insights from the ENSCCA Registry. *J Hepatol* 2022; **76**: 1109-1121 [PMID: 35167909 DOI: 10.1016/j.jhep.2021.12.010]
- 13 **Henson KE**, Elliss-Brookes L, Coupland VH, Payne E, Vernon S, Rous B, Rashbass J. Data Resource Profile: National Cancer Registration

- Dataset in England. *Int J Epidemiol* 2020; **49**: 16-16h [PMID: 31120104 DOI: 10.1093/ije/dyz076]
- 14 **Bright CJ**, Lawton S, Benson S, Bomb M, Dodwell D, Henson KE, McPhail S, Miller L, Rashbass J, Turnbull A, Smittenaar R. Data Resource Profile: The Systemic Anti-Cancer Therapy (SACT) dataset. *Int J Epidemiol* 2020; **49**: 15-151 [PMID: 31340008 DOI: 10.1093/ije/dyz137]
 - 15 **Sandhu S**, Sharpe M, Findlay Ú, Roe C, Broggio J, Spencer K, Thackray K. Cohort profile: radiotherapy dataset (RTDS) in England. *BMJ Open* 2023; **13**: e070699 [PMID: 37339842 DOI: 10.1136/bmjopen-2022-070699]
 - 16 **Herbert A**, Wijlaars L, Zylbersztejn A, Cromwell D, Hardelid P. Data Resource Profile: Hospital Episode Statistics Admitted Patient Care (HES APC). *Int J Epidemiol* 2017; **46**: 1093-1093i [PMID: 28338941 DOI: 10.1093/ije/dyx015]
 - 17 **National Disease Registration Service**. CAS-SOP #4.8 Linking treatment tables: chemotherapy, tumour resections and radiotherapy. [cited 22 June 2023]. Available from: <https://digital.nhs.uk/ndrs/our-work/ncras-work-programme/treatment-data/cas-sop-4.8>
 - 18 **Crooks CJ**, West J, Card TR. A comparison of the recording of comorbidity in primary and secondary care by using the Charlson Index to predict short-term and long-term survival in a routine linked data cohort. *BMJ Open* 2015; **5**: e007974 [PMID: 26048212 DOI: 10.1136/bmjopen-2015-007974]
 - 19 **Elliss-Brookes L**, McPhail S, Ives A, Greenslade M, Shelton J, Hiom S, Richards M. Routes to diagnosis for cancer - determining the patient journey using multiple routine data sets. *Br J Cancer* 2012; **107**: 1220-1226 [PMID: 22996611 DOI: 10.1038/bjc.2012.408]
 - 20 **Driver RJ**, Balachandrakumar V, Burton A, Shearer J, Downing A, Cross T, Morris E, Rowe IA. Validation of an algorithm using inpatient electronic health records to determine the presence and severity of cirrhosis in patients with hepatocellular carcinoma in England: an observational study. *BMJ Open* 2019; **9**: e028571 [PMID: 31292182 DOI: 10.1136/bmjopen-2018-028571]
 - 21 **Te Grotenhuis M**, Pelzer B, Eisinga R, Nieuwenhuis R, Schmidt-Catran A, König R. When size matters: advantages of weighted effect coding in observational studies. *Int J Public Health* 2017; **62**: 163-167 [PMID: 27796415 DOI: 10.1007/s00038-016-0901-1]
 - 22 **Braveman P**, Gottlieb L. The social determinants of health: it's time to consider the causes of the causes. *Public Health Rep* 2014; **129** Suppl 2: 19-31 [PMID: 24385661 DOI: 10.1177/00333549141291S206]
 - 23 **Galea S**, Tracy M, Hoggatt KJ, Dimaggio C, Karpati A. Estimated deaths attributable to social factors in the United States. *Am J Public Health* 2011; **101**: 1456-1465 [PMID: 21680937 DOI: 10.2105/AJPH.2010.300086]
 - 24 **Pruitt SL**, Shim MJ, Mullen PD, Vernon SW, Amick BC 3rd. Association of area socioeconomic status and breast, cervical, and colorectal cancer screening: a systematic review. *Cancer Epidemiol Biomarkers Prev* 2009; **18**: 2579-2599 [PMID: 19815634 DOI: 10.1158/1055-9965.EPI-09-0135]
 - 25 **Manser CN**, Bauerfeind P. Impact of socioeconomic status on incidence, mortality, and survival of colorectal cancer patients: a systematic review. *Gastrointest Endosc* 2014; **80**: 42-60.e9 [PMID: 24950641 DOI: 10.1016/j.gie.2014.03.011]
 - 26 **Maddison AR**, Asada Y, Urquhart R. Inequity in access to cancer care: a review of the Canadian literature. *Cancer Causes Control* 2011; **22**: 359-366 [PMID: 21221758 DOI: 10.1007/s10552-010-9722-3]
 - 27 **Sinding C**, Warren R, Fitzpatrick-Lewis D, Sussman J. Research in cancer care disparities in countries with universal healthcare: mapping the field and its conceptual contours. *Support Care Cancer* 2014; **22**: 3101-3120 [PMID: 25120008 DOI: 10.1007/s00520-014-2348-3]
 - 28 **Davis LE**, Coburn NG, Hallet J, Earle CC, Liu Y, Myrehaug S, Mahar AL. Material deprivation and access to cancer care in a universal health care system. *Cancer* 2020; **126**: 4545-4552 [PMID: 32745271 DOI: 10.1002/cncr.33107]
 - 29 **Jiang Y**, Jiang L, Li F, Li Q, Yuan S, Huang S, Fu Y, Yan X, Chen J, Li H, Li S, Liu J. The epidemiological trends of biliary tract cancers in the United States of America. *BMC Gastroenterol* 2022; **22**: 546 [PMID: 36581813 DOI: 10.1186/s12876-022-02637-8]

Retrospective Study

Effect of ultrasound-guided lumbar square muscle block on stress response in patients undergoing radical gastric cancer surgery

Xin-Ran Wang, Dan-Dan Xu, Meng-Jiao Guo, Yi-Xin Wang, Meng Zhang, Dong-Xiao Zhu

Specialty type: Oncology

Provenance and peer review:

Unsolicited article; Externally peer reviewed.

Peer-review model: Single blind

Peer-review report's scientific quality classification

Grade A (Excellent): 0

Grade B (Very good): B

Grade C (Good): C

Grade D (Fair): 0

Grade E (Poor): 0

P-Reviewer: Ramos AC, Brazil; Varon C, France

Received: September 12, 2023

Peer-review started: September 12, 2023

First decision: September 26, 2023

Revised: October 7, 2023

Accepted: November 25, 2023

Article in press: November 25, 2023

Published online: December 15, 2023



Xin-Ran Wang, Dan-Dan Xu, Meng-Jiao Guo, Yi-Xin Wang, Meng Zhang, Dong-Xiao Zhu, Department of Ultrasound, Affiliated Hospital of Jiangnan University, Wuxi 214122, Jiangsu Province, China

Corresponding author: Dong-Xiao Zhu, Doctor, Staff Physician, Department of Ultrasound, Affiliated Hospital of Jiangnan University, No. 1000 Hefeng Road, Wuxi 214122, Jiangsu Province, China. acm18990505@163.com

Abstract

BACKGROUND

Radical surgery is a common treatment for patients with gastric cancer; however, it can lead to postoperative complications and intestinal barrier dysfunction. Ultrasound-guided quadratus lumborum block is often used for postoperative analgesia, but its effects on stress response and intestinal barrier function are not well understood.

AIM

To investigate the effects of an ultrasound-guided quadratus lumborum block on stress response and intestinal barrier function in patients undergoing radical surgery for gastric cancer.

METHODS

A total of 100 patients undergoing radical surgery for gastric cancer were randomly categorized into observation and control groups. Plasma adrenaline and cortisol levels, intestinal mucosal barrier indexes, and complication rates were compared between the two groups before, during, and 1 day after surgery.

RESULTS

The observation group had significantly lower plasma adrenaline and cortisol levels during surgery and at 1 day postoperatively than that of the control group ($P < 0.05$). Additionally, intestinal barrier indexes (endotoxin and D-dimer) at 1 day postoperatively were significantly lower in the observation group than in the control group ($P < 0.05$).

CONCLUSION

Ultrasound-guided quadratus lumborum block could reduce stress response, protect intestinal barrier function, and decrease the incidence of complications in patients undergoing radical surgery for gastric cancer. This technique has the

potential for clinical applications.

Key Words: Ultrasound-guided quadratus lumborum block; Radical gastric cancer surgery; Stress response; Intestinal barrier function; Postoperative analgesia; Rehabilitation

©The Author(s) 2023. Published by Baishideng Publishing Group Inc. All rights reserved.

Core Tip: Ultrasound-guided quadratus lumborum block reduces stress response and preserves intestinal barrier function following radical surgery for gastric cancer, potentially lowering the associated complications. This technique shows promise in providing postoperative analgesia and for improving patient outcomes. It protects the intestinal barrier function and reduces the incidence of complications in patients who undergo radical gastric cancer surgery, highlighting its potential clinical use.

Citation: Wang XR, Xu DD, Guo MJ, Wang YX, Zhang M, Zhu DX. Effect of ultrasound-guided lumbar square muscle block on stress response in patients undergoing radical gastric cancer surgery. *World J Gastrointest Oncol* 2023; 15(12): 2093-2100

URL: <https://www.wjgnet.com/1948-5204/full/v15/i12/2093.htm>

DOI: <https://dx.doi.org/10.4251/wjgo.v15.i12.2093>

INTRODUCTION

Ultrasound-guided quadratus lumborum block exhibited promising effects in reducing stress response and improving intestinal barrier function in patients undergoing radical surgery for gastric cancer[1-5]. The decline in the plasma adrenaline and cortisol levels[5-10], improved intestinal barrier indexes, and reduced incidence of postoperative complications underscores the potential clinical application of this technique[11-15]. However, further studies are needed to optimize its clinical application[16-21], and explore its combination with other interventions to enhance postoperative recovery and minimize complications[22,23].

MATERIALS AND METHODS

Ultrasound-guided quadratus lumborum block has made significant progress as a pain management and rehabilitation promotion technique for clinical applications[24-27]. This study investigated the effects of ultrasound-guided quadratus lumborum block on stress response and intestinal barrier function in patients undergoing radical surgery for gastric cancer.

Furthermore, we did not evaluate the onset and maintenance times of the quadratus lumborum block; therefore, further studies are warranted to assess these parameters.

First, we anticipated that the ultrasound-guided quadratus lumborum block group would demonstrate improved outcomes in terms of postoperative physiological indicators and pain scores, reflecting a reduced stress response[28-30]. This could be partly attributed to the analgesic effect of the ultrasound-guided quadratus lumborum block, which diminishes pain transmission at the surgical site through local anesthesia, thereby reducing postoperative pain perception and stress response. Additionally, quadratus lumborum blocks may modulate stress response by blocking sympathetic activity and reducing the release of inflammatory mediators[31-33].

Second, regarding the assessment of intestinal barrier function, we anticipated that the ultrasound-guided quadratus lumborum block group would demonstrate enhanced outcomes[34], including reduced intestinal permeability and inflammatory response[35]. Surgical trauma and stress may lead to intestinal barrier dysfunction, increased intestinal permeability, and an inflammatory response, potentially leading to postoperative complications. Ultrasound-guided quadratus lumborum block may protect intestinal barrier function by reducing the inflammatory response to surgical trauma and maintaining intestinal blood perfusion[36,37]. In addition, some studies have suggested that these blocks may maintain intestinal health by regulating the balance of the intestinal microbiota. However, intestinal barrier function is influenced by a number of factors, with ultrasound-guided quadratus lumborum block being just one of them; other interventions and factors may also have an impact on intestinal barrier function[38,39].

First, the sample size may be limited, necessitating studies with larger sample sizes to further validate the reliability of our results. Second, the clinical application of ultrasound-guided quadratus lumborum blocks may involve the collaboration of multiple medical personnel, potentially introducing differences in operating techniques that could affect the results; hence, uniform operating standards are needed. In addition, this study only focused on the effects of postoperative stress and intestinal barrier function; other clinical outcomes and the long-term prognosis of patients require further investigation.

Table 1 Comparison of plasma inflammatory factor levels before and after treatment between the observation and control groups ($X \pm s$)

		Pro-adrenaline (pg/L)	Cortisol (ng/L)	IL-6 (ng/L)	C-reactive protein (mg/L)
Control group ($n = 50$)	Before treatment	1.16 \pm 0.12	24.55 \pm 2.54	36.47 \pm 1.64	34.22 \pm 1.64
	After treatment	0.88 \pm 0.18	21.66 \pm 2.16	30.08 \pm 1.72	27.84 \pm 1.19
Observation group ($n = 50$)	Before treatment	1.15 \pm 0.19	24.51 \pm 2.08	36.39 \pm 1.66	34.35 \pm 1.91
	After treatment	0.51 \pm 0.09	17.08 \pm 1.52	22.51 \pm 1.58	16.78 \pm 1.49
t/P		8.682/ $<$ 0.001	5.814/ $<$ 0.001	18.037/ $<$ 0.001	21.122/ $<$ 0.001
t/P		20.421/ $<$ 0.001	19.347/ $<$ 0.001	40.629/ $<$ 0.001	48.655/ $<$ 0.001
t/P post-treatment inter-group values		12.333/ $<$ 0.001	11.632/ $<$ 0.001	21.743/ $<$ 0.001	38.908/ $<$ 0.001

Values are expressed as mean \pm SD.

Table 2 Comparison of perioperative indicators between the observation and the control groups ($X \pm s$)

Group	n	Sufentanil dosage (μ g)	Post-operative awakening time (min)	Postoperative time in bed (h)	Time taken for anal discharge (h)
Observation group	50	25.56 \pm 4.56	14.52 \pm 1.72	21.26 \pm 3.41	12.26 \pm 1.65
Control group	50	71.12 \pm 7.45	25.62 \pm 2.51	30.23 \pm 4.56	20.17 \pm 2.36
t value	28.380	20.533	8.861	15.458	0.000
P value	0.000	0.000	0.000		

Table 3 Comparison of the incidence of adverse reactions between the observation and the control groups [n (%)]

	Leukopenia	Hepatic impairment	Nausea and vomiting	Bone marrow suppression	Renal impairment	Incidence
Control group ($n = 50$)	5 (11.11)	3 (6.67)	5 (11.11)	4 (8.89)	7 (15.56)	24 (53.33)
Observation group ($n = 50$)	2 (4.44)	1 (2.22)	1 (2.22)	1 (2.22)	2 (4.44)	7 (15.56)
χ^2						14.221
P value						0.000

RESULTS

Comparison of plasma epinephrine and cortisol levels and indicators of intestinal mucosal barrier between the two groups before, during, and 1 day after surgery

The plasma adrenaline, cortisol, interleukin-6, and C-reactive protein levels were significantly lower in both the groups after treatment in comparison to their levels before treatment, and the reduction in these indicators was more significant in the observation group than in the control group ($P < 0.05$, Table 1).

Perioperative indicators

Compared with the patients in the control group, those in the observation group demonstrated significantly improved outcomes in terms of sufentanil dosage, postoperative awakening time, postoperative time in bed, and time taken for anal discharge ($P < 0.05$, Table 2).

Statistics on complication rates

The incidence of adverse reactions was significantly lower in the observation group than in the control group ($P < 0.05$, Table 3).

Effect of ultrasound guidance on immunity of two groups of patients

Compared with the control group, the observation group exhibited a significant decrease in the CD4+/CD8+ ratio and

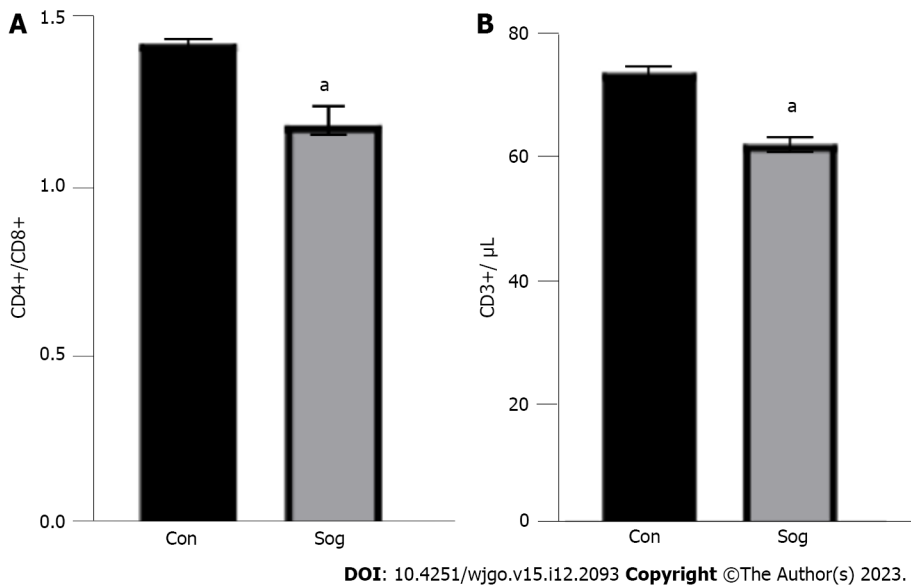


Figure 1 Effect of ultrasound on immunity of the observation and control groups. A and B: CD4+/CD8+ (A) and CD3+ (B) ($n = 50$, $^aP < 0.01$).

CD3+ count, indicating that ultrasound guidance exerts a substantial influence on the body's immune response and a positive effect on the recovery and prognosis of the disease. In patients undergoing radical gastrectomy, ultrasound-guided quadratus lumborum block, administered at the same dose, could achieve an ideal postoperative analgesic effect and significantly reduce postoperative immune function suppression (Figure 1).

DISCUSSION

General information

A total of 100 patients with gastric cancer who underwent radical surgery between February 2019 and July 2020 were enrolled in this study[40]. The inclusion criteria were as follows: (1) Confirmation of gastric cancer through pathological examination; (2) absence of allergies to anesthetic drugs; and (3) absence of contraindication for surgery or use of drugs affecting neuromuscular function. The patients were randomly categorized into two groups using the random number table method. The observation group included 50 patients (28 male and 22 female), aged 35–58 years (mean: 46.24 ± 1.63 years), with ASA classification grade I in 31 and grade II in 19 patients. The control group comprised 50 patients (27 male and 23 female), aged 33–58 years (mean: 45.98 ± 1.58 years), with ASA classification grade I in 32 and grade II in 18 patients.

Methodology

Before surgery patients in both the groups were prepared by administering oxygen at room air; promptly establishing intravenous access; and assessing vital signs, including electrocardiography, heart rate, and blood pressure.

In the control group, the anesthetic induction protocol comprised 0.05 mg/kg imipramine + 0.3 μg/kg sufentanil + 2.0 mg/kg propofol + 0.6 mg/kg rocuronium bromide. In the observation group, an ultrasound-guided quadratus lumborum block was performed alongside the standard anesthesia protocol. Postoperatively, both the groups were connected to a self-controlled analgesic pump delivering a mixture of 2 μg/kg sufentanil + 8 mg ondansetron mixed with 100 mL saline; the pump was devoid of a background dose, and delivered a single-pressed dose of 2 mL with a lock time of 15 min.

Observation indicators

The plasma epinephrine and cortisol levels, as well as indicators of intestinal mucosal barrier were compared between the two groups before, during, and one day postsurgery. The amount of sufentanil in both the groups was quantified, and the postoperative parameters, including awakening time, time in bed, and time taken for anal discharge were recorded in both the groups.

Additionally, the complication rate was determined at the time of discharge, and patient satisfaction was assessed using a self-designed questionnaire.

Data analysis

Statistical analyses were performed using the SPSS 21.0 software. The t-test was used to analyze measurement data, whereas the χ^2 test was used for count data. A P value of < 0.05 indicated a statistically significant difference.

CONCLUSION

Gastric cancer is a common malignancy, and radical surgery for gastric cancer is one of the main treatment modalities. Surgical trauma and stress reactions may lead to postoperative complications and intestinal barrier dysfunction. Ultrasound-guided quadratus lumborum block is widely used for providing postoperative analgesia and promoting recovery; however, its effects on stress response and intestinal barrier function are unclear. The laparoscopic approach offers many advantages, such as less trauma, faster postoperative recovery, and fewer postoperative complications; however, surgery inevitably causes stress and unavoidable postoperative pain; therefore, a suitable surgical anesthetic is needed to ensure a successful outcomes of surgery. In the past, laparoscopic surgery for gastric cancer has often been performed under general anesthesia, yielding good results; however, general anesthesia can easily lead to central sensitization, and require a considerable amount of analgesic drugs during surgery. The use of large amounts of analgesic drugs during surgery potentially cause nausea, vomiting, intestinal paralysis, and other adverse reactions, which can easily affect the smooth implementation of surgery and may even lead to failure. With the advancements in ultrasound technology and anesthesia practices, studies have demonstrated that the combination of an ultrasound-guided anterior lumbar muscle block with conventional general anesthesia during laparoscopic surgery can achieve improved satisfactory anesthetic and analgesic effects. However, its efficacy in reducing the use of analgesics and promoting postoperative recovery remains unclear. In this study, we aimed to investigate the effects of ultrasound-guided quadratus lumborum combined with general anesthesia in laparoscopic surgery for gastric cancer to provide a valuable reference for those involved in such procedures.

ARTICLE HIGHLIGHTS

Research background

Future studies should focus on optimizing the clinical application of ultrasound-guided quadratus lumborum block and exploring its efficacy in combination with other interventions to enhance postoperative recovery and minimize complications.

Research motivation

To investigate the effects of an ultrasound-guided quadratus lumborum block on stress response and intestinal barrier function in patients with gastric cancer.

Research objectives

The observation group exhibited significantly lower plasma adrenaline and cortisol levels during surgery and on the first day postoperatively compared to the control group ($P < 0.05$).

Research methods

A total of 100 patients who underwent radical surgery for gastric cancer were randomly assigned to either the observation or the control group (50 patients each). Plasma adrenaline and cortisol levels, intestinal mucosal barrier indexes, and complication rates were compared between the two groups before, during, and on the first day after surgery.

Research results

The observation group exhibited significantly lower plasma adrenaline and cortisol levels during surgery and on the first day postoperatively compared to the control group ($P < 0.05$).

Research conclusions

Ultrasound-guided quadratus lumborum block aids in preserving intestinal barrier function and reducing the incidence of postoperative complications, thereby demonstrating its potential clinical applicability.

Research perspectives

Radical surgery for gastric cancer can lead to postoperative complications and intestinal barrier dysfunction owing to surgical trauma and stress.

FOOTNOTES

Co-first authors: Xin-Ran Wang and Dan-Dan Xu.

Author contributions: Wang XR and Xu DD contributed equally to this work; Wang XR, Xu DD, Guo MJ, Wang YX, Zhang M, and Zhu DX designed the research study; Wang XR, Xu DD, Guo MJ, Wang YX, Zhang M, and Zhu DX performed the research; Xu DD and Guo MJ contributed new reagents and analytic tools; Wang XR, and Zhu DX analyzed the data and wrote the manuscript; All authors have read and approve the final manuscript. Wang XR and Xu DD contributed equally to this work as co-first authors. The decision to designate Wang XR and Xu DD as co-first authors is based in three primary reasons. First, the research was performed as a collaborative

effort, and the designation of co-first authors accurately reflects the distribution of responsibilities and burdens associated with the time and effort required to complete the study and the resultant manuscript. Designating two first authors will ensure effective communication and management of post-submission matters, which will enhance the paper's quality and reliability. Second, the research team consisted of authors with diverse expertise and skills from various fields, and the designation of two co-first authors best reflects this diversity. This also promotes the most comprehensive and in-depth examination of the research topic, ultimately enriching readers' understanding by offering various expert perspectives. Third, both Wang XR and Xu DD Made substantial and equal contributions throughout the research process. Selecting these researchers as co-first authors acknowledges and respects their equal contribution and exemplifies the collaborative spirit and teamwork within this study. In summary, we believe that designating Wang XR and Xu DD as co-first authors is fitting for our manuscript as it accurately reflects our team's collaborative spirit, equal contributions, and diversity.

Institutional review board statement: This study was reviewed and approved by the Affiliated Hospital of Jiangnan University.

Informed consent statement: Prior to the study, informed consent forms were obtained from all patients.

Conflict-of-interest statement: All authors have no conflicts of interest.

Data sharing statement: No additional data are available.

Open-Access: This article is an open-access article that was selected by an in-house Author and fully peer-reviewed by external reviewers. It is distributed in accordance with the Creative Commons Attribution NonCommercial (CC BY-NC 4.0) license, which permits others to distribute, remix, adapt, build upon this work non-commercially, and license their derivative works on different terms, provided the original work is properly cited and the use is non-commercial. See: <https://creativecommons.org/licenses/by-nc/4.0/>

Country/Territory of origin: China

ORCID number: Xin-Ran Wang 0009-0009-4581-5661; Dong-Xiao Zhu 0009-0008-8413-4431.

S-Editor: Lin C

L-Editor: A

P-Editor: Lin C

REFERENCES

- Balshem H**, Helfand M, Schünemann HJ, Oxman AD, Kunz R, Brozek J, Vist GE, Falck-Ytter Y, Meerpohl J, Norris S, Guyatt GH. GRADE guidelines: 3. Rating the quality of evidence. *J Clin Epidemiol* 2011; **64**: 401-406 [PMID: 21208779 DOI: 10.1016/j.jclinepi.2010.07.015]
- Fassnacht M**, Arlt W, Bancos I, Dralle H, Newell-Price J, Sahdev A, Tabarin A, Terzolo M, Tsagarakis S, Dekkers OM. Management of adrenal incidentalomas: European Society of Endocrinology Clinical Practice Guideline in collaboration with the European Network for the Study of Adrenal Tumors. *Eur J Endocrinol* 2016; **175**: G1-G34 [PMID: 27390021 DOI: 10.1530/EJE-16-0467]
- Zeiger MA**, Thompson GB, Duh QY, Hamrahian AH, Angelos P, Elaraj D, Fishman E, Kharlip J; American Association of Clinical Endocrinologists; American Association of Endocrine Surgeons. American Association of Clinical Endocrinologists and American Association of Endocrine Surgeons Medical Guidelines for the Management of Adrenal Incidentalomas: executive summary of recommendations. *Endocr Pract* 2009; **15**: 450-453 [PMID: 19632968 DOI: 10.4158/EP.15.5.450]
- Dinnes J**, Bancos I, Ferrante di Ruffano L, Chortis V, Davenport C, Bayliss S, Sahdev A, Guest P, Fassnacht M, Deeks JJ, Arlt W. MANAGEMENT OF ENDOCRINE DISEASE: Imaging for the diagnosis of malignancy in incidentally discovered adrenal masses: a systematic review and meta-analysis. *Eur J Endocrinol* 2016; **175**: R51-R64 [PMID: 27257145 DOI: 10.1530/EJE-16-0461]
- Ichijo T**, Ueshiba H, Nawata H, Yanase T. A nationwide survey of adrenal incidentalomas in Japan: the first report of clinical and epidemiological features. *Endocr J* 2020; **67**: 141-152 [PMID: 31694993 DOI: 10.1507/endocrj.EJ18-0486]
- Ebbehoj A**, Li D, Kaur RJ, Zhang C, Singh S, Li T, Atkinson E, Achenbach S, Khosla S, Arlt W, Young WF, Rocca WA, Bancos I. Epidemiology of adrenal tumours in Olmsted County, Minnesota, USA: a population-based cohort study. *Lancet Diabetes Endocrinol* 2020; **8**: 894-902 [PMID: 33065059 DOI: 10.1016/S2213-8587(20)30314-4]
- Hong AR**, Kim JH, Park KS, Kim KY, Lee JH, Kong SH, Lee SY, Shin CS, Kim SW, Kim SY. Optimal follow-up strategies for adrenal incidentalomas: reappraisal of the 2016 ESE-ENSAT guidelines in real clinical practice. *Eur J Endocrinol* 2017; **177**: 475-483 [PMID: 28870984 DOI: 10.1530/EJE-17-0372]
- Cyranska-Chyrek E**, Szczepanek-Parulska E, Olejarsz M, Ruchala M. Malignancy Risk and Hormonal Activity of Adrenal Incidentalomas in a Large Cohort of Patients from a Single Tertiary Reference Center. *Int J Environ Res Public Health* 2019; **16** [PMID: 31137898 DOI: 10.3390/ijerph16101872]
- Bancos I**, Taylor AE, Chortis V, Sitch AJ, Jenkinson C, Davidge-Pitts CJ, Lang K, Tsagarakis S, Macech M, Riester A, Deutschbein T, Pupovac ID, Kienitz T, Prete A, Papathomas TG, Gilligan LC, Bancos C, Reimondo G, Haissaguerre M, Marina L, Grytaas MA, Sajwani A, Langton K, Ivison HE, Shackleton CHL, Erickson D, Asia M, Palimeri S, Kondracka A, Spyroglou A, Ronchi CL, Simunov B, Delivanis DA, Sutcliffe RP, Tsiros I, Bednarczuk T, Reincke M, Burger-Stritt S, Feelders RA, Canu L, Haak HR, Eisenhofer G, Denney MC, Ueland GA, Ivovic M, Tabarin A, Terzolo M, Quinkler M, Kastelan D, Fassnacht M, Beuschlein F, Ambroziak U, Vassiliadi DA, O'Reilly MW, Young WF Jr, Biehl M, Deeks JJ, Arlt W; ENSAT EURINE-ACT Investigators. Urine steroid metabolomics for the differential diagnosis of adrenal incidentalomas in the EURINE-ACT study: a prospective test validation study. *Lancet Diabetes Endocrinol* 2020; **8**: 773-781 [PMID: 32711725 DOI: 10.1016/S2213-8587(20)30218-7]
- Cawood TJ**, Hunt PJ, O'Shea D, Cole D, Soule S. Recommended evaluation of adrenal incidentalomas is costly, has high false-positive rates and confers a risk of fatal cancer that is similar to the risk of the adrenal lesion becoming malignant; time for a rethink? *Eur J Endocrinol* 2009; **161**: 513-527 [PMID: 19439510 DOI: 10.1530/EJE-09-0234]

- 11 **Cho YY**, Suh S, Joung JY, Jeong H, Je D, Yoo H, Park TK, Min YK, Kim KW, Kim JH. Clinical characteristics and follow-up of Korean patients with adrenal incidentalomas. *Korean J Intern Med* 2013; **28**: 557-564 [PMID: 24009451 DOI: 10.3904/kjim.2013.28.5.557]
- 12 **Elhassan YS**, Alahdab F, Prete A, Delivanis DA, Khanna A, Prokop L, Murad MH, O'Reilly MW, Arlt W, Bancos I. Natural History of Adrenal Incidentalomas With and Without Mild Autonomous Cortisol Excess: A Systematic Review and Meta-analysis. *Ann Intern Med* 2019; **171**: 107-116 [PMID: 31234202 DOI: 10.7326/M18-3630]
- 13 **Morelli V**, Reimondo G, Giordano R, Della Casa S, Policola C, Palmieri S, Salcuni AS, Dolci A, Mendola M, Arosio M, Ambrosi B, Scillitani A, Ghigo E, Beck-Peccoz P, Terzolo M, Chiodini I. Long-term follow-up in adrenal incidentalomas: an Italian multicenter study. *J Clin Endocrinol Metab* 2014; **99**: 827-834 [PMID: 24423350 DOI: 10.1210/jc.2013-3527]
- 14 **Falcetta P**, Orsolini F, Benelli E, Agretti P, Vitti P, Di Cosmo C, Tonacchera M. Clinical features, risk of mass enlargement, and development of endocrine hyperfunction in patients with adrenal incidentalomas: a long-term follow-up study. *Endocrine* 2021; **71**: 178-188 [PMID: 32915435 DOI: 10.1007/s12020-020-02476-1]
- 15 **Yilmaz N**, Avsar E, Tazegul G, Sari R, Altunbas H, Balci MK. Clinical Characteristics and Follow-Up Results of Adrenal Incidentaloma. *Exp Clin Endocrinol Diabetes* 2021; **129**: 349-356 [PMID: 31958848 DOI: 10.1055/a-1079-4915]
- 16 **Hannemann A**, Wallaschofski H. Prevalence of primary aldosteronism in patient's cohorts and in population-based studies--a review of the current literature. *Horm Metab Res* 2012; **44**: 157-162 [PMID: 22135219 DOI: 10.1055/s-0031-1295438]
- 17 **Iacobone M**, Citton M, Scarpa M, Viel G, Boscaro M, Nitti D. Systematic review of surgical treatment of subclinical Cushing's syndrome. *Br J Surg* 2015; **102**: 318-330 [PMID: 25640696 DOI: 10.1002/bjs.9742]
- 18 **Park J**, De Luca A, Dutton H, Malcolm JC, Doyle MA. Cardiovascular Outcomes in Autonomous Cortisol Secretion and Nonfunctioning Adrenal Adenoma: A Systematic Review. *J Endocr Soc* 2019; **3**: 996-1008 [PMID: 31065617 DOI: 10.1210/je.2019-00090]
- 19 **Rossi R**, Tauchmanova L, Luciano A, Di Martino M, Battista C, Del Viscovo L, Nuzzo V, Lombardi G. Subclinical Cushing's syndrome in patients with adrenal incidentaloma: clinical and biochemical features. *J Clin Endocrinol Metab* 2000; **85**: 1440-1448 [PMID: 10770179 DOI: 10.1210/jcem.85.4.6515]
- 20 **Vassiliadi DA**, Tsagarakis S. Diagnosis and management of primary bilateral macronodular adrenal hyperplasia. *Endocr Relat Cancer* 2019; **26**: R567-R581 [PMID: 32053747 DOI: 10.1530/ERC-19-0240]
- 21 **Meloche-Dumas L**, Mercier F, Lacroix A. Role of unilateral adrenalectomy in bilateral adrenal hyperplasias with Cushing's syndrome. *Best Pract Res Clin Endocrinol Metab* 2021; **35**: 101486 [PMID: 33637447 DOI: 10.1016/j.beem.2021.101486]
- 22 **Osswald A**, Quinkler M, Di Dalmazi G, Deutschbein T, Rubinstein G, Ritzel K, Zopp S, Bertherat J, Beuschlein F, Reincke M. Long-Term Outcome of Primary Bilateral Macronodular Adrenocortical Hyperplasia After Unilateral Adrenalectomy. *J Clin Endocrinol Metab* 2019; **104**: 2985-2993 [PMID: 30844071 DOI: 10.1210/jc.2018-02204]
- 23 **Xu Y**, Rui W, Qi Y, Zhang C, Zhao J, Wang X, Wu Y, Zhu Q, Shen Z, Ning G, Zhu Y. The role of unilateral adrenalectomy in corticotropin-independent bilateral adrenocortical hyperplasias. *World J Surg* 2013; **37**: 1626-1632 [PMID: 23592061 DOI: 10.1007/s00268-013-2059-9]
- 24 **Oßwald A**, Plomer E, Dimopoulou C, Milian M, Blaser R, Ritzel K, Mickisch A, Knerr F, Stanojevic M, Hallfeldt K, Schopohl J, Kuhn KA, Stalla G, Beuschlein F, Reincke M. Favorable long-term outcomes of bilateral adrenalectomy in Cushing's disease. *Eur J Endocrinol* 2014; **171**: 209-215 [PMID: 24975318 DOI: 10.1530/EJE-14-0214]
- 25 **Szabo Yamashita T**, Sada A, Bancos I, Young WF Jr, Dy BM, Farley DR, Lyden ML, Thompson GB, McKenzie TJ. Differences in outcomes of bilateral adrenalectomy in patients with ectopic ACTH producing tumor of known and unknown origin. *Am J Surg* 2021; **221**: 460-464 [PMID: 32921404 DOI: 10.1016/j.amjsurg.2020.08.047]
- 26 **Thompson SK**, Hayman AV, Ludlam WH, Deveney CW, Loriaux DL, Sheppard BC. Improved quality of life after bilateral laparoscopic adrenalectomy for Cushing's disease: a 10-year experience. *Ann Surg* 2007; **245**: 790-794 [PMID: 17457173 DOI: 10.1097/01.sla.0000251578.03883.2f]
- 27 **Di Dalmazi G**, Berr CM, Fassnacht M, Beuschlein F, Reincke M. Adrenal function after adrenalectomy for subclinical hypercortisolism and Cushing's syndrome: a systematic review of the literature. *J Clin Endocrinol Metab* 2014; **99**: 2637-2645 [PMID: 24878052 DOI: 10.1210/jc.2014-1401]
- 28 **Else T**, Williams AR, Sabolch A, Jolly S, Miller BS, Hammer GD. Adjuvant therapies and patient and tumor characteristics associated with survival of adult patients with adrenocortical carcinoma. *J Clin Endocrinol Metab* 2014; **99**: 455-461 [PMID: 24302750 DOI: 10.1210/jc.2013-2856]
- 29 **Bilimoria KY**, Shen WT, Elaraj D, Bentrem DJ, Winchester DJ, Kebebew E, Sturgeon C. Adrenocortical carcinoma in the United States: treatment utilization and prognostic factors. *Cancer* 2008; **113**: 3130-3136 [PMID: 18973179 DOI: 10.1002/encr.23886]
- 30 **Kebebew E**, Reiff E, Duh QY, Clark OH, McMillan A. Extent of disease at presentation and outcome for adrenocortical carcinoma: have we made progress? *World J Surg* 2006; **30**: 872-878 [PMID: 16680602 DOI: 10.1007/s00268-005-0329-x]
- 31 **Lenders JW**, Duh QY, Eisenhofer G, Gimenez-Roqueplo AP, Grebe SK, Murad MH, Naruse M, Pacak K, Young WF Jr; Endocrine Society. Pheochromocytoma and paraganglioma: an endocrine society clinical practice guideline. *J Clin Endocrinol Metab* 2014; **99**: 1915-1942 [PMID: 24893135 DOI: 10.1210/jc.2014-1498]
- 32 **Kunz PL**, Reidy-Lagunes D, Anthony LB, Bertino EM, Brendtro K, Chan JA, Chen H, Jensen RT, Kim MK, Klimstra DS, Kulke MH, Liu EH, Metz DC, Phan AT, Sippel RS, Strosberg JR, Yao JC; North American Neuroendocrine Tumor Society. Consensus guidelines for the management and treatment of neuroendocrine tumors. *Pancreas* 2013; **42**: 557-577 [PMID: 23591432 DOI: 10.1097/MPA.0b013e31828e34a4]
- 33 **Dahia PL**. Pheochromocytoma and paraganglioma pathogenesis: learning from genetic heterogeneity. *Nat Rev Cancer* 2014; **14**: 108-119 [PMID: 24442145 DOI: 10.1038/nrc3648]
- 34 **Fishbein L**, Leshchiner I, Walter V, Danilova L, Robertson AG, Johnson AR, Lichtenberg TM, Murray BA, Ghayee HK, Else T, Ling S, Jefferys SR, de Cubas AA, Wenz B, Korpershoek E, Amelio AL, Makowski L, Rathmell WK, Gimenez-Roqueplo AP, Giordano TJ, Asa SL, Tischler AS; Cancer Genome Atlas Research Network, Pacak K, Nathanson KL, Wilkerson MD. Comprehensive Molecular Characterization of Pheochromocytoma and Paraganglioma. *Cancer Cell* 2017; **31**: 181-193 [PMID: 28162975 DOI: 10.1016/j.ccell.2017.01.001]
- 35 **Grubbs EG**, Rich TA, Ng C, Bhosale PR, Jimenez C, Evans DB, Lee JE, Perrier ND. Long-term outcomes of surgical treatment for hereditary pheochromocytoma. *J Am Coll Surg* 2013; **216**: 280-289 [PMID: 23317575 DOI: 10.1016/j.jamcollsurg.2012.10.012]
- 36 **Neumann HPH**, Tsoy U, Bancos I, Amodru V, Walz MK, Tirosh A, Kaur RJ, McKenzie T, Qi X, Bandgar T, Petrov R, Yukina MY, Roslyakova A, van der Horst-Schrivers ANA, Berends AMA, Hoff AO, Castroneves LA, Ferrara AM, Rizzati S, Mian C, Dvorakova S, Hasse-Lazar K, Kvachenyuk A, Peczkowska M, Loli P, Erenler F, Krauss T, Almeida MQ, Liu L, Zhu F, Recasens M, Wohllk N, Corssmit EPM, Shafiqullina Z, Calissendorff J, Grozinsky-Glasberg S, Kunavisarut T, Schalin-Jäntti C, Castinetti F, Vlcek P, Beltsevich D, Egorov VI, Schiavi F, Links TP, Lechan RM, Bausch B, Young WF Jr, Eng C; International Bilateral-Pheochromocytoma-Registry Group. Comparison of

- Pheochromocytoma-Specific Morbidity and Mortality Among Adults With Bilateral Pheochromocytomas Undergoing Total Adrenalectomy vs Cortical-Sparing Adrenalectomy. *JAMA Netw Open* 2019; **2**: e198898 [PMID: 31397861 DOI: 10.1001/jamanetworkopen.2019.8898]
- 37 **Maestroni U**, Ferretti S, Ziglioli F, Campobasso D, Cerasi D, Cortellini P. [Laparoscopic adrenalectomy in giant masses]. *Urologia* 2011; **78** Suppl 18: S54-S58 [PMID: 22081417 DOI: 10.5301/RU.2011.8776]
- 38 **Kebebew E**, Siperstein AE, Duh QY. Laparoscopic adrenalectomy: the optimal surgical approach. *J Laparoendosc Adv Surg Tech A* 2001; **11**: 409-413 [PMID: 11814133 DOI: 10.1089/10926420152761941]
- 39 **Anderson KL Jr**, Thomas SM, Adam MA, Pontius LN, Stang MT, Scheri RP, Roman SA, Sosa JA. Each procedure matters: threshold for surgeon volume to minimize complications and decrease cost associated with adrenalectomy. *Surgery* 2018; **163**: 157-164 [PMID: 29122321 DOI: 10.1016/j.surg.2017.04.028]
- 40 **Fischer A**, Schöffski O, Nießen A, Hamm A, Langan EA, Büchler MW, Billmann F. Retroperitoneoscopic adrenalectomy may be superior to laparoscopic transperitoneal adrenalectomy in terms of costs and profit: a retrospective pair-matched cohort analysis. *Surg Endosc* 2023; **37**: 8104-8115 [PMID: 37658201 DOI: 10.1007/s00464-023-10395-1]

Retrospective Study

Application of remimazolam transversus abdominis plane block in gastrointestinal tumor surgery

Jun Liu, Jian-Min Tian, Guo-Ze Liu, Jun-Na Sun, Peng-Fei Gao, Yong-Qiang Zhang, Xiu-Qin Yue

Specialty type: Oncology**Provenance and peer review:**

Unsolicited article; Externally peer reviewed.

Peer-review model: Single blind**Peer-review report's scientific quality classification**

Grade A (Excellent): 0

Grade B (Very good): B

Grade C (Good): C

Grade D (Fair): 0

Grade E (Poor): 0

P-Reviewer: Seeneevassen L, France; Vidal AF, Brazil**Received:** September 21, 2023**Peer-review started:** September 21, 2023**First decision:** October 9, 2023**Revised:** October 26, 2023**Accepted:** November 25, 2023**Article in press:** November 25, 2023**Published online:** December 15, 2023**Jun Liu, Jian-Min Tian, Guo-Ze Liu, Jun-Na Sun, Peng-Fei Gao, Yong-Qiang Zhang, Xiu-Qin Yue,** Department of Anesthesiology and Perioperative Medicine, The First Affiliated Hospital of Xinxiang Medical University, Weihui 453100, Henan Province, China**Corresponding author:** Jun Liu, MM, Doctor, Department of Anesthesiology and Perioperative Medicine, The First Affiliated Hospital of Xinxiang Medical University, No. 88 Jiankang Road, Weihui 453100, Henan Province, China. t604au@126.com**Abstract****BACKGROUND**

Transversus abdominis plane block (TAPB) is a block of the abdominal afferent nerve fibers between the internal oblique muscle and the transverse abdominal muscle achieved with local anesthetics. It can effectively block the conduction of the anterior nerve of the abdominal wall and exert a good analgesic effect. However, the effect of combining the block with remimazolam on anesthesia in patients undergoing gastrointestinal tumor surgery is still unclear.

AIM

To examine the effects of combining TAPB with remimazolam on the stress response and postoperative recovery of gastrointestinal tumor surgery patients.

METHODS

A retrospective analysis was conducted on the clinical data of 102 individuals diagnosed with gastrointestinal malignancies who underwent laparoscopic surgery under general anesthesia between April 2020 and June 2023. The patients were categorized into a control group ($n = 51$), receiving remimazolam for general anesthesia, and an observation group ($n = 51$), receiving TAPB combined with remimazolam for general anesthesia. A comparison was made between both groups in terms of hemodynamic parameters, stress markers, pain levels, recovery quality, analgesic effects, and adverse reactions during the perioperative period.

RESULTS

The observation group had significantly higher heart rates at time points 1 min after induction and upon leaving the operating room than the control group ($P < 0.05$). The mean arterial pressure at time point T1 in the observation group was significantly higher than that in the control group ($P < 0.05$). Five minutes after extubation, the levels of the hormones adrenaline and noradrenaline in the observation group were considerably lower than those in the control group ($P <$

0.05). At 12 h, 24 h, and 48 h following surgery, the visual analog scale scores of the observation group were considerably lower than those of the control group ($P < 0.05$). The observation group had shorter awakening and extubation times and lower Riker sedation-agitation scale scores than the control group ($P < 0.05$). The observation group exhibited considerably fewer effective pump presses, lower fentanyl dosages, and lower incidences of rescue analgesia within 24 h following surgery than the control group ($P < 0.05$).

CONCLUSION

The application effect of TAPB combined with remimazolam general anesthesia in anesthesia of patients undergoing gastrointestinal tumor surgery is good, which is helpful to promote faster recovery after operation.

Key Words: Transversus abdominis plane block; Remimazolam; General anesthesia; Gastrointestinal tumor surgery; Stress response

©The Author(s) 2023. Published by Baishideng Publishing Group Inc. All rights reserved.

Core Tip: Stress can lead to severe changes in hemodynamics during surgery and increase the risk of postoperative adverse events. In this study, the application value of transversus abdominis plane block (TAPB) combined with remimazolam general anesthesia in patients undergoing gastrointestinal tumor surgery was observed. The results showed that the application of TAPB combined with remimazolam general anesthesia had the advantages of stable anesthesia induction and small hemodynamic fluctuation, which was helpful to reduce the acute stress response of patients undergoing gastrointestinal tumor surgery and improve the quality of recovery.

Citation: Liu J, Tian JM, Liu GZ, Sun JN, Gao PF, Zhang YQ, Yue XQ. Application of remimazolam transversus abdominis plane block in gastrointestinal tumor surgery. *World J Gastrointest Oncol* 2023; 15(12): 2101-2110

URL: <https://www.wjgnet.com/1948-5204/full/v15/i12/2101.htm>

DOI: <https://dx.doi.org/10.4251/wjgo.v15.i12.2101>

INTRODUCTION

The gastrointestinal tract includes the stomach, duodenum, jejunum, ileum, cecum, colon, and rectum. Gastrointestinal tumors are the most common digestive tract tumors worldwide. Based on statistical data[1], gastric cancer is the second most prominent cause of cancer death in China, following lung cancer. Recently, there has been a notable increase in the occurrence of colorectal cancer, resulting in its inclusion among the five most prevalent forms of cancer. Since most gastrointestinal tumor patients have subtle symptoms in the early stages of the disease and are usually diagnosed at an intermediate or advanced stage, timely surgical intervention is necessary to control disease progression[2] before distant metastasis. Due to its minimal invasiveness, reduced pain, and faster recovery, laparoscopic surgery has been widely used in treating gastrointestinal tumors. However, carbon dioxide (CO₂) pneumoperitoneum is established during laparoscopic surgery, increasing intra-abdominal pressure. When the intra-abdominal pressure drops suddenly, it can lead to ischemia-reperfusion injury and a stress response, and the change in surgical position will also affect the body's homeostasis, causing severe postoperative pain and adversely affecting the patient's recovery[3]. Prior research has demonstrated that stress conditions can potentially augment the production and release of cortisol, epinephrine (E), norepinephrine (NE), and blood glucose in individuals. The drastic changes in hemodynamics can increase the risk of adverse events postoperatively, significantly affecting the effectiveness of surgical treatment and postoperative recovery [4]. Therefore, a reasonable anesthesia approach reduces stress responses during laparoscopic surgery and promotes faster postoperative recovery.

Transversus abdominis plane block (TAPB) provides regional anesthesia by effectively blocking the sensory nerve fibers within the abdominal cavity, explicitly targeting the area between the internal oblique and transverse abdominis muscles. It can effectively block the transmission of the anterior abdominal wall nerves, thus providing analgesic effects [5]. The relevant literature has shown that remimazolam can be safely and effectively used in outpatient gastrointestinal endoscopy and bronchoscopy. Its successful sedation rate is similar to that of propofol, but it is significantly safer. It can be used for anesthesia induction and maintenance[6]. There are few reports on the use of TAPB combined with remimazolam in laparoscopic surgery for the treatment of gastrointestinal tumors. The primary objective of this study was to examine the effects of the combination of TAPB and remimazolam for anesthesia on the stress responses and postoperative recovery of individuals undergoing gastrointestinal tumor surgery. The findings of this study can be used to establish a theoretical foundation for the prevention or reduction of stress responses in patients, as well as to provide evidence-based choices for clinical anesthesia.

MATERIALS AND METHODS

Subjects and methods

Study subjects: Medical information from a cohort of 104 patients diagnosed with gastrointestinal malignancies and who underwent laparoscopic surgery under general anesthesia at our institution from April 2021 to June 2023 was retrospectively acquired. The criteria for inclusion are outlined below: Confirmed diagnosis of gastrointestinal tumors; being suitable for laparoscopic surgery; American Society of Anesthesiologists classification II-III; 18-65 years old; and complete medical records. Patients with incomplete case data were excluded. In this study, the clinical data of 104 patients with gastrointestinal tumors who underwent laparoscopic surgery under general anesthesia were reviewed, including 52 patients in the observation group and 52 patients in the control group. In the observation group, 1 patient without gastrointestinal tumors was excluded; in the control group, 1 patient was excluded due to missing intraoperative hemodynamic data. Finally, 51 patients in the observation group and 51 patients in the control group were included in the statistical analysis. All participants submitted informed consent forms, and the study methodology followed the Helsinki Declaration.

Anesthesia methods

Preanesthetic preparation: All patients underwent relevant examinations preoperatively and were advised to fast for 6-8 h before surgery. Upon arrival to the operating room, peripheral intravenous access was established, and routine monitoring of the heart rate (HR), bispectral index (BIS), respiratory rate (RR), oxygen saturation, mean arterial pressure (MAP), and electrocardiography was commenced.

Anesthesia methods: Anesthesia Induction: The following drugs were sequentially administered intravenously for anesthesia induction: Remimazolam (0.2 mg/kg), cisatracurium (0.2-0.4 mg/kg), and sufentanil (0.4-0.6 µg/kg). After the BIS value fell below 60 and appropriate conditions for endotracheal intubation were ascertained, tracheal intubation was executed. Subsequently, the anesthetic device was attached to facilitate controlled respiration. The tidal volume was set at 8-10 mL/kg, the RR at 12-14 breaths per min, and the inspiratory-expiratory ratio at 1:2. During the surgery, respiratory parameters were adjusted to maintain the end-tidal carbon dioxide pressure-CO₂ between 30-40 mmHg. In the observation group, bilateral TAPB was performed 5 min after anesthesia induction by the side entry method. A linear ultrasound probe guided the needle into the transversus abdominis plane. The ultrasonic probe was positioned at a right angle to the anterior axillary line, within the space bounded by the iliac crest and the costal edge on one side. The probe was then adjusted until the three distinct muscles of the transverse abdominal muscle group were discernible. When the needle tip reached the plane of the transverse fascia of the abdomen, it was drawn back to confirm that there was no blood or air. Ropivacaine (20 mL of 0.375%) was injected into the fascial sheath between the internal oblique and transverse abdominalis muscles to obtain spindle-shaped hypoechoic images. The same procedure was repeated on the other side to complete the bilateral TAPB. The control group received only remimazolam.

Anesthesia maintenance: Intravenous remimazolam 0.4-1.2 mg/kg/h was administered, while cisatracurium was injected at a rate of 0.1 mg/kg/h. On the other hand, sufentanil 6-12 µg/kg/h was provided intravenously. The dosage of anesthetic drugs was adjusted based on the patient's BIS, MAP, and HR. The BIS value was maintained between 40-60. Atropine (0.3-0.5 mg) was administered if the patient's HR dropped below 50 beats per min, and esmolol (0.5 mg/kg) was administered if the HR exceeded 100 beats per min. Drugs were readministered if necessary.

Flurbiprofen (50 mg) was administered for postoperative analgesia during skin closure, and all patients received patient-controlled intravenous analgesia (PCIA) after surgery. The PCIA scheme consisted of sufentanil 100 µg, flurbiprofen 200 mg, and ondansetron hydrochloride 32 mg, mixed in a total volume of 100 mL. The initial infusion rate was set at 2 mL/h, followed by a self-controlled infusion rate of 1.5 mL/h. The maximum self-controlled infusion rate allowed was 8 mL/h, with a lockout period of 20 min. After the surgical procedure, the individuals were sent to the postanesthesia care unit (PACU) for observation and recovery. Tracheal extubation was successfully performed in all patients, and they were then moved back to the ward.

Observational parameters

(1) Hemodynamics comparison: MAP and HR were compared at different time points, including upon leaving the operating room (T3), immediately after tracheal intubation (T2), 1 min after induction (T1), and before anesthesia induction (T0); (2) Stress response: Blood samples were obtained from the radial artery of patients at two specific time points: 10 min before the introduction of anesthesia and 5 min following extubation. The concentrations of plasma NE and E were measured using an enzyme-linked immunosorbent assay; (3) Pain intensity: Pain intensity in both groups was evaluated at 4, 12, 24, and 48 h post surgery using the visual analog scale (VAS). The scores ranged from 0 to 10, with higher values denoting greater pain intensity; (4) Recovery quality: Recorded parameters included time to eye-opening, time to extubation, PACU stay duration, and Riker sedation-agitation score assessed at extubation. A Riker score ≥ 5 indicated agitation at extubation; and (5) Safety: The examiners monitored the number of successful activations of the Patient-Controlled Analgesia (PCA) pump, the amount of sufentanil administered, and the frequency of rescue analgesic administrations during the 24 h following the surgical procedure. The occurrence rates of vomiting, nausea, pruritus, and respiratory depression were compared between the two groups within 48 h after surgery.

Statistical analysis

We used SPSS 22.0 software to analyze the data. The measured information is presented as the mean \pm SD, and we compared them using *t* tests. Count data are expressed as numbers or percentages and were compared using chi-square

tests. The chi-square value was corrected if the theoretical frequency was ≤ 5 but ≥ 1 . Fisher's exact test was used if the theoretical frequency was < 1 . A P value less than 0.05 is indicative of a statistically significant difference.

RESULTS

A comparative analysis of the baseline characteristics between the two groups

Between the observation and control groups, there was no statistically significant variation in sex, age, or any other baseline characteristics ($P > 0.05$, Table 1).

A Comparison of both groups' HRs at various time points

The two groups had no significant differences in HR at the T0 and T2 time points ($P > 0.05$). Nevertheless, the observation group displayed substantially higher HRs at the T1 and T3 time points than the control group ($P > 0.05$, Table 2, Figure 1).

Comparison of MAP at different time points between the two groups

No statistically significant variation was observed in the MAP between the two categories at the T0, T2, and T3 time points ($P > 0.05$). Nevertheless, the MAP at the T1 time point exhibited a statistically significant elevation in the observation group compared to the control ($P < 0.05$, Table 3, Figure 2).

A comparative analysis of stress parameter levels at various time points between both groups

No statistically significant variations were observed in the levels of E and NE at 10 min prior to anesthesia induction between the two groups ($P > 0.05$). Nevertheless, the E and NE levels 5 min after extubation exhibited a notable decrease in the observation group compared to the control group ($P < 0.05$, Table 4).

VAS scores at various intervals following surgery in both groups

No statistically significant differences were observed in the VAS score between the two groups at the 4-h point following the surgical procedure ($P > 0.05$). Nevertheless, the VAS scores recorded at 12, 24, and 48 h post surgery showed a statistically significant decrease in the observation group ($P < 0.05$, Table 5, Figure 3).

Comparison of recovery quality in both groups

There were no statistically significant differences in the duration of PACU stay between the two groups, as indicated by a P value greater than 0.05. The observation group exhibited a significantly shorter eye-opening and time to extubation time than the control group. Additionally, the observation group had a substantially lower Riker sedation-agitation score ($P < 0.05$, Table 6).

Comparison of the postoperative analgesic situation within 24 h between the two groups

The observation group exhibited significantly lower effective PCA presses and sufentanil consumption within 24 h post surgery than the control group. Additionally, the observation group had a substantially lower number of cases requiring rescue analgesia ($P < 0.05$, Table 7).

Comparative analysis of the postoperative adverse effect frequency in the two cohorts

No statistically significant disparity was observed in the occurrence of postoperative nausea, vomiting, itching, or other unpleasant responses when comparing the two groups ($P > 0.05$, Table 8).

DISCUSSION

As the proportion of aging adults increases, the incidence of gastrointestinal tumors has been increasing yearly. Although laparoscopic surgery can prolong the survival time of patients, factors such as CO₂ pneumoperitoneum and positional changes during surgery can disturb the body's homeostasis, leading to stress responses and causing severe postoperative pain that significantly affects surgical outcomes and postoperative recovery. Research has shown that administering various anesthetic medications during the perioperative phase substantially influences the stress reactions exhibited by patients under general anesthesia. Propofol is currently the most widely used intravenous anesthetic drug worldwide. However, it has apparent inhibitory effects on circulatory and respiratory functions, which can lead to hemodynamic fluctuations during surgery. Long-term use of propofol has drawbacks, such as drug residue, especially in patients with poor cardiovascular function or the elderly[7,8]. Remimazolam, a new type of benzodiazepine sedative-hypnotic drug, has the advantages of rapid metabolism, no residual effects, and minimal impact on respiration and circulation. It has been well applied in short and outpatient surgeries and is expected to be an anesthetic drug for reducing patient stress responses. Phase IIb/III trial results comparing propofol and remimazolam demonstrated that patients who received remimazolam had a lower incidence of adverse cardiovascular events such as bradycardia and hypotension than those who received propofol, confirming the safety and efficacy of remimazolam[9]. However, the analgesic and sedative effects of remimazolam alone are similar to those of propofol. Thus, additional anesthetics must be combined with remimazolam to improve the analgesic and soothing effects, further reduce the intraoperative stress response, and

Table 1 An examination of the differences in the two groups' baseline features

Group	<i>n</i>	Sex (male/female, cases)	Age (yr, mean ± SD)	BMI (kg/m ² , mean ± SD)	Surgical time, (min, mean ± SD)	ASA classification (I/II/III, cases)
Observation group	51	33/18	49.58 ± 11.29	23.64 ± 1.54	216.15 ± 29.33	9/31/11
Control group	51	30/21	49.24 ± 11.58	23.28 ± 1.69	208.48 ± 31.67	12/33/6
<i>t/χ²</i>		0.374	0.150	1.124	1.269	1.962
<i>P</i> value		0.541	0.881	0.264	0.207	0.375

ASA: American Society of Anesthesiologists.

Table 2 Comparison of heart rate between the groups at various time points (beats per min, mean ± SD)

Group	<i>n</i>	T0	T1	T2	T3
Observation group	51	77.37 ± 11.49	76.85 ± 10.18	75.69 ± 9.84	77.12 ± 10.15
Control group	51	77.84 ± 11.25	71.54 ± 8.74	74.55 ± 9.62	72.61 ± 9.78
<i>t/χ²</i>		0.209	2.826	0.592	2.285
<i>P</i> value		0.835	0.006	0.555	0.024

T0: Before anesthesia induction; T1: 1 min after induction; T2: Immediately after tracheal intubation; T3: Upon leaving the operating room.

Table 3 A comparative analysis of mean arterial pressure at various time intervals within the groups (mmHg, mean ± SD)

Group	<i>n</i>	T0	T1	T2	T3
Observation group	51	96.54 ± 11.59	93.18 ± 10.27	91.48 ± 10.18	91.02 ± 10.23
Control group	51	96.11 ± 11.74	82.54 ± 9.85	90.22 ± 10.09	89.25 ± 9.58
<i>t/χ²</i>		0.259	3.834	0.628	0.902
<i>P</i> value		0.796	< 0.001	0.532	0.369

T0: Before anesthesia induction; T1: 1 min after induction; T2: Immediately after tracheal intubation; T3: Upon leaving the operating room.

Table 4 Shows a comparison of the stress parameter levels of the two groups at various time points (μmol/L, mean ± SD)

Group	<i>n</i>	E		NE	
		10 min before anesthesia induction	5 min after extubation	10 min before anesthesia induction	5 min after extubation
Observation group	51	0.45 ± 0.11	0.59 ± 0.15	3.19 ± 0.57	3.97 ± 0.45
Control group	51	0.43 ± 0.16	0.94 ± 0.09 ^a	3.14 ± 0.61	4.75 ± 0.63 ^a
<i>t/χ²</i>		0.736	14.289	0.428	7.195
<i>P</i> value		0.464	0.881	0.670	0.207

^a*P* < 0.05. Compared with 10 min before anesthesia induction in the same group. E: Epinephrine; NE: Norepinephrine.

stabilize hemodynamics during the perioperative period.

The TAPB technique requires the administration of local anesthetics into the fascial gap across the transversus abdominis muscle and the internal oblique. This action effectively obstructs the abdominal wall nerves traversing this specific plane, hence inducing regional nerve block and analgesic effects on the anterior-lateral abdominal wall[10]. The TAPB technique blocks pain signal transmission by acting on the peripheral nerves and nerve fibers in the transversus

Table 5 Evaluation of visual analog scale scores between both groups at different time points following surgery (score, mean ± SD)

Group	n	4 h following surgery	12 h following surgery	24 h following surgery	48 h following surgery
Observation group	51	3.65 ± 0.58	2.74 ± 0.47	1.97 ± 0.53	1.02 ± 0.41
Control group	51	3.87 ± 0.62	3.29 ± 0.23	2.54 ± 0.47	1.65 ± 0.32
t/ χ^2		1.851	7.506	5.746	8.651
P value		0.067	< 0.001	< 0.001	< 0.001

Table 6 Comparison of recovery quality between the two groups (mean ± SD)

Group	n	Time to eye-opening	Time to extubation	PACU stay duration	Riker sedation-agitation score (score)
Observation group	51	18.12 ± 6.52	22.34 ± 8.31	37.54 ± 7.49	4.02 ± 1.33
Control group	51	23.25 ± 4.89	28.92 ± 6.54	38.12 ± 8.74	4.73 ± 0.82
t/ χ^2		4.495	4.444	0.360	3.245
P value		< 0.001	< 0.001	0.720	0.002

PACU: Postanesthesia care unit.

Table 7 Comparison of postoperative analgesic effect within 24 h between the two groups

Group	n	Number of effective PCA presses within 24 h after surgery (mean ± SD)	Sufentanil consumption (μ g, mean ± SD)	Number of rescue analgesia cases (cases)
Observation group	51	3.52 ± 1.26	57.31 ± 5.82	3
Control group	51	6.11 ± 1.82	67.84 ± 4.37	13
χ^2		8.356	10.332	7.413
P value		< 0.001	< 0.001	0.007

PCA: Patient-controlled analgesia.

Table 8 Comparison of nausea and vomiting, skin itching, respiratory depression and hypotension between the two groups

Group	n	Nausea and vomiting	Skin itching	Respiratory depression	Hypotension
Observation group	51	3	0	0	0
Control group	51	5	0	2	0
χ^2		0.543	-	2.040	-
P value		0.461	-	0.153	-

abdominis plane, reducing postoperative pain perception. Moreover, TAPB can impede the transmission of nerve signals within the transversus abdominis plane, encompassing the intercostal nerves, inguinal nerves, and rectus abdominis nerves, consequently leading to the mitigation of pain postoperatively[11]. In recent years, with the continuous development of ultrasound-guided techniques, ultrasound-guided TAPB has been proven to effectively enhance the accuracy of needle insertion and enhance the analgesic and sedative effects of the blockade. Numerous studies have shown that TAPB can significantly alleviate postoperative pain and reduce opioid-related side effects, promoting postoperative recovery[12,13]. The present study investigated the use of TAPB combined with remimazolam in individuals undergoing laparoscopic surgery for gastrointestinal malignancies. The study's findings indicate a statistically significant increase in HR at both T1 and T3 in the observation group compared to the control group. This suggests that the combination of TAPB and remimazolam is effective in maintaining stable hemodynamics during surgery while exerting fewer inhibitory effects on the circulatory system than remimazolam alone.

The hypothalamic-pituitary-adrenal axis is the primary mechanism mediating the acute stress response in the body. When sympathetic activation occurs during the perioperative period due to surgical trauma, fear and anxiety, or hyperthermia, corticosteroid and catecholamine secretion, such as cortisol and E/NE, increases. The clinical manifest-

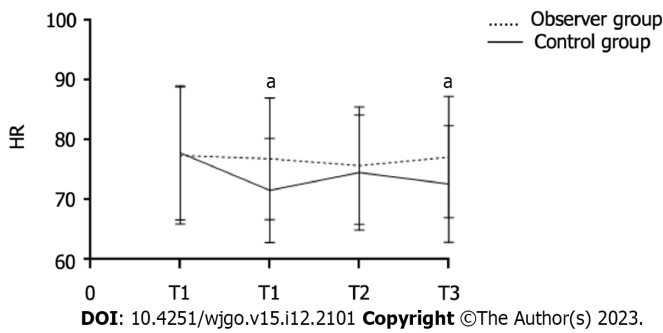


Figure 1 A Comparison of both groups' heart rates at various time points. ^a*P* < 0.05. HR: Heart rate; T1: 1 min after induction; T2: Immediately after tracheal intubation; T3: Upon leaving the operating room.

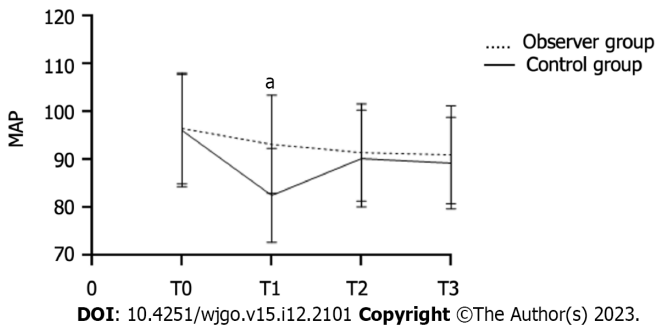


Figure 2 Comparison of mean arterial pressure at different time points between the two groups. ^a*P* < 0.05. MAP: Mean arterial pressure; T0: Before anesthesia induction; T1: 1 min after induction; T2: Immediately after tracheal intubation; T3: Upon leaving the operating room.

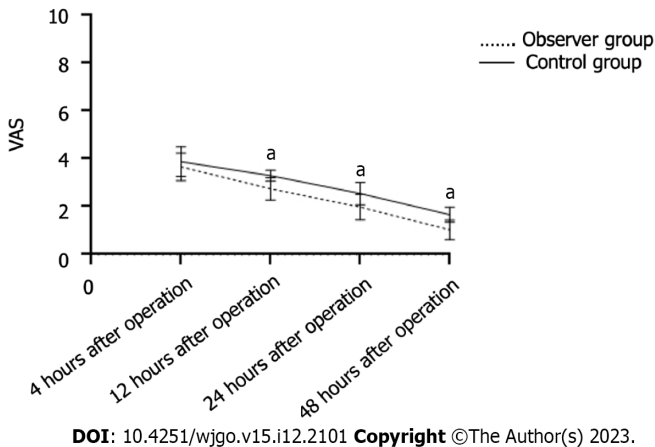


Figure 3 Visual analog scale scores at various intervals following surgery in both groups. ^a*P* < 0.05. VAS: Visual analog scale.

ations include hemodynamic fluctuations, increased myocardial oxygen consumption, changes in RR and increased metabolic rates. In severe cases, internal environment disturbances, acid-base imbalances, and even arrhythmias can occur[14,15]. The outcomes of the present study demonstrated a significant decrease in E and NE levels 5 min following extubation in the observation group compared to the control group. This suggests that the combination of TAPB and remimazolam may be more effective in mitigating patient stress responses than remimazolam alone.

The Riker Sedation-Agitation Scale was proposed by Riker in 1999 and is mainly used to assess the level of agitation during the recovery phase in patients undergoing treatment under general anesthesia. It has higher reliability and authenticity in evaluating the awakening status of mechanically ventilated patients compared to the widely used Ramsay Sedation Scale[16,17]. The present study's findings indicate that the time to eye opening and extubation was significantly shorter in the observation group than in the control group. The Riker sedation agitation score was notably lower in the observation group. Additionally, the VAS scores at 12, 24, and 48 h after surgery were significantly lower in the observation group, indicating that TAPB combined with remimazolam provides good analgesic and sedative effects, improves patient comfort during anesthesia recovery, and has a positive impact on improving the quality of recovery. In addition, compared to the control group, the observation group exhibited fewer PCA pump pushes and less sufentanil

intake during the 24 h following surgery. The number of patients requiring rescue analgesia was considerably lower in the observation group, providing additional evidence to support the effective analgesic outcome of TAPB combined with remimazolam for postoperative pain control.

CONCLUSION

TAPB combined with remimazolam can improve the hemodynamic stability of patients undergoing gastrointestinal tumor surgery, reduce the stress response, and promote postoperative recovery. This study has limitations, that is, the sample size is limited and only focuses on patients undergoing gastrointestinal tumor surgery. In the future, the sample size will be expanded to analyze the potential benefits of the combination of TAPB and remimazolam.

ARTICLE HIGHLIGHTS

Research background

Carbon dioxide pneumoperitoneum will be established in patients with gastrointestinal tumors during laparoscopic surgery, resulting in intra-abdominal hypertension, which is easy to cause stress response. At the same time, the change of posture will also aggravate the stress response, which will seriously affect the effect of surgical treatment and postoperative rehabilitation. Therefore, it is of great significance to adopt a reasonable anesthesia method to promote the postoperative recovery of patients. Transversus abdominis plane block (TAPB) can effectively block the conduction of the anterior nerve of the abdominal wall, resulting in analgesic effect. The success rate of remifentanyl analgesia is similar to that of propofol, and the safety is significantly better than that of propofol. It can be used in the induction and maintenance of general anesthesia. The combination of TAPB and remimazolam and remimazolam can provide a basis for the anesthetic regimen to reduce the stress response of laparoscopic patients with gastrointestinal tumors.

Research motivation

The use of different anesthetics during the perioperative period of gastrointestinal tumors has an important impact on the stress response caused by general anesthesia. In the past, propofol was mostly used, but its obvious inhibition of circulatory and respiratory function can easily lead to intraoperative hemodynamic fluctuations. In addition, the change of intraoperative position can easily lead to stress response in patients, causing severe postoperative pain, which has a serious impact on the surgical effect and postoperative recovery. Remimazolam has the advantages of fast metabolism, no residue and little influence on respiration and circulation. However, the analgesic and sedative effects of simple application of remifentanyl general anesthesia are similar to those of propofol. Therefore, it is necessary to combine the application of TAPB on the basis of remifentanyl general anesthesia to improve the analgesic effect. It is expected to become an important anesthetic and analgesic scheme for laparoscopic surgery of gastrointestinal tumors in the future.

Research objectives

This study mainly discussed the effect of TAPB combined with remimazolam general anesthesia on stress response and postoperative recovery in patients undergoing gastrointestinal tumor surgery. The results showed that the application of TAPB combined with remimazolam general anesthesia in gastrointestinal tumor surgery had the advantages of stable anesthesia induction, small hemodynamic fluctuation, low incidence of cardiovascular events, fast postoperative recovery and less agitation. It is helpful to reduce acute stress response, improve the quality of recovery, and the level of analgesia and sedation can meet the needs of surgery. In the future, it can be used as an anesthesia and analgesia program for patients undergoing laparoscopic surgery for gastrointestinal tumors.

Research methods

In this study, the clinical data of patients with gastrointestinal tumors who underwent laparoscopic surgery under general anesthesia were retrospectively analyzed. The patients were grouped according to different anesthesia schemes, and the hemodynamics, stress response and recovery quality of the observation group and the control group were compared. The data were analyzed by SPSS22.0 software to further clarify the application value of TAPB combined with remimazolam general anesthesia in patients undergoing gastrointestinal tumor surgery.

Research results

This study further clarified that TAPB combined with remimazolam general anesthesia can effectively alleviate the stress response of patients undergoing gastrointestinal tumor surgery. The level of analgesia and sedation is good, the intraoperative hemodynamic fluctuation is small, and the quality of recovery is good. However, this study is a retrospective analysis, and it is impossible to analyze the long-term effects of this anesthesia program and its application effect in other operations. In the future, the sample size will be further expanded to explore the application value of this anesthesia program.

Research conclusions

The application of TAPB combined with remifentanyl general anesthesia in gastrointestinal tumor surgery has the

advantages of stable anesthesia induction, small hemodynamic fluctuations, low incidence of cardiovascular events, rapid postoperative recovery and less agitation. It is helpful to reduce acute stress response, improve the quality of recovery, and the level of analgesia and sedation can meet the needs of surgery.

Research perspectives

In the future, the sample size will be expanded to explore the application value of TAPB combined with remifentanyl general anesthesia in other types of laparoscopic surgery anesthesia.

FOOTNOTES

Author contributions: Liu J, Tian JM, and Liu GZ initiated the project, Tian JM and Sun JN designed the experiment and conducted clinical data collection; Liu GZ and Gao PF performed postoperative follow-up and recorded data; Liu J, Sun JN, and Gao PF conducted a number of collation and statistical analysis, and wrote the original manuscript; Liu J, Zhang YQ and Yue XQ reviewed and approved the paper; all authors have read and approved the final manuscript.

Institutional review board statement: The study was reviewed and approved by the Institutional Review Board at First Affiliated Hospital of Xinxiang Medical University.

Informed consent statement: As the study used anonymous and pre-existing data, the requirement for the informed consent from patients was waived.

Conflict-of-interest statement: The authors declare that they have no conflict of interest.

Data sharing statement: No additional data are available.

Open-Access: This article is an open-access article that was selected by an in-house editor and fully peer-reviewed by external reviewers. It is distributed in accordance with the Creative Commons Attribution NonCommercial (CC BY-NC 4.0) license, which permits others to distribute, remix, adapt, build upon this work non-commercially, and license their derivative works on different terms, provided the original work is properly cited and the use is non-commercial. See: <https://creativecommons.org/licenses/by-nc/4.0/>

Country/Territory of origin: China

ORCID number: Jun Liu [0009-0004-2965-8663](https://orcid.org/0009-0004-2965-8663).

S-Editor: Qu XL

L-Editor: A

P-Editor: Zhang XD

REFERENCES

- Gao K, Wu J. National trend of gastric cancer mortality in China (2003-2015): a population-based study. *Cancer Commun (Lond)* 2019; **39**: 24 [PMID: [31046840](https://pubmed.ncbi.nlm.nih.gov/31046840/) DOI: [10.1186/s40880-019-0372-x](https://doi.org/10.1186/s40880-019-0372-x)]
- Chen QY, Zhong Q, Liu ZY, Huang XB, Que SJ, Zheng WZ, Li P, Zheng CH, Huang CM. Advances in laparoscopic surgery for the treatment of advanced gastric cancer in China. *Eur J Surg Oncol* 2020; **46**: e7-e13 [PMID: [32709375](https://pubmed.ncbi.nlm.nih.gov/32709375/) DOI: [10.1016/j.ejso.2020.07.015](https://doi.org/10.1016/j.ejso.2020.07.015)]
- Hyung WJ, Yang HK, Park YK, Lee HJ, An JY, Kim W, Kim HI, Kim HH, Ryu SW, Hur H, Kim MC, Kong SH, Cho GS, Kim JJ, Park DJ, Ryu KW, Kim YW, Kim JW, Lee JH, Han SU; Korean Laparoendoscopic Gastrointestinal Surgery Study Group. Long-Term Outcomes of Laparoscopic Distal Gastrectomy for Locally Advanced Gastric Cancer: The KLASS-02-RCT Randomized Clinical Trial. *J Clin Oncol* 2020; **38**: 3304-3313 [PMID: [32816629](https://pubmed.ncbi.nlm.nih.gov/32816629/) DOI: [10.1200/JCO.20.01210](https://doi.org/10.1200/JCO.20.01210)]
- Munteanu A, Munteanu D, Iancu M, Lupan I, Samasca G, Aldea C, Mocan T, Iancu C. Assessing immunological and surgical stress markers in patients undergoing digestive surgery for pancreatic, hepatic, and gastric tumors. *Journal of B.U.ON: official journal of the Balkan Union of Oncology* 2018; **23**: 1655 [DOI: [10.1016/j.pan.2016.05.331](https://doi.org/10.1016/j.pan.2016.05.331)]
- Peltrini R, Cantoni V, Green R, Greco PA, Calabria M, Bucci L, Corcione F. Efficacy of transversus abdominis plane (TAP) block in colorectal surgery: a systematic review and meta-analysis. *Tech Coloproctol* 2020; **24**: 787-802 [PMID: [32253612](https://pubmed.ncbi.nlm.nih.gov/32253612/) DOI: [10.1007/s10151-020-02206-9](https://doi.org/10.1007/s10151-020-02206-9)]
- Dai G, Pei L, Duan F, Liao M, Zhang Y, Zhu M, Zhao Z, Zhang X. Safety and efficacy of remimazolam compared with propofol in induction of general anesthesia. *Minerva Anesthesiol* 2021; **87**: 1073-1079 [PMID: [34263581](https://pubmed.ncbi.nlm.nih.gov/34263581/) DOI: [10.23736/S0375-9393.21.15517-8](https://doi.org/10.23736/S0375-9393.21.15517-8)]
- Tang S, Lu J, Xu C, Wei L, Mei S, Chen R, Meng QT. Feasibility and Safety of Remazolam versus Propofol When Inserting Laryngeal Masks Without Muscle Relaxants During Hysteroscopy. *Drug Des Devel Ther* 2023; **17**: 1313-1322 [PMID: [37152102](https://pubmed.ncbi.nlm.nih.gov/37152102/) DOI: [10.2147/DDDT.S408584](https://doi.org/10.2147/DDDT.S408584)]
- Liu G, Xiong Y. Analysis of Stress Response and Analgesic Effect of Remazolam Combined with Etomidate in Painless Gastroenteroscopy. *Contrast Media Mol Imaging* 2022; **2022**: 4863682 [PMID: [35992545](https://pubmed.ncbi.nlm.nih.gov/35992545/) DOI: [10.1155/2022/4863682](https://doi.org/10.1155/2022/4863682)]
- Doi M, Morita K, Takeda J, Sakamoto A, Yamakage M, Suzuki T. Efficacy and safety of remimazolam versus propofol for general anesthesia: a multicenter, single-blind, randomized, parallel-group, phase IIb/III trial. *J Anesth* 2020; **34**: 543-553 [PMID: [32417976](https://pubmed.ncbi.nlm.nih.gov/32417976/) DOI: [10.1007/s00540-020-02788-6](https://doi.org/10.1007/s00540-020-02788-6)]
- Tran DQ, Bravo D, Leurcharusmee P, Neal JM. Transversus Abdominis Plane Block: A Narrative Review. *Anesthesiology* 2019; **131**: 1166-

- 1190 [PMID: 31283738 DOI: 10.1097/ALN.0000000000002842]
- 11 **Kamel AAF**, Amin OAI, Ibrahim MAM. Bilateral Ultrasound-Guided Erector Spinae Plane Block Versus Transversus Abdominis Plane Block on Postoperative Analgesia after Total Abdominal Hysterectomy. *Pain Physician* 2020; **23**: 375-382 [PMID: 32709172 DOI: 10.36076/ppj.2020/23/375]
- 12 **Liu KY**, Lu YJ, Lin YC, Wei PL, Kang YN. Transversus abdominis plane block for laparoscopic colorectal surgery: A meta-analysis of randomised controlled trials. *Int J Surg* 2022; **104**: 106825 [PMID: 35953018 DOI: 10.1016/j.ijssu.2022.106825]
- 13 **Emile SH**, Elfeki H, Elbahrawy K, Sakr A, Shalaby M. Ultrasound-guided versus laparoscopic-guided subcostal transversus abdominis plane (TAP) block versus No TAP block in laparoscopic cholecystectomy; a randomized double-blind controlled trial. *Int J Surg* 2022; **101**: 106639 [PMID: 35487422 DOI: 10.1016/j.ijssu.2022.106639]
- 14 **Aly A**, Gouda J, Awadein A, Soliman HM, El-Fayoumi D. Serum cortisol and adrenocorticotrophic hormone (ACTH) in infants receiving topical and subconjunctival corticosteroids following cataract surgery. *Graefes Arch Clin Exp Ophthalmol* 2021; **259**: 3159-3165 [PMID: 33959809 DOI: 10.1007/s00417-021-05221-0]
- 15 **Milone M**, Desiderio A, Velotti N, Manigrasso M, Vertaldi S, Bracale U, D'Ambra M, Servillo G, De Simone G, De Palma FDE, Perruolo G, Raciti GA, Miele C, Beguinot F, De Palma GD. Surgical stress and metabolic response after totally laparoscopic right colectomy. *Sci Rep* 2021; **11**: 9652 [PMID: 33958669 DOI: 10.1038/s41598-021-89183-7]
- 16 **Feng X**, Zhao B, Wang Y. Effect Evaluation of Dexmedetomidine Intravenous Anesthesia on Postoperative Agitation in Patients with Craniocerebral Injury by Magnetic Resonance Imaging Based on Sparse Reconstruction Algorithm. *Contrast Media Mol Imaging* 2022; **2022**: 5161703 [PMID: 35833071 DOI: 10.1155/2022/5161703]
- 17 **Riker RR**, Picard JT, Fraser GL. Prospective evaluation of the Sedation-Agitation Scale for adult critically ill patients. *Crit Care Med* 1999; **27**: 1325-1329 [PMID: 10446827 DOI: 10.1097/00003246-199907000-00022]



Retrospective Study

The efficacy of full-thickness endoscopic resection of subepithelial tumors in the gastric cardia

En-Pan Xu, Zhi-Peng Qi, Bing Li, Zhong Ren, Ming-Yan Cai, Shi-Lun Cai, Zhen-Tao Lyv, Zhang-Han Chen, Jing-Yi Liu, Qiang Shi, Yun-Shi Zhong

Specialty type: Oncology

Provenance and peer review:

Unsolicited article; Externally peer reviewed.

Peer-review model: Single blind

Peer-review report's scientific quality classification

Grade A (Excellent): 0
Grade B (Very good): 0
Grade C (Good): C, C
Grade D (Fair): 0
Grade E (Poor): 0

P-Reviewer: Langner C, Austria;
Milone M, Italy

Received: September 10, 2023

Peer-review started: September 10, 2023

First decision: October 13, 2023

Revised: October 18, 2023

Accepted: October 30, 2023

Article in press: October 30, 2023

Published online: December 15, 2023



En-Pan Xu, Zhi-Peng Qi, Bing Li, Zhong Ren, Ming-Yan Cai, Shi-Lun Cai, Zhen-Tao Lyv, Zhang-Han Chen, Jing-Yi Liu, Qiang Shi, Yun-Shi Zhong, Endoscopy Center, Zhongshan Hospital Fudan University, Shanghai 200032, China

Corresponding author: Yun-Shi Zhong, MD, PhD, Doctor, Surgeon, Endoscopy Center, Zhongshan Hospital Fudan University, No. 180 Fenglin Road, Shanghai 200032, China.
zhong.yunshi@zs-hospital.sh.cn

Abstract

BACKGROUND

Gastric subepithelial tumors (SETs) may harbor potential malignancy. Although it is well recognized that large SETs should be resected, the precise treatment strategy remains controversial. Compared to surgical resection, endoscopic resection (ER) has many advantages; however, ER of SETs in the cardia is challenging.

AIM

To evaluate the safety and efficacy of endoscopic full-thickness resection (EFTR) for the treatment of gastric cardia SETs.

METHODS

We retrospectively reviewed data from all patients with SETs originating from the muscularis propria layer in the gastric cardia that were treated by EFTR or submucosal tunneling ER (STER) at Zhongshan Hospital Fudan University between November 2014 and May 2022. Baseline characteristics and clinical outcomes, including procedure times and complications rates, were compared between groups of patients receiving EFTR and STER.

RESULTS

A total of 171 tumors were successfully removed [71 (41.5%) tumors in the EFTR and 100 (58.5%) tumors in the STER group]. Gastrointestinal stromal tumors (GISTs) were the most common SET. The en bloc resection rate was 100% in the EFTR group *vs* 97.0% in STER group ($P > 0.05$). Overall, the EFTR group had a higher complete resection rate than the STER group (98.6% *vs* 91.0%, $P < 0.05$). The procedure time was also shorter in the EFTR group (44.63 ± 28.66 min *vs* 53.36 ± 27.34 , $P < 0.05$). The most common major complication in both groups was electrocoagulation syndrome. There was no significant difference in total complica-

ations between the two groups (21.1% *vs* 22.0%, $P = 0.89$).

CONCLUSION

EFTR of gastric cardia SETs is a very promising method to facilitate complete resection with similar complications and reduced operative times compared to STER. In cases of suspected GISTs or an unclear diagnosis, EFTR should be recommended to ensure complete resection.

Key Words: Endoscopic full-thickness resection; Submucosal tunneling endoscopic resection; Gastrointestinal stromal tumor; Gastric cardia; Gastric subepithelial tumors

©The Author(s) 2023. Published by Baishideng Publishing Group Inc. All rights reserved.

Core Tip: Efficacy of endoscopic full-thickness resection (EFTR) is safe and effective in the treatment of cardiac subepithelial tumors. Compared with submucosal tunneling endoscopic resection, EFTR can better completely resect subepithelial tumors and provide a better pathological diagnosis. When lesions with a high index of suspicion for gastrointestinal stromal tumors are found or there is an unclear diagnosis, EFTR should be recommended to ensure complete resection.

Citation: Xu EP, Qi ZP, Li B, Ren Z, Cai MY, Cai SL, Lyv ZT, Chen ZH, Liu JY, Shi Q, Zhong YS. The efficacy of full-thickness endoscopic resection of subepithelial tumors in the gastric cardia. *World J Gastrointest Oncol* 2023; 15(12): 2111-2119

URL: <https://www.wjgnet.com/1948-5204/full/v15/i12/2111.htm>

DOI: <https://dx.doi.org/10.4251/wjgo.v15.i12.2111>

INTRODUCTION

Gastric subepithelial tumors (SETs) are rare, accounting for less than 2% of all gastric tumors[1]. This group is comprised of different pathologies, commonly correlating with their location. Benign SETs are more frequently found in the cardia than in other locations[2].

With technological advancements, laparoscopic wedge resection is currently considered the best option for the treatment of gastric SETs[3]; however, it is difficult to resect SETs locating in the cardia and is associated with several complications, including leak, stenosis, and reflux[4,5]. Due to their typically benign nature and these postoperative risks, surgical resection of small, benign SETs is typically not mandatory.

Since the advent of submucosal tunneling endoscopic resection (ER) (STER), it has been widely used for SETs resection in the esophagus and cardia, and has achieved positive results[6-8]. The American Gastroenterological Association Clinical Practice Guidelines recommend using ER techniques to remove SETs[9]; however, in clinical application, damage to the tunneled surface mucosa may occur. This may be due to a large tumor and/or a lesion located in the deep layer of the muscularis propria (MP) (or even outside the cavity) or if the operating space in the tunnel is small, or the tunnel cannot be established at the tumor site. Additionally, submucosal fibrosis can lead to technical difficulty and tunnel establishment failure can occur.

Endoscopic full-thickness resection (EFTR) is a new surgical method of repairing the gastric wall after full-thickness resection so that endoscopic surgery is no longer limited by the depth of the tumor and submucosal fibrosis[10]. In 2009, EFTR without laparoscopic assistance for the treatment of gastrointestinal SET was first proposed. Since then, EFTR has been developed and widely applied clinically. Li *et al*[11] reported using dental floss and a hemoclip for assisted EFTR for SETs in the gastric fundus and demonstrated advantages in reducing surgical time and occurrence of post-endoscopic submucosal dissection (ESD) electrocoagulation syndrome (PEECS). Many studies have also proven that EFTR is safe and effective in the treatment of gastric SETs[12,13]; however, data regarding the clinical outcomes of EFTR for gastric cardia SETs are limited. Therefore, we evaluated the clinical outcomes of gastric cardia SETs treated by EFTR resection at our institution.

MATERIALS AND METHODS

Patients

We collected and reviewed data from patients with SETs originating from the MP layer in the gastric cardia, which were treated by EFTR or STER at Zhongshan Hospital Fudan University (Shanghai, China) between November 2014 and May 2022. The inclusion criteria were: (1) Proven diagnosis of SET by gastroscopy, endoscopic ultrasonography (EUS), and computed tomography (CT); (2) eligibility for endoscopic treatment; (3) lesion located in the cardia; and (4) final application of STER or EFTR. The exclusion criteria were: (1) Patients disagreement regarding resection; (2) malignant tumors with metastasis; and (3) coagulation disorders.

Informed patient consent was obtained from all patients. The study and procedures were conducted in accordance with the ethical standards of the Helsinki Declaration of 1975. This study was approved by the Institutional Review Board of Zhongshan Hospital (reference number: B2020-265).

EFTR and STER

EUS and/or CT were used to characterize the lesions in terms of size and other features prior to EFTR or STER. All patients were airway intubated under intravenous anesthesia, while vital signs were monitored. The ER method was selected based on the tumor characteristics. If the tumor deviates to the esophageal side, STER is used, and if the tumor deviates to the stomach side, EFTR is used. Some cases underwent EFTR while others underwent STER according to the patient's preference, after being informed of the merits and disadvantages of each technique. Description of the specific resection procedures can be found in the literature previously published by our center (Figure 1)[7,10].

Definitions

The surgical operator was categorized as a trainee with experience of 25 EFTR and STER procedures per year or as an expert with experience of > 25 procedures per year[11]. All were certified EFTR endoscopists. En bloc resection was characterized as the complete removal of a tumor without fragmentation. Complete resection was characterized as the en bloc removal of a lesion with the tumor extracted in a single piece and the capsule remaining intact[7]. Postoperative bleeding was characterized as hematemesis or melena within 14 d after completion of EFTR or STER. Hydrothorax was excess fluid in the pleural space, as confirmed by chest X-ray. Pneumoperitoneum was diagnosed by the presence of gas in the peritoneal cavity, observable on either X-ray or CT scan. Minor cases of pneumoperitoneum and minor hydrothorax had negligible clinical impact or symptoms and did not necessitate therapeutic intervention. Similar to PEECS, included as a minor complication here, was defined as fever (> 37.7 °C) and abdominal pain with localized tenderness without perforation confirmed by radiological exam within 7 d after EFTR or STER.

Follow up

Data were initially collected from medical records in our hospital. If patients have been discharged from our hospital, we make an effort to gather outcome information by contacting the patient or a family member by telephone. The minimum follow-up duration is 12 mo.

Statistical analysis

SPSS 21.0 software (IBM Corp, Armonk, NY, United States) was used for analysis. We compared categorical variables with the chi-square or Fisher's exact test. The Student's *t*-test or analysis of variance was used to compare continuous variables. Statistical analysis of independent risk factors for long operative times was assessed using a combination of univariate and multivariate analyses. A two-tailed *P* value < 0.05 was considered statistically significant.

RESULTS

Baseline characteristics

A total of 171 patients with SETs in the cardia were included in the study. Seventy-one (41.5%) patients underwent EFTR, while 100 (58.5%) received STER treatment. The clinical characteristics of these patients are presented in Table 1. The mean age of the EFTR and STER group was 51.32 ± 12.44 (median: 52; range: 43–61 years) and 50.29 ± 12.19 years (median: 51; range: 41–60 years), respectively. The average tumor size of the EFTR and STER group was 2.16 ± 1.81 cm (median: 1.5; range: 1.0–3.0 cm) and 2.09 ± 1.38 cm (median: 1.5; range: 1.2–2.5 cm), respectively. Six (8.5%) and 5 (5.0%) tumors showed extraluminal growth in the EFTR and STER groups. 59 (83.1%) patients underwent EFTR by expert surgeons, and 85 (85%) patients underwent EFTR by trainee surgeons. Patient characteristics and clinical data relating to tumors and procedures were similar between the EFTR and STER groups.

Outcome

The primary surgery-related outcomes from the two groups of patients are described in Table 2. All gastric cardia SETs were resected by ER. The en bloc resection rate was 100% in the EFTR group. There was no significant difference between the groups. EFTR had a higher completed resection rate than STER (98.6% vs 91.0%, *P* < 0.05). The procedure time was also shorter in the EFTR group (44.63 ± 28.66 min vs 53.36 ± 27.34, *P* < 0.05). In the EFTR group, there were 28 (39.4%) gastrointestinal stromal tumors (GISTs) and 43 (60.6%) leiomyomas. In the STER group, there were 7 (7%) GISTs, 88 (88%) leiomyomas, 3 (3%) lipomas, and 2 (2%) cysts. Metallic clips and endoloop was applied in 29 (40.8%) EFTR patients and 2 (2%) STER patients. There was no significant difference in total complications between two groups (21.1% vs 22.0%, *P* = 0.89). The most common complication in both groups was electrocoagulation syndrome. All complications were managed successfully by endoscopic methods and conservative treatment.

Subgroup analyses the risk for EFTR

Univariate and multivariate analyses showed that larger tumor size (> 2 cm) and extraluminal growth were significant risk factors for long procedure times (Table 3).

Table 1 Baseline characteristics of the 171 patients with submucosal tumors in gastric cardia treated by endoscopic full-thickness resection and submucosal tunneling endoscopic resection

Patients	EFTR	STER	P value
Age (yr)			0.59
mean ± SD	51.32 ± 12.44	50.29 ± 12.19	
Median (range)	52.00 (43.00-61.00)	51.00 (41.00-59.75)	
Sex			0.01
Male	24 (33.8%)	53 (53.0%)	
Female	47 (66.2%)	47 (47.0%)	
Lesion characteristics			
Size (cm)			0.78
mean ± SD	2.16 ± 1.81	2.09 ± 1.38	
Median (range)	1.50 (1.00-3.00)	1.50 (1.20-2.50)	
Extraluminal growth			0.37
Yes	6 (8.5%)	5 (5.0%)	
No	65 (91.5%)	95 (95.0%)	
Operator level			0.74
Experts	59 (83.1%)	85 (85.0%)	
Trainees	12 (16.9%)	15 (15.0%)	

EFTR: Endoscopic full-thickness resection; STER: Submucosal tunneling endoscopic resection.

Follow-up results

Of the 171 patients with gastric cardiac SETs, seven cases were lost to follow-up. The remaining 164 cases were followed for more than 12 mo. The median follow-up was 28 (range: 16-52.5) mo. All patients did not develop local recurrence or distant metastasis during follow-up.

DISCUSSION

The present work was the first time that the efficacy of EFTR for gastric cardia SETs was studied. Current methods to remove gastric SETs include surgical and ER. ER has several advantages over surgical approaches, such as being minimally invasive and incurring a shorter hospital stay[14,15]. The STER procedure was derived from peroral endoscopic myotomy and was initially reported in 2012[6]. A series of subsequent studies have reported that, compared to ESD, STER has benefits for the removal of SETs, such as maintaining the integrity of the mucosa, faster wound healing, and reduced risks of complications including perforation, extraluminal infection, and esophageal stenosis[16-18]. STER has also been reported as a successful treatment option for SETs located in the cardia or esophagogastric junction[19,20]. The advantages of shorter operative and hospitalization times and reduced cost are described[21].

STER requires the establishment of adequate operating space beyond the tumor in the tunnel. The tumor is then pushed into the distal portion of the submucosal tunnel during resection, separating the tumor from the deep MP and increasing the safety of the operation[22,23]. Performing the operation for SETs in the cardia is more complicated than in other parts owing to its specific anatomic characteristics[24]. There is a significant change in the angle of this gastric muscle layer. Therefore, the formation of the tunnel beyond the tumor requires a greater degree of curvature of the anterior part of the endoscope. Additionally, the gastric cavity is relatively narrow, which greatly increases the difficulty of resection[25,26]. Meanwhile, the blood supply at the cardia and gastric fundus is abundant. Thus, the risk of intraoperative bleeding is high, which also increases the difficulty of the operation[26]. In addition, in the lesser curvature or the anterior aspect of the cardia, when the tumor is located in the deep layer of the MP (or even growing extraluminally), and/or where a submucosal tunnel cannot be established, EFTR is needed.

EFTR, as a technical extension of ESD, offers distinct advantages, particularly when dealing with SETs deeply embedded within the MP layer or exhibiting extraluminal growth patterns. The characteristics of EFTR make it a very suitable form of treatment for SETs[12]. Our center previously reported the successful application of EFTR in 26 gastric SETs without laparoscopic assistance. No gastric bleeding, sign of peritonitis, or abdominal infections/abscesses occurred after EFTR[10]. In addition, we have improved the EFTR procedure by incorporating dental floss and a hemoclip, which facilitate countertraction. This improvement enables better visualization of the submucosal layer, resulting in a reduced

Table 2 A comparison of treatment outcomes between endoscopic full-thickness resection and submucosal tunneling endoscopic resection groups

Outcomes	EFTR	STER	P value
En bloc resection	71 (100%)	97 (97.0%)	0.14
Complete resection	70 (98.6%)	91 (91.0%)	0.04
Procedure time (min)	44.63 ± 28.66	53.36 ± 27.34	0.04
Procedure-related characteristics			
Suturing methods			0.01
Metallic clips	38 (53.5%)	98 (98.0%)	
Metallic clips with endoloop	29 (40.8%)	2 (2.0%)	
Stent	4 (5.6%)	0 (0%)	
Histopathology			0.01
GIST	28 (39.4%)	7 (7.0%)	
Leiomyoma	43 (60.6%)	88 (88.0%)	
Others	0 (0%)	5 (5.0%)	
Complications			0.89
Pneumoperitoneum	0 (0%)	0 (0%)	
Hydrothorax			
Minor hydrothorax	3 (4.2%)	4 (4.0%)	
Major hydrothorax	0 (0%)	0 (0%)	
PEECS	10 (14.1%)	18 (18.0%)	
Delayed bleeding	2 (2.8%)	0 (0%)	
Delayed perforation	0 (0%)	0 (0.0%)	
Follow-up			
Recurrence	0 (0%)	0 (0%)	
Metastasis	0 (0%)	0 (0%)	

EFTR: Endoscopic full-thickness resection; STER: Submucosal tunneling endoscopic resection; GIST: Gastrointestinal stromal tumor; PEECS: Post-endoscopic submucosal dissection electrocoagulation syndrome.

incidence of adverse events in the gastric fundus[11].

Similar to the data from our previous studies, EFTR in the gastric cardia had a 100% en bloc and 98.6% complete resection rate. The complete resection rate was higher than STER (98.6% *vs* 91.0%, *P* < 0.05). Complete ER of SETs is the key to ensuring successful operation and avoiding recurrence[26]. Upper gastrointestinal SETs are composed primarily of leiomyomas and GISTs[27]. GISTs have greater potential for malignancy and should be completely resected. An irregular shape and larger size have been shown to be the risk factors for STERs having piecemeal resection[28]. Most esophageal SETs are regular while the majority of cardiac SETs are irregular and lobulated[8], which makes it more difficult for STERs to be completely resected. Additionally, tumor resection by STER is limited by the diameter of the tunnel. Therefore, oversized tumors cannot be completely resected. Due to the anatomy, the tunnel has a turn at the cardia, which can easily lead to compression of the tumor and tumor rupture. Conversely, EFTR allows full-thickness excision of the complete gastrointestinal wall without a diameter limit and the risk for poor resection margins and residual tumor which increases the accuracy of histopathology measurement to direct future therapy[29]. In a meta-analysis including 952 G-SETs treated with EFTR, it was suggested that EFTR was a highly effective therapeutic option for removing deep G-SETs, with an R0 resection achieved in 99.3% of cases[30]. Therefore, for lesions that are highly suspicious for GIST or lesions that are not clearly diagnosed, EFTR should be recommended to ensure completed resection.

In our study, EFTR had a shorter procedure time than STER (44.63 ± 28.66 *vs* 53.36 ± 27.34 min, *P* < 0.05). Chen revealed that STER was relatively difficult and time consuming when used to resect gastric SETs because of limited space in the established submucosal tunnel[7]. They found that an irregular shape and large size were also risk factors for procedures requiring a long operative time. Therefore, irregular shaped and larger sized SETs were more suitable for EFTR. Additionally, compared to STER, EFTR required the creation of a tunnel. Also, there was no risk of the tumor being too large to rupture in the tunnel, which kept the tumor intact.

Table 3 The association of the clinicopathological characteristics of subepithelial tumors in gastric cardia treated by endoscopic full-thickness resection over the median procedure time

	Univariate analysis		Multivariate analysis	
	OR (95%CI)	P value	OR (95%CI)	P value
Age (yr)		0.37		
< 50	1 (reference)			
≥ 50	1.88 (0.48-7.46)			
Sex		0.41		
Male	1 (reference)			
Female	1.76 (0.46-6.68)			
Size (cm)		0.01		
< 2.0	1 (reference)		1 (reference)	0.02
≥ 2.0	6.58 (1.60-27.09)		3.75 (1.21-11.58)	
Extraluminal growth		0.048		0.04
No	1 (reference)		1 (reference)	
Yes	7.83 (1.02-60.03)		7.64 (1.15-50.83)	
Histopathology		0.42		
Others	1 (reference)			
Leiomyoma	1.85 (0.42-8.17)			
Metallic clips with endoloop		0.05		
No	1 (reference)			
Yes	3.68 (0.98-13.91)			
Operator level		0.19		
Trainees	1 (reference)			
Experts	0.31 (0.05-1.76)			

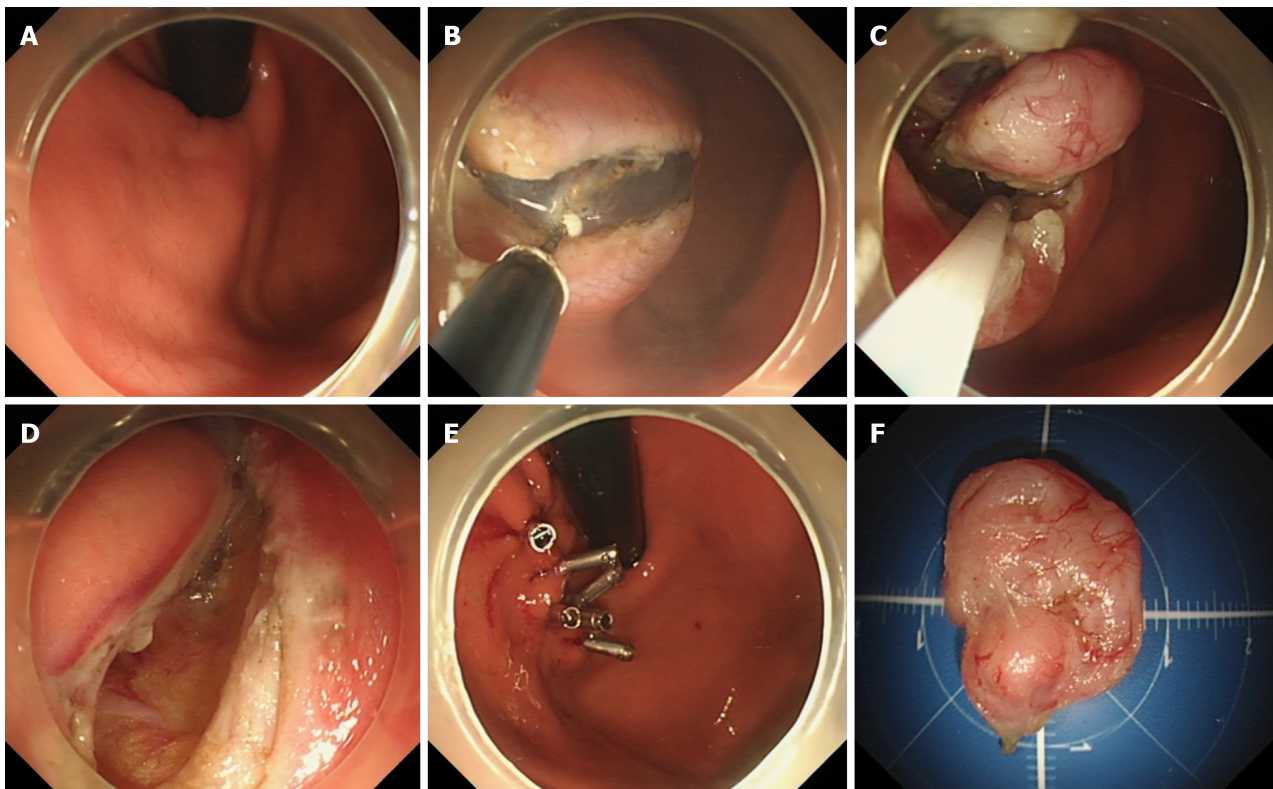
OR: Odds ratio; 95%CI: 95% confidence interval.

The key of the EFTR procedure is the successful closure of the wall defect after resection to prevent peritonitis and the need for surgical intervention[10]. Although a growing body of evidence has demonstrated that gastrointestinal defects after ER can be effectively managed by endoscopy, the closure of large gastrointestinal defects is still technically demanding for most endoscopists[31,32]. Several clips can close small defects. When the diameter of the defect is larger than the width of the open clip, and before applying metallic clips, the defect can first be reduced by air suction using the “suction-clip-suture” method[10]. If the defect is too large to be closed only by clips, a few new techniques have been used in the stomach, such as nylon loop suturing and the over-the-scope clip[33]. In our study, 53.5% patients underwent closure of the defect with clips. 40.8% patients had defect closure using metallic clips with an endoloop. Four patients with large defects had covered, retrievable self-expandable metallic stents used to close the defect. As we our previous study showed, no leakage occurred[33].

There are also having several limitations. The study was retrospective and was conducted at a single institution. Thus, prospective study will be needed to further verify our views. Additionally, gastric EFTR was first performed our center and center has many experienced surgeons in the field. It may be difficult for other hospitals with less experience to carry out the procedure.

CONCLUSION

In conclusion, EFTR was demonstrated to be a very promising method with which to facilitate complete resection and reduce operation time compared to STER in gastric cardia SETs. GISTs were the most common type of SETs in the cardia. When lesions with a high index of suspicion for GIST are found or there is an unclear diagnosis, EFTR should be recommended to ensure complete resection. EFTR by experienced surgeons was shown to be the better option in cases of gastric cardia SETs > 2 cm or with extraluminal growth.



DOI: 10.4251/wjgo.v15.i12.2111 Copyright ©The Author(s) 2023.

Figure 1 Processes of endoscopic full-thickness resection for gastric cardia subepithelial tumors. A: Endoscopic view of gastric cardia subepithelial tumor; B: Circumferential incision was made as deep as muscularis propria around the lesion with IT knife; C: Incision into serosal layer around the lesion was performed with Hook knife to create active perforation; D: Gastric wall defect was presented after lesion was resected; E: The gastric wound was closed with several metallic clips successfully; F: Resected tumor.

ARTICLE HIGHLIGHTS

Research background

The endoscopic full-thickness resection (EFTR) of cardiac subepithelial tumors (SETs) is still difficult.

Research motivation

To evaluate the safety and efficacy of EFTR for the treatment of gastric cardia SETs.

Research objectives

The objective was the comparison of treatment outcomes between EFTR and submucosal tunnel endoscopic resection (STER), and the factors of difficult of EFTR.

Research methods

We retrospectively analyzed the data of all patients with SET originating from the muscularis propria of the gastric cardia who underwent EFTR or STER from November 2014 to May 2022 at Zhongshan Hospital Fudan University.

Research results

Gastrointestinal stromal tumors were the most common SET. The EFTR group had a higher complete resection rate than the STER group (98.6% *vs* 91.0%, $P < 0.05$) and the procedure time was also shorter in the EFTR group (44.63 ± 28.66 min *vs* 53.36 ± 27.34 , $P < 0.05$). There was no significant difference in total complications between the two groups (21.1% *vs* 22.0%, $P = 0.89$).

Research conclusions

Compared to STER, EFTR for gastric cardia SETs is also safe and effective.

Research perspectives

For patients with suspected cardia gastrointestinal stromal tumor, EFTR can be used to achieve better complete resection. Of course, subsequent prospective studies should be conducted for verification this opinion.

FOOTNOTES

Co-first authors: En-Pan Xu and Zhi-Peng Qi.

Co-corresponding authors: Qiang Shi and Yun-Shi Zhong.

Author contributions: Xu EP and Qi ZP contributed equally to this work; Zhong YS and Shi Q designed the research study; Ren Z, Cai MY, Lyu ZT, Chen ZH and Liu JY performed the research; Xu EP, Qi ZP and Li B analyzed the data and wrote the manuscript; All authors have read and approve the final manuscript. Xu EP and Qi ZP contributed equally to this work as co-first authors. Zhong YS and Shi Q contributed equally to this work as co-corresponding authors. The reasons for designating Zhong YS and Shi Q as co-corresponding authors are threefold. First, the research was performed as a collaborative effort, and the designation of co-corresponding authorship accurately reflects the distribution of responsibilities and burdens associated with the time and effort required to complete the study and the resultant paper. This also ensures effective communication and management of post-submission matters, ultimately enhancing the paper's quality and reliability. Second, the overall research team encompassed authors with a variety of expertise and skills from different fields, and the designation of co-corresponding authors best reflects this diversity. This also promotes the most comprehensive and in-depth examination of the research topic, ultimately enriching readers' understanding by offering various expert perspectives. Third, Zhong YS and Shi Q contributed efforts of equal substance throughout the research process. The choice of these researchers as co-corresponding authors acknowledges and respects this equal contribution, while recognizing the spirit of teamwork and collaboration of this study. The are two reasons for designating Xu EP and Qi ZP as co-first authors. First, Qi ZP participated in the writing and revision of the manuscript and provided opinions during the writing process. Furthermore, the data results were analyzed with the help of Qi ZP. In summary, we believe that designating Zhong YS and Shi Q as co-corresponding authors and Xu EP and Qi ZP as co-first authors of is fitting for our manuscript as it accurately reflects our team's collaborative spirit, equal contributions, and diversity.

Supported by National Natural Science Foundation of China, No. 82273025; China Postdoctoral Science Foundation, No. 2022TQ0070 and No. 2022M710759; and Shanghai Municipal Commission of Science and Technology, No. 22JC1403003 and No. 22531903800.

Institutional review board statement: This study was approved by the Institutional Review Board of Zhongshan Hospital (Approval No. B2020-265).

Conflict-of-interest statement: The authors have no conflict of interest to declare.

Data sharing statement: Technical appendix, statistical code, and dataset available from the corresponding author at zhong.yunshi@zs-hospital.sh.cn.

Open-Access: This article is an open-access article that was selected by an in-house editor and fully peer-reviewed by external reviewers. It is distributed in accordance with the Creative Commons Attribution NonCommercial (CC BY-NC 4.0) license, which permits others to distribute, remix, adapt, build upon this work non-commercially, and license their derivative works on different terms, provided the original work is properly cited and the use is non-commercial. See: <https://creativecommons.org/licenses/by-nc/4.0/>

Country/Territory of origin: China

ORCID number: En-Pan Xu 0000-0001-7341-3437; Zhi-Peng Qi 0000-0002-1792-3595; Bing Li 0000-0002-8727-3591; Ming-Yan Cai 0000-0002-8155-3154; Shi-Lun Cai 0000-0002-5000-9658; Zhen-Tao Lvy 0000-0003-4460-0166; Qiang Shi 0000-0001-9958-2132; Yun-Shi Zhong 0000-0001-8382-3747.

S-Editor: Lin C

L-Editor: A

P-Editor: Xu ZH

REFERENCES

- 1 Cheng HL, Lee WJ, Lai IR, Yuan RH, Yu SC. Laparoscopic wedge resection of benign gastric tumor. *Hepatogastroenterology* 1999; **46**: 2100-2104 [PMID: 10430405]
- 2 Lee HH, Hur H, Jung H, Jeon HM, Park CH, Song KY. Analysis of 151 consecutive gastric submucosal tumors according to tumor location. *J Surg Oncol* 2011; **104**: 72-75 [PMID: 21031420 DOI: 10.1002/jso.21771]
- 3 Akahoshi K, Oya M, Koga T, Shiratsuchi Y. Current clinical management of gastrointestinal stromal tumor. *World J Gastroenterol* 2018; **24**: 2806-2817 [PMID: 30018476 DOI: 10.3748/wjg.v24.i26.2806]
- 4 Ko SY, Lee JS, Kim JJ, Park SM. Higher incidence of gastroesophageal reflux disease after gastric wedge resections of gastric submucosal tumors located close to the gastroesophageal junction. *Ann Surg Treat Res* 2014; **86**: 289-294 [PMID: 24949319 DOI: 10.4174/astr.2014.86.6.289]
- 5 Kim SG, Eom BW, Yoon H, Kook MC, Kim YW, Ryu KW. Necessity of Individualized Approach for Gastric Subepithelial Tumor Considering Pathologic Discrepancy and Surgical Difficulty Depending on the Gastric Location. *J Clin Med* 2022; **11** [PMID: 36012971 DOI: 10.3390/jcm11164733]
- 6 Xu MD, Cai MY, Zhou PH, Qin XY, Zhong YS, Chen WF, Hu JW, Zhang YQ, Ma LL, Qin WZ, Yao LQ. Submucosal tunneling endoscopic resection: a new technique for treating upper GI submucosal tumors originating from the muscularis propria layer (with videos). *Gastrointest Endosc* 2012; **75**: 195-199 [PMID: 22056087 DOI: 10.1016/j.gie.2011.08.018]
- 7 Chen T, Zhou PH, Chu Y, Zhang YQ, Chen WF, Ji Y, Yao LQ, Xu MD. Long-term Outcomes of Submucosal Tunneling Endoscopic

- Resection for Upper Gastrointestinal Submucosal Tumors. *Ann Surg* 2017; 265: 363-369 [PMID: 28059965 DOI: 10.1097/SLA.0000000000001650]
- 8 **Du C**, Chai N, Linghu E, Gao Y, Li Z, Li L, Zhai Y, Lu Z, Meng J, Tang P. Treatment of cardiac submucosal tumors originating from the muscularis propria layer: submucosal tunneling endoscopic resection versus endoscopic submucosal excavation. *Surg Endosc* 2018; 32: 4543-4551 [PMID: 29766300 DOI: 10.1007/s00464-018-6206-0]
 - 9 **Sharzchi K**, Sethi A, Savides T. AGA Clinical Practice Update on Management of Subepithelial Lesions Encountered During Routine Endoscopy: Expert Review. *Clin Gastroenterol Hepatol* 2022; 20: 2435-2443.e4 [PMID: 35842117 DOI: 10.1016/j.cgh.2022.05.054]
 - 10 **Zhou PH**, Yao LQ, Qin XY, Cai MY, Xu MD, Zhong YS, Chen WF, Zhang YQ, Qin WZ, Hu JW, Liu JZ. Endoscopic full-thickness resection without laparoscopic assistance for gastric submucosal tumors originated from the muscularis propria. *Surg Endosc* 2011; 25: 2926-2931 [PMID: 21424195 DOI: 10.1007/s00464-011-1644-y]
 - 11 **Li B**, Shi Q, Qi ZP, Yao LQ, Xu MD, Lv ZT, Yalikong A, Cai SL, Sun D, Zhou PH, Zhong YS. The efficacy of dental floss and a hemoclip as a traction method for the endoscopic full-thickness resection of submucosal tumors in the gastric fundus. *Surg Endosc* 2019; 33: 3864-3873 [PMID: 31376013 DOI: 10.1007/s00464-019-06920-w]
 - 12 **Cai MY**, Martin Carreras-Presas F, Zhou PH. Endoscopic full-thickness resection for gastrointestinal submucosal tumors. *Dig Endosc* 2018; 30 Suppl 1: 17-24 [PMID: 29658639 DOI: 10.1111/den.13003]
 - 13 **Ni L**, Liu X, Wu A, Yu C, Zou C, Xu G, Wang C, Gao X. Endoscopic full-thickness resection with clip- and snare-assisted traction for gastric submucosal tumours in the fundus: A single-centre case series. *Oncol Lett* 2023; 25: 151 [PMID: 36936023 DOI: 10.3892/ol.2023.13737]
 - 14 **Nishida T**, Kawai N, Yamaguchi S, Nishida Y. Submucosal tumors: comprehensive guide for the diagnosis and therapy of gastrointestinal submucosal tumors. *Dig Endosc* 2013; 25: 479-489 [PMID: 23902569 DOI: 10.1111/den.12149]
 - 15 **Kim SY**, Kim KO. Management of gastric subepithelial tumors: The role of endoscopy. *World J Gastrointest Endosc* 2016; 8: 418-424 [PMID: 27298713 DOI: 10.4253/wjge.v8.i11.418]
 - 16 **Song S**, Feng M, Zhou H, Liu M, Sun M. Submucosal Tunneling Endoscopic Resection for Large and Irregular Submucosal Tumors Originating from Muscularis Propria Layer in Upper Gastrointestinal Tract. *J Laparoendosc Adv Surg Tech A* 2018; 28: 1364-1370 [PMID: 30256158 DOI: 10.1089/lap.2017.0607]
 - 17 **Ye LP**, Zhang Y, Mao XL, Zhu LH, Zhou X, Chen JY. Submucosal tunneling endoscopic resection for small upper gastrointestinal subepithelial tumors originating from the muscularis propria layer. *Surg Endosc* 2014; 28: 524-530 [PMID: 24013472 DOI: 10.1007/s00464-013-3197-8]
 - 18 **Gong W**, Xiong Y, Zhi F, Liu S, Wang A, Jiang B. Preliminary experience of endoscopic submucosal tunnel dissection for upper gastrointestinal submucosal tumors. *Endoscopy* 2012; 44: 231-235 [PMID: 22354823 DOI: 10.1055/s-0031-1291720]
 - 19 **Chen H**, Xu Z, Huo J, Liu D. Submucosal tunneling endoscopic resection for simultaneous esophageal and cardia submucosal tumors originating from the muscularis propria layer (with video). *Dig Endosc* 2015; 27: 155-158 [PMID: 24444087 DOI: 10.1111/den.12227]
 - 20 **Liu BR**, Song JT, Kong LJ, Pei FH, Wang XH, Du YJ. Tunneling endoscopic muscularis dissection for subepithelial tumors originating from the muscularis propria of the esophagus and gastric cardia. *Surg Endosc* 2013; 27: 4354-4359 [PMID: 23765425 DOI: 10.1007/s00464-013-3023-3]
 - 21 **Li QY**, Meng Y, Xu YY, Zhang Q, Cai JQ, Zheng HX, Qing HT, Huang SL, Han ZL, Li AM, Huang Y, Zhang YL, Zhi FC, Cai RJ, Li Y, Gong W, Liu SD. Comparison of endoscopic submucosal tunneling dissection and thoracoscopic enucleation for the treatment of esophageal submucosal tumors. *Gastrointest Endosc* 2017; 86: 485-491 [PMID: 27899323 DOI: 10.1016/j.gie.2016.11.023]
 - 22 **Werner YB**, Rösch T. POEM and Submucosal Tunneling. *Curr Treat Options Gastroenterol* 2016; 14: 163-177 [PMID: 27059229 DOI: 10.1007/s11938-016-0086-y]
 - 23 **Zhang Q**, Cai JQ, Xiang L, Wang Z, de Liu S, Bai Y. Modified submucosal tunneling endoscopic resection for submucosal tumors in the esophagus and gastric fundus near the cardia. *Endoscopy* 2017; 49: 784-791 [PMID: 28658679 DOI: 10.1055/s-0043-111236]
 - 24 **Wang S**, Shen L. Efficacy of Endoscopic Submucosal Excavation for Gastrointestinal Stromal Tumors in the Cardia. *Surg Laparosc Endosc Percutan Tech* 2016; 26: 493-496 [PMID: 27846180 DOI: 10.1097/SLE.0000000000000330]
 - 25 **Jang YS**, Lee BE, Kim GH, Park DY, Jeon HK, Baek DH, Kim DU, Song GA. Factors Associated With Outcomes in Endoscopic Submucosal Dissection of Gastric Cardia Tumors: A Retrospective Observational Study. *Medicine (Baltimore)* 2015; 94: e1201 [PMID: 26252277 DOI: 10.1097/MD.0000000000001201]
 - 26 **Wang S**, Luo H, Shen L. Clinical Efficacy of Single-Channel Gastroscopy, Double-Channel Gastroscopy, and Double Gastroscopy for Submucosal Tumors in the Cardia and Gastric Fundus. *J Gastrointest Surg* 2020; 24: 1307-1313 [PMID: 31197688 DOI: 10.1007/s11605-019-04286-x]
 - 27 **Hong JB**, Choi CW, Kim HW, Kang DH, Park SB, Kim SJ, Kim DJ. Endoscopic resection using band ligation for esophageal SMT in less than 10 mm. *World J Gastroenterol* 2015; 21: 2982-2987 [PMID: 25780296 DOI: 10.3748/wjg.v21.i10.2982]
 - 28 **Mao XL**, Ye LP, Zheng HH, Zhou XB, Zhu LH, Zhang Y. Submucosal tunneling endoscopic resection using methylene-blue guidance for cardiac subepithelial tumors originating from the muscularis propria layer. *Dis Esophagus* 2017; 30: 1-7 [PMID: 27671744 DOI: 10.1111/dote.12536]
 - 29 **Li J**, Tang J, Lua GW, Chen J, Shi X, Liu F, Li Z. Safety and efficacy of endoscopic submucosal dissection of large (≥ 3 cm) subepithelial tumors located in the cardia. *Surg Endosc* 2017; 31: 5183-5191 [PMID: 28597288 DOI: 10.1007/s00464-017-5585-y]
 - 30 **Granata A**, Martino A, Ligresti D, Tuzzolino F, Lombardi G, Traina M. Exposed endoscopic full-thickness resection without laparoscopic assistance for gastric submucosal tumors: A systematic review and pooled analysis. *Dig Liver Dis* 2022; 54: 729-736 [PMID: 34654680 DOI: 10.1016/j.dld.2021.09.014]
 - 31 **Yamamoto Y**, Uedo N, Abe N, Mori H, Ikeda H, Kanzaki H, Hirasawa K, Yoshida N, Goto O, Morita S, Zhou P. Current status and feasibility of endoscopic full-thickness resection in Japan: Results of a questionnaire survey. *Dig Endosc* 2018; 30 Suppl 1: 2-6 [PMID: 29658648 DOI: 10.1111/den.13045]
 - 32 **Zhang Y**, Peng JB, Mao XL, Zheng HH, Zhou SK, Zhu LH, Ye LP. Endoscopic resection of large (≥ 4 cm) upper gastrointestinal subepithelial tumors originating from the muscularis propria layer: a single-center study of 101 cases (with video). *Surg Endosc* 2021; 35: 1442-1452 [PMID: 32989549 DOI: 10.1007/s00464-020-08033-1]
 - 33 **Zhang Y**, Yao L, Xu M, Berzin TM, Li Q, Chen W, Hu J, Wang Y, Cai M, Qin W, Xu J, Huang Y, Zhou P. Treatment of leakage via metallic stents placements after endoscopic full-thickness resection for esophageal and gastroesophageal junction submucosal tumors. *Scand J Gastroenterol* 2017; 52: 76-80 [PMID: 27632665 DOI: 10.1080/00365521.2016.1228121]

Basic Study

Hsa_circ_0136666 mediates the antitumor effect of curcumin in colorectal carcinoma by regulating CXCL1 via miR-1301-3p

Shi Chen, Wei Li, Chen-Gong Ning, Feng Wang, Li-Xing Wang, Chen Liao, Feng Sun

Specialty type: Cardiac and cardiovascular systems**Provenance and peer review:**

Unsolicited article; Externally peer reviewed.

Peer-review model: Single blind**Peer-review report's scientific quality classification**Grade A (Excellent): 0
Grade B (Very good): B
Grade C (Good): C
Grade D (Fair): 0
Grade E (Poor): 0**P-Reviewer:** Garcia K, Spain;
Schijven MP, Netherlands**Received:** July 27, 2023**Peer-review started:** July 27, 2023**First decision:** August 8, 2023**Revised:** September 22, 2023**Accepted:** October 16, 2023**Article in press:** October 16, 2023**Published online:** December 15, 2023**Shi Chen, Chen-Gong Ning, Feng Wang, Li-Xing Wang, Chen Liao, Feng Sun**, Department of Gastrointestinal Surgery, The Second Affiliated Hospital of Kunming Medical University, Kunming 650101, Yunnan Province, China**Wei Li**, Department of Blood Transfusion, The Second Affiliated Hospital of Kunming Medical University, Kunming 650101, Yunnan Province, China**Corresponding author:** Feng Sun, PhD, Doctor, Department of Gastrointestinal Surgery, The Second Affiliated Hospital of Kunming Medical University, No. 374 Yunnan-Myanmar Avenue, Wuhua District, Kunming 650101, Yunnan Province, China. sunfeng1971@163.com**Abstract****BACKGROUND**

This study investigate the anti-tumor effect of curcumin and whether its mediated by hsa_circ_0136666 through miR-1301-3p/CXCL1 in colorectal carcinoma (CRC). Through multiple experiments, we have drawn the conclusion that curcumin inhibited CRC development through the hsa_circ_0136666/miR-1301-3p/CXCL1 axis, hinting at a novel treatment option for curcumin to prevent CRC development.

AIM

To determine whether hsa_circ_0136666 involvement in curcumin-triggered CRC progression was mediated by sponging miR-1301-3p.

METHODS

Cell counting kit-8, colony-forming cell, 5-ethynyl-2'-deoxyuridine, and flow cytometry assays were carried out to determine cell proliferation, apoptosis, and cell cycle progression. Real-time quantitative polymerase chain reaction quantified hsa_circ_0136666, miR-1301-3p, and chemokine (C-X-C motif) ligand 1 (CXCL1), and western blot analysis determined CXCL1, B-cell lymphoma-2 (Bcl-2), and Bcl-2 related X protein (Bax) protein levels. CircBank or starbase software was first used for the prediction of miR-1301-3p binding with hsa_circ_0136666 and CXCL1, followed by RNA pull-down, RNA immunoprecipitation, and dual-luciferase reporter assay validation. *In vivo* experiments were implemented in a murine xenograft model.

RESULTS

Curcumin blocked CRC cell proliferation but boosted apoptosis. Moreover, ele-

vated hsa_circ_0136666 Levels were observed in CRC cells, which were reduced by curcumin. *In vitro*, hsa_circ_0136666 overexpression abolished the antitumor activity of CRC cells. Mechanical analysis revealed the ability of hsa_circ_0136666 to sponge miR-1301-3p to modulate *CXCL1* levels.

CONCLUSION

Curcumin inhibited CRC development through the hsa_circ_0136666/miR-1301-3p/*CXCL1* axis, hinting at a novel treatment option for curcumin to prevent CRC development.

Key Words: Curcumin; Hsa_circ_0136666; MiR-1301-3p; *CXCL1*; Colorectal carcinoma

©The Author(s) 2023. Published by Baishideng Publishing Group Inc. All rights reserved.

Core Tip: This study investigate the anti-tumor effect of curcumin and whether its mediated by hsa_circ_0136666 through miR-1301-3p/*CXCL1* in colorectal carcinoma (CRC). Through multiple experiments, we have drawn the conclusion that curcumin inhibited CRC development through the hsa_circ_0136666/miR-1301-3p/*CXCL1* axis, hinting at a novel treatment option for curcumin to prevent CRC development.

Citation: Chen S, Li W, Ning CG, Wang F, Wang LX, Liao C, Sun F. Hsa_circ_0136666 mediates the antitumor effect of curcumin in colorectal carcinoma by regulating *CXCL1* via miR-1301-3p. *World J Gastrointest Oncol* 2023; 15(12): 2120-2137

URL: <https://www.wjgnet.com/1948-5204/full/v15/i12/2120.htm>

DOI: <https://dx.doi.org/10.4251/wjgo.v15.i12.2120>

INTRODUCTION

Colorectal carcinoma (CRC), afflicting an estimated 104270 new cases and causing 52980 deaths in 2021 in the United States, is still considered the prime reason for cancer-related death in the United States[1,2]. Clinically, despite substantial advances made in surgical resection and adjuvant chemoradiotherapy, the conventional treatment method for CRC, the overall patient prognosis is still unfavorable[3,4]. Hence, it is urgent to find a more effective therapy that has high clinical significance for CRC patients. Currently, the chemo-preventive properties of traditional Chinese medicine have drawn great attention in cancer therapeutics. As a naturally occurring medicine, curcumin is derived from the medicinal plant *Curcuma longa* L.[5]. The salient features of curcumin include chemical stability, low toxicity, and extensive distribution, so the application of curcumin in the management of various diseases has gradually been understood[6,7]. Of note, curcumin exhibited powerful antitumor activity in diverse cancers[8-10], including CRC[11]. However, further investigation is needed regarding the mechanism through which curcumin affects CRC development.

Over the last decade, circular RNAs (circRNAs) have been identified as a novel noncoding RNA subgroup that are produced by exon or intron back-splicing and have a closed continuous loop[12,13]. CircRNAs are correlated with the initiation and development of various tumors, including CRC. For example, circ-FARSA aggravates malignant behavior by promoting CRC cell growth[14]. Consistently, circRNA_0000392 exerted oncogenic properties in CRC by regulating PIK3R3/AKT[15]. Hsa_circ_0136666 has been identified as a highly circRNA that is a carcinogenic factor in breast cancer and osteosarcoma[16,17]. Moreover, it facilitated CRC progression by enhancing cell growth and metastasis[18,19]. Interestingly, some studies indicated that curcumin could participate in the regulation of tumor progression by interacting with noncoding RNAs, including circRNAs[20,21]. However, the exact role played by hsa_circ_0136666 in curcumin-mediated CRC progression is still unclear.

Currently, the increasing focus on the competing endogenous RNA (ceRNA) hypothesis is that circRNAs serve as microRNA (miRNA) sponges to derepress target mRNA levels[22,23]. Here, some binding sites between hsa_circ_0136666 and miR-1301-3p were identified by bioinformatics analysis. In addition, miR-1301-3p has been suggested to dampen CRC cell growth ability[24]. Hence, this article aims to illuminate whether hsa_circ_0136666 involvement in curcumin-triggered CRC progression is mediated by sponging miR-1301-3p.

MATERIALS AND METHODS

Cultivation of cells

Under a consistent temperature (37 °C) and humidified atmosphere containing 5% CO₂, a normal human colon mucosal epithelial cell line (NCM460, ATCC, Manassas, VA, United States) and two CRC cell strains (SW480 and SW620, ATCC) were cultivated in DMEM (PAN Biotech, Aidenbach, Germany) that was mixed with FBS (10%; HyClone, Logan, UT, United States) and penicillin/streptomycin (1%; KeyGen, Nanjing, China). In addition, 20 μM curcumin (Sigma-Aldrich, St. Louis, MO, United States) was added to CRC cells for 24 h after dilution with dimethyl sulfoxide (DMSO, Sigma-Aldrich).

Cell counting kit-8 assay

Cell viability assessment was performed as per the cell counting kit (CCK)-8 reagent (Dojindo, Osaka, Japan) guidebook. A total of 2000 cells were plated into a 96-well culture plate for curcumin (20 μ M) treatment, followed by the addition of CCK-8 solution (0 μ L) into each well for another 4 h after 24 h of curcumin treatment. At 450 nm, the absorbance value was determined with the use of a microplate reader.

Colony-forming cell assay

After incubation for 2 wk, 5×10^2 treated or untreated cells in 6-well plates were mixed with paraformaldehyde (4%) and dyed with crystal violet (0.1%). After an incubation period of 30 min, the colony number was observed using a microscope.

Cell apoptosis assay

Apoptosis assessment was implemented based on the Annexin V-FITC/PI Apoptosis kit (Bender Med System, Vienna, Austria) manuals. In short, tumor cells were trypsinized, followed by resuspension in binding buffer. After the addition of Annexin V-FITC and PI at volumes of 5 μ L and 10 μ L, respectively, a FACSCalibur (BD Biosciences, Heidelberg, Germany) was applied for apoptosis detection according to the operation manual.

Real-time quantitative polymerase chain reaction

In this assay, total cellular RNAs prepared by TRIzol reagent (Invitrogen, Carlsbad, CA, United States) were quantified with a NanoDrop 2000 instrument (Thermo Scientific, Waltham, MA, United States) spectrophotometer, followed by synthesis into cDNA with a PrimeScript RT reagent kit (Takara, Tokyo, Japan) and the subsequent determination of the relative gene expression with the use of a SYBR Green PCR Kit (TaKaRa). After normalization against GAPDH (for circRNA and mRNA) and U6 (for miRNA), the relative fold changes were counted with the $2^{-\Delta\Delta Ct}$ formula. See [Table 1](#) for primers.

Cell transfection

For hsa_circ_0136666 stable upregulation, CRC cells were transfected with hsa_circ_0136666 overexpression vector (oe-hsa_circ_0136666, Geenseed Biotech, Guangzhou, China). In addition, 40 nM each of miR-1301-3p mimic and inhibitor, as well as chemokine (C-X-C motif) ligand 1 (CXCL1) small interfering RNA (si-CXCL1) and their corresponding controls (mimic NC, inhibitor NC, si-NC), were transfected. These oligonucleotides were provided by RiboBio (Guangzhou, China). Lipofectamine 3000 reagent (Invitrogen) was utilized for transfection, and further analysis was conducted after a 48-hour incubation.

5-Ethynyl-2'-deoxyuridine assay

Briefly, 5-Ethynyl-2'-deoxyuridine (EdU) (50 μ M, RiboBio) was placed into CRC cells (4×10^4 cells/well), followed by a 2-hour incubation. After immobilization in a formaldehyde solution (4%), the cells were treated with Apollo and 4',6-diamidino-2-phenylindole (DAPI). Finally, EdU-positive cells were counted by imaging five random fields using a fluorescence microscope (Olympus, Tokyo, Japan). Cell proliferation was calculated after normalizing the EdU-positive cell (red) count against the DAPI-stained cell (blue) count.

Cell cycle assay

In brief, CRC cells were trypsinized, followed by fixation in ice-cold ethanol overnight. The PBS-rinsed cells were then resuspended in PI (Bender Med System) for 30 min at 37 °C. Referring to the operation manual of FACSCalibur (BD Biosciences), the cell cycle distribution was assessed in this assay.

Western blot analysis

Cell lysates were prepared from 5×10^6 treated or untreated CRC cells in 6-well plates following the RIPA buffer (Beyotime, Nantong, China) instructions. After that, the specimens were subjected to SDS-PAGE (10%) and electrotransfer onto nitrocellulose membranes (Millipore, Molsheim, France). After being probed using the primary antibodies (Abcam, Cambridge, MA, United States): B-cell lymphoma-2 (Bcl-2; ab59348, 1:1000), Bcl-2 related X protein (Bax; ab53154, 1:1000), CXCL1 (1:100, ab206411), and β -actin (1:1000, ab8227) overnight, the immune complexes were treated with a 2-hour incubation with a secondary antibody (ab6721, 1:10000), followed by visualization with an ECL reagent (Amersham Biosciences, Pittsburg, PA, Sweden).

RNA pull-down assay

In short, probe-coated beads, generated by 2 h of room temperature incubation of the biotinylated hsa_circ_0136666 or NC probe (GenePharma, Shanghai, China) with magnetic beads, were incubated with SW480 and SW620 Lysates that were collected after sonication. Finally, the bead-bound RNA complexes were subjected to real-time quantitative PCR (RT-qPCR) analysis.

RNA immunoprecipitation assay

Briefly, SW480 and SW620 cells were cultured to 80% confluency through overnight incubation, followed by immersion in complete RNA immunoprecipitation (RIP) lysis buffer (Millipore). Then, the cell lysates were incubated with anti-Argonaute2 (Ago2) or immunoglobulin G (IgG) and 2 h of treatment with magnetic protein A/G beads. At length, the

Table 1 Primer sequences for real-time quantitative PCR

Names	Sequences (5'-3')
hsa_circ_0136666: Forward	AGGTGCTCACITGTCIGAAA
hsa_circ_0136666: Reverse	CAGATGTTTCATGGGTCCAT
hsa_circ_0000896: Forward	ACTTCATTGAGAGCTCCTTCTGG
hsa_circ_0000896: Reverse	CTTCAGAGTCCTCGAAGGAAGA
hsa_circ_0000392: Forward	TCAAGTACTGAGAAGAAAAAGCTG
hsa_circ_0000392: Reverse	GTCCTCGAGGCACACACAAT
miR-1301-3p: Forward	TTACAGCTGCCTGAGAGTGACTTA
miR-1301-3p: Reverse	CTCTACAGCTATATTGCCAGCCA
miR-34a-5p: Forward	TCCGAGTGGCAGTGTCTTAG
miR-34a-5p: Reverse	CTCAACTGGTGTCTGGAG
miR-216a-3p: Forward	ATAGTCACAGTGGTCTCTGG
miR-216a-3p: Reverse	CTCAACTGGTGTCTGGAG
CXCL1: Forward	AACCGAAGTCATAGCCACAC
CXCL1: Reverse	GTTGGATTGTACITGTTTCAGC
U6: Forward	CTCGCTCCGGCAGCACA
U6: Reverse	AACGCTTACGAATTTCGCT
GAPDH: Forward	GGTACCAGGGCTGCTTT
GAPDH: Reverse	GGAAGATGGTGATGGGATT

samples were isolated for RT-qPCR quantification of hsa_circ_0136666 and miR-1301-3p.

Dual-luciferase reporter assay

In brief, hsa_circ_0136666 and CXCL1 3' untranslated region (3'UTR) segments possessing miR-1301-3p-matched regions or mismatches were introduced into the psiCHECK2 vector (Promega, Madison, WI, United States) to generate hsa_circ_0136666 wild-type (wt)/mutant-type (mut) and CXCL1 3'UTR wt/mut reporter vectors. Subsequently, the indicated reporter vector (50 ng) was transfected into 293T cells (Sigma-Aldrich) with miR-1301-3p mimic or mimic NC (20 nM), followed by luciferase activity detection with the use of a dual-luciferase reporter (DLR) assay system (Promega).

Tumor xenograft assay

After obtaining the approval of the Animal Ethics Committee of the Second Affiliated Hospital of Kunming Medical University, we used BALB/C nude mice (Vital River Laboratory, Beijing, China) raised under a specific-pathogen-free environment for experiments. Male mice aged 5 wk were arranged in 4 groups (vector + DMSO, oe-hsa_circ_0136666 + DMSO, vector + curcumin, and oe-hsa_circ_0136666 + curcumin) with 6 mice in each group. SW480 cells (1×10^5) were transfected with vector or oe-hsa_circ_0136666, followed by subcutaneous inoculation into nude mice. Seven days later, these groups were treated with intraperitoneal DMSO or curcumin (25 mg/kg) injection twice a week. Additionally, a caliper was used to examine the tumor size once a week. All mice were euthanized on day 35 after inoculation, and their tumors were resected and weighed for further analysis. Additionally, immunohistochemical staining (IHCS) was executed in xenograft tissue sections as per the prior description[25], with Ki67- and proliferating cell nuclear antigen (PCNA)-specific antibodies to assess proliferation. In addition, section observation and image recording were performed using a BX51 system microscope (Olympus) and a digital microscope camera (DP70; Olympus), respectively.

Enzyme-linked immunosorbent assay

A CXCL1-dedicated enzyme-linked immunosorbent assay (ELISA) kit was used to quantify CXCL1. After curcumin (20 μ M, 24 h) treatment, the culture media of SW480 and SW620 cells were collected and measured using a human CXCL1 ELISA kit (ab190805, Abcam) according to the manufacturer's instructions.

Statistical methods

Data were obtained from experiments run independently in triplicate at least with the results analyzed using GraphPad Prism 7 (GraphPad Prism software, San Diego, CA, United States), and statistical significance was indicated by $P < 0.05$. Meanwhile, the mean \pm SD was used for statistical description of the data. Intergroup and multigroup differences were identified by two-tailed Student's *t* test and one-way analysis of variance (ANOVA) with Tukey's tests, respectively.

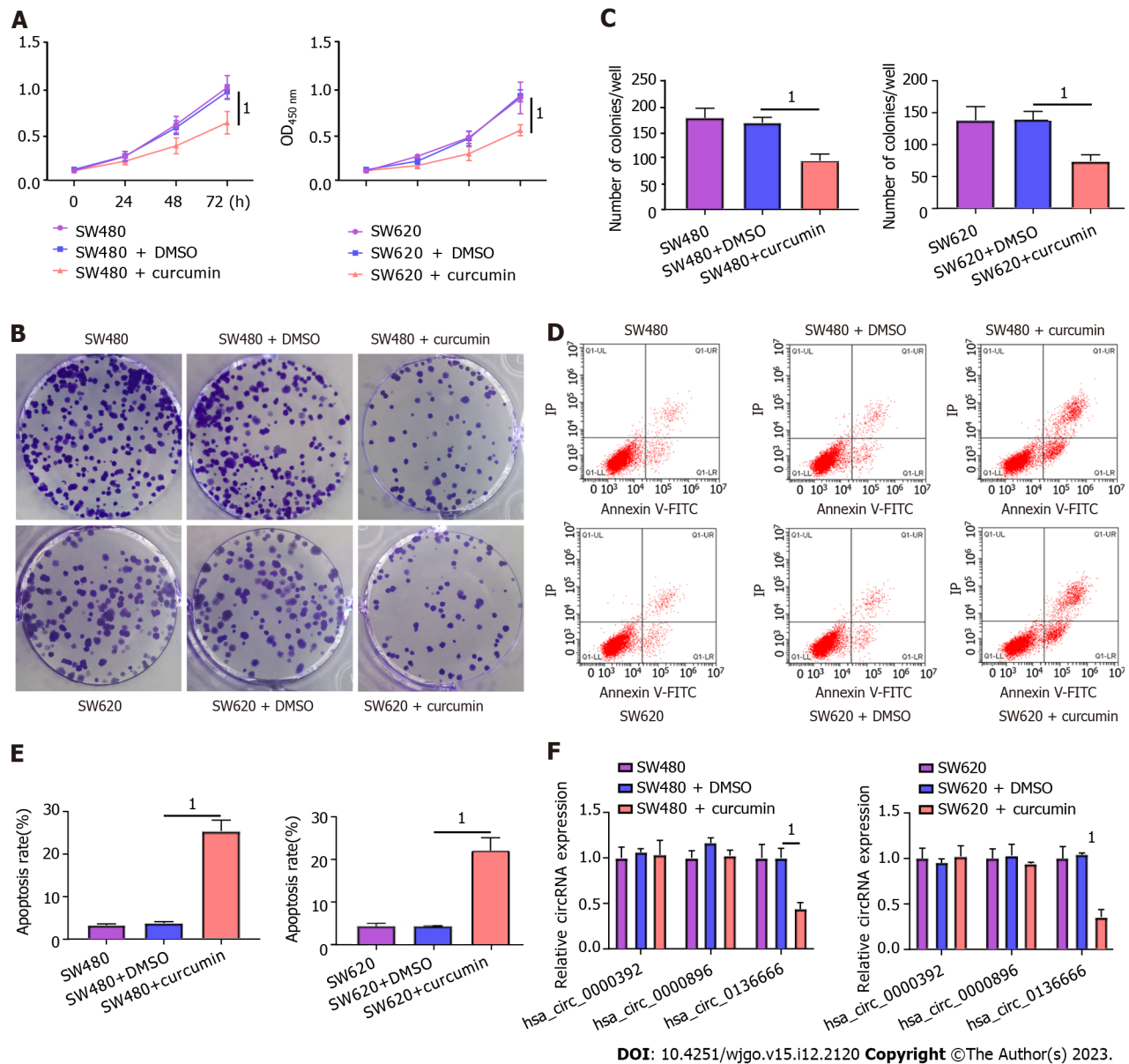
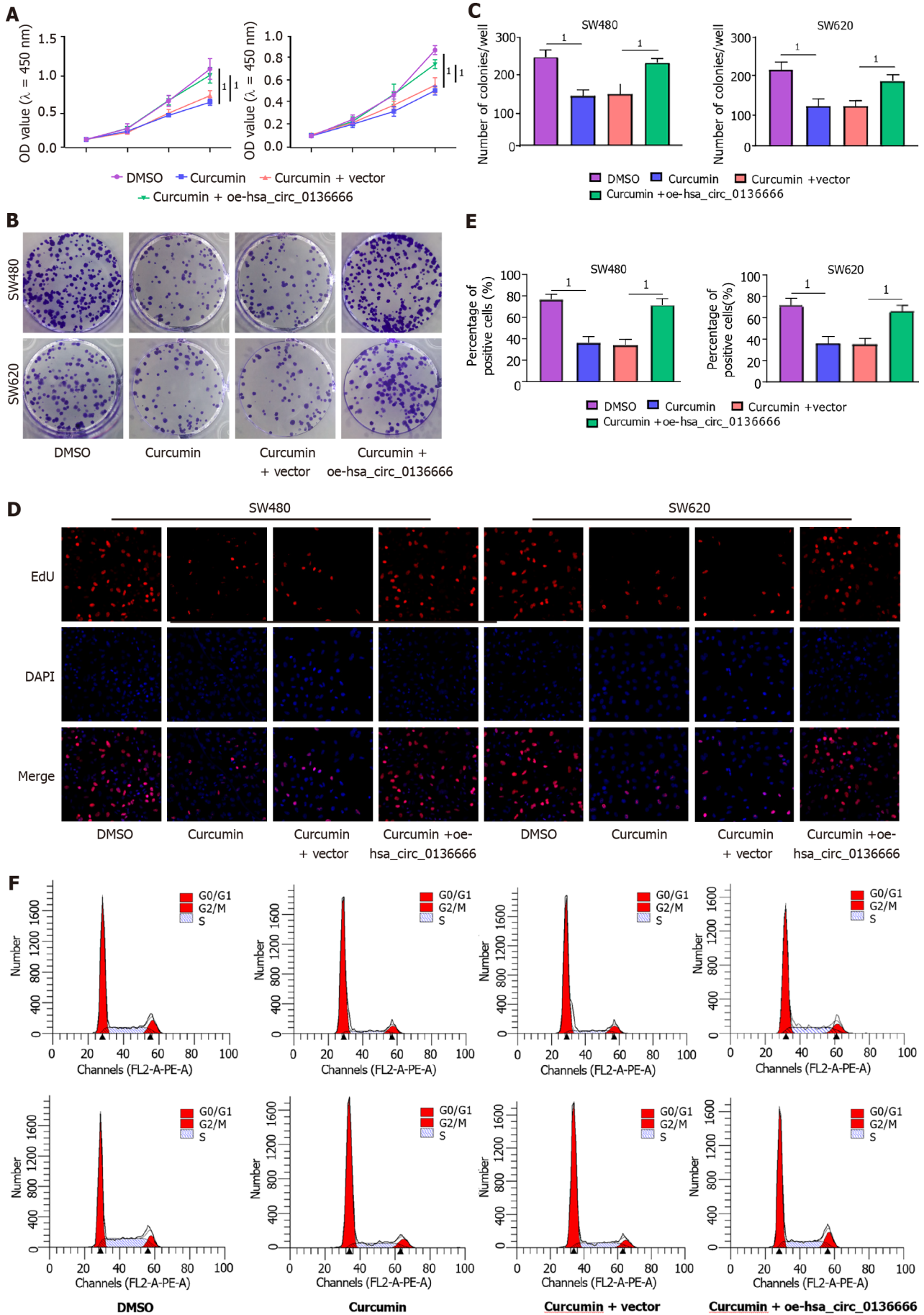


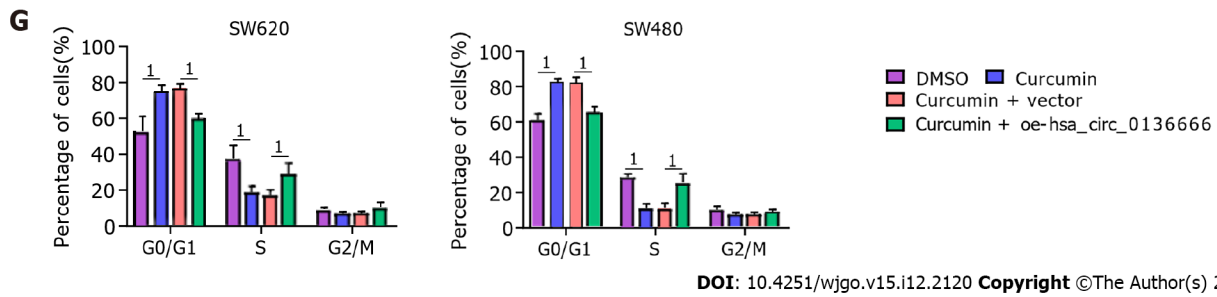
Figure 1 The impacts of curcumin treatment on colorectal carcinoma (SW480 and SW620) cell proliferation and apoptosis. Colorectal carcinoma (CRC) cells were treated with DMSO or curcumin (20 μ M). A: Cell viability was detected in treated or untreated SW480 and SW620 using cell counting kit-8 assays; B and C: Colony number assessment by colony-forming cell assays in treated or untreated SW480 and SW620; D and E: Apoptosis rate analysis in treated or untreated CRC cells by flow cytometry assays; F: Real-time quantitative PCR analysis of hsa_circ_0000392, hsa_circ_0000896, and hsa_circ_0136666 expression in treated or untreated SW480 and SW620 cells. ¹*P* < 0.05.

RESULTS

Curcumin repressed CRC cell proliferation and boosted apoptosis

First, CRC SW480 and SW620 cells were treated with 20 μ M curcumin to investigate the functional role played by curcumin in CRC. The CCK-8 results showed that 20 μ M curcumin intervention was not toxic to NCM460, a normal human colon mucosal epithelial cell line (Supplementary Figure 1). As presented in Figure 1A, decreased cell viability was observed due to curcumin intervention compared to both the control and DMSO-treated groups. Consistently, curcumin treatment distinctly reduced the colony number of SW480 and SW620 cells relative to their control groups (Figure 1B and C). Furthermore, the apoptosis rate in the curcumin group was markedly improved in comparison with that in the other groups (Figure 1D and E). In addition, previous studies indicated the involvement of hsa_circ_0000392, hsa_circ_0000896, and hsa_circ_0136666 in the regulation of CRC progression[26]. Interestingly, curcumin treatment significantly decreased hsa_circ_0136666 expression in SW480 and SW620 cells but had no effect on hsa_circ_0000392 or hsa_circ_0000896 expression (Figure 1F). Therefore, follow-up studies were conducted on hsa_circ_0136666. Together, these data indicated the suppressive role of curcumin in CRC development.



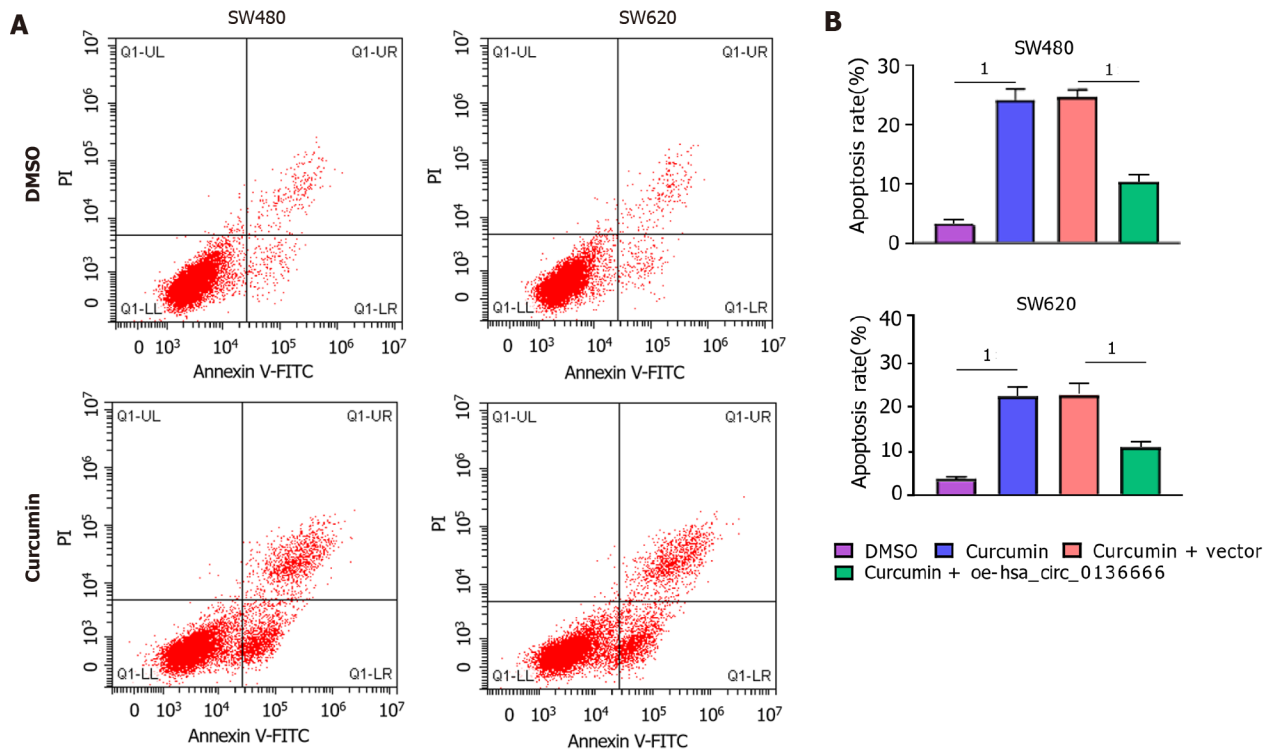


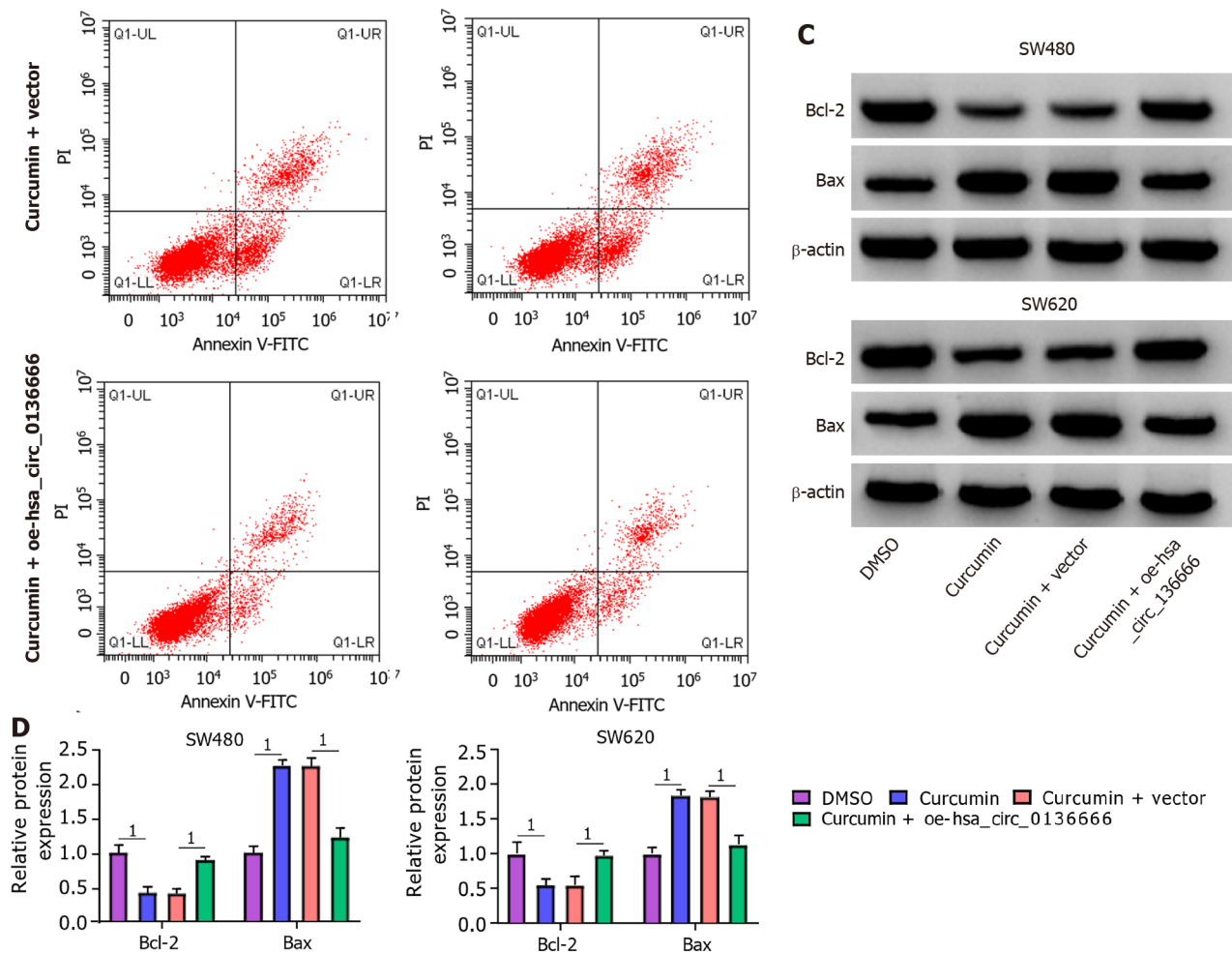
DOI: 10.4251/wjgo.v15.i12.2120 Copyright ©The Author(s) 2023.

Figure 2 Overexpressing *hsa_circ_0136666* overturned the effect of curcumin on proliferation in colorectal carcinoma SW480 and SW620 cells. Colorectal carcinoma cells were treated with DMSO, curcumin, curcumin + vector, and curcumin + *oe-hsa_circ_0136666*. A: Cell counting kit-8 assays examined SW480 and SW620 cell viability after treatment; B and C: Colony-forming cell assays detected colony numbers in treated SW480 and SW620; D and E: 5-Ethynyl-2'-deoxyuridine assays measured positive cells in treated SW480 and SW620; F and G: Flow cytometry assays analyzed cell cycle distribution in treated SW480 and SW620. * $P < 0.05$.

Overexpression of *hsa_circ_0136666* reversed curcumin-mediated CRC cell growth and apoptosis in vitro

Subsequently, the influence of *hsa_circ_0136666* and curcumin on CRC cell malignant biological behaviors was determined. First, the overexpression efficiency of *hsa_circ_0136666* was successful (Supplementary Figure 2A). The data suggested that *hsa_circ_0136666* upregulation could abrogate the inhibition of SW480 and SW620 cell viability and colony counts by curcumin (Figure 2A-C). Similarly, the reduction in EdU-positive cells caused by curcumin was also evidently ameliorated by *hsa_circ_0136666* overexpression (Figure 2D and E). In addition, curcumin treatment might block cell cycle progression in SW480 and SW620 cells, which was significantly counteracted by *oe-hsa_circ_0136666* transfection (Figure 2F and G). In addition, elevated *hsa_circ_0136666* significantly mitigated the positive effect of curcumin on the apoptosis rate in SW480 and SW620 cells (Figure 3A and B). Meanwhile, curcumin treatment induced a marked decrease in Bcl-2 (an anti-apoptosis factor) and a substantial increase in Bax (a pro-apoptosis factor), which was reversed by *hsa_circ_0136666* enrichment (Figure 3C and D). Collectively, *hsa_circ_0136666* upregulation abolished the impacts of curcumin on CRC cell growth and apoptosis.





DOI: 10.4251/wjgo.v15.i12.2120 Copyright ©The Author(s) 2023.

Figure 3 Upregulating *hsa_circ_0136666* overturned curcumin-mediated apoptosis promotion in colorectal carcinoma cells. SW480 and SW620 were treated with DMSO, curcumin, curcumin + vector, and curcumin + *oe-hsa_circ_0136666*. A and B: Flow cytometry assays tested apoptosis rate in treated SW480 and SW620; C and D: Western blot assays determined Bcl-2 and Bax protein levels in treated SW480 and SW620. $^1P < 0.05$.

Hsa_circ_0136666 directly interacted with miR-1301-3p

Then, we searched 3 potential target miRNAs of *hsa_circ_0136666*, namely, miR-34a-5p, miR-1301-3p, and miR-216-3p, from circBank. All these miRNAs were subjected to RNA pull-down analysis. In SW480 and SW620 cells, only miR-1301-3p was substantially pulled down by the biotinylated *hsa_circ_0136666* probe (Figure 4A). In addition, the RIP assay showed that *hsa_circ_0136666* and miR-1301-3p were both greatly enriched in Ago2 pellets *vs* the IgG control group (Figure 4B). Thus, miR-1301-3p was chosen for further research. Furthermore, their binding loci are presented in Figure 4C. Furthermore, the miR-1301-3p mimic transfection efficiency is displayed in Supplementary Figure 2B. Then, the DLR assay showed that the miR-1301-3p mimic could decrease *hsa_circ_0136666* wt luciferase activity in 293T cells, whereas it had no obvious impact on the mutant group (Figure 4D). Moreover, miR-1301-3p was enhanced by curcumin exposure in SW480 and SW620 cells compared with their control groups (Figure 4E), implying the participation of miR-1301-3p in curcumin-mediated CRC development. Overall, miR-1301-3p acted as a direct target of *hsa_circ_0136666*.

Hsa_circ_0136666 could reverse curcumin-triggered CRC cell proliferation and apoptosis by interacting with miR-1301-3p

Next, the influence of *hsa_circ_0136666*/miR-1301-3p on curcumin-mediated proliferation and apoptosis was further explored. According to the RT-qPCR assay, elevated *hsa_circ_0136666* repressed miR-1301-3p levels in CRC cells, while miR-1301-3p mimic cotransfection counteracted these effects (Figure 5A). Functionally, miR-1301-3p upregulation weakened the cell growth ability-promoting effect of *hsa_circ_0136666* in curcumin-treated SW480 and SW620 cells (Figure 5B-E). Similarly, *hsa_circ_0136666* overexpression-induced enhancement of cell cycle progression was partly abated by miR-1301-3p upregulation in curcumin-induced SW480 and SW620 cells (Figure 5F). In addition, miR-1301-3p mimic introduction promoted the suppressive action of *hsa_circ_0136666* overexpression against apoptosis in curcumin-stimulated CRC cells (Figure 5G and H), accompanied by lowered Bcl-2 and elevated Bax levels (Figure 5I and J). Overall, *hsa_circ_0136666* could partly regulate proliferation and apoptosis by targeting miR-1301-3p in curcumin-treated CRC cells.

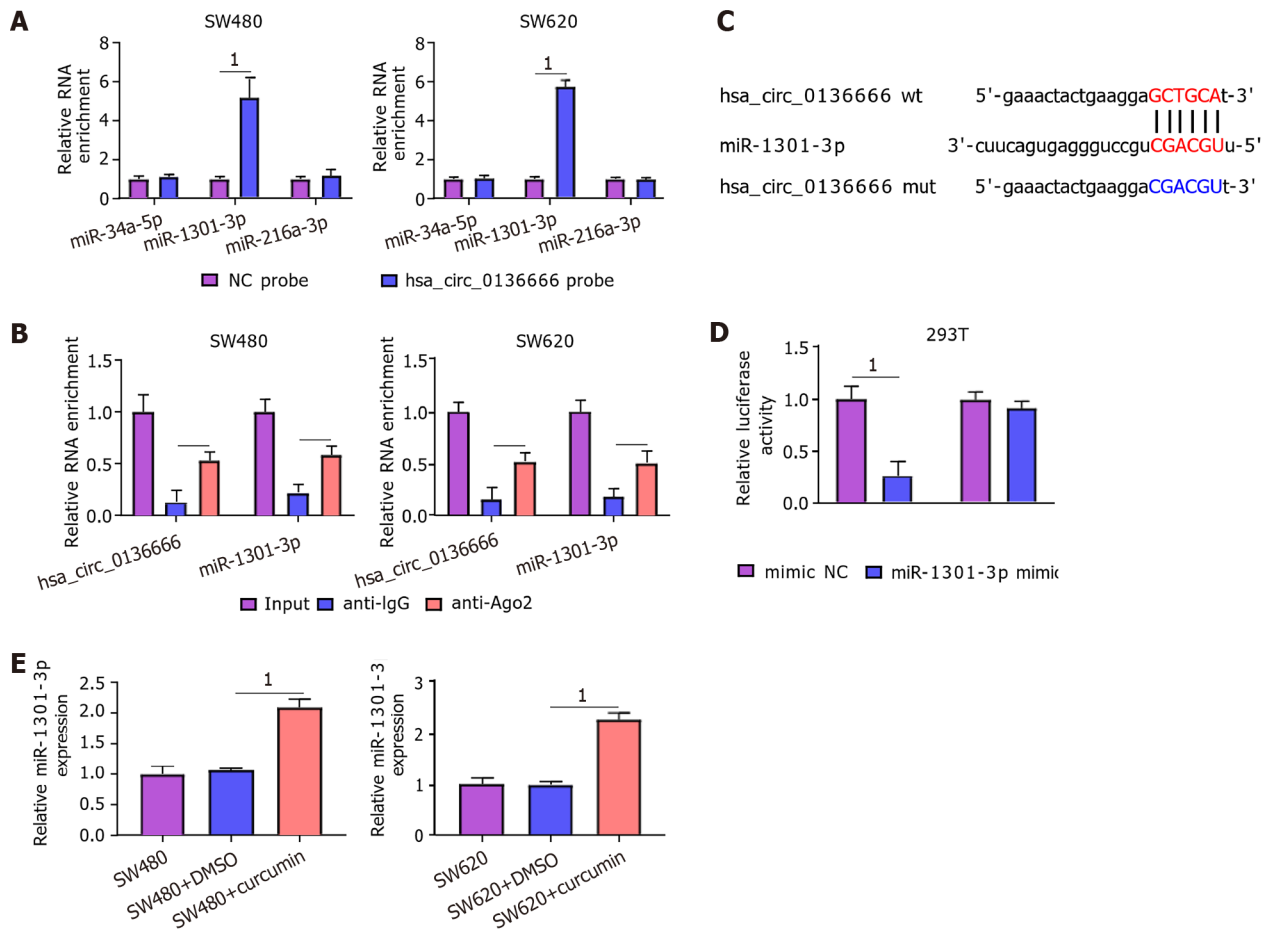
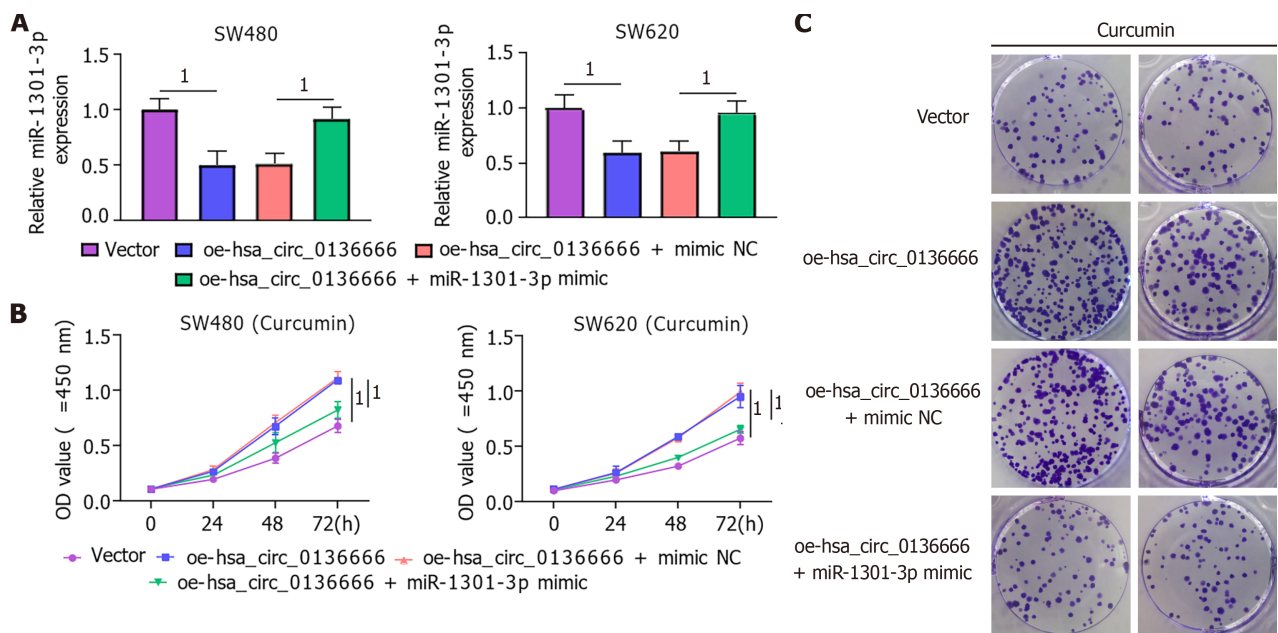
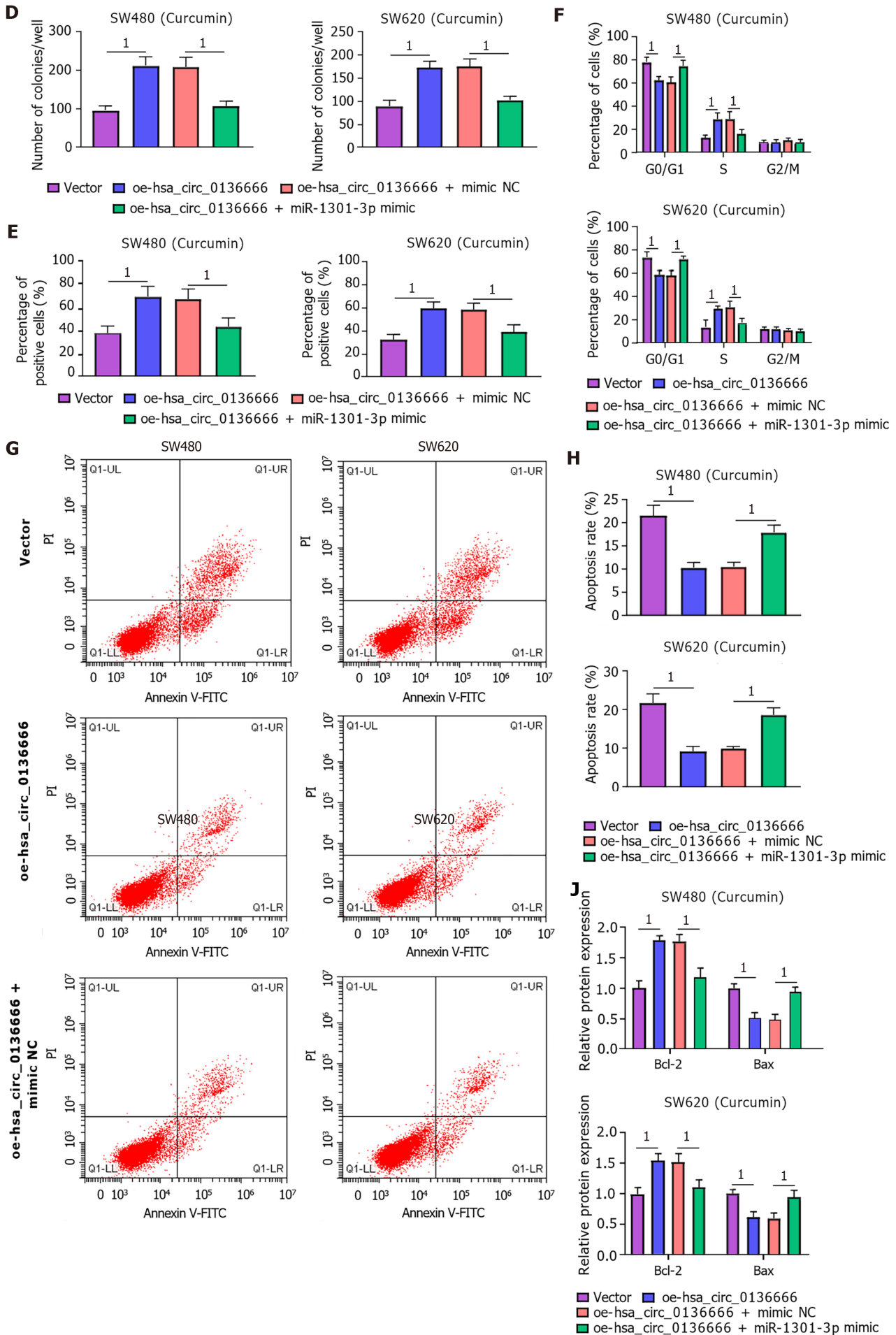


Figure 4 Hsa_circ_0136666 directly bound to miR-1301-3p. A: Real-time quantitative PCR (RT-qPCR) measured relative levels of 3 miRNA candidates in SW480 and SW620 lysates; B: RNA immunoprecipitation assays assessed miR-1301-3p endogenously associated with hsa_circ_0136666 in SW480 and SW620 extracts; C: Binding loci between hsa_circ_0136666 and miR-1301-3p and the hsa_circ_0136666 mut sequence; D: The binding relationship was verified by a dual-luciferase reporter assay; E: RT-qPCR assays quantified miR-1301-3p in SW480, SW480 + DMSO, SW480 + curcumin, SW620, SW620 + DMSO, and SW620 + curcumin. ¹*P* < 0.05. wt: Wild-type; mut: Mutant-type.





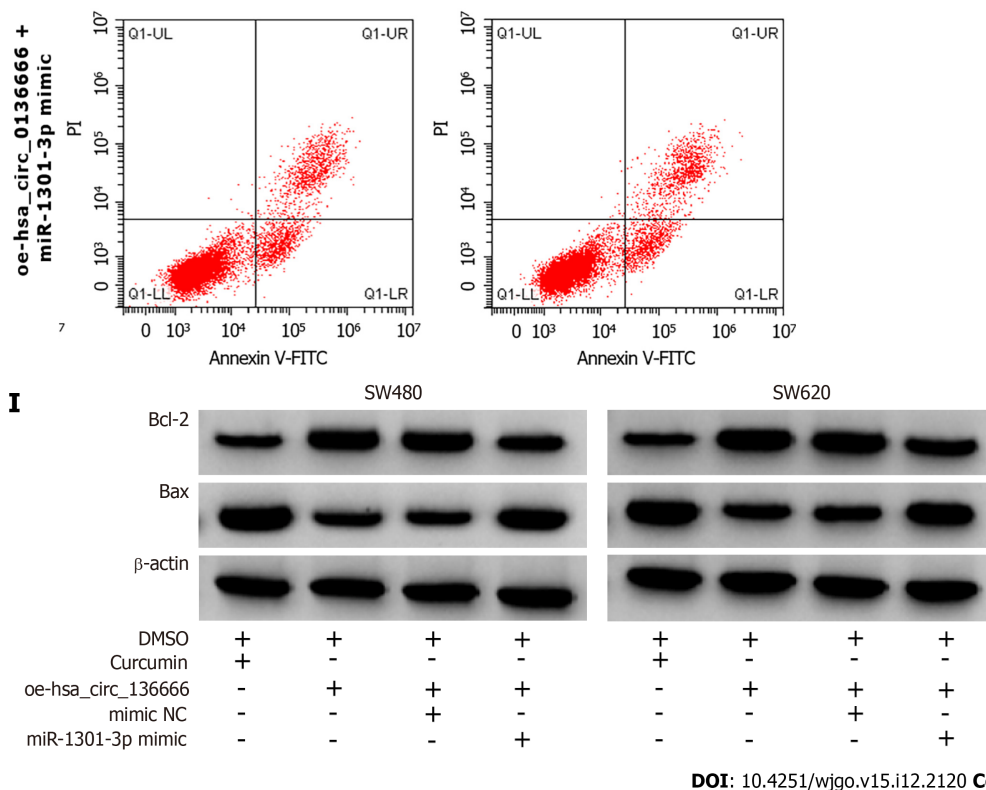


Figure 5 miR-1301-3p overturned the effect of hsa_circ_0136666 on growth and apoptosis in curcumin-treated colorectal carcinoma cells.

A: Real-time quantitative PCR assays quantified miR-1301-3p levels in SW480 and SW620 transfected with vector, oe-hsa_circ_0136666, oe-hsa_circ_0136666+mimic NC, and oe-hsa_circ_0136666 + miR-1301-3p mimic; B-J: Colorectal carcinoma cells were intervened by curcumin after transfection; B: Cell counting kit-8 assays measured cell viability; C and D: Colony-forming cell assays determined the colony number; E: 5-Ethynyl-2'-deoxyuridine assays examined positive cell count; F: Flow cytometry assays determined cell cycle distribution; G and H: Flow cytometry assays tested apoptosis; I and J: Western blot assays quantified Bcl-2 and Bax protein levels. * $P < 0.05$.

miR-1301-3p directly targeted CXCL1

According to starBase analysis, the CXCL1 3'UTR possessed some complementary loci with miR-1301-3p (Figure 6A). The DLR assay suggested that miR-1301-3p upregulation significantly hindered CXCL1 3'UTR reporter luciferase activity but not the mutant group (Figure 6B). Notably, CXCL1 Levels were significantly downregulated by curcumin treatment in CRC cells (Figure 6C). Moreover, ELISA showed that CXCL1 levels were obviously reduced by curcumin treatment in CRC cells (Supplementary Figure 3A). Moreover, elevated hsa_circ_0136666 could facilitate CXCL1 protein levels in CRC cells, and miR-1301-3p upregulation distinctly attenuated this effect (Figure 6D), implying the ability of hsa_circ_0136666 to modulate CXCL1 by sponging miR-1301-3p. Meanwhile, ELISA showed that hsa_circ_0136666 overexpression might increase CXCL1 secretion in CRC cells, which was reversed by miR-1301-3p overexpression (Supplementary Figure 3B). Overall, CXCL1 acted as a direct target of miR-1301-3p.

miR-1301-3p knockdown reversed the curcumin-induced increase in CRC cell growth and decrease in apoptosis by targeting CXCL1

The roles played by miR-1301-3p and CXCL1 in curcumin-mediated proliferation and apoptosis were explored. Simultaneously, the introduction of miR-1301-3p inhibitor and si-CXCL1 into SW480 and SW620 cells was performed, followed by transfection efficiency assessment (Figure 7A and B). Meanwhile, ELISA showed that the introduction of si-CXCL1 might reduce CXCL1 secretion in SW480 and SW620 cells (Supplementary Figure 3C). In addition, reduced miR-1301-3p could reinforce the CXCL1 protein level, while the cotransfection of si-CXCL1 counteracted the effect in SW480 and SW620 cells (Figure 7C). Additionally, ELISA showed that CXCL1 downregulation might significantly abolish the promotion of CXCL1 secretion by the miR-1301-3p inhibitor (Supplementary Figure 3D). Functionally, the augmented cell proliferative ability and cell cycle progression induced by miR-1301-3p downregulation were significantly relieved by CXCL1 knockdown in curcumin-treated SW480 and SW620 cells (Figure 7D-H). In addition, the introduction of si-CXCL1 abolished the negative action of miR-1301-3p knockdown against apoptosis in curcumin-exposed CRC cells (Figure 7I and J), manifested as decreased Bcl-2 and increased Bax levels (Figure 7K and L). In summary, miR-1301-3p regulated proliferation and apoptosis by interacting with CXCL1 in curcumin-treated CRC cells.

Curcumin repressed CRC cell growth by regulating hsa_circ_0136666 in vivo

We established mouse xenograft models of CRC to validate the functional effect of hsa_circ_0136666 and curcumin on *in vivo* tumor growth. As indicated by Figure 8A and B, curcumin could distinctly dampen tumor growth (reduced tumor

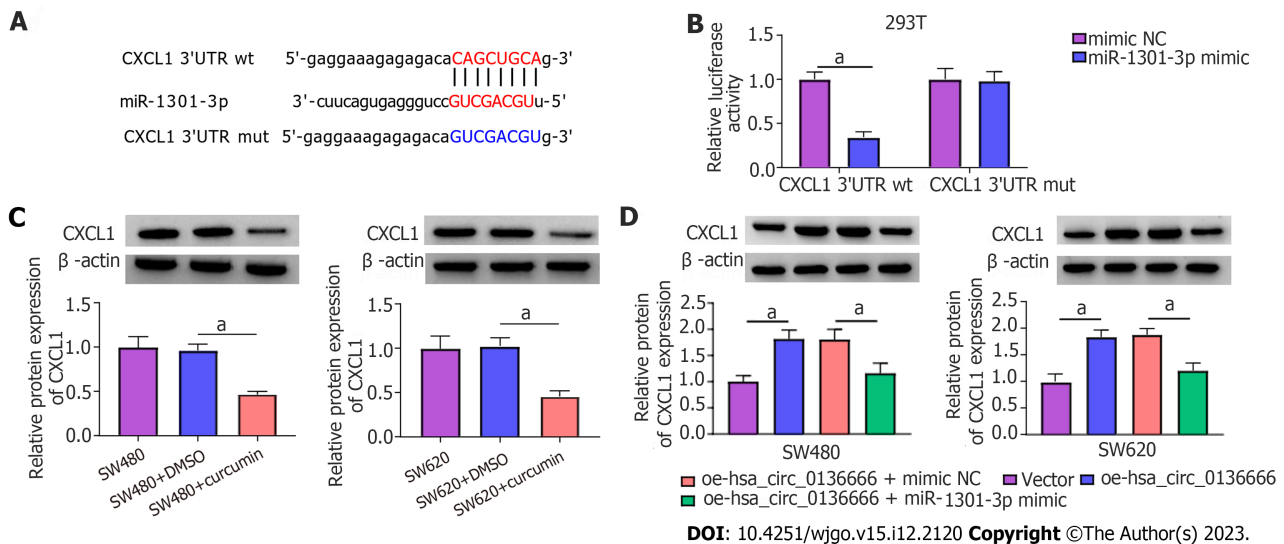


Figure 6 CXCL1 was miR-1301-3p's direct target. A: Putative binding sequences between miR-1301-3p and CXCL1 3'UTR, and mutant sites in CXCL1 3'UTR mut; B: Validation of prediction by dual-luciferase reporter assay; C: Western blot assay quantification of CXCL1 protein in SW480, SW480 + DMSO, SW480 + curcumin, SW620, SW620 + DMSO, and SW620 + curcumin; D: Western blot assay quantification of CXCL1 protein in SW480 and SW620 transfected with vector, oe-hsa_circ_0136666, oe-hsa_circ_0136666 + mimic NC, and oe-hsa_circ_0136666 + miR-1301-3p mimic. * $P < 0.05$. 3'UTR: 3' untranslated region; wt: Wild-type; mut: Mutant-type.

volume and weight), whereas the overexpression of hsa_circ_0136666 partially attenuated these effects in xenografts (Figure 8A and B). Furthermore, our data showed that curcumin injection could abate hsa_circ_0136666 and CXCL1 levels in tumor tissues derived from oe-hsa_circ_0136666-transfected SW480 cells (Figure 8C). Synchronously, miR-1301-3p displayed an opposite trend in this xenograft (Figure 8C and D). In addition, IHCS revealed that Ki-67 and PCNA (standard proliferation markers) levels were dampened by hsa_circ_0136666 deficiency in this xenograft (Figure 8E). Together, curcumin suppressed CRC cell growth by regulating hsa_circ_0136666 *in vivo*.

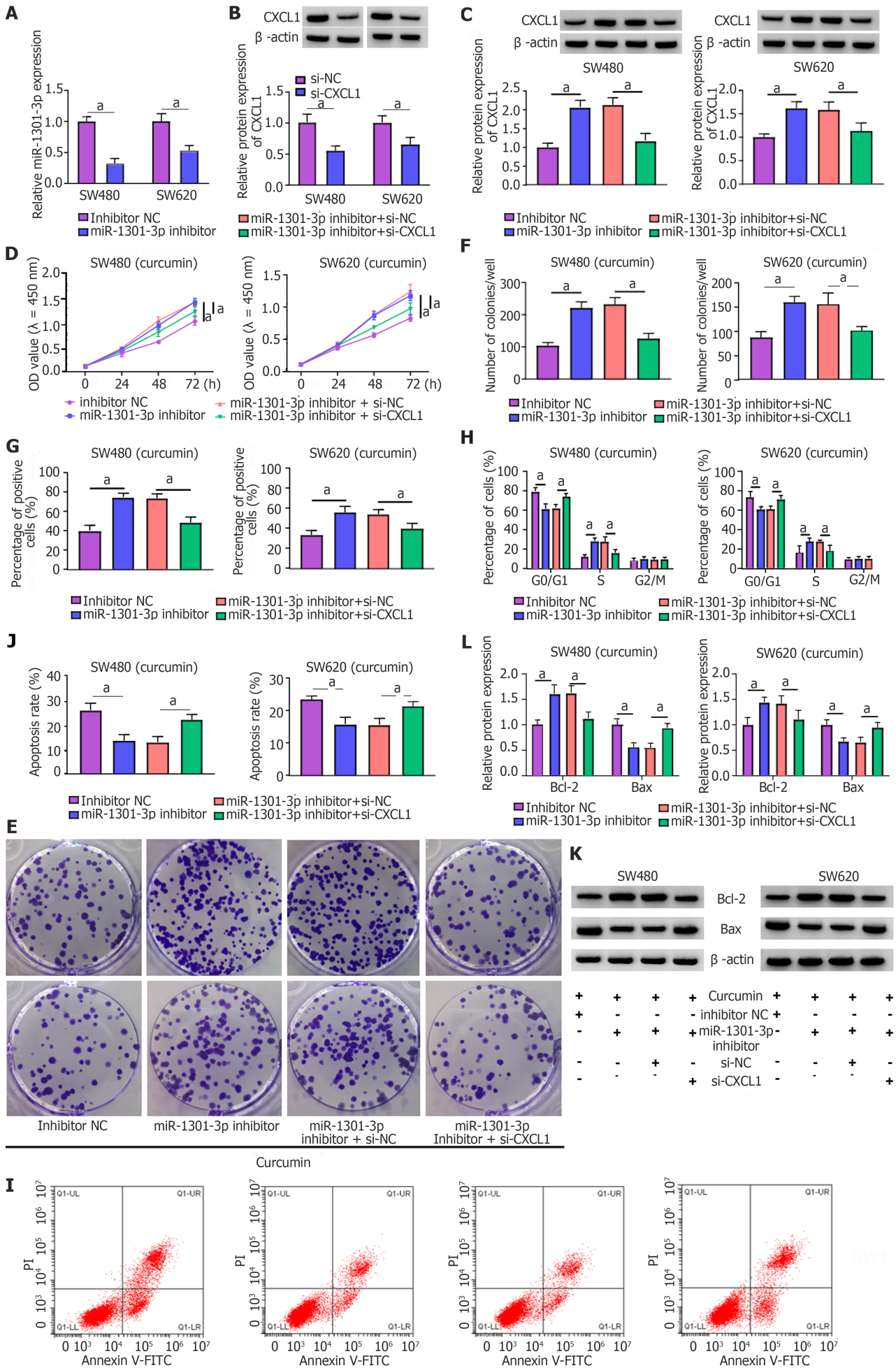
DISCUSSION

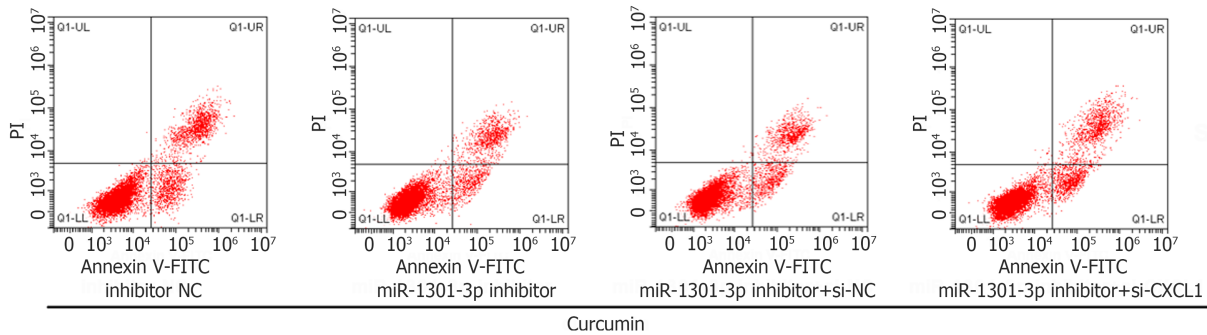
In this research, the role and mechanism of curcumin in CRC development were explored. Here, we found that curcumin repressed CRC cell proliferation and boosted apoptosis and first verified that it was associated with the hsa_circ_0136666/miR-1301-3p/CXCL1 regulatory network.

Work in several laboratories has revealed that curcumin, a natural polyphenolic compound, presents antioxidant, anti-inflammatory, and anticancer properties[27-29]. Recently, it has become evident that curcumin can repress tumor progression in a variety of cancers[30,31]. In terms of CRC, some studies have indicated that curcumin is a novel agent to prevent cancer development[32-34]. In this regard, the present study suggested the antiproliferative and pro-apoptotic actions of curcumin on CRC, consistent with previous reports[35,36]. Notably, previous documents discovered that circRNAs might be a potential mechanism through which curcumin modulates tumor development[20,21]. In this paper, we found that curcumin could reduce hsa_circ_0136666 levels in CRC cells for the first time. Moreover, recent studies have described that hsa_circ_0136666 acts as a carcinogenic factor by accelerating proliferation and metastasis in CRC[19, 37]. Functional analysis suggested that overexpressing hsa_circ_0136666 abolished the curcumin-triggered decline in CRC cell proliferative ability and augmentation of apoptosis *in vitro*. As expected, hsa_circ_0136666 upregulation also partly reversed the repressive action of curcumin on CRC cell growth *in vivo*. That is, the regulatory role of curcumin in the development of CRC might be correlated with hsa_circ_0136666.

CircRNAs are mostly stable transcripts with a large number of miRNA-binding loci, enabling them to act as miRNA sponges to repress miRNA modulation of downstream target genes in various human cancers[38,39]. In the current work, we first identified the role of miR-1301-3p as a novel miRNA target of hsa_circ_0136666. Similarly, miR-1301-3p was verified as a tumor-associated miRNA in thyroid papillary, breast, and bladder cancers[40-42]. miR-1301-3p has also been demonstrated to impede CRC cell proliferation and induce apoptosis[24]. Consistent with previous work, miR-1301-3p downregulation was also proven in CRC cells. Interestingly, we observed enhanced miR-1301-3p by curcumin. Furthermore, upregulating miR-1301-3p reversed the effects of hsa_circ_0136666 on curcumin-treated CRC cell growth and apoptosis. These findings imply that curcumin can hinder CRC development by a ceRNA effect of hsa_circ_0136666 and miR-1301-3p.

Analogously, the possible miR-1301-3p-interacting target gene was searched based on bioinformatics, and CXCL1 was validated. CXCL1 is a chemokine of epithelial origin in rodents and humans that elevates tumor epithelia-stromal interactions and boosts tumor growth and invasion[43]. Further studies have shown that CXCL1 plays a tumorigenic role in multiple cancers[44,45], including CRC[46]. Meanwhile, the participation of CXCL1 in the modulation of malignant tumor progression by curcumin has been demonstrated[47,48]. In concordance with these findings, CXCL1 was identified





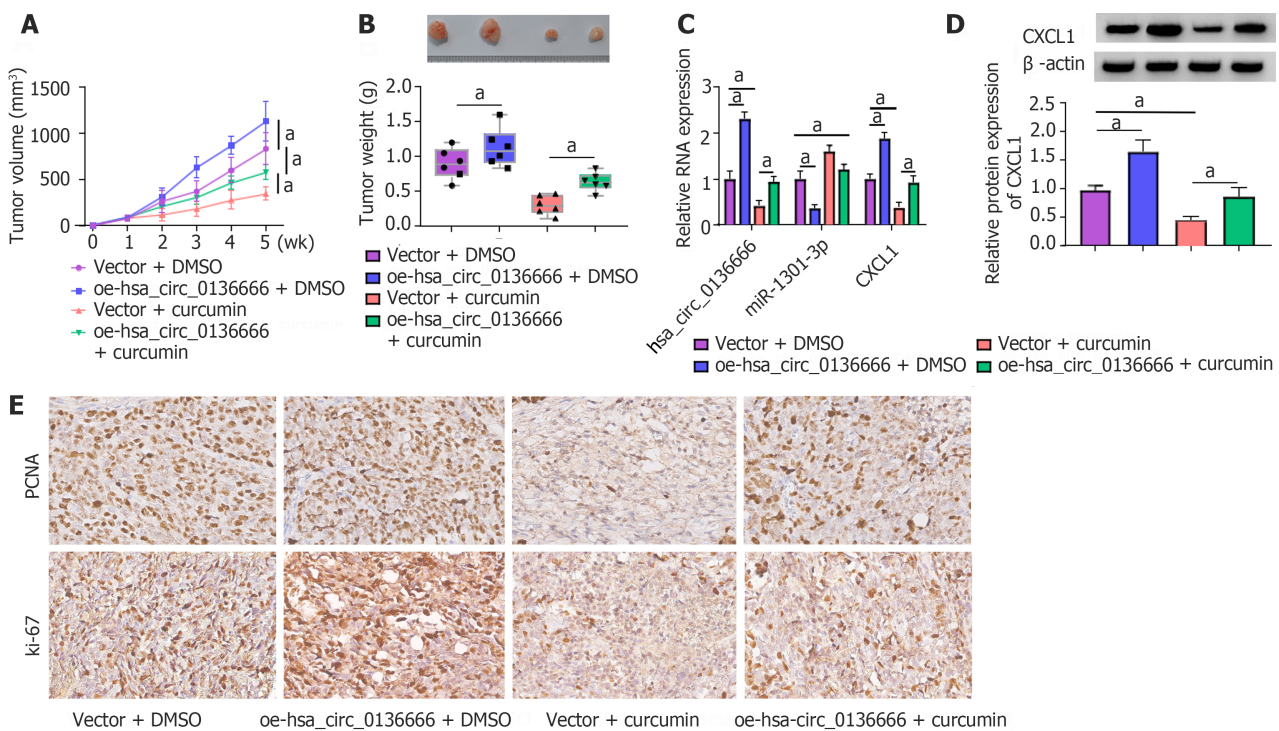
DOI: 10.4251/wjgo.v15.i12.2120 Copyright ©The Author(s) 2023.

Figure 7 Downregulating CXCL1 abrogated the influence of miR-1301-3p knockdown on curcumin-triggered colorectal carcinoma cell proliferation and apoptosis. A: Real-time quantitative PCR assay measurement of miR-1301-3p in inhibitor NC and miR-1301-3p inhibitor-transfected SW480 and SW620; B: Western blot assay of CXCL1 protein in si-NC or si-CXCL1-transfected SW480 and SW620; C: Western blot assay of CXCL1 protein in SW480 and SW620 after inhibitor NC, miR-1301-3p inhibitor, miR-1301-3p inhibitor + si-NC and miR-1301-3p inhibitor + si-CXCL1 transfection; D-L: Colorectal carcinoma cells were intervened by curcumin after transfection; D: Cell counting kit-8 assay of cell viability; E and F: Colony-forming cell assay of colony number; G: 5-Ethynyl-2'-deoxyuridine assay of positive cells; H: Flow cytometry assay of cell cycle distribution; I and J: Flow cytometry assay of apoptosis; K and L: Western blot assay of Bcl-2 and Bax protein levels. *P < 0.05.

to be downregulated by curcumin treatment. Synchronously, the miR-1301-3p inhibitor enhanced cell growth and repressed apoptosis in curcumin-stimulated CRC cells by targeting CXCL1. Additionally, hsa_circ_0136666 modulated CXCL1 by sponging miR-1301-3p, further verifying that hsa_circ_0136666 regulation of tumor development can be mediated through miR-1301-3p/CXCL1 signaling.

CONCLUSION

Hsa_circ_0136666 relieves curcumin-induced CRC cell growth and apoptosis partly *via* miR-1301-3p/CXCL1 signaling. This study elucidates a new mechanism of curcumin and sheds light on developing a new therapeutic for CRC treatment.



DOI: 10.4251/wjgo.v15.i12.2120 Copyright ©The Author(s) 2023.

Figure 8 Overexpressing hsa_circ_0136666 abolished the repression of curcumin on colorectal carcinoma growth *in vivo*. The nude mice were subcutaneously inoculated with SW480 introduced with vector or oe-hsa_circ_0136666, followed by intraperitoneal curcumin (25 mg/kg) injection one week

later. A and B: Tumour volume and tumour weight measurements in the xenografts; C: Real-time quantitative PCR assay quantification of hsa_circ_0136666, miR-1301-3p, and CXCL1 in xenografts; D: Western blot assay of CXCL1 protein in xenografts; E: Immunohistochemical staining of Ki-67 and proliferating cell nuclear antigen expression in xenografts. ¹P < 0.05. PCNA: Proliferating cell nuclear antigen.

ARTICLE HIGHLIGHTS

Research background

Colorectal carcinoma (CRC) is the most frequent-occurring malignant tumour in the United States. Curcumin exerts anti-tumor activity in CRC, but the underlying mechanism needs further elucidation. Meanwhile, over the last decade, circular RNAs (circRNAs) is correlated with the initiation and development of various tumors, containing CRC. Also, the increasing focus on the competing endogenous RNAs hypothesis is that circRNAs serve as microRNA sponges to derepress target mRNAs' levels.

Research motivation

Clinically, it is urgent to find a more effective therapy, which has high clinical significance for CRC patients. Currently, the chemo-preventive properties of traditional Chinese medicine have drawn great attention in cancer therapeutics. As a naturally occurring medicine, curcumin is derived from the medical plant *Curcuma longa L.* However, it needs further investigation regarding the mechanism through which curcumin affects CRC development.

Research objectives

This study aims at illuminating whether hsa_circ_0136666 involvement on curcumin-triggered CRC progression was mediated *via* sponging miR-1301-3p.

Research methods

CRC cells were adopted and treated with 20 μ M curcumin for 24 h. Then, for hsa_circ_0136666 stably upregulation, CRC cells were treated with hsa_circ_0136666 overexpression vector transfection or miR-1301-3p mimic and inhibitor. Real-time quantitative PCR was used to quantified the expression of hsa_circ_0136666, miR-1301-3p and CXCL1. Cell counting kit-8, colony-forming cell, 5-ethynyl-2'-deoxyuridine, and flow cytometry assays were carried out to determine cell proliferation, apoptosis, and cell cycle progression. The relationship between hsa_circ_0136666, miR-1301-3p and CXCL1 were validated by RNA pull-down, RIP, and dual-luciferase reporter assay. *In vivo* experiments were implemented by the murine xenograft model.

Research results

Curcumin treatment could distinctly reduce the colony number of SW480 and SW620 cells relative to their control groups. Furthermore, the apoptosis rate in the curcumin group was markedly improved in comparison with other groups. Interestingly, curcumin treatment significantly decreased hsa_circ_0136666 in SW480 and SW620 but had no effect on hsa_circ_0000392 and hsa_circ_0000896 expression. These data indicated the suppressive role of curcumin on CRC development. hsa_circ_0136666 upregulation could abolish the impacts of curcumin on CRC cell growth and apoptosis. Meanwhile, miR-1301-3p acted as a direct target of hsa_circ_0136666 and miR-1301-3p directly targeted CXCL1. Hsa_circ_0136666 could reverse curcumin-triggered CRC cell proliferation and apoptosis by interacting with miR-1301-3p while miR-1301-3p knockdown overturned curcumin-induced increase in CRC cell growth and decrease in apoptosis by targeting CXCL1. Curcumin repressed CRC cell growth *via* regulating hsa_circ_0136666 *in vivo*.

Research conclusions

Curcumin repressed CRC cell proliferation and boosted apoptosis, and first verified it was associated with the regulatory network of the hsa_circ_0136666/miR-1301-3p/CXCL1. Hsa_circ_0136666 relieves curcumin-induced CRC cell growth and apoptosis partly *via* the miR-1301-3p/CXCL1 signaling.

Research perspectives

This study elucidates a new mechanism of curcumin and sheds light on developing a new therapeutic for CRC treatment.

FOOTNOTES

Co-first authors: Shi Chen and Wei Li.

Author contributions: Chen S and Li W contributed equally to this work and are co-first authors, including design of the study, acquiring and analyzing data from experiments, and writing of the actual manuscript. Chen S, Li W, Li W and Wang F conceived and designed the experiments; Liao C, Chen S, Wang F and Ning CG performed the research; Ning CG, Wang LX, and Sun F contributed to the statistical analysis; Chen S, Li W, Wang F and Ning CG wrote the paper; including design of the study, acquiring and analyzing data from experiments, and writing of the actual manuscript. All authors read and approved the final manuscript.

Supported by National Natural Science Foundation of China, No. 81960508; Yunnan Province Wang Bin Expert Workstation, No.

202205AF150011.

Institutional review board statement: This study did not involve any human studies.

Institutional animal care and use committee statement: The experimental protocol was approved by the Animal Care and Use Committee of The Second Affiliated Hospital of Kunming Medical University.

Conflict-of-interest statement: All the authors report no relevant conflicts of interest for this article.

Data sharing statement: No additional data are available.

ARRIVE guidelines statement: The authors have read the ARRIVE guidelines, and the manuscript was prepared and revised according to the ARRIVE guidelines.

Open-Access: This article is an open-access article that was selected by an in-house editor and fully peer-reviewed by external reviewers. It is distributed in accordance with the Creative Commons Attribution NonCommercial (CC BY-NC 4.0) license, which permits others to distribute, remix, adapt, build upon this work non-commercially, and license their derivative works on different terms, provided the original work is properly cited and the use is non-commercial. See: <https://creativecommons.org/licenses/by-nc/4.0/>

Country/Territory of origin: China

ORCID number: Feng Sun 0009-0006-3770-6391.

S-Editor: Lin C

L-Editor: A

P-Editor: Wu RR

REFERENCES

- 1 Siegel RL, Miller KD, Fuchs HE, Jemal A. Cancer statistics, 2022. *CA Cancer J Clin* 2022; **72**: 7-33 [PMID: 35020204 DOI: 10.3322/caac.21708]
- 2 Siegel RL, Jakubowski CD, Fedewa SA, Davis A, Azad NS. Colorectal Cancer in the Young: Epidemiology, Prevention, Management. *Am Soc Clin Oncol Educ Book* 2020; **40**: 1-14 [PMID: 32315236 DOI: 10.1200/EDBK_279901]
- 3 Baidoun F, Elshihy K, Elkerai Y, Merjaneh Z, Khoudari G, Sarmini MT, Gad M, Al-Husseini M, Saad A. Colorectal Cancer Epidemiology: Recent Trends and Impact on Outcomes. *Curr Drug Targets* 2021; **22**: 998-1009 [PMID: 33208072 DOI: 10.2174/1389450121999201117115717]
- 4 Cardoso R, Guo F, Heisser T, De Schutter H, Van Damme N, Nilbert MC, Christensen J, Bouvier AM, Bouvier V, Launoy G, Woronoff AS, Cariou M, Robaszekiewicz M, Delafosse P, Poncet F, Walsh PM, Senore C, Rosso S, Lemmens VEPP, Elferink MAG, Tomšič S, Žagar T, Marques ALM, Marcos-Gragera R, Puigdemont M, Galceran J, Carulla M, Sánchez-Gil A, Chirlaque MD, Hoffmeister M, Brenner H. Overall and stage-specific survival of patients with screen-detected colorectal cancer in European countries: A population-based study in 9 countries. *Lancet Reg Health Eur* 2022; **21**: 100458 [PMID: 35832063 DOI: 10.1016/j.lanepe.2022.100458]
- 5 Ming T, Tao Q, Tang S, Zhao H, Yang H, Liu M, Ren S, Xu H. Curcumin: An epigenetic regulator and its application in cancer. *Biomed Pharmacother* 2022; **156**: 113956 [PMID: 36411666 DOI: 10.1016/j.biopha.2022.113956]
- 6 Mari M, Carrozza D, Ferrari E, Asti M. Applications of Radiolabelled Curcumin and Its Derivatives in Medicinal Chemistry. *Int J Mol Sci* 2021; **22** [PMID: 34299029 DOI: 10.3390/ijms22147410]
- 7 Abd El-Hack ME, El-Saadony MT, Swelum AA, Arif M, Abo Ghanima MM, Shukry M, Noreldin A, Taha AE, El-Tarabily KA. Curcumin, the active substance of turmeric: its effects on health and ways to improve its bioavailability. *J Sci Food Agric* 2021; **101**: 5747-5762 [PMID: 34143894 DOI: 10.1002/jsfa.11372]
- 8 Termini D, Den Hartogh DJ, Jaglanian A, Tsiani E. Curcumin against Prostate Cancer: Current Evidence. *Biomolecules* 2020; **10** [PMID: 33182828 DOI: 10.3390/biom10111536]
- 9 Ashrafzadeh M, Najafi M, Makvandi P, Zarrabi A, Farkhondeh T, Samarghandian S. Versatile role of curcumin and its derivatives in lung cancer therapy. *J Cell Physiol* 2020; **235**: 9241-9268 [PMID: 32519340 DOI: 10.1002/jcp.29819]
- 10 Rutz J, Janicova A, Woidacki K, Chun FK, Blaheta RA, Relja B. Curcumin-A Viable Agent for Better Bladder Cancer Treatment. *Int J Mol Sci* 2020; **21** [PMID: 32466578 DOI: 10.3390/ijms21113761]
- 11 Pricci M, Girardi B, Giorgio F, Losurdo G, Ierardi E, Di Leo A. Curcumin and Colorectal Cancer: From Basic to Clinical Evidences. *Int J Mol Sci* 2020; **21** [PMID: 32235371 DOI: 10.3390/ijms21072364]
- 12 Liu CX, Chen LL. Circular RNAs: Characterization, cellular roles, and applications. *Cell* 2022; **185**: 2016-2034 [PMID: 35584701 DOI: 10.1016/j.cell.2022.04.021]
- 13 Lei M, Zheng G, Ning Q, Zheng J, Dong D. Translation and functional roles of circular RNAs in human cancer. *Mol Cancer* 2020; **19**: 30 [PMID: 32059672 DOI: 10.1186/s12943-020-1135-7]
- 14 Lu C, Fu L, Qian X, Dou L, Cang S. Knockdown of circular RNA circ-FARSA restricts colorectal cancer cell growth through regulation of miR-330-5p/LASP1 axis. *Arch Biochem Biophys* 2020; **689**: 108434 [PMID: 32473899 DOI: 10.1016/j.abb.2020.108434]
- 15 Xu H, Liu Y, Cheng P, Wang C, Zhou W, Xu Y, Ji G. CircRNA_0000392 promotes colorectal cancer progression through the miR-193a-5p/PIK3R3/AKT axis. *J Exp Clin Cancer Res* 2020; **39**: 283 [PMID: 33317596 DOI: 10.1186/s13046-020-01799-1]
- 16 Liu LH, Tian QQ, Liu J, Zhou Y, Yong H. Upregulation of hsa_circ_0136666 contributes to breast cancer progression by sponging miR-1299 and targeting CDK6. *J Cell Biochem* 2019; **120**: 12684-12693 [PMID: 30993801 DOI: 10.1002/jcb.28536]

- 17 **Zhang C**, Zhou H, Yuan K, Xie R, Chen C. Overexpression of hsa_circ_0136666 predicts poor prognosis and initiates osteosarcoma tumorigenesis through miR-593-3p/ZEB2 pathway. *Aging (Albany NY)* 2020; **12**: 10488-10496 [PMID: 32424109 DOI: 10.18632/aging.103273]
- 18 **Li Y**, Zang H, Zhang X, Huang G. circ_0136666 Facilitates the Progression of Colorectal Cancer via miR-383/CREB1 Axis. *Cancer Manag Res* 2020; **12**: 6795-6806 [PMID: 32821160 DOI: 10.2147/CMAR.S251952]
- 19 **Jin C**, Wang A, Liu L, Wang G, Li G. Hsa_circ_0136666 promotes the proliferation and invasion of colorectal cancer through miR-136/SH2B1 axis. *J Cell Physiol* 2019; **234**: 7247-7256 [PMID: 30370521 DOI: 10.1002/jcp.27482]
- 20 **Xie W**, Chu M, Song G, Zuo Z, Han Z, Chen C, Li Y, Wang ZW. Emerging roles of long noncoding RNAs in chemoresistance of pancreatic cancer. *Semin Cancer Biol* 2022; **83**: 303-318 [PMID: 33207266 DOI: 10.1016/j.semcancer.2020.11.004]
- 21 **Yang J**, Zhu D, Liu S, Shao M, Liu Y, Li A, Lv Y, Huang M, Lou D, Fan Q. Curcumin enhances radiosensitization of nasopharyngeal carcinoma by regulating circRNA network. *Mol Carcinog* 2020; **59**: 202-214 [PMID: 31793078 DOI: 10.1002/mc.23143]
- 22 **Panda AC**. Circular RNAs Act as miRNA Sponges. *Adv Exp Med Biol* 2018; **1087**: 67-79 [PMID: 30259358 DOI: 10.1007/978-981-13-1426-1_6]
- 23 **Verduci L**, Strano S, Yarden Y, Blandino G. The circRNA-microRNA code: emerging implications for cancer diagnosis and treatment. *Mol Oncol* 2019; **13**: 669-680 [PMID: 30719845 DOI: 10.1002/1878-0261.12468]
- 24 **Xu G**, Wang H, Yuan D, Yao J, Meng L, Li K, Zhang Y, Dang C, Zhu K. RUNX1-activated upregulation of lncRNA RNCR3 promotes cell proliferation, invasion, and suppresses apoptosis in colorectal cancer via miR-1301-3p/AKT1 axis *in vitro* and *in vivo*. *Clin Transl Oncol* 2020; **22**: 1762-1777 [PMID: 32239427 DOI: 10.1007/s12094-020-02335-5]
- 25 **Jiang G**, Wu AD, Huang C, Gu J, Zhang L, Huang H, Liao X, Li J, Zhang D, Zeng X, Jin H. Isorhapontigenin (ISO) Inhibits Invasive Bladder Cancer Formation *In Vivo* and Human Bladder Cancer Invasion *In Vitro* by Targeting STAT1/FOXO1 Axis. *Cancer Prev Res (Phila)* 2016; **9**: 567-580 [PMID: 27080594 DOI: 10.1158/1940-6207.CAPR-15-0338]
- 26 **Zhang S**, Sun J, Gu M, Wang G, Wang X. Circular RNA: A promising new star for the diagnosis and treatment of colorectal cancer. *Cancer Med* 2021; **10**: 8725-8740 [PMID: 34796685 DOI: 10.1002/cam4.4398]
- 27 **Hasanzadeh S**, Read MI, Bland AR, Majeed M, Jamialahmadi T, Sahebkar A. Curcumin: an inflammasome silencer. *Pharmacol Res* 2020; **159**: 104921 [PMID: 32464325 DOI: 10.1016/j.phrs.2020.104921]
- 28 **Fernández-Lázaro D**, Mielgo-Ayuso J, Seco Calvo J, Córdova Martínez A, Caballero García A, Fernandez-Lazaro CI. Modulation of Exercise-Induced Muscle Damage, Inflammation, and Oxidative Markers by Curcumin Supplementation in a Physically Active Population: A Systematic Review. *Nutrients* 2020; **12** [PMID: 32075287 DOI: 10.3390/nu12020501]
- 29 **Koroth J**, Nirgude S, Tiwari S, Gopalakrishnan V, Mahadeva R, Kumar S, Karki SS, Choudhary B. Investigation of anti-cancer and migrastatic properties of novel curcumin derivatives on breast and ovarian cancer cell lines. *BMC Complement Altern Med* 2019; **19**: 273 [PMID: 31638975 DOI: 10.1186/s12906-019-2685-3]
- 30 **Zhang X**, Zhang C, Ren Z, Zhang F, Xu J, Zhang X, Zheng H. Curcumin Affects Gastric Cancer Cell Migration, Invasion and Cytoskeletal Remodeling Through Gli1-β-Catenin. *Cancer Manag Res* 2020; **12**: 3795-3806 [PMID: 32547215 DOI: 10.2147/CMAR.S244384]
- 31 **Ohnishi Y**, Sakamoto T, Zhengguang L, Yasui H, Hamada H, Kubo H, Nakajima M. Curcumin inhibits epithelial-mesenchymal transition in oral cancer cells via c-Met blockade. *Oncol Lett* 2020; **19**: 4177-4182 [PMID: 32391111 DOI: 10.3892/ol.2020.11523]
- 32 **Weng W**, Goel A. Curcumin and colorectal cancer: An update and current perspective on this natural medicine. *Semin Cancer Biol* 2022; **80**: 73-86 [PMID: 32088363 DOI: 10.1016/j.semcancer.2020.02.011]
- 33 **Ruiz de Porras V**, Layos L, Martínez-Balibrea E. Curcumin: A therapeutic strategy for colorectal cancer? *Semin Cancer Biol* 2021; **73**: 321-330 [PMID: 32942023 DOI: 10.1016/j.semcancer.2020.09.004]
- 34 **Gupta MK**, Vadde R, Sarojamma V. Curcumin - A Novel Therapeutic Agent in the Prevention of Colorectal Cancer. *Curr Drug Metab* 2019; **20**: 977-987 [PMID: 31589120 DOI: 10.2174/1389200220666191007153238]
- 35 **Calibasi-Kocal G**, Pakdemirli A, Bayrak S, Ozupek NM, Sever T, Basbinar Y, Ellidokuz H, Yigitbasi T. Curcumin effects on cell proliferation, angiogenesis and metastasis in colorectal cancer. *J BUON* 2019; **24**: 1482-1487 [PMID: 31646795]
- 36 **Ismail NI**, Othman I, Abas F, H Lajis N, Naidu R. Mechanism of Apoptosis Induced by Curcumin in Colorectal Cancer. *Int J Mol Sci* 2019; **20** [PMID: 31108984 DOI: 10.3390/ijms20102454]
- 37 **Wang G**, Li Y, Zhu H, Huo G, Bai J, Gao Z. Circ-PRKDC Facilitates the Progression of Colorectal Cancer Through miR-198/DDR1 Regulatory Axis. *Cancer Manag Res* 2020; **12**: 12853-12865 [PMID: 33364834 DOI: 10.2147/CMAR.S273484]
- 38 **Misir S**, Hepokur C, Aliyazicioglu Y, Enguita FJ. Circular RNAs serve as miRNA sponges in breast cancer. *Breast Cancer* 2020; **27**: 1048-1057 [PMID: 32715419 DOI: 10.1007/s12282-020-01140-w]
- 39 **Zhou J**, Wang L, Sun Q, Chen R, Zhang C, Yang P, Tan Y, Peng C, Wang T, Jin C, Ji J, Jin K, Sun Y. Hsa_circ_0001666 suppresses the progression of colorectal cancer through the miR-576-5p/PCDH10 axis. *Clin Transl Med* 2021; **11**: e565 [PMID: 34841662 DOI: 10.1002/ctm2.565]
- 40 **Peng X**, Yan B, Shen Y. MiR-1301-3p inhibits human breast cancer cell proliferation by regulating cell cycle progression and apoptosis through directly targeting ICT1. *Breast Cancer* 2018; **25**: 742-752 [PMID: 29951881 DOI: 10.1007/s12282-018-0881-5]
- 41 **Qiao DH**, He XM, Yang H, Zhou Y, Deng X, Cheng L, Zhou XY. miR-1301-3p suppresses tumor growth by downregulating PCNA in thyroid papillary cancer. *Am J Otolaryngol* 2021; **42**: 102920 [PMID: 33454555 DOI: 10.1016/j.amjoto.2021.102920]
- 42 **Liu Y**, Wu G. NNT-AS1 enhances bladder cancer cell growth by targeting miR-1301-3p/PODXL axis and activating Wnt pathway. *NeuroUrol Urodyn* 2020; **39**: 547-557 [PMID: 31782983 DOI: 10.1002/nau.24238]
- 43 **Miyake M**, Lawton A, Goodison S, Urquidi V, Rosser CJ. Chemokine (C-X-C motif) ligand 1 (CXCL1) protein expression is increased in high-grade prostate cancer. *Pathol Res Pract* 2014; **210**: 74-78 [PMID: 24252309 DOI: 10.1016/j.prp.2013.08.013]
- 44 **Wang N**, Liu W, Zheng Y, Wang S, Yang B, Li M, Song J, Zhang F, Zhang X, Wang Q, Wang Z. CXCL1 derived from tumor-associated macrophages promotes breast cancer metastasis via activating NF-κB/SOX4 signaling. *Cell Death Dis* 2018; **9**: 880 [PMID: 30158589 DOI: 10.1038/s41419-018-0876-3]
- 45 **Yu S**, Yi M, Xu L, Qin S, Li A, Wu K. CXCL1 as an Unfavorable Prognosis Factor Negatively Regulated by DACH1 in Non-small Cell Lung Cancer. *Front Oncol* 2019; **9**: 1515 [PMID: 31998654 DOI: 10.3389/fonc.2019.01515]
- 46 **Wang D**, Sun H, Wei J, Cen B, DuBois RN. CXCL1 Is Critical for Premetastatic Niche Formation and Metastasis in Colorectal Cancer. *Cancer Res* 2017; **77**: 3655-3665 [PMID: 28455419 DOI: 10.1158/0008-5472.CAN-16-3199]
- 47 **Howells LM**, Iwujii COO, Irving GRB, Barber S, Walter H, Sidat Z, Griffin-Teall N, Singh R, Foreman N, Patel SR, Morgan B, Steward WP,

Gescher A, Thomas AL, Brown K. Curcumin Combined with FOLFOX Chemotherapy Is Safe and Tolerable in Patients with Metastatic Colorectal Cancer in a Randomized Phase IIa Trial. *J Nutr* 2019; **149**: 1133-1139 [PMID: 31132111 DOI: 10.1093/jn/nxz029]

- 48 Killian PH, Kronski E, Michalik KM, Barbieri O, Astigiano S, Sommerhoff CP, Pfeffer U, Nerlich AG, Bachmeier BE. Curcumin inhibits prostate cancer metastasis *in vivo* by targeting the inflammatory cytokines CXCL1 and -2. *Carcinogenesis* 2012; **33**: 2507-2519 [PMID: 23042094 DOI: 10.1093/carcin/bgs312]



Basic Study

Combined TIM-3 and PD-1 blockade restrains hepatocellular carcinoma development by facilitating CD4⁺ and CD8⁺ T cell-mediated antitumor immune responses

Xu-Sheng Zhang, Hong-Cai Zhou, Peng Wei, Long Chen, Wei-Hu Ma, Lin Ding, Shi-Cai Liang, Ben-Dong Chen

Specialty type: Oncology

Provenance and peer review:

Unsolicited article; Externally peer reviewed.

Peer-review model: Single blind

Peer-review report's scientific quality classification

Grade A (Excellent): 0

Grade B (Very good): B

Grade C (Good): C

Grade D (Fair): 0

Grade E (Poor): 0

P-Reviewer: Arvanitakis K, Greece; Cuno C, Spain

Received: September 5, 2023

Peer-review started: September 5, 2023

First decision: September 15, 2023

Revised: October 9, 2023

Accepted: November 8, 2023

Article in press: November 8, 2023

Published online: December 15, 2023



Xu-Sheng Zhang, Hong-Cai Zhou, Peng Wei, Long Chen, Wei-Hu Ma, Lin Ding, Shi-Cai Liang, School of Clinical Medicine, Ningxia Medical University, Yinchuan 750004, Ningxia Hui Autonomous Region, China

Ben-Dong Chen, Department of Hepatobiliary Surgery, The General Hospital of Ningxia Medical University, Yinchuan 750004, Ningxia Hui Autonomous Region, China

Ben-Dong Chen, Hepatobiliary Pancreatic Surgical, Ningxia Hepatobiliary Pancreatic Surgical Diseases Clinical Research Center, Yinchuan 750004, Ningxia Hui Autonomous Region, China

Corresponding author: Ben-Dong Chen, MD, Doctor, Department of Hepatobiliary Surgery, The General Hospital of Ningxia Medical University, No. 804 Shengli Street, Yinchuan 750004, Ningxia Hui Autonomous Region, China. bendong8511@nyfy.com.cn

Abstract

BACKGROUND

Immune checkpoint inhibitors (ICIs) targeting programmed cell death protein 1 (PD-1) and T cell immunoglobulin and mucin domain-containing protein 3 (TIM-3) are beneficial to the resumption of anti-tumor immunity response and hold extreme potential as efficient therapies for certain malignancies. However, ICIs with a single target exhibit poor overall response rate in hepatocellular carcinoma (HCC) patients due to the complex pathological mechanisms of HCC.

AIM

To investigate the effects of combined TIM-3 and PD-1 blockade on tumor development in an HCC mouse model, aiming to identify more effective immunotherapies and provide more treatment options for HCC patients.

METHODS

The levels of PD-1 and TIM-3 on CD4⁺ and CD8⁺ T cells from tumor tissues, ascites, and matched adjacent tissues from HCC patients were determined with flow cytometry. An HCC xenograft mouse model was established and treated with anti-TIM-3 monoclonal antibody (mAb) and/or anti-PD-1 mAb. Tumor growth in each group was measured. Hematoxylin and eosin staining and immunohistochemical staining were used to evaluate T cell infiltration in tumors.

The percentage of CD4⁺ and CD8⁺ T cells in tissue samples from mice was tested with flow cytometry. The percentages of PD-1⁺CD8⁺, TIM-3⁺CD8⁺, and PD-1⁺TIM-3⁺ CD8⁺ T cells was accessed by flow cytometry. The levels of the cytokines including tumor necrosis factor alpha (TNF- α), interferon- γ (IFN- γ), interleukin (IL)-6, and IL-10 in tumor tissues were gauged with enzyme-linked immunosorbent assay kits.

RESULTS

We confirmed that PD-1 and TIM-3 expression was substantially upregulated in CD4⁺ and CD8⁺ T cells isolated from tumor tissues and ascites of HCC patients. TIM-3 mAb and PD-1 mAb treatment both reduced tumor volume and weight, while combined blockade had more substantial anti-tumor effects than individual treatment. Then we showed that combined therapy increased T cell infiltration into tumor tissues, and downregulated PD-1 and TIM-3 expression on CD8⁺ T cells in tumor tissues. Moreover, combined treatment facilitated the production of T cell effector cytokines TNF- α and IFN- γ , and reduced the production of immunosuppressive cytokines IL-10 and IL-6 in tumor tissues. Thus, we implicated that combined blockade could ameliorate T cell exhaustion in HCC mouse model.

CONCLUSION

Combined TIM-3 and PD-1 blockade restrains HCC development by facilitating CD4⁺ and CD8⁺ T cell-mediated antitumor immune responses.

Key Words: Hepatocellular carcinoma; T cell immunoglobulin and mucin domain-containing protein 3; Programmed cell death protein 1; CD4⁺ T cells; CD8⁺ T cells

©The Author(s) 2023. Published by Baishideng Publishing Group Inc. All rights reserved.

Core Tip: This study investigated the effects of combined blockade of T cell immunoglobulin and mucin domain-containing protein 3 (TIM-3) and programmed cell death protein 1 (PD-1) on tumor development in a hepatocellular carcinoma (HCC) mouse model. We showed that combined TIM-3 and PD-1 blockade had more substantial inhibitory effects on tumor growth in mice compared with individual blockade. The combined therapy increased T cell infiltration and ameliorated CD4⁺ and CD8⁺ T cell exhaustion in HCC mouse model. Our findings proposed an effective immunotherapy and may provide more treatment options for HCC patients.

Citation: Zhang XS, Zhou HC, Wei P, Chen L, Ma WH, Ding L, Liang SC, Chen BD. Combined TIM-3 and PD-1 blockade restrains hepatocellular carcinoma development by facilitating CD4⁺ and CD8⁺ T cell-mediated antitumor immune responses. *World J Gastrointest Oncol* 2023; 15(12): 2138-2149

URL: <https://www.wjgnet.com/1948-5204/full/v15/i12/2138.htm>

DOI: <https://dx.doi.org/10.4251/wjgo.v15.i12.2138>

INTRODUCTION

Hepatocellular carcinoma (HCC) is the fourth most intractable tumor in clinic worldwide[1]. The majority of HCC patients have advanced-stage diagnoses, which are frequently accompanied by distant metastases[2,3]. Surgical resection, chemotherapy and local ablative therapy are three conventional methods used in clinical HCC treatment, but which have limited effects on advanced HCC patients, such as tumor recurrence, drug resistance, and unsatisfactory survival rate and prognosis[4-6]. It's general known that the aggressive tumor progression is intimately related to immune escape mediated by multiple mechanisms[7,8]. Recently, multiple novel immune therapies, such as blockade of immune checkpoints and adoptive T-cell transfer, have been identified as efficient and safe therapies for malignant tumors with long-term survival and acceptable toxicity, which have attracted more attention and provide novel directions for HCC treatment[9,10]. Therefore, it's essential to identify more effective immunotherapies and provide more treatment options to achieve satisfactory survival rate and prognosis for HCC patients.

The tumor microenvironment has been frequently studied in cancer research. It's generally known that tumor-infiltrating lymphocytes (TILs) contribute to anti-tumor immunity and affect the cancer progression of patients[11,12]. Changes in TIL numbers, localization and phenotypes are indispensable indicators of cancer progression and immunotherapy efficacy[13]. Among them, T cells are essential for identifying and destroying tumor cells. The increased T cell infiltration is a positive prognostic indicator in HCC immunotherapy management[14]. Cytotoxic CD8⁺ T cells can eliminate malignant cancer cells and is an important defense line for anti-tumor immunity[15]. Additionally, there is evidence that CD4⁺ T cells can eliminate malignant cancer cells[16]. Nevertheless, persistent tumor antigen stimulation can cause T cell exhaustion and loss of function, resulting in tumor immune escape[17].

It is generally recognized that exhausted T cells are accompanied by frequent expression of various co-inhibitory receptors, such as programmed cell death protein 1 (PD-1), T cell immunoglobulin and mucin domain-containing protein

3 (TIM-3)[18]. These receptors can inhibit T cell function by interacting with their specific ligands, which are also called immune checkpoints. It has been previously revealed that blockage of immune checkpoints is beneficial to the resumption of anti-tumor immunity response and holds extreme potential as an efficient method for certain malignancies including advanced melanoma and lung cancer[19,20]. Currently, immune checkpoint inhibitors (ICIs) targeting PD-1 exhibits encouraging outcomes for HCC immunotherapy in clinic[21]. These inhibitors are essentially monoclonal antibodies (mAb) and have received increased attention. However, due to the complex pathological mechanisms of HCC, ICIs with a single target exhibit poor overall response rate in HCC patients[22]. Therefore, combination therapy with more targets may be a better option to achieve better clinical outcomes.

Given the limited studies study about TIM-3 blockade in HCC, our study first characterized the expression of PD-1 and TIM-3 in CD4+ and CD8+ T cells from clinical HCC samples. Then we focused on investigating the effects of combined blockade of TIM-3 and PD-1 on T cell immunological function and cancer development in an HCC mouse model.

MATERIALS AND METHODS

Clinical specimens

We recruited 20 HCC patients (12 males and 8 females; age 63.7 ± 7.3 years) at the General Hospital of Ningxia Medical University between February 2022 and May 2022. Tumor tissues, paired non-tumor adjacent tissues, and malignant ascites were collected during surgery. None of the patients received chemoradiotherapy or immunotherapy before surgery. This study was conducted with the approval of the Ethics Committee of the General Hospital of Ningxia Medical University. All participants provided clinical specimens and signed the informed consent forms (Table 1).

Animals and cell line

Healthy male BALB/c nude mice (18-20 g) were obtained from the experimental animal center of Ningxia Medical University. They were maintained in standard laboratory environment with a 12 h light/dark cycle, 22-25 °C temperature, 55%-60% humidity, and free access to food and water. HepG2 cells were obtained from ATCC (Manassas, VA, United States), and cultured in DMEM containing 10% foetal bovine serum and 1% antibiotics at 37 °C in 5% CO₂.

Isolation of mononuclear cells from tissues and ascites

Mononuclear cell suspensions from tumor and adjacent tissues were obtained according to previously described method [23,24]. In general, tumor and adjacent tissues were mechanically fragmented and digested in RPMI 1640 with 1 mg/mL collagenase IV, 0.04 mg/mL DNase I, and 0.4 mg/mL hyaluronidase for 1 h at 37 °C. The obtained mixture was filtered using cell strainers with a 70 µm pore size to acquire cells. Moreover, ascites supernatant was collected using a centrifuge set at $400 \times g$ for 10 min. Afterwards, mononuclear cells in the tissue suspension and ascites were separated and collected by Ficoll density gradient centrifugation with Lymphoprep (Stemcell Technologies, Canada). Cells were then washed and resuspended in RPMI 1640.

Flow cytometry

The isolated mononuclear cells were stained with fluorescence-conjugated mAb in the dark at 4 °C for 20 min. The fluorescence-conjugated mAb provided by eBioscience (San Diego, United States) were as follows: Fluorescein isothiocyanate (FITC)-conjugated CD4, FITC-conjugated CD8, allophycocyanin-conjugated PD-1, phycoerythrin-conjugated TIM-3, and the corresponding isotype controls. Flow cytometry was conducted with a flow cytometer (BD Biosciences, CA, United States). FlowJo software (Treestar, CA, United States) was used to analyze the data. Antigen expression is represented by the fluorescence intensity on dual-parameter scattergrams.

Animal studies

After acclimatization to the environment for one week, 4×10^5 HepG2 cells were subcutaneously injected into the right flank of mice. These model mice were divided into four treatment groups ($n = 8$ each group). Mice were administrated with immunoglobulin G (IgG) isotype control (100 µg), anti-TIM-3 mAb (100 µg) or/and anti-PD1 mAb (100 µg) in a volume of 200 µL *via* intraperitoneal injection twice a week for sustained 4 wk. These mAbs were all purchased from BioXcell (New Hampshire, United States). Tumor volume was calculated every week. Peripheral blood was collected before euthanasia and kept in an anticoagulant tube. Then tumor tissues, spleen, and thymus were completely separated and weight was recorded. All animal experiments in this study were approved by the Ethics Committee of the General Hospital of Ningxia Medical University.

Immune organ indices

The spleen or thymus index can roughly estimate the strength of immune function. They were calculated by the following equation: Spleen/thymus index (mg/g) = the weight of spleen/thymus (mg)/body weight (g).

Hematoxylin and eosin staining

Paraffin-embedded tissues were prepared and cut into 4 µm thick slices. Tissue slices were deparaffinized with xylene, dehydrated, and stained with hematoxylin and eosin (HE) solution. After cleaning and sealing with neutral resin, slices were photographed under light microscope.

Table 1 Patient characteristics

Patient characteristics		<i>n</i>
Age (yr)	< 60	14
	≥ 60	6
Gender	Male	12
	Female	8
Pathologic stage	Stage I	4
	Stage II	12
	Stage III	4

Immunohistochemical staining

After deparaffinization with xylene and rehydration, 4 μm paraffin-embedded tissue slices were mixed with sodium citrate solution and heated in a microwave oven, followed by adding 3% H₂O₂ for 10 min of inactivation. Thereafter, the slices were incubated with primary antibodies against CD4 (ab133616, Abcam) and CD8 (ab217344, Abcam) overnight at 4 °C, and secondary antibody for 1 h. Next, the slices were developed with a diaminobenzidine immunohistochemistry color development kit (Beyotime, Shanghai, China). Finally, positive staining was imaged under a light microscope and analyzed with the ImageJ software (NIH, Maryland, United States).

Mononuclear cell isolation

Cell supernatants from tumor tissues were obtained according to the method we mentioned above. Moreover, the obtained spleens were softly pulverized by filtering through a 200-gauge steel mesh, and digested in FACS lysis solution. The mixture was centrifuged and washed with phosphate buffered saline. Then, mononuclear cells in tumor and spleen tissue suspensions were obtained by density gradient centrifugation. Peripheral mononuclear cells were isolated with mouse lymphocyte separation medium (Solarbio, Shanghai, China).

Cytokine level detection

Tumor tissues were lysed, and the supernatant was collected by centrifugation. The levels of the cytokines including tumor necrosis factor alpha (TNF-α), interferon-γ (IFN-γ), interleukin (IL)-6, and IL-10 in tumor tissues were gauged with corresponding enzyme-linked immunosorbent assay kits.

Statistical analysis

Data from at least triplicate independent experiments were presented as mean ± SD and analyzed with SPSS 22.0 software. Student's *t*-test or one-way analysis of variance (ANOVA) was used to analyze comparisons among groups. *P* < 0.05 was considered statistically significant.

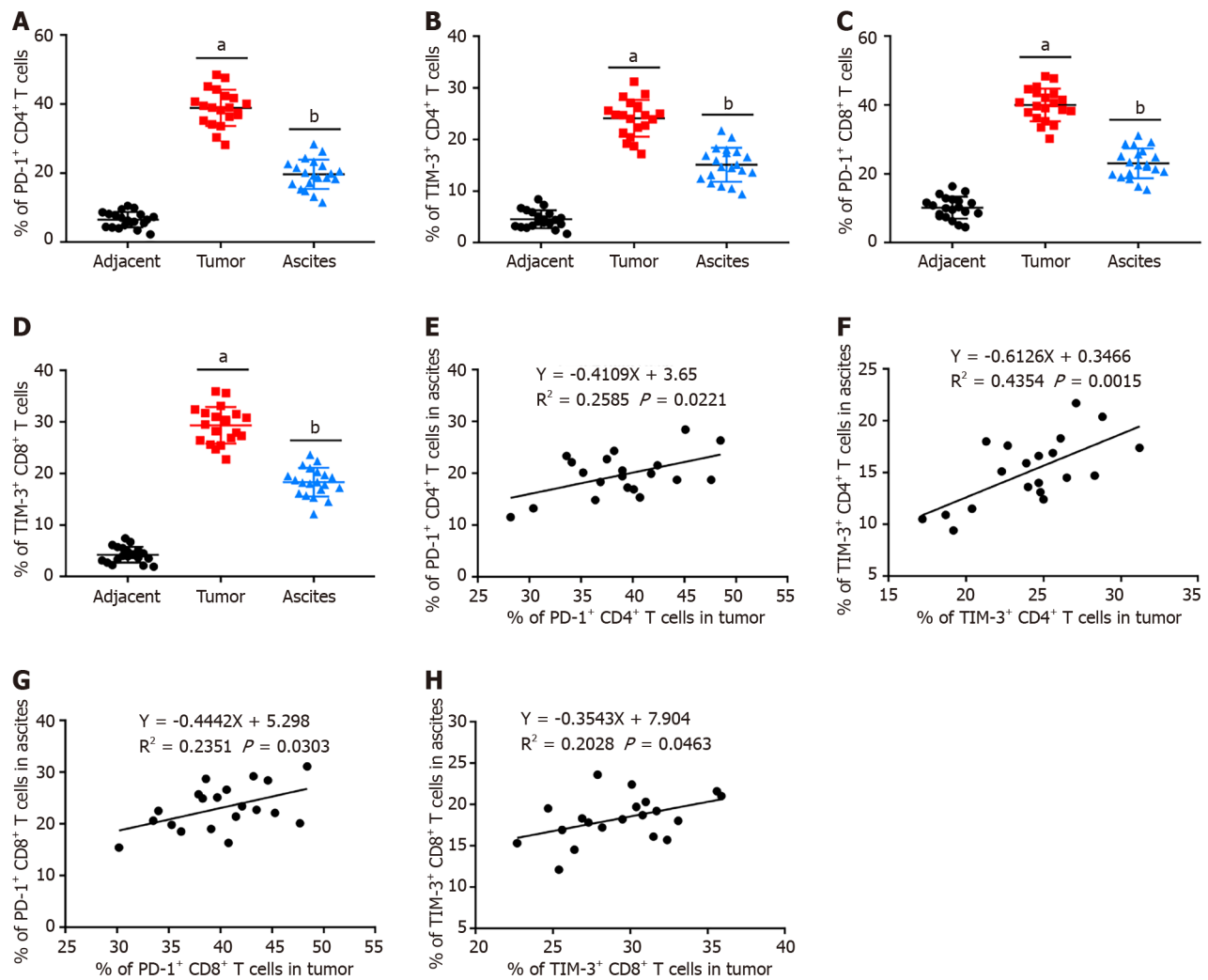
RESULTS

PD-1 and TIM-3 were upregulated in T cells from HCC patients

We first determined PD-1 and TIM-3 levels on CD4⁺ and CD8⁺ T cells from HCC patients by flow cytometry. As exhibited in Figures 1A-D, compared with matched adjacent tissues, they were both conspicuously upregulated in CD4⁺ and CD8⁺ T cells from tumor tissues. Our results also implied that PD-1 and TIM-3 were also highly expressed in conveniently available clinical ascites samples. Afterwards, we observed that their expression on T cells in tumor tissues was positively correlated with that in ascites (Figures 1E-H).

Combined TIM-3 and PD-1 blockade restrained xenograft tumor growth in mice

Anti-PD-1 agents have been used in clinic for HCC treatment[25,26]. However, the effects of anti-TIM-3 agents have not been fully clarified. We next determined the anti-tumor activities of anti-TIM-3 mAb, anti-PD-1 mAb and their combination in HCC. A xenograft mouse model of HCC was established. Tumor images were presented in Figure 2A, and it was observed that TIM-3 and PD-1 mAb treatment both reduced tumor volume (Figure 2B) and weight (Figure 2C) compared with IgG treatment. Moreover, combined blockade had more substantial anti-tumor effects than individual treatment. In addition, the spleen index (Figure 2D) was obviously elevated and the thymus index (Figure 2E) was decreased in model mice, indicating the impaired immunity in model mice. However, individual or combination treatment substantially reduced the spleen index and increased the thymus index in mice, while the effects of combination treatment were more significant. Our results illustrated that combined blockade restrained xenograft tumor growth and ameliorated the tumor immunosuppressive microenvironment in mice.



DOI: 10.4251/wjgo.v15.i12.2138 Copyright ©The Author(s) 2023.

Figure 1 Programmed cell death protein 1 and T cell immunoglobulin and mucin domain-containing protein 3 were upregulated in CD4⁺ and CD8⁺ T cells isolated from hepatocellular carcinoma patients. Mononuclear cells were isolated from tumor tissues, ascites, and matched adjacent tissues of hepatocellular carcinoma (HCC) patients. A and B: Programmed cell death protein 1 (PD-1) (A) and T cell immunoglobulin and mucin domain-containing protein 3 (TIM-3) (B) expression on CD4⁺ T cells in tumor tissues, ascites, and matched adjacent tissues of HCC patients (n = 20) was assessed with flow cytometry; C and D: PD-1 (C) and TIM-3 (D) expression on CD8⁺ T cells in tumor tissues, ascites, and matched adjacent tissues of HCC patients (n = 20) was assessed with flow cytometry; E and F: PD-1 expression on CD4⁺ (E) cells and CD8⁺ (F) T cells in tumor tissues was positively correlated with that in ascites; G and H: TIM-3 expression on CD4⁺ cells and CD8⁺ T cells in tumor tissues was positively correlated with that in ascites. Data from at least three independent experiments were presented as mean ± SD. ^aP < 0.01, tumor group compared with the adjacent group; ^bP < 0.01, ascites group compared with the adjacent group. PD-1: Programmed cell death protein 1; TIM-3: T cell immunoglobulin and mucin domain-containing protein 3.

Combined TIM-3 and PD-1 blockade activated CD4⁺ and CD8⁺ T cell infiltration into tumor tissues

We next investigated the effects of combined blockade on TILs in tumor microenvironment. HE staining illustrated that combined blockade alleviated the apoptotic characteristics of TILs and increased the number of TILs. Particularly, these changes were more obvious in the combination treatment group (Figure 3A). Additionally, immunohistochemical staining indicated that combined blockade improved the number of CD4⁺ (Figures 3B and C) and CD8⁺ (Figures 3D and E) T cells in mice. Our results revealed that combined blockade could prominently activate T cell infiltration.

Combined TIM-3 and PD-1 blockade increased the percentage of CD4⁺ and CD8⁺ T cells in mice

The main immunosuppressive mechanism of cancer cells is intimately related to CD4⁺ and CD8⁺ T cells[15,16]. The percentage of CD4⁺ and CD8⁺ T cells in tumor tissues, peripheral blood and spleen was then tested with flow cytometry. As expected, TIM-3 and PD-1 blockade prominently increased the percentage of CD4⁺ (Figures 4A-C) and CD8⁺ (Figures 4D-F) T cells in all collected samples of mice, especially the combined group, which exhibited more significant alterations. Therefore, we proposed that combined blockade could increase the percentage of CD4⁺ and CD8⁺ T cells and improve anti-tumor immune responses.

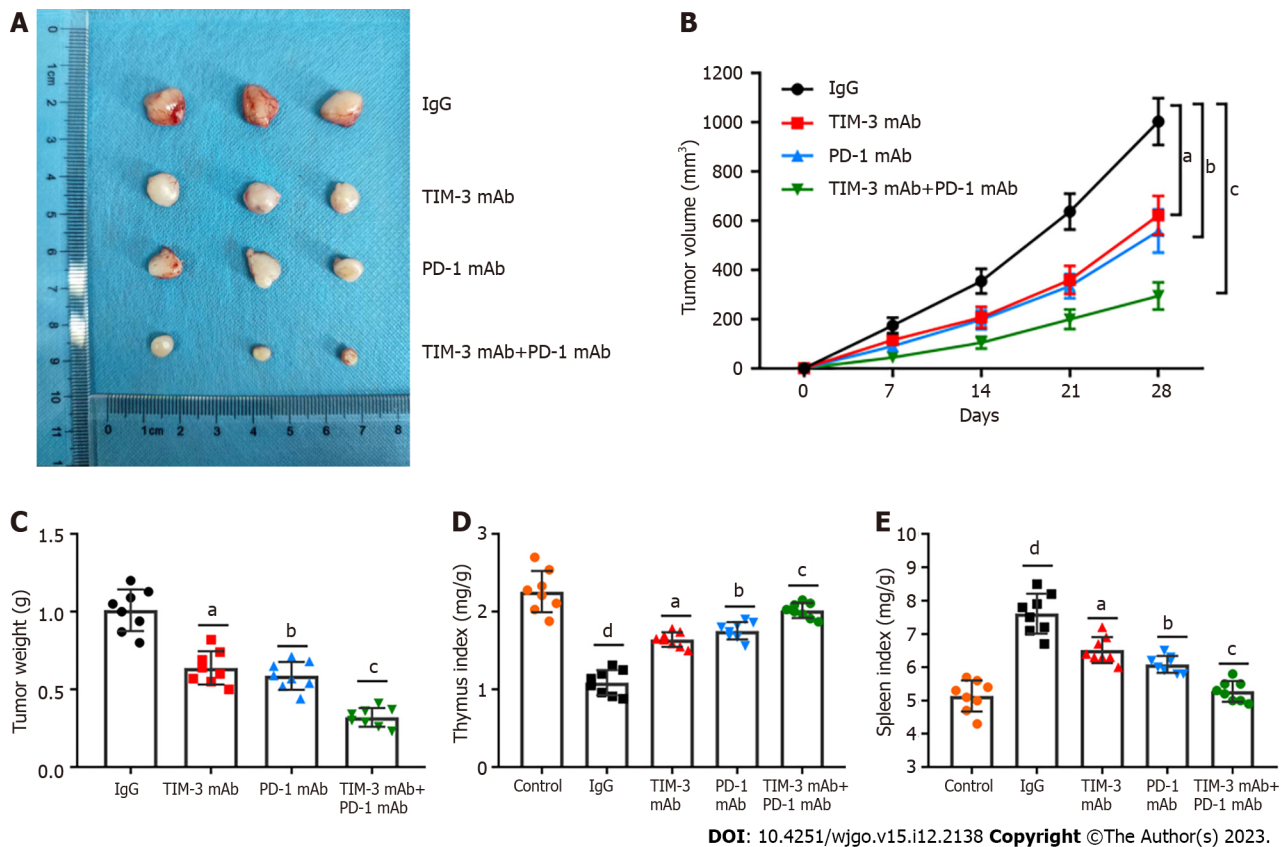


Figure 2 Combined T cell immunoglobulin and mucin domain-containing protein 3 and programmed cell death protein 1 blockade restrained xenograft tumor growth in mice. A xenograft mouse model of hepatocellular carcinoma was established by subcutaneously injecting HepG2 cells into mice. These model mice were treated with immunoglobulin G (IgG) isotype control (IgG group; $n = 8$), anti-T cell immunoglobulin and mucin domain-containing protein 3 (TIM-3) monoclonal antibody (mAb) (TIM-3 mAb group; $n = 8$), anti-programmed cell death protein 1 (PD-1) mAb (PD-1 mAb group; $n = 8$), and combined anti-TIM-3 mAb and anti-PD-1 mAb (TIM-3 mAb + PD-1 mAb group; $n = 8$) for 4 wk. A: Tumor images in the four groups; B: Tumor volume; C: Tumor weight of mice in the four groups were recorded; D and E: The spleen index (D) and thymus index (E) were determined after euthanasia. Data from at least three independent experiments were presented as mean \pm SD. ^a $P < 0.01$, compared with healthy control mice; ^a $P < 0.01$, ^b $P < 0.01$, ^c $P < 0.01$, compared with the immunoglobulin G isotype control group. PD-1: Programmed cell death protein 1; TIM-3: T cell immunoglobulin and mucin domain-containing protein 3; IgG: Immunoglobulin G; mAb: Monoclonal antibody.

Combined TIM-3 and PD-1 blockade ameliorated T cell exhaustion

T cell exhaustion is a vital immune escape mechanism in tumor microenvironment, and is accompanied by increased co-inhibitory receptor expression[27,28]. Therefore, we determined the roles of combined blockade in T cell exhaustion phenotypes in a xenograft mouse model. PD-1+CD8+ and TIM-3+CD8+ T cells in tumor tissues were assessed. Our results clearly indicated that PD-1 blockade prominently decreased PD-1+CD8+ T cell levels (Figures 5A and D) compared with IgG treatment, while anti-TIM-3 blockade restrained TIM-3+CD8+ T cell numbers (Figures 5B and E) in tumor tissues. Moreover, combined treatment simultaneously reduced PD-1+CD8+ T cell and TIM-3+CD8+ T cell numbers. Additionally, combined blockade obviously inhibited PD-1+TIM-3+CD8+ T cell numbers (Figures 5C and F). Collectively, our results suggested that combined blockade could ameliorate the exhausted CD8+ T cell phenotype in the immunosuppressive microenvironment of HCC.

Combined TIM-3 and PD-1 blockade affected immune effector chemokines in mice

Solvent cytokines provide another crucial distinctive marker for T cell exhaustion. We detected the levels of critical T cell effector cytokines, IFN- γ and TNF- α , and immunosuppressive cytokines, IL-10 and IL-6 in tumor tissues of all groups of mice. It was revealed that the individual blockade of TIM-3 and PD-1 prominently facilitated IFN- γ and TNF- α production (Figures 6A and B), and reduced IL-10 and IL-6 levels (Figures 6C and D). Importantly, such changes were more obvious in the combined group. Thus, the above results highlighted the crucial effect of combined blockade on restoring exhausted CD8+ T cell mediated anti-tumor capability.

DISCUSSION

To date, multiple effective and safe immunotherapies have achieved gratifying survival rate and prognosis for HCC patients. which have attracted more attention and provide novel directions for HCC treatment. It's generally identified

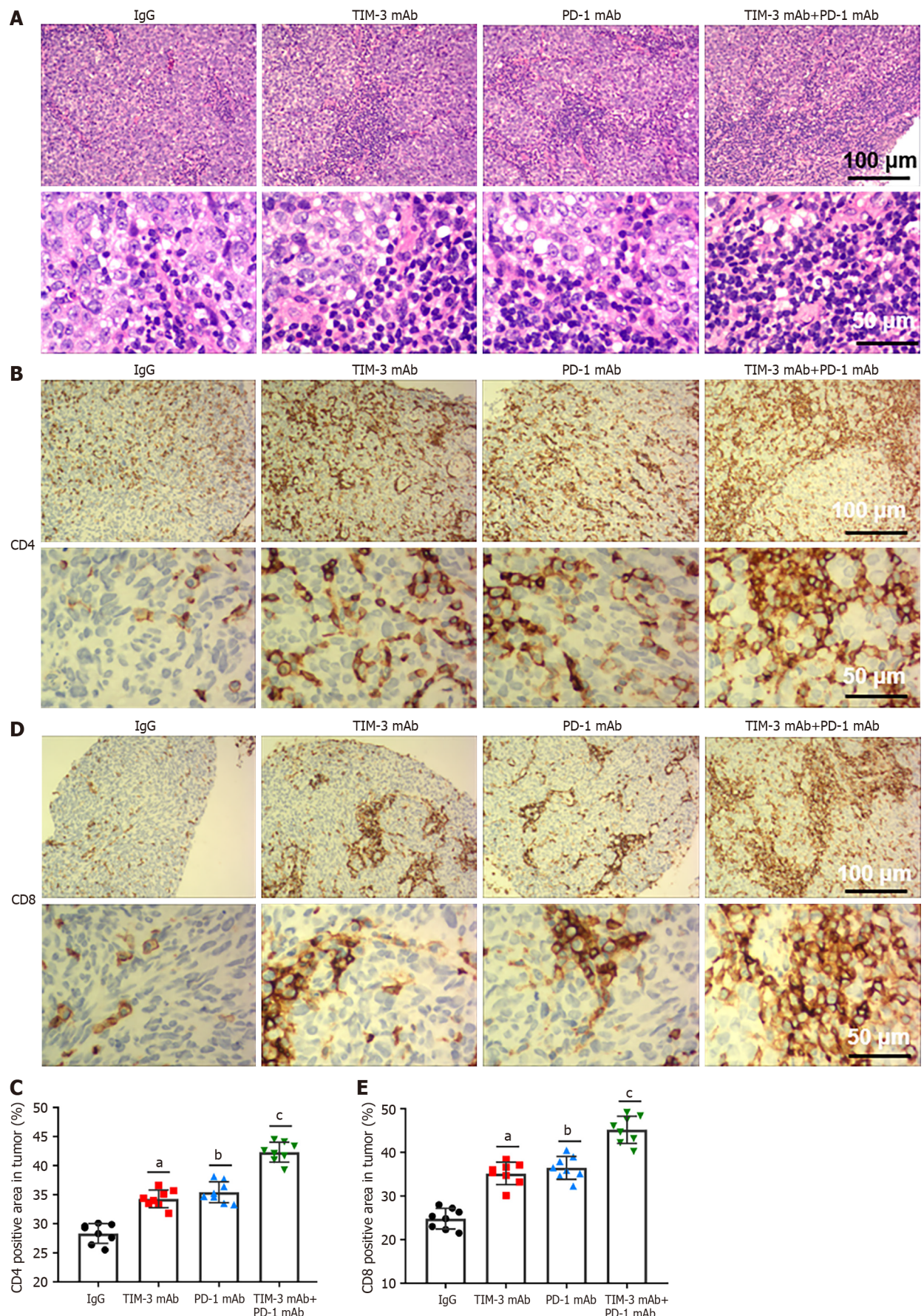
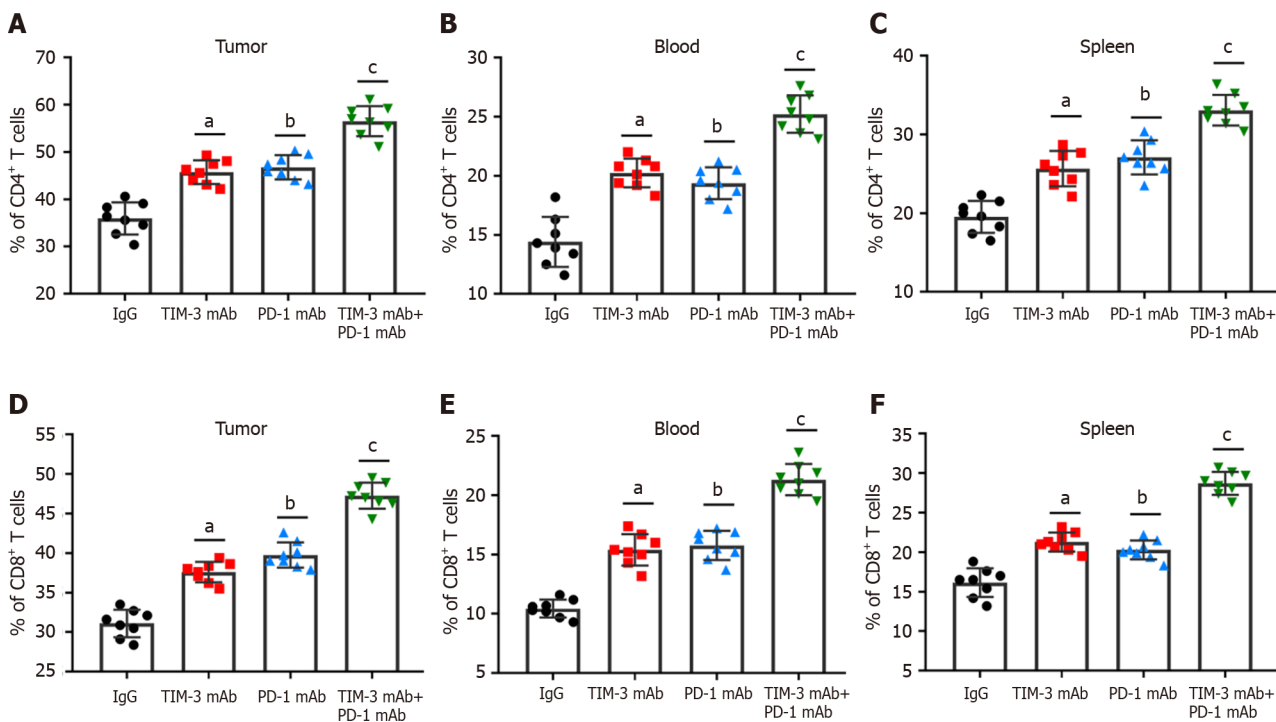


Figure 3 Combined blockade activated CD4⁺ and CD8⁺ T cell infiltration into tumor tissues. A: The infiltration of tumor-infiltrating lymphocytes into tumor tissues was evaluated with hematoxylin and eosin staining; B-E: Immunohistochemical staining was employed to assess CD4⁺ (B, C) and CD8⁺ (D, E) T cell

numbers in tumor tissues. Data from at least three independent experiments were presented as mean \pm SD. ^a $P < 0.01$, ^b $P < 0.01$, ^c $P < 0.01$, compared with the immunoglobulin G isotype control group. PD-1: Programmed cell death protein 1; TIM-3: T cell immunoglobulin and mucin domain-containing protein 3; IgG: Immunoglobulin G; mAb: Monoclonal antibody.



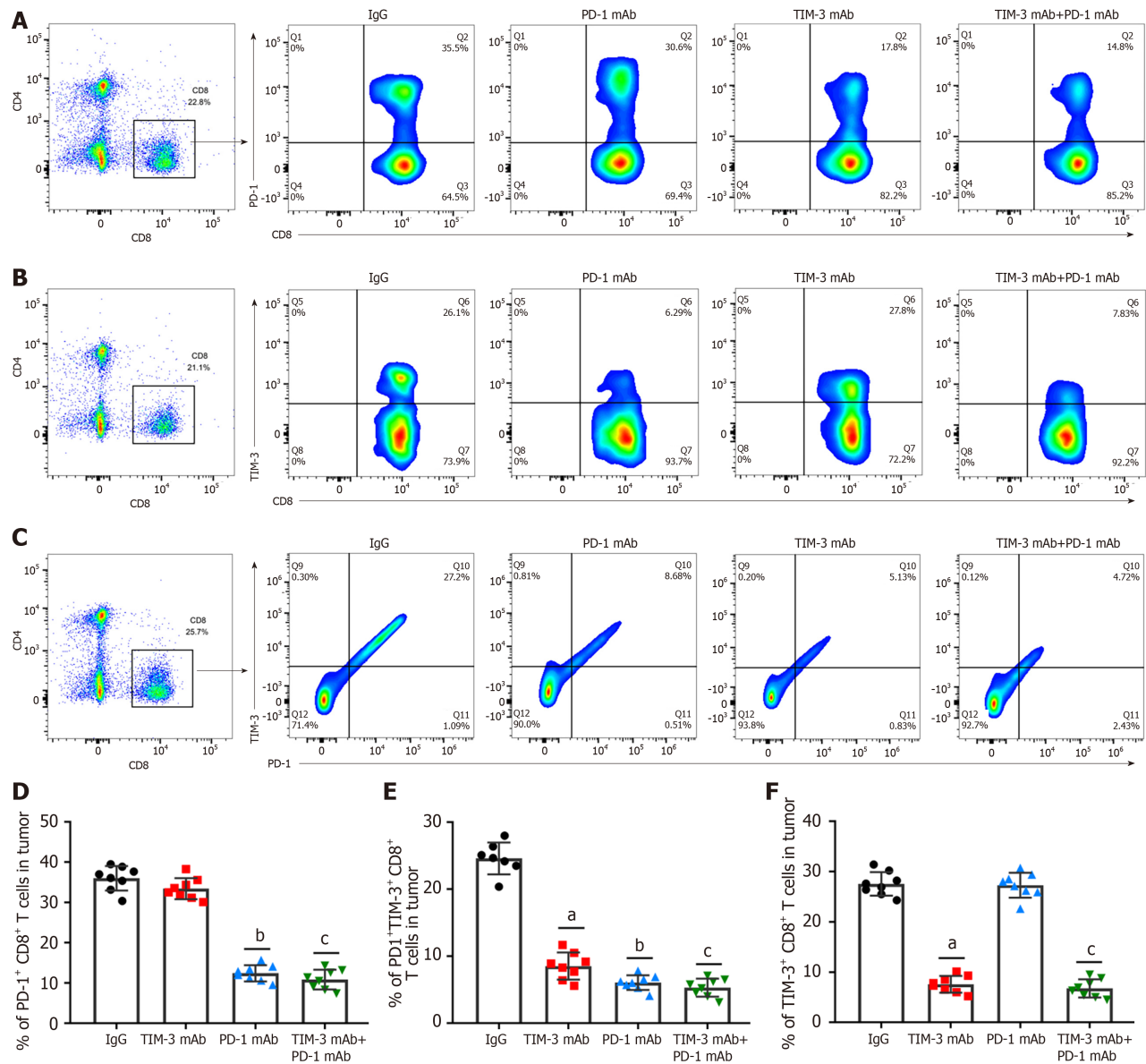
DOI: 10.4251/wjgo.v15.i12.2138 Copyright ©The Author(s) 2023.

Figure 4 Combined blockade increased the percentage of CD4⁺ and CD8⁺ T cells in mice. A-C: The percentage of CD4⁺ T cells in tumor tissues (A), peripheral blood (B) and spleen (C) of mice in four groups was tested with flow cytometry. E and F: The percentage of CD8⁺ T cells in (D) tumor tissues, peripheral blood (E) and spleen (F) of mice in four groups was tested with flow cytometry. Data from at least three independent experiments were presented as mean \pm SD. ^a $P < 0.01$, ^b $P < 0.01$, ^c $P < 0.01$, compared with the immunoglobulin G isotype control group. PD-1: Programmed cell death protein 1; TIM-3: T cell immunoglobulin and mucin domain-containing protein 3; IgG: Immunoglobulin G; mAb: Monoclonal antibody.

that increased TIL infiltration in tumor microenvironment has consistently been linked to improved outcomes for HCC patients in clinic[14]. The ability of tumor specific effector CD4⁺ and CD8⁺ T cells is intimately associated with their numbers, localization, and phenotype[15,16]. T cells are essential for identifying and destroying tumor cells. However, persistent tumor antigen stimulation can cause T cell exhaustion and loss of function, resulting in tumor immune escape [17]. Meanwhile, it has been reported that increased co-inhibitory receptor expression induces T cell exhaustion phenotype, leading to T cell immunodeficiency[18]. Thus, restoring T cell functions through blockade of immune checkpoints continues to be a dominant approach for cancer treatment. To date, advanced development of ICIs has been achieved, and multiple ICIs targeting PD-1 have been applied for HCC patients[25,26]. However, PD-1/PD-L1 is just one of numerous complex elements of anti-tumor immunity, and only blockade of PD-1 has the limitation of unsatisfactory curative effects and drug resistance. Therefore, the combination of multiple ICIs may have additive effects and become a better option to treat advanced HCC.

TIM-3 was identified as a promising immune checkpoint molecule. The therapeutic method of TIM-3 blockade has been studied in multiple human tumor immunotherapies, especially in combination with other immune checkpoints[29]. It has been previously found that multiple co-inhibitory receptors, including PD-1 and TIM-3, are prominently upregulated on CD4⁺ and CD8⁺ T cells from tumor tissues of HCC patients[24]. Moreover, TIM-3 and PD-1 positive CD8⁺ T cells were indicated to be related to adverse outcomes for HCC[23]. However, TIM-3 blockade is relatively poorly studied in HCC. Our study first collected clinical samples from HCC patients, and confirmed that PD-1 and TIM-3 expression was substantially upregulated in CD4⁺ and CD8⁺ T cells isolated from tumor tissues and ascites compared with matched adjacent tissues. Ascites are conveniently available clinical samples, and our results support the adoption of ascites as an alternative site for TIM-3 recognition and patient stratification to manage TIM-3 blockers.

A previous meta-analysis revealed that TIM-3 upregulation was linked to adverse prognosis in individuals with various cancers, and they proposed that TIM-3 might be a dominant target[30]. Notably, TIM-3 blockade in combination with radiation could improve anti-tumor efficacy in an HCC mouse model[31]. Our study suggested that individual TIM-3 mAb and PD-1 mAb treatment both reduced tumor volume and weight, while combined blockade had more substantial tumor suppressive effect than individual treatment. In addition, the combination therapy also reduced the spleen index and increased the thymus index in mice, indicating the improvement in the immunosuppressive tumor microenvi-



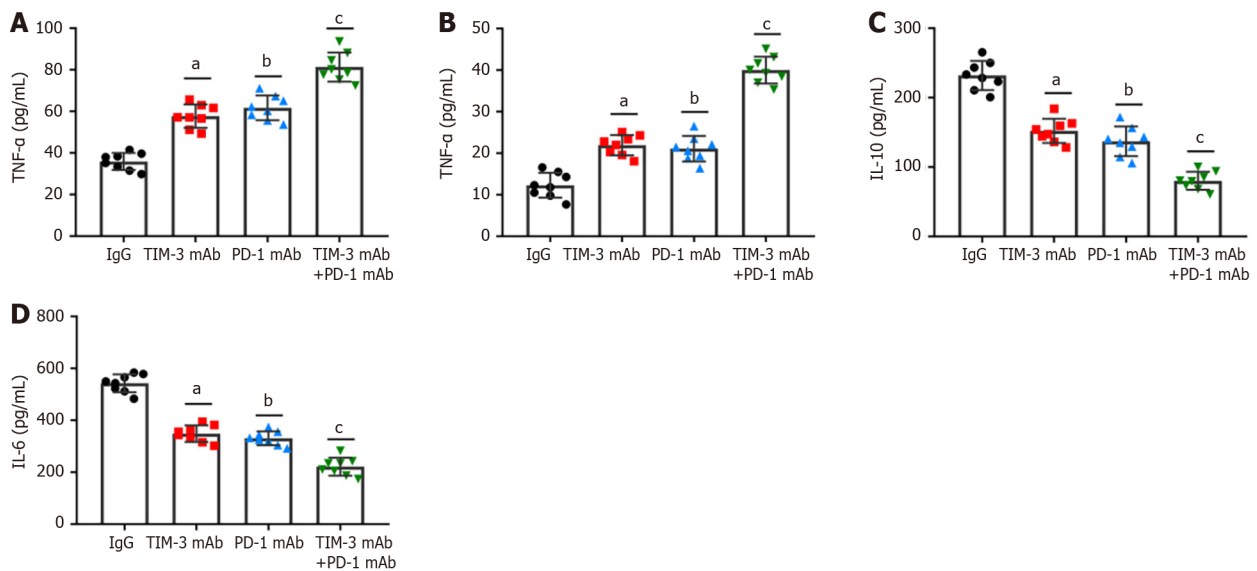
DOI: 10.4251/wjgo.v15.i12.2138 Copyright ©The Author(s) 2023.

Figure 5 Combined blockade ameliorated T cell exhaustion. A and D: The percentages of programmed cell death protein 1 (PD-1)+CD8+ T cells; B and E: T cell immunoglobulin and mucin domain-containing protein 3 (TIM-3)+CD8+ T cells; C and F: PD-1+TIM-3+CD8+ T cells in the tumor tissues of mice in the four groups was assessed with flow cytometry. Data from at least three independent experiments were presented as mean ± SD. ^aP < 0.01, ^bP < 0.01, ^cP < 0.01, compared with the immunoglobulin G isotype control group. PD-1: Programmed cell death protein 1; TIM-3: T cell immunoglobulin and mucin domain-containing protein 3; IgG: Immunoglobulin G; mAb: Monoclonal antibody.

onment. More importantly, combined blockade prominently upregulated CD4+ and CD8+ T cells and activated cell infiltration into tumor tissues. Additionally, our results showed that combined blockade can simultaneously downregulate PD-1 and TIM-3 expression on CD8+ T cells. Likewise, PD-1+TIM-3+ CD8+ T cell numbers in tumor tissues were obviously reduced by combination therapy. Meanwhile, combined blockade also facilitated IFN-γ and TNF-α production, and reduced the production of IL-10 and IL-6 in tumor tissues. Therefore, we implicated that combined blockade could ameliorate T cell exhaustion in HCC model mice.

CONCLUSION

Taken together, our study proposed that the combined blockade of TIM-3 and PD-1 had an additive anti-tumor effect on an HCC mouse model compared with individual treatment. Combined therapy improved anti-tumor immune responses in HCC mouse model by increasing CD4+ and CD8+ T cell infiltration, down-regulating the co-inhibitory receptors TIM-3 and PD-1, and ameliorating T cell exhaustion. We hope that our findings will benefit to the clinical treatment of HCC.



DOI: 10.4251/wjgo.v15.i12.2138 Copyright ©The Author(s) 2023.

Figure 6 Combined blockade of T cell immunoglobulin and mucin domain-containing protein 3 and programmed cell death protein 1 affected immune effector chemokines in mice. A-D: The levels of T cell effector cytokines interferon- γ (A) and (B) tumor necrosis factor- α , and immunosuppressive cytokines interleukin (IL)-10 (C) and IL-6 (D) in tumor tissues of mice in four groups were gauged with enzyme-linked immunosorbent assay kits. Data from at least three independent experiments were presented as mean \pm SD. ^a $P < 0.01$, ^b $P < 0.01$, ^c $P < 0.01$, compared with the immunoglobulin G isotype control group. PD-1: Programmed cell death protein 1; TIM-3: T cell immunoglobulin and mucin domain-containing protein 3; IgG: Immunoglobulin G. IL: Interleukin; TNF- α : Tumor necrosis factor- α ; IFN- γ : Interferon- γ ; mAb: Monoclonal antibody.

ARTICLE HIGHLIGHTS

Research background

Hepatocellular carcinoma (HCC) is the fourth intractable tumors in clinic worldwide. Recently, immune checkpoint inhibitors (ICIs), a novel immune therapy, has been identified as an efficient and safe therapy for malignant tumors, which have attracted more attention and give novel directions for HCC treatment.

Research motivation

ICIs targeting programmed cell death protein 1 (PD-1) and T cell immunoglobulin and mucin domain-containing protein 3 (TIM-3) are benefit to the resume of anti-tumor immunity response and hold extreme potential as efficient therapies for certain malignancies. Given the complex pathological mechanisms of HCC, ICIs with a single target exhibit poor overall response rate in HCC patients. Therefore, it's of great significance to identify more effective immunotherapies and provide more treatment options to achieve gratifying survival rate and prognosis for HCC patients.

Research objectives

This study investigated the effects of combined TIM-3 and PD-1 blockade on tumor development in an HCC mouse model, aiming to identify more effective immunotherapies and provide more treatment options for HCC patients.

Research methods

We first detected the levels of PD-1 CD4⁺, PD-1 CD8⁺, TIM-3 CD4⁺, and TIM-3 CD8⁺ in tumor tissues, ascites, and matched adjacent tissues from HCC patients. Next, we investigated the effects of combined and individual blockade of TIM-3 and PD-1 on an HCC xenograft mouse model. Tumor growth and CD4⁺ and CD8⁺ T cell-mediated antitumor immune responses were assessed.

Research results

PD-1 and TIM-3 expression was upregulated in CD4⁺ and CD8⁺ T cells isolated from tumor tissues and ascites of HCC patients. TIM-3 mAb and PD-1 mAb treatment both reduced tumor volume and weight, while combined blockade had more substantial anti-tumor effects compared with individual treatment. The combined therapy increased T cell infiltration into tumor tissues, and ameliorated CD4⁺ and CD8⁺ T cell exhaustion in HCC mouse model.

Research conclusions

Combined TIM-3 and PD-1 blockade has more substantial anti-tumor effects compared with individual blockade. Combined TIM-3 and PD-1 blockade restrains HCC development by facilitating CD4⁺ and CD8⁺ T cell-mediated antitumor immune responses.

Research perspectives

We need to explore the effects of combination of multiple ICIs to provide better options for HCC treatment.

FOOTNOTES

Co-first authors: Xu-Sheng Zhang and Peng Wei.

Author contributions: Zhang XS, Wei P, and Liang SC were responsible for research design; Zhou HC, Peng Wei, and Long Chen contributed to the conducting the experiments; Zhang XS, Ding L, Chen BD, and Liang SC involved in the data acquisition; Chen L, Ma WH, and Ding L participated in the data analysis; Zhou HC, Ma WH, and Chen BD wrote the manuscript; and all the authors have contributed to the completion of this paper.

Supported by the First-Class Discipline Construction Founded Project of Ningxia Medical University and the School of Clinical Medicine, No. 2020008.

Institutional review board statement: This study was conducted with the approval of the Ethics Committee of the General Hospital of Ningxia Medical University. All participants provided clinical specimens and signed the informed consent forms.

Institutional animal care and use committee statement: All animal care and experimental procedures were approved by the Ethics Committee of the General Hospital of Ningxia Medical University.

Conflict-of-interest statement: All the authors report no relevant conflicts of interest for this article.

Data sharing statement: All the data obtained in the current study were available from the corresponding authors on reasonable request.

ARRIVE guidelines statement: The authors have read the ARRIVE guidelines, and the manuscript was prepared and revised according to the ARRIVE guidelines.

Open-Access: This article is an open-access article that was selected by an in-house editor and fully peer-reviewed by external reviewers. It is distributed in accordance with the Creative Commons Attribution NonCommercial (CC BY-NC 4.0) license, which permits others to distribute, remix, adapt, build upon this work non-commercially, and license their derivative works on different terms, provided the original work is properly cited and the use is non-commercial. See: <https://creativecommons.org/licenses/by-nc/4.0/>

Country/Territory of origin: China

ORCID number: Ben-Dong Chen [0009-0007-9960-1146](https://orcid.org/0009-0007-9960-1146).

S-Editor: Wang JJ

L-Editor: A

P-Editor: Yu HG

REFERENCES

- 1 **Harris PS**, Hansen RM, Gray ME, Massoud OI, McGuire BM, Shoreibah MG. Hepatocellular carcinoma surveillance: An evidence-based approach. *World J Gastroenterol* 2019; **25**: 1550-1559 [PMID: [30983815](https://pubmed.ncbi.nlm.nih.gov/30983815/) DOI: [10.3748/wjg.v25.i13.1550](https://doi.org/10.3748/wjg.v25.i13.1550)]
- 2 **Zhang Y**, Liu Z, Ji K, Li X, Wang C, Ren Z, Liu Y, Chen X, Han X, Meng L, Li L, Li Z. Clinical Application Value of Circulating Cell-free DNA in Hepatocellular Carcinoma. *Front Mol Biosci* 2021; **8**: 736330 [PMID: [34660697](https://pubmed.ncbi.nlm.nih.gov/34660697/) DOI: [10.3389/fmolb.2021.736330](https://doi.org/10.3389/fmolb.2021.736330)]
- 3 **Li S**, Wang P, Qiu J, Xie Y, Yin D, Deng K. Comparison of IDEAL-IQ and IVIM-DWI for Differentiating between Alpha Fetoprotein-Negative Hepatocellular Carcinoma and Focal Nodular Hyperplasia. *Oncologie* 2022; **24**: 1-12 [DOI: [10.32604/oncologie.2022.022815](https://doi.org/10.32604/oncologie.2022.022815)]
- 4 **Zhang W**, Zhang B, Chen XP. Adjuvant treatment strategy after curative resection for hepatocellular carcinoma. *Front Med* 2021; **15**: 155-169 [PMID: [33754281](https://pubmed.ncbi.nlm.nih.gov/33754281/) DOI: [10.1007/s11684-021-0848-3](https://doi.org/10.1007/s11684-021-0848-3)]
- 5 **Wang K**, Wang C, Jiang H, Zhang Y, Lin W, Mo J, Jin C. Combination of Ablation and Immunotherapy for Hepatocellular Carcinoma: Where We Are and Where to Go. *Front Immunol* 2021; **12**: 792781 [PMID: [34975896](https://pubmed.ncbi.nlm.nih.gov/34975896/) DOI: [10.3389/fimmu.2021.792781](https://doi.org/10.3389/fimmu.2021.792781)]
- 6 **Yan D**, Li C, Zhou Y, Yan X, Zhi W, Qian H, Han Y. Exploration of Combinational Therapeutic Strategies for HCC Based on TCGA HCC Database. *Oncologie* 2023; **24** [DOI: [10.32604/oncologie.2022.020357](https://doi.org/10.32604/oncologie.2022.020357)]
- 7 **Liu Z**, Liu X, Liang J, Liu Y, Hou X, Zhang M, Li Y, Jiang X. Immunotherapy for Hepatocellular Carcinoma: Current Status and Future Prospects. *Front Immunol* 2021; **12**: 765101 [PMID: [34675942](https://pubmed.ncbi.nlm.nih.gov/34675942/) DOI: [10.3389/fimmu.2021.765101](https://doi.org/10.3389/fimmu.2021.765101)]
- 8 **Shu X**, Wang Q, Wu Q. The Eph/Ephrin System in Hepatocellular Carcinoma: Functional Roles and Potential Therapeutic Targets. *Oncologie* 2022; **24**: 427-439 [DOI: [10.32604/oncologie.2022.023248](https://doi.org/10.32604/oncologie.2022.023248)]
- 9 **Jiang Y**, Han QJ, Zhang J. Hepatocellular carcinoma: Mechanisms of progression and immunotherapy. *World J Gastroenterol* 2019; **25**: 3151-3167 [PMID: [31333308](https://pubmed.ncbi.nlm.nih.gov/31333308/) DOI: [10.3748/wjg.v25.i25.3151](https://doi.org/10.3748/wjg.v25.i25.3151)]
- 10 **Keilson JM**, Knochelmann HM, Paulos CM, Kudchadkar RR, Lowe MC. The evolving landscape of immunotherapy in solid tumors. *J Surg Oncol* 2021; **123**: 798-806 [PMID: [33595890](https://pubmed.ncbi.nlm.nih.gov/33595890/) DOI: [10.1002/jso.26416](https://doi.org/10.1002/jso.26416)]
- 11 **Pajjens ST**, Vledder A, de Bruyn M, Nijman HW. Tumor-infiltrating lymphocytes in the immunotherapy era. *Cell Mol Immunol* 2021; **18**:

- 842-859 [PMID: 33139907 DOI: 10.1038/s41423-020-00565-9]
- 12 **Yu S**, Lv H, Zhang J, Zhang H, Ju W, Jiang Y, Lin L. Heparanase/Syndecan-1 Axis Regulates the Grade of Liver Cancer and Proliferative Ability of Hepatocellular Carcinoma Cells. *Oncologie* 2022; **24**: 1-3 [DOI: 10.32604/oncologie.2022.024882]
 - 13 **Maibach F**, Sadozai H, Seyed Jafari SM, Hunger RE, Schenk M. Tumor-Infiltrating Lymphocytes and Their Prognostic Value in Cutaneous Melanoma. *Front Immunol* 2020; **11**: 2105 [PMID: 33013886 DOI: 10.3389/fimmu.2020.02105]
 - 14 **Liu YT**, Sun ZJ. Turning cold tumors into hot tumors by improving T-cell infiltration. *Theranostics* 2021; **11**: 5365-5386 [PMID: 33859752 DOI: 10.7150/thno.58390]
 - 15 **Reina-Campos M**, Scharping NE, Goldrath AW. CD8(+) T cell metabolism in infection and cancer. *Nat Rev Immunol* 2021; **21**: 718-738 [PMID: 33981085 DOI: 10.1038/s41577-021-00537-8]
 - 16 **Oh DY**, Fong L. Cytotoxic CD4(+) T cells in cancer: Expanding the immune effector toolbox. *Immunity* 2021; **54**: 2701-2711 [PMID: 34910940 DOI: 10.1016/j.immuni.2021.11.015]
 - 17 **Blank CU**, Haining WN, Held W, Hogan PG, Kallies A, Lugli E, Lynn RC, Philip M, Rao A, Restifo NP, Schietinger A, Schumacher TN, Schwartzberg PL, Sharpe AH, Speiser DE, Wherry EJ, Youngblood BA, Zehn D. Defining 'T cell exhaustion'. *Nat Rev Immunol* 2019; **19**: 665-674 [PMID: 31570879 DOI: 10.1038/s41577-019-0221-9]
 - 18 **Ando M**, Ito M, Srirat T, Kondo T, Yoshimura A. Memory T cell, exhaustion, and tumor immunity. *Immunol Med* 2020; **43**: 1-9 [PMID: 31822213 DOI: 10.1080/25785826.2019.1698261]
 - 19 **Marconcini R**, Spagnolo F, Stucci LS, Ribero S, Marra E, Rosa F, Picasso V, Di Guardo L, Cimminiello C, Cavalieri S, Orgiano L, Tanda E, Spano L, Falcone A, Queirolo P; Italian Melanoma Intergroup (IMI). Current status and perspectives in immunotherapy for metastatic melanoma. *Oncotarget* 2018; **9**: 12452-12470 [PMID: 29552325 DOI: 10.18632/oncotarget.23746]
 - 20 **Saigi M**, Albuquerque-Bejar JJ, Sanchez-Céspedes M. Determinants of immunological evasion and immunotherapy inhibition response in non-small cell lung cancer: the genetic front. *Oncogene* 2019; **38**: 5921-5932 [PMID: 31253869 DOI: 10.1038/s41388-019-0855-x]
 - 21 **Wang J**, Li J, Tang G, Tian Y, Su S, Li Y. Clinical outcomes and influencing factors of PD-1/PD-L1 in hepatocellular carcinoma. *Oncol Lett* 2021; **21**: 279 [PMID: 33732355 DOI: 10.3892/ol.2021.12540]
 - 22 **Li Q**, Han J, Yang Y, Chen Y. PD-1/PD-L1 checkpoint inhibitors in advanced hepatocellular carcinoma immunotherapy. *Front Immunol* 2022; **13**: 1070961 [PMID: 36601120 DOI: 10.3389/fimmu.2022.1070961]
 - 23 **Ma J**, Zheng B, Goswami S, Meng L, Zhang D, Cao C, Li T, Zhu F, Ma L, Zhang Z, Zhang S, Duan M, Chen Q, Gao Q, Zhang X. PD1(Hi) CD8(+) T cells correlate with exhausted signature and poor clinical outcome in hepatocellular carcinoma. *J Immunother Cancer* 2019; **7**: 331 [PMID: 31783783 DOI: 10.1186/s40425-019-0814-7]
 - 24 **Zhou G**, Sprengers D, Boor PPC, Doukas M, Schutz H, Mancham S, Pedroza-Gonzalez A, Polak WG, de Jonge J, Gaspersz M, Dong H, Thielemans K, Pan Q, IJzermans JNM, Bruno MJ, Kwekkeboom J. Antibodies Against Immune Checkpoint Molecules Restore Functions of Tumor-Infiltrating T Cells in Hepatocellular Carcinomas. *Gastroenterology* 2017; **153**: 1107-1119.e10 [PMID: 28648905 DOI: 10.1053/j.gastro.2017.06.017]
 - 25 **D'Alessio A**, Rimassa L, Cortellini A, Pinato DJ. PD-1 Blockade for Hepatocellular Carcinoma: Current Research and Future Prospects. *J Hepatocell Carcinoma* 2021; **8**: 887-897 [PMID: 34386437 DOI: 10.2147/JHC.S284440]
 - 26 **Chen Z**, Lu X, Koral K. The clinical application of camrelizumab on advanced hepatocellular carcinoma. *Expert Rev Gastroenterol Hepatol* 2020; **14**: 1017-1024 [PMID: 32762583 DOI: 10.1080/17474124.2020.1807939]
 - 27 **Nagasaki J**, Togashi Y. A variety of 'exhausted' T cells in the tumor microenvironment. *Int Immunol* 2022; **34**: 563-570 [PMID: 35460561 DOI: 10.1093/intimm/dxac013]
 - 28 **Dolina JS**, Van Braeckel-Budimir N, Thomas GD, Salek-Ardakani S. CD8(+) T Cell Exhaustion in Cancer. *Front Immunol* 2021; **12**: 715234 [PMID: 34354714 DOI: 10.3389/fimmu.2021.715234]
 - 29 **Zhao L**, Cheng S, Fan L, Zhang B, Xu S. TIM-3: An update on immunotherapy. *Int Immunopharmacol* 2021; **99**: 107933 [PMID: 34224993 DOI: 10.1016/j.intimp.2021.107933]
 - 30 **Qin S**, Dong B, Yi M, Chu Q, Wu K. Prognostic Values of TIM-3 Expression in Patients With Solid Tumors: A Meta-Analysis and Database Evaluation. *Front Oncol* 2020; **10**: 1288 [PMID: 32850398 DOI: 10.3389/fonc.2020.01288]
 - 31 **Kim KJ**, Lee HW, Seong J. Combination therapy with anti-T-cell immunoglobulin and mucin-domain containing molecule 3 and radiation improves antitumor efficacy in murine hepatocellular carcinoma. *J Gastroenterol Hepatol* 2021; **36**: 1357-1365 [PMID: 33217056 DOI: 10.1111/jgh.15319]



Basic Study

Association between heat shock factor protein 4 methylation and colorectal cancer risk and potential molecular mechanisms: A bioinformatics study

Wen-Jing Zhang, Ke-Lin Yue, Jing-Zhai Wang, Yu Zhang

Specialty type: Oncology

Provenance and peer review:

Unsolicited article; Externally peer reviewed.

Peer-review model: Single blind

Peer-review report's scientific quality classification

Grade A (Excellent): 0

Grade B (Very good): B, B

Grade C (Good): C

Grade D (Fair): 0

Grade E (Poor): E

P-Reviewer: Duraes LC, United States; El-Arabey AA, Egypt; Rotondo JC, Italy; Shinozaki M, Japan

Received: July 28, 2023

Peer-review started: July 28, 2023

First decision: September 26, 2023

Revised: October 16, 2023

Accepted: November 17, 2023

Article in press: November 17, 2023

Published online: December 15, 2023



Wen-Jing Zhang, Department of Medical Oncology, The First People's Hospital of Yunnan Province, Affiliated Hospital of Kunming University of Science and Technology, Kunming 650032, Yunnan Province, China

Ke-Lin Yue, Jing-Zhai Wang, Yu Zhang, Department of Gastroenterology, The First People's Hospital of Yunnan Province, Affiliated Hospital of Kunming University of Science and Technology, Kunming 650032, Yunnan Province, China

Corresponding author: Yu Zhang, MD, PhD, Associate Professor, Department of Gastroenterology, The First People's Hospital of Yunnan Province, Affiliated Hospital of Kunming University of Science and Technology, No. 157 Jinbi Road, Kunming 650032, Yunnan Province, China. yuzhang320@sina.com

Abstract

BACKGROUND

We previously demonstrated that heat shock factor protein 4 (HSF4) facilitates colorectal cancer (CRC) progression. DNA methylation, a major modifier of gene expression and stability, is involved in CRC development and outcome.

AIM

To investigate the correlation between *HSF4* methylation and CRC risk, and to uncover the underlying molecular mechanisms.

METHODS

Differences in β values of *HSF4* methylation loci in multiple malignancies and their correlation with *HSF4* mRNA expression were analyzed based on Shiny Methylation Analysis Resource Tool. *HSF4* methylation-related genes were identified by LinkedOmics in CRC, and Gene Ontology and Kyoto Encyclopedia of Genes and Genomes enrichment analyses were performed. Protein-protein interaction network of *HSF4* methylation-related genes was constructed by String database and MCODE algorithm.

RESULTS

A total of 19 CpG methylation loci were identified in *HSF4*, and their β values were significantly increased in CRC tissues and exhibited a positive correlation with *HSF4* mRNA expression. Unfortunately, the prognostic and diagnostic

performance of these CpG loci in CRC patients was mediocre. In CRC, there were 1694 *HSF4* methylation-related genes; 1468 of which displayed positive and 226 negative associations, and they were involved in regulating phenotypes such as immune, inflammatory, and metabolic reprogramming. *EGFR*, *RELA*, *STAT3*, *FCGR3A*, *POLR2K*, and *AXIN1* are hub genes among the *HSF4* methylation-related genes.

CONCLUSION

HSF4 is highly methylated in CRC, but there is no significant correlation between it and the prognosis and diagnosis of CRC. *HSF4* methylation may serve as one of the ways in which *HSF4* mediates the CRC process.

Key Words: Colorectal cancer; DNA methylation; Prognosis; Diagnosis; Bioinformatics; Heat shock factor protein 4

©The Author(s) 2023. Published by Baishideng Publishing Group Inc. All rights reserved.

Core Tip: Colorectal cancer (CRC) is a common malignant tumor of the gastrointestinal tract with clinical manifestations of diarrhea, constipation, and abdominal pain. We previously demonstrated that heat shock factor protein 4 (*HSF4*) accelerates the malignant biological behavior of CRC cells *in vivo* and *in vitro*. This study reveals that *HSF4* is highly methylated and associated with *HSF4* overexpression in CRC. Although the diagnostic and prognostic value of *HSF4* methylation is poor, it may be involved in the process of CRC by mediating the expression of *HSF4* or related genes. Combined with the finding of our previous study, the present study suggests that the high expression of *HSF4* mRNA and protein and its oncogenic effects are likely to be associated with *HSF4* methylation.

Citation: Zhang WJ, Yue KL, Wang JZ, Zhang Y. Association between heat shock factor protein 4 methylation and colorectal cancer risk and potential molecular mechanisms: A bioinformatics study. *World J Gastrointest Oncol* 2023; 15(12): 2150-2168

URL: <https://www.wjgnet.com/1948-5204/full/v15/i12/2150.htm>

DOI: <https://dx.doi.org/10.4251/wjgo.v15.i12.2150>

INTRODUCTION

Colorectal cancer (CRC) is a malignant tumor of the digestive tract that occurs in the rectum, cecum, and entire colon, with symptoms such as abdominal pain, difficulty passing stool, constipation, or diarrhea[1]. According to the latest statistics from the World Health Organization[2], CRC has become the third most common malignancy worldwide after lung cancer and breast cancer, with about 200000 new cases occurring worldwide each year, of which, 916000 die from CRC. According to the American Society of Clinical Oncology[3], the 5-year survival rate for patients with CRC is approximately 65%. Nevertheless, most CRC patients have already developed distal metastases by the time they receive a definitive diagnosis, which leads to a shrinking 5-year survival rate to 14%[3]. Consequently, the search for new biomarkers will facilitate the timely diagnosis of CRC and provide new insights into the mechanisms of CRC occurrence and development.

DNA methylation is a process of chemical modification of DNA that affects biological processes such as gene expression, cell differentiation and development[4-6]. In epigenetics, DNA methylation is an important marker of cellular genetic information and is widely applied in cancer prediction and diagnosis[7,8]. For CRC, the United States Food and Drug Administration currently approves SEPT9 (blood samples) and a combination of *NDRG4* and *BMP3* (stool samples) as commercially available biomarkers related to methylation[9]. In addition, *APC*, *SFRP1*, *SFRP2*, *SDC2*, *MGMT*, *VIM* and *NDRG4* are methylation-related candidate markers of CRC[10]. Mechanistically, DNA methylation can inhibit gene transcription or activate gene expression, thereby affecting protein synthesis to mediate the cancer process. For instance, teashirt zinc finger homeobox 3 (*TSHZ3*) promoter methylation effectively suppresses *TSHZ3* expression, which facilitates CRC growth and metastasis[11]. Heparanase 2 (*HPSE2*) is highly methylated in CRC and is associated with poor patient prognosis, and high methylation of *HPSE2* reduces *HPSE2* expression, which inhibits the p53/p21 signaling cascade and facilitates proliferation of CRC cells *in vivo* and *in vitro*[12]. Heat shock response (HSR), an ancient cellular self-protective response, helps tumor cells to survive and proliferate smoothly under the stimulation of adverse microenvironment, oxidative stress and other stressors[13]. Heat shock factor protein 4 (*HSF4*), a member of the heat shock transcription factor family, plays an important role in HSR by preventing abnormal protein folding and aggregation to maintain intracellular protein homeostasis[13,14]. *HSF4* has been identified as a cancer-promoting factor in lymphoma [15], breast cancer[16], and cervical cancer[17]. Our previous study demonstrated that *HSF4* is significantly upregulated in CRC, which predicts poor patient prognosis, and that it promotes CRC progression by enhancing the activity of c-MET and downstream ERK1/2 and AKT signaling pathways[18]. Nevertheless, whether DNA methylation is involved in *HSF4*-mediated CRC progression remains to be investigated.

This study investigated the correlation between *HSF4* methylation and *HSF4* expression, and its prognostic and diagnostic value in CRC, and aimed to identify the potential molecular mechanisms associated with *HSF4* methylation through bioinformatics analysis. The aim was to provide a theoretical basis and a novel perspective for *HSF4* as a methylation-related biomarker for future CRC diagnosis and treatment.

Table 1 Basic information of the dataset in this study

Web	Sample source	Sample type	Platform	Samples number
SMART	TCGA_COAD	Tissue	Methylation 450K	Normal = 34, tumor = 288
SMART	TCGA_32 cancer types	Tissue	Methylation 450K	Normal = 676, tumor = 8604
LinkedOmics	TCGA_COADREAD	Tissue	Methylation 27K	Tumor = 233

MATERIALS AND METHODS

Differential analysis of *HSF4* methylation and its prognostic and diagnostic value

The Shiny Methylation Analysis Resource Tool (SMART) APP is an interactive and user-friendly web application for comprehensive analysis of DNA methylation in the The Cancer Genome Atlas (TCGA) project, with data from TCGA (<https://portal.gdc.cancer.gov/>)[19]. The level of methylation at each CpG loci of *HSF4* was assessed using the β value, which is the ratio of the methylation of the allele to the intensity of unmethylation, ranging from 0 to 1. In this study, we analyzed differences in the β values of 19 methylation probes associated with *HSF4* in 33 malignancies by SMART, including COAD, READ, BRCA, LAML, LGG, LIHC, BLCA, CESC, CHOL, KIRP, SKCM, LUAD, ACC, DLBC, KIRC, PCPG, OV, ESCA GBM, STAD, UCEC, UCS, HNSC, TGCT, THCA, THYM, KICH, PRAD, SARC, LUSC, MESO, PAAD, and UVM. Wilcoxon rank sum test was performed for difference analysis of β values, and data was adjusted using the Benjamini-Hochberg method. In addition, β values of 19 *HSF4*-related methylation probes were analyzed differentially in COAD stages and their correlation with *HSF4* mRNA expression based on SMART. The differential analysis of β values in COAD stages was performed based on ANOVA, and the correlation between β values of each probe and *HSF4* mRNA expression was performed based on Pearson. The COAD dataset in SMART was extracted and *HSF4* methylation in prognostic and diagnostic value of COAD was assessed by survival (<https://cran.r-project.org/web/packages/survival/index.html>) and pROC[20]/timeROC[21] R packages, respectively. Kaplan-Meier survival curves, Receiver operating characteristic (ROC) curves and time-dependent ROC curves were visualized with the ggplot2 R package[22]. Patient information is shown in Table 1.

Identification of *HSF4* methylation-related genes and their enrichment analysis

LinkedOmics is a publicly available portal that includes three analysis modules, LinkFinder, LinkInterpreter and LinkCompare, to support users in performing multi-omics analysis in cancer, with data from TCGA (<https://www.cancer.gov/ccg/research/genome-sequencing/tcga>) and Clinical Proteomic Tumor Analysis Consortium (<https://proteomics.cancer.gov/programs/cptac>)[23]. In this study, genes associated with *HSF4* methylation were identified at COAD through LinkedOmics. *HSF4* methylation-associated genes were identified by Spearman and subjected to correction by the Benjamini-Hochberg method. Finally, *HSF4* methylation-related genes were displayed by volcano plot and heatmap. Enrichment analysis of *HSF4* methylation-related genes was performed by hypergeometric distribution algorithm based on Gene Ontology (GO)[24] and Kyoto Encyclopedia of Genes and Genomes (KEGG)[25] databases, and presented by bubble and histogram plots. The above results was visualized with the ggplot2 R package[22].

Protein-protein interaction network construction for *HSF4* methylation-associated genes

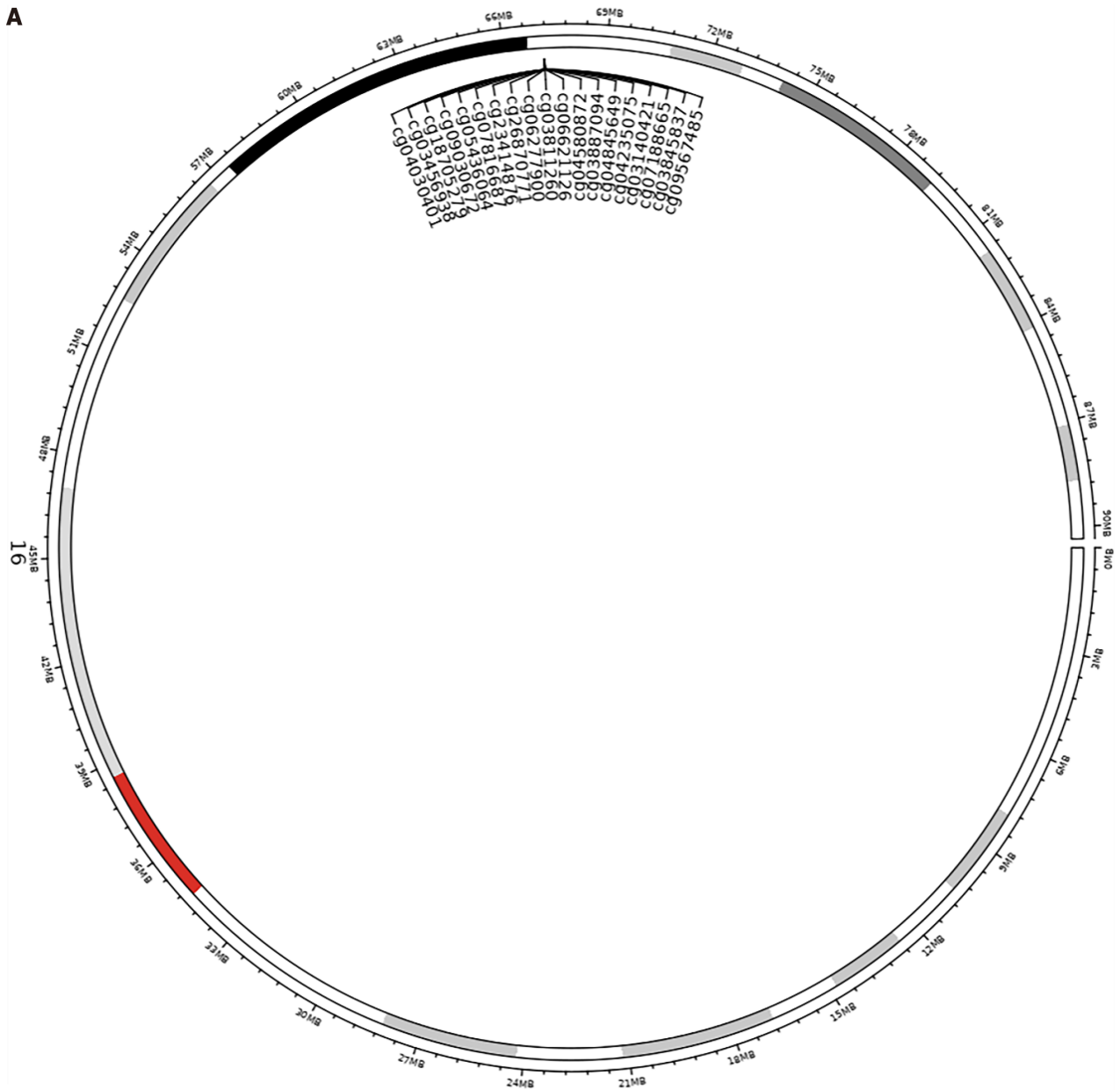
The protein-protein interaction (PPI) network construction for *HSF4* methylation-related genes was based on the String database[26], CytoScape software[27] and the MCODE plugin[28]. Briefly, *HSF4* methylation-related genes obtained from LinkedOmics were extracted, and the interactions of these genes were predicted from the String database. The minimum required interaction score of the String database was set to highest confidence. The interactions were imported into CytoScape software (version:3.8.2) for visualization and clustering analysis of the PPI network was performed by the MCODE algorithm. The parameters of MCODE are degree cutoff = 2, node density cutoff = 0.1, node score cutoff = 0.2, K-core = 2, Max depth = 100.

RESULTS

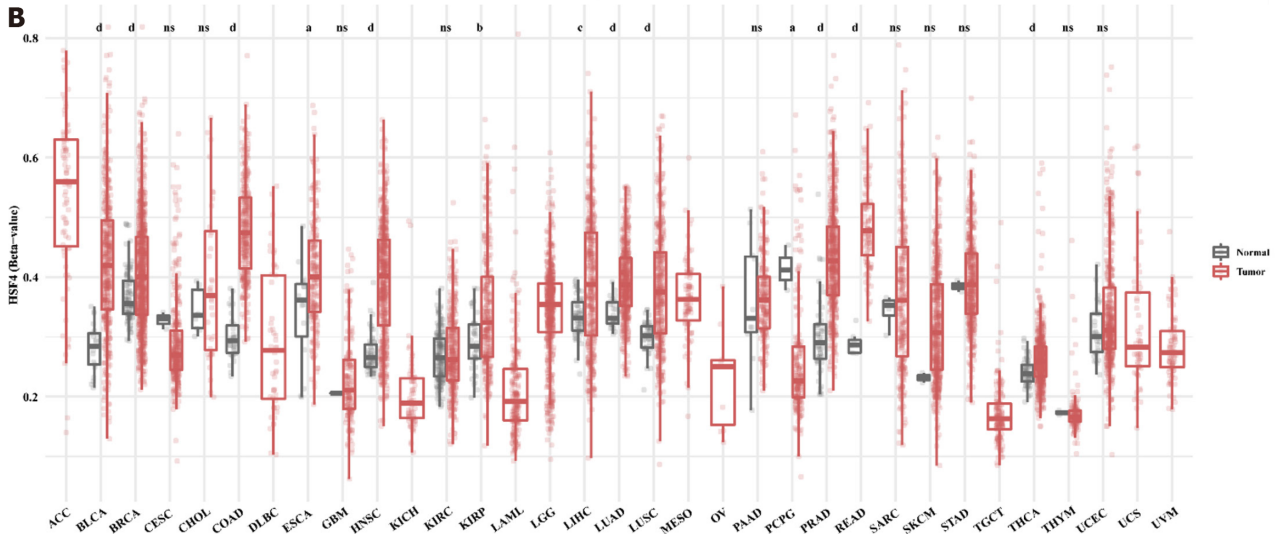
Identification of *HSF4* methylation levels

HSF4 is located on chromosome 16 with 19 CpG loci, with 14 on CpG island, three on N Shore and two on S Shore (Figure 1). Differential analysis revealed that β values of *HSF4* CpG-aggregation methylation were significantly enhanced in most malignancies, including COAD, and READ (Figure 1B). Similarly, the β values of each CpG site were significantly higher in most malignant tumors than in the corresponding paracancerous tissues (Supplementary Figure 1). It is notable that all CpG loci of *HSF4* had significantly elevated β values in these malignancies only in COAD (Supplementary Figure 1 and Figure 2). In READ, only two probes, cg07188665 and cg09567485, exhibited no significant difference in β values. We analyzed the methylation levels of *HSF4* CpG loci in different tumor stages. The β values of cg06277900, cg03811260, cg04580872, cg06621126, cg03887094 and cg09567485 probes were significantly different at various stages of COAD (Supplementary Figure 2). Therefore, we further explored the correlation between *HSF4* methylation and *HSF4* expression. In COAD, the β values of the probes displayed a significant positive correlation with *HSF4* expression, except

A



B



DOI: 10.4251/wjgo.v15.i12.2150 Copyright ©The Author(s) 2023.

Figure 1 Pan-cancer analysis of heat shock factor protein 4 methylation levels. A: Schematic representation of the distribution of eat shock factor protein 4 (*HSF4*) methylated CpG loci. B: Differential analysis of the β values of 19 CpG methylation loci of *HSF4* in multiple malignancies. ^a $P < 0.05$, ^b $P < 0.01$, ^c $P <$

0.001, and ^d*P* < 0.0001; ns: No significant difference.

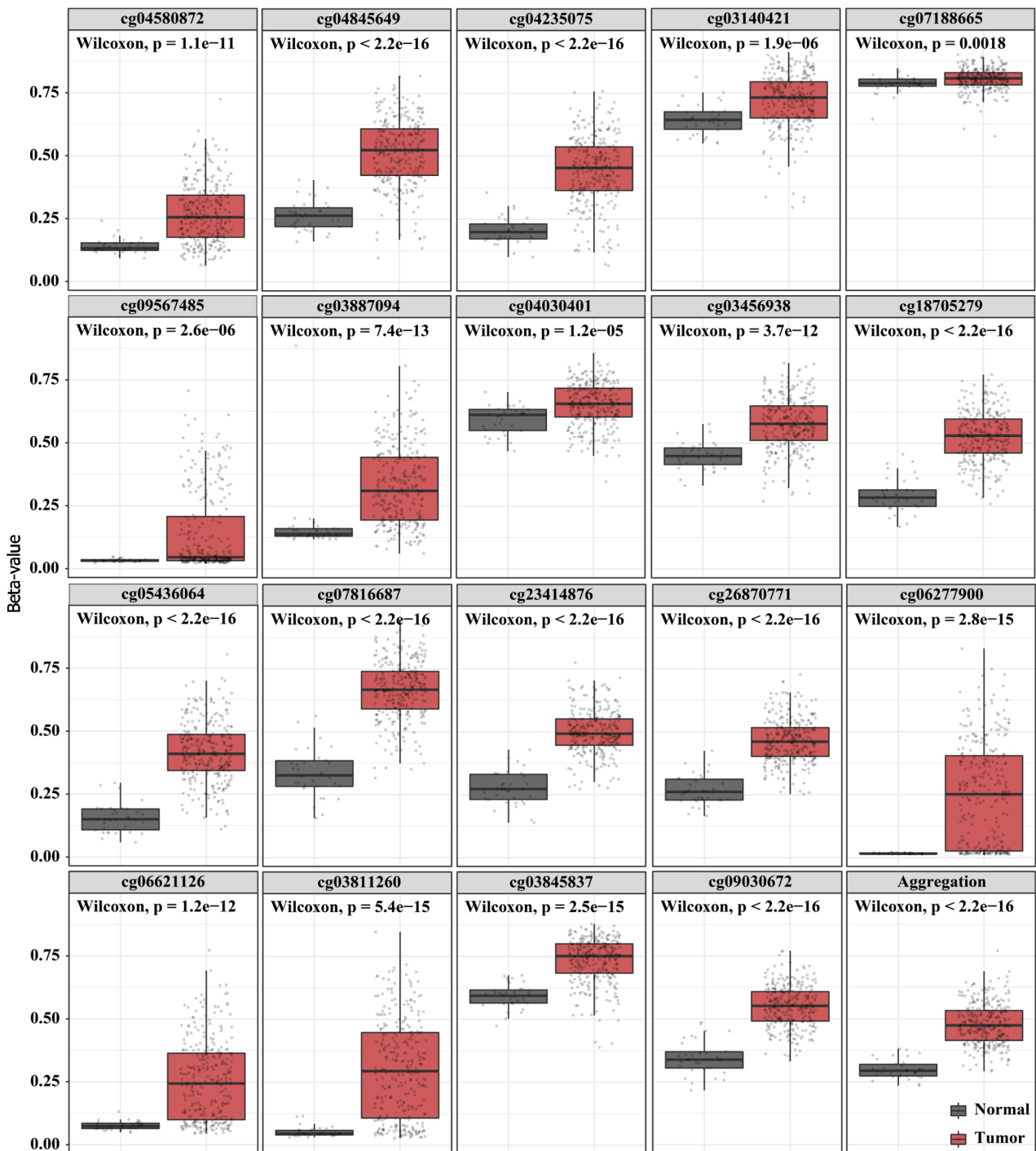


Figure 2 Differential analysis of β values of 19 probes related to heat shock factor protein 4 methylation in colon adenocarcinoma and paraneoplastic tissues. The β values of all 19 probes were significantly increased in the tissues of colon adenocarcinoma (COAD) patients. Black is paraneoplastic tissue, and red is COAD tissue.

for cg07188665 (Figure 3). Combined with our previous findings, we believe that *HSF4* promotes the CRC process at least through DNA methylation.

***HSF4* methylation correlates poorly with CRC prognosis and diagnosis**

In view of the differences in *HSF4* methylation in CRC, we further analyzed the prognostic and diagnostic value of *HSF4* methylation. Kaplan-Meier curves indicated no significant difference in survival among COAD patients with high and

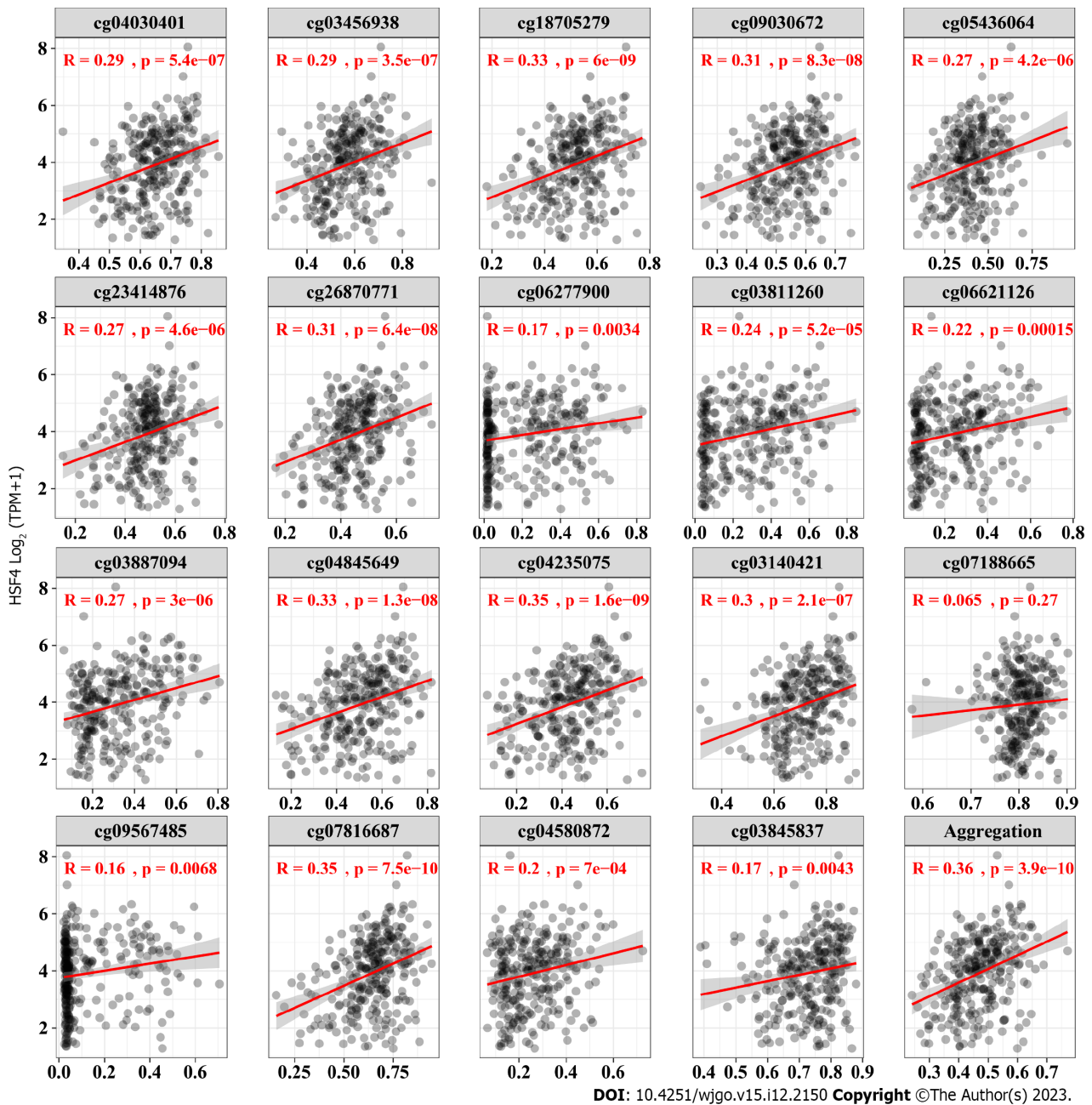
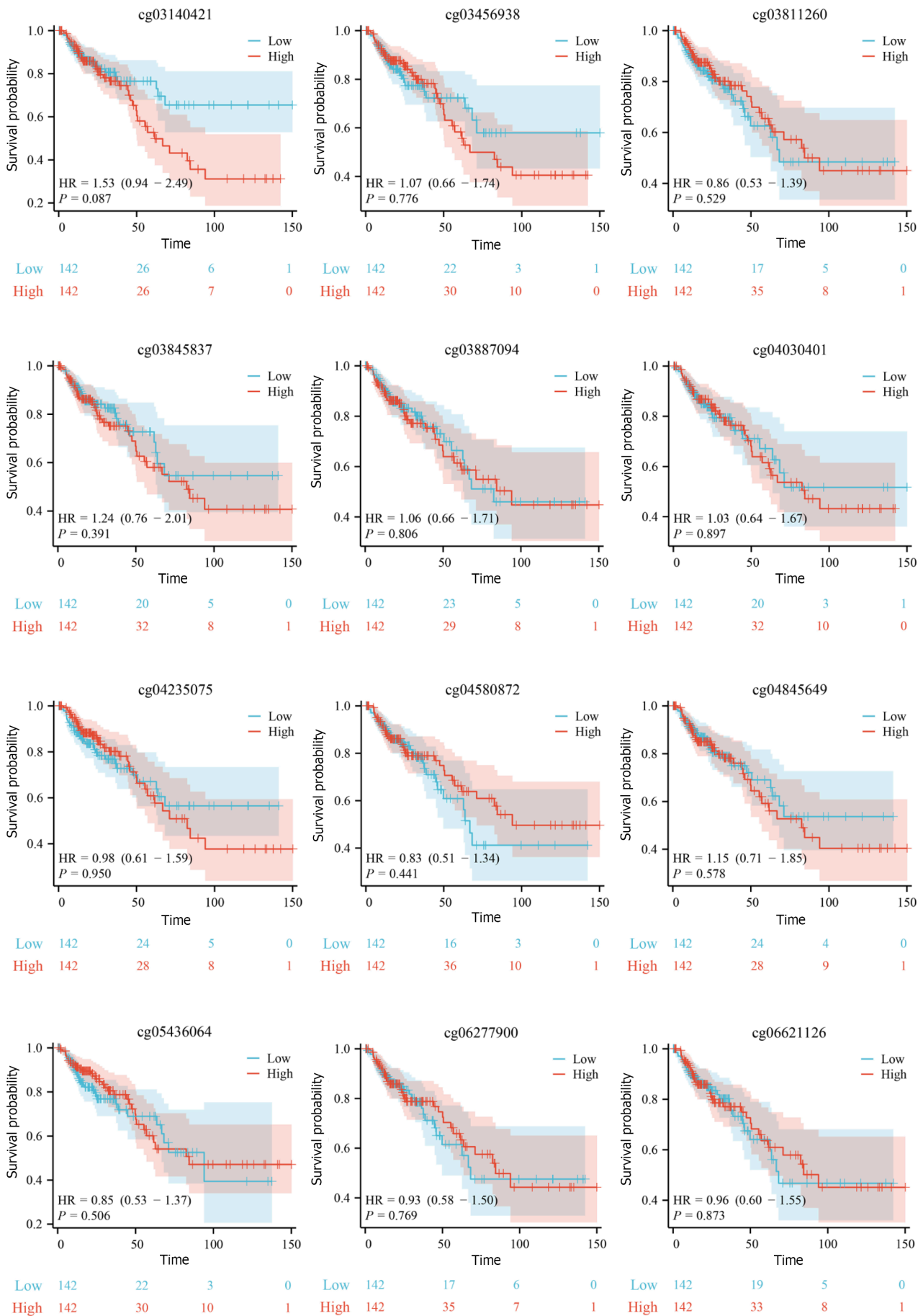


Figure 3 Correlation analysis of heat shock factor protein 4 expression and heat shock factor protein 4 methylation levels. The β values of all 19 probes exhibited a significant positive correlation with the expression of heat shock factor protein 4 (*HSF4*) mRNA. The x-axis is the β value of 19 probes, and y-axis is \log_2 (TPM + 1) of *HSF4* mRNA.

low methylation levels for each CpG loci (Figure 4). Nevertheless, most patients with hypermethylated CpG loci had better prognosis. The ROC curve revealed that the area under the curve (AUC) of each CpG loci ranged from 0.498 to 0.574 in COAD patients, suggesting the mediocre diagnostic value of *HSF4* methylation in COAD patients (Figure 5A). The time-dependent ROC curves suggested that the AUC of each CpG loci was greater with increasing time (Figure 5B). The above results indicated that the performance of *HSF4* methylation as a prognostic and diagnostic biomarker in CRC was ordinary, which may have been caused by relatively low accumulation of single genes.

Identification of *HSF4* methylation-related genes in CRC and their functional enrichment analysis

We analyzed the genes associated with *HSF4* methylation in CRC by LinkedOmics. The expression of 1468 genes was positively correlated with *HSF4* methylation levels, and expression of 226 genes was negatively correlated with *HSF4* methylation levels in the COAD cohort (Figure 6A). The heatmap illustrated the top 50 genes with absolute correlation coefficients (Figures 6B and C). To further understand the functions and pathways involved in these genes, we performed GO and KEGG enrichment analysis. GO identified that the proteins encoded by these genes were mainly extracellular matrix, and associated with processes such as positive regulation of mitogen-activated protein kinase cascade, tumor necrosis factor superfamily cytokine production, neutrophil mediated cytotoxicity, and chemokine activity (Figure 6D). KEGG enrichment revealed that *HSF4* methylation-related genes were involved in pathways including chemokine



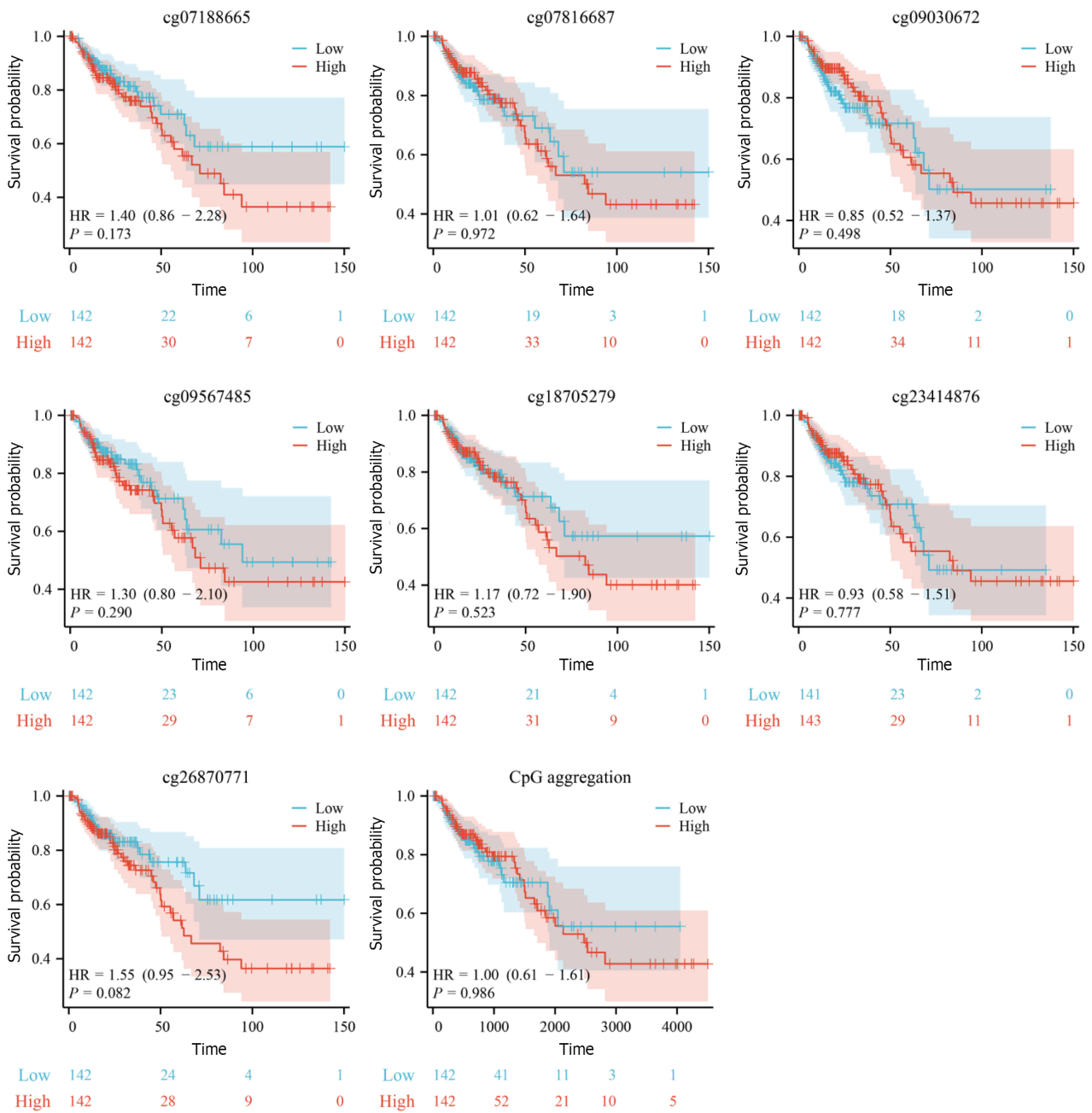
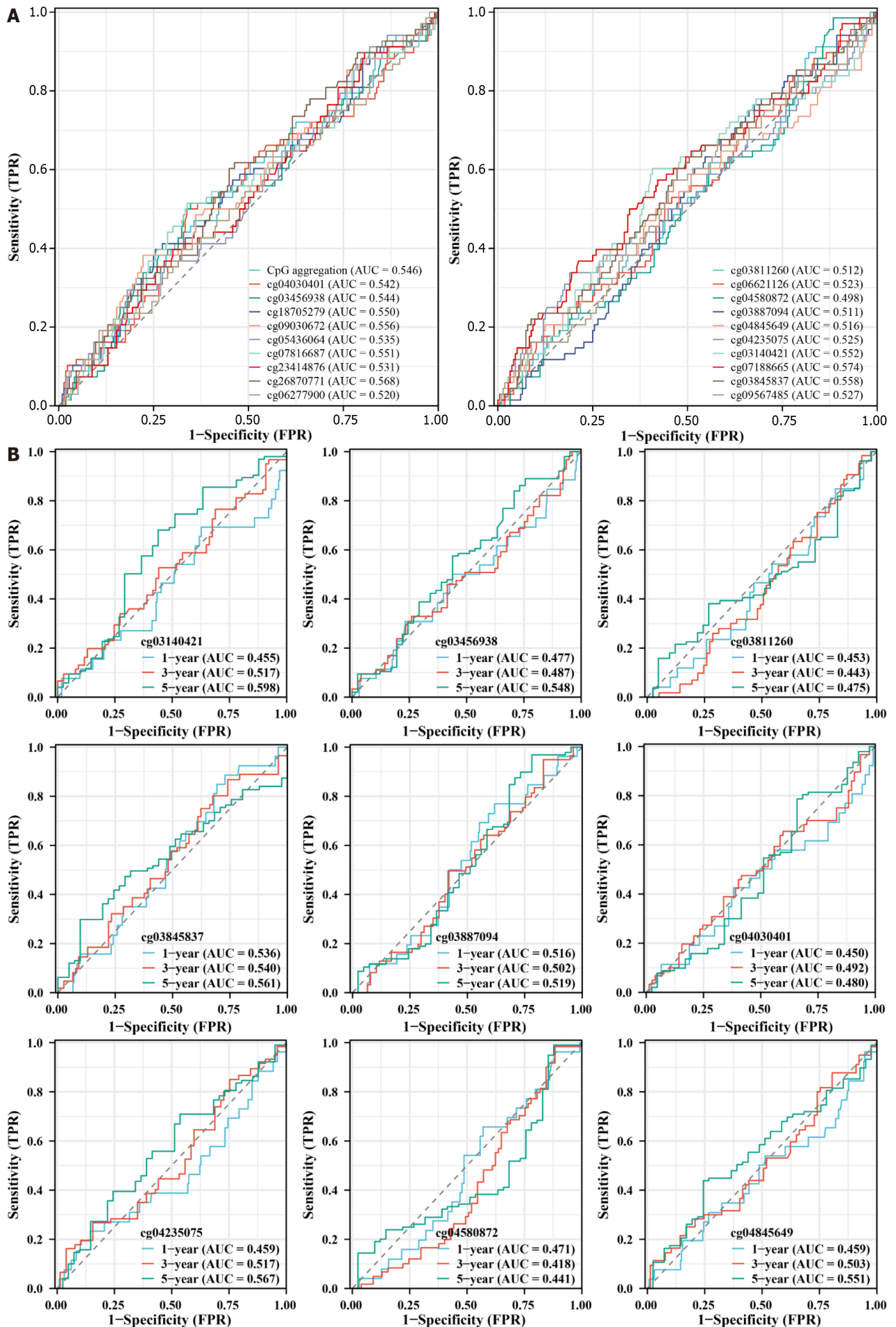


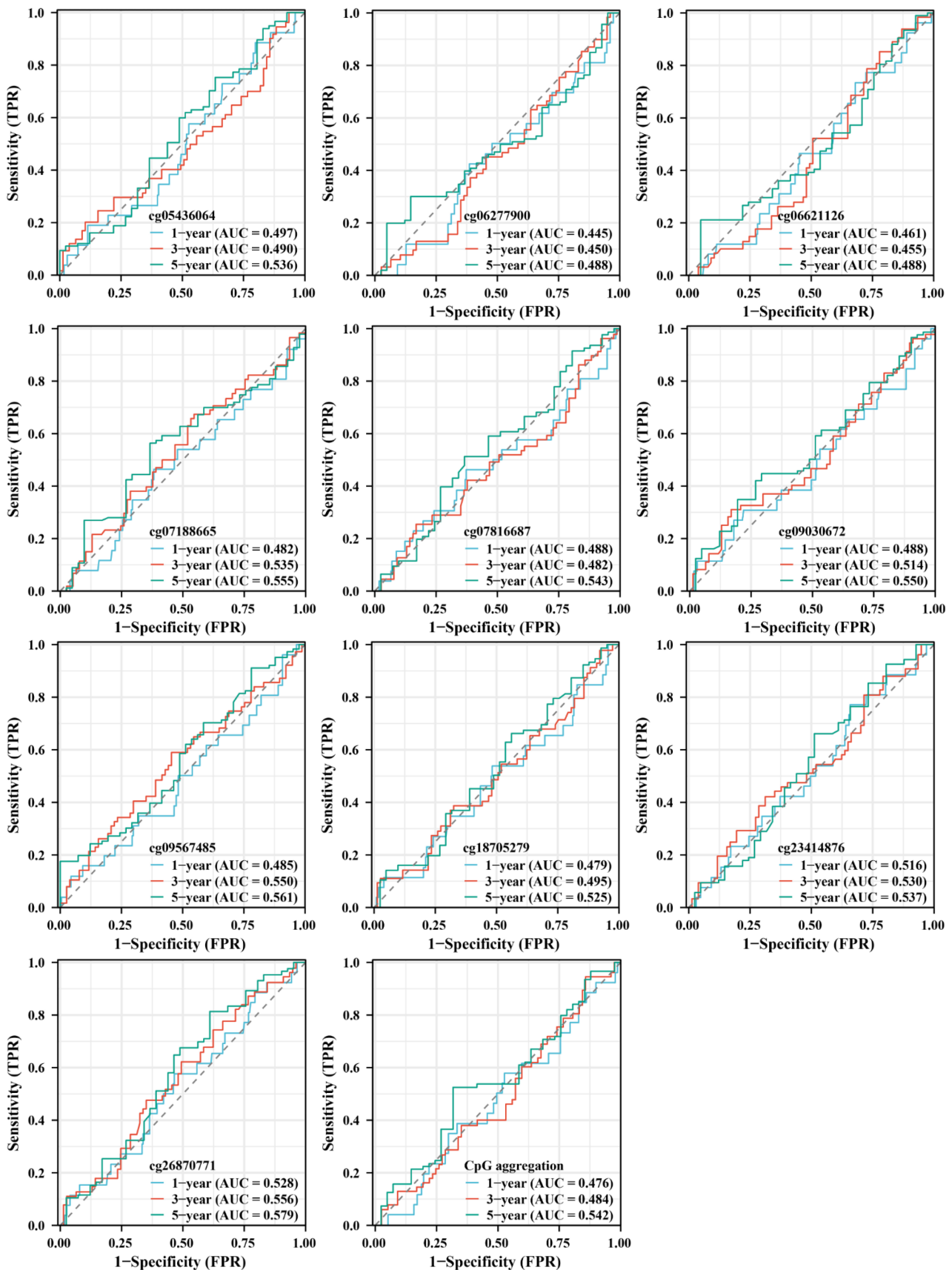
Figure 4 Correlation analysis of heat shock factor protein 4 methylation and prognosis of patients with colon adenocarcinoma. Kaplan Meier survival curves illustrating the survival of colon adenocarcinoma patients with high and low beta values for the 19 probes. The blue curve represents the cohort with low β values, and the red curve stands for the cohort with high β values.

signaling pathway, calcium signaling pathway, glycosphingolipid biosynthesis - lacto and neolacto series, inflammatory bowel disease and inflammatory bowel disease (Figure 6E). It is suggested that HSF4 methylation mediates the phenotypic involvement of immune, inflammatory, and metabolic reprogramming in the CRC process.

PPI network of HSF4 methylation-associated genes in CRC

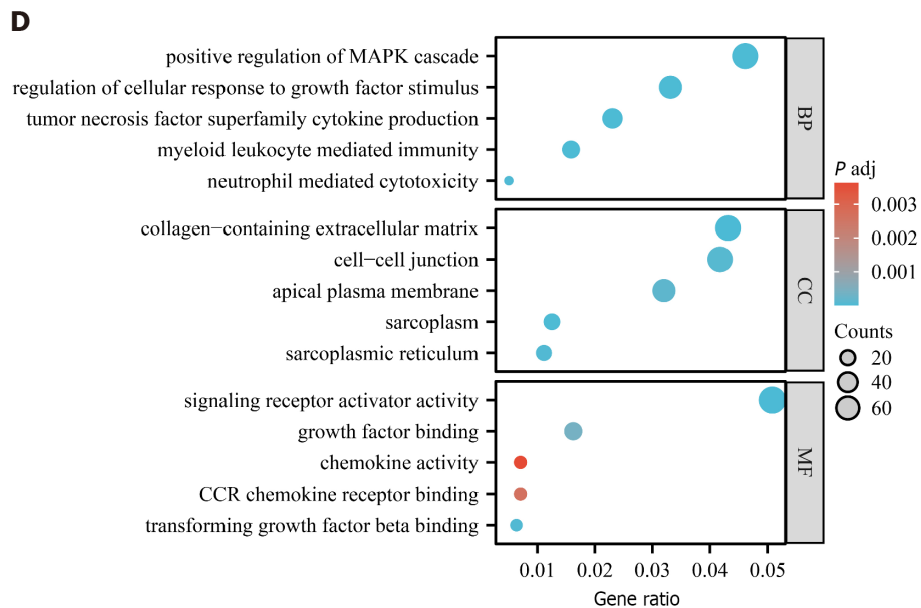
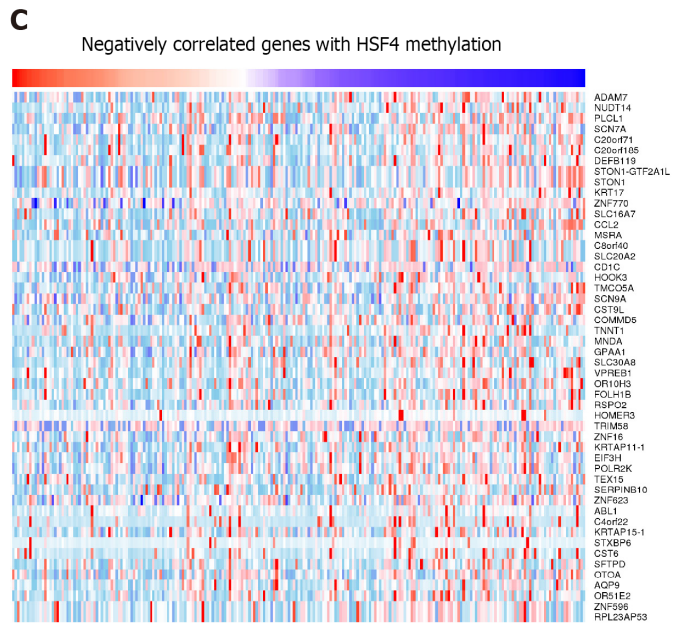
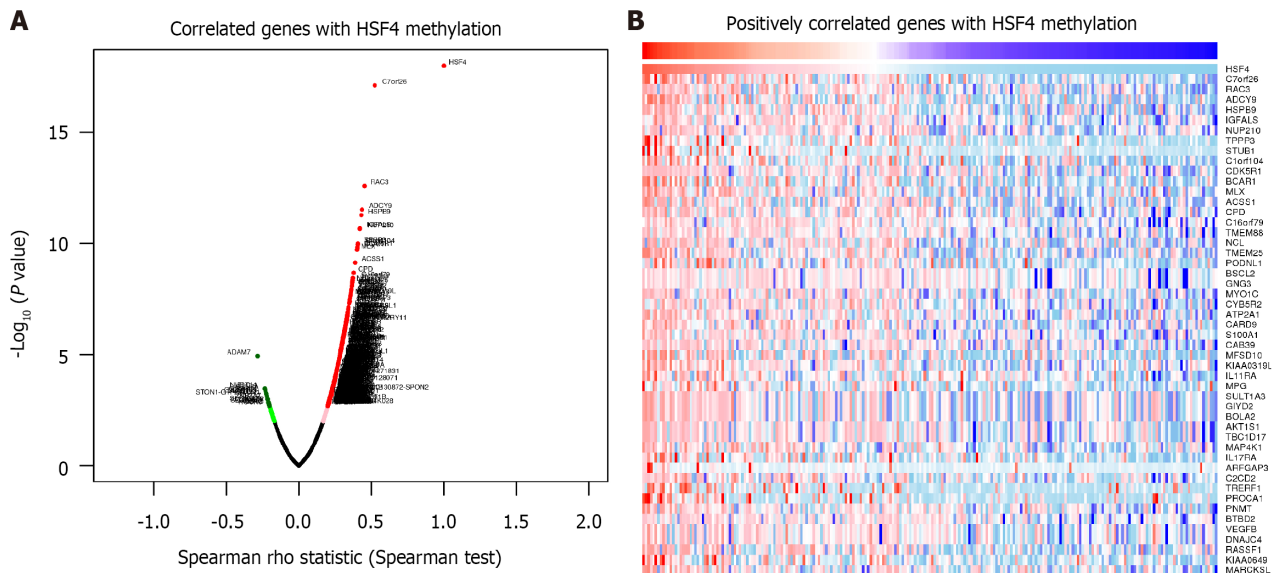
To identify the hub genes in HSF4 methylation-related genes, we constructed a relevant PPI network based on the String database and the MCODE algorithm. The PPI network constructed for HSF4 methylation positively correlated genes contained 422 nodes and 702 edges, and 22 clustering networks were obtained (Figure 7A). The top 20 genes in this network with the highest number of edges are displayed in Figure 7B, where EGFR, RELA, STAT3, ESR1, and F2 had the highest number of edges. The top 10 interworking networks with clustering scores are illustrated in Figure 7C. The network consisting of NUP98, SUMO3, IPO8, and HSPA6 had the highest clustering score, which contained 11 nodes and 35 edges (Figure 7C). In the same way, the network constructed for negatively associated genes contained 110 genes, 122 interactions and five clusters (Figure 8A). The edge numbers TOP5 of FCGR3A, POLR2K, AXIN1, CCL2 and COPS5 had eight, seven, six, five and five edges, respectively (Figure 8B). The five clustering networks composed of genes and interactions are shown in Figure 8C. It is suggested that these genes are involved in HSF4 methylation mediation of the





DOI: 10.4251/wjgo.v15.i12.2150 Copyright ©The Author(s) 2023.

Figure 5 Correlation analysis of heat shock factor protein 4 methylation and diagnosis in patients with colonic adenocarcinoma. A: Receiver operating characteristic (ROC) curves exhibiting the diagnostic value of 19 heat shock factor protein 4 (*HSF4*) methylation-associated probes in colon adenocarcinoma patients. B: Time-dependent ROC curves displaying the area under the curve of *HSF4* methylation at 1, 3 and 5 years. AUC: Area under the curve; TPR: True positive rate; FPR: False positive rate.



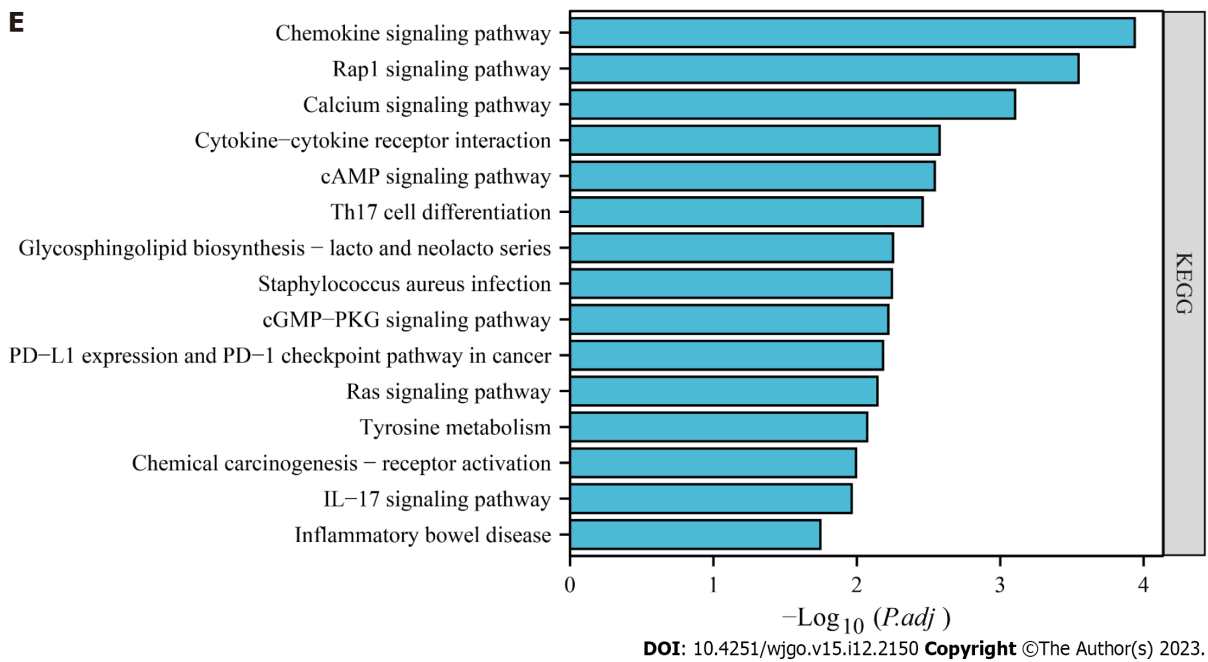


Figure 6 Identification of heat shock factor protein 4 methylation-related genes and their enrichment analysis in colorectal cancer. A: Volcano plot showing genes positively and negatively associated with heat shock factor protein 4 (*HSF4*) methylation in colorectal cancer. B, C: Expression profiles of the top 50 genes ranked by absolute correlation coefficient of *HSF4* methylation-related genes. B is the expression profile of genes positively associated with *HSF4* methylation; C is the expression profile of genes negatively associated with *HSF4* methylation. D: Bubble plots exhibiting the GO enrichment results of all *HSF4* methylation-related genes. E: Possible pathways involved in *HSF4* methylation-related genes obtained by Kyoto Encyclopedia of Genes and Genomes enrichment analysis. *HSF4*: Heat shock factor protein 4; BP: Biological process; CC: Cell component; MF: Molecular function; PD-L1: Programmed cell death-Ligand 1; PD-1: Programmed death 1; IL-17: Interleukin-17.

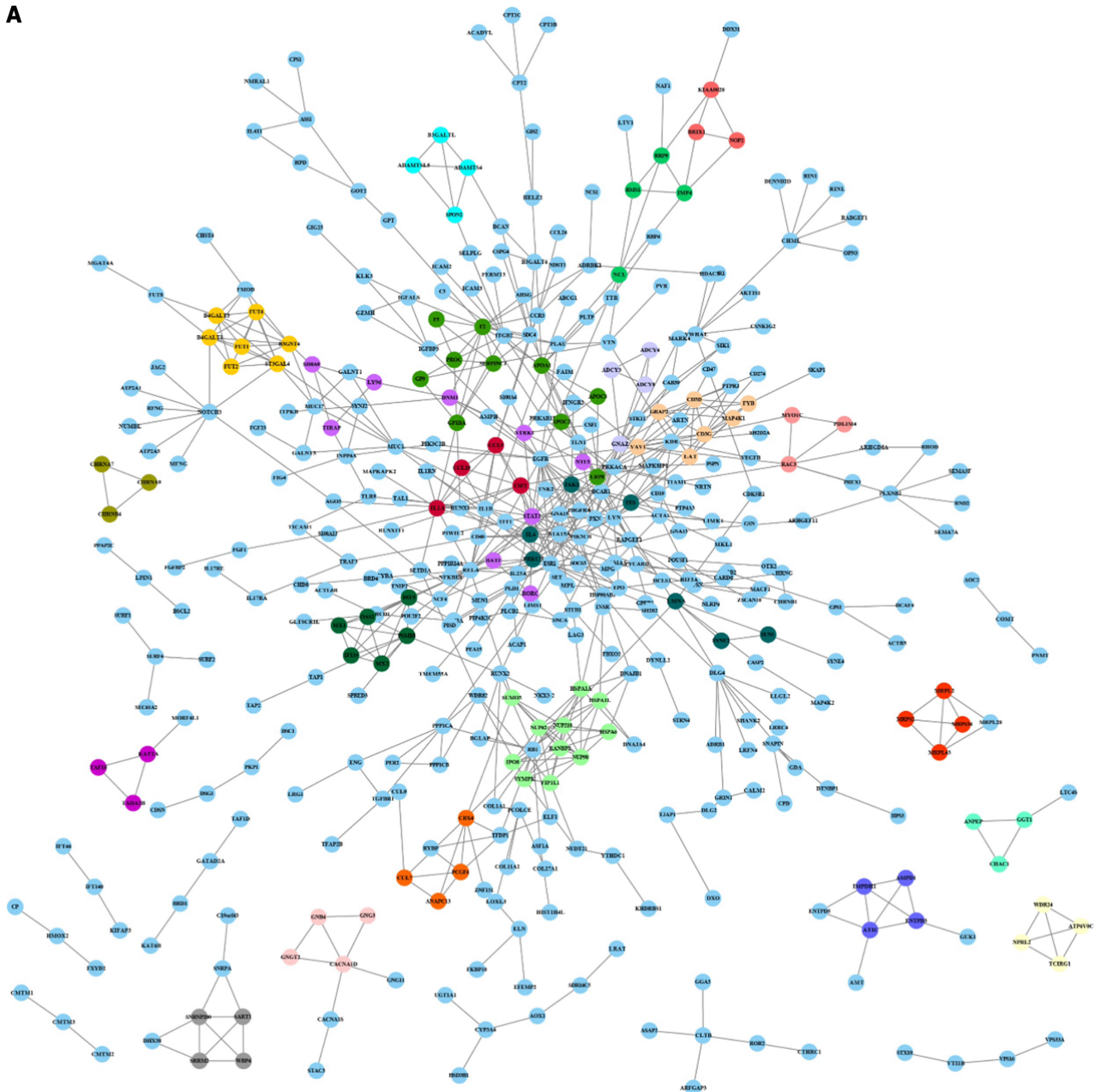
CRC process.

DISCUSSION

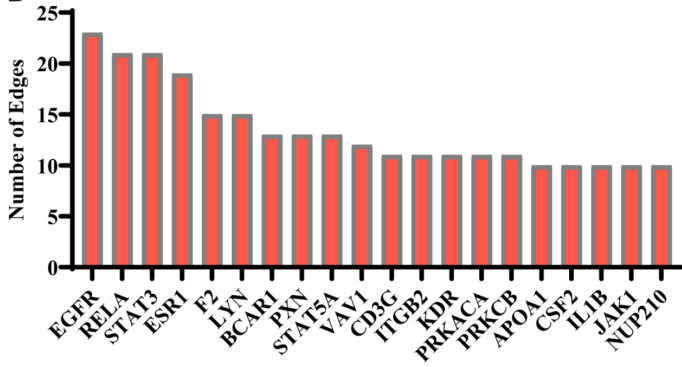
CRC is the second leading cause of cancer-related deaths worldwide. CRC is the outcome of progressive accumulation of a series of mutations and epigenetic changes in the rectum, cecum, and colon, leading to the development of colorectal adenoma and invasive adenocarcinoma. DNA methylation, one of the major epigenetic modifications, has been partially identified as a commercial diagnostic and prognostic biomarker for CRC. We have previously identified *HSF4* as an oncogenic gene in CRC[18]. Therefore, we tapped the diagnostic and prognostic value of *HSF4* and its possible molecular mechanisms in CRC. Unfortunately, *HSF4*, like most single-gene markers[29-32], has a mediocre diagnostic and prognostic value for its methylation levels in CRC. As in previous studies[29-32], this may be due to the small sample size analyzed or the insufficient accumulation of single gene methylation. Therefore, we analyzed the role of *HSF4* methylation in CRC at the molecular mechanism level. It is noteworthy that we identified 1694 genes associated with *HSF4* methylation, and their possible involvement in immune, inflammatory, and metabolic reprogramming. In addition, the constructed PPI network demonstrated that *EGFR*, *RELA*, *STAT3*, *ESR1*, *FCGR3A*, *AXIN1*, *CCL2*, and *COPS5* are hub genes among *HSF4* methylation-related genes.

Most of these hub genes have been demonstrated to be involved in the CRC process and have been applied as therapies for CRC. For instance, *EGFR* is a transmembrane receptor that plays a regulatory role in tumor cell function by binding to EGFs, promoting cell proliferation, differentiation, and survival[33]. Currently, monoclonal antibodies against *EGFR*, such as cetuximab or panitumumab, are utilized in the clinical treatment of patients with metastatic CRC[34,35]. *RELA*, also known as p53 or nuclear factor (NF)- κ B p53, is known to be a key transcription factor in tumors, and it mediates immune and inflammatory responses to facilitate cancer cell survival and metastasis, which leads to it being a key target in tumor therapy[36,37]. Similarly, *FCGR3A* belongs to the Fc γ receptor family, which is mainly expressed on the surface of natural killer cells, monocytes, and macrophages and plays an important role in antibody-mediated immune responses[38]. Polymorphisms in *FCGR3A* are associated with progression-free survival in patients with metastatic CRC treated with cetuximab[39,40]. *COPS5*, also known as CSN5 or JAB1, is one of the constituent proteins of the COP9 signalosome, is a nuclear-plasmid transmembrane protein with multiple functions, and is involved in the regulation of various cellular processes such as cell proliferation, differentiation, apoptosis, and DNA replication and repair[41]. It has been demonstrated that *COPS5* plays a role as a pro-cancer factor in CRC by regulating Wnt and PI14K/AKT pathways[42-44]. Some of these hub genes have also been proven to be related to HSF family proteins. For example, HSR-induced activation of HSP1 is regulated by the NF- κ B, which activates transcription of HSPA1A[45]. In turn, HSP1 inhibits the activation of NF- κ B pathway[46,47]. Stephanou and Latchman[48] showed that the activation of *STAT3* alone

A



B



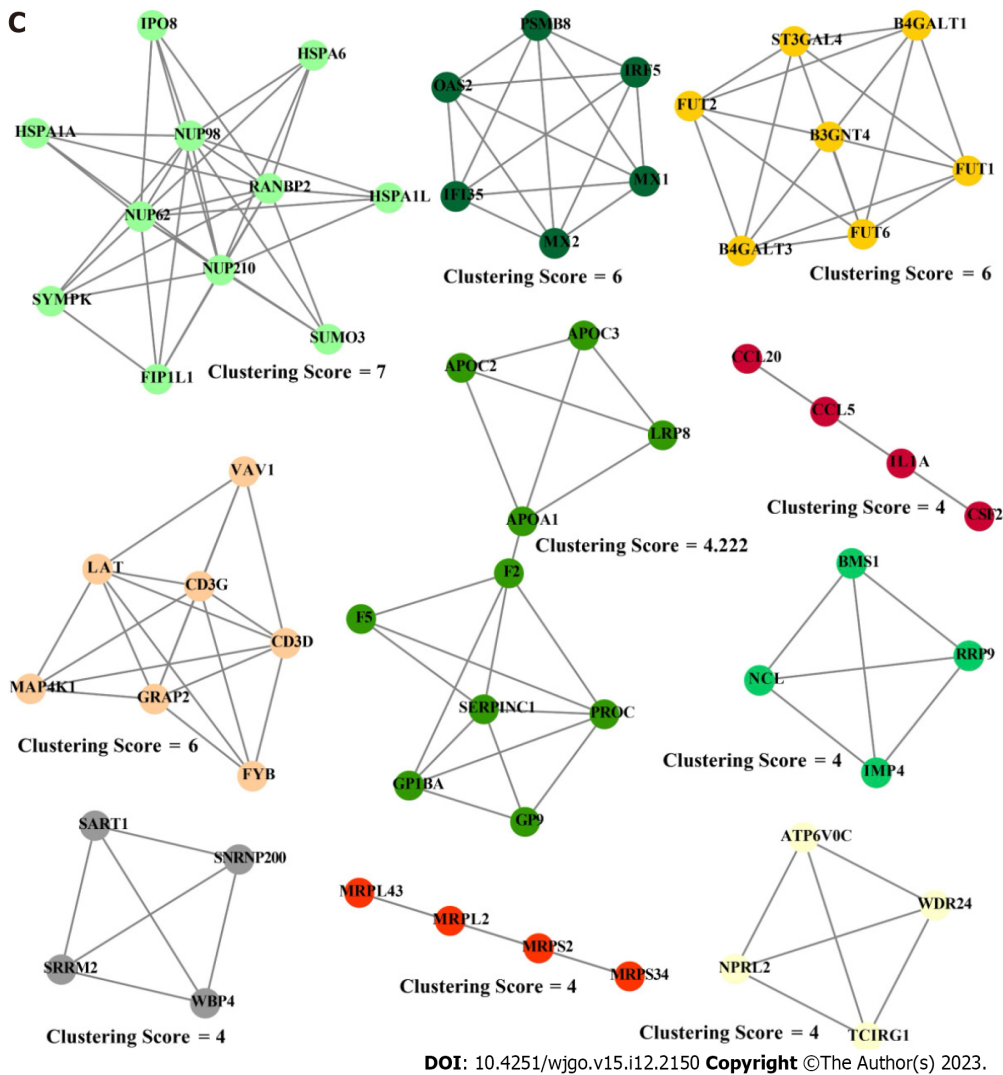


Figure 7 Protein-protein interaction network construction of heat shock factor protein 4 methylation positively associated genes. A: Protein-protein interaction (PPI) network of heat shock factor protein 4 methylation positively related genes constructed based on String database and MCODE algorithm. B: Top 20 genes in PPI network in terms of edge number. C: The top 10 clustering networks in terms of clustering scores obtained by the MCODE algorithm.

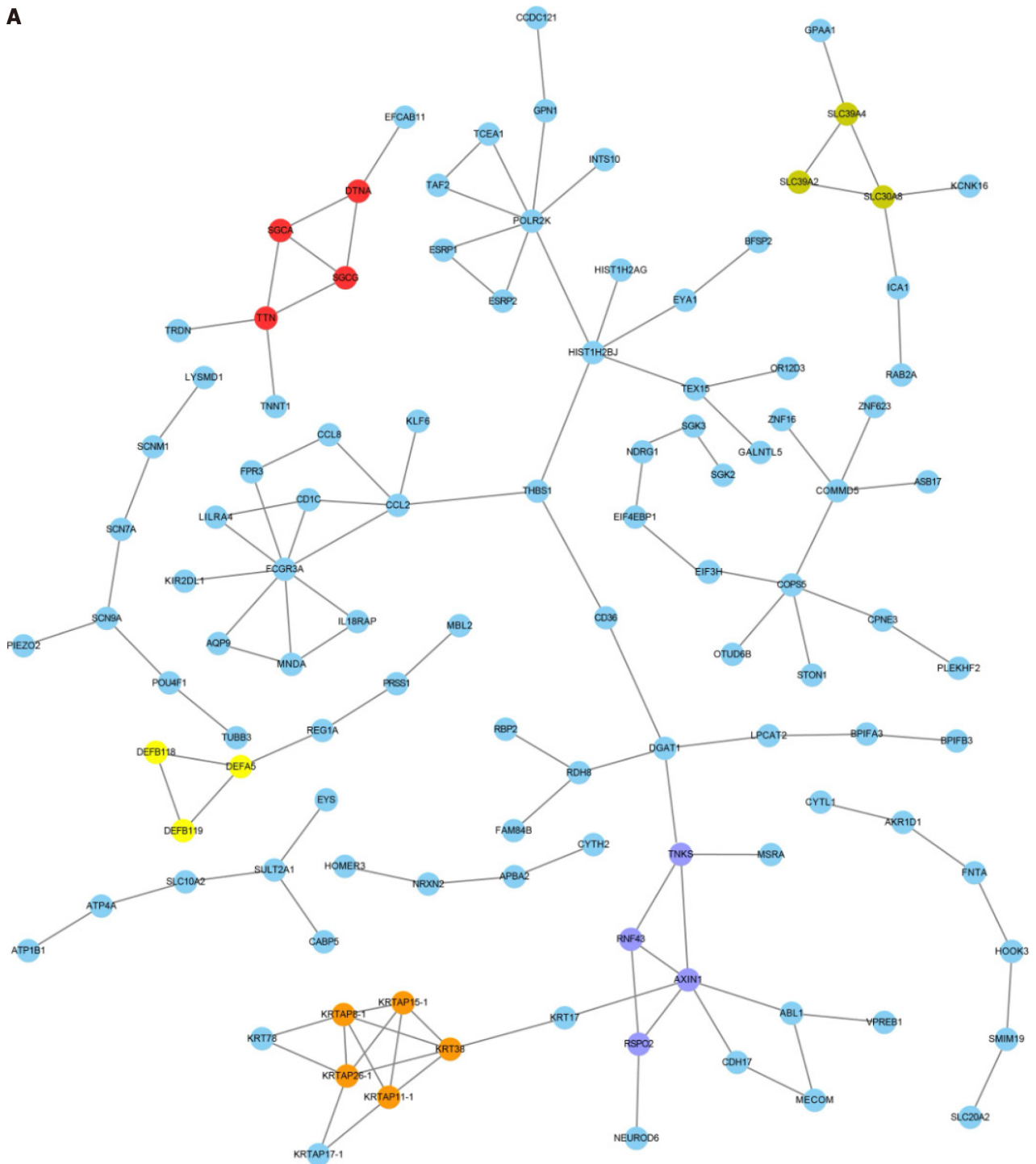
facilitates the mobilization of the HSP promoter. Nevertheless, whether *HSF4* methylation-mediated alterations in *HSF4* expression are crosstalk with these hub genes in CRC remains to be further investigated.

Unfortunately, there were some limitations to this study. For instance, the sample size was small, and a larger sample might reveal satisfactory diagnostic and prognostic values[49,50]. Exploring the correlation between *HSF4* methylation and CRC subtypes or *HSF4*-related gene methylation combinations may improve the value of *HSF4* in CRC[9,49]. It is essential to verify *HSF4* methylation in CRC tissues by methylation sequencing or microarrays, which could support the findings of this study[51]. Although we demonstrated that *HSF4* methylation levels exhibited a positive correlation with *HSF4* mRNA expression, *in vivo* and *in vitro* experiments are lacking for validation. In the same way, the molecular mechanisms associated with *HSF4* methylation remain to be explored *in vivo* and *in vitro*. The tumor immune microenvironment (TME) consists of immune cells, blood vessels, and extracellular matrix, and has a dual role in the growth and metastasis of tumor cells[52,53]. HSF family proteins, especially HSF1, have been demonstrated to mediate tumor cell associated immune responses in the TME[54,55]. This predicts that the function of *HSF4* in CRC-associated TME is also worthy of investigation.

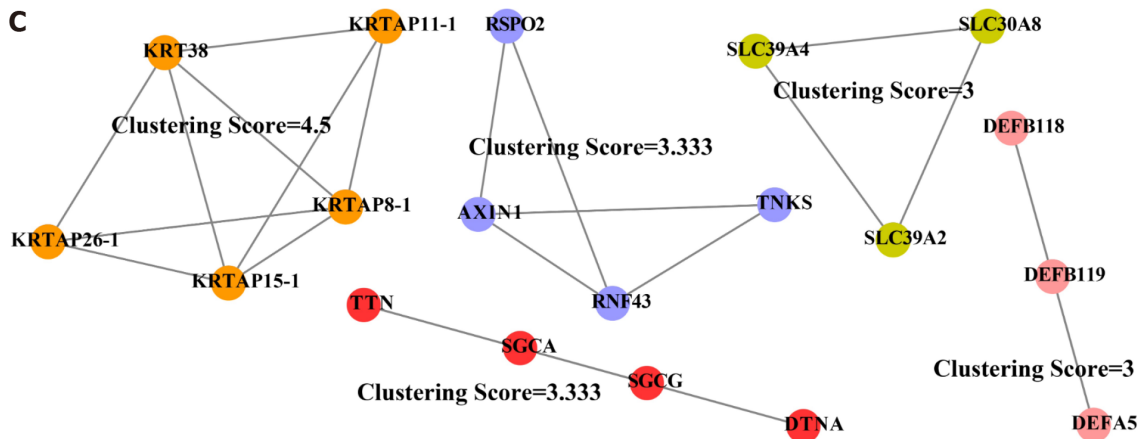
CONCLUSION

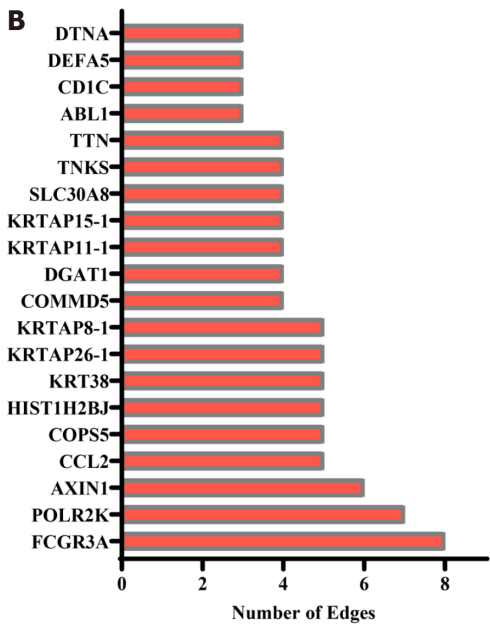
In conclusion, this study reveals that *HSF4* is highly methylated in CRC and is associated with *HSF4* overexpression. Although *HSF4* methylation has poor diagnostic and prognostic value, it may be involved in the CRC process by mediating expression of *HSF4* or related genes with potential mechanisms. Combined with our previously described findings[18], the present study believes that high expression of *HSF4* mRNA and protein and its oncogenic effects are most probably due to *HSF4* methylation (Figure 9). Specific mechanisms need to be confirmed by more *in vivo* and *in vitro*

A



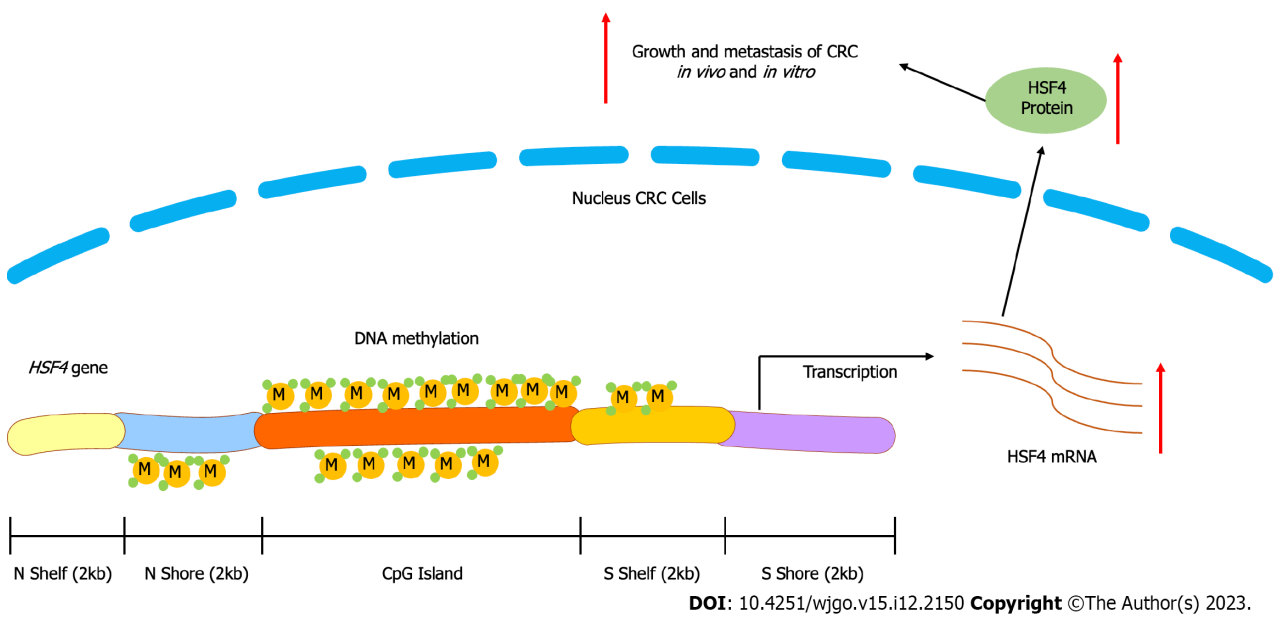
C





DOI: 10.4251/wjgo.v15.i12.2150 Copyright ©The Author(s) 2023.

Figure 8 Protein-protein interaction network construction of heat shock factor protein 4 methylation negatively associated genes. A: Representative images of the protein-protein interaction (PPI) network of heat shock factor protein 4 methylation negatively associated genes. B: The bar chart displaying edge number of each gene in the PPI network. C: Gene composition and interactions of clustering networks obtained by the MCODE algorithm.



DOI: 10.4251/wjgo.v15.i12.2150 Copyright ©The Author(s) 2023.

Figure 9 Diagrammatic representation of this study. CRC: Colorectal cancer; HSF4: Heat shock factor protein 4.

experiments.

ARTICLE HIGHLIGHTS

Research background

DNA methylation is involved in the regulation of gene expression and has been implicated in development and outcome of colorectal cancer (CRC).

Research motivation

We previously demonstrated that heat shock factor protein 4 (HSF4) expression is abnormally high, and contributes to the

malignant biological behavior of CRC *in vivo* and *in vitro*. However, the correlation of *HSF4* methylation with *HSF4* expression and prognosis of CRC patients, and other potential molecular mechanisms need to be further investigated.

Research objectives

The present study was proposed to investigate the correlation between *HSF4* methylation and CRC risk, and to uncover the underlying molecular mechanisms.

Research methods

Identification of *HSF4* methylation sites, and analysis of the differences in β values of *HSF4* methylation sites and their correlation with *HSF4* mRNA expression were performed using Shiny Methylation Analysis Resource Tool Web. The genes associated with *HSF4* methylation were identified by LinkedOmics Web for CRC, and Gene Ontology and Kyoto Encyclopedia of Genes and Genomes enrichment analyses were performed to reveal the functions and signaling that these associated genes may be involved in. The String database and MCODE algorithm were performed to construct protein-protein interaction (PPI) networks of *HSF4* methylation-related genes.

Research results

The *HSF4* gene had 19 CpG methylation sites, and their β -values were significantly higher in CRC tissues, positively correlating with *HSF4* mRNA expression. The β value of the *HSF4* methylation site was not associated with the prognosis of CRC patients. Notably, there are 1694 genes in CRC tissues whose expression is associated with *HSF4* methylation and which are involved in immune, inflammatory, and metabolic reprogramming. EGFR, STAT3 and AXIN1 are hub genes in the PPI network constructed by these *HSF4* methylation-related genes.

Research conclusions

The *HSF4* gene is highly methylated in CRC, and is associated with the overexpression of *HSF4* mRNA. *HSF4* methylation may be involved in the process of CRC by mediating the expression of *HSF4* or related genes.

Research perspectives

The finding will provide a theoretical basis and a new perspective on *HSF4* as a methylation-related biomarker for future CRC diagnosis and treatment.

FOOTNOTES

Author contributions: Zhang WJ and Zhang Y conceived and designed the experiments; Zhang WJ, Yue KL, and Wang JZ analyzed the data; Zhang Y contributed to the data curation; Zhang WJ wrote original draft preparation; Yue KL, Wang JZ, and Zhang Y participated in the writing-review and editing.

Supported by National Natural Science Foundation of China, No. 82260601; Joint Foundation of Kunming Medical University and Yunnan Provincial Science and Technology Department, No. 202201AY070001-256; Grant for Clinical Medical Center of Yunnan Provincial Health Commission, No. 2021LCZXXF-XH03; and Young Academic Talents Cultivation Foundation of Yunnan Province, No. 202205AC160070.

Institutional review board statement: This study did not involve any animal and human experimentation.

Conflict-of-interest statement: All the authors report no relevant conflicts of interest for this article.

Data sharing statement: No additional data are available.

Open-Access: This article is an open-access article that was selected by an in-house editor and fully peer-reviewed by external reviewers. It is distributed in accordance with the Creative Commons Attribution NonCommercial (CC BY-NC 4.0) license, which permits others to distribute, remix, adapt, build upon this work non-commercially, and license their derivative works on different terms, provided the original work is properly cited and the use is non-commercial. See: <https://creativecommons.org/licenses/by-nc/4.0/>

Country/Territory of origin: China

ORCID number: Yu Zhang [0000-0002-1523-3849](https://orcid.org/0000-0002-1523-3849).

S-Editor: Wang JJ

L-Editor: A

P-Editor: Zhang XD

REFERENCES

- 1 Dekker E, Tanis PJ, Vleugels JLA, Kasi PM, Wallace MB. Colorectal cancer. *Lancet* 2019; **394**: 1467-1480 [PMID: 31631858 DOI: 10.1016/S0140-6736(19)32319-0]
- 2 Singh D, Vignat J, Lorenzoni V, Eslahi M, Ginsburg O, Lauby-Secretan B, Arbyn M, Basu P, Bray F, Vaccarella S. Global estimates of incidence and mortality of cervical cancer in 2020: a baseline analysis of the WHO Global Cervical Cancer Elimination Initiative. *Lancet Glob Health* 2023; **11**: e197-e206 [PMID: 36528031 DOI: 10.1016/S2214-109X(22)00501-0]
- 3 Morris VK, Kennedy EB, Baxter NN, Benson AB 3rd, Cercek A, Cho M, Ciombor KK, Cremolini C, Davis A, Deming DA, Fakih MG, Gholami S, Hong TS, Jaiyesimi I, Klute K, Lieu C, Sanoff H, Strickler JH, White S, Willis JA, Eng C. Treatment of Metastatic Colorectal Cancer: ASCO Guideline. *J Clin Oncol* 2023; **41**: 678-700 [PMID: 36252154 DOI: 10.1200/JCO.22.01690]
- 4 Mattei AL, Bailly N, Meissner A. DNA methylation: a historical perspective. *Trends Genet* 2022; **38**: 676-707 [PMID: 35504755 DOI: 10.1016/j.tig.2022.03.010]
- 5 Law PP, Holland ML. DNA methylation at the crossroads of gene and environment interactions. *Essays Biochem* 2019; **63**: 717-726 [PMID: 31782496 DOI: 10.1042/EBC20190031]
- 6 Locke WJ, Guanzone D, Ma C, Liew YJ, Duesing KR, Fung KYC, Ross JP. DNA Methylation Cancer Biomarkers: Translation to the Clinic. *Front Genet* 2019; **10**: 1150 [PMID: 31803237 DOI: 10.3389/fgene.2019.01150]
- 7 Saghafinia S, Mina M, Riggi N, Hanahan D, Ciriello G. Pan-Cancer Landscape of Aberrant DNA Methylation across Human Tumors. *Cell Rep* 2018; **25**: 1066-1080.e8 [PMID: 30355485 DOI: 10.1016/j.celrep.2018.09.082]
- 8 Nishiyama A, Nakanishi M. Navigating the DNA methylation landscape of cancer. *Trends Genet* 2021; **37**: 1012-1027 [PMID: 34120771 DOI: 10.1016/j.tig.2021.05.002]
- 9 Jung G, Hernández-Illán E, Moreira L, Balaguer F, Goel A. Epigenetics of colorectal cancer: biomarker and therapeutic potential. *Nat Rev Gastroenterol Hepatol* 2020; **17**: 111-130 [PMID: 31900466 DOI: 10.1038/s41575-019-0230-y]
- 10 Müller D, Györfy B. DNA methylation-based diagnostic, prognostic, and predictive biomarkers in colorectal cancer. *Biochim Biophys Acta Rev Cancer* 2022; **1877**: 188722 [PMID: 35307512 DOI: 10.1016/j.bbcan.2022.188722]
- 11 Zhou Y, Wang S, Yin X, Gao G, Wang Q, Zhi Q, Han Y, Kuang Y. TSHZ3 functions as a tumor suppressor by DNA methylation in colorectal cancer. *Clin Res Hepatol Gastroenterol* 2021; **45**: 101725 [PMID: 34089916 DOI: 10.1016/j.clinre.2021.101725]
- 12 Zhang H, Xu C, Shi C, Zhang J, Qian T, Wang Z, Ma R, Wu J, Jiang F, Feng J. Hypermethylation of heparanase 2 promotes colorectal cancer proliferation and is associated with poor prognosis. *J Transl Med* 2021; **19**: 98 [PMID: 33663522 DOI: 10.1186/s12967-021-02770-0]
- 13 Lang BJ, Guerrero ME, Prince TL, Okusha Y, Bonorino C, Calderwood SK. The functions and regulation of heat shock proteins; key orchestrators of proteostasis and the heat shock response. *Arch Toxicol* 2021; **95**: 1943-1970 [PMID: 34003342 DOI: 10.1007/s00204-021-03070-8]
- 14 Syafruddin SE, Ling S, Low TY, Mohtar MA. More Than Meets the Eye: Revisiting the Roles of Heat Shock Factor 4 in Health and Diseases. *Biomolecules* 2021; **11** [PMID: 33807297 DOI: 10.3390/biom11040523]
- 15 Jin X, Eroglu B, Cho W, Yamaguchi Y, Moskophidis D, Mivechi NF. Inactivation of heat shock factor Hsf4 induces cellular senescence and suppresses tumorigenesis in vivo. *Mol Cancer Res* 2012; **10**: 523-534 [PMID: 22355043 DOI: 10.1158/1541-7786.MCR-11-0530]
- 16 Chen R, Liliental JE, Kowalski PE, Lu Q, Cohen SN. Regulation of transcription of hypoxia-inducible factor-1 α (HIF-1 α) by heat shock factors HSF2 and HSF4. *Oncogene* 2011; **30**: 2570-2580 [PMID: 21258402 DOI: 10.1038/onc.2010.623]
- 17 Tu N, Hu Y, Mivechi NF. Heat shock transcription factor (Hsf)-4b recruits Brg1 during the G1 phase of the cell cycle and regulates the expression of heat shock proteins. *J Cell Biochem* 2006; **98**: 1528-1542 [PMID: 16552721 DOI: 10.1002/jcb.20865]
- 18 Zhang W, Zhang X, Cheng P, Yue K, Tang M, Li Y, Guo Q, Zhang Y. HSF4 promotes tumor progression of colorectal cancer by transactivating c-MET. *Mol Cell Biochem* 2023; **478**: 1141-1150 [PMID: 36229759 DOI: 10.1007/s11010-022-04582-2]
- 19 Li Y, Ge D, Lu C. The SMART App: an interactive web application for comprehensive DNA methylation analysis and visualization. *Epigenetics Chromatin* 2019; **12**: 71 [PMID: 31805986 DOI: 10.1186/s13072-019-0316-3]
- 20 Robin X, Turck N, Hainard A, Tiberti N, Lisacek F, Sanchez JC, Müller M. pROC: an open-source package for R and S+ to analyze and compare ROC curves. *BMC Bioinformatics* 2011; **12**: 77 [PMID: 21414208 DOI: 10.1186/1471-2105-12-77]
- 21 Blanche P, Dartigues JF, Jacqmin-Gadda H. Estimating and comparing time-dependent areas under receiver operating characteristic curves for censored event times with competing risks. *Stat Med* 2013; **32**: 5381-5397 [PMID: 24027076 DOI: 10.1002/sim.5958]
- 22 Ito K, Murphy D. Application of ggplot2 to Pharmacometric Graphics. *CPT Pharmacometrics Syst Pharmacol* 2013; **2**: e79 [PMID: 24132163 DOI: 10.1038/psp.2013.56]
- 23 Vasaikar SV, Straub P, Wang J, Zhang B. LinkedOmics: analyzing multi-omics data within and across 32 cancer types. *Nucleic Acids Res* 2018; **46**: D956-D963 [PMID: 29136207 DOI: 10.1093/nar/gkx1090]
- 24 Mi H, Muruganujan A, Ebert D, Huang X, Thomas PD. PANTHER version 14: more genomes, a new PANTHER GO-slim and improvements in enrichment analysis tools. *Nucleic Acids Res* 2019; **47**: D419-D426 [PMID: 30407594 DOI: 10.1093/nar/gky1038]
- 25 Kanehisa M, Furumichi M, Sato Y, Ishiguro-Watanabe M, Tanabe M. KEGG: integrating viruses and cellular organisms. *Nucleic Acids Res* 2021; **49**: D545-D551 [PMID: 33125081 DOI: 10.1093/nar/gkaa970]
- 26 Szklarczyk D, Kirsch R, Koutrouli M, Nastou K, Mehryary F, Hachilif R, Gable AL, Fang T, Doncheva NT, Pyysalo S, Bork P, Jensen LJ, von Mering C. The STRING database in 2023: protein-protein association networks and functional enrichment analyses for any sequenced genome of interest. *Nucleic Acids Res* 2023; **51**: D638-D646 [PMID: 36370105 DOI: 10.1093/nar/gkac1000]
- 27 Otasek D, Morris JH, Bouças J, Pico AR, Demchak B. Cytoscape Automation: empowering workflow-based network analysis. *Genome Biol* 2019; **20**: 185 [PMID: 31477170 DOI: 10.1186/s13059-019-1758-4]
- 28 Bader GD, Hogue CW. An automated method for finding molecular complexes in large protein interaction networks. *BMC Bioinformatics* 2003; **4**: 2 [PMID: 12525261 DOI: 10.1186/1471-2105-4-2]
- 29 Shao C, Dai W, Li H, Tang W, Jia S, Wu X, Luo Y. The relationship between RASSF1A gene promoter methylation and the susceptibility and prognosis of melanoma: A meta-analysis and bioinformatics. *PLoS One* 2017; **12**: e0171676 [PMID: 28207831 DOI: 10.1371/journal.pone.0171676]
- 30 Laugsand EA, Brenne SS, Skorpen F. DNA methylation markers detected in blood, stool, urine, and tissue in colorectal cancer: a systematic review of paired samples. *Int J Colorectal Dis* 2021; **36**: 239-251 [PMID: 33030559 DOI: 10.1007/s00384-020-03757-x]
- 31 Vedeld HM, Nesbakken A, Lothe RA, Lind GE. Re-assessing ZNF331 as a DNA methylation biomarker for colorectal cancer. *Clin*

- Epigenetics* 2018; **10**: 70 [PMID: 29854011 DOI: 10.1186/s13148-018-0503-2]
- 32 **Gogna P**, King WD. The relationship between colorectal cancer risk factors and LINE-1 DNA methylation in healthy colon tissue. *Epigenomics* 2020; **12**: 1087-1093 [PMID: 32790479 DOI: 10.2217/epi-2019-0340]
- 33 **Sigismund S**, Avanzato D, Lanzetti L. Emerging functions of the EGFR in cancer. *Mol Oncol* 2018; **12**: 3-20 [PMID: 29124875 DOI: 10.1002/1878-0261.12155]
- 34 **Zhou J**, Ji Q, Li Q. Resistance to anti-EGFR therapies in metastatic colorectal cancer: underlying mechanisms and reversal strategies. *J Exp Clin Cancer Res* 2021; **40**: 328 [PMID: 34663410 DOI: 10.1186/s13046-021-02130-2]
- 35 **Piawah S**, Venook AP. Targeted therapy for colorectal cancer metastases: A review of current methods of molecularly targeted therapy and the use of tumor biomarkers in the treatment of metastatic colorectal cancer. *Cancer* 2019; **125**: 4139-4147 [PMID: 31433498 DOI: 10.1002/ncr.32163]
- 36 **Patel M**, Horgan PG, McMillan DC, Edwards J. NF- κ B pathways in the development and progression of colorectal cancer. *Transl Res* 2018; **197**: 43-56 [PMID: 29550444 DOI: 10.1016/j.trsl.2018.02.002]
- 37 **Peng C**, Ouyang Y, Lu N, Li N. The NF- κ B Signaling Pathway, the Microbiota, and Gastrointestinal Tumorigenesis: Recent Advances. *Front Immunol* 2020; **11**: 1387 [PMID: 32695120 DOI: 10.3389/fimmu.2020.01387]
- 38 **Wang TT**, Ravetch JV. Functional diversification of IgGs through Fc glycosylation. *J Clin Invest* 2019; **129**: 3492-3498 [PMID: 31478910 DOI: 10.1172/JCI130029]
- 39 **Zhang W**, Gordon M, Schultheis AM, Yang DY, Nagashima F, Azuma M, Chang HM, Borucka E, Lurje G, Sherrod AE, Iqbal S, Groshen S, Lenz HJ. FCGR2A and FCGR3A polymorphisms associated with clinical outcome of epidermal growth factor receptor expressing metastatic colorectal cancer patients treated with single-agent cetuximab. *J Clin Oncol* 2007; **25**: 3712-3718 [PMID: 17704420 DOI: 10.1200/jco.2006.08.8021]
- 40 **Pander J**, Gelderblom H, Antonini NF, Tol J, van Krieken JH, van der Straaten T, Punt CJ, Guchelaar HJ. Correlation of FCGR3A and EGFR germline polymorphisms with the efficacy of cetuximab in KRAS wild-type metastatic colorectal cancer. *Eur J Cancer* 2010; **46**: 1829-1834 [PMID: 20418097 DOI: 10.1016/j.ejca.2010.03.017]
- 41 **Liu G**, Claret FX, Zhou F, Pan Y. Jab1/COPS5 as a Novel Biomarker for Diagnosis, Prognosis, Therapy Prediction and Therapeutic Tools for Human Cancer. *Front Pharmacol* 2018; **9**: 135 [PMID: 29535627 DOI: 10.3389/fphar.2018.00135]
- 42 **Zhou R**, Shao Z, Liu J, Zhan W, Gao Q, Pan Z, Wu L, Xu L, Ding Y, Zhao L. COPS5 and LASP1 synergistically interact to downregulate 14-3-3 σ expression and promote colorectal cancer progression via activating PI3K/AKT pathway. *Int J Cancer* 2018; **142**: 1853-1864 [PMID: 29226323 DOI: 10.1002/ijc.31206]
- 43 **Jumpertz S**, Hennes T, Asare Y, Schütz AK, Bernhagen J. CSN5/JAB1 suppresses the WNT inhibitor DKK1 in colorectal cancer cells. *Cell Signal* 2017; **34**: 38-46 [PMID: 28229932 DOI: 10.1016/j.cellsig.2017.02.013]
- 44 **Schütz AK**, Hennes T, Jumpertz S, Fuchs S, Bernhagen J. Role of CSN5/JAB1 in Wnt/ β -catenin activation in colorectal cancer cells. *FEBS Lett* 2012; **586**: 1645-1651 [PMID: 22668871 DOI: 10.1016/j.febslet.2012.04.037]
- 45 **Sasi BK**, Sonawane PJ, Gupta V, Sahu BS, Mahapatra NR. Coordinated transcriptional regulation of Hspa1a gene by multiple transcription factors: crucial roles for HSF-1, NF-Y, NF- κ B, and CREB. *J Mol Biol* 2014; **426**: 116-135 [PMID: 24041570 DOI: 10.1016/j.jmb.2013.09.008]
- 46 **Shang L**, Wang L, Shi X, Wang N, Zhao L, Wang J, Liu C. HMGB1 was negatively regulated by HSF1 and mediated the TLR4/MyD88/NF- κ B signal pathway in asthma. *Life Sci* 2020; **241**: 117120 [PMID: 31825792 DOI: 10.1016/j.lfs.2019.117120]
- 47 **Chen Y**, Currie RW. Small interfering RNA knocks down heat shock factor-1 (HSF-1) and exacerbates pro-inflammatory activation of NF- κ B and AP-1 in vascular smooth muscle cells. *Cardiovasc Res* 2006; **69**: 66-75 [PMID: 16061216 DOI: 10.1016/j.cardiores.2005.07.004]
- 48 **Stephanou A**, Latchman DS. Transcriptional regulation of the heat shock protein genes by STAT family transcription factors. *Gene Expr* 1999; **7**: 311-319 [PMID: 10440232]
- 49 **Petit J**, Carroll G, Zhao J, Roper E, Pockney P, Scott RJ. Evaluation of epigenetic methylation biomarkers for the detection of colorectal cancer using droplet digital PCR. *Sci Rep* 2023; **13**: 8883 [PMID: 37264006 DOI: 10.1038/s41598-023-35631-5]
- 50 **Fang Q**, Yuan Z, Hu H, Zhang W, Wang G, Wang X. Genome-wide discovery of circulating cell-free DNA methylation biomarkers for colorectal cancer detection. *Clin Epigenetics* 2023; **15**: 119 [PMID: 37501075 DOI: 10.1186/s13148-023-01518-5]
- 51 **Ye Z**, Song G, Liang J, Yi S, Gao Y, Jiang H. Optimized screening of DNA methylation sites combined with gene expression analysis to identify diagnostic markers of colorectal cancer. *BMC Cancer* 2023; **23**: 617 [PMID: 37400791 DOI: 10.1186/s12885-023-10922-2]
- 52 **Lv B**, Wang Y, Ma D, Cheng W, Liu J, Yong T, Chen H, Wang C. Immunotherapy: Reshape the Tumor Immune Microenvironment. *Front Immunol* 2022; **13**: 844142 [PMID: 35874717 DOI: 10.3389/fimmu.2022.844142]
- 53 **El-Arabey AA**, Abdalla M, Abd-Allah AR. SnapShot: TP53 status and macrophages infiltration in TCGA-analyzed tumors. *Int Immunopharmacol* 2020; **86**: 106758 [PMID: 32663767 DOI: 10.1016/j.intimp.2020.106758]
- 54 **Shan Q**, Ma F, Wei J, Li H, Ma H, Sun P. Physiological Functions of Heat Shock Proteins. *Curr Protein Pept Sci* 2020; **21**: 751-760 [PMID: 31713482 DOI: 10.2174/138920372066619111113726]
- 55 **Calderwood SK**, Hightower LE. Report on the VIIth International Symposium on Heat Shock Proteins in Biology & Medicine. *Cell Stress Chaperones* 2015; **20**: 213-216 [PMID: 25542250 DOI: 10.1007/s12192-014-0562-z]



Basic Study

Evaluating the causal relationship between human blood metabolites and gastroesophageal reflux disease

Jia-Yan Hu, Mi Lv, Kun-Li Zhang, Xi-Yun Qiao, Yu-Xi Wang, Feng-Yun Wang

Specialty type: Oncology

Provenance and peer review:

Unsolicited article; Externally peer reviewed.

Peer-review model: Single blind

Peer-review report's scientific quality classification

Grade A (Excellent): A, A

Grade B (Very good): 0

Grade C (Good): 0

Grade D (Fair): 0

Grade E (Poor): 0

P-Reviewer: Caboclo JLF, Brazil; Yücel O, Turkey

Received: July 29, 2023

Peer-review started: July 29, 2023

First decision: September 23, 2023

Revised: October 1, 2023

Accepted: October 30, 2023

Article in press: October 30, 2023

Published online: December 15, 2023



Jia-Yan Hu, Mi Lv, Kun-Li Zhang, Xi-Yun Qiao, Yu-Xi Wang, Feng-Yun Wang, Institute of Digestive Diseases, Xiyuan Hospital, China Academy of Chinese Medical Sciences, Xiyuan Hospital, China Academy of Chinese Medical Sciences, Beijing 100091, China

Corresponding author: Feng-Yun Wang, PhD, Chief Doctor, Professor, Institute of Digestive Diseases, Xiyuan Hospital, China Academy of Chinese Medical Sciences, Xiyuan Hospital, China Academy of Chinese Medical Sciences, No. 1 Courtyard, Xiyuan Playground, Haidian District, Beijing 100091, China. wfy811@163.com

Abstract

BACKGROUND

Gastroesophageal reflux disease (GERD) affects approximately 13% of the global population. However, the pathogenesis of GERD has not been fully elucidated. The development of metabolomics as a branch of systems biology in recent years has opened up new avenues for the investigation of disease processes. As a powerful statistical tool, Mendelian randomization (MR) is widely used to explore the causal relationship between exposure and outcome.

AIM

To analyze of the relationship between 486 blood metabolites and GERD.

METHODS

Two-sample MR analysis was used to assess the causal relationship between blood metabolites and GERD. A genome-wide association study (GWAS) of 486 metabolites was the exposure, and two different GWAS datasets of GERD were used as endpoints for the base analysis and replication and meta-analysis. Bonferroni correction is used to determine causal correlation features ($P < 1.03 \times 10^{-4}$). The results were subjected to sensitivity analysis to assess heterogeneity and pleiotropy. Using the MR Steiger filtration method to detect whether there is a reverse causal relationship between metabolites and GERD. In addition, metabolic pathway analysis was conducted using the online database based MetaboAnalyst 5.0 software.

RESULTS

In MR analysis, four blood metabolites are negatively correlated with GERD: Levulinate (4-oxovalerate), stearate (18:0), adrenate (22:4n6) and p-acetamidophenylglucuronide. However, we also found a positive correlation between four blood metabolites and GERD: Kynurenine, 1-linoleoylglycerophosphoethan-

olamine, butyrylcarnitine and guanosine. And bonferroni correction showed that butyrylcarnitine (odds ratio 1.10, 95% confidence interval: 1.05-1.16, $P = 7.71 \times 10^{-5}$) was the most reliable causal metabolite. In addition, one significant pathway, the “glycerophospholipid metabolism” pathway, can be involved in the pathogenesis of GERD.

CONCLUSION

Our study found through the integration of genomics and metabolomics that butyrylcarnitine may be a potential biomarker for GERD, which will help further elucidate the pathogenesis of GERD and better guide its treatment. At the same time, this also contributes to early screening and prevention of GERD. However, the results of this study require further confirmation from both basic and clinical real-world studies.

Key Words: Blood metabolites; Gastroesophageal reflux disease; Mendelian randomization; Causality; Pathogenesis; Biomarkers; Metabolic pathway

©The Author(s) 2023. Published by Baishideng Publishing Group Inc. All rights reserved.

Core Tip: At present, there is no study on blood metabolomics of gastroesophageal reflux disease (GERD). This may be the first study combining metabolomics and genomics to explore the causal relationship between serum metabolites and GERD. We found that there was a significant correlation between eight metabolites and GERD, among which butyrylcarnitine was the most reliable pathogenic metabolite (odds ratio 1.10, 95% confidence interval: 1.05-1.16). Glycerophospholipid metabolism may be involved in the pathogenesis of GERD. The results provide a reference direction for the early screening, prevention and treatment of GERD and the design of future clinical research.

Citation: Hu JY, Lv M, Zhang KL, Qiao XY, Wang YX, Wang FY. Evaluating the causal relationship between human blood metabolites and gastroesophageal reflux disease. *World J Gastrointest Oncol* 2023; 15(12): 2169-2184

URL: <https://www.wjgnet.com/1948-5204/full/v15/i12/2169.htm>

DOI: <https://dx.doi.org/10.4251/wjgo.v15.i12.2169>

INTRODUCTION

Gastroesophageal reflux disease (GERD) refers to a disease in which gastric contents reflux into the esophagus, causing corresponding esophageal symptoms and/or complications. This condition affects approximately 13% of the global population[1]. GERD is not life-threatening, but it impairs patients' quality of life and increases the risk of other esophageal complications such as esophagitis, Barrett's esophagus (BE), and esophageal adenocarcinoma[2]. Previous epidemiological studies have identified several possible risk factors for GERD, including smoking, alcohol consumption and diabetes[3-5], which have played a role in the prevention of GERD. However, there are no studies on the blood metabolomics of GERD.

The development of metabolomics as a branch of systems biology in recent years has opened up new avenues for the investigation of disease processes. By identifying altered metabolites or metabolic pathways, metabolomics can specifically shed light on the molecular causes of disease[6]. Unlike genomics, transcriptomics or proteomics, metabolomics describes the concentration and flux of low molecular metabolites present in biological fluids or tissues[7]. It allows a global assessment of the cellular state in a real environment, taking into account gene expression, genetic regulation, changes in the kinetic activity and regulation of enzymes, and changes in metabolic responses[8]. Due to metabolic fluctuations downstream of changes in DNA, RNA, and protein levels, metabolomics provides a sensitive and comprehensive interpretation of biological systems. Metabolomics has now been widely used to characterize specific metabolic phenotypes associated with digestive diseases and has identified many metabolites[9-11]. To our knowledge, there are no thorough investigations that systematically examine the causative association between blood metabolites and GERD, although Liu *et al*[12] described 23 metabolic abnormalities related to GERD. Based on the information currently available, it is not possible to identify the metabolite profile that contributes to the development of GERD due to the inherent limitations of traditional observational research.

As a powerful statistical tool, Mendelian randomization (MR) is widely used to explore the causal relationship between exposure and outcome[13]. In particular, MR was able to circumvent the drawbacks of randomized controlled experiments by choosing exposure-related single nucleotide polymorphisms (SNPs) as instrumental variables (IVs)[14]. Because genetic variants are randomly assigned during meiosis, MR was able to largely avoid confounding factors by using this alternative to IVs that mimic randomized controlled trials[15]. In addition, genotype formation occurs before the onset of the disease and is usually not affected by disease progression. Thus, reverse causality is unlikely. In this study, we used MR analysis to thoroughly investigate the causal relationships between 486 blood metabolites and GERD using data from a genome-wide association study (GWAS). Additionally, we identified the metabolic pathways that cause GERD. In addition to advancing our understanding of the pathophysiological mechanisms underlying GERD, the integration of metabolomics and genomics offers fresh perspectives on the early detection and management of the

disease.

MATERIALS AND METHODS

Study design

An effective MR study should follow three assumptions: (1) IVs are closely related to exposure factors; (2) IVs are not related to confounding factors; and (3) IVs are not related to outcomes and affect outcome only *via* exposures[16]. Two independent GWAS alliances give the genetic information of GERD, subjected to preliminary and replication analyses, followed by meta-analysis. The overview of the study is showed in [Figure 1](#).

GWAS data for 486 blood metabolites and GERD

Genetic data for blood metabolites were obtained from the Metabolomics GWAS server (<https://metabolomics.helmholtz-muenchen.de/gwas/>). Shin *et al*[17] identified nearly 2.1 million SNPs of 486 metabolites related to human genetic variation through genome-wide association scanning and high-throughput metabolic analysis. Of the 486 metabolites, 107 are defined as unknown because their chemical properties are still unclear. Another 309 metabolites were chemically identified and assigned to eight broad metabolomes, including amino acid, carbohydrate, cofactors and vitamin, energy, lipid, nucleotide, peptide, and xenobiotic metabolism. The detailed names of 486 metabolites are shown in [Supplementary Table 1](#), among which the chemical properties of the metabolites named X - are unknown.

Download GERD's GWAS summary data from IEU (<https://gwas.mrcieu.ac.uk/>). The GWAS directory login number is ebi-a-GCST9000514. Specifically, GWAS data containing 2320781 SNPs were obtained from a previous GERD-related GWAS study conducted by Ong *et al*[18] and colleagues with a total sample size of 602604 Europeans containing 129080 cases and 473524 controls. The above GWAS data were used for the preliminary analysis of GERD. To validate our results by conducting replication analysis and meta-analysis, we repeated the MR analysis using the GERD data (54854 GERD patients and 401473 healthy controls) published by Wu *et al*[19]. This data is publicly available on the website: <https://cnsgenomics.com/content/data>.

Instruments selection

We performed a series of steps to select eligible genetic variants associated with metabolites. Given the small number of metabolite-related SNPs, we relaxed the significance threshold of $P < 1 \times 10^{-5}$ to select metabolite-related SNPs. We then clumped SNPs by removing linkage disequilibrium ($R^2 > 0.1$ and within 500kb). This criterion has been widely applied in previous studies[20-22]. To satisfy hypothesis (3), we removed the SNPs associated with the results in the IVs ($P < 1 \times 10^{-5}$). We eliminate bias caused by weak IVs by calculating the R^2 and F statistics for each SNP to measure statistical strength. SNPs with $F < 10$ were defined as weak genetic variants and were deleted. We further coordinated the SNPs of exposure and outcome, and removed the SNPs with palindromic effects and allele discordance (*e.g.* A/G *vs* A/C). Then, the final results were subjected to MR analysis.

Statistical analysis and sensitivity analysis

The causal relationship between blood metabolites and GERD was mainly assessed based on the results of random-effect inverse variance weighted (IVW). IVW is based on the hypothesis that there is no horizontal pleiotropy for all SNPs and the results from the pooled analysis of Walden ratios for all genetic variants, under the premise that IVW provides the most accurate assessment of causal effects[23]. Therefore, we used IVW-based estimates to initially screen for blood metabolites that have a causal effect on GERD. To obtain more reliable results, we used two additional methods to further evaluate metabolites with significant estimates (IVW derived $P < 0.05$). The MR-Egger and weighted median (WM) methods are used as complementary analyses. These two methods can provide more robust estimates under the relaxed. WM assumes that at least half of the tools are valid[24] and MR-Egger provides horizontal pleiotropy and heterogeneity detection in the presence of horizontal pleiotropy for all SNPs[25]. When consistent with the InSIDE hypothesis (IVs intensity independent of direct effects), MR-Egger regression can provide unbiased estimates[26].

For the initially determined significant estimates (IVW $P < 0.05$), sensitivity analysis will be performed to assess any deviation from the MR hypothesis. Horizontal pleiotropy was observed when IVs affected the results through other pathways than exposure. Horizontal pleiotropy was assessed based on the Egger intercept. Cochran Q test was used to test for the presence of heterogeneity. Heterogeneity was considered to exist when $P < 0.05$, $I^2 > 25\%$ [27]. For data with significant associations, Radial MR was used to identify heterogeneous values, and MR analysis was repeated after eliminating heterogeneous SNPs to obtain more accurate results[28]. Finally, we used MR-PRESSO to check again for the presence of heterogeneous SNPs[29]. We used leave-one-out (LOO) analysis to ensure the robustness of the results. By discarding each SNP in turn and then performing MR analysis to assess whether the results are heavily influenced by a single SNP.

In conclusion, we rigorously screened blood metabolites with potential causal relationship with GERD by multiple criteria: (1) Significant P -values for preliminary analysis (IVW derived $P < 0.05$); (2) The direction and amplitude of the three MR methods were consistent; (3) There was no heterogeneity or level pleiotropy in Mr results; and (4) MR estimates are not significantly confounded by individual SNPs.

Replication and metaanalysis

To fully assess the robustness of candidate metabolites identified based on the above criteria, we repeated the IVW

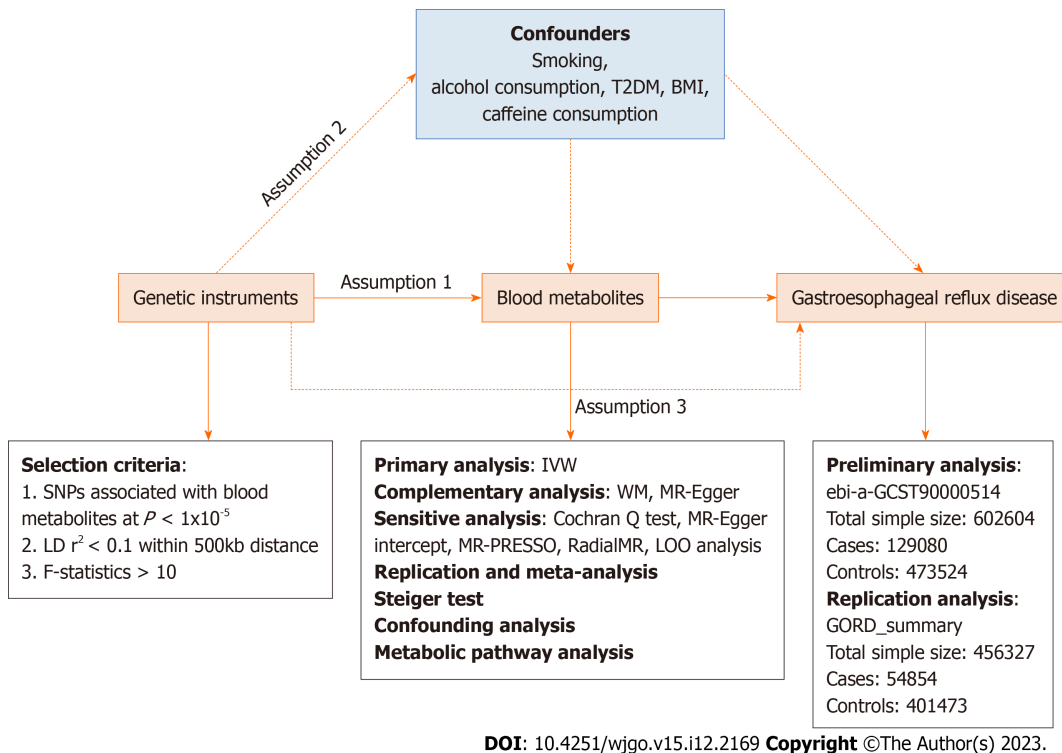


Figure 1 Overview of this Mendelian randomization analysis. Assumption 1, genetic instruments are strongly associated with the exposures of interest; Assumption 2, genetic instruments are independent of confounding factors; Assumption 3, genetic instruments are not associated with outcome and affect outcome only via exposures. IVW: Inverse variance weighted; LD: Linkage disequilibrium; LOO analysis: Leave-one-out analysis; MR-PRESSO: MR-Pleiotropy RESidual sum and outlier; SNPs: Single nucleotide polymorphisms; WM: Weighted median; BMI: Body mass index; T2DM: Type 2 diabetes mellitus.

analysis in another GERD cohort. In brief, the data from IEU with code ebi-a-GCST90000514 was used for the preliminary analysis and the data with the title GORD_summary was used for the replication analysis. Meta-analyses were based on a random-effects IVW model and performed on Review Manager 5.4 software.

Evaluation of genetic directionality

We verified whether the observed causality was biased by reversal of causality using the Steiger test[30]. Using the Steiger test, we determined whether the included SNPs explained the variability of GERD better than the detected metabolites. When the combination of SNPs was found to contribute more to the genetic risk of GERD than metabolites (Steiger $P > 0.05$), it indicated that the direction of causal inference may be biased.

Confounding analysis

Although we evaluated the horizontal pleiotropy of Mr results through a series of sensitivity analyses to detect any SNPs that violated the MR hypothesis, there may also be a small number of residual confounding SNPs. Therefore, we examined the IVs of metabolites on the PhenoScanner V2 website (<http://www.phenoscanner.medschl.cam.ac.uk/>) to assess whether each SNP was associated with known risk factors for GERD, such as smoking, alcohol consumption, type 2 diabetes, and body mass index (BMI). If any SNP was observed to be associated with the above confounding factors ($P < 1 \times 10^{-5}$), then MR analysis was repeated after removing these SNPs to verify the reliability of the results.

Metabolic pathway analysis

To clarify the biological mechanisms underlying the effects of blood metabolites on GERD, we further performed metabolic pathway analysis using MetaboAnalyst 5.0 (<https://www.metaboanalyst.ca/>)[29] to explore the potential pathogenesis of GERD.

RESULTS

Preliminary analysis

After strict control of the quality of IVs, SNPs of 25 metabolites were obtained. Filtered IVs contain 5 to 162 SNPs (X-11452 consists of 5 SNPs, while tryptophan sulfate consists of 162 SNPs). All metabolite-related SNPs had F-statistics greater than 10, which shows the strong power of the IVs. **Supplementary Table 2** displays the specific IV data. Prior to MR analysis, radial MR locates and eliminates all outliers (**Supplementary Table 3**). IVW analysis initially identified 25 metabolites with a potential causal relationship with GERD, including 17 metabolites with known chemical identity and 8

metabolites with unknown chemical identity. These 17 known metabolites include amino acids, cofactors, vitamins, lipids, nucleotides, and xenobiotic metabolism factors (Figure 2). Among the 17 known metabolic traits, butyrylcarnitine was significantly associated with GERD after Bonferroni correction. Twenty-one metabolites that passed the strict screening requirements were used for the follow-up analysis by sensitivity analysis (Figure 3). In short, the MR estimates derived from WM and MR-Egger regression presented consistent directions and amplitudes, supporting the robustness of causality (Table 1). *P* values and *I*² associated with Cochran Q indicated that no heterogeneity was found. In addition, the MR-Egger intercept term indicated a low risk of horizontal pleiotropy (Table 1). The LOO analysis did not find any high-impact SNPs biasing the pooled effect estimates (Supplementary Figure 1), and 21 metabolites that met the above criteria were included in the next study.

Replication and meta-analysis

The meta-analysis further identified 14 metabolites (8 known and 6 unknown) that could affect GERD (Figure 4). In detail, levulinate (4-oxovalerate) [odds ratio (OR) 0.80, 95% confidence interval (CI): 0.72-0.89, *P* < 0.0001], stearate (18:0) (OR 0.77, 95%CI: 0.64-0.92, *P* = 0.004), adrenate (22:4n6) (OR 0.83, 95%CI: 0.74-0.94, *P* = 0.004), p-acetamidophenyl-glucuronide (OR 0.99, 95%CI: 0.99-1.00, *P* = 0.0002), X-11247 (OR 0.92, 95%CI: 0.88-0.96, *P* = 0.0006), X-12786 (OR 0.90, 95%CI: 0.82-0.98, *P* = 0.01) decreased risk of GERD, while kynurenine (OR 1.20, 95%CI: 1.07-1.35, *P* = 0.002), 1-linoleoylglycerophosphoethanolamine (OR 1.17, 95%CI: 1.05-1.31, *P* = 0.004), butyrylcarnitine (OR 1.09, 95%CI: 1.05-1.13, *P* < 0.0001), guanosine (OR 1.10, 95%CI: 1.03-1.18, *P* = 0.003), X-09108 (OR 1.40, 95%CI: 1.13-1.74, *P* = 0.002), X-11452 (OR 1.14, 95%CI: 1.02-1.29, *P* = 0.03), X-12063 (OR 1.07, 95%CI: 1.03-1.11, *P* = 0.0008), and X-12456 (OR 1.12, 95%CI: 1.06-1.19, *P* = 0.0001) increased susceptibility to GERD.

Genetic basis for the causal association

We further investigated genetic variants affecting metabolite levels and GERD. The 39 SNPs of IVs for butyrylcarnitine are shown in Table 2. Among them, rs4767937 showed a strong correlation with butyrylcarnitine (β = 0.1052; SE = 0.0035, *P* = 1.00×10^{-200}). Notably, it had the strongest association with GERD (β = 0.0142; SE = 0.0048, *P* = 0.0032). The effect of this SNP on butyrylcarnitine and GERD suggests that the relevant genetic loci may provide valuable information for the biological mechanism of GERD, and butyrylcarnitine may be an important functional mediator of the biological processes affecting GERD.

Direction validation

We performed the Steiger test to verify the direction of the effect from metabolites to GERD. The Steiger *P* value indicates that the identified causality is not biased by reverse causality. The results are shown in Supplementary Table 4.

Confounding analysis

We used Phenoscanner to examine all SNPs associated with the metabolites that were positive on initial screening (IVW < 0.05) (including glycine, N-acetylglycine, and 1-palmitoylglycerol (1-monopalmitin)) to test the validity of Hypothesis 2 (IVs are independent of confounders). The data were disregarded since the exclusion of glycine and N-acetylglycine was meaningless because rs715 was related to BMI and rs1260326 in 1-palmitoylglycerol (1-monopalmitin) was connected with alcohol use. Supplementary Table 5 displays the findings for the remaining 25 metabolites. In total, 14 SNPs were found to be associated with common GERD risk variables; however, even after eliminating these SNPs, the estimates were still significant. Two well-known metabolites, adrenate (22:4n6) and 1-linoylglycerophosphoethanolamine*, were unaffected by any confounding factors.

Metabolic pathway analysis

Unfortunately, we only found 1 metabolic pathway that may be involved in the etiology of GERD (Supplementary Table 6), despite the existence of 8 recognized metabolites. One possible metabolic pathway in the pathophysiology of GERD is the glycerolipid metabolism pathway, which includes 1-linoleoylglycerophosphoethanolamine. Many of the metabolites that we discovered have also not yet been attributed to any of the metabolic pathways that are already listed in the kyoto encyclopedia of genes and genomes databases or The Small Molecule Pathway databases. Therefore, further research is needed to explore whether these metabolites are involved in the biological processes related to GERD occurrence.

DISCUSSION

In this study, we integrated two large-scale GWAS datasets to explore the causal effects of 486 blood metabolites on GERD through a rigorous MR design. Our study found 14 blood metabolites associated with GERD, among which butyrylcarnitine showed a significant positive correlation with GERD. This relationship is not affected by confounding factors such as smoking, alcohol consumption, BMI, and can be well replicated using samples from other data sources. In addition, we identified a metabolic pathway that may be involved in the biological mechanisms of GERD. This may be the first study to explore the causal relationship between serum metabolites and GERD by combining metabolomics and genomics. Given the unclear pathogenesis of GERD and the lack of blood metabolomics research related to GERD, this study is of great significance.

Table 1 Supplementary and sensitivity analyses for causality from blood metabolites on gastroesophageal reflux disease

Metabolites	n	MR analysis			Heterogeneity		Pleiotropy	
		Method	OR (95%CI)	P value	Q	P value	Intercept	P value
Amino acid								
Tryptophan	162	ME	0.72 (0.37-1.40)	0.34	160	0.58	0.002	0.07
		WM	1.42 (1.11-1.82)	0.006				
Kynurenine	33	ME	1.19 (0.78-1.81)	0.44	31	0.88	0.002	0.96
		WM	1.16 (0.90-1.48)	0.24				
Levulinate (4-oxovalerate)	52	ME	0.96 (0.73-1.27)	0.80	50	0.94	0.002	0.15
		WM	0.86 (0.67-1.09)	0.20				
Indoleacetate	16	ME	0.79 (0.60-1.05)	0.13	14	0.74	0.003	0.72
		WM	0.83 (0.67-1.04)	0.11				
Cofactors and Vitamin								
Ascorbate (Vitamin C)	12	ME	1.06 (0.89-1.25)	0.54	10	0.48	0.006	0.94
		WM	1.05 (0.98-1.13)	0.17				
Lipid								
Stearate (18:0)	31	ME	0.82 (0.51-1.32)	0.43	29	0.49	0.003	0.51
		WM	0.78 (0.60-1.01)	0.06				
1-linoleoylglycerophosphoethanolamine	13	ME	1.16 (0.80-1.68)	0.44	11	0.85	0.004	0.99
		WM	1.24 (1.03-1.50)	0.03				
1-stearoylglycerol (1-monostearin)	20	ME	1.42 (0.62-3.25)	0.42	18	0.49	0.006	0.90
		WM	1.16 (0.90-1.50)	0.25				
1-palmitoylglycerol (1-monopalmitin)	11	ME	0.88 (0.48-1.60)	0.68	9	0.89	0.005	0.27
		WM	1.09 (0.83-1.43)	0.54				
7-alpha-hydroxy-3-oxo-4-cholestenoate (7-Hoca)	11	ME	1.12 (0.52-2.41)	0.78	9	0.36	0.006	0.23
		WM	0.70 (0.48-1.01)	0.06				
Butyrylcarnitine	39	ME	1.06 (0.99-1.15)	0.11	37	0.30	0.002	0.26
		WM	1.07 (1.00-1.14)	0.04				
2-palmitoylglycerophosphocholine*	21	ME	0.91 (0.72-1.14)	0.41	19	0.76	0.002	0.50
		WM	0.97 (0.79-1.20)	0.80				
10-nonadecenoate (19:1n9)	7	ME	0.95 (0.60-1.50)	0.83	5	0.52	0.006	0.19
		WM	1.27 (1.00-1.61)	0.05				
1-stearoylglycerophosphocholine	9	ME	1.55 (0.85-2.83)	0.20	7	0.87	0.006	0.53
		WM	1.30 (1.01-1.67)	0.04				
Adrenate (22:4n6)	11	ME	0.75 (0.50-1.12)	0.19	9	0.20	0.005	0.66
		WM	0.74 (0.60-0.91)	0.004				
Nucleotide								
Guanosine	11	ME	1.31 (1.06-1.64)	0.04	9	0.99	0.005	0.16
		WM	1.16 (1.05-1.29)	0.005				
Xenobiotics								
p-acetamidophenylglucuronide	32	ME	1.00 (0.99-1.00)	0.41	30	0.25	0.004	0.60
		WM	1.00 (0.99-1.00)	0.75				
Unknow								

X-09108	9	ME	1.31 (0.72-2.37)	0.41	7	0.71	0.005	0.61
		WM	1.31 (0.89-1.93)	0.17				
X-11247	18	ME	0.92 (0.78-1.10)	0.37	16	0.68	0.004	0.82
		WM	0.91 (0.83-0.99)	0.03				
X-11452	5	ME	1.02 (0.67-1.56)	0.93	3	0.45	0.008	0.58
		WM	1.15 (0.97-1.36)	0.10				
X-11787	33	ME	0.84 (0.64-1.12)	0.25	31	0.94	0.002	0.84
		WM	0.89 (0.72-1.11)	0.31				
X-12007	18	ME	1.10 (1.03-1.17)	0.01	16	0.68	0.003	0.39
		WM	1.07 (1.01-1.13)	0.02				
X-12063	21	ME	1.06 (0.98-1.16)	0.16	19	0.30	0.002	0.60
		WM	1.10 (1.03-1.17)	0.004				
X-12456	21	ME	1.26 (1.07-1.49)	0.01	19	0.86	0.003	0.09
		WM	1.10 (0.99-1.22)	0.07				
X-12786	12	ME	0.95 (0.78-1.14)	0.58	10	0.87	0.003	0.48
		WM	0.91 (0.80-1.05)	0.20				

MR: Mendelian randomization; ME: MR-egger; WM: Weighted median; CI: Confidence interval; OR: Odd ratio.

The onset of GERD mainly consists of two mechanisms: the invasion of reflux and the destruction of the anti-reflux barrier at the esophageal junction. Usually, the anti reflux defense mechanism of the esophagus is in balance with the erosive effect of reflux substances on the esophageal mucosa. When the person's defense mechanism decreases or the damaging effect increases, the balance is disrupted, which may lead to the occurrence of GERD[31]. At present, the exploration of the pathogenesis of GERD is still at the macro level, and multiple studies suggest that abnormal esophageal sphincter function, esophageal hiatal hernia, and esophageal motility disorders play important roles[32-34]. However, the specific mechanism by which esophageal hiatal hernia participates in GERD is unclear, and a series of issues such as the causal relationship between esophageal peristaltic dysfunction and GERD and whether it is involved in the occurrence of esophagitis, remain poorly understood[35]. Therefore, more research is needed to help better elucidate the pathogenesis of GERD. Twenty-four-hour pH impedance monitoring, gastrointestinal endoscopy, and PPI testing are the gold standards for the clinical diagnosis and treatment of GERD, but the first two diagnostic methods are invasive and may cause a series of adverse reactions, such as headache and nausea. Therefore, there is an urgent need for accurate and effective biomarkers for the clinical diagnosis and early prevention of GERD. Metabolomics technology reveals the changes that have occurred in the body, serving as a bridge between genotype and phenotype, enabling researchers to understand diseases from a microscopic perspective. It is worth noting that blood metabolites reflect both endogenous and exogenous processes of disease occurrence[36]. For example, Matthew's study found differences in serum metabolites among GERD, BE, and high grade dysplasia/esophageal adenocarcinoma (EA) patients that could help distinguish patients at different stages of EA progression[37]. At present, there is still a significant lack of blood metabolomics research on GERD. Therefore, we conducted a key MR study to clarify the causal relationship between blood metabolites and GERD and the metabolic pathways involved, thus providing reference directions for further elucidating the pathogenesis of GERD and early screening and treatment.

A key clinical contribution of this study is the discovery of biomarkers. Our study supports a positive correlation between butyrylcarnitine and the risk of GERD from a causal perspective by combining genetics and metabolomics. Butyrylcarnitine belongs to the acyl carnitine group, which is composed of incomplete fatty acids β prooxidant compounds produced by oxidation. At present, there are no reports on the relationship between butyrylcarnitine and GERD, and we cannot accurately explain this relationship either. However, the carnitine shuttle pathway carries long-chain fatty acids from the cytoplasm to the mitochondria for later β oxidation, which necessitates acetyl-CoA and results in the esterification of L-carnitine to produce acyl carnitine derivatives[38]. The disturbance of the carnitine shuttle may lead to impaired mitochondrial function, which may reduce the ability of cells to process reactive oxygen species and increase the levels of inflammatory cytokines, leading to increased cell dysfunction and cell death[39]. This change may trigger GERD. On the other hand, weakened antioxidant capacity leads to a poor ability to prevent esophageal mucosal damage, which can also increase the severity of GERD[40,41]. Second, butyrylcarnitine is closely related to common GERD risk factors such as diabetes, obesity, anxiety and depression and other mental diseases. Studies have shown that butyrylcarnitine is involved in diet-induced insulin resistance, which in turn is related to the oxidation rate of fatty acids exceeding that of tricarboxylic acids and respiratory chains, leading to the accumulation of FAO intermediates such as acyl carnitine in mitochondria, and abnormal insulin signaling[42]. This indicates that butyryl carnitine plays an important role in the occurrence and development of diabetes. In addition, previous studies have found a positive

Table 2 Genetic predictors of butyrylcarnitine and their association with GERD

SNP	Gene	CHR	A1	A2	Butyrylcarnitine			GERD		
					Beta	SE	P value	Beta	SE	P value
rs10849832	OASL	12	C	T	0.0499	0.0067	1.06E-13	0.0106	0.0083	0.2040
rs10849846	P2RX7	12	C	T	0.0511	0.0097	1.34E-07	0.0079	0.0115	0.4916
rs11065202	CABP1	12	C	T	-0.1297	0.004	1.00E-200	-0.0087	0.0049	0.0751
rs11065208	MLEC	12	A	G	-0.0683	0.0106	1.17E-10	-0.0075	0.0134	0.5745
rs11065270	SPPL3	12	C	T	0.0603	0.0069	1.65E-18	0.0198	0.0091	0.0298
rs1109732	RP11-210L7.1	12	A	G	-0.0606	0.014	1.47E-05	-0.0004	0.0187	0.9848
rs1171617	SLC16A9	10	T	G	0.0358	0.0047	1.61E-14	0.0049	0.0057	0.3849
rs1186055	P2RX7	12	C	A	-0.0344	0.0043	1.30E-15	-0.0042	0.0054	0.4358
rs12025912	KIF17	1	C	T	0.0228	0.0053	1.76E-05	-0.0005	0.0069	0.9418
rs12255141	VTI1A	10	A	G	-0.0272	0.0062	1.15E-05	-0.0093	0.0081	0.2478
rs12257526	GRID1	10	C	T	0.0248	0.0058	1.74E-05	0.0105	0.0074	0.1580
rs12368199	OASL	12	A	G	0.1211	0.0052	1.67E-121	0.0062	0.0067	0.3564
rs12562686	RP11-410C4.4	1	A	C	-0.036	0.0084	1.74E-05	-0.0014	0.0103	0.8883
rs1336584	CTA-21C21.1	1	C	T	-0.018	0.0042	1.91E-05	-0.0079	0.0049	0.1064
rs1469231	NECAP1P1	7	A	G	-0.0188	0.0043	1.00E-05	-0.0098	0.0053	0.0653
rs1557852	RNA5SP192	5	G	A	-0.0181	0.0042	1.53E-05	-0.0067	0.0051	0.1904
rs17050084	AC007131.2	2	C	T	-0.0413	0.0096	1.90E-05	-0.0270	0.0123	0.0274
rs17507671	RNU4-1	12	C	T	-0.0512	0.0096	1.03E-07	0.0036	0.0108	0.7423
rs17686203	WAC	10	C	T	-0.0518	0.0118	1.06E-05	0.0118	0.0142	0.4093
rs1873745	C8orf37-AS1	8	A	G	-0.0195	0.0044	1.01E-05	-0.0098	0.0059	0.0972
rs1955919	LINC01765	1	A	G	-0.0467	0.0106	1.13E-05	-0.0253	0.0123	0.0389
rs1957910	PRKCH	14	A	G	0.0376	0.0088	1.96E-05	-0.0046	0.0093	0.6255
rs208294	-	-	-	-	0.0315	0.0036	1.08E-18	0.0058	0.0048	0.2293
rs2631693	FSIP1	15	C	G	-0.0233	0.0053	1.14E-05	-0.0085	0.0071	0.2302
rs273914	SLC22A4	5	T	A	0.0236	0.0041	1.17E-08	0.0016	0.0050	0.7519
rs278136	CIT	12	C	T	-0.0259	0.0043	1.96E-09	0.0040	0.0057	0.4776
rs3767512	CACNA1S	1	A	G	0.0625	0.0146	1.91E-05	0.0252	0.0177	0.1544
rs3817190	CAMKK2	12	A	T	0.0249	0.0047	1.14E-07	-0.0008	0.0049	0.8770
rs4146382	AC019050.1	2	C	T	-0.0186	0.0043	1.25E-05	-0.0001	0.0052	0.9912
rs4766962	COX6A1	12	A	T	0.0516	0.0043	1.70E-33	0.0078	0.0051	0.1238
rs4767937	SPPL3	12	C	G	0.1052	0.0035	1.00E-200	0.0142	0.0048	0.0032
rs4870883	FER1L6	8	A	T	-0.0262	0.006	1.41E-05	0.0057	0.0053	0.2824
rs4943508	LINC01048	13	C	T	0.0153	0.0035	1.38E-05	0.0098	0.0048	0.0431
rs646454	SGO1-AS1	3	T	C	0.0257	0.0059	1.17E-05	-0.0079	0.0074	0.2851
rs6468765	KB-1410C5.3	8	C	T	0.0156	0.0035	1.02E-05	-0.0078	0.0049	0.1082
rs6496996	RN7SL599P	15	A	G	0.0197	0.0045	1.05E-05	0.0035	0.0060	0.5583
rs7295193	TMEM117	12	C	T	-0.0288	0.0067	1.58E-05	0.0115	0.0088	0.1884
rs7303401	HNF1A-AS1	12	A	T	-0.0692	0.006	1.38E-30	-0.0106	0.0077	0.1678
rs7954772	SLC38A4	12	A	T	0.0182	0.0042	1.22E-05	-0.0009	0.0050	0.8617
rs7979473	HNF1A	12	G	A	0.0184	0.0042	1.20E-05	0.0078	0.0050	0.1184

GERD: Gastroesophageal reflux disease; SNP: Single nucleotide polymorphism; CHR: Chromosome.

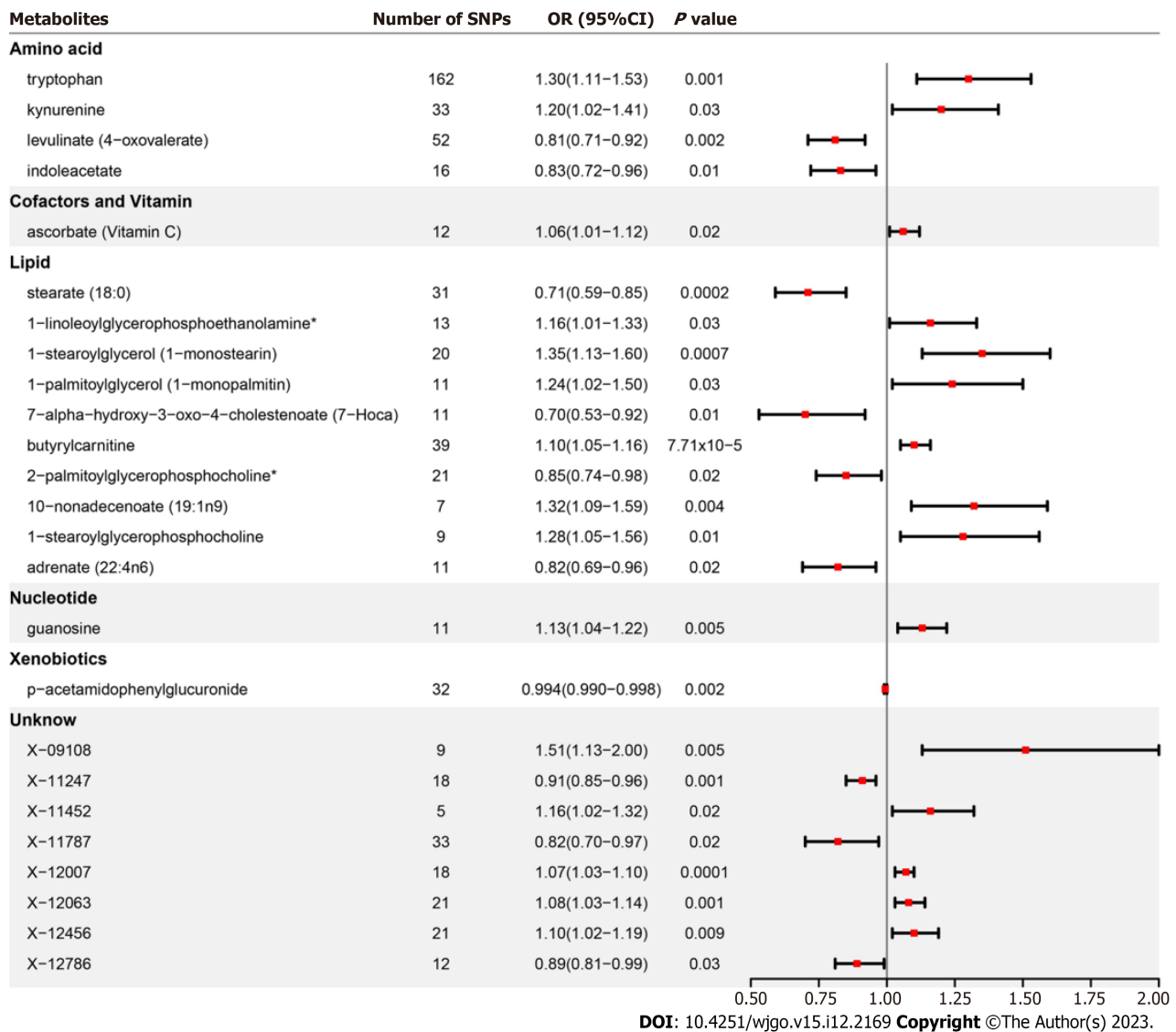
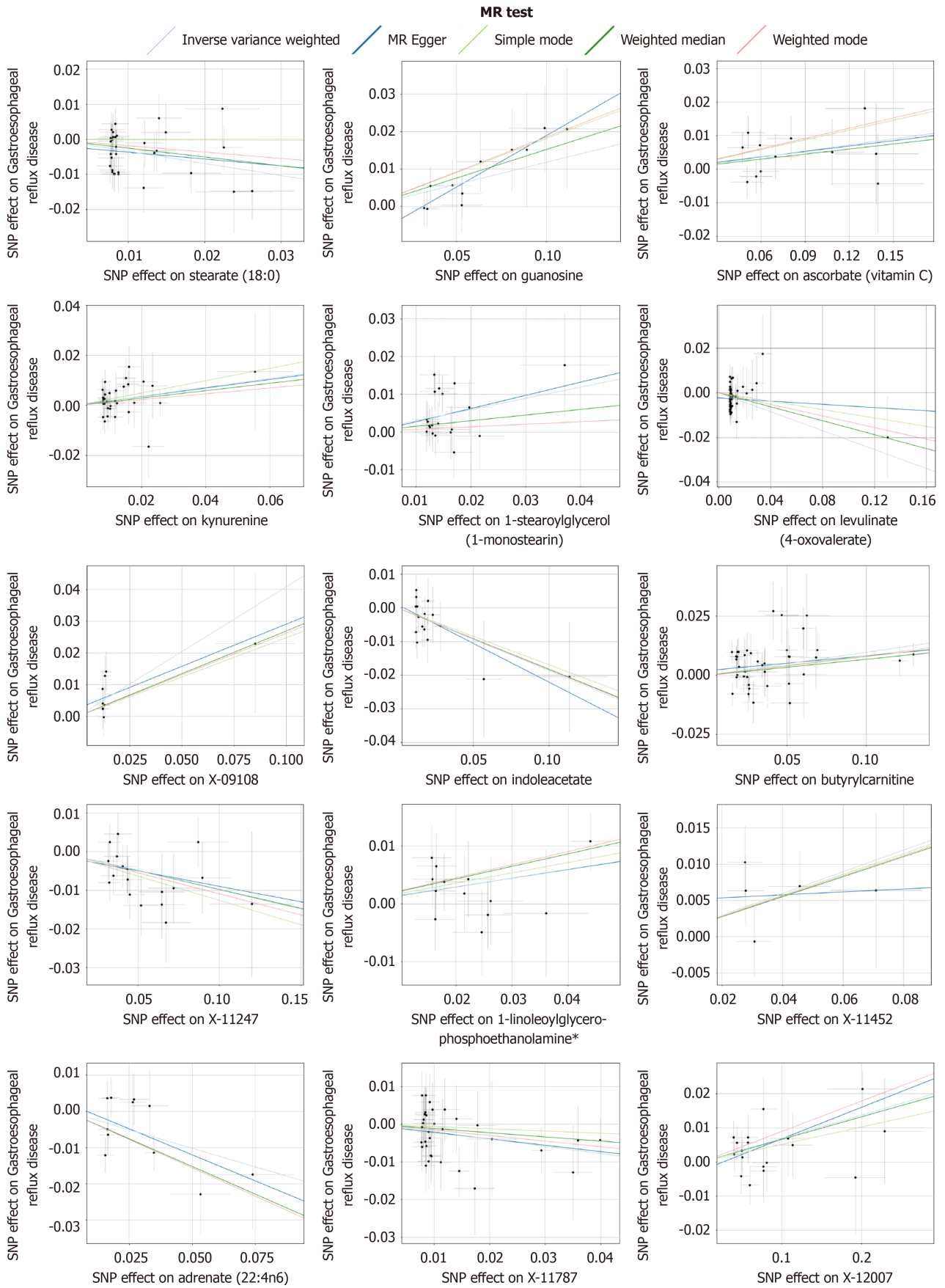
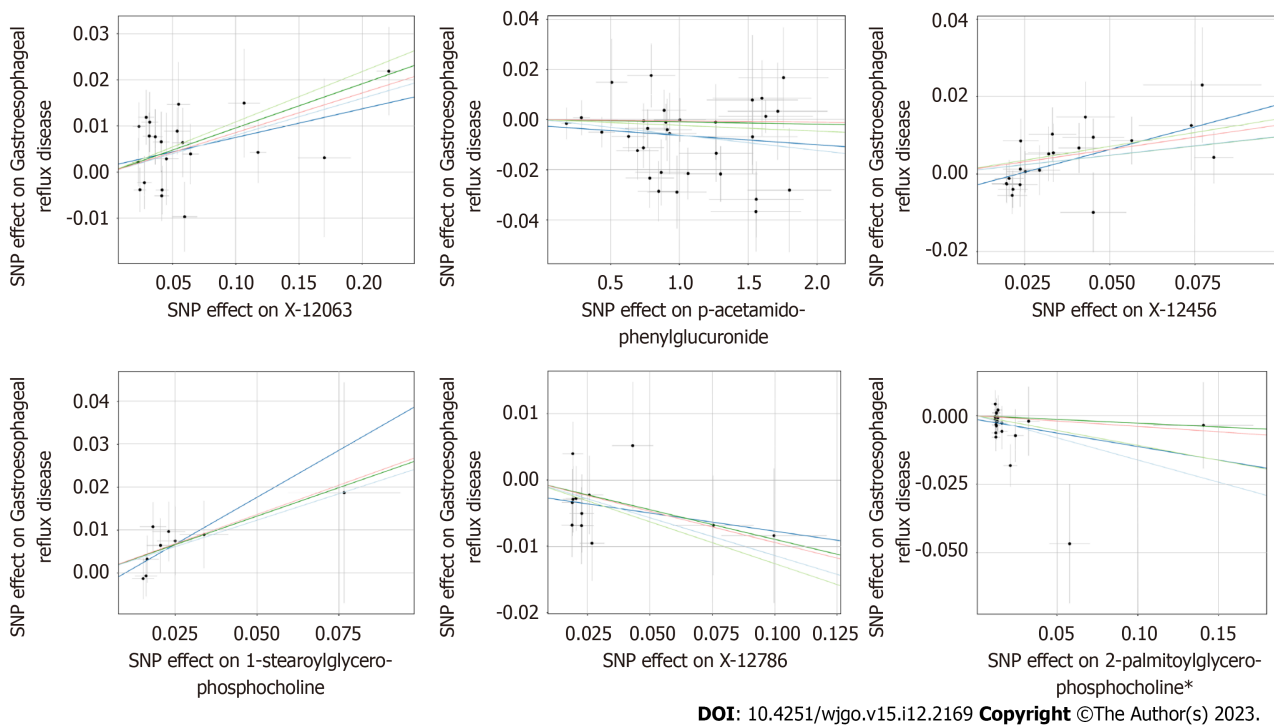


Figure 2 Forest plot for the causality of blood metabolites on gastroesophageal reflux disease derived from inverse variance weighted analysis. CI: Confidence interval; OR: Odd ratio.

correlation between butyrylcarnitine and obesity, showing similar results in both children and adults[43,44]. This result has been reported in individuals of Asian and European ancestry[45]. Obesity can lead to an increase in the number of brief relaxations of the lower esophageal sphincter, esophageal motility disorders, hiatal hernia, and elevated intra-abdominal pressure and is associated with complications such as BE and EA in GERD[46]. In addition, butyrylcarnitine has been found to be involved in the development of depression. Du et al[47] found that increasing neuronal differentiation is associated with symptoms of depression in later years, and the increase in neuronal differentiation is jointly regulated by an increase in butyrylcarnitine levels and a decrease in the levels of the glycerophospholipid PC35:1 (16:0/199:1). Zhao's study found cognitive improvement and decreased levels of butyrylcarnitine in schizophrenia patients treated with olanzapine[48]. These findings provide strong evidence for the involvement of butyrylcarnitine in the occurrence of mental illness. Therefore, we speculate that butyrylcarnitine may participate in the occurrence of GERD by increasing the risk factors for GERD. Finally, an increase in butyrylcarnitine is related to an increase in visceral fat content [49]. For example, research has found that compared to healthy controls, patients with steatosis and steatohepatitis have significantly higher levels of butyrylcarnitine[50]. Metabolically active visceral adipose tissue secretes adipokines and inflammatory cytokines, which may induce GERD and its complications. A recent MR study also confirmed a positive correlation between visceral adipose tissue accumulation and an increased risk of GERD[51]. In summary, butyrylcarnitine may participate in the occurrence of GERD through multiple pathways. Unfortunately, there is currently a lack of direct evidence linking butyrylcarnitine with GERD, including the pathogenesis of the latter. Our research for the first time discovered a relationship between genetics and metabolomics, which is also a key focus of our future research.





DOI: 10.4251/wjgo.v15.i12.2169 Copyright ©The Author(s) 2023.

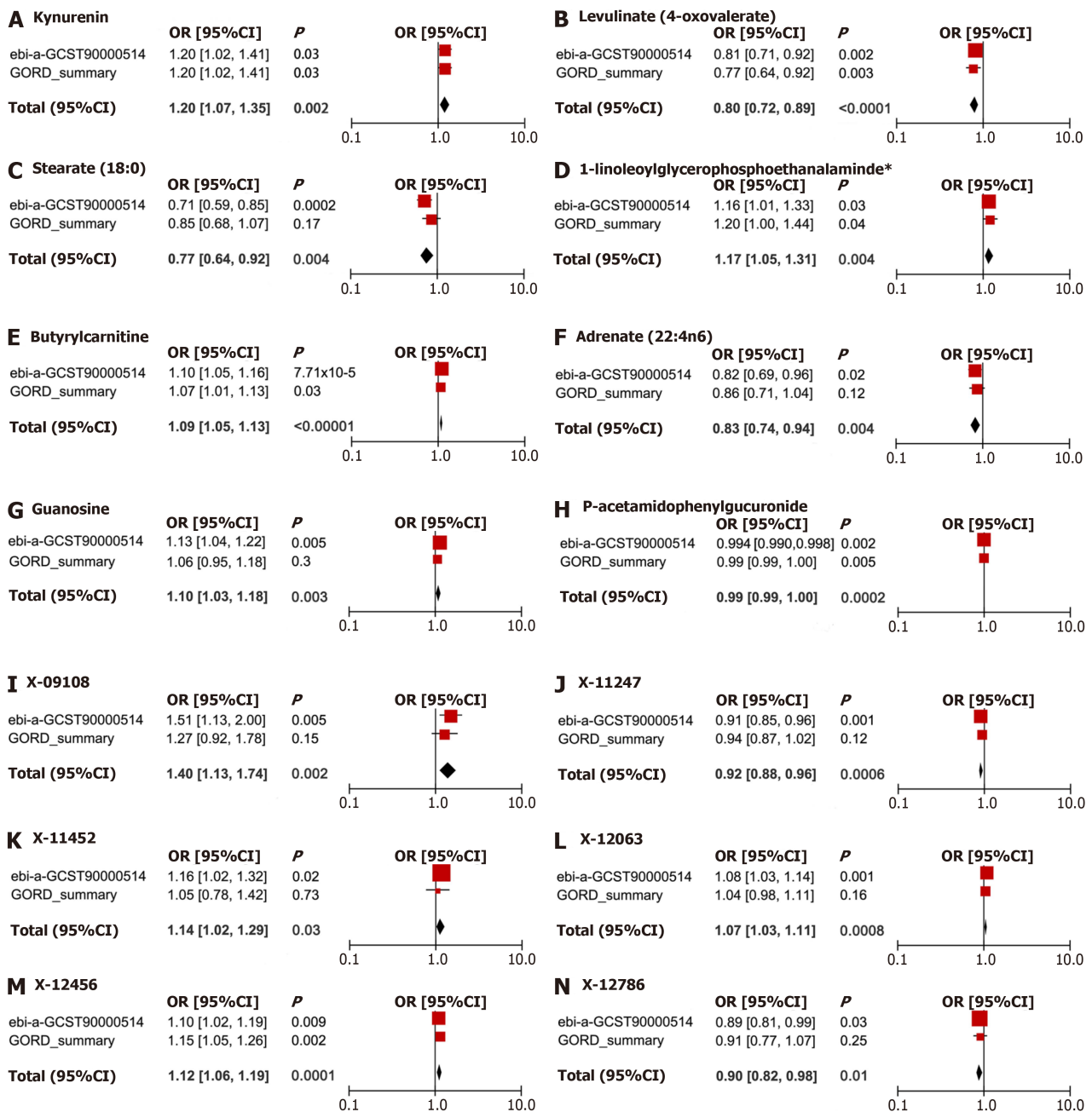
Figure 3 Scatterplot of significantly associated (inverse variance weighted derived $P < 0.05$) and directionally consistent estimates. SNP: Single nucleotide polymorphisms.

Metabolomics has a noninvasive advantage compared to gastroscopy and pathological tissue biopsy, as it can determine the material basis for the occurrence and development of GERD and further speculate on the metabolic pathways involved. This research method combining microdetection and macroanalysis has strong technical support and extensive practical significance.

Genetic factors played a central role in our study of the relationship between metabolites and GERD, and SNP rs4767937 (corresponding to the *spl3* gene) was most significantly associated with butyrylcarnitine and GERD. *SPPL3* is widely expressed in the human gastrointestinal tract, most notably in the esophagus[52]. Its main function is the intramembrane cleavage of aspartic proteases and it acts as an exonuclease by mediating the release and secretion of protein hydrolysis from the active site ectodomain of glycan-modified glycosidases and glycosyltransferases[53,54]. Unfortunately, there have been no reports on *SPPL3* and GERD or its risk factors and complications, and the specific pathological mechanisms of *SPPL3* in GERD remain to be explored.

The only metabolic pathway identified in our study was that of glycerolipid metabolism, which involves 1-linoleoylglycerophosphoethanolamine. 1-Linoleoylglycerophosphoethanolamine is an important component of phosphatidylethanolamine (PE), which is composed of fatty acids, ethanolamine, phosphoric acid and glycerol[55]. As a lipid chaperone, PE participates in the folding of some membrane proteins and is considered to be closely related to anxiety. Reichel's study found that alcohol dependent patients often have anxiety when abstaining from alcohol, and their plasma PE concentration is also higher after abstaining from alcohol[56]. In addition, Yang *et al*[21] explored the relationship between metabolites and some psychiatric disorders and found that 1-linoleoylglycerophosphoethanolamine was associated with the risk of major depression, which was further confirmed in a later study[57]. Therefore, it is probable that 1-linoleoylglycerophosphoethanolamine, similar to butyrylcarnitine, can influence depression to mediate the onset of GERD. In addition, an early study found that lansoprazole, one of the drugs of choice for GERD treatment, inhibited cytosolic PHOSPHO1 (a phosphatase that breaks down phosphocholine and phosphoethanolamine) in a noncompetitive manner[58]. This provides some reference for revealing the relationship between the two. Regarding glycerolipid metabolism, the signaling properties of glycerolipids have been elucidated in many fields from neuroscience and cancer to diabetes and obesity. The triglyceride metabolic pathway is the main route of action for several drugs. For example, LLKL, a new traditional Chinese medicine formulation, is able to exert hypoglycemic and gut microbiota-regulating effects by inhibiting triglyceride metabolism[59]. Unfortunately, however, no abnormalities in lipid metabolism have been reported in GERD. Given the lack of previous studies, the specific effects of GERD-related metabolites on GERD derived from this study need to be explored in detail under experimental conditions.

This MR analysis has several advantages. First, this is the most systematic and complete study to date on exploring the causal relationship between blood metabolites and GERD. Second, our results are convincing. The three MR estimates are highly consistent in direction and sensitivity analysis. The strict MR analysis allows us to avoid the rigorous MR analyses allow us to avoid the pitfalls of previous studies, such as reverse causality and confounding disturbances, and ensure the robustness of our results. Third, the reliability of the results was further verified by replication analysis and meta-analysis of additional GWAS data. Fourth, our study offers fresh insights into the molecular pathways underlying the pathogenesis of GERD by combining genomics and metabolomics.



DOI: 10.4251/wjgo.v15.i12.2169 Copyright ©The Author(s) 2023.

Figure 4 Meta-analysis of significantly associated (inverse variance weighted derived $P < 0.05$) between metabolites and gastro-esophageal reflux disease. CI: Confidence interval; OR: Odd ratio.

There are also some limitations to this study. First, given the small number of metabolite-related SNPs, our MR analysis set a slightly relaxed threshold. However, the F statistic of all SNPs associated with metabolites was greater than 10, indicating that IVS have a strong power. Furthermore, the Steiger test results' consistent causal direction support lends credence to our lenient threshold choice. Second, for the MR analysis, we solely used GWAS data from people with European ancestry in order to reduce the impact of ethnic differences. Therefore, it merits further investigation and validation to determine whether our findings hold true for other populations. Third, our study did not perform subgroup analysis on GERD. Because the existing dataset does not distinguish between GERD subtypes, which could be further subdivided when the data are more complete, there may be differences between subtypes. Moreover, although MR analysis provides valuable insights into the etiology, our findings should be rigorously confirmed by randomized controlled trials and basic research before clinical application.

CONCLUSION

In summary, this MR study revealed that eight known blood metabolites are causally associated with GERD, with

butyrylcarnitine showing a significant association signal after Bonferroni correction. Our study also highlights the extent to which genetic factors (such as SPPL3) contribute to changes in metabolic levels and the development of GERD. Glycerolipid metabolism has also been found to be possibly related to the biological processes behind GERD. Although further validation of experimental data is needed, the discovery of these serum metabolites provides valuable insights into the early screening, prevention and treatment of GERD and the design of future clinical studies. This combined genomic and metabolomic MR analysis also provides a reference direction for exploring the etiology and pathogenesis of GERD. Future research should also include genetic and metabolomic data related to GERD related diseases. For example, non erosive reflux disease, reflux esophagitis, BE, and hiatal hernia. At the same time, it is necessary to compare the genetic and metabolomic differences among various diseases, which will help clarify the relationship between diseases and better explain GERD.

ARTICLE HIGHLIGHTS

Research background

Gastroesophageal reflux disease (GERD) affects approximately 13% of the global population. However, the pathogenesis of GERD has not been fully elucidated. The development of metabolomics as a branch of systems biology in recent years has opened up new avenues for the investigation of disease processes. As a powerful statistical tool, Mendelian randomization (MR) is widely used to explore the causal relationship between exposure and outcome.

Research motivation

At present, there is still a significant lack of blood metabolomics research on GERD.

Research objectives

We used MR analysis to thoroughly investigate the causal relationships between 486 blood metabolites and GERD using data from a genome-wide association study (GWAS). Additionally, we identified the metabolic pathways that cause GERD. In addition to advancing our understanding of the pathophysiological mechanisms underlying GERD, the integration of metabolomics and genomics offers fresh perspectives on the early detection and management of the disease.

Research methods

Two-sample MR analysis was used to assess the causal relationship between blood metabolites and GERD. A GWAS of 486 metabolites was the exposure, and two different GWAS datasets of GERD were used as endpoints for the base analysis and replication and meta-analysis. Using the MR Steiger filtration method to detect whether there is a reverse causal relationship between metabolites and GERD. In addition, metabolic pathway analysis was conducted using the online database based MetaboAnalyst 5.0 software.

Research results

The results of this study indicated significant associations between eight metabolites, levulinate (4-oxovalerate) [odds ratio (OR) 0.80, 95% confidence interval (CI): 0.72-0.89, $P < 0.0001$], stearate (18:0) (OR 0.77, 95% CI: 0.64-0.92, $P = 0.004$), adrenate (22:4n6) (OR 0.83, 95% CI: 0.74-0.94, $P = 0.004$), p-acetamidophenylglucuronide (OR 0.99, 95% CI: 0.99-1.00, $P = 0.0002$), kynurenine (OR 1.20, 95% CI: 1.07-1.35, $P = 0.002$), 1-linoleoylglycerophosphoethanolamine (OR 1.17, 95% CI: 1.05-1.31, $P = 0.004$), butyrylcarnitine (OR 1.09, 95% CI: 1.05-1.13, $P < 0.0001$), and guanosine (OR 1.10, 95% CI: 1.03-1.18, $P = 0.003$), and GERD. Bonferroni correction showed that butyrylcarnitine (OR 1.10, 95% CI: 1.05-1.16, $P = 7.71 \times 10^{-5}$) was the most reliable causal metabolite. Glycerophospholipid metabolism may be involved in the pathogenesis of GERD.

Research conclusions

Through the integration of genomics and metabolomics, we found that butyrylcarnitine may be a potential biomarker for GERD.

Research perspectives

The relationship between GERD and butyrylcarnitine needs further confirmation from basic and clinical real-world studies. Future research should also include genetic and metabolomic data related to GERD related diseases. For example, non erosive reflux disease, reflux esophagitis, BE, and hiatal hernia. At the same time, it is necessary to compare the genetic and metabolomic differences among various diseases, which will help clarify the relationship between diseases and better explain GERD.

ACKNOWLEDGEMENTS

We first appreciate the original GWAS data provided by So-Youn Shin *et al* and Jue-Sheng Ong *et al* and Yeda Wu *et al* and the GWAS Catalog database.

FOOTNOTES

Author contributions: Hu JY and Lv M designed the research; Hu JY, Zhang KL, Qiao XY collected and analyzed the data; Hu JY, Lv M and Zhang KL drafted the manuscript; Qiao XY, Wang YX and Wang FY revised the manuscript; Wang FY for the entire text; all authors contributed to the article and approved the submitted version.

Supported by National Natural Science Foundation of China, No. 82174363.

Institutional review board statement: Only publicly available genome-wide association study (GWAS) data were used in this study, and the Ethics approval and consent to participate could be available in the original GWAS study.

Conflict-of-interest statement: The authors report no conflicts of interest.

Data sharing statement: All data generated or during this study are included in this published article and the supplementary materials. genome-wide association study (GWAS) summary statistics for human blood metabolites were publicly available at <https://metabolomics.helmholtz-muenchen.de/gwas/>. GWAS summary statistics for gastroesophageal reflux disease can be found here: <https://cnsgenomics.com/content/data> and <https://gwas.mrcieu.ac.uk/>.

Open-Access: This article is an open-access article that was selected by an in-house editor and fully peer-reviewed by external reviewers. It is distributed in accordance with the Creative Commons Attribution NonCommercial (CC BY-NC 4.0) license, which permits others to distribute, remix, adapt, build upon this work non-commercially, and license their derivative works on different terms, provided the original work is properly cited and the use is non-commercial. See: <https://creativecommons.org/licenses/by-nc/4.0/>

Country/Territory of origin: China

ORCID number: Jia-Yan Hu 0000-0001-6525-6371; Mi Lv 0000-0002-1715-8643; Feng-Yun Wang 0000-0002-4058-7905.

S-Editor: Qu XL

L-Editor: A

P-Editor: Xu ZH

REFERENCES

- Richter JE, Rubenstein JH. Presentation and Epidemiology of Gastroesophageal Reflux Disease. *Gastroenterology* 2018; **154**: 267-276 [PMID: 28780072 DOI: 10.1053/j.gastro.2017.07.045]
- Mehta RS, Staller K, Chan AT. Review of Gastroesophageal Reflux Disease. *JAMA* 2021; **325**: 1472 [PMID: 33847719 DOI: 10.1001/jama.2021.1438]
- Mehta RS, Nguyen LH, Ma W, Staller K, Song M, Chan AT. Association of Diet and Lifestyle With the Risk of Gastroesophageal Reflux Disease Symptoms in US Women. *JAMA Intern Med* 2021; **181**: 552-554 [PMID: 33393976 DOI: 10.1001/jamainternmed.2020.7238]
- Ness-Jensen E, Hveem K, El-Serag H, Lagergren J. Lifestyle Intervention in Gastroesophageal Reflux Disease. *Clin Gastroenterol Hepatol* 2016; **14**: 175-82.e1 [PMID: 25956834 DOI: 10.1016/j.cgh.2015.04.176]
- Yuan S, Larsson SC. Adiposity, diabetes, lifestyle factors and risk of gastroesophageal reflux disease: a Mendelian randomization study. *Eur J Epidemiol* 2022; **37**: 747-754 [PMID: 35119566 DOI: 10.1007/s10654-022-00842-z]
- Johnson CH, Ivanisevic J, Siuzdak G. Metabolomics: beyond biomarkers and towards mechanisms. *Nat Rev Mol Cell Biol* 2016; **17**: 451-459 [PMID: 26979502 DOI: 10.1038/nrm.2016.25]
- Gowda GA, Zhang S, Gu H, Asiago V, Shanaiah N, Raftery D. Metabolomics-based methods for early disease diagnostics. *Expert Rev Mol Diagn* 2008; **8**: 617-633 [PMID: 18785810 DOI: 10.1586/14737159.8.5.617]
- Griffin JL, Shookcor JP. Metabolic profiles of cancer cells. *Nat Rev Cancer* 2004; **4**: 551-561 [PMID: 15229480 DOI: 10.1038/nrc1390]
- O'Keefe SJ. Diet, microorganisms and their metabolites, and colon cancer. *Nat Rev Gastroenterol Hepatol* 2016; **13**: 691-706 [PMID: 27848961 DOI: 10.1038/nrgastro.2016.165]
- Bajaj JS, Reddy KR, O'Leary JG, Vargas HE, Lai JC, Kamath PS, Tandon P, Wong F, Subramanian RM, Thuluvath P, Fagan A, White MB, Gavis EA, Sehrawat T, de la Rosa Rodriguez R, Thacker LR, Sikaroodi M, Garcia-Tsao G, Gillevet PM. Serum Levels of Metabolites Produced by Intestinal Microbes and Lipid Moieties Independently Associated With Acute-on-Chronic Liver Failure and Death in Patients With Cirrhosis. *Gastroenterology* 2020; **159**: 1715-1730.e12 [PMID: 32687928 DOI: 10.1053/j.gastro.2020.07.019]
- Di'Narzo AF, Houten SM, Kosoy R, Huang R, Vaz FM, Hou R, Wei G, Wang W, Comella PH, Dodatko T, Rogatsky E, Stojmirovic A, Brodmerkel C, Perrigoue J, Hart A, Curran M, Friedman JR, Zhu J, Agrawal M, Cho J, Ungaro R, Dubinsky MC, Sands BE, Suárez-Fariñas M, Schadt EE, Colombel JF, Kasarskis A, Hao K, Argmann C. Integrative Analysis of the Inflammatory Bowel Disease Serum Metabolome Improves Our Understanding of Genetic Etiology and Points to Novel Putative Therapeutic Targets. *Gastroenterology* 2022; **162**: 828-843.e11 [PMID: 34780722 DOI: 10.1053/j.gastro.2021.11.015]
- Li Liu, Sheng Xie, Li-jian Liu. Plasma metabolomics study and clinical observation in patients with gastroesophageal reflux disease. *Journal of Guangxi University (Natural Science Edition)* 2022; **47**: 254-261 [DOI: 10.1016/j.jval.2022.04.444]
- Zuccolo L, Holmes MV. Commentary: Mendelian randomization-inspired causal inference in the absence of genetic data. *Int J Epidemiol* 2017; **46**: 962-965 [PMID: 28025256 DOI: 10.1093/ije/dyw327]
- Richmond RC, Davey Smith G. Mendelian Randomization: Concepts and Scope. *Cold Spring Harb Perspect Med* 2022; **12** [PMID: 34426474 DOI: 10.1101/cshperspect.a040501]
- Burgess S, Butterworth A, Thompson SG. Mendelian randomization analysis with multiple genetic variants using summarized data. *Genet*

- Epidemiol* 2013; **37**: 658-665 [PMID: [24114802](#) DOI: [10.1002/gepi.21758](#)]
- 16 **Boef AG**, Dekkers OM, le Cessie S. Mendelian randomization studies: a review of the approaches used and the quality of reporting. *Int J Epidemiol* 2015; **44**: 496-511 [PMID: [25953784](#) DOI: [10.1093/ije/dyv071](#)]
- 17 **Shin SY**, Fauman EB, Petersen AK, Krumstiek J, Santos R, Huang J, Arnold M, Erte I, Forgetta V, Yang TP, Walter K, Menni C, Chen L, Vasquez L, Valdes AM, Hyde CL, Wang V, Ziemek D, Roberts P, Xi L, Grundberg E; Multiple Tissue Human Expression Resource (MuTHER) Consortium, Waldenberger M, Richards JB, Mohnhey RP, Milburn MV, John SL, Trimmer J, Theis FJ, Overington JP, Suhre K, Brosnan MJ, Gieger C, Kastenmüller G, Spector TD, Soranzo N. An atlas of genetic influences on human blood metabolites. *Nat Genet* 2014; **46**: 543-550 [PMID: [24816252](#) DOI: [10.1038/ng.2982](#)]
- 18 **Ong JS**, An J, Han X, Law MH, Nandakumar P; 23andMe Research team; Esophageal cancer consortium, Schumacher J, Gockel I, Bohmer A, Jankowski J, Palles C, Olsen CM, Neale RE, Fitzgerald R, Thrift AP, Vaughan TL, Buas MF, Hinds DA, Gharahkhani P, Kendall BJ, MacGregor S. Multitrait genetic association analysis identifies 50 new risk loci for gastro-oesophageal reflux, seven new loci for Barrett's oesophagus and provides insights into clinical heterogeneity in reflux diagnosis. *Gut* 2022; **71**: 1053-1061 [PMID: [34187846](#) DOI: [10.1136/gutjnl-2020-323906](#)]
- 19 **Wu Y**, Murray GK, Byrne EM, Sidorenko J, Visscher PM, Wray NR. GWAS of peptic ulcer disease implicates *Helicobacter pylori* infection, other gastrointestinal disorders and depression. *Nat Commun* 2021; **12**: 1146 [PMID: [33608531](#) DOI: [10.1038/s41467-021-21280-7](#)]
- 20 **Choi KW**, Chen CY, Stein MB, Klimentidis YC, Wang MJ, Koenen KC, Smoller JW; Major Depressive Disorder Working Group of the Psychiatric Genomics Consortium. Assessment of Bidirectional Relationships Between Physical Activity and Depression Among Adults: A 2-Sample Mendelian Randomization Study. *JAMA Psychiatry* 2019; **76**: 399-408 [PMID: [30673066](#) DOI: [10.1001/jamapsychiatry.2018.4175](#)]
- 21 **Yang J**, Yan B, Zhao B, Fan Y, He X, Yang L, Ma Q, Zheng J, Wang W, Bai L, Zhu F, Ma X. Assessing the Causal Effects of Human Serum Metabolites on 5 Major Psychiatric Disorders. *Schizophr Bull* 2020; **46**: 804-813 [PMID: [31919502](#) DOI: [10.1093/schbul/sbz138](#)]
- 22 **Cai J**, Li X, Wu S, Tian Y, Zhang Y, Wei Z, Jin Z, Chen X, Chen WX. Assessing the causal association between human blood metabolites and the risk of epilepsy. *J Transl Med* 2022; **20**: 437 [PMID: [36180952](#) DOI: [10.1186/s12967-022-03648-5](#)]
- 23 **Pierce BL**, Burgess S. Efficient design for Mendelian randomization studies: subsample and 2-sample instrumental variable estimators. *Am J Epidemiol* 2013; **178**: 1177-1184 [PMID: [23863760](#) DOI: [10.1093/aje/kwt084](#)]
- 24 **Bowden J**, Davey Smith G, Haycock PC, Burgess S. Consistent Estimation in Mendelian Randomization with Some Invalid Instruments Using a Weighted Median Estimator. *Genet Epidemiol* 2016; **40**: 304-314 [PMID: [27061298](#) DOI: [10.1002/gepi.21965](#)]
- 25 **Bowden J**, Davey Smith G, Burgess S. Mendelian randomization with invalid instruments: effect estimation and bias detection through Egger regression. *Int J Epidemiol* 2015; **44**: 512-525 [PMID: [26050253](#) DOI: [10.1093/ije/dyv080](#)]
- 26 **Burgess S**, Thompson SG. Interpreting findings from Mendelian randomization using the MR-Egger method. *Eur J Epidemiol* 2017; **32**: 377-389 [PMID: [28527048](#) DOI: [10.1007/s10654-017-0255-x](#)]
- 27 **Greco M FD**, Minelli C, Sheehan NA, Thompson JR. Detecting pleiotropy in Mendelian randomisation studies with summary data and a continuous outcome. *Stat Med* 2015; **34**: 2926-2940 [PMID: [25950993](#) DOI: [10.1002/sim.6522](#)]
- 28 **Bowden J**, Spiller W, Del Greco M F, Sheehan N, Thompson J, Minelli C, Davey Smith G. Improving the visualization, interpretation and analysis of two-sample summary data Mendelian randomization via the Radial plot and Radial regression. *Int J Epidemiol* 2018; **47**: 1264-1278 [PMID: [29961852](#) DOI: [10.1093/ije/dyy101](#)]
- 29 **Verbanck M**, Chen CY, Neale B, Do R. Detection of widespread horizontal pleiotropy in causal relationships inferred from Mendelian randomization between complex traits and diseases. *Nat Genet* 2018; **50**: 693-698 [PMID: [29686387](#) DOI: [10.1038/s41588-018-0099-7](#)]
- 30 **Hemani G**, Tilling K, Davey Smith G. Orienting the causal relationship between imprecisely measured traits using GWAS summary data. *PLoS Genet* 2017; **13**: e1007081 [PMID: [29149188](#) DOI: [10.1371/journal.pgen.1007081](#)]
- 31 **Savarino V**, Marabotto E, Zentilin P, Furnari M, Bodini G, De Maria C, Tolone S, De Bortoli N, Frazzoni M, Savarino E. Pathophysiology, diagnosis, and pharmacological treatment of gastro-oesophageal reflux disease. *Expert Rev Clin Pharmacol* 2020; **13**: 437-449 [PMID: [32253948](#) DOI: [10.1080/17512433.2020.1752664](#)]
- 32 **Schlottmann F**, Andolfi C, Herbelli FA, Rebecchi F, Allaix ME, Patti MG. GERD: Presence and Size of Hiatal Hernia Influence Clinical Presentation, Esophageal Function, Reflux Profile, and Degree of Mucosal Injury. *Am Surg* 2018; **84**: 978-982 [PMID: [29981634](#)]
- 33 **Lin S**, Li H, Fang X. Esophageal Motor Dysfunctions in Gastroesophageal Reflux Disease and Therapeutic Perspectives. *J Neurogastroenterol Motil* 2019; **25**: 499-507 [PMID: [31587540](#) DOI: [10.5056/jnm19081](#)]
- 34 **Savarino E**, Bredenoord AJ, Fox M, Pandolfino JE, Roman S, Gyawali CP; International Working Group for Disorders of Gastrointestinal Motility and Function. Expert consensus document: Advances in the physiological assessment and diagnosis of GERD. *Nat Rev Gastroenterol Hepatol* 2017; **14**: 665-676 [PMID: [28951582](#) DOI: [10.1038/nrgastro.2017.130](#)]
- 35 **Zheng Z**, Shang Y, Wang N, Liu X, Xin C, Yan X, Zhai Y, Yin J, Zhang J, Zhang Z. Current Advancement on the Dynamic Mechanism of Gastroesophageal Reflux Disease. *Int J Biol Sci* 2021; **17**: 4154-4164 [PMID: [34803489](#) DOI: [10.7150/ijbs.65066](#)]
- 36 **Rappaport SM**, Barupal DK, Wishart D, Vineis P, Scalbert A. The blood exposome and its role in discovering causes of disease. *Environ Health Perspect* 2014; **122**: 769-774 [PMID: [24659601](#) DOI: [10.1289/ehp.1308015](#)]
- 37 **Buas MF**, Gu H, Djukovic D, Zhu J, Onstad L, Reid BJ, Raftery D, Vaughan TL. Candidate serum metabolite biomarkers for differentiating gastroesophageal reflux disease, Barrett's esophagus, and high-grade dysplasia/esophageal adenocarcinoma. *Metabolomics* 2017; **13** [PMID: [28190989](#) DOI: [10.1007/s11306-016-1154-y](#)]
- 38 **Sharma S**, Black SM. CARNITINE HOMEOSTASIS, MITOCHONDRIAL FUNCTION, AND CARDIOVASCULAR DISEASE. *Drug Discov Today Dis Mech* 2009; **6**: e31-e39 [PMID: [20648231](#) DOI: [10.1016/j.ddmcc.2009.02.001](#)]
- 39 **Mitchell SL**, Uppal K, Williamson SM, Liu K, Burgess LG, Tran V, Umfress AC, Jarrell KL, Cooke Bailey JN, Agarwal A, Pericak-Vance M, Haines JL, Scott WK, Jones DP, Brantley MA Jr. The Carnitine Shuttle Pathway is Altered in Patients With Neovascular Age-Related Macular Degeneration. *Invest Ophthalmol Vis Sci* 2018; **59**: 4978-4985 [PMID: [30326066](#) DOI: [10.1167/iovs.18-25137](#)]
- 40 **Cheng HH**, Chang CS, Wang HJ, Wang WC. Interleukin-1beta and -10 polymorphisms influence erosive reflux esophagitis and gastritis in Taiwanese patients. *J Gastroenterol Hepatol* 2010; **25**: 1443-1451 [PMID: [20659236](#) DOI: [10.1111/j.1440-1746.2010.06310.x](#)]
- 41 **Rieder F**, Biancani P, Harnett K, Yerian L, Falk GW. Inflammatory mediators in gastroesophageal reflux disease: impact on esophageal motility, fibrosis, and carcinogenesis. *Am J Physiol Gastrointest Liver Physiol* 2010; **298**: G571-G581 [PMID: [20299604](#) DOI: [10.1152/ajpgi.00454.2009](#)]
- 42 **Schooneman MG**, Vaz FM, Houten SM, Soeters MR. Acylcarnitines: reflecting or inflicting insulin resistance? *Diabetes* 2013; **62**: 1-8 [PMID: [23258903](#) DOI: [10.2337/db12-0466](#)]

- 43 **Butte NF**, Liu Y, Zakeri IF, Mohney RP, Mehta N, Voruganti VS, Göring H, Cole SA, Comuzzie AG. Global metabolomic profiling targeting childhood obesity in the Hispanic population. *Am J Clin Nutr* 2015; **102**: 256-267 [PMID: 26085512 DOI: 10.3945/ajcn.115.111872]
- 44 **Park S**, Sadanala KC, Kim EK. A Metabolomic Approach to Understanding the Metabolic Link between Obesity and Diabetes. *Mol Cells* 2015; **38**: 587-596 [PMID: 26072981 DOI: 10.14348/molcells.2015.0126]
- 45 **Moore SC**, Matthews CE, Sampson JN, Stolzenberg-Solomon RZ, Zheng W, Cai Q, Tan YT, Chow WH, Ji BT, Liu DK, Xiao Q, Boca SM, Leitzmann MF, Yang G, Xiang YB, Sinha R, Shu XO, Cross AJ. Human metabolic correlates of body mass index. *Metabolomics* 2014; **10**: 259-269 [PMID: 25254000 DOI: 10.1007/s11306-013-0574-1]
- 46 **Chang P**, Friedenberg F. Obesity and GERD. *Gastroenterol Clin North Am* 2014; **43**: 161-173 [PMID: 24503366 DOI: 10.1016/j.gtc.2013.11.009]
- 47 **Du Preez A**, Lefèvre-Arbogast S, González-Domínguez R, Houghton V, de Lucia C, Low DY, Helmer C, Féart C, Delcourt C, Proust-Lima C, Pallàs M, Sánchez-Pla A, Urpi-Sardà M, Ruigrok SR, Altendorfer B, Aigner L, Lucassen PJ, Korosi A, Manach C, Andres-Lacueva C, Samieri C, Thuret S. Impaired hippocampal neurogenesis in vitro is modulated by dietary-related endogenous factors and associated with depression in a longitudinal ageing cohort study. *Mol Psychiatry* 2022; **27**: 3425-3440 [PMID: 35794184 DOI: 10.1038/s41380-022-01644-1]
- 48 **Zhao L**, Liu H, Wang W, Wang Y, Xiu M, Li S. Carnitine metabolites and cognitive improvement in patients with schizophrenia treated with olanzapine: a prospective longitudinal study. *Front Pharmacol* 2023; **14**: 1255501 [PMID: 37663259 DOI: 10.3389/fphar.2023.1255501]
- 49 **Pallister T**, Jackson MA, Martin TC, Glastonbury CA, Jennings A, Beaumont M, Mohney RP, Small KS, MacGregor A, Steves CJ, Cassidy A, Spector TD, Menni C, Valdes AM. Untangling the relationship between diet and visceral fat mass through blood metabolomics and gut microbiome profiling. *Int J Obes (Lond)* 2017; **41**: 1106-1113 [PMID: 28293020 DOI: 10.1038/ijo.2017.70]
- 50 **Kalhan SC**, Guo L, Edmison J, Dasarathy S, McCullough AJ, Hanson RW, Milburn M. Plasma metabolomic profile in nonalcoholic fatty liver disease. *Metabolism* 2011; **60**: 404-413 [PMID: 20423748 DOI: 10.1016/j.metabol.2010.03.006]
- 51 **Zhao X**, Ding R, Su C, Yue R. Sleep traits, fat accumulation, and glycemic traits in relation to gastroesophageal reflux disease: A Mendelian randomization study. *Front Nutr* 2023; **10**: 1106769 [PMID: 36895273 DOI: 10.3389/fnut.2023.1106769]
- 52 **Fagerberg L**, Hallström BM, Oksvold P, Kampf C, Djureinovic D, Odeberg J, Habuka M, Tahmasebpoor S, Danielsson A, Edlund K, Asplund A, Sjöstedt E, Lundberg E, Szgyarto CA, Skogs M, Takanan JO, Berling H, Tegel H, Mulder J, Nilsson P, Schwenk JM, Lindskog C, Danielsson F, Mardinoglu A, Sivertsson A, von Feilitzen K, Forsberg M, Zwahlen M, Olsson I, Navani S, Huss M, Nielsen J, Ponten F, Uhlén M. Analysis of the human tissue-specific expression by genome-wide integration of transcriptomics and antibody-based proteomics. *Mol Cell Proteomics* 2014; **13**: 397-406 [PMID: 24309898 DOI: 10.1074/mcp.M113.035600]
- 53 **Voss M**, Künzel U, Higel F, Kuhn PH, Colombo A, Fukumori A, Haug-Kröper M, Klier B, Grammer G, Seidl A, Schröder B, Obst R, Steiner H, Lichtenthaler SF, Haass C, Fluhrer R. Shedding of glycan-modifying enzymes by signal peptide peptidase-like 3 (SPPL3) regulates cellular N-glycosylation. *EMBO J* 2014; **33**: 2890-2905 [PMID: 25354954 DOI: 10.15252/embj.201488375]
- 54 **Kuhn PH**, Voss M, Haug-Kröper M, Schröder B, Schepers U, Bräse S, Haass C, Lichtenthaler SF, Fluhrer R. Secretome analysis identifies novel signal Peptide peptidase-like 3 (Sppl3) substrates and reveals a role of Sppl3 in multiple Golgi glycosylation pathways. *Mol Cell Proteomics* 2015; **14**: 1584-1598 [PMID: 25827571 DOI: 10.1074/mcp.M115.048298]
- 55 **Calzada E**, Onguka O, Claypool SM. Phosphatidylethanolamine Metabolism in Health and Disease. *Int Rev Cell Mol Biol* 2016; **321**: 29-88 [PMID: 26811286 DOI: 10.1016/bs.iremb.2015.10.001]
- 56 **Reichel M**, Hönig S, Liebisch G, Lüth A, Kleuser B, Gulbins E, Schmitz G, Kornhuber J. Alterations of plasma glycerophospholipid and sphingolipid species in male alcohol-dependent patients. *Biochim Biophys Acta* 2015; **1851**: 1501-1510 [PMID: 26291032 DOI: 10.1016/j.bbalip.2015.08.005]
- 57 **Xiao G**, He Q, Liu L, Zhang T, Zhou M, Li X, Chen Y, Qin C. Causality of genetically determined metabolites on anxiety disorders: a two-sample Mendelian randomization study. *J Transl Med* 2022; **20**: 475 [PMID: 36266699 DOI: 10.1186/s12967-022-03691-2]
- 58 **Delomenède M**, Buchet R, Mebarek S. Lansoprazole is an uncompetitive inhibitor of tissue-nonspecific alkaline phosphatase. *Acta Biochim Pol* 2009; **56**: 301-305 [PMID: 19543559]
- 59 **Li M**, Ding L, Hu YL, Qin LL, Wu Y, Liu W, Wu LL, Liu TH. Herbal formula LLKL ameliorates hyperglycaemia, modulates the gut microbiota and regulates the gut-liver axis in Zucker diabetic fatty rats. *J Cell Mol Med* 2021; **25**: 367-382 [PMID: 33215869 DOI: 10.1111/jcmm.16084]



Basic Study

Paired-related homeobox 1 induces epithelial-mesenchymal transition in oesophageal squamous cancer

Jin-Bao Guo, Ming Du, Bin Wang, Li Zhong, Zhong-Xue Fu, Jin-Lai Wei

Specialty type: Oncology

Provenance and peer review:

Unsolicited article; Externally peer reviewed.

Peer-review model: Single blind

Peer-review report's scientific quality classification

Grade A (Excellent): 0

Grade B (Very good): B

Grade C (Good): C, C

Grade D (Fair): 0

Grade E (Poor): 0

P-Reviewer: Rojas A, Chile; Tanabe S, Japan; Jeong KY, South Korea

Received: August 15, 2023

Peer-review started: August 15, 2023

First decision: October 9, 2023

Revised: October 16, 2023

Accepted: November 9, 2023

Article in press: November 9, 2023

Published online: December 15, 2023



Jin-Bao Guo, Ming Du, Bin Wang, Department of Thoracic Surgery, The First Affiliated Hospital of Chongqing Medical University, Chongqing 400016, China

Li Zhong, Department of Obstetrics and Gynaecology, The First Affiliated Hospital of Chongqing Medical University, Chongqing 400016, China

Zhong-Xue Fu, Jin-Lai Wei, Department of Gastrointestinal Surgery, The First Affiliated Hospital of Chongqing Medical University, Chongqing 400016, China

Corresponding author: Li Zhong, PhD, Academic Editor, Doctor, Researcher, Department of Obstetrics and Gynaecology, The First Affiliated Hospital of Chongqing Medical University, No. 1 Youyi Road, Yuanjiagang Street, Chongqing 400016, China. zhongli401@126.com

Abstract

BACKGROUND

It is unclear that paired-related homeobox 1 (PRRX1) induces epithelial-mesenchymal transition (EMT) in oesophageal cancer and the specific function of PRRX1 in oesophageal cancer metastasis.

AIM

To assess the significance of PRRX1 expression and investigate the mechanism of EMT in oesophageal cancer metastasis.

METHODS

Detect the expression of PRRX1 by immunohistochemistry in oesophageal tumour tissues and adjacent normal oesophageal tissues; the PRRX1 short hairpin RNA (shRNA) or blank vector lentiviral gene delivery system was transfected into cells; cell proliferation assay, soft agar colony formation assays, cell invasion and migration assays and animal studies were used to observe cells biological characteristics *In vitro* and *in vivo*; XAV939 and LiCl were used to alter the activity of Wnt/ β -catenin pathway. Immunofluorescence staining and western blot analysis were used to detect protein expression of EMT markers and Wnt/ β -catenin pathway.

RESULTS

PRRX1 is expressed at high levels in oesophageal cancer specimens and is closely related to tumour metastasis in patients with oesophageal cancer. Regulation of PRRX1 expression might exert obvious effects on cell proliferation, especially the

migration and invasion of oesophageal cancer cells. Moreover, silencing PRRX1 expression using a shRNA produced the opposite effects. In addition, when PRRX1 was overexpressed, inhibition of the Wnt/ β -catenin pathway with XAV939 negated the effect of PRRX1 on EMT, whereas when PRRX1 was downregulated, activation of the Wnt/ β -catenin pathway with LiCl impaired the effect on EMT.

CONCLUSION

PRRX1 is upregulated in oesophageal cancer is closely correlated with cancer metastasis. Additionally, PRRX1 induces EMT in oesophageal cancer metastasis through activation of Wnt/ β -catenin signalling.

Key Words: Paired-related homeobox 1; Oesophageal squamous cancer; Epithelial-mesenchymal transition; Cancer metastasis

©The Author(s) 2023. Published by Baishideng Publishing Group Inc. All rights reserved.

Core Tip: This study aims to assess the significance of paired-related homeobox 1 (PRRX1) expression and investigate the mechanism of epithelial-mesenchymal transition (EMT) in oesophageal cancer metastasis. PRRX1 is expressed at high levels in oesophageal cancer specimens and is closely related to tumour metastasis in patients with oesophageal cancer. Regulation of PRRX1 expression might exert obvious effects on cell proliferation, especially the migration and invasion of oesophageal cancer cells. Moreover, silencing PRRX1 expression using a short hairpin RNA produced the opposite effects. In addition, when PRRX1 was overexpressed, inhibition of the Wnt/ β -catenin pathway with XAV939 negated the effect of PRRX1 on EMT, whereas when PRRX1 was downregulated, activation of the Wnt/ β -catenin pathway with LiCl impaired the effect on EMT. These observations indicate that PRRX1 is upregulated in oesophageal cancer is closely correlated with cancer metastasis. Additionally, PRRX1 induces EMT in oesophageal cancer metastasis through activation of Wnt/ β -catenin signalling.

Citation: Guo JB, Du M, Wang B, Zhong L, Fu ZX, Wei JL. Paired-related homeobox 1 induces epithelial-mesenchymal transition in oesophageal squamous cancer. *World J Gastrointest Oncol* 2023; 15(12): 2185-2196

URL: <https://www.wjgnet.com/1948-5204/full/v15/i12/2185.htm>

DOI: <https://dx.doi.org/10.4251/wjgo.v15.i12.2185>

INTRODUCTION

Oesophageal cancer is one of the most common cancers with high morbidity and mortality. Oesophageal cancer includes squamous-cell carcinoma and adenocarcinoma. At present, the treatment strategies of oesophageal carcinoma mainly include surgery, chemotherapy, radiotherapy and molecular targeted therapy. However, the prognosis remains poor and overall Five-year survival rate is very low, with metastasis and recurrence being the main causes[1]. Metastasis is a sign of the progression of malignant tumours and remains the greatest challenge for cancer treatment[2]. Epithelial-mesenchymal transition (EMT) is a set of complex and variable transitional states between the epithelial and mesenchymal phenotypes, which acts a key role in carcinoma metastasis, and increasing reports show that metastasis is caused by EMT in pre-invasive stage of most primary cancer[3]. According to reports, the ability of cancer cells to invade and metastasize can be obtained by transforming into the mesenchymal phenotype. EMT is a type of transdifferentiation characterized by decreased expression of epithelial markers such as E-cadherin and increased expression of mesenchymal markers such as N-cadherin and vimentin[4]. The invasive ability of cancer cells is obtained by transforming into a mesenchymal phenotype, accompanied by changes of EMT markers (N-cadherin, E-cadherin and vimentin) were observed[4]. EMT is caused by the changes of genetic, epigenetic changes and the tumour microenvironment. WIST1, SNAIL, ZEB1 and ZEB2 are EMT inducers involved in EMT in most of cancer[5-7]. It is reported that the EMT is a key step in inducing the metastasis of highly aggressive cancer cells, and its molecular mechanism must be extensively investigated.

Recently, paired-related homeobox 1 (PRRX1), which is revealed as a EMT inducer, could induce EMT in some cancers. Surprisingly, the function of PRRX1 is markedly different in these cancer types, and high expression of PRRX1 may predict less metastasis in breast cancer and a better prognosis in breast cancer[8]. At the same time, we observed the opposite relationship in gastric cancer[9], which was also found in pancreatic cancer and colorectal cancer[10,11]. Researchers have not determined whether PRRX1 induces EMT in oesophageal cancer and the specific function of PRRX1 in oesophageal squamous cancer metastasis.

MATERIALS AND METHODS

Patients and tissue samples

One hundred primary oesophageal squamous cancer tissue samples were collected from the Department of Thoracic Surgery of the First Affiliated Hospital of Chongqing Medical University (Chongqing, China). The patients did not

receive preoperative chemotherapy or radiotherapy. These patients with oesophageal squamous cancer were performed on radical resection. This study was reviewed and ratified by the Research Ethics Committee of Chongqing Medical University.

Immunohistochemistry

To detect the expression of PRRX1, immunohistochemical staining was performed with the immunohistochemical SP kit (ZSGB-BIO, Beijing, China). The sections were deparaffinized, heated in a microwave oven at 90 °C for 20 min for antigen retrieval, incubated with 3% hydrogen peroxide for 25 min, then blocked by serum at 37 °C for 30 min. The sections were incubated with the primary antibody overnight at 4 °C and then incubated with the secondary antibody at 37 °C for 40 min. Next, the sections on the glass slide were incubated with streptavidin-HRP at 37 °C for 30 min and chromogen 3,3'-diaminobenzidine for 15 min and then counterstained with haematoxylin. The staining for the target protein was observed under a microscope.

Two independent pathologists judged and scored staining in 10 random fields of view. As mentioned above, the staining was semi-quantitatively graded by determining the percentage of positively stained cells (0 points indicates 0%-5%, 1 point indicates 6%-25%, 2 points indicates 26%-50%, and 3 points indicates > 50%) and expression intensity score (1 point = weak intensity, 2 points = medium intensity, and 3 points = strong intensity). A total score > 3 points was considered significant overexpression and was considered positive for data analysis.

Cell culture and antibodies

The human oesophageal squamous carcinoma cell lines EC109 and EC9706 were purchased from the Key Laboratory of General Surgery. The cell lines were maintained in RPMI 1640 medium (Gibco, United States) containing 10% foetal bovine serum (HyClone, China) and cultured at 37 °C in a humidified atmosphere containing 5% CO₂ and 95% air. Cells were treated with 10 μmol/L XAV939 (a Wnt/β-catenin signalling inhibitor) or 20 mmol/L LiCl (a Wnt/β-catenin signalling activator) for 24 h to determine the effects of Wnt/β-catenin signalling on the function of PRRX1.

The antibodies against the following proteins were used: PRRX1 (OriGene, United States), N-cadherin, E-cadherin, Vimentin, and anti-lamin B1 (Sigma-Aldrich, United States), β-actin (Beyotime, China), HRP-conjugated goat anti-mouse IgG, Alexa Fluor 549-conjugated goat anti-rabbit IgG (H + L), and HRP-conjugated goat anti-rabbit IgG (ZSGB-BIO, Beijing, China).

Plasmid construction and transfection

The PRRX1 short hairpin RNA (shRNA) was constructed in a recombinant adenovirus gene delivery system by GeneChem Biomedical Co., Ltd. (Shanghai, China), and the negative control was delivered by a blank vector lentiviral gene delivery system. The PRRX1 shRNA or blank vector lentiviral gene delivery system was transfected into cells, and then referred to as the PRRX1(i) or MOCK group, respectively.

Cell proliferation assay and soft agar colony formation assays

The cells were incubated in a 96-well plate at a density of 2×10^3 cells per well. After 1, 2, 3, 4, 5, 6 and 7 d, 20 μL of MTT dye (Sigma-Aldrich) were added to each well and incubated at 37 °C for 4 h before dimethyl sulfoxide was added to each well. The absorbance was measured spectrophotometrically with a microplate reader (Bio-Rad, Hercules, CA, United States).

Soft agar colony formation assays were performed to evaluate the colony formation capacity. Cells were cultured in 6-well plates were cultured containing 0.35% agarose (RPMI medium 1640 mixed with agarose) at a density of 2×10^3 cells per well. After 3 wk, the colonies were manually counted under a microscope.

Cell invasion and migration assays

Twenty-four-well Transwell chambers with an 8-μm pore size (Corning, New York, NY, United States) were coated with BD Matrigel Basement Membrane Matrix (BD Biosciences, San Diego, CA, United States), maintained overnight at 4 °C, and then polymerized at 37 °C. The transwell chambers used in the migration assay were not coated with Matrigel. Cells were plated in transwell chambers at a density of 1×10^5 cells per well and incubated. After 20 h, the cells that passed through the transwell were stained with 4% paraformaldehyde and then stained with haematoxylin-eosin (HE). By counting the number of stained cells in the four quadrants from each insert and averaging the obtained triplicate values, the number of cells invaded or migrated through Matrigel was quantified.

Immunofluorescence staining

Cells were incubated in dishes. After 24 h, cells were fixed with 4% paraformaldehyde for 30 min, then permeabilized with 0.04% Triton X-100 for 10 min, and then blocked by 5% bovine serum albumin for 30 min. Cells were incubated with the primary antibody at 37 °C for 1 h, incubated with the appropriate Alexa Fluor 549-conjugated secondary antibody at 37 °C for 1 h, and counterstained with 4',6-diamidino-2-phenylindole for 1 h. Immunofluorescence images were captured using a fluorescence microscope.

Animal studies

BALB/c nude mice were used to the role of PRRX1 on detect tumorigenicity and tumor formation in oesophageal tumour formation. Three groups (EC9706, EC9706 MOCK and EC9706 PRRX1(i)) were expanded and subcutaneously inoculated into the flanks of nude mice (3×10^5 cells). Tumour diameters were measured using Vernier callipers every week, and the tumour volumes were calculated using the following formula: $V(\text{mm}^3) = \text{length} \times \text{width}^2/2$. After 6 wk, the mice were

euthanized by Carbon Dioxide Euthanasia.

A total of 1×10^4 cells was injected into the tail vein of each nude mouse to assay the effect of PRRX1 on oesophageal cancer cell metastasis *in vivo*. Necropsies were performed after 30 d, and the number of lung metastasis nodules in each mouse was counted.

Western blot analysis

Whole-cell extracts were prepared in lysis buffer (Beyotime, China), and the nuclear and cytoplasmic fractions were separated with a nuclear and cytoplasmic protein extraction kit (Beyotime, China). Then, 40 μ g of protein were loaded into each well, electrophoretically separated, and transferred to membranes. The membranes were then incubated with primary antibodies for 10 h at 4 °C and then incubated with secondary antibodies for 1 h at 37 °C. Finally, each band was analysed using an ECL chemiluminescence detection system (ChemiDoc™ XRS imager, Bio-Rad, United States).

Statistical analysis

Statistical analyses were performed by SPSS v. 20 and GraphPad Prism 6 software. Student's *t* test, was used to calculate significant differences. Pearson's correlation coefficients and the χ^2 test, as appropriate. Overall survival was analysed using the logrank test and KaplanMeier analysis. Values of $P < 0.05$ were considered statistically significant.

RESULTS

PRRX1 expression is upregulated in oesophageal squamous cancer and related to shorter overall survival

We determined the PRRX1 expression level in oesophageal squamous tumour tissues and adjacent normal oesophageal tissues by performing immunohistochemistry. Compared with adjacent normal oesophageal tissues, PRRX1 was expressed at significantly higher levels in oesophageal squamous tumour tissues (Figures 1A-D). The expression level of PRRX1 in 100 oesophageal squamous cancer specimens was investigated. As shown in Figure 1E, during the 5-year follow-up, 55.9% of patients with low PRRX1 expression survived, and only 37.9% of patients with high PRRX1 expression survived ($P < 0.05$). As shown in Table 1, PRRX1 was expressed at significantly higher levels in oesophageal tumour tissues than in adjacent normal oesophageal tissues ($P < 0.05$). The correlations between the expression levels of PRRX1 and the clinicopathological features of patients with oesophageal cancer were analysed (as shown in Table 2). Strong correlations were observed between the expression of PRRX1 and T-stage and lymph node metastasis and pTNM stage of tumour invasion ($P < 0.05$). In addition, the expression of PRRX1 had no relationship with the age, gender, tumor location and histologic grade of oesophageal squamous cancer ($P > 0.05$).

PRRX1 modulates cell proliferation, colony formation, invasion and migration in oesophageal cancer

High PRRX1 expression was detected in EC109 and EC9706 cells. After shRNA vector transfection, stable oesophageal cancer cell lines were established, in which the expression of PRRX1 was continuously inhibited. The PRRX1(i) groups were confirmed to express the PRRX1 protein at lower levels after transfection with the PRRX1 shRNA vector lentivirus. PRRX1 expression was more obviously inhibited in EC9706 PRRX1(i) cells than in EC109 PRRX1(i) cells (as shown in Figure 2), and thus EC9706 cells were used in follow-up biological experiments using oesophageal cancer cells.

Cell proliferation was assessed using the MTT assay. The proliferation of EC9706 cells was significantly decreased on days 4, 5, 6, and 7 after silencing endogenous PRRX1 (Figure 3A). Silencing the expression of PRRX1 inhibits the growth of oesophageal cancer cells. The soft agar colony formation assay revealed the effect of PRRX1 on the colony formation ability of oesophageal cancer cells. Smaller and fewer colonies were formed by EC9706 cells after PRRX1 was downregulated (Figure 3B).

Cell migration and invasion assays were executed. In Figure 3C, compared with the EC9706 and EC9706 MOCK groups, the number of cells migrating through the Transwell was significantly reduced after PRRX1 silencing ($P < 0.05$). In addition, as shown in Figure 3D, the number of cells passing through Matrigel was significantly reduced after PRRX1 was downregulated compared with the EC9706 and EC9706 MOCK groups ($P < 0.05$). Based on these results, PRRX1 increases the proliferation, colony formation, invasion and migration of oesophageal cancer cells.

PRRX1 induces EMT in oesophageal cancer

In the EC109 PRRX1(i) and EC9706 PRRX1(i) groups, the level of the PRRX1 protein was obviously reduced, but no significant difference in the expression of PRRX1 was observed between the MOCK group and parental cell group. Then, the levels of EMT markers were also distinctly changed. The expression of N-cadherin and vimentin was significantly decreased; in contrast, E-cadherin expression was significantly increased in EC109 PRRX1(i) and EC9706 PRRX1(i) cells (Figure 2). Similar results were also obtained from the immunofluorescence staining experiment (Figure 4). The change in the level of the PRRX1 protein was accompanied by changes in the expression of EMT markers. These results reveal that PRRX1 induces EMT in oesophageal cancer cells.

PRRX1 regulates the Wnt/ β -catenin pathway in oesophageal cancer

β -catenin as the key protein in the Wnt/ β -catenin pathway, and the expression of β -catenin was significantly decreased in EC109 PRRX1(i) and EC9706 PRRX1(i) cells (Figure 2). Therefore, PRRX1 may affect the Wnt/ β -catenin pathway in oesophageal cancer cells. PRRX1 silencing accompanied an obvious reduction in the total β -catenin level, especially the nuclear level of β -catenin (Figure 2). An obvious reduction in the nuclear level of β -catenin was also observed (Figure 4).

Table 1 Expression of paired-related homeobox 1 in 100 cases of esophageal cancer and adjacent normal esophageal tissues (χ^2 -test)

Protein	Esophageal cancer tissues	Esophageal cancer adjacent normal tissues	P value
PRRX1			
+	62	43	0.007
-	38	57	

PRRX1: Paired-related homeobox 1.

Table 2 Correlation between paired-related homeobox 1 immunostaining and clinicopathologic features in 100 cases of esophageal cancer tissues (χ^2 -test)

Parameters	n	PRRX1		P value
		+	-	
Age (yr)				0.529
< 60	30	20	10	
≥ 60	70	42	28	
Gender				0.813
Male	67	41	26	
Female	33	21	12	
Tumor location				0.626
Upper	19	10	9	
Middle	60	39	21	
Lower	21	13	8	
T-stage				0.024
T1-T2	29	13	16	
T3-T4	71	49	22	
Histologic grade				0.423
Well	17	9	8	
Middle	58	35	23	
Poor	25	18	7	
Lymph node metastasis				0.014
Negative	35	16	19	
Positive	65	46	19	
pTNM stage				0.009
I	14	5	9	
II	26	12	14	
III	44	34	10	
IV	16	11	5	

Both depth of tumor invasion and tumor node metastasis (TNM) stage: According to 2018 TNM classification of malignant tumors by the International Union Against Cancer. TNM: Tumor node metastasis; PRRX1: Paired-related homeobox 1.

Further research showed that the total and nuclear levels of the β -catenin protein were decreased after cells were treated with XAV939 (an inhibitor of Wnt/ β -catenin signalling), meanwhile, significantly increased after cells were treated with LiCl (an activator of Wnt/ β -catenin signalling) (Figure 5). This information suggests that PRRX1 is involved in regulating the Wnt/ β -catenin pathway in oesophageal cancer cells.

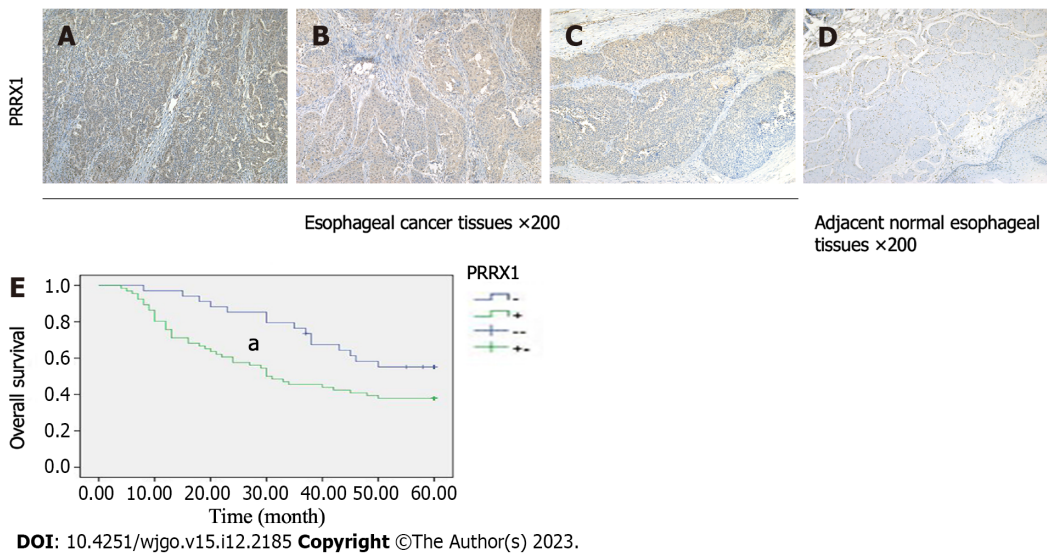


Figure 1 Paired-related homeobox 1 expression is upregulated in oesophageal cancer and related to shorter overall survival. A: Immunohistochemical detection of the expression of paired-related homeobox 1 (PRRX1) in oesophageal cancer specimens with a high ($\times 200$); B: Middle ($\times 200$); C: Low grade ($\times 200$); D: Immunohistochemical detection of the expression of PRRX1 in adjacent normal oesophageal tissues ($\times 200$); E: Logrank test and Kaplan-Meier analysis of the association of PRRX1 expression with the overall survival of patients with oesophageal cancer. ^a $P < 0.05$. PRRX1: Paired-related homeobox 1.

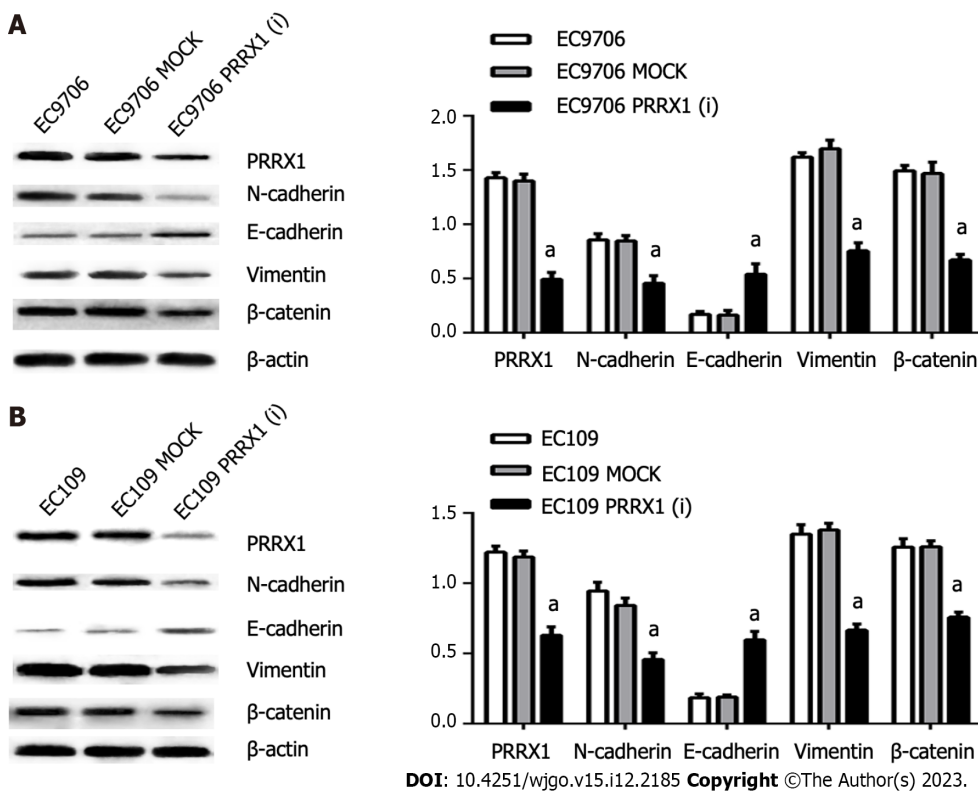
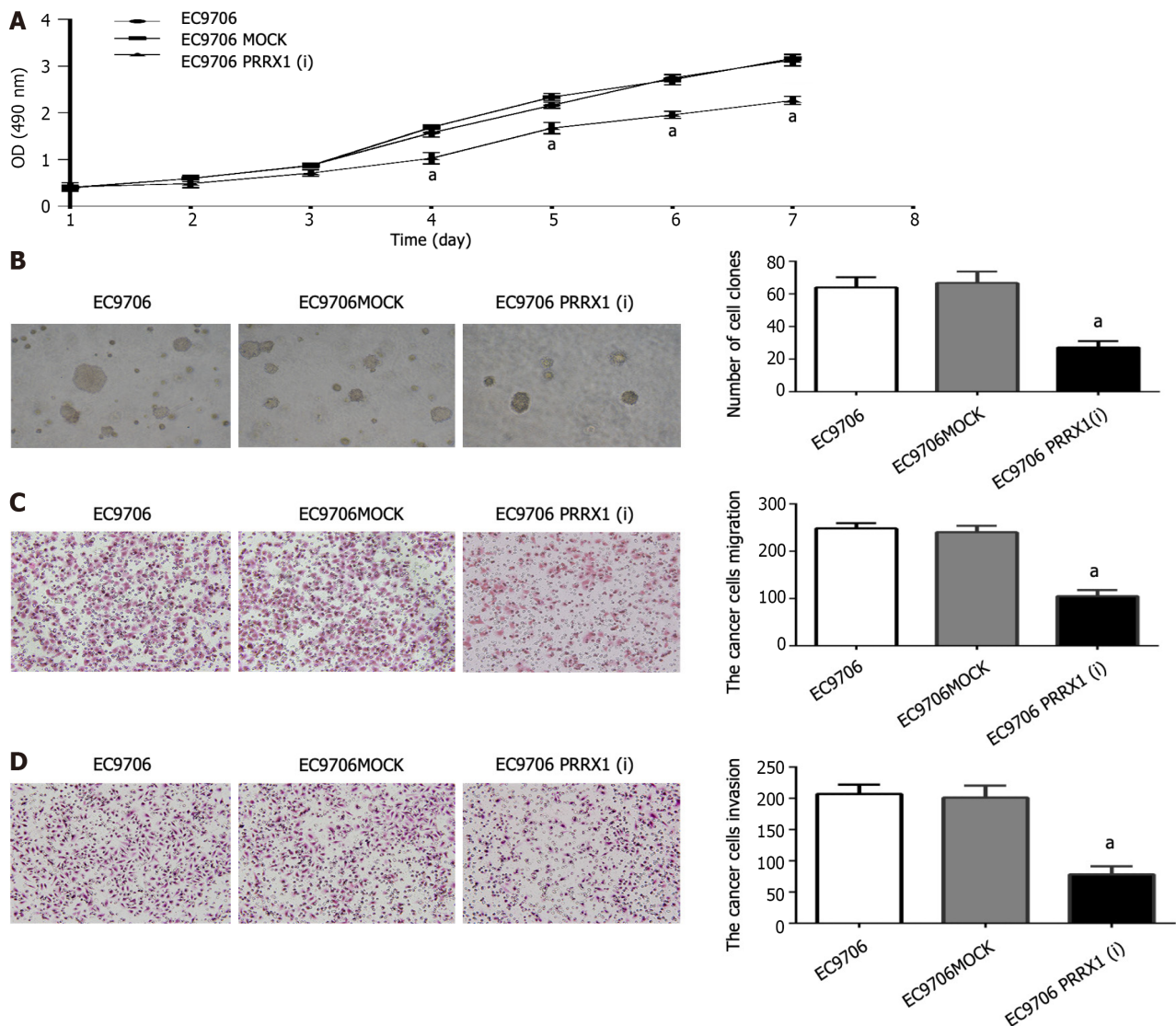


Figure 2 Paired-related homeobox 1 not only induces epithelial-mesenchymal transition but also regulates Wnt/ β -catenin signalling. A and B: The protein levels of paired-related homeobox 1, epithelial-mesenchymal transition markers (E-cadherin, Vimentin, and N-cadherin), total β -catenin and nuclear β -catenin in various groups of EC9706 and EC109 cells were examined using western blotting. ^a $P < 0.05$. PRRX1: Paired-related homeobox 1.

PRRX1 induces EMT in oesophageal cancer via the Wnt/ β -catenin pathway

After the level of the PRRX1 protein was obviously reduced in EC109 PRRX1(i) and EC9706 PRRX1(i) cells, a significant increase in E-cadherin levels and significant reductions in levels of the vimentin, N-cadherin, total β -catenin proteins were examined (Figure 2). As shown in Figure 5, the activator of Wnt/ β -catenin signalling LiCl increased the levels of the total and nuclear β -catenin proteins. Concomitantly, levels of the N-cadherin and vimentin proteins were significantly increased, the level of the E-cadherin protein was decreased, and the level of the PRRX1 protein was not changed in EC109 PRRX1(i) and EC9706 PRRX1(i) cells. At the same time, after the inhibition of Wnt/ β -catenin signalling



DOI: 10.4251/wjgo.v15.i12.2185 Copyright ©The Author(s) 2023.

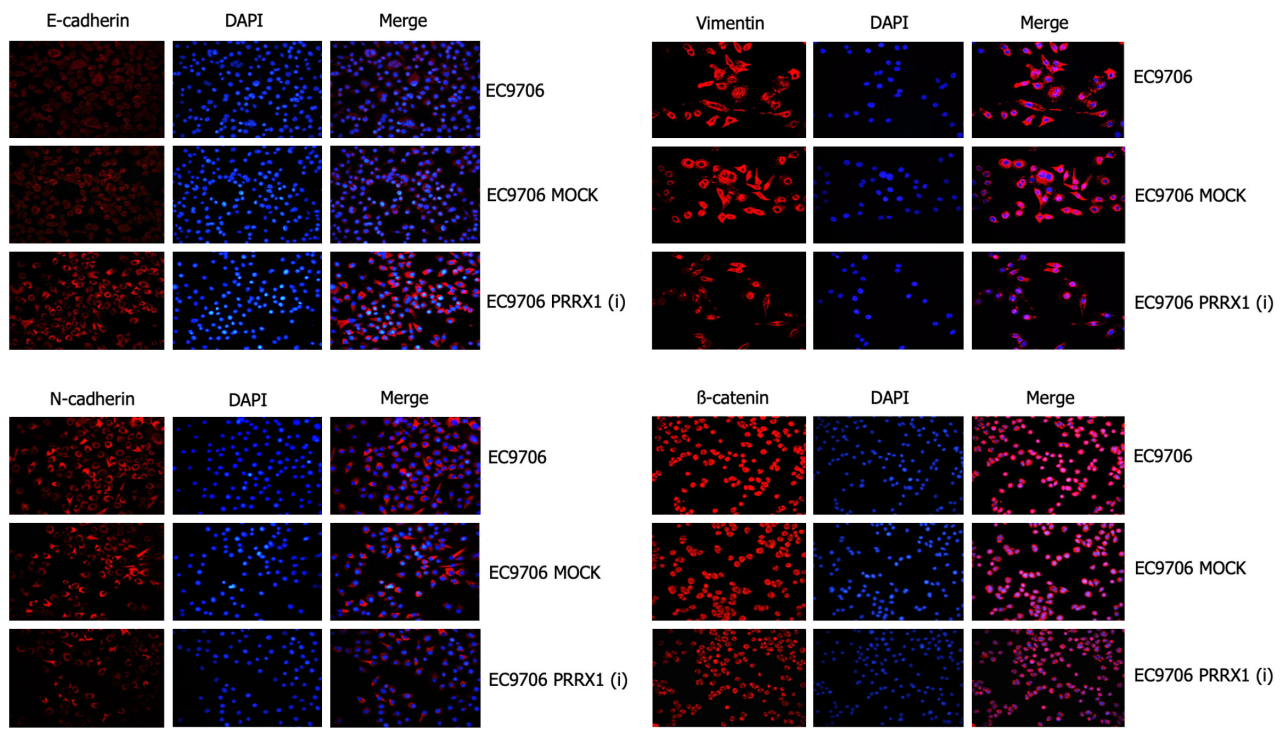
Figure 3 Paired-related homeobox 1 modulates proliferation, colony formation, migration and invasion in oesophageal cancer cells. A: The MTT assay. Paired-related homeobox 1 (PRRX1) affected EC9706 cell proliferation; B: Soft agar colony formation assay. PRRX1 affected the ability of EC9706 cells to form colonies in soft agar, and the number of colonies was different in various groups of EC9706 cells; C: Cellular migration assays. PRRX1 affected the migration of EC9706 cells. The number of migrating EC9706 cells in various groups was different. Cells were stained with hematoxylin and eosin; D: Cellular invasion assays. PRRX1 affected the invasive properties of EC9706 cells. The number of invasive EC9706 cells in various groups was different. Cells were stained with hematoxylin and eosin. ^a $P < 0.05$. PRRX1: Paired-related homeobox 1.

with XAV939, the total and nuclear levels of the β -catenin protein were decreased, levels of the vimentin and N-cadherin proteins were decreased, the expression of the E-cadherin protein was increased, and the level of the PRRX1 protein was not altered in EC109 and EC9706 cells. PRRX1 not only induced EMT but also altered the activity of the Wnt/ β -catenin pathway. After further study, activation of the Wnt/ β -catenin pathway potentially restores the effects of PRRX1 on inhibiting EMT, whereas inhibiting the activity of the Wnt/ β -catenin pathway enhances the effect of the downregulation of PRRX1 on EMT.

PRRX1 promotes oesophageal cancer cell proliferation and metastasis in vivo

Xenografts of EC9706, EC9706 MOCK and EC9706 PRRX1(i) cells were established in nude mice to test the function of PRRX1 in tumorigenesis, and solid tumours developed after 6 wk. In the EC9706 PRRX1(i) group, the tumour volumes and weights were significantly smaller than those in the EC9706 and EC9706 MOCK groups (Figure 6A).

The number of lung metastatic foci was evaluated to explore the role of PRRX1 in oesophageal cancer cell metastasis *in vivo*, and a smaller number of lung metastatic nodules was observed in animals injected with PRRX1-silenced cells than in animals injected with control cells (Figure 6B).



DOI: 10.4251/wjgo.v15.i12.2185 Copyright ©The Author(s) 2023.

Figure 4 Cellular immunofluorescence staining. The protein levels of epithelial-mesenchymal transition markers (E-cadherin, N-cadherin, and Vimentin) and β -catenin in cells were stained red, and the nucleus was stained blue with 4',6-diamidino-2-phenylindole. PRRX1: Paired-related homeobox 1; DAPI: 4',6-diamidino-2-phenylindole.

DISCUSSION

EMT plays a key role in tumour progression[12]. During EMT, epithelial cells obtain mesenchymal characteristics with the loss of epithelial cell markers (E-cadherin) and the acquisition of mesenchymal cell markers (vimentin and N-cadherin). EMT is activated or reversed (mesenchymal to epithelial transition, MET) by cells, revealing a form of plasticity that also leads to stemness and drug resistance[13]. EMT is related to tumour metastasis, which is accompanied by the activation of signalling networks[14]. EMT is reported to be important in the invasion and metastasis of cancer cells[3].

PRRX1 was reported for the first time to enhance the DNA binding activity of serum response factors[15]. PRRX1 induces EMT by inhibiting the expression of E-cadherin[8,10]. PRRX1 also plays a key role in the process of pancreatic regeneration and carcinogenesis[11]. In oesophageal squamous cancer tumours, PRRX1 is expressed at higher levels than that in adjacent normal tissue, and the expression of PRRX1 is significantly correlated with the T-stage, lymph node metastasis and pTNM stage of oesophageal squamous cancer. High PRRX1 expression is related to a shorter overall survival. This study is a small sample size study, follow-up studies need a larger sample size to reduce bias. Oesophageal cancer cells (EC9706 and EC109) with high PRRX1 expression not only exhibit a spindle-like shape but also display a loss of E-cadherin expression and high vimentin and N-cadherin expression. After downregulating the expression of PRRX1, oesophageal cancer cells (EC9706 and EC109) upregulated the expression of E-cadherin and downregulated the expression of vimentin and N-cadherin, showing an oval-like shape. These results indicate that oesophageal cancer cells with downregulation of PRRX1 undergo the MET and that EMT can be reversed to the MET[16]. At the same time, we also observed that PRRX1 silencing suppressed cell proliferation, colony formation, migration and invasion *in vitro*, and downregulating PRRX1 also inhibited proliferation and metastasis *in vivo*. During EMT, epithelial features of cancer cells are inhibited, and the expression of mesenchymal genes is upregulated. Then, an invasive and metastatic phenotype is acquired. EMT is presumed to play a central role in cancer metastasis[17]. Based on these results, PRRX1 not only maintains EMT but also promotes cancer metastasis in oesophageal cancer. PRRX1 also induces EMT during carcinogenesis; therefore, EMT may play an important role in PRRX1-mediated tumour invasion and metastasis[10,18].

However, the molecular mechanism by which PRRX1 regulates EMT in oesophageal squamous cancer is unclear[10]. In this study, it was found that the expression and localization of β -catenin in oesophageal cancer was related to the expression of PRRX1. And the aberrant expression of β -catenin may be a potential unfavourable factor contributing to the occurrence and development of oesophageal cancer[19]. β -catenin functions as a key mediator in the Wnt/ β -catenin signalling pathway. After activating Wnt/ β -catenin signalling, β -catenin escapes proteasomal degradation and is transported to the nucleus, where it binds to its target genes and promotes a variety of carcinogenic pathways[20]. The Wnt/ β -catenin signalling pathway plays an important role in the progression, metastasis and invasion of oesophageal cancer[21]. The Wnt/ β -catenin signalling pathway regulates multiple biological processes, such as cardiac valve formation and cell proliferation, as well as EMT in gastrulation and cancer[22,23]. When Wnt/ β -catenin signalling is activated, the destruction complex is inhibited, β -catenin could gradually accumulate, and then translocate to the nucleus.

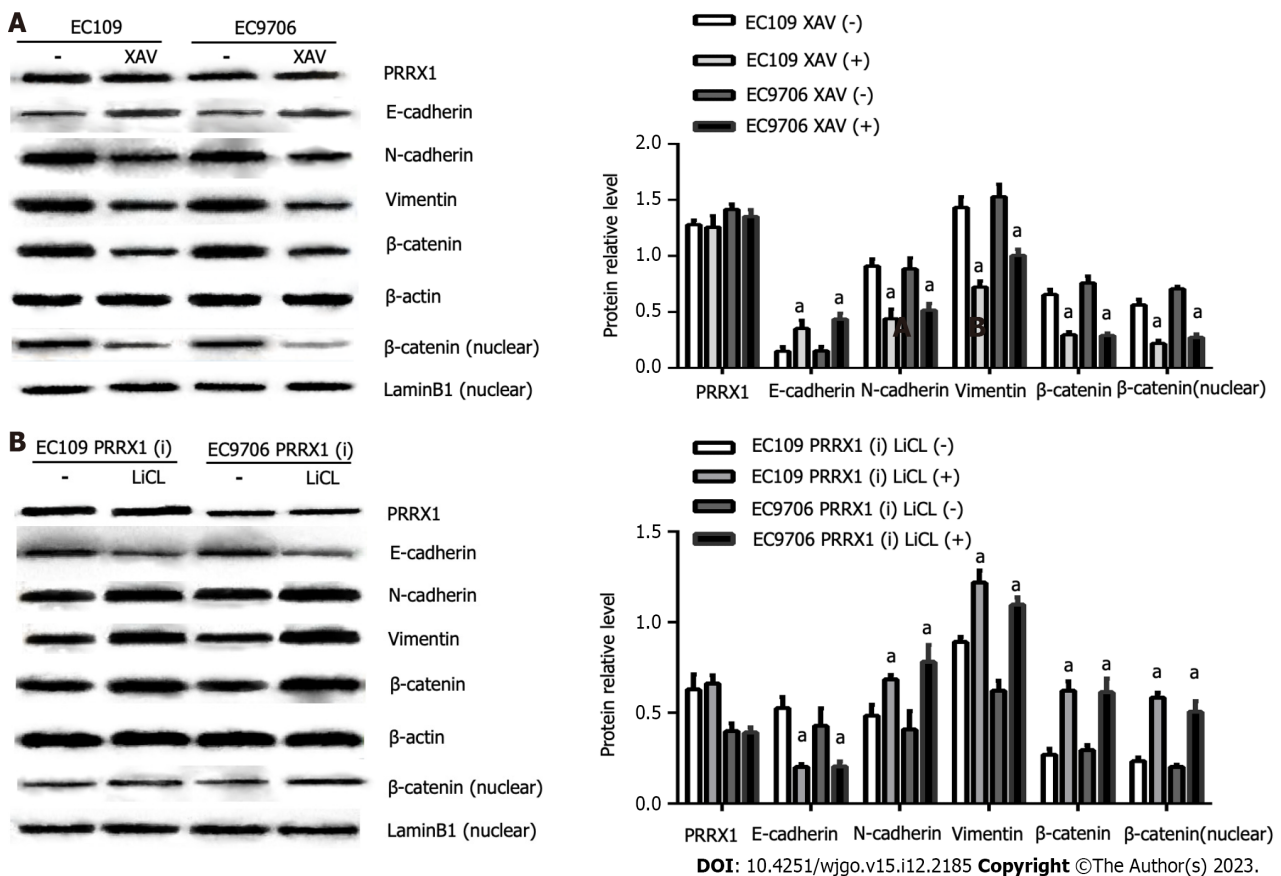


Figure 5 Paired-related homeobox 1 regulates epithelial-mesenchymal transition via the Wnt/β-catenin pathway. A: The protein levels of paired-related homeobox 1 (PRRX1), epithelial-mesenchymal transition (EMT) markers (E-cadherin, Vimentin, and N-cadherin), total β-catenin and nuclear β-catenin in different groups of EC109 and EC9706 cells (treated with 10 μM XAV939) were examined using western blotting; B: The protein levels of the EMT markers total β-catenin nuclear β-catenin, and PRRX1 in different groups of EC109 PRRX1(i) and EC9706 PRRX1(i) cells (treated with 20 mmol/L LiCl) were examined using western blotting. *P < 0.05. PRRX1: Paired-related homeobox 1.

The loss of E-cadherin expression may be caused by the translocation of β-catenin into the nucleus[23,24]. High PRRX1 expression was accompanied by increased levels of β-catenin in the nucleus of oesophageal cancer cells and activation of the Wnt/β-catenin signalling pathway in the present study. Following PRRX1 downregulation, β-catenin expression was downregulated, and more obviously, β-catenin levels in the nucleus were decreased. In addition, XAV939, which as an inhibitor of Wnt/β-catenin signalling, inhibited the activity of Wnt/β-catenin signalling by preventing β-catenin translocation into the nucleus[25]. High PRRX1 expression in oesophageal cancer cells induces EMT, and the effect on EMT was neutralized by XAV939. At the same time, LiCl-mediated activation of the Wnt/β-catenin pathway weakens the effect of PRRX1 downregulation on EMT. These results indicate that PRRX1 regulates Wnt/β-catenin signalling in oesophageal cancer and that Wnt/β-catenin signalling regulates the PRRX1-induced EMT.

In summary, the upregulation of PRRX1 is a common event in oesophageal cancer that is closely related to the metastasis of oesophageal squamous cancer. PRRX1 induces EMT by activating Wnt/β-catenin signalling and stimulates the invasion and metastasis of oesophageal cancer, which leads to poor prognosis of patients with oesophageal cancer. Our results are consistent with those observed in pancreatic cancer and colorectal and gastric cancer[9], but differ from the findings in breast cancer[8]. Perhaps these data suggest that the function of PRRX1 is different in different cancers. More research is needed on PRRX1. PRRX1 is regulated by transforming growth factor-β and microRNAs[8,26]. PRRX1 isoforms regulate the DNA damage response in pancreatic cancer cells in cooperation with FOXM1[27]. Cellular phenotypic plasticity and dormancy of head and neck squamous cell carcinoma are regulated by PRRX1[28]. In hepatocellular carcinoma, the downregulation of PRRX1 predicts a poor prognosis, and PRRX1 regulates the p53-dependent signalling pathway[29].

CONCLUSION

Given the importance of PRRX1 in EMT and the Wnt/β-catenin pathway in esophageal squamous cancer, our findings not only provide a better understanding of the molecular mechanisms of PRRX1 in esophageal squamous cancer metastasis, but also provide a better understanding of the role of PRRX1 in cancer metastasis, it also suggests some potential therapeutic intervention targets[11].

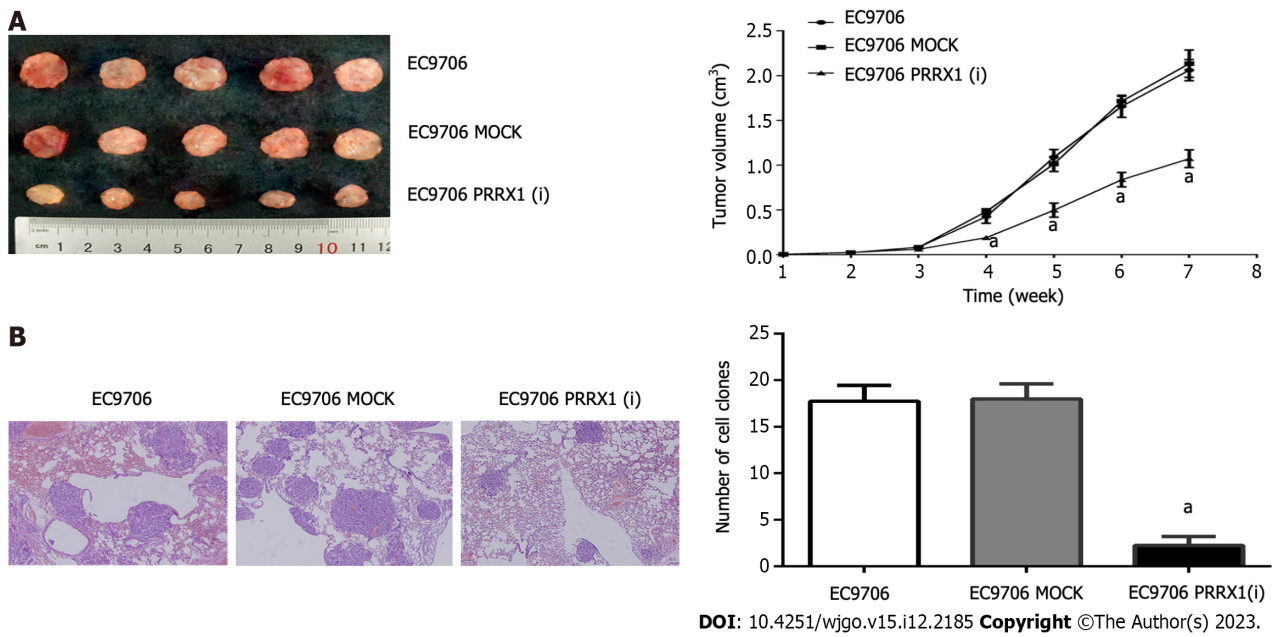


Figure 6 Paired-related homeobox 1 downregulation inhibits cell proliferation and lung metastasis *in vivo*. A: Paired-related homeobox 1 (PRRX1) affected EC9706 cell proliferation *in vivo*. The tumour volume was measured weekly; B: The number of metastatic lung nodules was different in the various EC9706 groups. **P* < 0.05. PRRX1: Paired-related homeobox 1.

ARTICLE HIGHLIGHTS

Research background

Esophageal cancer is one of the most common cancers with high morbidity and mortality. It is unclear that paired-related homeobox 1 (PRRX1) induces epithelial-mesenchymal transition (EMT) in oesophageal cancer and the specific function of PRRX1 in oesophageal cancer metastasis.

Research motivation

This study is to assess the significance of PRRX1 expression and investigate the mechanism of EMT in oesophageal cancer metastasis.

Research objectives

One hundred primary oesophageal cancer tissue samples were collected from Thoracic Surgery and the human oesophageal squamous carcinoma cell lines EC109 and EC9706.

Research methods

The expression of PRRX1 by the chemical test of immunohistochemical tissue is in the esophageal tumor tissue. The PRRX1 short hair holder RNA (SHRNA) or blank virus gene delivery system is transfected into the cells. Cell proliferation measurement, the formation of soft agar colonies, cell invasion and migration measurement, and animal research are used to observe the cell biological characteristics of internal and internal body. Mouse experimental testing and metastasis of esophageal tumors in the body. Immunofluorescence staining and protein marks analysis is used to detect protein expression of EMT labeling and Wnt/ β -catenin. XAV939 and LiCl are used to change the activity of Wnt/ β -catenin pathway.

Research results

PRRX1 is expressed in high levels in the specimen of esophageal cancer and is closely related to the metastasis and prognosis of the tumor metastasis and prognosis of patients with esophageal cancer. The regulation of PRRX1 may have a significant impact on cell proliferation, especially the migration and invasion of esophageal cancer cells. The expression of PRRX1 is closely related to EMT and Wnt/ β -catenin. Further experiments, using shRNA to silence the expression of PRRX1 have the opposite effect. In addition, when PRRX1 was expressed, the inhibitory effect of XAV939 on WNT/ β -catenin's inhibitory has denied the effect of PRRX1 on EMT. When the expression of PRRX1 was downregulated, the Wnt/ β -catenin pathway with LiCl impaired the effect on EMT.

Research conclusions

In oesophageal cancer, PRRX1 is closely related to the metastasis and prognosis of tumor. PRRX1 can improve the ability to value and metastasize tumors. PRRX1 regulate EMT increases the ability of tumors. Further research found that PRRX1 regulates EMT through the Wnt/ β -catenin signal.

Research perspectives

The expression of PRRX1 is closely related to the metastasis and prognosis of esophageal cancer, which also shows that PRRX1 may become a potential esophageal cancer treatment target. Our studies have confirmed that PRRX1 is regulating EMT through WNT/ β -catenin. More PRRX1 regulation mechanisms and downstream target areas need to be more in-depth research.

FOOTNOTES

Author contributions: Guo JB and Zhong L designed the research and wrote the paper; Wei JL performed the research and analyzed results; Du M, Wang B, and Fu ZX edited the manuscript and provided critical comments.

Institutional review board statement: All experimental protocols were approved by the Ethics Committee the First Affiliated Hospital of Chongqing Medical University (Approval number 2021-033).

Institutional animal care and use committee statement: All experimental protocols were approved by the Ethics Committee the First Affiliated Hospital of Chongqing Medical University (Approval number 2021-033).

Conflict-of-interest statement: All the authors report no relevant conflicts of interest for this article.

Data sharing statement: Technical appendix, statistical code, and dataset available from the corresponding author at zhongli401@126.com.

ARRIVE guidelines statement: The authors have read the ARRIVE guidelines, and the manuscript was prepared and revised according to the ARRIVE guidelines.

Open-Access: This article is an open-access article that was selected by an in-house editor and fully peer-reviewed by external reviewers. It is distributed in accordance with the Creative Commons Attribution NonCommercial (CC BY-NC 4.0) license, which permits others to distribute, remix, adapt, build upon this work non-commercially, and license their derivative works on different terms, provided the original work is properly cited and the use is non-commercial. See: <https://creativecommons.org/licenses/by-nc/4.0/>

Country/Territory of origin: China

ORCID number: Jin-Bao Guo 0000-0002-4147-7708; Li Zhong 0009-0003-1440-6933.

S-Editor: Wang JJ

L-Editor: A

P-Editor: Zhang XD

REFERENCES

- 1 He S, Xu J, Liu X, Zhen Y. Advances and challenges in the treatment of esophageal cancer. *Acta Pharm Sin B* 2021; **11**: 3379-3392 [PMID: 34900524 DOI: 10.1016/j.apsb.2021.03.008]
- 2 Stuelten CH, Parent CA, Montell DJ. Cell motility in cancer invasion and metastasis: insights from simple model organisms. *Nat Rev Cancer* 2018; **18**: 296-312 [PMID: 29546880 DOI: 10.1038/nrc.2018.15]
- 3 Pastushenko I, Blanpain C. EMT Transition States during Tumor Progression and Metastasis. *Trends Cell Biol* 2019; **29**: 212-226 [PMID: 30594349 DOI: 10.1016/j.tcb.2018.12.001]
- 4 Bakir B, Chiarella AM, Pitarresi JR, Rustgi AK. EMT, MET, Plasticity, and Tumor Metastasis. *Trends Cell Biol* 2020; **30**: 764-776 [PMID: 32800658 DOI: 10.1016/j.tcb.2020.07.003]
- 5 Yochum ZA, Cades J, Wang H, Chatterjee S, Simons BW, O'Brien JP, Khetarpal SK, Lemtiri-Chlieh G, Myers KV, Huang EH, Rudin CM, Tran PT, Burns TF. Targeting the EMT transcription factor TWIST1 overcomes resistance to EGFR inhibitors in EGFR-mutant non-small-cell lung cancer. *Oncogene* 2019; **38**: 656-670 [PMID: 30171258 DOI: 10.1038/s41388-018-0482-y]
- 6 Pan Z, Cai J, Lin J, Zhou H, Peng J, Liang J, Xia L, Yin Q, Zou B, Zheng J, Qiao L, Zhang L. A novel protein encoded by circFND3B inhibits tumor progression and EMT through regulating Snail in colon cancer. *Mol Cancer* 2020; **19**: 71 [PMID: 32241279 DOI: 10.1186/s12943-020-01179-5]
- 7 Lindner P, Paul S, Eckstein M, Hampel C, Muenzner JK, Erlenbach-Wuensch K, Ahmed HP, Mahadevan V, Brabletz T, Hartmann A, Vera J, Schneider-Stock R. EMT transcription factor ZEB1 alters the epigenetic landscape of colorectal cancer cells. *Cell Death Dis* 2020; **11**: 147 [PMID: 32094334 DOI: 10.1038/s41419-020-2340-4]
- 8 Ocaña OH, Córcoles R, Fabra A, Moreno-Bueno G, Acloque H, Vega S, Barrallo-Gimeno A, Cano A, Nieto MA. Metastatic colonization requires the repression of the epithelial-mesenchymal transition inducer Prrx1. *Cancer Cell* 2012; **22**: 709-724 [PMID: 23201163 DOI: 10.1016/j.ccr.2012.10.012]
- 9 Guo J, Fu Z, Wei J, Lu W, Feng J, Zhang S. PRRX1 promotes epithelial-mesenchymal transition through the Wnt/ β -catenin pathway in gastric cancer. *Med Oncol* 2015; **32**: 393 [PMID: 25428393 DOI: 10.1007/s12032-014-0393-x]
- 10 Takahashi Y, Sawada G, Kurashige J, Uchi R, Matsumura T, Ueo H, Takano Y, Akiyoshi S, Eguchi H, Sudo T, Sugimachi K, Doki Y, Mori M, Mimori K. Paired related homoeobox 1, a new EMT inducer, is involved in metastasis and poor prognosis in colorectal cancer. *Br J Cancer*

- 2013; **109**: 307-311 [PMID: 23807160 DOI: 10.1038/bjc.2013.339]
- 11 **Reichert M**, Takano S, von Burstin J, Kim SB, Lee JS, Ihida-Stansbury K, Hahn C, Heeg S, Schneider G, Rhim AD, Stanger BZ, Rustgi AK. The Prx1 homeodomain transcription factor plays a central role in pancreatic regeneration and carcinogenesis. *Genes Dev* 2013; **27**: 288-300 [PMID: 23355395 DOI: 10.1101/gad.204453.112]
 - 12 **Brabletz T**, Kalluri R, Nieto MA, Weinberg RA. EMT in cancer. *Nat Rev Cancer* 2018; **18**: 128-134 [PMID: 29326430 DOI: 10.1038/nrc.2017.118]
 - 13 **Karacosta LG**, Anchang B, Kimmey S, van de Rijn M, Shrager JB, Bendall SC, Plevritis SK, Abstract 4997: Identifying dynamic EMT states and constructing a proteomic EMT landscape of lung cancer using single cell multidimensional analysis. *Cancer Res* 2018; **78**: 4997 [DOI: 10.1158/1538-7445.AM2018-4997]
 - 14 **Thiery JP**. Epithelial-mesenchymal transitions in tumour progression. *Nat Rev Cancer* 2002; **2**: 442-454 [PMID: 12189386 DOI: 10.1038/nrc822]
 - 15 **Grueneberg DA**, Natesan S, Alexandre C, Gilman MZ. Human and Drosophila homeodomain proteins that enhance the DNA-binding activity of serum response factor. *Science* 1992; **257**: 1089-1095 [PMID: 1509260 DOI: 10.1126/science.257.5073.1089]
 - 16 **Xue H**, Tian GY. MiR-429 regulates the metastasis and EMT of HCC cells through targeting RAB23. *Arch Biochem Biophys* 2018; **637**: 48-55 [PMID: 29191386 DOI: 10.1016/j.abb.2017.11.011]
 - 17 **Ramesh V**, Brabletz T, Ceppi P. Targeting EMT in Cancer with Repurposed Metabolic Inhibitors. *Trends Cancer* 2020; **6**: 942-950 [PMID: 32680650 DOI: 10.1016/j.trecan.2020.06.005]
 - 18 **Takano S**, Reichert M, Heeg S, Bakir B, Rhim AD, Stanger B, Rustgi AK. 339 The Prx1 Homeobox Transcription Factor Regulates Invasion and EMT in Pancreatic Cancer. *Gastroenterology* 2013; **144**: S-71 [DOI: 10.1016/S0016-5085(13)60263-2]
 - 19 **Deng F**, Zhou K, Cui W, Liu D, Ma Y. Clinicopathological significance of wnt/ β -catenin signaling pathway in esophageal squamous cell carcinoma. *Int J Clin Exp Pathol* 2015; **8**: 3045-3053 [PMID: 26045816]
 - 20 **Vallée A**, Lecarpentier Y. Crosstalk Between Peroxisome Proliferator-Activated Receptor Gamma and the Canonical WNT/ β -Catenin Pathway in Chronic Inflammation and Oxidative Stress During Carcinogenesis. *Front Immunol* 2018; **9**: 745 [PMID: 29706964 DOI: 10.3389/fimmu.2018.00745]
 - 21 **Qian Y**, Liang X, Kong P, Cheng Y, Cui H, Yan T, Wang J, Zhang L, Liu Y, Guo S, Cheng X, Cui Y. Elevated DHODH expression promotes cell proliferation *via* stabilizing β -catenin in esophageal squamous cell carcinoma. *Cell Death Dis* 2020; **11**: 862 [PMID: 33060568 DOI: 10.1038/s41419-020-03044-1]
 - 22 **Astudillo P**. Extracellular matrix stiffness and Wnt/ β -catenin signaling in physiology and disease. *Biochem Soc Trans* 2020; **48**: 1187-1198 [PMID: 32412078 DOI: 10.1042/BST20200026]
 - 23 **Liu J**, Xiao Q, Xiao J, Niu C, Li Y, Zhang X, Zhou Z, Shu G, Yin G. Wnt/ β -catenin signalling: function, biological mechanisms, and therapeutic opportunities. *Signal Transduct Target Ther* 2022; **7**: 3 [PMID: 34980884 DOI: 10.1038/s41392-021-00762-6]
 - 24 **Pal I**, Rajesh Y, Banik P, Dey G, Dey KK, Bharti R, Naskar D, Chakraborty S, Ghosh SK, Das SK, Emdad L, Kundu SC, Fisher PB, Mandal M. Prevention of epithelial to mesenchymal transition in colorectal carcinoma by regulation of the E-cadherin- β -catenin-vinculin axis. *Cancer Lett* 2019; **452**: 254-263 [PMID: 30904616 DOI: 10.1016/j.canlet.2019.03.008]
 - 25 **Bian J**, Dannappel M, Wan C, Firestein R. Transcriptional Regulation of Wnt/ β -Catenin Pathway in Colorectal Cancer. *Cells* 2020; **9** [PMID: 32961708 DOI: 10.3390/cells9092125]
 - 26 **Lee YJ**, Kang CW, Oh JH, Kim J, Park JP, Moon JH, Kim EH, Lee S, Kim SH, Ku CR, Lee EJ. Downregulation of miR-216a-5p and miR-652-3p is associated with growth and invasion by targeting JAK2 and PRRX1 in GH-producing pituitary tumours. *J Mol Endocrinol* 2021; **68**: 51-62 [PMID: 34738916 DOI: 10.1530/JME-21-0070]
 - 27 **Marchand B**, Pitarresi JR, Reichert M, Suzuki K, Laczkó D, Rustgi AK. PRRX1 isoforms cooperate with FOXM1 to regulate the DNA damage response in pancreatic cancer cells. *Oncogene* 2019; **38**: 4325-4339 [PMID: 30705403 DOI: 10.1038/s41388-019-0725-6]
 - 28 **Jiang J**, Zheng M, Zhang M, Yang X, Li L, Wang SS, Wu JS, Yu XH, Wu JB, Pang X, Tang YJ, Tang YL, Liang XH. PRRX1 Regulates Cellular Phenotype Plasticity and Dormancy of Head and Neck Squamous Cell Carcinoma Through miR-642b-3p. *Neoplasia* 2019; **21**: 216-229 [PMID: 30622052 DOI: 10.1016/j.neo.2018.12.001]
 - 29 **Fan M**, Shen J, Liu H, Wen Z, Yang J, Yang P, Liu K, Chang Y, Duan J, Lu K. Downregulation of PRRX1 *via* the p53-dependent signaling pathway predicts poor prognosis in hepatocellular carcinoma. *Oncol Rep* 2017; **38**: 1083-1090 [PMID: 28677793 DOI: 10.3892/or.2017.5785]



Intensive follow-up vs conventional follow-up for patients with non-metastatic colorectal cancer treated with curative intent: A meta-analysis

Li-Li Cui, Shi-Qi Cui, Zhong Qu, Zhen-Qing Ren

Specialty type: Oncology

Provenance and peer review:

Unsolicited article; Externally peer reviewed.

Peer-review model: Single blind

Peer-review report's scientific quality classification

Grade A (Excellent): 0
Grade B (Very good): B
Grade C (Good): C
Grade D (Fair): 0
Grade E (Poor): 0

P-Reviewer: Kobayashi S, Japan;
Moshref L, Saudi Arabia

Received: June 21, 2023

Peer-review started: June 21, 2023

First decision: September 6, 2023

Revised: September 22, 2023

Accepted: October 30, 2023

Article in press: October 30, 2023

Published online: December 15, 2023



Li-Li Cui, Department of Operating Room, Jiangsu Taizhou People's Hospital, Taizhou 225300, Jiangsu Province, China

Shi-Qi Cui, Department of Oncology, Sir Run Run Shaw Hospital, Zhejiang University School of Medicine, Hangzhou 310020, Zhejiang Province, China

Zhong Qu, Department of Endoscopy Center, Sir Run Run Shaw Hospital, Zhejiang University School of Medicine, Hangzhou 310020, Zhejiang Province, China

Zhen-Qing Ren, Department of Nursing, Jiangsu Taizhou People's Hospital, Taizhou 225300, Jiangsu Province, China

Corresponding author: Zhen-Qing Ren, MA, Department of Nursing, Jiangsu Taizhou People's Hospital, No. 366 Taihu Road, Pharmaceutical and High-tech Zone, Taizhou 225300, Jiangsu Province, China. 635818285@qq.com

Abstract

BACKGROUND

The frequency and content of follow-up strategies remain controversial for colorectal cancer (CRC), and scheduled follow-ups have limited value.

AIM

To compare intensive and conventional follow-up strategies for the prognosis of non-metastatic CRC treated with curative intent using a meta-analysis.

METHODS

PubMed, Embase, and the Cochrane Library databases were systematically searched for potentially eligible randomized controlled trials (RCTs) from inception until April 2023. The Cochrane risk of bias was used to assess the methodological quality of the included studies. The hazard ratio, relative risk, and 95% confidence interval were used to calculate survival and categorical data, and pooled analyses were performed using the random-effects model. Additional exploratory analyses were performed for sensitivity, subgroups, and publication bias.

RESULTS

Eighteen RCTs involving 8533 patients with CRC were selected for the final

analysis. Intensive follow-up may be superior to conventional follow-up in improving overall survival, but this difference was not statistically significant. Moreover, intensive follow-up was associated with an increased incidence of salvage surgery compared to conventional follow-up. In addition, there was no significant difference in the risk of recurrence between intensive and conventional follow-up strategies, whereas intensive follow-up was associated with a reduced risk of interval recurrence compared to conventional follow-up. Finally, the effects of intensive and conventional follow-up strategies differed when stratified by tumor location and follow-up duration.

CONCLUSION

Intensive follow-up may have a beneficial effect on the overall survival of patients with non-metastatic CRC treated with curative intent.

Key Words: Intensive follow-up; Conventional follow-up; Colorectal cancer; Curative intent; Meta-analysis

©The Author(s) 2023. Published by Baishideng Publishing Group Inc. All rights reserved.

Core Tip: This systematic review and meta-analysis aimed to determine the effects of intensive *vs* conventional follow-up strategies on the prognosis of patients with colorectal cancer (CRC) treated with curative intent by examining randomized controlled trials (RCTs). This study found that an intensive follow-up strategy might have beneficial effects on overall survival. Moreover, an intensive follow-up strategy was associated with an increased incidence of salvage surgery and a reduced risk of interval survival. Further large-scale RCTs should assess the effects of intensive follow-up with a specific frequency and content for non-metastatic CRC treated with curative intent.

Citation: Cui LL, Cui SQ, Qu Z, Ren ZQ. Intensive follow-up *vs* conventional follow-up for patients with non-metastatic colorectal cancer treated with curative intent: A meta-analysis. *World J Gastrointest Oncol* 2023; 15(12): 2197-2211

URL: <https://www.wjgnet.com/1948-5204/full/v15/i12/2197.htm>

DOI: <https://dx.doi.org/10.4251/wjgo.v15.i12.2197>

INTRODUCTION

Colorectal cancer (CRC) is the third most frequently diagnosed cancer, which accounted for more than 1.9 million cases and 900000 cancer-related deaths worldwide in 2000, thereby causing a great public health burden[1,2]. The incidence and prognosis of CRC have improved because of the use of population-based screening programs and understanding the necessity of a healthy lifestyle. Early diagnosis and treatment are significantly related to CRC prognosis[3]. The 5-year survival rate is 90% for stage I-II CRC and is reduces to 14% for stage IV CRC[4]. The standard treatment for early-stage CRC is curative surgery, and tumor node metastasis is an important predictor of early-stage CRC prognosis and other prognostic factors, including tumor location and clinicopathological results[5-7]. Nevertheless, 10%-20% of patients develop recurrent disease, and an additional follow-up strategy should be applied to improve CRC prognosis.

Curative surgery aims for the early detection of treatable recurrence and improving CRC prognosis. Generally, there is a long follow-up duration for patients with CRC treated through curative surgery. However, the frequency and content of follow-ups remain controversial for CRC, and scheduled follow-ups have limited value[8-10]. A prior meta-analysis found that the use of intensive follow-up strategies could improve overall survival compared to conventional follow-up strategies. However, the pooled analyses did not yield a conclusive solution[11]. Moreover, stratified analyses based on studies and patient characteristics were not performed. Therefore, this systematic review and meta-analysis was conducted to determine the effects of intensive *vs* conventional follow-up strategies on the prognosis of patients with CRC treated with curative intent. The study chose randomized controlled trials (RCTs) for its data.

MATERIALS AND METHODS

Search strategy and selection criteria

This study was conducted according to the Preferred Reporting Items for Systematic Reviews and Meta-Analysis guidelines[12]. RCTs comparing the effects of intensive and conventional follow-up strategies for non-metastatic CRC treated with curative intent were eligible for our study, and the publication language was restricted to English. We systematically searched PubMed, Embase, and the Cochrane library for eligible trials throughout April 2023, and we used the following search terms: ("colorectal neoplasms") AND ("recurrence" OR "metastasis" OR "survival analysis" OR "mortality" OR "prognosis") AND ("follow up" OR "episode of care" OR "surveillance") AND ("randomized controlled trials"). Trials that had already been completed but had not yet been published were also searched on the ClinicalTrials.gov website (NIH, United States). Manual searches were also performed on the reference lists of the relevant reviews to identify any new trials that met the inclusion criteria.

Two reviewers independently conducted the literature search and trial screening, and conflicts between the reviewers were resolved *via* discussions. Studies were included if they met the following criteria: (1) Patients: All patients with non-metastatic CRC who were treated with curative intent surgery; (2) Intervention: Intensive follow-up strategy; (3) Control: Conventional follow-up strategy; (4) Outcome: The study should report at least one outcome of overall survival, cancer-specific survival, relapse-free survival, salvage surgery, recurrence, and interval recurrences; and (5) Study design: All included studies had to have an RCT design.

Data collection and quality assessment

The following data were independently collected from the included trials: First author's name, publication year, region, sample size, mean age, proportion of males, tumor stage (Dukes' stage A/B/C), tumor location (colon cancer/rectal cancer), treatments (curative intent surgery and subsequent adjuvant treatments), intervention, control, follow-up, and reported outcomes (overall survival, cancer-specific survival, relapse-free survival, salvage surgery, recurrence, and interval recurrences). The Cochrane risk of bias was used to assess methodological quality, including random sequence generation, allocation concealment, blinding of participants and personnel, blinding of outcome assessment, incomplete outcome data, selective reporting, and other biases[13]. Each item was defined as having a low, high, or an unclear risk of bias. Two reviewers independently performed the abstracted data and methodological quality assessments, and a third reviewer who referred to the original article settled inconsistent results.

Statistical analysis

The effects of intensive *vs* conventional follow-up strategies on survival and categorical data were assigned as hazard ratios (HR), relative risks (RR), and 95% confidence intervals (CI), and pooled analyses were performed using the random-effects model because it considers the underlying variations across the included trials[14,15]. Heterogeneity among the included trials was evaluated using I^2 and Q statistics, and significant heterogeneity was defined as $I^2 > 50%$ or $P < 0.10$ [16,17]. The stability of the pooled analyses were determined using sensitivity analysis through the sequential removal of a single trial[18]. Subgroup analyses of the investigated outcomes were performed based on sample size, mean age, proportion of males, tumor location, and follow-up duration, and the differences between subgroups were assessed using the interaction *t*-test, which assumes that the data distribution was normal[19]. Moreover, the ratio of HR (RHR) to RR (RRR) between the subgroups was assessed among patients without specific characteristics[20]. Funnel plots, Egger's test, and Begg's test were used to assess potential publication bias[21,22]. All reported *P* values for the pooled analyses were 2-sided, and the inspection level was 0.05. Statistical analyses were performed using the STATA software (version 10.0; Stata Corporation, College Station, TX, United States).

RESULTS

Literature search and study selection

A total of 2671 articles were identified from the initial electronic search, and 1743 studies were retained after duplicate articles were removed. Subsequently, 1698 studies were excluded because they reported irrelevant topics, and the remaining 45 studies were retrieved for full-text evaluation. Reviewing the reference lists yielded two potentially eligible studies, and 46 articles were subjected to detailed evaluation. After this, 28 studies were excluded because they reported the same population ($n = 15$), did not have an RCT design ($n = 9$), or included cancers at other stages ($n = 4$). The remaining 18 RCTs were included in the final meta-analysis[23-40]. Details of the study selection process are shown in Figure 1.

Trials' characteristics

Table 1 summarizes the baseline characteristics of the identified trials and patients involved. A total of 8533 patients with CRC were included from 18 RCTs, and the sample sizes ranged from 106 to 2509. Seventeen of the included trials were performed in Western countries, including Australia and European countries, whereas the remaining one trial was conducted in China. The follow-up duration ranged from 1.0-10.0 years. Details of the methodological quality of the included trials are listed in Table 2. Most of the included trials were of moderate to high quality, and three were of low quality.

Overall survival

Sixteen trials reported the effects of intensive *vs* conventional follow-up strategies on overall survival. There was no significant difference between intensive and conventional follow-up strategies for the improvement of overall survival (HR = 0.90; 95%CI: 0.81-1.01; $P = 0.062$; Figure 2A), and no evidence of heterogeneity was observed across the included trials ($I^2 = 0.0%$; $P = 0.643$). Sensitivity analysis indicated that an intensive follow-up strategy might be associated with an improvement in overall survival compared to a conventional follow-up strategy (Supplementary material). Subgroup analyses found that intensive follow-up was superior to conventional follow-up in overall survival if the sample size was < 500 , proportion of males was $< 60.0%$, and follow-up duration was ≥ 5.0 years (Table 3). There were no significant differences between subgroups when stratified by sample size (RHR = 1.19; 95%CI: 0.95-1.48; $P = 0.135$), mean age (RHR = 1.07; 95%CI: 0.84-1.35; $P = 0.584$), proportion of males (RHR = 1.11; 95%CI: 0.89-1.39; $P = 0.339$), tumor location (RHR = 1.07; 95%CI: 0.84-1.36; $P = 0.584$), and follow-up (RHR = 0.86; 95%CI: 0.69-1.06; $P = 0.163$). No significant publication bias for overall survival was observed (P value for Egger's test: 0.753; P value for Begg's test: 0.558; Supplementary material).

Table 1 The baseline characteristics of included trials and recruited patients

Ref.	Region	Sample size	Age (yr)	Male (%)	Stage (A/B/C)	Tumor location (C/R)	Treatments	Intervention	Control	Follow-up duration
Mäkelä <i>et al</i> [23], 1995	Finland	106	66.0	49.1	(A/B/C) 28/48/30	75/31	Radical resection denotes surgical removal of all macroscopic tumor tissue with microscopically evaluated clearance of the surgical margins	Flexible sigmoidoscopy with video imaging every 3 mo, colonoscopy at 3 mo, then annually. They also had ultrasound of the liver and primary site at 6 mo, then annually	Rigid sigmoidoscopy and barium enema annually	5.0 yr
Ohlsson <i>et al</i> [24], 1995	Sweden	107	65.6	47.7	(A/B/C) 19/47/41	71/36	Resection with curative intent and early postoperative colonoscopy	Performed at each visit were clinical exam, rigid proctosigmoidoscopy, CEA, alkaline phosphatase, gamma-glutamyl transferase, faecal haemoglobin, and CXR. Examination of anastomosis was performed at 9, 21, and 42 mo. Colonoscopy was performed at 3, 15, 30, and 60 mo. CT of the pelvis was performed at 3, 6, 12, 18, and 24 mo	Written instructions recommending that they leave faecal samples with the district nurse for examination every 3 mo during the first 2 yr then once a year. They contact the surgical department if they had any symptoms	5.5-8.8 yr
Kjeldsen <i>et al</i> [25], 1997	Denmark	597	< 76.0	54.6	(A/B/C) 138/293/166	314/283	Radical primary surgery and no residual neoplasia was detected by complete colonoscopy or incomplete colonoscopy plus double-contrast barium enema, chest radiograph, histological examination of all resection margins in surgical specimens, biopsy of lesions, and inspection and palpation of the liver during surgery	Examinations at 6, 12, 18, 30, 36, 48, 60, 120, 150, and 180 mo after radical surgery (medical history, clinical examination, digital rectal examination, gynaecological examination, Haemocult-II test, colonoscopy, CXR, haemoglobin level, erythrocyte sedimentation rate, and liver enzymes)	Examinations at 60, 120, and 180 mo (medical history, clinical examination, digital rectal examination, gynaecological examination, Haemocult-II test, colonoscopy, CXR, haemoglobin level, erythrocyte sedimentation rate, and liver enzymes)	5.0-10.0 yr
Pietra <i>et al</i> [26], 1998	Italy	207	63.3	53.6	(A/B/C) 0/122/85	139/68	Curative resection defined as one in which no macroscopic tumor remained at the end of the operation and in which histopathologic examination of the operative specimen showed no tumor at the lines of resection	Examinations at 3, 6, 9, 12, 15, 18, 21, 24, 30, 36, 42, 48, 54, and 60 mo, then annually thereafter. There was clinical examination, ultrasound, CEA, and CXR at each visit. Annual CT of the liver and colonoscopy were performed	Examinations at 6 and 12 mo, then annually. At each visit, clinical examination, CEA, and ultrasound were performed. They had annual CXR, yearly colonoscopy, and CT scan	5.0 yr
Schoemaker <i>et al</i> [27], 1998	Australia	325	68.0	63.7	(A/B/C) 71/153/101	238/87	Curative resection	Yearly CXR, CT of the liver, and colonoscopy	Clinical grounds or after screening test abnormality, and at 5 yr of follow-up, to exclude a reservoir of undetected recurrences	5.0 yr
Secco <i>et al</i> [28], 2002	Italy	337	65.1	48.4	(A or B/C) 201/136	NA	Putative curative surgery alone, which defined as macroscopic excision of the primary tumour, peritumoral tissues and palpable locoregional lymph nodes	Clinic visits and serum CEA, abdomen/pelvic US scans, and CXR. Participants with rectal carcinoma had rigid sigmoidoscopy and CXR	Minimal follow-up programme performed by physicians	4.0-5.1 yr
Rodríguez-Moranta <i>et al</i> [29], 2006	Spain	259	68.0	62.2	(II/III) 157/102	194/65	Curative resection, complete colon study was achieved with colonoscopy to determine the presence of synchronous lesions. If colonoscopy of the entire bowel could not be performed before resection, a postoperative colonoscopy was	Seen with history, examination, and bloods (including CEA) at 3, 6, 9, 12, 15, 18, 21, 24, 27, 30, 33, 36, 39, 42, 45, 48, 51, 54, 57, and 60 mo; US/CT at 6, 12, 18, 24, 30, 36, 42, 48, and 56 mo; CXR and colonoscopy at 12, 24, 36, 48, and 56 mo	Seen with history, examination, and bloods (including CEA) at 3, 6, 9, 12, 15, 18, 21, 24, 27, 30, 33, 36, 39, 42, 45, 48, 51, 54, 57, and 60 mo	4.0 yr

							warranted				
Wattchow <i>et al</i> [30], 2006	Australia	203	NA	53.6	(A/B/C) 47/96/60	203/0	Curative surgery and completion of postsurgical chemotherapy	Every 3 mo for the first 2 yr postoperatively, then every 6 mo for the next 3 yr	Asking a list of set questions about symptoms, physical examination, annual faecal occult blood testing, and colonoscopy every 3 yr	2.0 yr	
Sobhani <i>et al</i> [31], 2008	France	130	60.1	NA	IV: 17	75/55	Curative surgery, compliance with adjuvant chemotherapy, and the absence of disease progression and/or missed synchronous metastases were checked	PET performed at 9 and 15 mo and conventional follow-up	Conventional follow-up	2.0 yr	
Wang <i>et al</i> [32], 2009	China	326	54.5	54.3	(A/B/C) 100/133/93	171/155	Curative surgery, which was defined as one in which no macroscopic tumor remained at the end of the operation and in which histopathologic examination of the operative specimen demonstrated no tumor at the margins of resection	Colonoscopy at each visit	Colonoscopy at 6 mo, 30 mo, and 60 mo from randomisation	5.3-6.5 yr	
Strand <i>et al</i> [33], 2011	Sweden	110	68.0	53.6	(I/II/III/IV) 26/40/36/8	0/110	Curative surgery, all patients had a first postoperative visit with the surgeon for information on histology and adjuvant therapy. Consecutive patients were asked to participate at various postoperative controls starting after the adjuvant chemotherapy was terminated	Surgeon-led follow-up	Nurse-led follow-up	5.0 yr	
Augestad <i>et al</i> [34], 2013	Norway	110	65.4	59.1	(A/B/C) 24/55/32	110/0	Surgery and received postsurgical adjuvant chemotherapy	Surgeon follow-up	GP follow-up	2.0 yr	
Primrose <i>et al</i> [35], 2014	United Kingdom	1202	69.2	61.2	(A/B/C) 254/553/354	811/359	Curative surgery, and adjuvant treatment if indicated, with no evidence of residual disease on investigation	CEA testing every 3 mo for 2 yr, then every 6 mo for 3 yr with a single CT scan of the chest/abdomen/pelvis if requested at study entry by clinician; CT scan of the chest/abdomen/pelvis every 6 mo for 2 yr, then annually for 3 yr, plus colonoscopy at 2 yr; CEA and CT follow-up: Both blood and imaging as above, plus colonoscopy at 2 yr	No scheduled follow-up except a single CT scan of the chest/ abdomen/pelvis if requested at study entry by a clinician	3.4 yr	
Treasure <i>et al</i> [36], 2014	United Kingdom	216	63.0	59.3	(A/B/C) 10/95/101	NA	Curative resection for adenocarcinoma of the colon or rectum and who were fit and willing to adhere to the postoperative monitoring routine	CEA rise triggered the “second-look” surgery, with intention to remove any recurrence discovered	Conventional follow-up	2.0 yr	
Rosati <i>et al</i> [37], 2016	Italy	1228	63.9	60.7	(B/C) 617/611	933/295	Curative intent, with adjuvant radio-chemotherapy if indicated	4, 8, 12, 16, 20, 24, 30, 36, 42, 48, and 60 monthly office visits and history and clinical examination, FBC, CEA, and CA 19-9; colonoscopy and CXR at 12, 24, 36, 48, and 60 mo; liver US at 4, 8, 12, 16, 24, 36, 48, and 60 mo; for rectal participants, pelvic CT at 4, 12, 24, and 48 mo	4, 8, 12, 16, 20, 24, 30, 42, 48, and 60 monthly office visits, including history, examination, and CEA; colonoscopy at 12 and 48 mo; liver US at 4 and 16 mo; rectal cancer participants in addition had rectoscopy at 4 mo, CXR at 12 mo, and liver US at 8 and 16 mo. A single pelvic CT was allowed if a radiation oncologist required it as baseline following adjuvant treatment	5.2 yr	

Wille-Jørgensen <i>et al</i> [38], 2018	Denmark and Uruguay	2509	64.9	55.0	(II/III) 1352/1157	884/1625	Curative intent, with adjuvant treatment if indicated, a colon and rectum free of neoplasia verified by perioperative barium enema or a colonoscopy within 3 mo after surgery	Multislice contrast-enhanced CT of the thorax and abdomen and CEA at 6, 12, 18, 24, and 36 mo after surgery	Multislice contrast-enhanced CT of the thorax and abdomen and CEA at 12 and 36 mo after surgery	3.0 yr
Rahr <i>et al</i> [39], 2019	Denmark	196	70.0	63.8	(I/II/III/IV) 47/66/49/16	140/56	Elective surgery for verified or suspected CRC were screened by a study nurse for cardiopulmonary comorbidity at the preoperative visit	Routine follow-up with one extra medical visit and additional visits to the Cardiology and Respiratory Medicine Clinics 1 and 3 mo postoperatively	Routine follow-up	1.0 yr
Monteil <i>et al</i> [40], 2021	France	365	65.0	54.8	(I/II/III/IV) 2/176/185/2	290/75	Curative surgery, with adjuvant treatment if indicated	PET/CT and conventional follow-up every 3 mo	CEA, liver echography, and alternated between lung radiography and CT scans	3.0 yr

PET-CT: Positron emission tomography/computed tomography; CXR: Chest radiography; CEA: Carcinoembryonic antigen; CA: Carbohydrate antigen; US: Ultrasound.

Cancer-specific survival

Ten trials reported the effects of intensive *vs* conventional follow-up strategies on cancer-specific survival. No significant difference between intensive and conventional follow-up strategies was observed for improvement in cancer-specific survival (HR = 0.98; 95%CI: 0.83-1.15; $P = 0.785$; **Figure 2B**), and unimportant heterogeneity was detected across the included trials ($I^2 = 17.8\%$; $P = 0.280$). Sensitivity analysis indicated that the pooled analyses were stable and not altered by the sequential removal of a single trial (**Supplementary material**). The results of the subgroup analyses were consistent with those of the overall analysis in all subgroups (**Table 3**). Moreover, the differences between subgroups were not statistically significant when stratified by sample size (RHR = 1.04; 95%CI: 0.70-1.54; $P = 0.837$), mean age (RHR = 1.23; 95%CI: 0.84-1.79; $P = 0.281$), proportion of males (RHR = 1.09; 95%CI: 0.75-1.60; $P = 0.645$), tumor location (RHR = 1.35; 95%CI: 0.89-2.05; $P = 0.155$), and follow-up (RHR = 0.82; 95%CI: 0.58-1.15; $P = 0.245$). There was no significant publication bias for cancer-specific survival (P value for Egger's test: 0.492; P value for Begg's test: 0.858; **Supplementary material**).

Relapse-free survival

Fifteen trials reported the effects of intensive *vs* conventional follow-up strategies on relapse-free survival. There was no significant difference between intensive and conventional follow-up strategies for improvement in relapse-free survival (HR = 1.08; 95%CI: 0.97-1.22; $P = 0.168$; **Figure 2C**), and non-significant heterogeneity was observed among the included trials ($I^2 = 10.8\%$; $P = 0.333$). Sensitivity analysis revealed that intensive follow-up may be associated with poor relapse-free survival after excluding the trial performed by Schoemaker *et al* [27] (**Supplementary material**). Subgroup analyses indicated that an intensive follow-up strategy was associated with poor relapse-free survival when the sample size was ≥ 500 (**Table 3**). Furthermore, there were no significant differences between subgroups when stratified by sample size (RHR = 1.24; 95%CI: 0.99-1.56; $P = 0.063$), mean age (RHR = 1.02; 95%CI: 0.79-1.31; $P = 0.885$), proportion of males (RHR = 1.08; 95%CI: 0.80-1.45; $P = 0.633$), tumor location (RHR = 1.04; 95%CI: 0.81-1.32; $P = 0.778$), and follow-up (RHR = 0.87; 95%CI: 0.68-1.11; $P = 0.265$). No significant publication bias was observed for relapse-free survival (P value for Egger's test: 0.189; P value for Begg's test: 0.621; **Supplementary material**).

Salvage surgery

Fourteen trials reported the effects of intensive *vs* conventional follow-up strategies on the incidence of salvage surgery. We noted that intensive follow-up significantly increased the risk of salvage surgery compared to a conventional follow-

Table 2 The methodological quality assessment of included trials

Ref.	Random sequence generation	Allocation concealment	Blinding of participants and personnel	Blinding of outcome assessment	Incomplete outcome data	Selective reporting	Other bias
Mäkelä <i>et al</i> [23], 1995	Unclear	Unclear	Low risk	Unclear	Low risk	Unclear	Unclear
Ohlsson <i>et al</i> [24], 1995	Unclear	Unclear	Low risk	Unclear	Low risk	Unclear	Unclear
Kjeldsen <i>et al</i> [25], 1997	Unclear	Unclear	Unclear	High risk	Low risk	Unclear	Unclear
Pietra <i>et al</i> [26], 1998	Unclear	Unclear	Low risk	Unclear	High risk	Unclear	Unclear
Schoemaker <i>et al</i> [27], 1998	Low risk	High risk	Low risk	Low risk	Low risk	Unclear	Unclear
Secco <i>et al</i> [28], 2002	Unclear	Unclear	Unclear	Low risk	Unclear	Unclear	Unclear
Rodríguez-Moranta <i>et al</i> [29], 2006	Low risk	Low risk	Unclear	Unclear	Low risk	Unclear	Unclear
Wattchow <i>et al</i> [30], 2006	Low risk	Low risk	Low risk	Low risk	Low risk	Unclear	Unclear
Sobhani <i>et al</i> [31], 2008	Unclear	Unclear	Low risk	Low risk	Low risk	Unclear	Unclear
Wang <i>et al</i> [32], 2009	Unclear	Unclear	High risk	High risk	Unclear	Unclear	Unclear
Strand <i>et al</i> [33], 2011	Unclear	Unclear	Low risk	Low risk	Unclear	Unclear	Unclear
Augestad <i>et al</i> [34], 2013	Unclear	Low risk	Low risk	Low risk	Low risk	Unclear	Unclear
Primrose <i>et al</i> [35], 2014	Low risk	Low risk	Unclear	Low risk	Low risk	Low risk	Unclear
Treasure <i>et al</i> [36], 2014	Low risk	Low risk	Low risk	Low risk	Unclear	Low risk	Low risk
Rosati <i>et al</i> [37], 2016	Unclear	Unclear	Unclear	Unclear	Low risk	Unclear	Unclear
Wille-Jørgensen <i>et al</i> [38], 2018	Low risk	Low risk	Low risk	Low risk	Unclear	Low risk	Low risk
Rahr <i>et al</i> [39], 2019	Low risk	Unclear	Unclear	Unclear	Low risk	Unclear	Unclear
Monteil <i>et al</i> [40], 2021	Unclear	Unclear	Unclear	Low risk	Low risk	Unclear	Unclear

up strategy (RR = 1.99; 95%CI: 1.57-2.53; $P < 0.001$; Figure 2D), and unimportant heterogeneity was detected among the included trials ($I^2 = 25.0\%$; $P = 0.184$). The pooled analyses for the incidence of salvage surgery were robust and not altered by any specific trial (Supplementary material). The results of the subgroup analyses were consistent with those of the overall analysis, and significant differences between the intensive and conventional follow-up strategies were observed in all subgroups (Table 3). We noted that intensive *vs* conventional follow-up strategies on salvage surgery in tumor location [colon/rectal ratio (C/R)] $\geq 70.0\%$ was lower than tumor location (C/R) $< 70.0\%$ (RRR = 0.54; 95%CI: 0.31-0.92; $P = 0.022$). There was no significant publication bias for salvage surgery (P value for Egger's test: 0.419; P value for Begg's test: 1.000; Supplementary material).

Recurrence

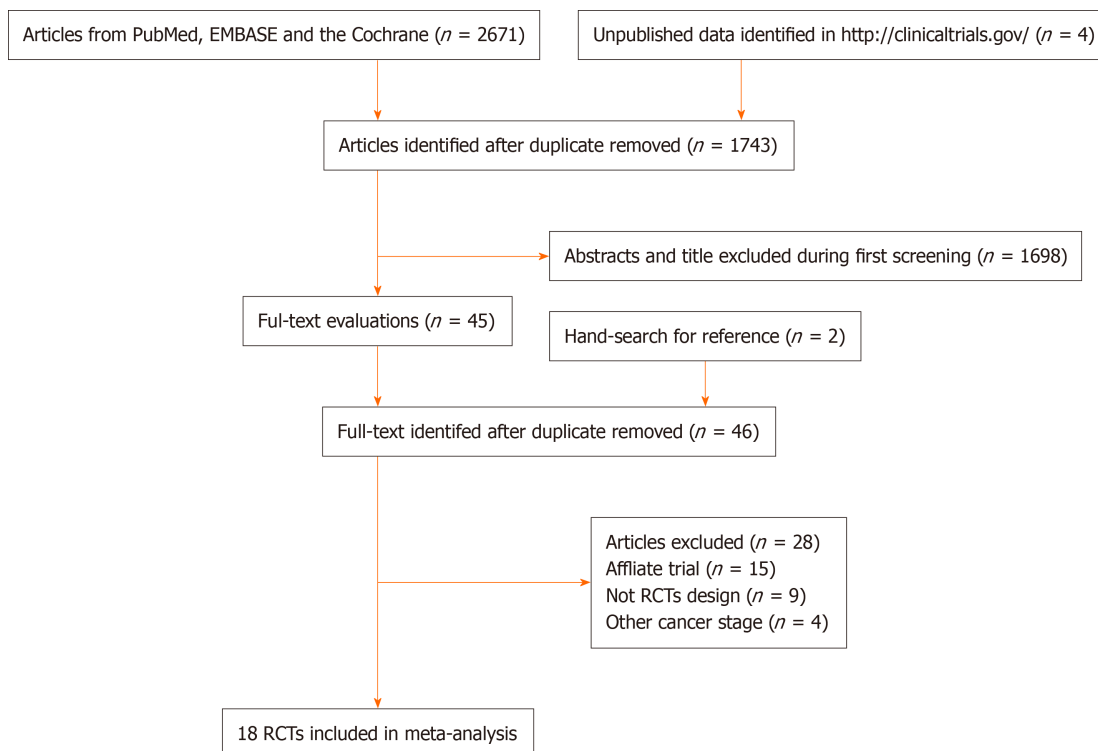
Fifteen trials reported the effects of intensive *vs* conventional follow-up strategies on the risk of recurrence. We noted that the intensive follow-up strategy had no significant effect on the risk of recurrence (RR = 1.13; 95%CI: 0.98-1.31; $P = 0.094$; Figure 2E), and significant heterogeneity was observed across the included trials ($I^2 = 51.6\%$; $P = 0.011$). Sensitivity analysis indicated that the intensive follow-up strategy was associated with an elevated risk of recurrence when the trial conducted by Secco *et al*[28] was excluded (Supplementary material). Subgroup analyses suggested that the intensive follow-up strategy was associated with an increased risk of recurrence when the sample size was ≥ 500 and the mean age was < 65.0 years (Table 3). Moreover, the differences between subgroups were not statistically significant when stratified

Table 3 Subgroup analyses for investigated outcomes

Outcomes	Factors	Subgroups	No. of studies	HR or RR and 95%CI	P value	I ² (%)	P value for I ²	Interaction P value	RHR or RRR with 95%CI		
Overall survival	Sample size	≥ 500	4	0.96 (0.84-1.10)	0.579	0.0	0.581	0.135	1.19 (0.95-1.48)		
		< 500	12	0.81 (0.68-0.97)	0.019	0.0	0.693				
	Mean age (yr)	≥ 65.0	9	0.94 (0.78-1.14)	0.538	0.0	0.563			0.584	1.07 (0.84-1.35)
		< 65.0	6	0.88 (0.77-1.02)	0.082	7.7	0.367				
	Male (%)	≥ 60.0	5	0.97 (0.81-1.16)	0.758	0.0	0.503			0.339	1.11 (0.89-1.39)
		< 60.0	11	0.87 (0.76-0.99)	0.035	0.0	0.620				
	Tumor location (C/R)	≥ 70.0	8	0.93 (0.78-1.11)	0.429	0.0	0.742			0.584	1.07 (0.84-1.36)
		< 70.0	7	0.87 (0.74-1.02)	0.082	16.9	0.301				
Follow-up (yr)	≥ 5.0	8	0.84 (0.72-0.97)	0.017	0.0	0.635	0.163	0.86 (0.69-1.06)			
	< 5.0	8	0.98 (0.84-1.15)	0.837	0.0	0.658					
Cancer-specific survival	Sample size	≥ 500	4	0.99 (0.83-1.17)	0.866	0.0	0.804	0.837	1.04 (0.70-1.54)		
		< 500	6	0.95 (0.67-1.36)	0.782	49.4	0.079				
	Mean age (yr)	≥ 65.0	5	1.12 (0.80-1.57)	0.515	29.3	0.226			0.281	1.23 (0.84-1.79)
		< 65.0	5	0.91 (0.77-1.08)	0.276	0.0	0.510				
	Male (%)	≥ 60.0	3	1.05 (0.77-1.43)	0.750	0.0	0.603			0.645	1.09 (0.75-1.60)
		< 60.0	7	0.96 (0.77-1.20)	0.732	37.6	0.142				
	Tumor location (C/R)	≥ 70.0	4	1.23 (0.84-1.81)	0.281	23.9	0.268			0.155	1.35 (0.89-2.05)
		< 70.0	6	0.91 (0.78-1.07)	0.254	0.0	0.560				
Follow-up (yr)	≥ 5.0	5	0.89 (0.72-1.10)	0.288	0.0	0.464	0.245	0.82 (0.58-1.15)			
	< 5.0	5	1.09 (0.83-1.42)	0.552	35.9	0.182					
Relapse-free survival	Sample size	≥ 500	4	1.18 (1.02-1.36)	0.025	18.8	0.296	0.063	1.24 (0.99-1.56)		
		< 500	11	0.95 (0.80-1.14)	0.589	0.0	0.583				
	Mean age (yr)	≥ 65.0	9	1.10 (0.89-1.36)	0.388	23.5	0.234			0.885	1.02 (0.79-1.31)
		< 65.0	6	1.08 (0.95-1.23)	0.220	3.6	0.394				
	Male (%)	≥ 60.0	4	1.14 (0.87-1.50)	0.340	51.1	0.105			0.633	1.08 (0.80-1.45)
		< 60.0	11	1.06 (0.94-1.20)	0.364	0.0	0.569				
	Tumor location (C/R)	≥ 70.0	6	1.15 (0.94-1.40)	0.171	9.5	0.355			0.778	1.04 (0.81-1.32)
		< 70.0	7	1.11 (0.96-1.28)	0.159	6.2	0.380				
Follow-up (yr)	≥ 5.0	8	1.01 (0.86-1.18)	0.917	0.0	0.597	0.265	0.87 (0.68-1.11)			
	< 5.0	7	1.16 (0.96-1.39)	0.120	27.9	0.215					
Salvage surgery	Sample size	≥ 500	3	2.12 (1.05-4.29)	0.036	71.7	0.029	0.990	1.00 (0.48-2.11)		
		< 500	11	2.11 (1.67-2.66)	< 0.001	0.0	0.567				
	Mean age (yr)	≥ 65.0	8	1.95 (1.42-2.69)	< 0.001	0.0	0.910			0.675	0.89 (0.50-1.56)
		< 65.0	6	2.20 (1.38-3.50)	0.001	65.8	0.012				
	Male (%)	≥ 60.0	4	1.64 (1.06-2.53)	0.026	38.1	0.183			0.256	0.75 (0.45-1.23)
		< 60.0	9	2.19 (1.72-2.80)	< 0.001	0.0	0.726				
	Tumor location (C/R)	≥ 70.0	6	1.44 (1.08-1.91)	0.013	0.0	0.759			0.022	0.54 (0.31-0.92)
		< 70.0	6	2.69 (1.71-4.24)	< 0.001	24.0	0.254				
Follow-up (yr)	≥ 5.0	7	1.69 (1.15-2.48)	0.007	28.2	0.213	0.189	0.73 (0.46-1.16)			
	< 5.0	7	2.30 (1.79-2.97)	< 0.001	0.0	0.591					

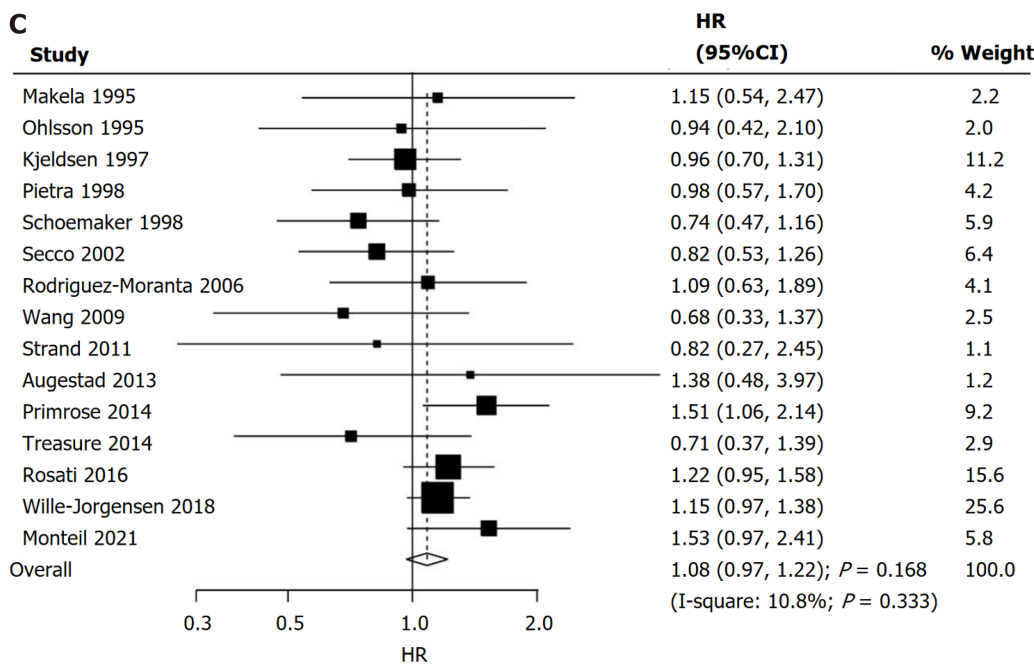
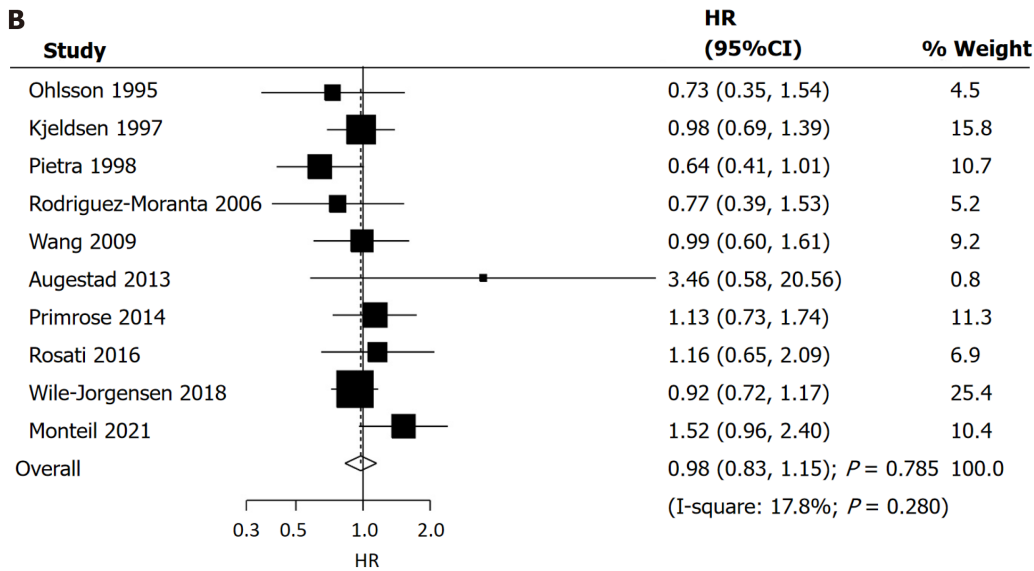
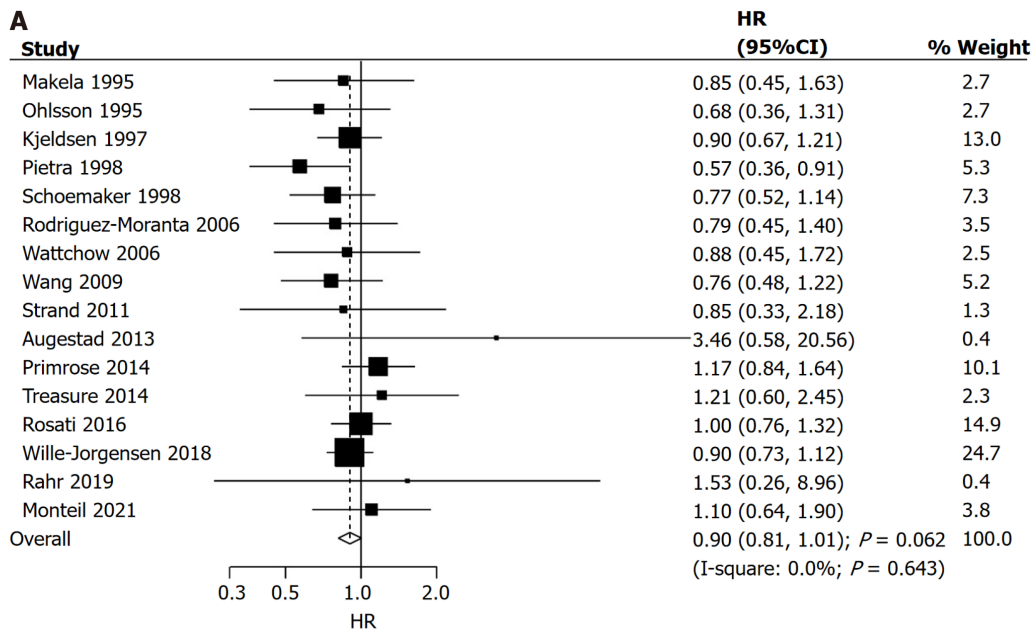
Recurrence	Sample size	≥ 500	4	1.38 (1.00-1.89)	0.048	82.1	0.001	0.075	1.37 (0.97-1.93)
		< 500	11	1.01 (0.89-1.15)	0.891	0.0	0.585		
	Mean age (yr)	≥ 65.0	8	1.23 (0.87-1.73)	0.238	75.4	< 0.001	0.645	1.09 (0.76-1.56)
		< 65.0	6	1.13 (1.01-1.26)	0.027	0.0	0.808		
	Male (%)	≥ 60.0	3	1.54 (0.71-3.30)	0.273	89.7	< 0.001	0.357	1.44 (0.66-3.12)
		< 60.0	11	1.07 (0.97-1.18)	0.185	0.0	0.618		
	Tumor location (C/R)	≥ 70.0	6	1.13 (0.96-1.32)	0.130	0.0	0.461	0.583	0.92 (0.68-1.24)
		< 70.0	8	1.23 (0.95-1.59)	0.116	64.3	0.006		
	Follow-up (yr)	≥ 5.0	8	1.09 (0.95-1.25)	0.223	0.0	0.715	0.317	0.85 (0.62-1.17)
		< 5.0	7	1.28 (0.97-1.71)	0.085	76.3	< 0.001		
Interval recurrence	Sample size	≥ 500	3	0.74 (0.45-1.20)	0.221	74.8	0.019	0.060	1.76 (0.98-3.18)
		< 500	4	0.42 (0.30-0.58)	< 0.001	0.0	0.557		
	Mean age (yr)	≥ 65.0	3	0.45 (0.34-0.60)	< 0.001	0.0	0.423	0.173	0.65 (0.35-1.21)
		< 65.0	4	0.69 (0.40-1.19)	0.182	62.0	0.048		
	Male (%)	≥ 60.0	2	0.77 (0.32-1.85)	0.558	86.9	0.006	0.424	1.48 (0.57-3.87)
		< 60.0	4	0.52 (0.35-0.77)	0.001	47.6	0.126		
	Tumor location (C/R)	≥ 70.0	2	1.12 (0.75-1.67)	0.586	0.0	0.435	0.007	1.96 (1.21-3.20)
		< 70.0	4	0.57 (0.43-0.75)	< 0.001	0.0	0.412		
	Follow-up (yr)	≥ 5.0	4	0.76 (0.47-1.23)	0.265	57.1	0.072	0.044	1.77 (1.02-3.07)
		< 5.0	3	0.43 (0.33-0.57)	< 0.001	0.0	0.795		

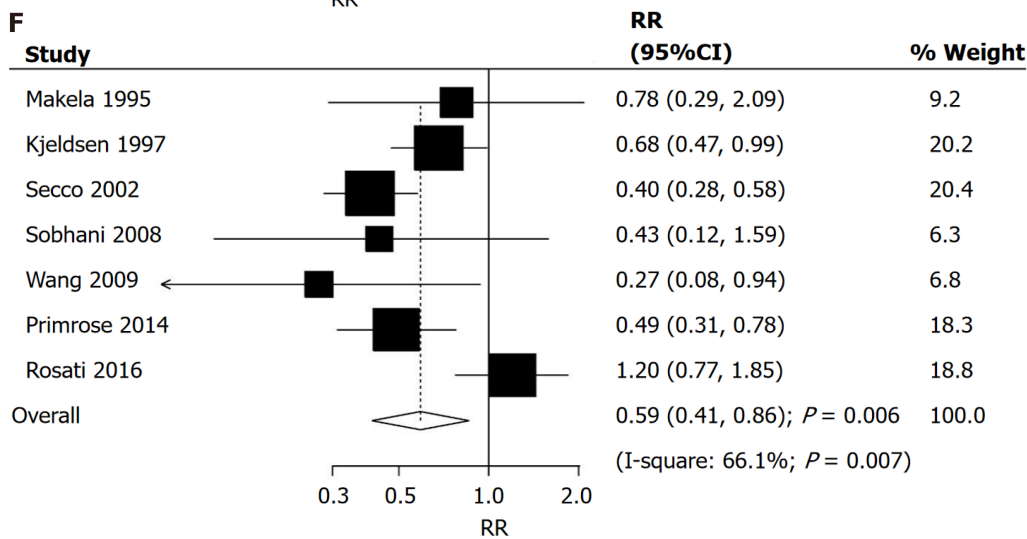
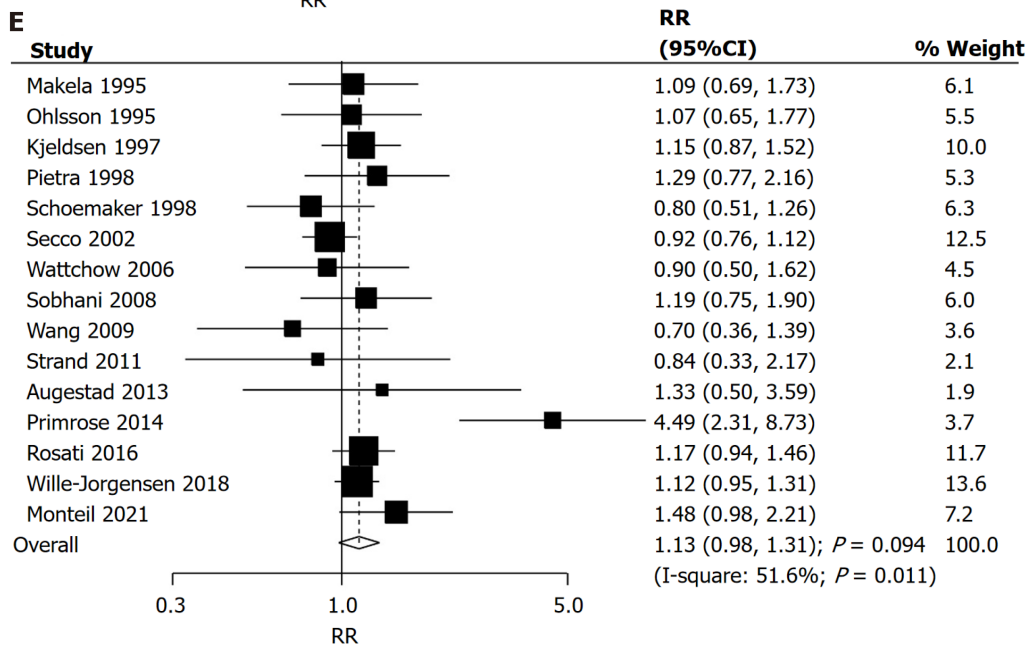
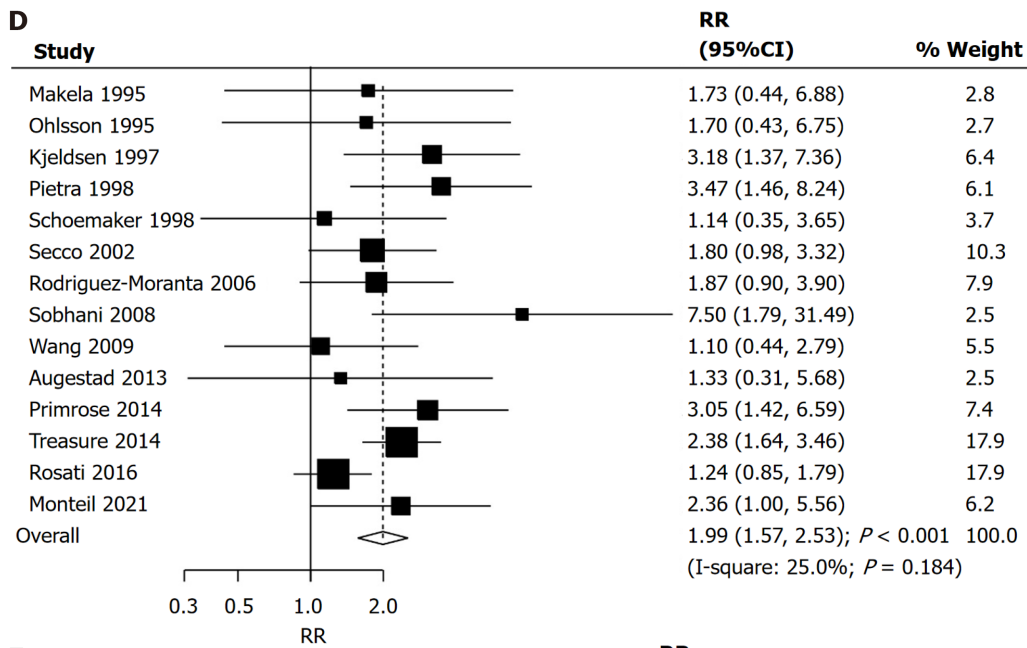
CI: Confidence interval; HR: Hazard ratio; RR: Risk ratio; RHR: Ratio of hazard ratio; RRR: Ratio of risk ratio; C/R: Colon/rectal ratio.



DOI: 10.4251/wjgo.v15.i12.2197 Copyright ©The Author(s) 2023.

Figure 1 The PRISMA flowchart for the literature search and study selection process. RCT: Randomized controlled trial.





DOI: 10.4251/wjgo.v15.i12.2197 Copyright ©The Author(s) 2023.

Figure 2 Intensive vs conventional follow-up strategies. A: On overall survival; B: On cancer-specific survival; C: On relapse-free survival; D: On salvage

surgery; E: On recurrence; F: On interval recurrences. HR: Hazard ratio; CI: Confidence interval; RR: Risk ratio.

by sample size (RRR = 1.37; 95%CI: 0.970-1.93; $P = 0.075$), mean age (RRR = 1.09; 95%CI: 0.76-1.56; $P = 0.645$), proportion of males (RRR = 1.44; 95%CI: 0.66-3.12; $P = 0.357$), tumor location (RRR = 0.92; 95%CI: 0.68-1.24; $P = 0.583$), and follow-up (RRR = 0.85; 95%CI: 0.62-1.17; $P = 0.317$). No significant publication bias was observed for recurrence (P value for Egger's test: 0.492; P value for Begg's test: 0.843; [Supplementary material](#)).

Interval recurrence

Seven trials reported the effects of intensive *vs* conventional follow-up strategies on the risk of interval recurrence. We noted that intensive follow-up significantly reduced the risk of interval recurrence compared to conventional follow-up (RR = 0.59; 95%CI: 0.41-0.86; $P = 0.006$; [Figure 2F](#)), and significant heterogeneity was observed among the included trials ($I^2 = 66.1\%$; $P = 0.007$). The sensitivity analysis indicated that the pooled analyses were not altered when a particular trial was excluded ([Supplementary material](#)). Subgroup analyses found that intensive *vs* conventional follow-up strategies were associated with a lower risk of interval recurrence if the sample size was < 500, mean age was ≥ 65.0 , proportion of males was < 60.0, tumor location (C/R) was < 70.0%, and follow-up duration was < 5.0 years ([Table 3](#)). Moreover, the effects of intensive *vs* conventional follow-up strategies on the risk of interval recurrence in the subgroups of tumor location (C/R) $\geq 70.0\%$ (RRR = 1.96; 95%CI: 1.21-3.20; $P = 0.007$) and follow-up ≥ 5.0 years (RRR = 1.77; 95%CI: 1.02-3.07; $P = 0.044$) were greater than the corresponding subgroups. There was no significant publication bias for interval recurrence (P value for Egger's test: 0.790; P value for Begg's test: 1.000; [Supplementary material](#)).

DISCUSSION

Numerous studies have addressed the effects of intensive *vs* conventional follow-up strategies on the prognosis of patients with non-metastatic CRC treated with curative intent. However, the study results are controversial. This comprehensive quantitative meta-analysis identified 8533 patients with CRC from 18 RCTs, and the patients had a broad range of characteristics. We noted that the intensive follow-up strategy was not associated with overall survival, cancer-specific survival, relapse-free survival, or recurrence compared to the conventional follow-up strategy. Moreover, intensive follow-up significantly increased the incidence of salvage surgery and reduced the risk of interval recurrence compared to conventional follow-up. Finally, the effects of intensive and conventional follow-up strategies differed when stratified by tumor location and follow-up duration.

Several systematic reviews and meta-analyses have compared the effects of intensive treatment with those of conventional follow-up strategies on the prognosis of patients with non-metastatic CRC treated with curative intent[11,41]. The results of a meta-analysis conducted by Zhao *et al*[11] were consistent with those of a Cochrane review, and the investigated outcomes were similar. A Cochrane review found that using an intensive follow-up strategy did not affect survival outcomes but could increase the incidence of salvage surgeries[41]. Although the analysis in this study was comprehensive, stratified analyses were performed only through the intervention protocol and according to the study or patient characteristics. Therefore, this study was conducted to compare the effects of intensive *vs* conventional follow-up strategies on the prognosis of non-metastatic CRC treated with curative intent by examining published RCTs.

The summary result did not reveal significant differences between intensive and conventional follow-up strategies for improving overall survival. However, this pooled analysis was not stable, and the sensitivity analysis revealed a potentially beneficial role of intensive follow-up on overall survival. A potential reason for this could be that recurrent cases can be detected early and further curative procedures can be applied among patients who receive an intensive follow-up strategy, which could improve the prognosis of CRC after curative surgery. Moreover, patients in the intensive follow-up group showed an increased frequency of clinic visits, tests, and examinations, which could improve CRC prognosis[41]. Furthermore, subgroup analyses found that the beneficial effects of intensive follow-up strategies were mainly relevant when the sample size was < 500, proportion of males was < 60.0%, and follow-up duration was ≥ 5.0 , which could be explained by the fact that patients with rectal cancer need longer follow-up durations owing to the delayed liver and lung recurrences[42]. Finally, intensive follow-up might be superior to conventional follow-up among women because the difference in lifestyle and compliance among women was better than that among men.

There were no significant differences between the intensive and conventional follow-up strategies in improving cancer-specific survival and relapse-free survival. These results were consistent with those of prior meta-analyses[11,41]. However, subgroup analyses found that intensive follow-up was associated with poor relapse-free survival when the sample size was ≥ 500 patients. The potential reason for this could be the large sample size with sufficient power to detect potential differences, and that residual cancer could be detected through a more thorough follow-up[43]. Similar to a previous meta-analysis, we noted that intensive follow-up significantly increased the incidence of salvage surgery, which could be explained by the early detection of recurrent cases, and salvage surgery was performed for patients with recurring issues.

Although there was no significant difference in the risk of recurrence between groups, intensive follow-up significantly reduced the risk of interval recurrence. Moreover, intensive follow-up was associated with an increased risk of recurrence when the sample size was ≥ 500 and the mean age was < 65.0 years. A potential reason for the risk of recurrence could be that the recurrent cases were consistent and could be affected by the colon/rectal cancer ratio[42]. Moreover, most recurrent cases occurred within 36 mo, and the mean age of the patients was significantly related to the tumor stage[44].

Interval recurrence was defined as symptomatic recurrence, and recurrent presentation in asymptomatic cases was observed when using an intensive follow-up strategy.

This study has several limitations. First, the disease status and treatments across the included trials were different, which could affect the prognosis of CRC after curative surgery. Second, the follow-up protocol differed among the included trials, and the frequency and content of examination could affect the prognosis of CRC. Third, there was substantial heterogeneity for recurrence and interval recurrence, which was not fully explained using sensitivity and subgroup analyses. Finally, there are inherent limitations of meta-analyses on published articles, including inevitable publication bias and restricted detailed analyses.

CONCLUSION

This study found that an intensive follow-up strategy might have beneficial effects on the overall survival of patients with CRC. Moreover, an intensive follow-up strategy was associated with an increased incidence of salvage surgery and a reduced risk of interval survival. Further large-scale studies should be performed to explore suitable follow-up plans after CRC surgery.

ARTICLE HIGHLIGHTS

Research background

Colorectal cancer (CRC) is the third most frequently diagnosed cancer, and the prognosis of CRC at early stage was relative better. The frequency and content of follow-up strategies play an important role on the prognosis of CRC, and intensive follow-up may improve the prognosis of CRC.

Research motivation

Assess the effects of intensive with conventional follow-up strategies for CRC patients after curative intention using a meta-analysis.

Research objectives

This study aimed to compare the overall survival, cancer-specific survival, relapse-free survival, salvage surgery, recurrence, and interval recurrences between intensive and conventional follow-up strategies for non-metastatic CRC treated with curative intent.

Research methods

The eligible trials were identified from PubMed, Embase, and the Cochrane Library databases from inception until April 2023. All of pooled analyses were calculated using the random-effects model, which considering the underlying varies across included trials.

Research results

We noted intensive follow-up play a beneficial effects in improving overall survival, and interval recurrence as compared with conventional follow-up. Moreover, the incidence of salvage surgery was significantly increased for patients received intensive follow-up.

Research conclusions

This study found intensive follow-up was superior than conventional follow-up for CRC patients after curative intention, which should introduce in clinical practice.

Research perspectives

The results of this study based on randomized controlled trials, and the evidence level for pooled conclusions was high.

FOOTNOTES

Author contributions: Cui LL and Ren ZQ conceived the study concept and participated in its design, data extraction, statistical analysis; Cui LL, Cui SQ, Qu Z, and Ren ZQ contributed to the manuscript drafting, and editing; Cui SQ and Qu Z participated in the literature research; and all authors read and approved the final manuscript.

Conflict-of-interest statement: All the authors report no relevant conflicts of interest for this article.

PRISMA 2009 Checklist statement: The authors have read the PRISMA 2009 Checklist, and the manuscript was prepared and revised according to the PRISMA 2009 Checklist.

Open-Access: This article is an open-access article that was selected by an in-house editor and fully peer-reviewed by external reviewers. It is distributed in accordance with the Creative Commons Attribution NonCommercial (CC BY-NC 4.0) license, which permits others to distribute, remix, adapt, build upon this work non-commercially, and license their derivative works on different terms, provided the original work is properly cited and the use is non-commercial. See: <https://creativecommons.org/licenses/by-nc/4.0/>

Country/Territory of origin: China

ORCID number: Li-Li Cui 0009-0002-6404-5884; Shi-Qi Cui 0009-0006-4950-6063; Zhong Qu 0009-0002-5608-9633; Zhen-Qing Ren 0000-0003-2816-5395.

S-Editor: Wang JJ

L-Editor: A

P-Editor: Xu ZH

REFERENCES

- World Health Organization.** International Agency for Research on Cancer. Global Cancer Observatory. [cited 10 June 2023]. Available from: <https://gco.aws-csu.iarc.who.int/>
- GBD 2017 Colorectal Cancer Collaborators.** The global, regional, and national burden of colorectal cancer and its attributable risk factors in 195 countries and territories, 1990-2017: a systematic analysis for the Global Burden of Disease Study 2017. *Lancet Gastroenterol Hepatol* 2019; **4**: 913-933 [PMID: 31648977 DOI: 10.1016/S2468-1253(19)30345-0]
- National Cancer Institute.** SEER Cancer Statistics Review, 1975–2016. [cited 10 June 2023]. Available from: https://seer.cancer.gov/archive/csr/1975_2016/
- Siegel RL, Miller KD, Jemal A.** Cancer statistics, 2019. *CA Cancer J Clin* 2019; **69**: 7-34 [PMID: 30620402 DOI: 10.3322/caac.21551]
- Sakin A, Sahin S, Sakin A, Karatas F, Sengul Samanci N, Yasar N, Arici S, Demir C, Geredeli C, Dikker O, Cihan S.** Mean platelet volume and platelet distribution width correlates with prognosis of early colon cancer. *J BUON* 2020; **25**: 227-239 [PMID: 32277636]
- Baqar AR, Wilkins S, Staples M, Angus Lee CH, Oliva K, McMurrick P.** The role of preoperative CEA in the management of colorectal cancer: A cohort study from two cancer centres. *Int J Surg* 2019; **64**: 10-15 [PMID: 30822523 DOI: 10.1016/j.ijso.2019.02.014]
- Skanccke M, Arnott SM, Amdur RL, Siegel RS, Obias VJ, Umapathi BA.** Lymphovascular Invasion and Perineural Invasion Negatively Impact Overall Survival for Stage II Adenocarcinoma of the Colon. *Dis Colon Rectum* 2019; **62**: 181-188 [PMID: 30640833 DOI: 10.1097/DCR.0000000000001258]
- Figueredo A, Rumble RB, Maroun J, Earle CC, Cummings B, McLeod R, Zuraw L, Zwaal C;** Gastrointestinal Cancer Disease Site Group of Cancer Care Ontario's Program in Evidence-based Care. Follow-up of patients with curatively resected colorectal cancer: a practice guideline. *BMC Cancer* 2003; **3**: 26 [PMID: 14529575 DOI: 10.1186/1471-2407-3-26]
- Verberne CJ, Zhan Z, van den Heuvel E, Grossmann I, Doornbos PM, Havenga K, Manusama E, Klaase J, van der Mijle HC, Lamme B, Bosscha K, Baas P, van Ooijen B, Nieuwenhuijzen G, Marinelli A, van der Zaag E, Wasowicz D, de Bock GH, Wiggers T.** Intensified follow-up in colorectal cancer patients using frequent Carcino-Embryonic Antigen (CEA) measurements and CEA-triggered imaging: Results of the randomized "CEAwatch" trial. *Eur J Surg Oncol* 2015; **41**: 1188-1196 [PMID: 26184850 DOI: 10.1016/j.ejso.2015.06.008]
- Jones RP, McWhirter D, Fretwell VL, McAvoy A, Hardman JG.** Clinical follow-up does not improve survival after resection of stage I-III colorectal cancer: A cohort study. *Int J Surg* 2015; **17**: 67-71 [PMID: 25827817 DOI: 10.1016/j.ijso.2015.03.017]
- Zhao Y, Yi C, Zhang Y, Fang F, Faramand A.** Intensive follow-up strategies after radical surgery for nonmetastatic colorectal cancer: A systematic review and meta-analysis of randomized controlled trials. *PLoS One* 2019; **14**: e0220533 [PMID: 31361784 DOI: 10.1371/journal.pone.0220533]
- Panic N, Leoncini E, de Belvis G, Ricciardi W, Boccia S.** Evaluation of the endorsement of the preferred reporting items for systematic reviews and meta-analysis (PRISMA) statement on the quality of published systematic review and meta-analyses. *PLoS One* 2013; **8**: e83138 [PMID: 24386151 DOI: 10.1371/journal.pone.0083138]
- Higgins JPT, Green S.** Cochrane handbook for systematic reviews of interventions version 5.1.0. [cited 10 June 2023]. Available from: <http://handbook-5-1.cochrane.org/>
- DerSimonian R, Laird N.** Meta-analysis in clinical trials. *Control Clin Trials* 1986; **7**: 177-188 [PMID: 3802833 DOI: 10.1016/0197-2456(86)90046-2]
- Ades A, Lu G, Higgins J.** The interpretation of random-effects metaanalysis in decision models. *Med Decis Mak* 2005; **25**: 646-654 [DOI: 10.1177/0272989X05282643]
- Deeks J, Higgins JPT, Altman D.** Analyzing data and undertaking meta-analyses. In: Higgins J, Green S, editors. *Cochrane Handbook for Systematic Reviews of Interventions 5.0.1*. Oxford: The Cochrane Collaboration; 2008
- Higgins JP, Thompson SG, Deeks JJ, Altman DG.** Measuring inconsistency in meta-analyses. *BMJ* 2003; **327**: 557-560 [PMID: 12958120 DOI: 10.1136/bmj.327.7414.557]
- Tobias A.** Assessing the influence of a single study in the meta-analysis estimate. *Stata Tech Bull* 1999; **8**
- Altman DG, Bland JM.** Interaction revisited: the difference between two estimates. *BMJ* 2003; **326**: 219 [PMID: 12543843 DOI: 10.1136/bmj.326.7382.219]
- Huxley RR, Woodward M.** Cigarette smoking as a risk factor for coronary heart disease in women compared with men: a systematic review and meta-analysis of prospective cohort studies. *Lancet* 2011; **378**: 1297-1305 [PMID: 21839503 DOI: 10.1016/S0140-6736(11)60781-2]
- Egger M, Davey Smith G, Schneider M, Minder C.** Bias in meta-analysis detected by a simple, graphical test. *BMJ* 1997; **315**: 629-634 [PMID: 9310563 DOI: 10.1136/bmj.315.7109.629]
- Begg CB, Mazumdar M.** Operating characteristics of a rank correlation test for publication bias. *Biometrics* 1994; **50**: 1088-1101 [PMID: 7786990]

- 23 **Mäkelä JT**, Laitinen SO, Kairaluoma MI. Five-year follow-up after radical surgery for colorectal cancer. Results of a prospective randomized trial. *Arch Surg* 1995; **130**: 1062-1067 [PMID: 7575117 DOI: 10.1001/archsurg.1995.01430100040009]
- 24 **Ohlsson B**, Breland U, Ekberg H, Graffner H, Tranberg KG. Follow-up after curative surgery for colorectal carcinoma. Randomized comparison with no follow-up. *Dis Colon Rectum* 1995; **38**: 619-626 [PMID: 7774474 DOI: 10.1007/BF02054122]
- 25 **Kjeldsen BJ**, Kronborg O, Fenger C, Jørgensen OD. A prospective randomized study of follow-up after radical surgery for colorectal cancer. *Br J Surg* 1997; **84**: 666-669 [PMID: 9171758]
- 26 **Pietra N**, Sarli L, Costi R, Ouchemi C, Grattarola M, Peracchia A. Role of follow-up in management of local recurrences of colorectal cancer: a prospective, randomized study. *Dis Colon Rectum* 1998; **41**: 1127-1133 [PMID: 9749496 DOI: 10.1007/BF02239434]
- 27 **Schoemaker D**, Black R, Giles L, Tooouli J. Yearly colonoscopy, liver CT, and chest radiography do not influence 5-year survival of colorectal cancer patients. *Gastroenterology* 1998; **114**: 7-14 [PMID: 9428212 DOI: 10.1016/s0016-5085(98)70626-2]
- 28 **Secco GB**, Fardelli R, Gianquinto D, Bonfante P, Baldi E, Ravera G, Derchi L, Ferraris R. Efficacy and cost of risk-adapted follow-up in patients after colorectal cancer surgery: a prospective, randomized and controlled trial. *Eur J Surg Oncol* 2002; **28**: 418-423 [PMID: 12099653 DOI: 10.1053/ejso.2001.1250]
- 29 **Rodríguez-Moranta F**, Saló J, Arcusa A, Boadas J, Piñol V, Bessa X, Batiste-Alentorn E, Lacy AM, Delgado S, Maurel J, Piqué JM, Castells A. Postoperative surveillance in patients with colorectal cancer who have undergone curative resection: a prospective, multicenter, randomized, controlled trial. *J Clin Oncol* 2006; **24**: 386-393 [PMID: 16365182 DOI: 10.1200/JCO.2005.02.0826]
- 30 **Wattchow DA**, Weller DP, Esterman A, Pilotto LS, McGorm K, Hammett Z, Platell C, Silagy C. General practice vs surgical-based follow-up for patients with colon cancer: randomised controlled trial. *Br J Cancer* 2006; **94**: 1116-1121 [PMID: 16622437 DOI: 10.1038/sj.bjc.6603052]
- 31 **Sobhani I**, Tiret E, Lebtahi R, Aparicio T, Itti E, Montravers F, Vaylet C, Rougier P, André T, Gornet JM, Cherqui D, Delbaldo C, Panis Y, Talbot JN, Meignan M, Le Guludec D. Early detection of recurrence by 18FDG-PET in the follow-up of patients with colorectal cancer. *Br J Cancer* 2008; **98**: 875-880 [PMID: 18301402 DOI: 10.1038/sj.bjc.6604263]
- 32 **Wang T**, Cui Y, Huang WS, Deng YH, Gong W, Li CJ, Wang JP. The role of postoperative colonoscopic surveillance after radical surgery for colorectal cancer: a prospective, randomized clinical study. *Gastrointest Endosc* 2009; **69**: 609-615 [PMID: 19136105 DOI: 10.1016/j.gie.2008.05.017]
- 33 **Strand E**, Nygren I, Bergkvist L, Smedh K. Nurse or surgeon follow-up after rectal cancer: a randomized trial. *Colorectal Dis* 2011; **13**: 999-1003 [PMID: 20478003 DOI: 10.1111/j.1463-1318.2010.02317.x]
- 34 **Augustad KM**, Norum J, Dehof S, Aspevik R, Ringberg U, Nestvold T, Vonon B, Skrøvseth SO, Lindsetmo RO. Cost-effectiveness and quality of life in surgeon versus general practitioner-organised colon cancer surveillance: a randomised controlled trial. *BMJ Open* 2013; **3** [PMID: 23564936 DOI: 10.1136/bmjopen-2012-002391]
- 35 **Primrose JN**, Perera R, Gray A, Rose P, Fuller A, Corkhill A, George S, Mant D; FACS Trial Investigators. Effect of 3 to 5 years of scheduled CEA and CT follow-up to detect recurrence of colorectal cancer: the FACS randomized clinical trial. *JAMA* 2014; **311**: 263-270 [PMID: 24430319 DOI: 10.1001/jama.2013.285718]
- 36 **Treasure T**, Monson K, Fiorentino F, Russell C. The CEA Second-Look Trial: a randomised controlled trial of carcinoembryonic antigen prompted reoperation for recurrent colorectal cancer. *BMJ Open* 2014; **4**: e004385 [PMID: 24823671 DOI: 10.1136/bmjopen-2013-004385]
- 37 **Rosati G**, Ambrosini G, Barni S, Andreoni B, Corradini G, Luchena G, Daniele B, Gaion F, Oliverio G, Duro M, Martignoni G, Pinna N, Sozzi P, Pancera G, Solina G, Pavia G, Pignata S, Johnson F, Labianca R, Apolone G, Zaniboni A, Monteforte M, Negri E, Torri V, Mosconi P, Fossati R; GILDA working group. A randomized trial of intensive versus minimal surveillance of patients with resected Dukes B2-C colorectal carcinoma. *Ann Oncol* 2016; **27**: 274-280 [PMID: 26578734 DOI: 10.1093/annonc/mdv541]
- 38 **Wille-Jørgensen P**, Syk I, Smedh K, Laurberg S, Nielsen DT, Petersen SH, Renehan AG, Horváth-Puhó E, Pahlman L, Sørensen HT; COLOFOL Study Group. Effect of More vs Less Frequent Follow-up Testing on Overall and Colorectal Cancer-Specific Mortality in Patients With Stage II or III Colorectal Cancer: The COLOFOL Randomized Clinical Trial. *JAMA* 2018; **319**: 2095-2103 [PMID: 29800179 DOI: 10.1001/jama.2018.5623]
- 39 **Rahr HB**, Streym S, Kryh-Jensen CG, Hougaard HT, Knudsen AS, Kristensen SH, Ejlersen E. Screening and systematic follow-up for cardiopulmonary comorbidity in elective surgery for colorectal cancer: a randomised feasibility study. *World J Surg Oncol* 2019; **17**: 127 [PMID: 31331339 DOI: 10.1186/s12957-019-1668-7]
- 40 **Monteil J**, Le Brun-Ly V, Cachin F, Zasadny X, Seitz JF, Mundler O, Selvy M, Smith D, Rullier E, Lavau-Denes S, Lades G, Labrunie A, Lecaille C, Valli N, Leobon S, Terrebbonne E, Deluche E, Tubiana-Mathieu N. Comparison of 18FDG-PET/CT and conventional follow-up methods in colorectal cancer: A randomised prospective study. *Dig Liver Dis* 2021; **53**: 231-237 [PMID: 33153929 DOI: 10.1016/j.dld.2020.10.012]
- 41 **Jeffery M**, Hickey BE, Hider PN. Follow-up strategies for patients treated for non-metastatic colorectal cancer. *Cochrane Database Syst Rev* 2019; **9**: CD002200 [PMID: 31483854 DOI: 10.1002/14651858.CD002200.pub4]
- 42 **Sadahiro S**, Suzuki T, Ishikawa K, Nakamura T, Tanaka Y, Masuda T, Mukoyama S, Yasuda S, Tajima T, Makuuchi H, Murayama C. Recurrence patterns after curative resection of colorectal cancer in patients followed for a minimum of ten years. *Hepatogastroenterology* 2003; **50**: 1362-1366 [PMID: 14571738]
- 43 **Morris EJ**, Sandin F, Lambert PC, Bray F, Klint A, Linklater K, Robinson D, Pahlman L, Holmberg L, Möller H. A population-based comparison of the survival of patients with colorectal cancer in England, Norway and Sweden between 1996 and 2004. *Gut* 2011; **60**: 1087-1093 [PMID: 21303917 DOI: 10.1136/gut.2010.229575]
- 44 **Ryuk JP**, Choi GS, Park JS, Kim HJ, Park SY, Yoon GS, Jun SH, Kwon YC. Predictive factors and the prognosis of recurrence of colorectal cancer within 2 years after curative resection. *Ann Surg Treat Res* 2014; **86**: 143-151 [PMID: 24761423 DOI: 10.4174/astr.2014.86.3.143]

Prognostic value of T cell immunoglobulin and mucin-domain containing-3 expression in upper gastrointestinal tract tumors: A meta-analysis

Jing-Jing Yan, Bing-Bing Liu, Yan Yang, Meng-Ru Liu, Han Wang, Zhen-Quan Deng, Zhi-Wei Zhang

Specialty type: Oncology

Provenance and peer review:

Unsolicited article; Externally peer reviewed.

Peer-review model: Single blind

Peer-review report's scientific quality classification

Grade A (Excellent): A, A

Grade B (Very good): 0

Grade C (Good): 0

Grade D (Fair): D

Grade E (Poor): 0

P-Reviewer: Huang B, China; Rizzo A, Italy

Received: August 12, 2023

Peer-review started: August 12, 2023

First decision: September 12, 2023

Revised: September 25, 2023

Accepted: October 16, 2023

Article in press: October 16, 2023

Published online: December 15, 2023



Jing-Jing Yan, Bing-Bing Liu, Yan Yang, Meng-Ru Liu, Han Wang, College of Clinical Medicine, Hebei University of Engineering, Handan 056000, Hebei Province, China

Zhen-Quan Deng, Department of Oncology, Handan First Hospital, Handan 056002, Hebei Province, China

Zhi-Wei Zhang, Department of Oncology, Affiliated Hospital of Hebei University of Engineering, Handan 056000, Hebei Province, China

Corresponding author: Zhi-Wei Zhang, MD, PhD, Attending Doctor, Department of Oncology, Affiliated Hospital of Hebei University of Engineering, No. 81 Congtai Road, Congtai District, Handan 056000, Hebei Province, China. zhangzw128@126.com

Abstract

BACKGROUND

There is a lack of robust prognostic markers for upper gastrointestinal (GI) tract cancers, including esophageal, gastric, and esophagogastric junction cancers. T cell immunoglobulin and mucin-domain containing-3 (TIM3) plays a key immunomodulatory role and is linked to the prognosis of various cancers. However, the significance of TIM3 in upper GI tract tumors is still uncertain.

AIM

To investigate the prognostic value of TIM3 expression in upper GI tract tumors.

METHODS

A literature search was conducted on the PubMed, Embase, and Web of Science databases for relevant studies published until June 2023. After screening and quality assessment, studies that met the criteria were included in the meta-analysis. Statistical methods were used for the pooled analysis to assess the association of TIM3 expression in upper GI tract tumors with the prognosis and clinicopathological parameters. The results were reported with the hazard ratio (HR) and 95% confidence interval (CI).

RESULTS

Nine studies involving 2556 patients with upper GI tract cancer were included. High TIM3 expression was associated with a worse prognosis in upper GI tract cancer (HR: 1.17, 95%CI: 1.01-1.36). Positive expression of TIM3 in gastric cancer

was correlated with the T and N stage, but the difference was not statistically significant. However, TIM3 overexpression was significantly correlated with the TNM stage (odds ratio: 1.21, 95%CI: 0.63-2.33; $P < 0.05$). TIM3 expression showed no association with the other clinicopathological parameters.

CONCLUSION

High expression of TIM3 in the upper GI tract cancer is associated with a worse prognosis and advanced T or N stages, indicating its potential value as a prognostic biomarker. These findings may provide a basis for the personalized treatment of upper GI tract cancers.

Key Words: Immune checkpoint; T cell immunoglobulin-3; Upper gastrointestinal tract cancer; Overall survival; Clinicopathological features

©The Author(s) 2023. Published by Baishideng Publishing Group Inc. All rights reserved.

Core Tip: Immune checkpoint receptor inhibitors have transformed cancer treatment in a wide range of tumor types, and T cell immunoglobulin and mucin-domain containing-3 (TIM3) is one of these immune checkpoint receptors. The study initially evaluated the survival-prognostic effect of TIM3 in upper gastrointestinal tract tumors by conducting a meta-analysis, aggregating data from several independent studies, and providing the latest comprehensive insights into the field. We believe that the results of this study will further advance immunotherapy and provide some value to future research.

Citation: Yan JJ, Liu BB, Yang Y, Liu MR, Wang H, Deng ZQ, Zhang ZW. Prognostic value of T cell immunoglobulin and mucin-domain containing-3 expression in upper gastrointestinal tract tumors: A meta-analysis. *World J Gastrointest Oncol* 2023; 15(12): 2212-2224

URL: <https://www.wjgnet.com/1948-5204/full/v15/i12/2212.htm>

DOI: <https://dx.doi.org/10.4251/wjgo.v15.i12.2212>

INTRODUCTION

The high incidence of cancer is a major public health concern worldwide[1]. An analysis of cancer statistics in 2022 revealed a declining trend in the incidence and mortality rates of malignant tumors in the United States[2]. However, upper gastrointestinal (GI) tract tumors, including esophageal cancer, gastric cancer, and esophagogastric junction cancer, continue to pose a serious threat to health. Gastric cancer is the fifth most common cancer worldwide, and the fourth highest contributor to cancer-associated mortality. Worldwide, esophageal cancer ranks seventh in terms of incidence and sixth in terms of mortality[3].

Recent data have suggested a gradual decrease in the incidence of gastric cancer in China. However, it remains the fourth most commonly occurring cancer and the third most common cause of cancer-associated mortality in China, whereas esophageal cancer is among the top five causes of cancer-related deaths[4].

A diverse range of treatment methods are presently available for upper GI tract tumors. In addition to traditional treatments (surgery, chemotherapy, and radiotherapy), targeted therapy, immunotherapy, and combination therapy have exhibited promising results in certain subsets of patients. However, despite these novel therapeutic approaches, the prognosis of patients with middle- and advanced-stage upper GI tract tumors remains unsatisfactory. In recent years, immunotherapy using immune checkpoint inhibitors has transformed the treatment landscape for various types of cancers. Combination therapy containing immunotherapy has been the first-line treatment for advanced upper GI tract tumors. Approximately 15%-20% of patients with gastric adenocarcinoma overexpress human epidermal growth factor receptor 2 (HER2). While trastuzumab was once favored for treating HER2-positive advanced gastric cancer, the DESTINY-Gastric01 study highlighted trastuzumab deruxtecan as a superior option[5]. The MOUSEION series indicates that immunotherapy benefits both men and women, but women may show a reduced response to monotherapy[6]. Moreover, combining two immune checkpoint inhibitors yields better outcomes, and while not all gastric cancer patients show a positive response, those with high microsatellite instability or Epstein-Barr virus positivity exhibit a strong response to pembrolizumab[7]. The synergy of chemotherapy and immunotherapy, especially targeting the DNA damage response pathway, offers promising prospects in gastric cancer treatment[8]. Furthermore, immune checkpoints represent a contemporary research hotspot among prognostic markers.

Immune checkpoints are inhibitory molecules that can modulate the immune system to reduce unwanted autoimmune responses, thereby helping maintain self-tolerance and regulating the timing of physiological immune responses in peripheral tissues[9]. In the cancer microenvironment, T lymphocytes play a central role in cell-mediated cytotoxicity. Activated T cells express inhibitory receptors, such as cytotoxic T-lymphocyte-associated protein 4 (CTLA-4) and programmed cell death protein 1 (PD-1). Cancer cells express ligands, such as programmed death-ligand 1 (PD-L1), which can combine with PD-1 and further weaken the antitumor effects of T cells[10,11]. The blockade of immune checkpoints can have powerful and durable antitumor effects.

In March 2011, the United States Food and Drug Administration approved ipilimumab, a monoclonal CTLA-4 antibody, for the treatment of patients with late-stage melanoma[12]. PD-1/PD-L1 blockers are among the most successful checkpoint inhibitors[13]. PD-1 or PD-L1 inhibitors have been approved as first- or second-line treatment for several cancers, such as non-small cell lung cancer, melanoma, and gastric cancer[14]. Therefore, immune checkpoint inhibitors are presently an important component of comprehensive cancer therapy.

At present, the most commonly used immune checkpoint molecular targets are PD-1, CTLA-4, lymphocyte activation gene-3 (LAG-3), and T cell immunoglobulin-3 (TIM3). Among these, TIM3, also referred to as hepatitis A virus-cell receptor 2, is a transmembrane protein that negatively regulates type 1 immunity and plays an important regulatory role in carcinogenesis and development[15]. This suppresses the activity of T cells and other immune cells by binding to its ligand galectin-9 (Gal-9), thereby regulating the intensity and duration of the immune response[16].

Recent studies have demonstrated high TIM3 expression in upper GI tract tumor tissues, and its close association with overall survival (OS). For example, studies have reported a correlation between TIM3 expression level and the prognosis of gastric[17-20] and esophageal[21-25] cancers. However, the prognostic value of TIM3 in gastroesophageal junction cancer has not been reported. The results suggest the important role of TIM3 in these tumors.

Therefore, a meta-analysis was conducted to comprehensively assess the relationship between TIM3 expression level and the prognosis and clinicopathological parameters of upper GI tract tumors.

MATERIALS AND METHODS

Search strategy and study selection

A literature search was performed in the PubMed, Web of Science, and Embase databases for studies published as of June 30, 2023. The keywords used were “TIM3,” “gastric cancer,” and “esophageal cancer.” No studies have investigated TIM3 expression in gastroesophageal junction cancer. In addition, to prevent the omission of relevant literature, especially focused literature, we used a new tool, Reference Citation Analysis (<https://www.referencecitationanalysis.com>), to analyze the articles. Next, a systematic approach was used to select eligible studies and extract relevant data. The reference lists of the selected articles were screened to identify additional studies that met the criteria for inclusion in the present meta-analysis. Only publicly available published data were used for the present study, precluding any concerns related to personal privacy or ethical issues. The present meta-analysis is registered on the PROSPERO website (<https://www.crd.york.ac.uk/PROSPERO/>; Registration No. CRD42023438756).

Study selection criteria

Studies that met the following criteria were eligible for inclusion: (1) Case-control studies, cohort studies, or clinical trials; (2) patients with upper GI cancer; (3) diagnosis confirmed by histopathology; (4) detection of TIM3 expression by immunohistochemistry (IHC); and (5) variables reported of TIM3 expression levels and cancer prognosis-related outcomes (such as OS).

The exclusion criteria were: (1) *In vitro* studies or animal experiments; (2) inability to extract the required data from the published results; (3) non-reporting of survival outcomes; and (4) patients who received chemotherapy or radiotherapy before the assessment of TIM3 expression.

Data extraction and quality assessment

Two researchers independently extracted the data pertaining to the following variables from each study: Study design, sample size, demographic characteristics (including age, sex, nationality, and ethnicity), clinicopathological parameters (T stage, lymph node metastasis, tumor-node-metastasis [TNM] stage, and grade of differentiation), and prognostic indices (such as OS). The specifics of the TNM staging were meticulously documented. The methods and thresholds for determining TIM3 expression, primarily through IHC, were outlined. Using the Newcastle-Ottawa Scale (NOS) for quality assessment, only studies that scored between 6 to 9 points, denoting high quality, were included in the meta-analysis.

Statistical analyses

Pooled analyses of data obtained from the included studies were performed using STATA statistical software, version 15.2. $P < 0.05$ was considered statistically significant for all analyses. The pooled hazard ratios (HRs) and 95% confidence interval (CIs) were calculated to assess the association between TIM3 expression and the prognosis and clinicopathological parameters (sex, age, T stage, lymph node metastasis, TNM stage, and grade of differentiation) of GI tract cancer. The individual HR estimates were pooled into a summary HR. The assumption of homogeneity was tested by performing Cochran's Q-statistic and I^2 test for heterogeneity. $P < 0.05$ in the Q-test or $I^2 > 50\%$ was considered indicative of significant heterogeneity. In case of significant heterogeneity, the random-effects model was used for the meta-analysis; otherwise, the fixed-effects model was used. HR or odds ratio (OR) > 1 (indicating worse prognosis for cases with TIM3 expression positivity) was considered statistically significant when the 95%CI did not overlap 1. In case of significant heterogeneity among the included studies, subgroup analysis or sensitivity analysis was performed to identify the source of heterogeneity and explore the impact of potential factors on the results. The results were presented as forest plots. The effect of potential publication bias on the results of the meta-analysis was assessed by drawing funnel plots, and performing the Begg's rank correlation test.

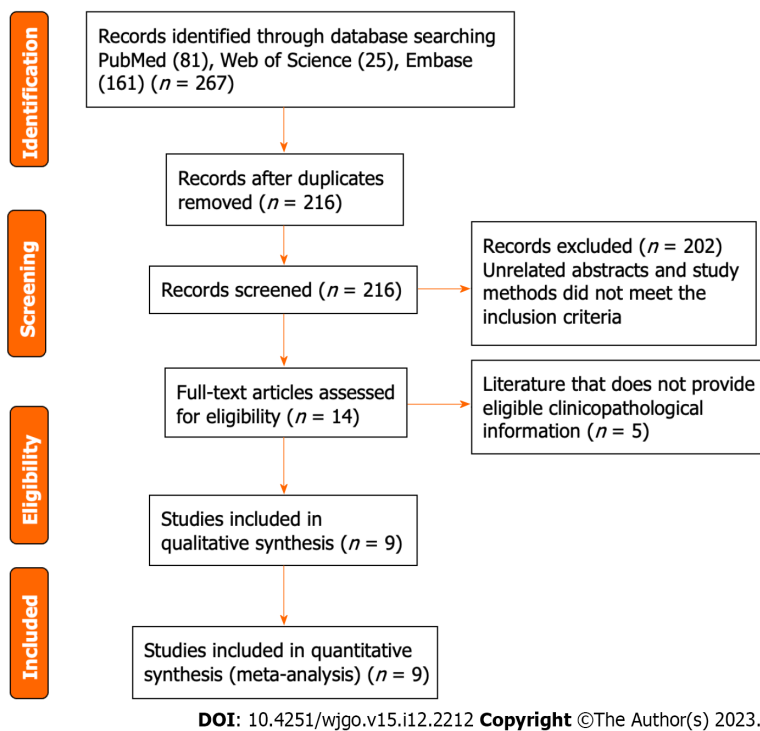


Figure 1 Flow diagram for the study selection criteria and process.

RESULTS

Selection of trials

The flow diagram illustrating the study selection process and criteria is presented in Figure 1. A total of 267 studies that investigated the association of TIM3 expression in upper GI tract cancer with both prognosis and clinicopathological parameters were retrieved during the database search. Among these studies, 51 duplicate publications were excluded. Of the remaining 216 articles, 202 were excluded after the review of the abstracts and study methods, since these did not meet the inclusion criteria. Subsequently, the full texts of the remaining 14 articles were reviewed. Of these 14 studies, 5 that did not provide qualifying clinicopathological information were excluded. Finally, the remaining nine studies, which enrolled 2556 patients, were included in the pooled analysis. These studies were published between 2013 and 2022. In each of the eligible studies, TIM3 expression in upper GI tract cancer was reported to be associated with OS. All studies were considered high quality based on the NOS assessment (average score: 8). Table 1 summarizes the characteristics of the selected studies.

Association between TIM3 expression and OS

Nine studies were included in the pooled analysis of the association between TIM3 expression and OS (Figure 2). It was noteworthy that no significant positive results were obtained from the literature data provided by Wang *et al*[18] and Park *et al*[19]. Nonetheless, these results revealed that high TIM3 expression was associated with a worse prognosis of upper GI tract tumors, with a pooled HR of 1.17 (95%CI: 1.01-1.36). To further investigate the prognostic significance of TIM3 in different types of upper GI tumors, we performed the analyses grouped by cancer type (Supplementary Figures 1 and 2). In addition, there were two papers in which the data were obviously biased. To further illustrate the situation, we showed the result after removing these two papers (Supplementary Figure 3), and found that high TIM3 expression was significantly associated with poorer survival of upper GI cancers. The abovementioned results indicate that high expression of TIM3 may be a predictor of poor prognosis, shorter survival, and a higher risk of recurrence in patients with upper GI cancers.

Association between TIM3 expression and clinicopathological characteristics

All studies included in the meta-analysis had analyzed data on TIM3 expression, and at least one clinicopathological parameter for upper GI tract tumors (Figures 3 and 4, Table 2). TIM3 expression was associated with the T and N stage, and was significantly correlated with the TNM stage. However, among the other clinicopathological parameters, TIM3 expression was not associated with sex, age, tumor location, size, or grade.

On analysis of the T stage for assessing the degree of primary tumor invasiveness, TIM3 expression was found to be associated with the T stage (T1-2 *vs* T3-4, OR: 1.39, 95%CI: 1.06-1.83; fixed effects model). Furthermore, TIM3 expression was higher in the T3-4 group compared to the T1-2 group, although the difference was not statistically significant ($P > 0.05$). This result suggests the potential role of TIM3 expression in the depth of tumor invasion of upper GI tract tumors. The analysis of the distribution of involved lymph nodes (stage N) revealed that TIM3 expression was greater in the N2-3

Table 1 Characteristics of studies included for the meta-analysis

Reference	Yr	Country	Ethnicity	Age	Method	Study design	Stage	Cancer type	Cut-off values	n (E +)	Follow-up time in mo (range)	OS (HR with 95%CI)	NOS
Jiang <i>et al</i> [17]	2013	China	Asian	60	IHC	Retrospective	1-4	Gastric cancer	HSCORE > 0	305 (60.0%)	Median 40 (3-135)	0.60 (0.35–1.01)	9
Wang <i>et al</i> [18]	2018	China	Asian	61.6	IHC	Retrospective	1-4	Gastric cancer	Median number of stained cells	587 (49.9%)	Median 48 (1-117)	1.71 (1.327–2.203)	9
Park <i>et al</i> [19]	2021	Korea	Asian	59	IHC	Retrospective	2-3	Gastric cancer	Immunostaining 5%	385 (61.6%)	NA	0.30 (0.13–0.68)	7
Chen <i>et al</i> [20]	2022	China	Asian	65	IHC	Retrospective	2-3	Gastric cancer	Median number of stained cells	496 (49.0%)	Median 37 (4-76)	2.236 (1.427–3.504)	7
Shan <i>et al</i> [21]	2016	China	Asian	55	IHC	Retrospective	1-4	ESCC	3 points	64 (85.9%)	Median 31 (7-105)	1 (0.932-1.072)	8
Hou <i>et al</i> [22]	2017	China	Asian	58	IHC	Retrospective	2-3	ESCC	3 points	45 (22.2%)	< 100	1.102 (0.292–4.157)	7
Duan <i>et al</i> [23]	2018	China	Asian	58	IHC	Retrospective	1-4	ESCC	1%	95 (37.9%)	Median 32 (3-84)	0.405 (0.148–1.103)	9
Hong <i>et al</i> [24]	2019	Korea	Asian	64	IHC	Retrospective	1-4	ESCC	1%	396 (50.8%)	Median 24.8 (0.5-210.0)	1.60 (1.13–2.27)	8
Zhao <i>et al</i> [25]	2020	China	Asian	65	IHC	Retrospective	1-4	ESCC	HSCORE > 3	183 (47.5%)	NA	2.620 (1.569–4.375)	8

HSCORE system = Stain intensity × percentage of stained cells. CI: Confidence interval; E +: T cell immunoglobulin and mucin-domain containing-3 positive expression; ESCC: Esophageal squamous cell carcinoma; HR: Hazard ratio; IHC: Immunohistochemistry; NA: Not applicable; NOS: New-Ottawa scale; OS: Overall survival.

group compared to the N0-1 group (N0-1 *vs* N2-3, OR: 1.5, 95%CI: 1.11–2.01; random effects model), although the difference was not statistically significant ($P > 0.05$). Furthermore, the results suggested that TIM3 expression may be correlated with the N stage in upper GI tract tumors. However, further studies are required to explore this association. In further analyses, TIM3 overexpression was found to be correlated with the TNM stage, since TIM3 expression was higher in the III/IV stage of gastric cancer compared to the I/II stage (I/II *vs* III/IV, OR: 1.21, 95%CI: 0.63–2.33, random-effects model). Therefore, TIM3 overexpression may play an important role in the development of upper GI tract tumors.

Sensitivity analysis and publication bias assessment

In the sensitivity analysis, the pooled analysis results remained stable and consistent across the different statistical models and methods, reinforcing the reliability of the results. Furthermore, the funnel plot and Begg's rank correlation test revealed no significant effect of potential publication bias on the results of the meta-analysis (Figure 5).

DISCUSSION

Upper GI tract tumors are a group of malignant tumors with a high incidence and associated mortality. The pathogenic mechanism of these tumors is complex, and intricately linked to the immune system. The immune system plays a crucial role in the initiation, advancement, and spread of cancer[26,27]. As cancer advances, exosomes released by the tumor cells

Table 2 Sub-group analysis of the association between T cell immunoglobulin and mucin-domain containing-3 and the clinicopathological parameters

Subgroups	OR (95%CI)	P value	Studies, n	Patients, n
Sex: Female <i>vs</i> male	0.92 (0.75-1.14)	0.388	7	1866
Age: Elderly <i>vs</i> non-elderly	1.07 (0.79-1.44)	0.061	6	1771
Tumor location: Top and middle <i>vs</i> bottom	1.07 (0.85-1.35)	0.605	4	1311
Tumor size: 4 <i>vs</i> < 4	0.77 (0.53-1.12)	0.202	4	1192
T stage: T1-2 <i>vs</i> T3-4	1.39 (1.06-1.83)	0.6	3	865
N stage: N0-1 <i>vs</i> N2-3	1.5 (1.11-2.01)	0.803	3	865
TNM Stage: III/IV <i>vs</i> I/II	1.21 (0.63-2.33)	< 0.001	7	1866
Grade: G1 <i>vs</i> G2 + G3	0.7 (0.40-1.22)	0.427	3	323

CI: Confidence interval; OR: Odds ratio; TNM: Tumor-node-metastasis.

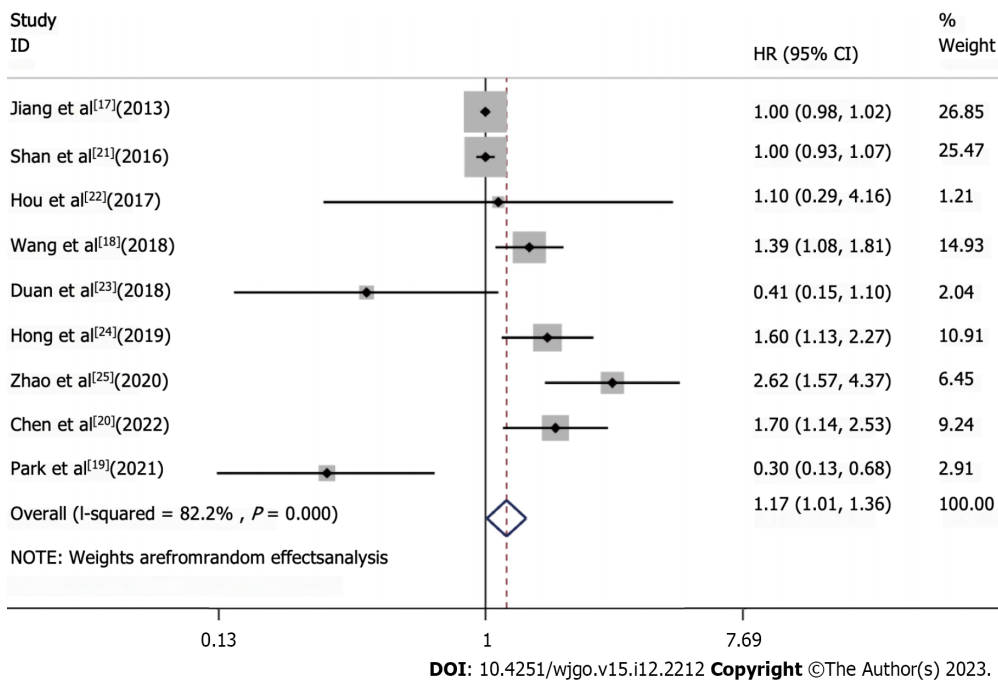
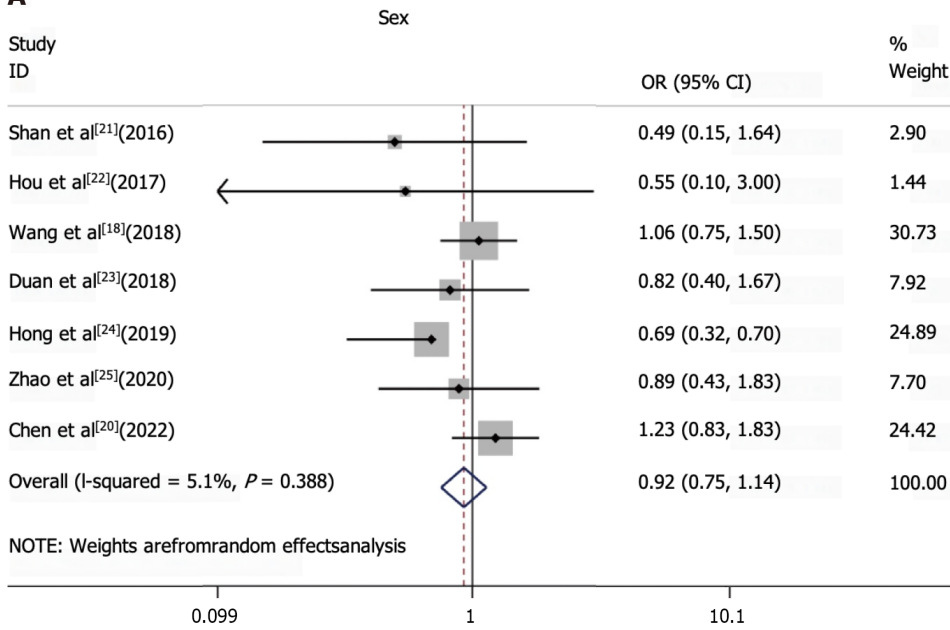


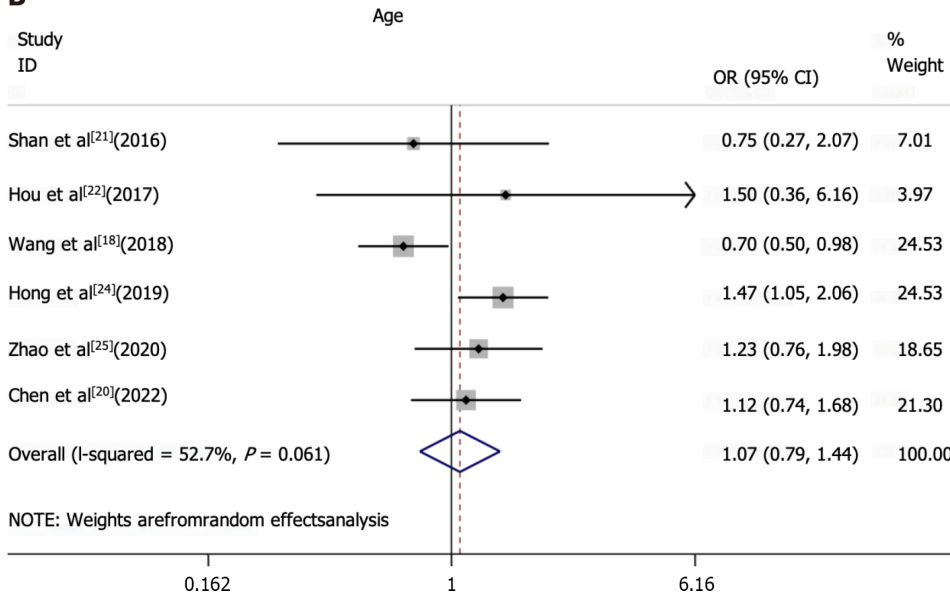
Figure 2 Meta-analysis of the association between T cell immunoglobulin and mucin-domain containing-3 expression and overall survival. Hazard ratio forest plot for the association between the T cell immunoglobulin and mucin-domain containing-3 expression and overall survival in upper gastrointestinal tract tumors.

not only facilitate tumor immune evasion but also serve as biomarkers of autoimmune response[28]. Notably, serum pepsinogen, a biomarker, is widely believed to reflect the pathological changes in the stomach[29]. Biomarkers are indispensable in cancer diagnosis and treatment, aiding in early diagnosis, evaluating therapeutic efficacy, predicting disease progression, and offering vital information for personalized treatment. The immunomodulatory molecule TIM3, which is an important immune checkpoint[30,31], plays a key role in tumor immune evasion and treatment resistance, and is expressed in both serum and tumors. Furthermore, TIM3 can suppress tumor immune responses by modulating the function of T helper 1 CD4 T cells and cytotoxic CD8 T cells[32]. Studies conducted in the context of melanoma, and head and neck cancers have revealed that TIM3 can limit the antitumor immunity[33,34]. TIM3 enhances the growth of hepatocellular carcinoma by inducing the functional blockade of natural killer cells[35]. Furthermore, TIM3 has been identified as a marker of microsatellite-stable colorectal carcinoma with immune failure and distinct clinicopathological features[36]. Moreover, TIM3, which acts with its ligand CEA cell adhesion molecule 1, can suppress T cells, thereby downregulating antitumor immunity[37,38]. Of note, the serum levels of TIM3 and Gal-9 are significantly elevated in patients with systemic mastocytosis, suggesting the potential value of TIM3 in the diagnosis and treatment of this condition[39]. However, the prognostic significance of TIM3 in upper GI tract tumors remain inconsistent. Therefore, we conducted a meta-analysis of the available evidence to comprehensively evaluate the potential prognostic value of TIM3 in patients with upper GI tract tumors. These findings may provide insights for guiding clinical treatment decisions and

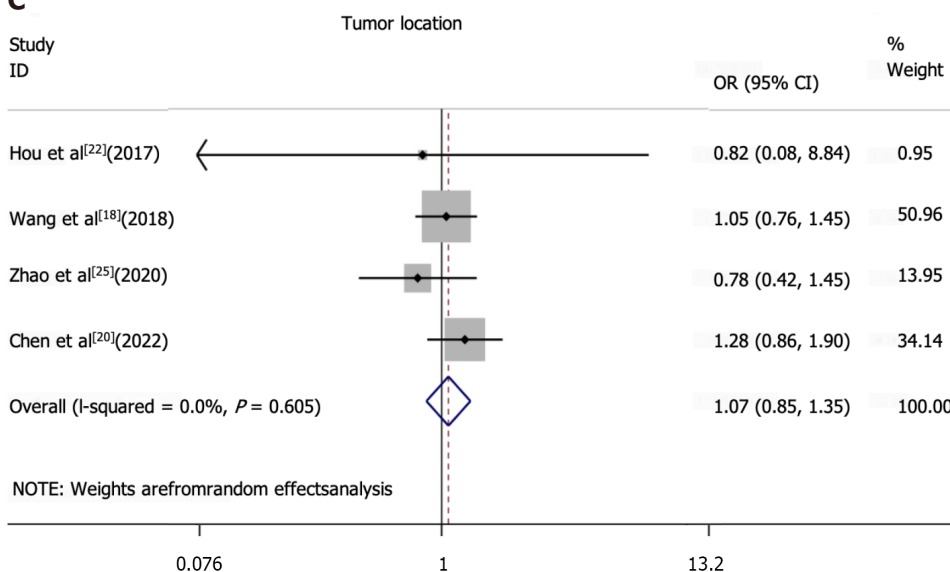
A



B



C



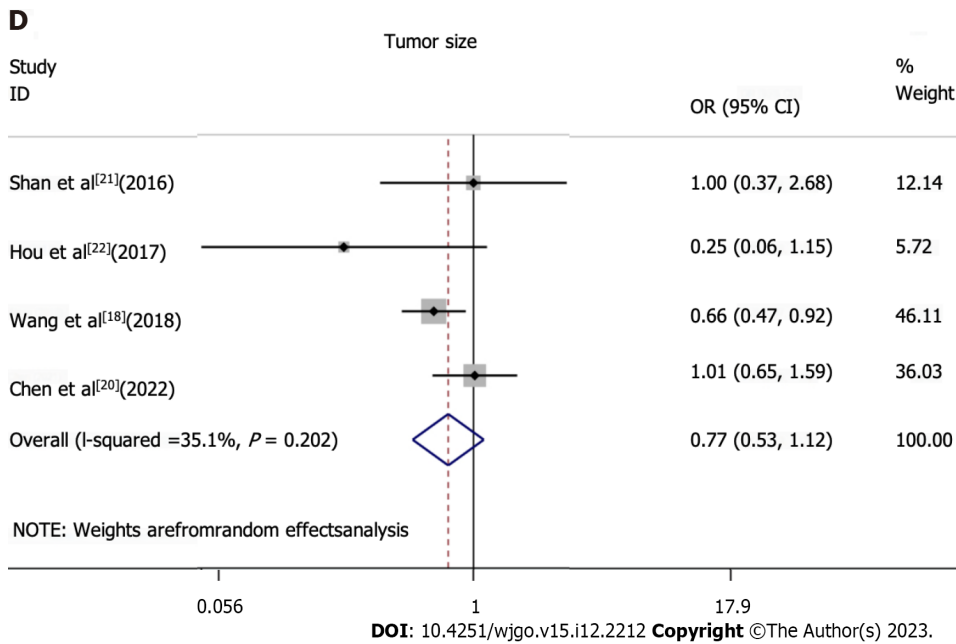


Figure 3 Association between T cell immunoglobulin and mucin-domain containing-3 expression and clinicopathological characteristics was analyzed. Forest plots with Odds ratio (OR) and 95% confidence interval (CI) were drawn for the association of T cell immunoglobulin and mucin-domain containing-3 expression with clinicopathological characteristics. A: Sex; B: Age; C: Tumor location; D: Tumor size.

individualized therapy.

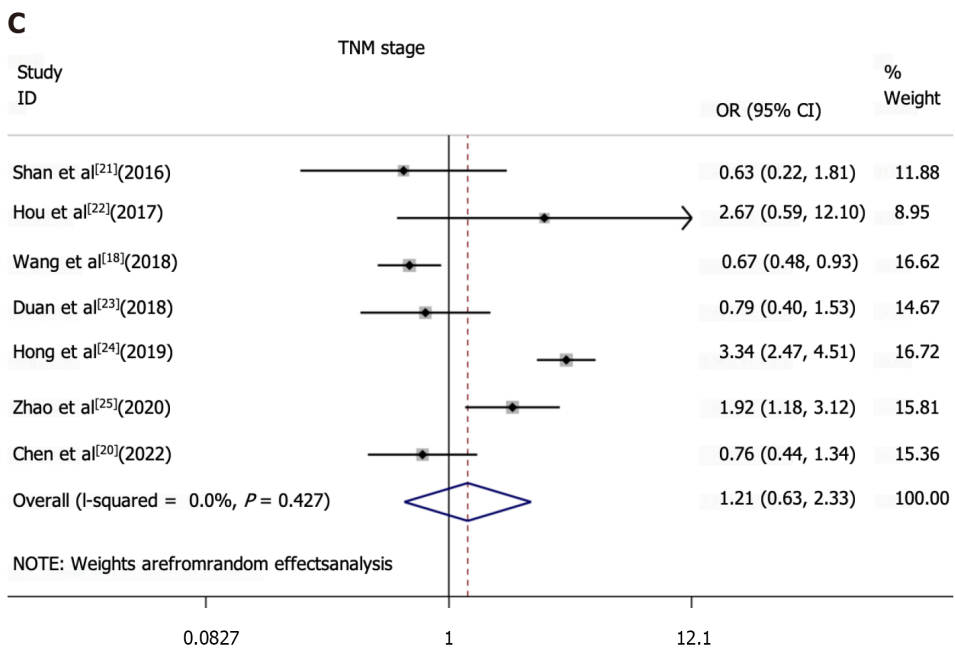
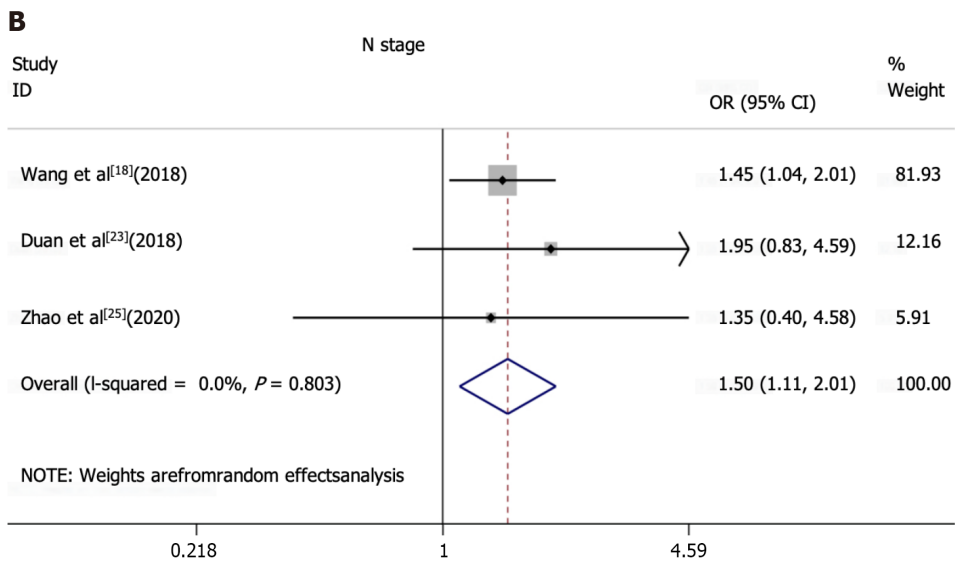
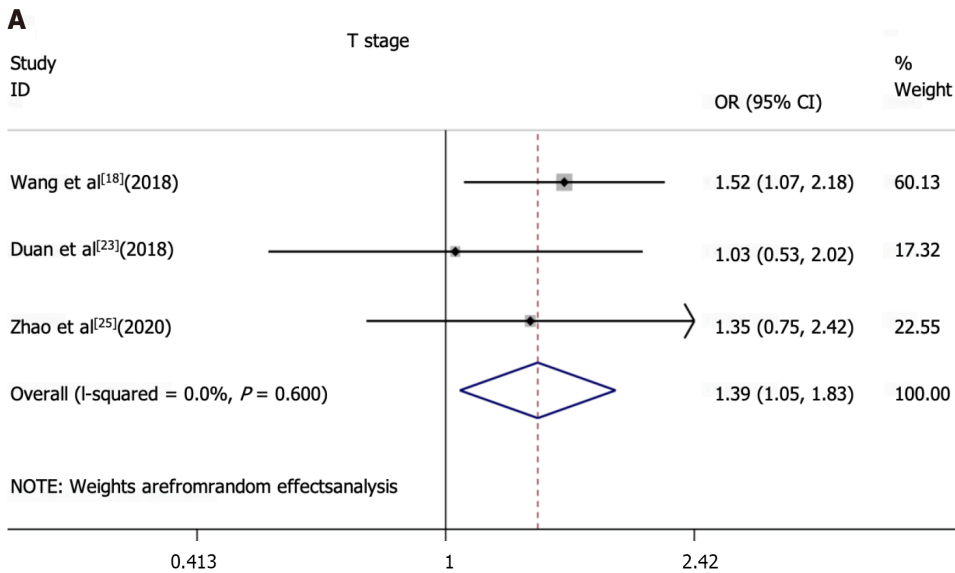
A total of nine independent studies, which enrolled 2556 patients with upper GI tract tumors, were included. In the pooled analysis, high TIM3 expression was associated with worse prognosis. Specifically, a poorer prognosis was observed in patients with high TIM3 expression, with an HR of 1.17 (95%CI: 1.01-1.36). This suggests that high TIM3 expression may be a predictor of poor prognosis, and is associated with shorter survival and higher risk of recurrence in these patients. Of note, as shown in [Figure 5](#), the results were not very good. Hence, the investigators searched for the reason, and identified some deviations on the data obtained from two studies (Wang *et al*[18] and Park *et al*[19]). A graph was drawn to determine the effects of deleting these two articles, and it was observed that the results were very relevant to the drawn conclusions. Thus, it would be worthwhile to further investigate TIM3. It was notable that previous studies have identified the combination of TIM3, LAG-3, and others as potential biomarkers[40].

In the subgroup analysis, high expression of TIM3 was associated with a worse prognosis of patients with esophageal, gastric, and combined esophagogastric cancers. This highlights the potential role of TIM3 in the development and progression of these tumor types, and underlines its clinical relevance as a potential marker for prognostic assessment and treatment selection.

High expression of TIM3 may suggest immune escape and an immunosuppressive milieu in the tumor microenvironment. In this study, we found a significant correlation between high expression of TIM3 and the TNM staging of upper GI tumors. Given the pivotal role of TIM3 in tumor immune evasion and treatment resistance, we hypothesize that high expression of TIM3 may be intricately linked with the TNM staging of the tumor. TIM3 inhibits T cell activation and function, and induces immune tolerance by binding to its ligand Gal-9. Gal-9 promotes the persistence of PD-1 + TIM3 + T cells by binding to PD-1, and impairing Gal-9/TIM3-induced cell death[41]. Furthermore, TIM3 and Gal9 have exhibited the potential as predictive biomarkers in different cancers. In-depth characterization of the TIM3/Gal9 signaling in cancers, and its underlying mechanisms can help identify patients who are likely to respond to the blockade of this pathway, and facilitate the design of combination therapies[42]. High expression of TIM3 may lead to the suppression of immune response, and diminishing host immune clearance of tumors, thereby promoting tumor growth and proliferation. This may explain the association between high TIM3 expression and poor prognosis of upper GI tract tumors. This further emphasizes the significance of TIM3 as a potential therapeutic target and prognostic biomarker.

Through a meta-analysis approach, our study comprehensively assessed the prognostic significance of TIM3 in upper GI tract tumors. Our findings suggest that TIM3 might be a biomarker warranting further attention. It not only offers a novel reference for classifying and staging upper GI tract tumors but may also shed light on the potential immunotherapeutic strategies for these tumors. Especially as immunotherapy becomes a focal point of cancer treatment, TIM3, as one of the immune checkpoints and a regulator of T-cell responses in the tumor microenvironment, may become an important test similar to PD-1/PD-L1. Such checkpoints are commonly associated with immune escape in cancer patients, and therefore, therapies targeting them may provide significant clinical benefits.

Before embarking on this research, the existing literature presented conflicting views regarding the role of TIM3 in upper GI tract tumors. At present, we do not fully understand the specific role of TIM3 in various upper GI tract tumors and its potential interactions with other immune checkpoints, such as PD-1/PD-L1. We aim to consolidate a stronger evidence base in this area by systematically conducting meta-analyses covering a wider range of literature, employing state-of-the-art statistical techniques, and taking into account a variety of potential confounding factors. Recognizing the



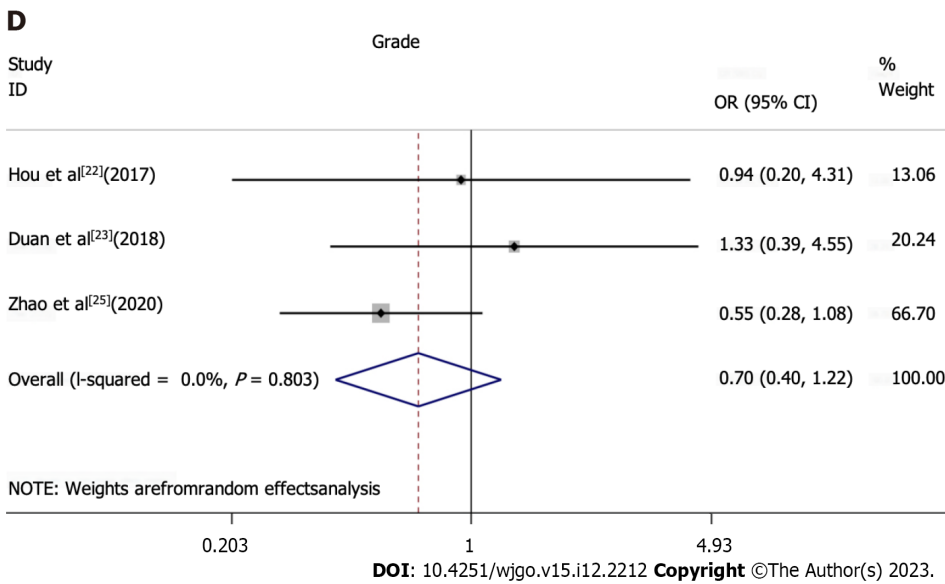


Figure 4 Association between T cell immunoglobulin and mucin-domain containing-3 expression and clinicopathological characteristics was analyzed. Forest plots of odds ratio (OR) and 95% confidence interval (CI) were performed for correlation between T cell immunoglobulin and mucin-domain containing-3 expression and Tumor staging and grade of tissue differentiation. A: T stage; B: N stage; C: TNM stage; D: Grade of tissue differentiation.

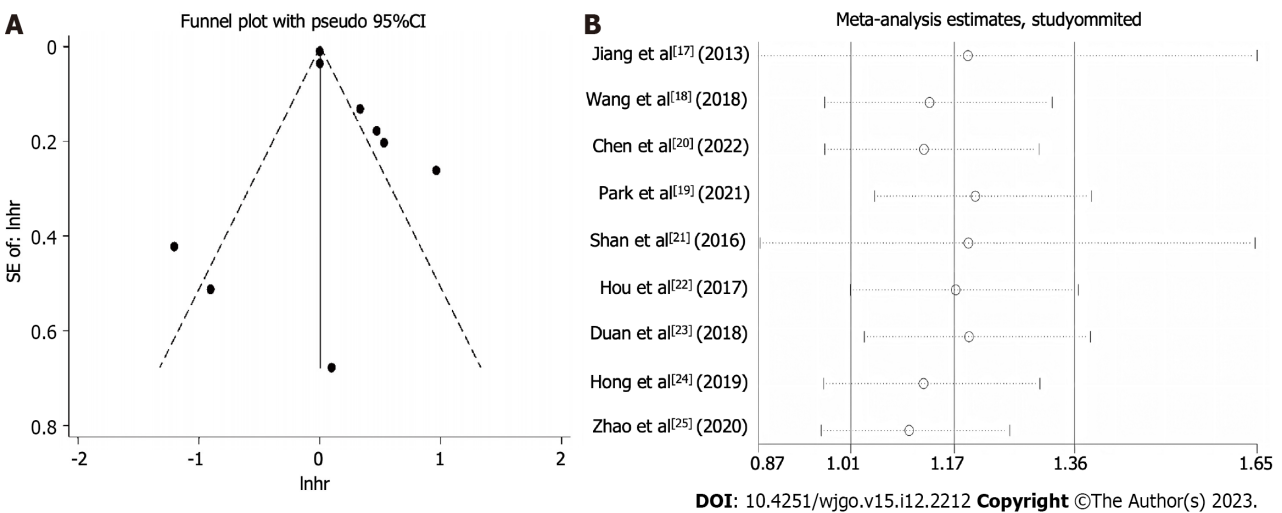


Figure 5 Assessment of publication bias and sensitivity analysis. A: Funnel plot that assessed the effect of potential publication bias on the meta-analysis results; B: Sensitivity analysis that evaluated the impact of omitting individual studies on the pooled effect size estimate to determine the association between the T cell immunoglobulin and mucin-domain containing-3 expression and prognosis in upper gastrointestinal tumors. HR: Hazard ratio.

role of TIM3 as an immunomodulatory molecule and its expression trends in different tumors, we believe that studies around TIM3 will increase in the future. The benefits of TIM3-targeted therapeutic strategies may not be limited to upper GI tract tumors but also to other cancer types. In addition, TIM3-focused combination therapies, such as those paired with PD-1/PD-L1 inhibitors, may become a hot research topic. As more studies unravel the function of TIM3 and its interrelationships with other immune checkpoints, it may become an important target in cancer therapy. TIM3 is expected to serve as a biomarker to predict prognosis and provide guidance for immunotherapy and even chemotherapy.

Although our study provides strong evidence for the role of TIM3 in upper GI tract tumors, it also has its limitations. First, the studies included in the meta-analysis were conducted only in Asian populations. Thus, our conclusions may not be entirely generalizable to other ethnic groups. Second, the studies included in the meta-analysis were somewhat heterogeneous in terms of study design, sample source, and experimental method. Moreover, the experimental method used was IHC, which is a less accurate method for quantitative analysis compared to other protein analysis methods. In addition, TIM3-related clinical drugs are not widely available, and further drug development is needed.

CONCLUSION

In conclusion, the meta-analysis results suggest that high TIM3 expression in upper GI tract tumors is strongly associated with poor prognosis. The findings underline the role of TIM3 as a potential prognostic marker, which may provide guidance in the development of individualized treatment and immunotherapy strategies. However, more studies are needed to explore the prognostic value of TIM3 expression in upper GI tract tumors. Furthermore, unraveling its underlying mechanisms may provide a theoretical basis for the development of therapeutic strategies that target TIM3.

ARTICLE HIGHLIGHTS

Research background

T cell immunoglobulin and mucin-domain containing-3 (TIM3) is an immune checkpoint molecule. The prognostic value of TIM3 expression in upper gastrointestinal (GI) tract tumors has not been comprehensively analyzed.

Research motivation

The study clarifies the prognostic value of TIM3 in upper GI tumors and assesses whether TIM3 could be used as a research target to guide future clinical treatment.

Research objectives

The study investigates the immunohistochemical expression of TIM3 in upper GI tract tumors and assesses its clinical and prognostic value.

Research methods

The PubMed, Web of Science, and Embase databases were searched for subject terms, including “TIM3,” “gastric cancer,” and “esophageal cancer.” Data analyses were performed using STATA 15.2. The results were expressed as hazard ratio (HR) and odds ratio (OR), with the respective 95% confidence interval (CI). Heterogeneity was assessed using the I^2 statistic.

Research results

High TIM3 expression was associated with a worse prognosis in upper GI tract cancers (HR: 1.17, 95%CI: 1.01-1.36). TIM3 overexpression was significantly correlated with the TNM stage (OR: 1.21, 95%CI: 0.63-2.33; $P < 0.05$). TIM3 expression showed no association with other clinicopathological parameters.

Research conclusions

High expression of TIM3 in upper GI tract cancers is associated with a poorer prognosis and advanced T or N stage.

Research perspectives

None of the studies included in the meta-analysis evaluated the prognostic value of TIM3 expression in esophagogastric junction cancer. In addition, the small sample size of the studies was a limitation and the effect of confounding factors on the results cannot be ruled out. However, the results revealed a significant association between high expression of TIM3 and poor survival outcomes in upper GI tract tumors. Our analysis suggests that TIM3, as an immune checkpoint receptor, may be a useful prognostic marker and a potential therapeutic target worthy of further research.

FOOTNOTES

Author contributions: Zhang ZW conceptualized, designed, and revised the manuscript; Yan JJ searched the literature, collected the data, organized the data, and drafted the manuscript; Liu BB collected the data; Yang Y and Deng ZQ checked and collated the data; Liu MR and Wang H performed the statistical analyses; All authors approved the final version of the manuscript.

Supported by the Science and Technology Research Project of Colleges and Universities of Hebei Province, No. QN2020234; the Precision Medicine Joint Cultivation Fund Project of Natural Science Foundation of Hebei Province, No. H2021402007; the Clinical Medicine Talent Cultivation Project of Health Commission of Hebei Province, No. 2020; and the Medical Science Research Project of Health Commission of Hebei Province, No. 20211392.

Conflict-of-interest statement: The authors have no conflicts of interest to declare.

PRISMA 2009 Checklist statement: The authors have read the PRISMA 2009 checklist, and subsequently prepared and revised it.

Open-Access: This article is an open-access article that was selected by an in-house editor and fully peer-reviewed by external reviewers. It is distributed in accordance with the Creative Commons Attribution NonCommercial (CC BY-NC 4.0) license, which permits others to distribute, remix, adapt, build upon this work non-commercially, and license their derivative works on different terms, provided the

original work is properly cited and the use is non-commercial. See: <https://creativecommons.org/licenses/by-nc/4.0/>

Country/Territory of origin: China

ORCID number: Jing-Jing Yan 0000-0002-2883-1872; Bing-Bing Liu 0000-0002-8091-8908; Yan Yang 0000-0001-5017-3899; Meng-Ru Liu 0000-0003-0758-7142; Han Wang 0000-0002-9101-0655; Zhen-Quan Deng 0009-0001-3055-5512; Zhi-Wei Zhang 0000-0001-9262-1004.

S-Editor: Li L

L-Editor: Filipodia

P-Editor: Zhang XD

REFERENCES

- 1 Siegel RL, Miller KD, Wagle NS, Jemal A. Cancer statistics, 2023. *CA Cancer J Clin* 2023; **73**: 17-48 [PMID: 36633525 DOI: 10.3322/caac.21763]
- 2 Xia C, Dong X, Li H, Cao M, Sun D, He S, Yang F, Yan X, Zhang S, Li N, Chen W. Cancer statistics in China and United States, 2022: profiles, trends, and determinants. *Chin Med J (Engl)* 2022; **135**: 584-590 [PMID: 35143424 DOI: 10.1097/CM9.0000000000002108]
- 3 Sung H, Ferlay J, Siegel RL, Laversanne M, Soerjomataram I, Jemal A, Bray F. Global Cancer Statistics 2020: GLOBOCAN Estimates of Incidence and Mortality Worldwide for 36 Cancers in 185 Countries. *CA Cancer J Clin* 2021; **71**: 209-249 [PMID: 33538338 DOI: 10.3322/caac.21660]
- 4 Zheng R, Zhang S, Zeng H, Wang S, Sun K, Chen R, Li L, Wei W, He J. Cancer incidence and mortality in China, 2016. *J Natl Cancer Cent* 2022; **2**: 1-9
- 5 Ricci AD, Rizzo A, Rojas Llimpe FL, Di Fabio F, De Biase D, Rihawi K. Novel HER2-Directed Treatments in Advanced Gastric Carcinoma: Another Paradigm Shift? *Cancers (Basel)* 2021; **13** [PMID: 33916206 DOI: 10.3390/cancers13071664]
- 6 Santoni M, Rizzo A, Mollica V, Matrana MR, Rosellini M, Faloppi L, Marchetti A, Battelli N, Massari F. The impact of gender on The efficacy of immune checkpoint inhibitors in cancer patients: The MOUSEION-01 study. *Crit Rev Oncol Hematol* 2022; **170**: 103596 [PMID: 35031442 DOI: 10.1016/j.critrevonc.2022.103596]
- 7 Santoni M, Rizzo A, Kucharz J, Mollica V, Rosellini M, Marchetti A, Tassinari E, Monteiro FSM, Soares A, Molina-Cerrillo J, Grande E, Battelli N, Massari F. Complete remissions following immunotherapy or immuno-oncology combinations in cancer patients: the MOUSEION-03 meta-analysis. *Cancer Immunol Immunother* 2023; **72**: 1365-1379 [PMID: 36633661 DOI: 10.1007/s00262-022-03349-4]
- 8 Ricci AD, Rizzo A, Brandi G. DNA damage response alterations in gastric cancer: knocking down a new wall. *Future Oncol* 2021; **17**: 865-868 [PMID: 33508962 DOI: 10.2217/fo-2020-0989]
- 9 Pardoll DM. The blockade of immune checkpoints in cancer immunotherapy. *Nat Rev Cancer* 2012; **12**: 252-264 [PMID: 22437870 DOI: 10.1038/nrc3239]
- 10 Li B, Chan HL, Chen P. Immune Checkpoint Inhibitors: Basics and Challenges. *Curr Med Chem* 2019; **26**: 3009-3025 [PMID: 28782469 DOI: 10.2174/0929867324666170804143706]
- 11 Tang Q, Chen Y, Li X, Long S, Shi Y, Yu Y, Wu W, Han L, Wang S. The role of PD-1/PD-L1 and application of immune-checkpoint inhibitors in human cancers. *Front Immunol* 2022; **13**: 964442 [PMID: 36177034 DOI: 10.3389/fimmu.2022.964442]
- 12 Lipson EJ, Drake CG. Ipilimumab: an anti-CTLA-4 antibody for metastatic melanoma. *Clin Cancer Res* 2011; **17**: 6958-6962 [PMID: 21900389 DOI: 10.1158/1078-0432.CCR-11-1595]
- 13 Yi M, Zheng X, Niu M, Zhu S, Ge H, Wu K. Combination strategies with PD-1/PD-L1 blockade: current advances and future directions. *Mol Cancer* 2022; **21**: 28 [PMID: 35062949 DOI: 10.1186/s12943-021-01489-2]
- 14 Chang E, Pelosof L, Lemery S, Gong Y, Goldberg KB, Farrell AT, Keegan P, Veeraraghavan J, Wei G, Blumenthal GM, Amiri-Kordestani L, Singh H, Fashoyin-Aje L, Gormley N, Kluetz PG, Pazdur R, Beaver JA, Theoret MR. Systematic Review of PD-1/PD-L1 Inhibitors in Oncology: From Personalized Medicine to Public Health. *Oncologist* 2021; **26**: e1786-e1799 [PMID: 34196068 DOI: 10.1002/onco.13887]
- 15 Monney L, Sabatos CA, Gaglia JL, Ryu A, Waldner H, Chernova T, Manning S, Greenfield EA, Coyle AJ, Sobel RA, Freeman GJ, Kuchroo VK. Th1-specific cell surface protein Tim-3 regulates macrophage activation and severity of an autoimmune disease. *Nature* 2002; **415**: 536-541 [PMID: 11823861 DOI: 10.1038/415536a]
- 16 Zheng S, Song J, Linghu D, Yang R, Liu B, Xue Z, Chen Q, Liu C, Zhong D, Hung MC, Sun L. Galectin-9 blockade synergizes with ATM inhibition to induce potent anti-tumor immunity. *Int J Biol Sci* 2023; **19**: 981-993 [PMID: 36778120 DOI: 10.7150/ijbs.79852]
- 17 Jiang J, Jin MS, Kong F, Cao D, Ma HX, Jia Z, Wang YP, Suo J, Cao X. Decreased galectin-9 and increased Tim-3 expression are related to poor prognosis in gastric cancer. *PLoS One* 2013; **8**: e81799 [PMID: 24339967 DOI: 10.1371/journal.pone.0081799]
- 18 Wang Y, Zhao E, Zhang Z, Zhao G, Cao H. Association between Tim3 and Gal9 expression and gastric cancer prognosis. *Oncol Rep* 2018; **40**: 2115-2126 [PMID: 30106451 DOI: 10.3892/or.2018.6627]
- 19 Park Y, Seo AN, Koh J, Nam SK, Kwak Y, Ahn SH, Park DJ, Kim HH, Lee HS. Expression of the immune checkpoint receptors PD-1, LAG3, and TIM3 in the immune context of stage II and III gastric cancer by using single and chromogenic multiplex immunohistochemistry. *Oncoimmunology* 2021; **10**: 1954761 [PMID: 34367732 DOI: 10.1080/2162402X.2021.1954761]
- 20 Chen K, Gu Y, Cao Y, Fang H, Lv K, Liu X, He X, Wang J, Lin C, Liu H, Zhang H, He H, Xu J, Li H, Li R. TIM3(+) cells in gastric cancer: clinical correlates and association with immune context. *Br J Cancer* 2022; **126**: 100-108 [PMID: 34725458 DOI: 10.1038/s41416-021-01607-3]
- 21 Shan B, Man H, Liu J, Wang L, Zhu T, Ma M, Xv Z, Chen X, Yang X, Li P. TIM-3 promotes the metastasis of esophageal squamous cell carcinoma by targeting epithelial-mesenchymal transition via the Akt/GSK-3 β /Snail signaling pathway. *Oncol Rep* 2016; **36**: 1551-1561 [PMID: 27430162 DOI: 10.3892/or.2016.4938]
- 22 Hou N, Ma J, Li W, Zhao L, Gao Q, Mai L. T-cell immunoglobulin and mucin domain-containing protein-3 and galectin-9 protein expression: Potential prognostic significance in esophageal squamous cell carcinoma for Chinese patients. *Oncol Lett* 2017; **14**: 8007-8013 [PMID: 29344243 DOI: 10.3892/ol.2017.7188]

- 23 **Duan J**, Xie Y, Qu L, Wang L, Zhou S, Wang Y, Fan Z, Yang S, Jiao S. A nomogram-based immunoprofile predicts overall survival for previously untreated patients with esophageal squamous cell carcinoma after esophagectomy. *J Immunother Cancer* 2018; **6**: 100 [PMID: 30285868 DOI: 10.1186/s40425-018-0418-7]
- 24 **Hong MH**, Shin SJ, Shin SK, Kim DJ, Zo JI, Shim YM, Lee SE, Cho BC, Park SY, Choi YL, Kim HR. High CD3 and ICOS and low TIM-3 expression predict favourable survival in resected oesophageal squamous cell carcinoma. *Sci Rep* 2019; **9**: 20197 [PMID: 31882943 DOI: 10.1038/s41598-019-56828-7]
- 25 **Zhao Y**, Chen D, Wang W, Zhao T, Wen J, Zhang F, Duan S, Chen C, Sang Y, Zhang Y, Chen Y. Significance of TIM-3 Expression in Resected Esophageal Squamous Cell Carcinoma. *Ann Thorac Surg* 2020; **109**: 1551-1557 [PMID: 31987829 DOI: 10.1016/j.athoracsur.2019.12.017]
- 26 **Aragon-Sanabria V**, Kim GB, Dong C. From Cancer Immunoediting to New Strategies in Cancer Immunotherapy: The Roles of Immune Cells and Mechanics in Oncology. *Adv Exp Med Biol* 2018; **1092**: 113-138 [PMID: 30368751 DOI: 10.1007/978-3-319-95294-9_7]
- 27 **Janssen LME**, Ramsay EE, Logsdon CD, Overwijk WW. The immune system in cancer metastasis: friend or foe? *J Immunother Cancer* 2017; **5**: 79 [PMID: 29037250 DOI: 10.1186/s40425-017-0283-9]
- 28 **Jiang J**, Li J, Zhou X, Zhao X, Huang B, Qin Y. Exosomes Regulate the Epithelial-Mesenchymal Transition in Cancer. *Front Oncol* 2022; **12**: 864980 [PMID: 35359397 DOI: 10.3389/fonc.2022.864980]
- 29 **Qin Y**, Geng JX, Huang B. Clinical value of serum pepsinogen in the diagnosis and treatment of gastric diseases. *World J Gastrointest Oncol* 2023; **15**: 1174-1181 [PMID: 37546552 DOI: 10.4251/wjgo.v15.i7.1174]
- 30 **Das M**, Zhu C, Kuchroo VK. Tim-3 and its role in regulating anti-tumor immunity. *Immunol Rev* 2017; **276**: 97-111 [PMID: 28258697 DOI: 10.1111/imr.12520]
- 31 **Borcherding N**, Kolb R, Gullicksrud J, Vikas P, Zhu Y, Zhang W. Keeping Tumors in Check: A Mechanistic Review of Clinical Response and Resistance to Immune Checkpoint Blockade in Cancer. *J Mol Biol* 2018; **430**: 2014-2029 [PMID: 29800567 DOI: 10.1016/j.jmb.2018.05.030]
- 32 **Sabins NC**, Chornoguz O, Leander K, Kaplan F, Carter R, Kinder M, Bachman K, Verona R, Shen S, Bhargava V, Santulli-Marotto S. TIM-3 Engagement Promotes Effector Memory T Cell Differentiation of Human Antigen-Specific CD8 T Cells by Activating mTORC1. *J Immunol* 2017; **199**: 4091-4102 [PMID: 29127145 DOI: 10.4049/jimmunol.1701030]
- 33 **Pagliano O**, Morrison RM, Chauvin JM, Banerjee H, Davar D, Ding Q, Tanegashima T, Gao W, Chakka SR, DeBlasio R, Lowin A, Kara K, Ka M, Zidi B, Amin R, Raphael I, Zhang S, Watkins SC, Sander C, Kirkwood JM, Bosenberg M, Anderson AC, Kuchroo VK, Kane LP, Korman AJ, Rajpal A, West SM, Han M, Bee C, Deng X, Schebye XM, Strop P, Zarour HM. Tim-3 mediates T cell trogocytosis to limit antitumor immunity. *J Clin Invest* 2022; **132** [PMID: 35316223 DOI: 10.1172/JCI152864]
- 34 **Liu JF**, Wu L, Yang LL, Deng WW, Mao L, Wu H, Zhang WF, Sun ZJ. Blockade of TIM3 relieves immunosuppression through reducing regulatory T cells in head and neck cancer. *J Exp Clin Cancer Res* 2018; **37**: 44 [PMID: 29506555 DOI: 10.1186/s13046-018-0713-7]
- 35 **Tan S**, Xu Y, Wang Z, Wang T, Du X, Song X, Guo X, Peng J, Zhang J, Liang Y, Lu J, Gao C, Wu Z, Li C, Li N, Gao L, Liang X, Ma C. Tim-3 Hampers Tumor Surveillance of Liver-Resident and Conventional NK Cells by Disrupting PI3K Signaling. *Cancer Res* 2020; **80**: 1130-1142 [PMID: 31848194 DOI: 10.1158/0008-5472.CAN-19-2332]
- 36 **Klapholz M**, Drage MG, Srivastava A, Anderson AC. Presence of Tim3(+) and PD-1(+) CD8(+) T cells identifies microsatellite stable colorectal carcinomas with immune exhaustion and distinct clinicopathological features. *J Pathol* 2022; **257**: 186-197 [PMID: 35119692 DOI: 10.1002/path.5877]
- 37 **Huang YH**, Zhu C, Kondo Y, Anderson AC, Gandhi A, Russell A, Dougan SK, Petersen BS, Melum E, Pertel T, Clayton KL, Raab M, Chen Q, Beauchemin N, Yazaki PJ, Pyzik M, Ostrowski MA, Glickman JN, Rudd CE, Ploegh HL, Franke A, Petsko GA, Kuchroo VK, Blumberg RS. CEACAM1 regulates TIM-3-mediated tolerance and exhaustion. *Nature* 2015; **517**: 386-390 [PMID: 25363763 DOI: 10.1038/nature13848]
- 38 **Yu S**, Ren X, Meng F, Guo X, Tao J, Zhang W, Liu Z, Fu R, Li L. TIM3/CEACAM1 pathway involves in myeloid-derived suppressor cells induced CD8(+) T cells exhaustion and bone marrow inflammatory microenvironment in myelodysplastic syndrome. *Immunology* 2023; **168**: 273-289 [PMID: 35470423 DOI: 10.1111/imm.13488]
- 39 **Konantz M**, Williams M, Merkel T, Reiss A, Dirnhofer S, Meyer SC, Valent P, George TI, Tzankov A, Hartmann K. Increased TIM-3 and galectin-9 serum levels in patients with advanced systemic mastocytosis. *J Allergy Clin Immunol* 2023; **152**: 1019-1024 [PMID: 37423405 DOI: 10.1016/j.jaci.2023.07.001]
- 40 **Burugu S**, Dancsok AR, Nielsen TO. Emerging targets in cancer immunotherapy. *Semin Cancer Biol* 2018; **52**: 39-52 [PMID: 28987965 DOI: 10.1016/j.semcancer.2017.10.001]
- 41 **Yang R**, Sun L, Li CF, Wang YH, Yao J, Li H, Yan M, Chang WC, Hsu JM, Cha JH, Hsu JL, Chou CW, Sun X, Deng Y, Chou CK, Yu D, Hung MC. Galectin-9 interacts with PD-1 and TIM-3 to regulate T cell death and is a target for cancer immunotherapy. *Nat Commun* 2021; **12**: 832 [PMID: 33547304 DOI: 10.1038/s41467-021-21099-2]
- 42 **Kandel S**, Adhikary P, Li G, Cheng K. The TIM3/Gal9 signaling pathway: An emerging target for cancer immunotherapy. *Cancer Lett* 2021; **510**: 67-78 [PMID: 33895262 DOI: 10.1016/j.canlet.2021.04.011]

Association of *MBOAT7* rs641738 polymorphism with hepatocellular carcinoma susceptibility: A systematic review and meta-analysis

Min Lai, Ya-Lu Qin, Qiong-Yu Jin, Wen-Jing Chen, Jia Hu

Specialty type: Oncology

Provenance and peer review:

Unsolicited article; Externally peer reviewed.

Peer-review model: Single blind

Peer-review report's scientific quality classification

Grade A (Excellent): 0

Grade B (Very good): B, B

Grade C (Good): 0

Grade D (Fair): 0

Grade E (Poor): 0

P-Reviewer: Tsoulfas G, Greece; Yoshioka K, Japan

Received: August 27, 2023

Peer-review started: August 27, 2023

First decision: October 18, 2023

Revised: October 23, 2023

Accepted: November 17, 2023

Article in press: November 17, 2023

Published online: December 15, 2023



Min Lai, Qiong-Yu Jin, Wen-Jing Chen, Jia Hu, Department of Gastroenterology, the Third Affiliated Hospital of Chengdu Medical College/Chengdu Pidu District People's Hospital, Chengdu 611730, Sichuan Province, China

Ya-Lu Qin, Department of Cardiology, the Affiliated Third Hospital of Chengdu Traditional Chinese Medicine University/Chengdu Pidu District Hospital of Traditional Chinese Medicine, Chengdu 611730, Sichuan Province, China

Corresponding author: Min Lai, MD, Doctor, Department of Gastroenterology, the Third Affiliated Hospital of Chengdu Medical College/Chengdu Pidu District People's Hospital, No. 666 Section 2, Deyuan North Road, Pidu District, Chengdu 611730, Sichuan Province, China. laimin1128Lm@126.com

Abstract

BACKGROUND

The *MBOAT7* rs641738 single-nucleotide polymorphism (SNP) has been proven to influence various liver diseases, but its association with hepatocellular carcinoma (HCC) susceptibility has been debated. To address this discrepancy, we conducted the current systematic review and meta-analysis.

AIM

To perform a systematic review and meta-analysis on association of *MBOAT7* SNP and HCC susceptibility.

METHODS

We performed a systematic review in PubMed, Web of Science, Scopus, and EMBASE; applied specific inclusion and exclusion criteria; and extracted the data. Meta-analysis was conducted with the *meta* package in R. Sensitivity and subgroup analyses were also performed. This meta-analysis was registered in PROSPERO (CRD42023458046).

RESULTS

Eight studies were included in the systematic review, and 12 cohorts from 6 studies were included in the meta-analysis. Our meta-analysis revealed an association between the *MBOAT7* SNP and HCC susceptibility in both the dominant [odds ratio (OR): 1.14, 95% confidence interval (95%CI): 1.02-1.26, $P = 0.020$] and recessive (OR: 1.21, 95%CI: 1.05-1.39, $P = 0.008$) models. Subgroup analysis revealed that stratification of the included patients by geographical origin showed a significant association in Asia (OR: 1.20, 95%CI: 1.03-1.39).

CONCLUSION

This meta-analysis underscores the contribution of the *MBOAT7* rs641738 SNP to hepatocarcinogenesis, especially in Asian populations, which warrants further investigation.

Key Words: *MBOAT7*; Single-nucleotide polymorphisms; Hepatocellular carcinoma; Systematic review; Meta-analysis; Asian populations

©The Author(s) 2023. Published by Baishideng Publishing Group Inc. All rights reserved.

Core Tip: We conducted the current systematic review and meta-analysis to address the association between *MBOAT7* rs641738 SNP and HCC susceptibility. We demonstrated the correlation between *MBOAT7* rs641738 SNP and HCC susceptibility both in the dominant and recessive models, and subgroup analysis revealed the significant association especially in Asia populations, which could guide clinical practice in the identification of at-risk population.

Citation: Lai M, Qin YL, Jin QY, Chen WJ, Hu J. Association of *MBOAT7* rs641738 polymorphism with hepatocellular carcinoma susceptibility: A systematic review and meta-analysis. *World J Gastrointest Oncol* 2023; 15(12): 2225-2236

URL: <https://www.wjgnet.com/1948-5204/full/v15/i12/2225.htm>

DOI: <https://dx.doi.org/10.4251/wjgo.v15.i12.2225>

INTRODUCTION

Hepatocellular carcinoma (HCC), which ranks as the fourth leading cause of cancer-related mortality worldwide, presents a substantial challenge in the health care landscape[1]. Over 80% of HCC cases occur in low-resource and middle-resource countries, particularly in eastern Asia, where medical and social care resources are often constrained[2, 3]. To address this challenge, early detection, improved management, and careful monitoring of high-risk populations are essential strategies.

Germline DNA single-nucleotide polymorphisms (SNPs) likely represent etiology-specific host factors that determine HCC susceptibility, including SNPs within *PNPLA3* (patatin like phospholipase domain containing 3), *TM6SF2* (transmembrane 6 superfamily 2), and *MBOAT7* (membrane-bound O-acyltransferase domain-containing 7)[4]. The association between the *PNPLA3* rs738409 SNP and HCC has already been demonstrated by Singal *et al*[5], who indicated that *PNPLA3* is an independent risk factor for HCC. Furthermore, the association between the *TM6SF2* rs58542926 SNP and HCC has been illustrated by Tang *et al*[6], who also suggested a significant association of the *TM6SF2* SNP with HCC risk.

Interestingly, another previously studied SNP is the missense rs641738 C > T variant positioned downstream of the *MBOAT7* locus. The *MBOAT7* rs641738 SNP has been proven to influence histological liver damage in alcoholic liver disease, nonalcoholic fatty liver disease (NAFLD), hepatitis C, and hepatitis B[7]. However, its association with HCC has been debated. Thabet *et al*[8] performed a large case-control study in patients with hepatitis C virus (HCV)-related HCC and found that the role of rs641738 is limited to the early stages of liver disease but not to further progression or occurrence of HCC. Conversely, Donati *et al*[9] found that the *MBOAT7* rs641738 T allele may predispose patients without cirrhosis to HCC.

To address this discrepancy, we conducted the current systematic review and meta-analysis on the association of the *MBOAT7* SNP and HCC susceptibility, aiming to provide an updated and comprehensive assessment of the evolving evidence in this area.

MATERIALS AND METHODS

Search strategy

We performed a systematic review using the following search strategy in four different databases (PubMed, Web of Science, Scopus, and EMBASE, searched in August 2023): (1): Neoplasms, Hepatic OR Neoplasms, Liver OR Liver Neoplasm OR Neoplasm, Liver OR Hepatic Neoplasms OR Hepatic Neoplasm OR Neoplasm, Hepatic OR Cancer of Liver OR Hepatocellular Cancer OR Cancers, Hepatocellular OR Hepatocellular Cancers OR Hepatic Cancer OR Cancer, Hepatic OR Cancers, Hepatic OR Hepatic Cancers OR Liver Cancer OR Cancer, Liver OR Cancers, Liver OR Liver Cancers OR Cancer of the Liver OR Cancer, Hepatocellular; (2): Membrane bound O-acyltransferase domain-containing 7 protein, human OR *MBOAT7* protein, human OR *MBOAT7* OR membrane bound O-acyltransferase domain-containing 7; and (3): (1) AND (2).

Study selection

The inclusion criteria were as follows: (1) Case-control or cohort study evaluating the association between MBOAT7 rs641738 and HCC risk; and (2) reported odds ratios (ORs) and 95% confidence intervals (95% CIs) and/or allele frequencies and/or genotypes. If duplicate research reports were retrieved, the most comprehensive report was selected to avoid repeated statistics. Studies were excluded if they met one of the following criteria: (1) Review, comment, or conference abstract; and (2) insufficient data to estimate OR and 95% CI.

The following data were extracted from each included study: Author, publication year, country, cohort characteristics, sample size, genotype distribution, allele distribution, minor allele frequency, genotyping method, genetic models, adjustment, and Hardy-Weinberg equilibrium (HWE) data. Two authors independently assessed the studies, and disagreements were resolved through discussion with a third author.

Statistical analysis for meta-analysis

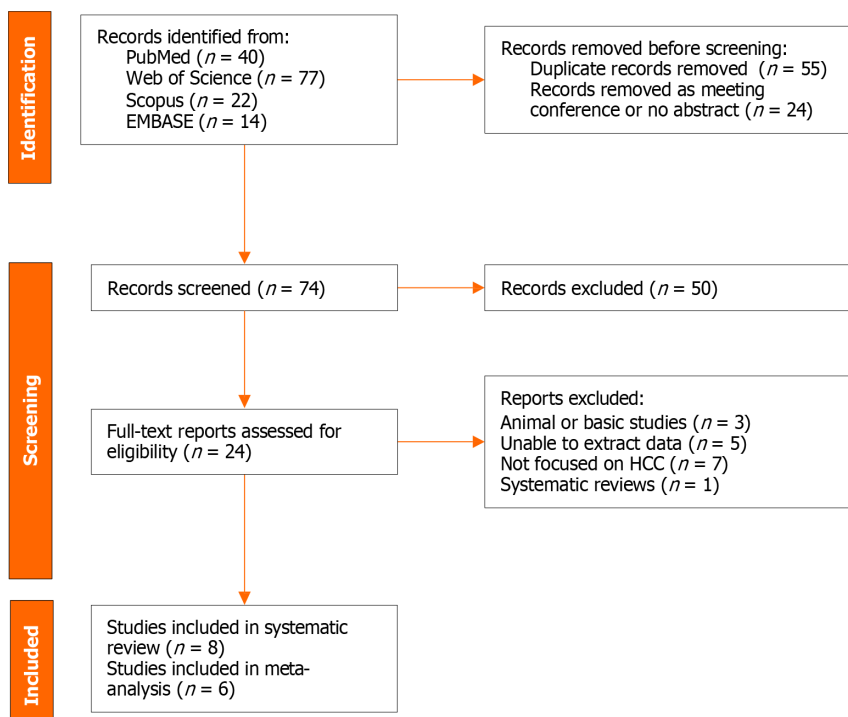
We further conducted a meta-analysis using the cohorts of the included studies. We used the *HardyWeinberg* package (1.7.5) to calculate HWE in the control group of each cohort and performed the meta-analysis using the "metabin", "metagen", and "metainf" functions of the meta package (6.5-0) in R (4.3.0). Between-study heterogeneity was examined using the *Q* test and quantified using *I*². If *I*² > 50%, heterogeneity was considered significant, and a random-effects model was applied. Otherwise, a common-effects model was used. Sensitivity analysis was carried out by re-estimating pooled ORs and 95% CIs after excluding each eligible study in turn to assess the stability of the pooled results. Publication bias was evaluated using a funnel plot.

This meta-analysis was performed according to the guidelines of the PRISMA[10]. The meta-analysis was registered in PROSPERO (CRD42023458046).

RESULTS

Systematic review of association of MBOAT7 rs641738 polymorphism with HCC susceptibility

A total of 153 records were found in four different databases; 40 records were found in PubMed, 77 in the Web of Science, 22 in Scopus, and 14 in EMBASE. After removing 55 duplicates and 24 meeting conferences or records without abstracts, we rigorously reviewed the titles and abstracts of the remaining 74 records. We assessed 24 full-text reports for eligibility and included 8 studies in the systematic review (Figure 1).



DOI: 10.4251/wjgo.v15.i12.2225 Copyright ©The Author(s) 2023.

Figure 1 Flow diagram for literature search and study selection.

Detailed information on the included studies is shown in Table 1. Our systematic review encompassed a comprehensive analysis of eight studies, spanning from 2016 to 2022, that explored the connection between the MBOAT7 rs641738 polymorphism and HCC. Notably, the majority of these studies (*n* = 6) were conducted outside of Asia. Of these,

Table 1 Systematic review of MBOAT7 rs641738 and hepatocellular carcinoma susceptibility

Ref.	Country	Cohort characteristics	Study design	Genotyping method	Genetic model(s)	Main results	Conclusion
Thabet <i>et al</i> [8], 2016	Multi-countries	HCV-related HCC	1706 with chronic HCV infection, divided into two cohorts: Discovery cohort ($n = 931$) and validation cohort ($n = 775$)	TaqMan	Dominant model	No significant association was observed with HCC (OR: 0.96; 95%CI: 0.58-1.57)	The role of rs641738 is limited to the early stages of liver disease, but not to further progression or occurrence of HCC
Donati <i>et al</i> [9], 2017	Multi-countries	NAFLD, HCV, and alcohol-related HCC	Italian ($n = 765$) and United Kingdom ($n = 358$) NAFLD patients; combined cohort of chronic hepatitis C ($n = 597$) or alcoholic liver disease ($n = 524$)	TaqMan	Additive models	In Italian NAFLD patients, the T allele was associated with NAFLD-HCC (OR: 1.65, 95%CI: 1.08-2.55; $n = 765$). In United Kingdom & Italian NAFLD cohort with non-cirrhotic NAFLD, the T allele remained associated with HCC (OR: 2.10, 95%CI: 1.33-3.31; $n = 913$). In combined cohort of chronic hepatitis C or alcoholic liver disease, the T allele was independently associated with HCC risk (OR: 1.93, 95%CI: 1.07-3.58; $n = 1121$)	The MBOAT7 rs641738 T allele may predispose to HCC in patients without cirrhosis
Stickel <i>et al</i> [11], 2018	Multi-countries	Alcohol-related cirrhotic HCC	751 cases with alcohol-related cirrhosis and HCC and 1165 controls with alcohol-related cirrhosis without HCC	TaqMan	Additive models	The risk associated with carriage of MBOAT7 rs641738 was not significant (OR: 1.04, 95%CI: 0.88-1.24)	Neither heterozygous nor homozygous carriage of the MBOAT7 rs641738 T allele was associated with HCC risk
Raksayot <i>et al</i> [14], 2019	Thailand	HBV, HCV, and NBNC-related HCC	Healthy controls ($n = 105$), HBV-related HCC ($n = 270$), HCV-related HCC ($n = 131$), and NBNC-related HCC ($n = 129$)	TaqMan	NA	The genotype distribution and T allele frequencies of MBOAT7 rs641738 were similar between groups (NBNC-HCC vs NBNC-cirrhosis OR: 0.86, 95%CI: 0.51-1.46)	The data did not reveal any association between MBOAT7 rs641738 and the development of NBNC-HCC
Wang <i>et al</i> [16], 2021	China	Unspecified	779 HCC cases and 1412 cancer-free controls (controls consist of 678 persistent HBV carriers and 734 spontaneously recovered subjects)	MassARRAY	Dominant, additive, recessive, and allelic models	The results suggested no association between MBOAT7-TMC4 rs641738 and HCC risk in most genetic models	The work highlights that MBOAT7-TMC4 rs641738 is not associated with the risk of HCC
Bianco <i>et al</i> [12], 2021	Multi-countries	NAFLD-related HCC	At-risk individuals (NAFLD cohort, $n = 2566$ and a replication cohort of 427 German patients with NAFLD). The general population (UKBB cohort, $n = 364048$).	TaqMan & United Kingdom BiLEVE and UKBB Axiom array	NA	In NAFLD cohort, OR: 1.0, 95%CI: 0.7-1.5; in overall UKBB, OR: 1.3, 95%CI: 0.9-1.8; in non-viral UKBB, OR: 1.3, 95%CI 0.9-1.9	Variants in PNPLA3-TM6SF2-GCKR-MBOAT7 were combined in a hepatic fat PRS and PRS predicted HCC more robustly than single variants
Liu <i>et al</i> [13], 2022	United Kingdom	MAFLD-related HCC	160979 participants were diagnosed as having MAFLD	United Kingdom BiLEVE and UKBB Axiom array	NA	Model 2: Adjusted for gender, age, assessment center, genotyping chip, smoking status, physical activity level, overall health rating, average household income, and alcohol consumption. CT vs CC: OR: 1.16, 95%CI: 0.84-1.62; TT vs CC: OR: 1.36, 95%CI: 0.95-1.95	MAFLD is independently associated with an increased risk of both intrahepatic and extrahepatic events. The impact of MAFLD on hepatic health events was amplified by variants in fatty liver disease related genes, among which the genetic variations in PNPLA3, TM6SF2, and MBOAT7 play prominent roles
Nahon <i>et al</i>	French	Compensated	Cohort 1 ($n = 659$):	TaqMan	NA	In HCV-cured cohort, CT/TT	A 7-SNP genetic risk

<i>al</i> [15], 2023	cirrhosis (HCV or alcohol)-related HCC	Compensated cirrhosis with HCV sustained virologic response. Cohort 2 ($n = 486$): Compensated alcohol-related cirrhosis	<i>vs</i> CC: Subhazard ratio: 1.43, 95%CI: 0.68-3.01; In alcohol cohort, CI/TT <i>vs</i> CC: Subhazard ratio: 1.83, 95%CI: 0.85-3.94 (Fine-Gray regression modelling)	score was established, which contains <i>PNPLA3</i> , <i>TM6SF2</i> , <i>HSD17B13</i> , <i>APOE</i> , <i>MBOAT7</i> , and <i>WNT3A-WNT9A</i> variants
----------------------	--	--	--	---

HCV: Hepatitis C virus; HCC: Hepatocellular carcinoma; NAFLD: Nonalcoholic fatty liver disease; HBV: Hepatitis B virus; NBNC: Non-hepatitis B and non-hepatitis C; MAFLD: Metabolic dysfunction-associated fatty liver disease; PRS: Polygenic risk score; OR: Odds ratio; 95%CI: 95% confidence interval; UKBB: United Kingdom Biobank; SNP: Single-nucleotide polymorphism; NA: Not available.

one study[8] concentrated solely on HCV-related HCC, while another[11] exclusively addressed alcohol-related HCC. Furthermore, two studies focused on HCC arising from NAFLD[12] or metabolic dysfunction-associated fatty liver disease[13], while another two[9,14] investigated a mixed cohort of NAFLD, viral, and alcohol-related HCC. One study [15] encompassed HCC occurring in the context of compensated cirrhosis (HCV or alcohol), and one[16] did not specify the particular characteristics of the included patient cohort. The genetic analysis techniques employed were diverse, with the TaqMan genotyping method being utilized in most studies ($n = 5$), with one study employing the MassARRAY[16] and two[12,13] employing United Kingdom Biobank Axiom array methodologies. A subset of studies ($n = 4$) explicitly delineated the genetic models employed in their analysis. Specifically, two studies[9,11] employed additive models, one [8] adopted a dominant model, and another[16] performed an investigation across dominant, additive, recessive, and allelic models. Conversely, the remaining four studies did not expound upon the genetic models utilized.

Overall, the prevailing trend in the majority of studies ($n = 7$) indicated a lack of significant association between the *MBOAT7* rs641738 variant and HCC. Among these, Thabet *et al*[8] examined a cohort of 1706 patients with chronic HCV infection, suggesting that the role of rs641738 was confined to the early stages of liver disease rather than the progression or emergence of HCC. In contrast, Donati *et al*[9] conducted an investigation on 765 Italian and 358 United Kingdom NAFLD patients, and they postulated that the *MBOAT7* rs641738 T allele might predispose individuals to HCC in the absence of cirrhosis. Notably, they discovered that the T allele was autonomously associated with HCC risk in a combined cohort characterized by chronic HCV infection or alcoholic liver disease. To reconcile these divergent findings, both Stickel *et al*[11] and Raksayot *et al*[14] pursued separate inquiries, focusing on alcohol-related and virus-related HCC. Intriguingly, both studies arrived at unanimous negative outcomes. In a similar vein, Wang *et al*[16] undertook a case-control study with unspecified cohort attributes, and they predominantly identified negative associations across various genetic models. The remaining three[12,13,15] studies adopted the polygenic risk score (PRS) approach, which encompassed key genes such as *PNPLA3*, *TM6SF2*, and *MBOAT7*. Through PRS analysis, these investigations successfully stratified patients into distinct risk levels for HCC. However, they consistently observed that *MBOAT7*'s standalone predictive capability was comparatively weak.

Meta-analysis of association of MBOAT7 rs641738 polymorphism with HCC susceptibility

In the meta-analysis, 12 cohorts from 6 studies were rigorously assessed to elucidate the connection between the *MBOAT7* rs641738 polymorphism and HCC. To ensure data quality, we excluded the Italian NAFLD-related and HCV-related HCC cohorts from the study by Donati *et al*[9] due to HWE P values < 0.05 . Additionally, we excluded the alcohol-related HCC cohort from the same study due to limited sample size ($n = 12$). Employing the "metabin" function, we performed calculations for ORs and 95% CIs, except for the combined Italian and United Kingdom NAFLD-related HCC cohort and the United Kingdom Biobank (nonviral) cohort in the study by Bianco *et al*[12], in which genotype counts were unspecified. We adopted both dominant and recessive models in the meta-analysis. Cohort characteristics are summarized in Table 2.

Intriguingly, our meta-analysis revealed an association between the *MBOAT7* rs641738 C > T polymorphism and HCC susceptibility in the dominant model (Figure 2). The pooled OR was 1.14 (95%CI: 1.02-1.26, $P = 0.020$) in the common-effects model used due to low heterogeneity ($I^2 = 33\%$, $P = 0.15$). Robustness was confirmed in the recessive model (Supplementary Figure 1), with a pooled OR of 1.21 (95%CI: 1.05-1.39, $P = 0.008$). Influential analysis *via* the leave-one-out method confirmed the stability of our results (Figure 3). Exclusion of the study by Donati *et al*[9] significantly reduced heterogeneity ($I^2 = 0\%$), and the funnel plot indicated this cohort as a source of heterogeneity (Figure 4). Similar outcomes were observed in the recessive model (Supplementary Figures 2 and 3); after omitting Donati *et al*[9] or Raksayot *et al*[14], the heterogeneity was significantly reduced ($I^2 = 0\%$), and the P value remained < 0.05 in every situation, indicating the robustness of our results.

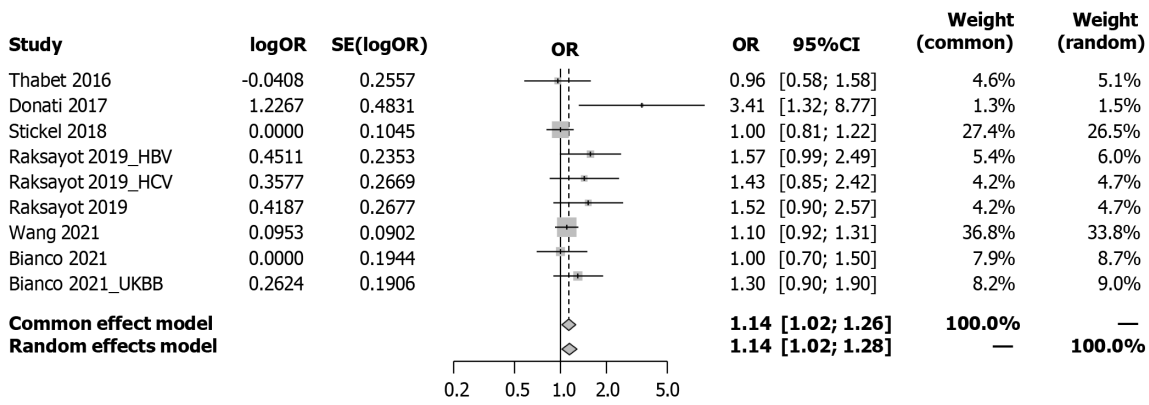
Subgroup analysis considered viral-related and nonviral-related HCC (Figure 5), revealing no significant associations in either the viral (OR: 1.30, 95%CI: 0.98-1.73) or nonviral subgroup (OR: 1.09, 95%CI: 0.93-1.27). Similar trends were observed in the recessive model (Supplementary Figure 4); in the viral subgroup, the OR was 1.09 (95%CI: 0.69-1.73), while in the nonviral subgroup, the OR was 1.14 (95%CI: 0.96-1.34). Studies were categorized into 5 groups by etiology: HCV, alcohol, NAFLD, hepatitis B virus (HBV), and NAFLD plus alcohol (Figure 6). No significant associations were found in the HCV, HBV, alcohol, or NAFLD subgroup. Notably, in the NAFLD plus alcohol subgroup, the OR was 1.37 (95%CI: 1.01-1.86); however, the same phenomenon was not observed with the recessive model (Supplementary Figure 5). Further stratification by the geographical origin of included patients showed a significant association in Asia (OR: 1.20, 95%CI: 1.03-1.39) but not in Europe (Figure 7). In the recessive model, similar results were observed in the Asia subgroup (OR: 1.43, 95%CI: 1.06-1.94, Supplementary Figure 6). This observation underscores the need for more investigation

Table 2 Studies included in meta-analysis

Ref.	Country	Cohort characteristics	Cases	Controls	Genotype (CC/CT/TT)		Allele (C/T)		Minor allele frequency		Adjustment	HWE of control (<i>P</i> value)
					Case	Control	Case	Control	Case	Control		
Thabet <i>et al</i> [8], 2016	Multi	HCV-related HCC	75	1706	24/35/16	531/822/353	83/67	1884/1528	0.45 (T)	0.45 (T)	Age, gender, BMI, and Child-Pugh score	0.305
Donati <i>et al</i> [9], 2017	Italian	NAFLD-related HCC	132	633	26/69/37	213/285/135	121/143	711/555	0.46 (C)	0.44 (T)	Age, gender, obesity, T2DM, and presence of advanced fibrosis	0.036
Donati <i>et al</i> [9], 2017	Italian & United Kingdom	Non-cirrhotic NAFLD-related HCC	41	872	5/21/15	280/422/170	31/51	982/762	0.38 (C)	0.44 (T)	NA	0.664
Donati <i>et al</i> [9], 2017	Italian	HCV-related HCC	13	584	1/7/5	177/259/148	9/17	613/555	0.35 (C)	0.48 (T)	Age, gender, and genetic variants	0.009
Donati <i>et al</i> [9], 2017	Italian	Alcohol-related HCC	12	512	1/8/3	150/251/111	10/14	551/473	0.42 (C)	0.46 (T)	Age, gender, and genetic variants	0.805
Stickel <i>et al</i> [11], 2018	Switzerland, Germany & United Kingdom	Alcohol-related cirrhotic HCC	751	1165	203/363/185	314/583/268	769/733	1211/1119	0.49 (T)	0.48 (T)	Age, gender, BMI, and T2DM	0.967
Raksayot <i>et al</i> [14], 2019	Thailand	HBV-related HCC	270	105	140/114/16	66/34/5	394/146	166/44	0.27 (T)	0.21 (T)	NA	0.943
Raksayot <i>et al</i> [14], 2019	Thailand	HCV-related HCC	131	105	71/53/7	66/34/5	195/67	166/44	0.26 (T)	0.21 (T)	NA	0.943
Raksayot <i>et al</i> [14], 2019	Thailand	NBNC-related HCC (containing NAFLD and alcoholic liver disease)	129	105	68/46/15	66/34/5	182/76	166/44	0.30 (T)	0.21 (T)	NA	0.943
Wang <i>et al</i> [16], 2021	China	Unspecified	779	1405	426/295/58	800/528/77	1147/411	2128/682	0.26 (T)	0.24 (T)	Age, gender, smoking status, and drinking status	0.437
Bianco <i>et al</i> [12], 2021	Italian & United Kingdom	NAFLD-related HCC	226	2338	NA	NA	NA	NA	NA	NA	Age, gender, BMI, and T2DM	NA
Bianco <i>et al</i> [12], 2021	United Kingdom	UKBB (Non-viral)	202	363,846	NA	NA	NA	NA	NA	NA	Age, gender, BMI, T2DM, ethnicity, array batch, and assessment center	NA

HCV: Hepatitis C virus; HCC: Hepatocellular carcinoma; HWE: Hardy-Weinberg equilibrium; NAFLD: Nonalcoholic fatty liver disease; HBV: Hepatitis B virus; T2DM: Type 2 diabetes mellitus; BMI: Body mass index; UKBB: United Kingdom BioBank; NBNC: Non-hepatitis B and non-hepatitis C; NA: Not available.

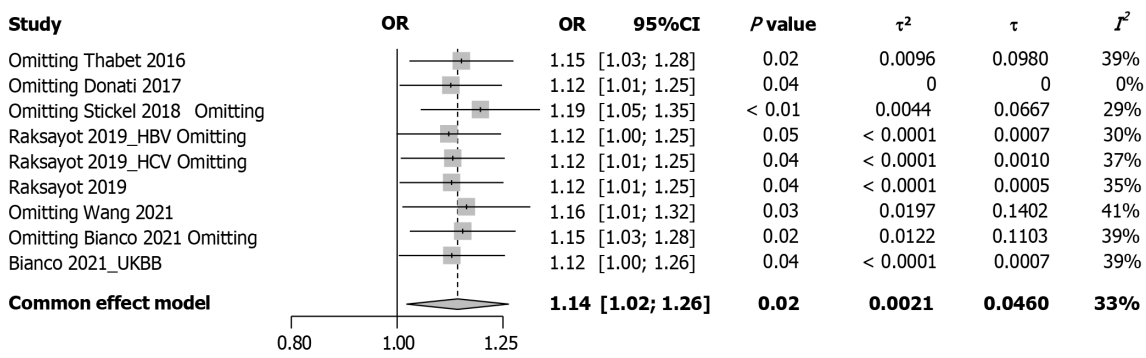
within the Asian population regarding *MBOAT7* polymorphisms and HCC susceptibility.



Heterogeneity: $I^2 = 33\%$, $\tau^2 = 0.0021$, $P = 0.15$

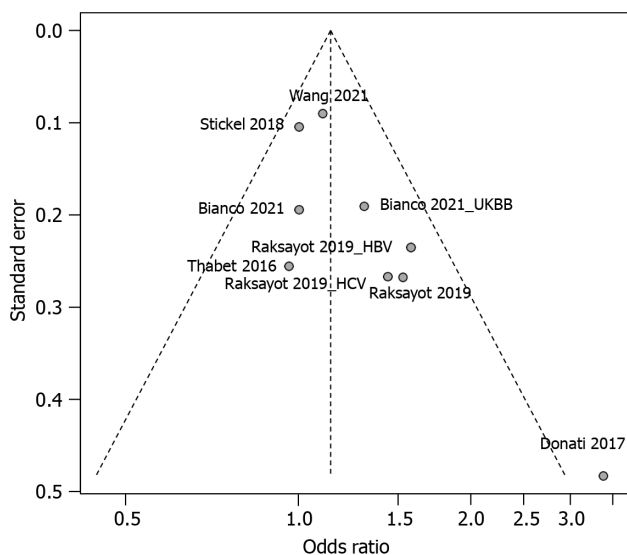
DOI: 10.4251/wjgo.v15.i12.2225 Copyright ©The Author(s) 2023.

Figure 2 Forest plot of association between MBOAT7 rs641738 and hepatocellular carcinoma risk under the dominant model. OR: Odds ratio; 95%CI: 95% confidence interval; HBV: Hepatitis B virus; HCV: Hepatitis C virus; UKBB: United Kingdom Biobank.



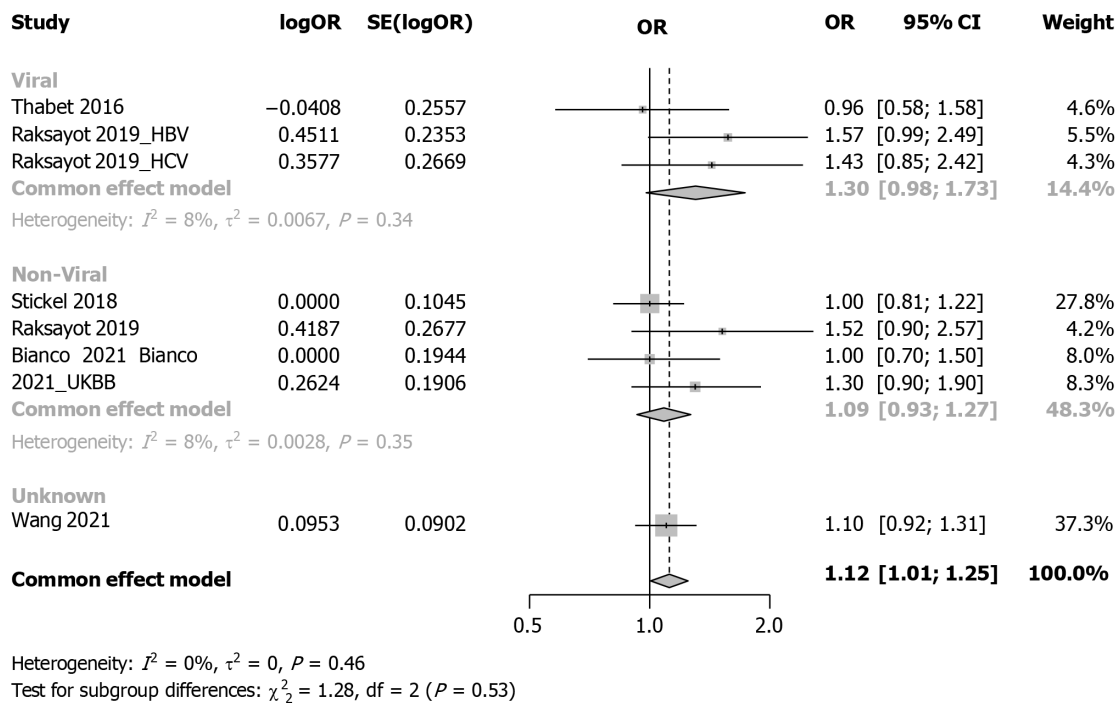
DOI: 10.4251/wjgo.v15.i12.2225 Copyright ©The Author(s) 2023.

Figure 3 Forest plot of influence analysis under the dominant model. OR: Odds ratio; 95%CI: 95% confidence interval; HBV: Hepatitis B virus; HCV: Hepatitis C virus; UKBB: United Kingdom Biobank.



DOI: 10.4251/wjgo.v15.i12.2225 Copyright ©The Author(s) 2023.

Figure 4 Funnel plot of included studies in meta-analysis under the dominant model. HBV: Hepatitis B virus; HCV: Hepatitis C virus; UKBB: United Kingdom Biobank.



DOI: 10.4251/wjgo.v15.i12.2225 Copyright ©The Author(s) 2023.

Figure 5 Forest plot of subgroup analysis under the dominant model (stratification by viral or non-viral related hepatocellular carcinoma). OR: Odds ratio; 95%CI: 95% confidence interval; HBV: Hepatitis B virus; HCV: Hepatitis C virus; UKBB: United Kingdom Biobank.

DISCUSSION

In this systematic review and meta-analysis, a total of 2761 HCC cases and 373376 controls were included. Our results suggested that the *MBOAT7* rs641738 polymorphism was positively associated with HCC susceptibility in both dominant and recessive models. Our subgroup analysis indicated that the *MBOAT7* rs641738 SNP contributes to hepatocarcinogenesis, especially among Asian populations, warranting further exploration of the underlying mechanisms.

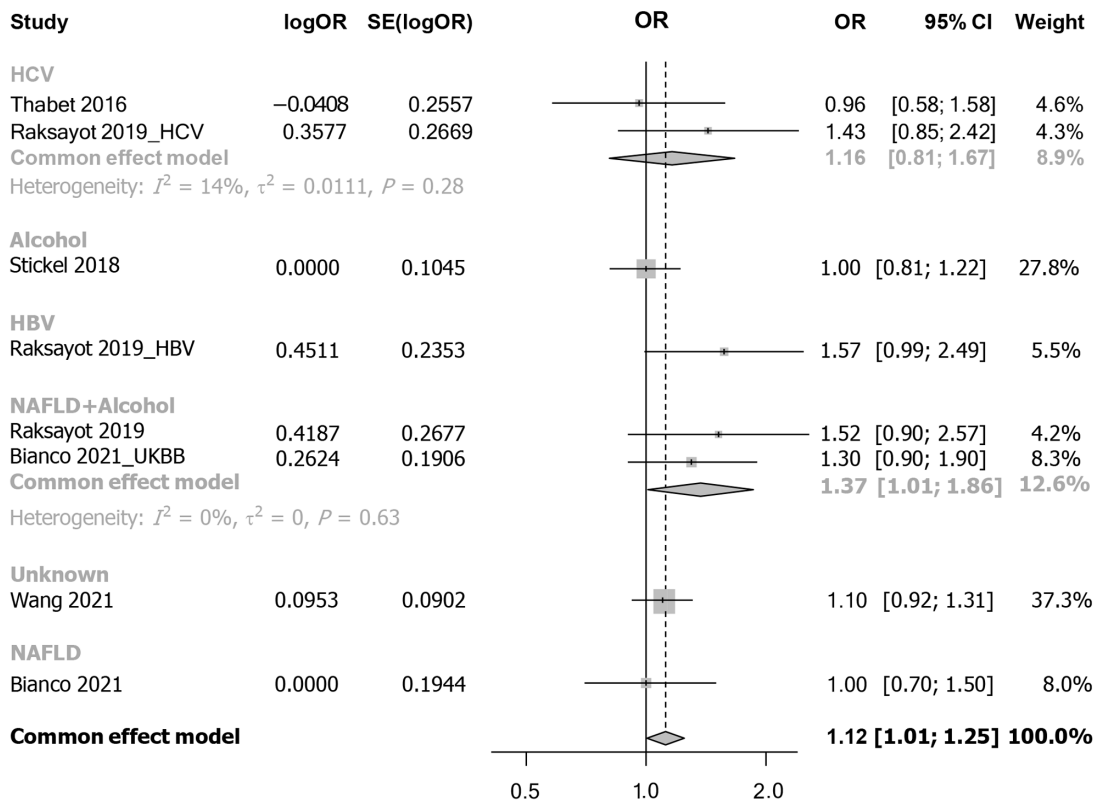
The *MBOAT7* rs641738 SNP contributes to hepatocarcinogenesis, which is supported by basic scientific evidence. Longo *et al*[17] generated a full knockout of *MBOAT7* in HepG2 cells (human HCC cell line) and observed an imbalance in mitochondrial dynamics, and the silencing of both *MBOAT7* and *TM6SF2* impaired mitochondrial activity with a shift toward metabolic reprogramming, which led to hepatocarcinogenesis. Moreover, *MBOAT7*- and *TM6SF2*-silenced cells exhibited increased cell survival, proliferation, and invasiveness.

Multiple studies have been conducted to investigate the association between the PRS and HCC susceptibility, and most of them reached a positive conclusion. Most studies established PRS models including genes such as *PNPLA3*, *HSD17B13*, *TM6SF2*, *MBOAT7*, and *GCKR*. Thrift *et al*[18] evaluated the association of PRS with HCC in 1644 patients in the United State and found that HCC risk increased by 134% per unit increase in PRS [hazard ratio (HR): 2.30; 95%CI: 1.35-3.92]. Similarly, Degasperri *et al*[19] included 509 patients with HCV cirrhosis and found that the PRS was an independent predictor of HCC (HR: 2.30, $P = 0.04$). In contrast, single genetic risk variants were not useful in stratifying HCC risk. Importantly, the PRS method represents a comprehensive assessment of the multiple aspects involved in cancer development. However, the inclusivity of gene sets within the PRS framework remains inconsistent, necessitating further fundamental investigations to refine the approach.

There remain some limitations in this study. First, the included studies in our meta-analysis exhibited diverse etiologies of HCC, which could influence our outcomes. To address this variability, we conducted subgroup analyses and found that the conspicuously positive outcomes might be attributed to studies focused on Asian patients. Additionally, HCC susceptibility could be influenced by patient characteristics, such as age, sex, and smoking habits. Due to the unavailability of the original data of the included studies, this could generate bias in the interpretation of the results. However, the sensitivity analyses confirmed the robustness of our results.

CONCLUSION

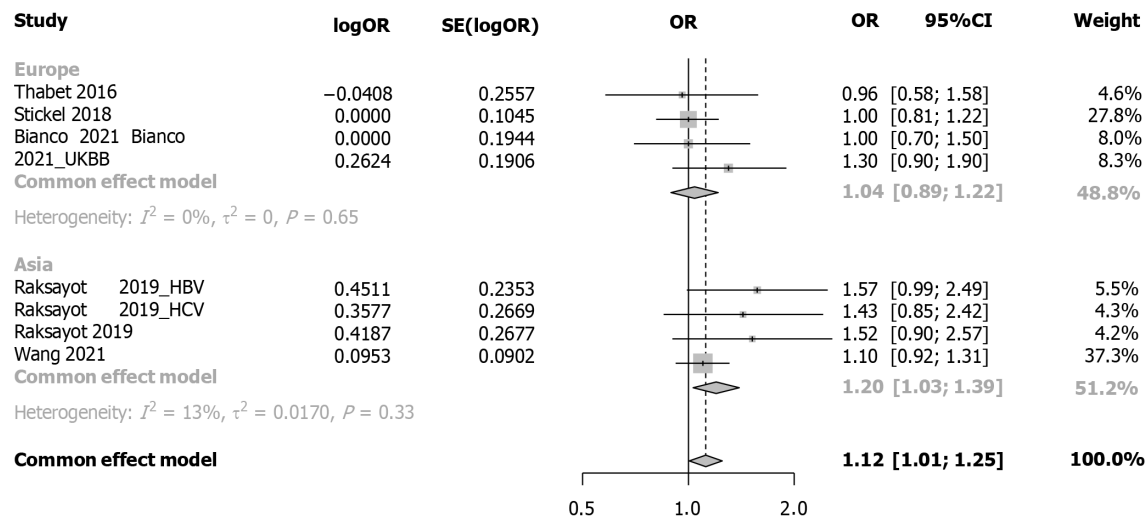
In summary, this meta-analysis underscores the contribution of the *MBOAT7* rs641738 SNP to hepatocarcinogenesis, especially in Asian populations, which warrants further investigation.



Heterogeneity: $I^2 = 0\%$, $\tau^2 = 0$, $P = 0.46$
 Test for subgroup differences: $\chi^2_5 = 5.34$, $df = 5$ ($P = 0.38$)

DOI: 10.4251/wjgo.v15.i12.2225 Copyright ©The Author(s) 2023.

Figure 6 Forest plot of subgroup analysis under the dominant model (stratification by detailed etiology). OR: Odds ratio; 95%CI: 95% confidence interval; HBV: Hepatitis B virus; HCV: Hepatitis C virus; UKBB: United Kingdom Biobank.



Heterogeneity: $I^2 = 0\%$, $\tau^2 = 0$, $P = 0.46$
 Test for subgroup differences: $\chi^2_1 = 1.63$, $df = 1$ ($P = 0.20$)

DOI: 10.4251/wjgo.v15.i12.2225 Copyright ©The Author(s) 2023.

Figure 7 Forest plot of subgroup analysis under the dominant model (stratification by geographical origin). OR: Odds ratio; 95%CI: 95% confidence interval; HBV: Hepatitis B virus; HCV: Hepatitis C virus; UKBB: United Kingdom Biobank.

ARTICLE HIGHLIGHTS

Research background

The *MBOAT7* rs641738 single-nucleotide polymorphism (SNP) has been proven to influence various liver diseases, but its association with hepatocellular carcinoma (HCC) susceptibility has been debated. To address this discrepancy, we conducted the current systematic review and meta-analysis.

Research motivation

Investigating whether *MBOAT7* SNP has an association with HCC susceptibility could help identify at-risk population.

Research objectives

We conducted a systematic review and meta-analysis on the association of the *MBOAT7* SNP and HCC susceptibility, aiming to provide an updated and comprehensive assessment of the evolving evidence in this area.

Research methods

We performed a systematic review in PubMed, Web of Science, Scopus, and EMBASE; applied specific inclusion and exclusion criteria; and extracted the data. Meta-analysis was conducted with the *meta* package in R. Sensitivity and subgroup analyses were also performed.

Research results

Eight studies were included in the systematic review, and 12 cohorts from 6 studies were included in the meta-analysis. Our meta-analysis revealed an association between the *MBOAT7* SNP and HCC susceptibility in both the dominant [odds ratio (OR): 1.14, 95% confidence interval (95%CI): 1.02-1.26, $P = 0.020$] and recessive (OR: 1.21, 95%CI: 1.05-1.39, $P = 0.008$) models. Subgroup analysis revealed that stratification of the included patients by geographical origin showed a significant association in Asia (OR: 1.20, 95%CI: 1.03-1.39).

Research conclusions

This meta-analysis underscores the contribution of the *MBOAT7* rs641738 SNP to hepatocarcinogenesis, especially in Asian populations, which warrants further investigation.

Research perspectives

Future research should focus on what is the specific molecular biological mechanism of *MBOAT7* rs641738 SNP leading to HCC and how to prevent it.

FOOTNOTES

Co-first authors: Min Lai and Ya-Lu Qin.

Author contributions: Lai M and Qin YL conceived, designed, and refined the study protocol; Lai M, Qin YL, Jin QY, Chen WJ, and Hu J were involved in the data collection; Lai M, Qin YL, and Jin QY analyzed the data; Lai M and Qin YL drafted the manuscript; all authors were involved in the critical review of the results and have contributed to, read, and approved the final manuscript. Lai M and Qin YL contributed equally to this work as co-first authors. The reasons for designating Lai M and Qin YL as co-first authors are threefold. First, the research was performed as a collaborative effort, and the designation of co-first authorship accurately reflects the distribution of responsibilities and burdens associated with the time and effort required to complete the study and the resultant paper. This also ensures effective communication and management of post-submission matters, ultimately enhancing the paper's quality and reliability. Second, the overall research team encompassed authors with a variety of expertise and skills from different fields, and the designation of co-first authors best reflects this diversity. This also promotes the most comprehensive and in-depth examination of the research topic, ultimately enriching readers' understanding by offering various expert perspectives. Third, Lai M and Qin YL contributed efforts of equal substance throughout the research process. The choice of these researchers as co-first authors acknowledges and respects this equal contribution, while recognizing the spirit of teamwork and collaboration of this study. In summary, we believe that designating Lai M and Qin YL as co-first authors is fitting for our manuscript as it accurately reflects our team's collaborative spirit, equal contributions, and diversity.

Conflict-of-interest statement: The authors have nothing to disclose.

PRISMA 2009 Checklist statement: The authors have read the PRISMA 2020 Checklist, and the manuscript was prepared and revised according to the PRISMA 2020 Checklist.

Open-Access: This article is an open-access article that was selected by an in-house editor and fully peer-reviewed by external reviewers. It is distributed in accordance with the Creative Commons Attribution NonCommercial (CC BY-NC 4.0) license, which permits others to distribute, remix, adapt, build upon this work non-commercially, and license their derivative works on different terms, provided the original work is properly cited and the use is non-commercial. See: <https://creativecommons.org/licenses/by-nc/4.0/>

Country/Territory of origin: China

ORCID number: Min Lai 0009-0009-8712-0980.

S-Editor: Lin C

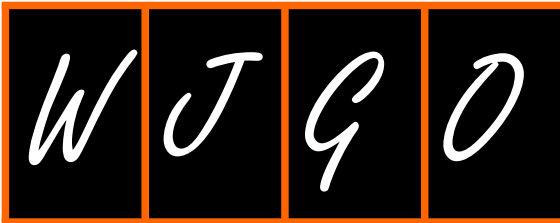
L-Editor: Wang TQ

P-Editor: Zhao S

REFERENCES

- Global Burden of Disease Cancer Collaboration**, Fitzmaurice C, Allen C, Barber RM, Barregard L, Bhutta ZA, Brenner H, Dicker DJ, Chimed-Orchir O, Dandona R, Dandona L, Fleming T, Forouzanfar MH, Hancock J, Hay RJ, Hunter-Merrill R, Huynh C, Hosgood HD, Johnson CO, Jonas JB, Khubchandani J, Kumar GA, Kutz M, Lan Q, Larson HJ, Liang X, Lim SS, Lopez AD, MacIntyre MF, Marczak L, Marquez N, Mokdad AH, Pinho C, Pourmalek F, Salomon JA, Sanabria JR, Sandar L, Sartorius B, Schwartz SM, Shackelford KA, Shibuya K, Stanaway J, Steiner C, Sun J, Takahashi K, Vollset SE, Vos T, Wagner JA, Wang H, Westerman R, Zeeb H, Zocckler L, Abd-Allah F, Ahmed MB, Alabed S, Alam NK, Aldhahri SF, Alem G, Alemayohu MA, Ali R, Al-Raddadi R, Amare A, Amoako Y, Artaman A, Asayesh H, Atnaftu N, Awasthi A, Saleem HB, Barac A, Bedi N, Bensenor I, Berhane A, Bernabé E, Betsu B, Binagwaho A, Boneya D, Campos-Nonato I, Castañeda-Orjuela C, Catalá-López F, Chiang P, Chibueze C, Chitheer A, Choi JY, Cowie B, Damte S, das Neves J, Dey S, Dharmaratne S, Dhillon P, Ding E, Driscoll T, Ekwueme D, Endries AY, Farvid M, Farzadfar F, Fernandes J, Fischer F, G/Hiwot TT, Gebru A, Gopalani S, Hailu A, Horino M, Horita N, Hussein A, Huybrechts I, Inoue M, Islami F, Jakovljevic M, James S, Javanbakht M, Jee SH, Kasaeian A, Kedir MS, Khader YS, Khang YH, Kim D, Leigh J, Linn S, Lunevicius R, El Razek HMA, Malekzadeh R, Malta DC, Marcenes W, Markos D, Melaku YA, Meles KG, Mendoza W, Mengiste DT, Meretoja TJ, Miller TR, Mohammad KA, Mohammadi A, Mohammed S, Moradi-Lakeh M, Nagel G, Nand D, Le Nguyen Q, Nolte S, Ogbo FA, Oladimeji KE, Oren E, Pa M, Park EK, Pereira DM, Plass D, Qorbani M, Radfar A, Rafay A, Rahman M, Rana SM, Søreide K, Satpathy M, Sawhney M, Sepanlou SG, Shaikh MA, She J, Shiue I, Shore HR, Shrimpe MG, So S, Soneji S, Stathopoulou V, Stroumpoulis K, Sufiyan MB, Sykes BL, Tabarés-Seisdedos R, Tadese F, Tedla BA, Tessema GA, Thakur JS, Tran BX, Ukwaja KN, Uzochukwu BSC, Vlassov VV, Weiderpass E, Wubshet Terefe M, Yebo HG, Yimam HH, Yonemoto N, Younis MZ, Yu C, Zaidi Z, Zaki MES, Zenebe ZM, Murray CJL, Naghavi M. Global, Regional, and National Cancer Incidence, Mortality, Years of Life Lost, Years Lived With Disability, and Disability-Adjusted Life-years for 32 Cancer Groups, 1990 to 2015: A Systematic Analysis for the Global Burden of Disease Study. *JAMA Oncol* 2017; **3**: 524-548 [PMID: 27918777 DOI: 10.1001/jamaoncol.2016.5688]
- El-Serag HB**. Epidemiology of viral hepatitis and hepatocellular carcinoma. *Gastroenterology* 2012; **142**: 1264-1273.e1 [PMID: 22537432 DOI: 10.1053/j.gastro.2011.12.061]
- Yang JD**, Hainaut P, Gores GJ, Amadou A, Plymoth A, Roberts LR. A global view of hepatocellular carcinoma: trends, risk, prevention and management. *Nat Rev Gastroenterol Hepatol* 2019; **16**: 589-604 [PMID: 31439937 DOI: 10.1038/s41575-019-0186-y]
- Fujiwara N**, Hoshida Y. Hepatocellular Carcinoma Risk Stratification by Genetic Profiling in Patients with Cirrhosis. *Semin Liver Dis* 2019; **39**: 153-162 [PMID: 30912093 DOI: 10.1055/s-0039-1681031]
- Singal AG**, Manjunath H, Yopp AC, Beg MS, Marrero JA, Gopal P, Waljee AK. The effect of PNPLA3 on fibrosis progression and development of hepatocellular carcinoma: a meta-analysis. *Am J Gastroenterol* 2014; **109**: 325-334 [PMID: 24445574 DOI: 10.1038/ajg.2013.476]
- Tang S**, Zhang J, Mei TT, Guo HQ, Wei XH, Zhang WY, Liu YL, Liang S, Fan ZP, Ma LX, Lin W, Liu YR, Qiu LX, Yu HB. Association of TM6SF2 rs58542926 T/C gene polymorphism with hepatocellular carcinoma: a meta-analysis. *BMC Cancer* 2019; **19**: 1128 [PMID: 31752753 DOI: 10.1186/s12885-019-6173-4]
- Thabet K**, Chan HLY, Petta S, Mangia A, Berg T, Boonstra A, Brouwer WP, Abate ML, Wong VW, Nazmy M, Fischer J, Liddle C, George J, Eslam M. The membrane-bound O-acyltransferase domain-containing 7 variant rs641738 increases inflammation and fibrosis in chronic hepatitis B. *Hepatology* 2017; **65**: 1840-1850 [PMID: 28109005 DOI: 10.1002/hep.29064]
- Thabet K**, Asimakopoulos A, Shojaei M, Romero-Gomez M, Mangia A, Irving WL, Berg T, Dore GJ, Grønbaek H, Sheridan D, Abate ML, Bugianesi E, Weltman M, Mollison L, Cheng W, Riordan S, Fischer J, Spengler U, Nattermann J, Wahid A, Rojas A, White R, Douglas MW, McLeod D, Powell E, Liddle C, van der Poorten D, George J, Eslam M; International Liver Disease Genetics Consortium. MBOAT7 rs641738 increases risk of liver inflammation and transition to fibrosis in chronic hepatitis C. *Nat Commun* 2016; **7**: 12757 [PMID: 27630043 DOI: 10.1038/ncomms12757]
- Donati B**, Dongiovanni P, Romeo S, Meroni M, McCain M, Miele L, Petta S, Maier S, Rosso C, De Luca L, Vanni E, Grimaudo S, Romagnoli R, Colli F, Ferri F, Mancina RM, Iruzubieta P, Craxi A, Fracanzani AL, Grieco A, Corradini SG, Aghemo A, Colombo M, Soardo G, Bugianesi E, Reeves H, Anstee QM, Fargion S, Valenti L. MBOAT7 rs641738 variant and hepatocellular carcinoma in non-cirrhotic individuals. *Sci Rep* 2017; **7**: 4492 [PMID: 28674415 DOI: 10.1038/s41598-017-04991-0]
- Page MJ**, McKenzie JE, Bossuyt PM, Boutron I, Hoffmann TC, Mulrow CD, Shamseer L, Tetzlaff JM, Akl EA, Brennan SE, Chou R, Ghanville J, Grimshaw JM, Hróbjartsson A, Lalu MM, Li T, Loder EW, Mayo-Wilson E, McDonald S, McGuinness LA, Stewart LA, Thomas J, Tricco AC, Welch VA, Whiting P, Moher D. The PRISMA 2020 statement: an updated guideline for reporting systematic reviews. *BMJ* 2021; **372**: n71 [PMID: 33782057 DOI: 10.1136/bmj.n71]
- Stickel F**, Buch S, Nischalke HD, Weiss KH, Gotthardt D, Fischer J, Rosendahl J, Marot A, Elamly M, Casper M, Lammert F, McQuillan A, Zopf S, Spengler U, Marhenke S, Kirstein MM, Vogel A, Eyer F, von Felden J, Wege H, Buch T, Schafmayer C, Braun F, Deltenre P, Berg T, Morgan MY, Hampe J. Genetic variants in PNPLA3 and TM6SF2 predispose to the development of hepatocellular carcinoma in individuals with alcohol-related cirrhosis. *Am J Gastroenterol* 2018; **113**: 1475-1483 [PMID: 29535416 DOI: 10.1038/s41395-018-0041-8]
- Bianco C**, Jamialahmadi O, Pelusi S, Baselli G, Dongiovanni P, Zanoni I, Santoro L, Maier S, Liguori A, Meroni M, Borroni V, D'Ambrosio R, Spagnuolo R, Alisi A, Federico A, Bugianesi E, Petta S, Miele L, Vespasiani-Gentilucci U, Anstee QM, Stickel F, Hampe J, Fischer J, Berg T, Fracanzani AL, Soardo G, Reeves H, Prati D, Romeo S, Valenti L. Non-invasive stratification of hepatocellular carcinoma risk in non-alcoholic fatty liver using polygenic risk scores. *J Hepatol* 2021; **74**: 775-782 [PMID: 33248170 DOI: 10.1016/j.jhep.2020.11.024]
- Liu Z**, Suo C, Shi O, Lin C, Zhao R, Yuan H, Jin L, Zhang T, Chen X. The Health Impact of MAFLD, a Novel Disease Cluster of NAFLD, Is Amplified by the Integrated Effect of Fatty Liver Disease-Related Genetic Variants. *Clin Gastroenterol Hepatol* 2022; **20**: e855-e875 [PMID: 33387670 DOI: 10.1016/j.cgh.2020.12.033]

- 14 **Raksayot M**, Chuaypen N, Khlaiphuengsin A, Pinjaroen N, Treeprasertsuk S, Poovorawan Y, Tanaka Y, Tangkijvanich P. Independent and additive effects of PNPLA3 and TM6SF2 polymorphisms on the development of non-B, non-C hepatocellular carcinoma. *J Gastroenterol* 2019; **54**: 427-436 [PMID: 30506232 DOI: 10.1007/s00535-018-01533-x]
- 15 **Nahon P**, Bamba-Funck J, Layese R, Trépo E, Zucman-Rossi J, Cagnot C, Ganne-Carrié N, Chaffaut C, Guyot E, Ziol M, Sutton A, Audureau E; ANRS CO12 CirVir and CIRRAL groups. Integrating genetic variants into clinical models for hepatocellular carcinoma risk stratification in cirrhosis. *J Hepatol* 2023; **78**: 584-595 [PMID: 36427656 DOI: 10.1016/j.jhep.2022.11.003]
- 16 **Wang P**, Li Y, Li L, Zhong R, Shen N. MBOAT7-TMC4 rs641738 Is Not Associated With the Risk of Hepatocellular Carcinoma or Persistent Hepatitis B Infection. *Front Oncol* 2021; **11**: 639438 [PMID: 34113561 DOI: 10.3389/fonc.2021.639438]
- 17 **Longo M**, Meroni M, Paolini E, Erconi V, Carli F, Fortunato F, Ronchi D, Piciotti R, Sabatini S, Macchi C, Alisi A, Miele L, Soardo G, Comi GP, Valenti L, Ruscica M, Fracanzani AL, Gastaldelli A, Dongiovanni P. TM6SF2/PNPLA3/MBOAT7 Loss-of-Function Genetic Variants Impact on NAFLD Development and Progression Both in Patients and in In Vitro Models. *Cell Mol Gastroenterol Hepatol* 2022; **13**: 759-788 [PMID: 34823063 DOI: 10.1016/j.jcmgh.2021.11.007]
- 18 **Thrift AP**, Kanwal F, Liu Y, Khaderi S, Singal AG, Marrero JA, Loo N, Asrani SK, Luster M, Al-Sarraj A, Ning J, Tsavachidis S, Gu X, Amos CI, El-Serag HB. Risk stratification for hepatocellular cancer among patients with cirrhosis using a hepatic fat polygenic risk score. *PLoS One* 2023; **18**: e0282309 [PMID: 36854015 DOI: 10.1371/journal.pone.0282309]
- 19 **Degasperi E**, Galmozzi E, Pelusi S, D'Ambrosio R, Soffredini R, Borghi M, Perbellini R, Facchetti F, Iavarone M, Sangiovanni A, Valenti L, Lampertico P. Hepatic Fat-Genetic Risk Score Predicts Hepatocellular Carcinoma in Patients With Cirrhotic HCV Treated With DAAs. *Hepatology* 2020; **72**: 1912-1923 [PMID: 32762045 DOI: 10.1002/hep.31500]



Conversion immunotherapy for deficient mismatch repair locally unresectable colon cancer: A case report

Zhen Sun, He Liu, Guan-Nan Zhang, Yi Xiao

Specialty type: Oncology

Provenance and peer review:

Unsolicited article; Externally peer reviewed.

Peer-review model: Single blind

Peer-review report's scientific quality classification

Grade A (Excellent): 0

Grade B (Very good): B

Grade C (Good): 0

Grade D (Fair): D, D

Grade E (Poor): 0

P-Reviewer: Rizzo A, Italy; Shalaby MN, Egypt

Received: October 26, 2023

Peer-review started: October 26, 2023

First decision: October 30, 2023

Revised: October 31, 2023

Accepted: November 5, 2023

Article in press: November 5, 2023

Published online: December 15, 2023



Zhen Sun, Guan-Nan Zhang, Yi Xiao, Division of Colorectal Surgery, Department of General Surgery, Peking Union Medical College Hospital, Chinese Academy of Medical Sciences and Peking Union Medical College, Beijing 100730, China

He Liu, Department of Gastrointestinal Surgery, The People's Hospital of Huangdao District, Qingdao 266400, Shandong Province, China

Corresponding author: Yi Xiao, PhD, Chief Doctor, Division of Colorectal Surgery, Department of General Surgery, Peking Union Medical College Hospital, Chinese Academy of Medical Sciences and Peking Union Medical College, No. 1 Shuai Fu Yuan, Dongcheng District, Beijing 100730, China. xiaoy@pumch.cn

Abstract

BACKGROUND

Owing to the special features of biologics, deficient mismatch repair (dMMR) in patients with colon cancer has achieved little treatment efficacy from chemoradiotherapy. Immunotherapy has shown promising results for the treatment of colon cancer. The high response rate observed suggests a great option for patients presenting with unresectable tumors, as it allows for better oncological resection. Here, we aimed to highlight the significant effects of immunotherapy on dMMR in colon cancer.

CASE SUMMARY

A 54-year-old man diagnosed with locally unresectable dMMR colon cancer received preoperative immunotherapy (three cycles of pembrolizumab) and achieved a pathological complete response after surgery.

CONCLUSION

Immunotherapy can be used as a conversion treatment for locally unresectable colon cancer with dMMR.

Key Words: Colon cancer; Immunotherapy; Pathological complete response; Case report

©The Author(s) 2023. Published by Baishideng Publishing Group Inc. All rights reserved.

Core Tip: Surgery remains the primary radical therapy for colon cancer and resection radicality is one of the most important predictors for survival. Preoperative chemotherapy has been proven to ameliorate resection radicality and survival. Due to the special features of biologics, deficient mismatch repair (dMMR) colon cancer patients achieved little treatment efficacy from chemoradiotherapy. Up to now, immunotherapy has shown promising responses in colon cancer. We aim to draw attention to the significant effect of immunotherapy on dMMR colon cancer.

Citation: Sun Z, Liu H, Zhang GN, Xiao Y. Conversion immunotherapy for deficient mismatch repair locally unresectable colon cancer: A case report. *World J Gastrointest Oncol* 2023; 15(12): 2237-2241

URL: <https://www.wjgnet.com/1948-5204/full/v15/i12/2237.htm>

DOI: <https://dx.doi.org/10.4251/wjgo.v15.i12.2237>

INTRODUCTION

Surgery remains the primary radical therapy for colon cancer[1,2], and resection radicality is an important predictor of local recurrence and overall survival[3]. Owing to the delayed administration of adjuvant chemotherapy, postoperative complications can cause poor oncological outcomes in patients with colorectal cancer (CRC)[4]. Hence, resection radicality should be improved, and the incidence of surgical complications should be reduced. Preoperative chemotherapy improves resection radicality and survival[5-8]. However, owing to the special features of biologics, patients with deficient mismatch repair (dMMR) colon cancer have achieved little treatment efficacy with chemoradiotherapy[9]. Immunotherapy has previously shown promising results for colon cancer[10-13]. Hence, we aimed to draw attention to its significant effect on dMMR in colon cancer. This study was written in compliance with the SCARE Guideline[14].

CASE PRESENTATION

Chief complaints

A 54-year-old man presented to the hospital with difficulty in defecating.

History of present illness

Symptoms started 2 mo before the patient was diagnosed with colon cancer in May 2023.

History of past illness

The patient had undergone colectomy twice owing to a poorly-differentiated adenocarcinoma of the splenic flexure colon (unknown pTNM stage) in 2007 and a moderate- to poorly-differentiated adenocarcinoma of the cecum (pT4aN2a) in 2008. Postoperative adjuvant chemotherapy was administered after both surgeries.

Personal and family history

The patient denied any family history of malignant tumors.

Physical examination

Physical examination revealed normal vital signs. The digital anal examination result was also normal.

Laboratory examinations

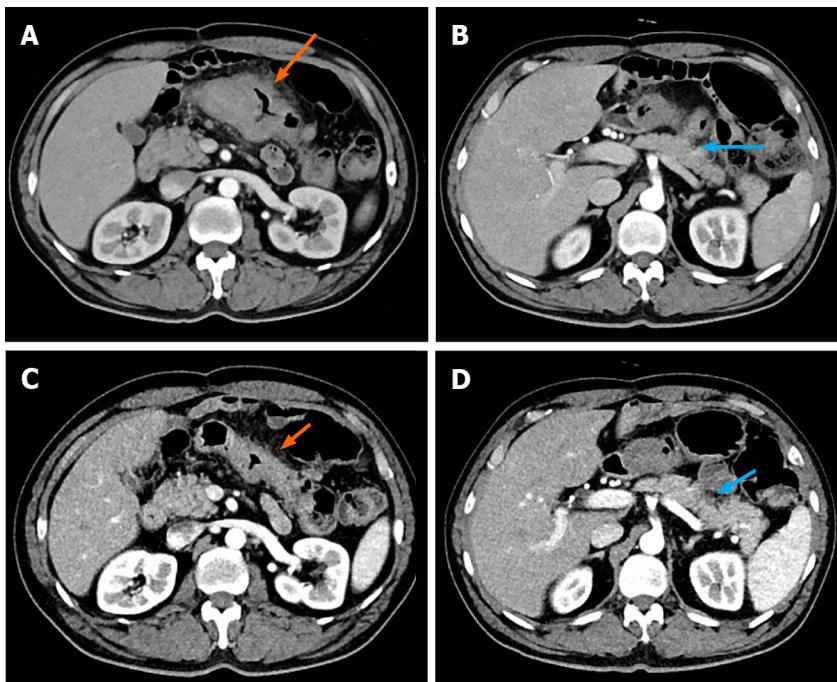
Laboratory results showed normal carcinoembryonic antigen and carbohydrate antigen 19-9. No abnormality was found in routine blood analyses.

Imaging examinations

Colonoscopy revealed a large, cauliflower-like mass in the transverse colon. Histopathological examination of the biopsy specimen revealed a poorly-differentiated adenocarcinoma with dMMR. Contrast-enhanced abdominal computed tomography (CT) demonstrated a bulky tumor measuring > 10 cm in the transverse colon (Figure 1A), and several enlarged lymph nodes in the mesentery. CT did not reveal metastases to distant sites.

FINAL DIAGNOSIS

Considering the invasion of the pancreatic capsule (Figure 1B), negative margins were not ascertained intraoperatively.



DOI: 10.4251/wjgo.v15.i12.2237 Copyright ©The Author(s) 2023.

Figure 1 Computed tomography scans taken before and after immunotherapy. A and B: Before immunotherapy (arrows); C and D: After immunotherapy. The orange arrows showed the location and range of the tumor, while the blue arrows showed invasion of the pancreatic capsule.

TREATMENT

Preoperative immunotherapy is recommended for conversion to resection. The patient received three cycles of pembrolizumab immunotherapy without complaints. Post-treatment CT showed significant regression of the tumor (Figure 1C and D), as assessed by our team.

Thus, the patient underwent open transverse colectomy with D2 lymph node dissection two weeks after the end of immunotherapy. The previous ileocolonic anastomosis was resected during surgery.

As shown in Figure 2A, gross examination revealed invasion of the serosal surface by the tumor. Interestingly, pathological examination showed that the tumor regression grade was 0, indicating complete regression with no residual tumor cells, including the lymph nodes (Figure 2B). The final stage in this patient was a pathologic complete response (pCR).

OUTCOME AND FOLLOW-UP

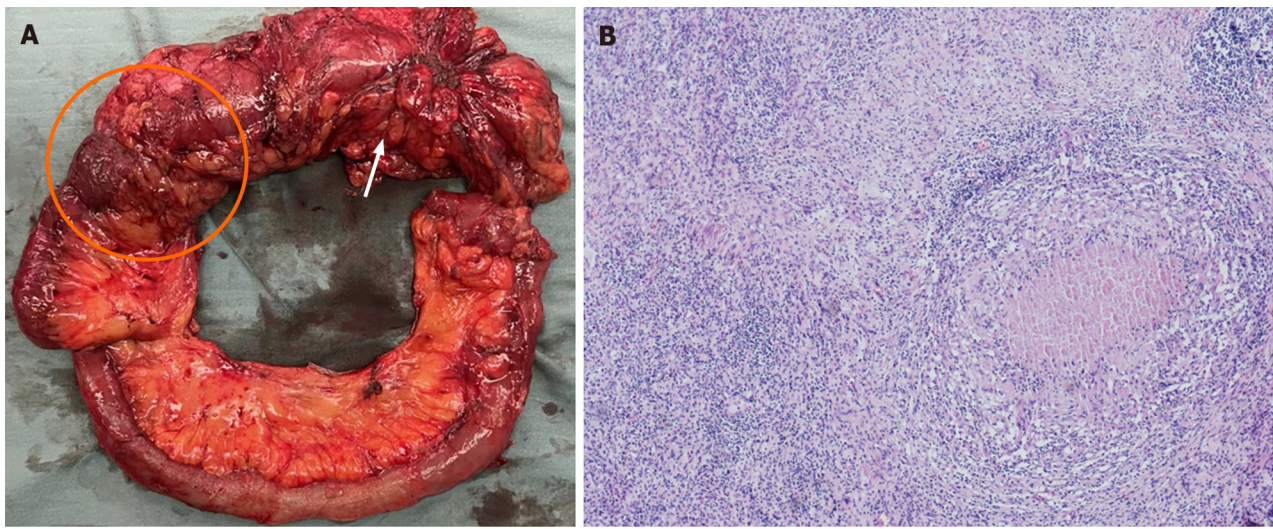
Delayed gastric emptying (DGE) occurred, and a transnasal feeding tube was placed for nutritional support. The patient was discharged from the hospital on the 39th day after surgery, when the DGE was alleviated.

DISCUSSION

To the best of our knowledge, this case is the first to provide evidence of the efficacy of immunotherapy as a conversion regimen for locally unresectable colon cancer with dMMR.

The hallmark of dMMR is the inability to repair spontaneous mutations during DNA replication, leading to hypermutation and increased tumor mutation burden[15]. Currently, dMMR is one of the major predictive biomarkers of the benefits of immune checkpoint inhibitor (ICI) benefit[16]. Thus, MMR status should be regularly tested for colon cancer to guide personalized treatment. ICI therapy aims to overcome tumor immune escape by targeting immune inhibitory molecules expressed on the surfaces of the tumor and immune cells.

Since numerous questions remain regarding dMMR and its impact on the efficacy of immunotherapy, several clinical trials have been launched to determine the optimal treatment for patients with colon cancer. NICHE-1 was the first neoadjuvant immunotherapy study to show pathological responses in 100% of dMMR tumors[10]. The PICC trial[12] reported a pCR rate of 65% in patients with locally advanced dMMR CRC who received immunotherapy. Pei *et al*[17] reported that 90.9% of patients with locally advanced dMMR CRC achieved pCR after neoadjuvant immunotherapy. The NICHE-2 study subsequently reported that the rates of major pathological response and pCR for locally advanced dMMR colon cancer were 95% and 67%, respectively[11]. It also reported the first survival data in which none of the patients had



DOI: 10.4251/wjgo.v15.i12.2237 Copyright ©The Author(s) 2023.

Figure 2 Gross pathological examination and hematoxylin and eosin staining. A: Gross pathological examination showed the tumor (orange arrow) and previous ileocolonic anastomosis (orange circle); B: Hematoxylin and eosin staining slide (magnification: $\times 40$) showed that the lesion was tumor-free.

recurrence at a median follow-up of 13 mo, suggesting the advantage of neoadjuvant immunotherapy. More than the potential survival benefit of immunotherapy, Han *et al*[18] reported that neoadjuvant immunotherapy significantly reduced open surgery (83.3% *vs* 72.2%, $P < 0.001$) and multi-visceral resection rate ($P = 0.025$) for CRC patients. Hence, this therapy could minimize the extent of surgery and improve postoperative recovery.

The high response rate observed in patients suggests that surgery combined with neoadjuvant immunotherapy is a promising option for CRC surgeons to use in dMMR colon cancers which appear unresectable. This method is also likely to achieve better oncologic resection and organ-sparing strategies. However, the optimal duration of immunotherapy and the timing of surgery remain to be determined. Moreover, a long-term follow-up is required to assess the effects of immunotherapy on the survival of a selected subset of patients with dMMR colon cancer.

CONCLUSION

Immunotherapy can be used as a conversion treatment for locally unresectable dMMR colon cancer. However, further evidence from clinical trials is required to confirm these findings.

FOOTNOTES

Author contributions: Sun Z and Liu H collected data and drafted the manuscript; Zhang GN participated in data acquisition and interpretation; Xiao Y revised and finalized the manuscript; all authors have read and approved the final manuscript.

Supported by National High Level Hospital Clinical Research Funding, No. 2022-PUMCH-C-027.

Informed consent statement: Written informed consent was obtained from the patient for publication of this report and any accompanying images.

Conflict-of-interest statement: Written informed consent was obtained from the patient for publication of this report and any accompanying images.

CARE Checklist (2016) statement: The authors read the CARE Checklist (2016) and the manuscript was prepared and revised according to this checklist.

Open-Access: This article is an open-access article that was selected by an in-house editor and fully peer-reviewed by external reviewers. It is distributed in accordance with the Creative Commons Attribution NonCommercial (CC BY-NC 4.0) license, which permits others to distribute, remix, adapt, build upon this work non-commercially, and license their derivative works on different terms, provided the original work is properly cited and the use is non-commercial. See: <https://creativecommons.org/licenses/by-nc/4.0/>

Country/Territory of origin: China

ORCID number: Zhen Sun 0000-0001-7430-8081; Guan-Nan Zhang 0000-0001-8685-5015; Yi Xiao 0000-0002-4309-1227.

S-Editor: Yan JP

L-Editor: A

P-Editor: Yu HG

REFERENCES

- 1 Vogel JD, Felder SI, Bhama AR, Hawkins AT, Langenfeld SJ, Shaffer VO, Thorsen AJ, Weiser MR, Chang GJ, Lightner AL, Feingold DL, Paquette IM. The American Society of Colon and Rectal Surgeons Clinical Practice Guidelines for the Management of Colon Cancer. *Dis Colon Rectum* 2022; **65**: 148-177 [PMID: 34775402 DOI: 10.1097/DCR.0000000000002323]
- 2 Argilés G, Taberero J, Labianca R, Hochhauser D, Salazar R, Iveson T, Laurent-Puig P, Quirke P, Yoshino T, Taieb J, Martinelli E, Arnold D; ESMO Guidelines Committee. Localised colon cancer: ESMO Clinical Practice Guidelines for diagnosis, treatment and follow-up. *Ann Oncol* 2020; **31**: 1291-1305 [PMID: 32702383 DOI: 10.1016/j.annonc.2020.06.022]
- 3 Chang H, Yu X, Xiao WW, Wang QX, Zhou WH, Zeng ZF, Ding PR, Li LR, Gao YH. Neoadjuvant chemoradiotherapy followed by surgery in patients with unresectable locally advanced colon cancer: a prospective observational study. *Onco Targets Ther* 2018; **11**: 409-418 [PMID: 29398921 DOI: 10.2147/OTT.S150367]
- 4 Miyamoto Y, Hiyoshi Y, Tokunaga R, Akiyama T, Daitoku N, Sakamoto Y, Yoshida N, Baba H. Postoperative complications are associated with poor survival outcome after curative resection for colorectal cancer: A propensity-score analysis. *J Surg Oncol* 2020; **122**: 344-349 [PMID: 32346880 DOI: 10.1002/jso.25961]
- 5 de Gooyer JM, Verstegen MG, 't Lam-Boer J, Radema SA, Verhoeven RHA, Verhoef C, Schreinemakers MJM, de Wilt JHW. Neoadjuvant Chemotherapy for Locally Advanced T4 Colon Cancer: A Nationwide Propensity-Score Matched Cohort Analysis. *Dig Surg* 2020; **37**: 292-301 [PMID: 31661689 DOI: 10.1159/000503446]
- 6 Yuan Y, Xiao WW, Xie WH, Cai PQ, Wang QX, Chang H, Chen BQ, Zhou WH, Zeng ZF, Wu XJ, Liu Q, Li LR, Zhang R, Gao YH. Neoadjuvant chemoradiotherapy for patients with unresectable radically locally advanced colon cancer: a potential improvement to overall survival and decrease to multivisceral resection. *BMC Cancer* 2021; **21**: 179 [PMID: 33607964 DOI: 10.1186/s12885-021-07894-6]
- 7 Niu SQ, Li RZ, Yuan Y, Xie WH, Wang QX, Chang H, Lu ZH, Ding PR, Li LR, Wu XJ, Zeng ZF, Xiao WW, Gao YH. Neoadjuvant chemoradiotherapy in patients with unresectable locally advanced sigmoid colon cancer: clinical feasibility and outcome. *Radiat Oncol* 2021; **16**: 93 [PMID: 34030722 DOI: 10.1186/s13014-021-01823-4]
- 8 Laursen M, Dohrn N, Gögenur I, Klein MF. Neoadjuvant chemotherapy in patients undergoing colonic resection for locally advanced nonmetastatic colon cancer: A nationwide propensity score matched cohort study. *Colorectal Dis* 2022; **24**: 954-964 [PMID: 35285992 DOI: 10.1111/codi.16116]
- 9 Morton D, Seymour M, Magill L, Handley K, Glasbey J, Glimelius B, Palmer A, Seligmann J, Laurberg S, Murakami K, West N, Quirke P, Gray R; FOXTROT Collaborative Group. Preoperative Chemotherapy for Operable Colon Cancer: Mature Results of an International Randomized Controlled Trial. *J Clin Oncol* 2023; **41**: 1541-1552 [PMID: 36657089 DOI: 10.1200/JCO.22.00046]
- 10 Chalabi M, Fanchi LF, Dijkstra KK, Van den Berg JG, Aalbers AG, Sikorska K, Lopez-Yurda M, Grootsholten C, Beets GL, Snaebjornsson P, Maas M, Mertz M, Veninga V, Bounova G, Broeks A, Beets-Tan RG, de Wijkerslooth TR, van Lent AU, Marsman HA, Nuijten E, Kok NF, Kuiper M, Verbeek WH, Kok M, Van Leerdam ME, Schumacher TN, Voest EE, Haanen JB. Neoadjuvant immunotherapy leads to pathological responses in MMR-proficient and MMR-deficient early-stage colon cancers. *Nat Med* 2020; **26**: 566-576 [PMID: 32251400 DOI: 10.1038/s41591-020-0805-8]
- 11 Chalabi M, Verschoor YL, van den Berg JG, Sikorska K, Beets G, Lent AV, Grootsholten MC, Aalbers A, Buller N, Marsman H, Hendriks E, Burger PWA, Aukema T, Oosterling S, Beets-Tan R, Schumacher TN, van Leerdam M, Voest EE, Haanen JBAG. LBA7 Neoadjuvant immune checkpoint inhibition in locally advanced MMR-deficient colon cancer: The NICHE-2 study. *Ann Oncol* 2022; **33** Suppl 7: S808-S869 [DOI: 10.1016/j.annonc.2022.08.016]
- 12 Hu H, Kang L, Zhang J, Wu Z, Wang H, Huang M, Lan P, Wu X, Wang C, Cao W, Hu J, Huang Y, Huang L, Shi L, Cai Y, Shen C, Ling J, Xie X, He X, Dou R, Zhou J, Ma T, Zhang X, Luo S, Deng W, Ling L, Liu H, Deng Y. Neoadjuvant PD-1 blockade with toripalimab, with or without celecoxib, in mismatch repair-deficient or microsatellite instability-high, locally advanced, colorectal cancer (PICC): a single-centre, parallel-group, non-comparative, randomised, phase 2 trial. *Lancet Gastroenterol Hepatol* 2022; **7**: 38-48 [PMID: 34688374 DOI: 10.1016/S2468-1253(21)00348-4]
- 13 Verschoor YL, Van den Berg JE, Beets G, Sikorska K, Aalbers A, van Lent A, Grootsholten C, Huibregtse I, Marsman H, Oosterling S, van de Belt M, Kok M, Schumacher T, van Leerdam ME, Haanen JBAG, Voest EE, Chalabi M. Neoadjuvant nivolumab, ipilimumab, and celecoxib in MMR-proficient and MMR-deficient colon cancers: Final clinical analysis of the NICHE study. *J Clin Oncol* 2022; **40**: 3511-3511 [DOI: 10.1200/JCO.2022.40.16_suppl.3511]
- 14 Agha RA, Franchi T, Sohrabi C, Mathew G, Kerwan A; SCARE Group. The SCARE 2020 Guideline: Updating Consensus Surgical Case Report (SCARE) Guidelines. *Int J Surg* 2020; **84**: 226-230 [PMID: 33181358 DOI: 10.1016/j.ijvs.2020.10.034]
- 15 Kavun A, Veselovsky E, Lebedeva A, Belova E, Kuznetsova O, Yakushina V, Grigoreva T, Mileyko V, Fedyanin M, Ivanov M. Microsatellite Instability: A Review of Molecular Epidemiology and Implications for Immune Checkpoint Inhibitor Therapy. *Cancers (Basel)* 2023; **15** [PMID: 37190216 DOI: 10.3390/cancers15082288]
- 16 Llosa NJ, Cruise M, Tam A, Wicks EC, Hechenbleikner EM, Taube JM, Blosser RL, Fan H, Wang H, Lubber BS, Zhang M, Papadopoulos N, Kinzler KW, Vogelstein B, Sears CL, Anders RA, Pardoll DM, Housseau F. The vigorous immune microenvironment of microsatellite instable colon cancer is balanced by multiple counter-inhibitory checkpoints. *Cancer Discov* 2015; **5**: 43-51 [PMID: 25358689 DOI: 10.1158/2159-8290.CD-14-0863]
- 17 Pei F, Wu J, Zhao Y, He W, Yao Q, Huang M, Huang J. Single-Agent Neoadjuvant Immunotherapy With a PD-1 Antibody in Locally Advanced Mismatch Repair-Deficient or Microsatellite Instability-High Colorectal Cancer. *Clin Colorectal Cancer* 2023; **22**: 85-91 [PMID: 36528470 DOI: 10.1016/j.clcc.2022.11.004]
- 18 Han K, Tang JH, Liao LE, Jiang W, Sui QQ, Xiao BY, Li WR, Hong ZG, Li Y, Kong LH, Li DD, Zhang XS, Pan ZZ, Steele SR, Ding PR. Neoadjuvant Immune Checkpoint Inhibition Improves Organ Preservation in T4bM0 Colorectal Cancer With Mismatch Repair Deficiency: A Retrospective Observational Study. *Dis Colon Rectum* 2023; **66**: e996-e1005 [PMID: 35485833 DOI: 10.1097/DCR.0000000000002466]



Published by **Baishideng Publishing Group Inc**
7041 Koll Center Parkway, Suite 160, Pleasanton, CA 94566, USA
Telephone: +1-925-3991568
E-mail: office@baishideng.com
Help Desk: <https://www.f6publishing.com/helpdesk>
<https://www.wjgnet.com>

